MCL-406/V

60-23865 (LC)

TT60-23865

AD649484

TRANSLATION

THE MACHINING OF HARDENED STEELS

By L. M. Re[illegible]kiy

July 1960

455 Pages

PREPARED BY
LIAISON OFFICE
TECHNICAL INFORMATION CENTER
MCLTD
WRIGHT-PATTERSON AIR FORCE BASE, OHIO

This translation was prepared under the auspices of the Liaison Office, Technical Information Center, Wright-Patterson AFB, Ohio. The fact of translation does not guarantee editorial accuracy, nor does it indicate USAF approval or disapproval of the material translated.

Comments pertaining to this translation should be addressed to:

Liaison Office
Technical Information Center
MCLTD
Wright-Patterson Air Force Base, Ohio

MCL-406/V

THE MACHINING OF HARDENED STEELS

BY: L. M. Reznitskiy

July 1960

455 pages

MCL-406/V

L. M. Reznitskiy
Kand. Tekhn. Nauk

MEKHANICHESKAYA OBRABOTKA ZAKALENNYKH STALEY

Mashgiz
Gosudarstvennoe Nauchno-Tekhnicheskoye Izdatel'stvo
Mashinostroitel'noy Literatury
Moscow 1958 Leningrad
398 pages

This book is devoted to the machining of hardened structural alloy steels. It sets forth the results of investigations and data on progressive industrial experience in the turning, end-milling, drilling, rose and flute reaming, and cutting of threads in hardened steels. It contains practical recommendations on tool design and geometry selection, and cutting routines.

The book is designed for use by the engineering and technological personnel of machine-building enterprises. It may also be valuable to the scientific personnel and students of institutes of machine-building technology and polytechnic institutes in the field.

Readers: A.M.Vul'f, Docent, Candidate in Engineering Sciences; and V.D.Morozov, Docent, Candidate in Engineering Sciences.

Editor: E.D.Maydel'man, Engineer

MASHGIZ, LENINGRAD DIVISION

Editorial Office for Literature on the Technology of Machinery Manufacture

Chief of Editorial Office: Ye.P.Naumov, Engineer

PREFACE

Today, machine-building is characterized by an effort to expand to the maximum the number of parts of machines and mechanical devices made of heat-treated high-hardness steels. However, the proportion of such parts to the whole is as yet insignificant and does not correspond to the great potentials for utilization of the mechanical properties of hardened steels.

Earlier concepts of the mechanical properties of hardened steels have undergone a fundamental change. It has been established by Ya.B.Fridman (Bibl.4) that high-hardness heat-treated steels which are highly brittle to tensile testing prove ductile in other tests, such as torsion testing. The studies of B.D.Grozin (Bibl.5) have revealed that such steels display plastic deformation when subjected to unequal universal compression.

The need for a considerable expansion of the use of hardened steels in the manufacture of machinery is also confirmed by investigations of surface properties. These show that machining of hardened steel parts results in a microgeometry of the surface and in physical and mechanical properties of the surface layer that give these parts very high service characteristics.

The hardening process causes strains in parts subjected to it, resulting in distortion of the geometric form. This makes it necessary that, after heat-treatment, such parts be subjected to a removal of the allowance, which comes to 3 - 4 mm and more per diameter.

Until recently only one method of machining high-hardness steels was known:

grinding. This seriously inhibited any extension of the field of application of hardened parts in machines and mechanical devices.

Subsequently, it was shown by research and production experience that a steel brought to any degree of hardness may be machined successfully by means of cermet cutting tools. Designers now have more latitude in specifying hardened parts in their machines and mechanical devices, without fearing the difficulties involved in machining such parts.

The process of manufacturing these parts - prior to the final heat treatment - should provide allowances for quenching strains. Machining by cermet tools permits a substantial reduction in the allowance to be removed by grinding, or even to omit this operation in its entirety. In both cases, a considerable saving is achieved.

The use of cermet tools to machine hardened steels results in a high surface finish. At average rates of feed, the surface finish achieved by mere turning of hardened steels corresponds to that attainable by rough grinding and, at slow rates of feed, to that attainable by finish-grinding.

The surface finish attainable by end-milling of hardened steels is also not inferior to that of finish-ground surfaces.

The investigations, showing that treatment of hardened steels by cermet tools results in surface layers of a considerably better quality than that produced by grinding, are of major significance.

Not long ago the entire literature on the machining of hardened steels was confined to a small number of articles in journals and magazines. The situation has now changed. In addition to K.F.Romanov's book on rose and flute reaming (Bibl.68), P.A.Markelov's book on end-milling (Bibl.60)* and the author's papers on turning and thread cutting (Bibl.53, 54), brief treatments of various methods of machining hard-

*P.A.Markelov's book devoted to high-speed end-milling of steels with cermet tools gives some space to the machining of hardened steels.

ened steels will be found in the standards for high-speed cutting routines issued by the former Ministry of Machine-Tool Manufacture (Bibl.27,66).

Interesting studies have been published by N.S.Logak on fine-turning (Bibl.21), by N.N.Zorev on the cutting force in turning (Bibl.27, 74), by M.N.Larin on the turning of hardened steels with introduction of electric current into the cutting zone (Bibl.56). Moreover, the essentials of theses for the degree of Candidate in Engineering Sciences dealing with the turning of hardened steels, submitted by V.S.Mamayev, A.A.Maslov, A.D.Makarov and Ye.A.Belousov (Bibl.18, 24, 26, 30) have been published. A paper by A.V.Silant'yev (Bibl.40) on profile turning and one by V.I.Zhikharev (Bibl.51) on turning hardened steels with cermet cutters, have been published.

The literature has given adequate treatment to the turning of hardened steels. Experimental findings and industrial experience in this field make it possible confidently to offer recommendations with respect to determination of tool geometry and machining conditions.

The number of investigations into other forms of machining of hardened steels has been considerably lower. Despite the substantial significance of the cited papers by K.F.Romanov and P.A.Markelov, the data they contain cannot serve as the basis for the development of entirely dependable recommendations.

Information on the drilling of hardened steels is limited entirely to the works of B.G.Levin (Bibl.65) and B.A.Ignatov (Bibl.67).

The foregoing will explain the limited nature of the data on end-milling, rose and flute reaming and particularly drilling - all as compared to turning - in the standards of the Scientific Research Bureau for Engineering Standards (NIBTN). Continuation of research in these fields is an important objective in the further development of the machining of hardened steels.

The need to systematize the theoretical and practical data accumulated to this moment on various methods of machining hardened steels, and to compile them in a single handbook, is evident. This is the objective of the present study.

Chapter I, containing data on alloy steels presents today's concepts on the mechanical properties of hardened steels.

Chapter II contains data on cermets, hard alloys, and mineral ceramics. An understanding of the process of machining hardened steels requires a knowledge of all the peculiarities of hard alloys. An attempt has been made by the author to compile all available latest data in this Chapter, so as to make it unnecessary for the reader to refer to other sources. The Chapter also contains a description of foreign brands of hard alloys.

Chapters III-VIII discuss the present status of scientific and practical knowledge in this field and give manufacturing suggestions on choice of design and the geometric parameters of the cutting part of the tool.

Chapter IX offers a series of generalizing conclusions on the data in this book and considers the problem of the physical nature of high-speed machining, based on an analysis of the process of machining hardened steels. The results of an investigation by N.N.Zorev of the cutting force in the turning of hardened steels is of considerable theoretical interest.

The author will welcome all comments and information on shortcomings found in this work.

CHAPTER I

MECHANICAL PROPERTIES OF HARDENED STRUCTURAL ALLOY STEELS

1. Classification of Alloy Steels

Alloy steels are usually classified in accordance with one of the following characteristics:

a) Structure in the normalized condition, resulting from accelerated cooling;

b) Structure in the annealed state, resulting from slow cooling;

c) End use.

Under the first of these, alloy steels are broken down into five classes: austenitic, martensitic, pearlitic (the former being the major classes), carbidic, and ferritic.

Determination of whether a given steel falls into one of these major classes is arrived at by heating specimens of 15 - 20 mm thickness to the austenitic state and then cooling them in the air. If the test steel acquired an austenitic or martensitic structure under these conditions, it is classified correspondingly. Steels of pearlitic as well as of sorbite or troostite structure are grouped in the pearlitic class.

The characteristic of steels in the carbidic class is not the basic structure of the cooled specimen, but the presence of a considerable volume of alloying carbides which are formed only when the steel has an adequate level of carbide-forming elements and carbon.

The ferritic class includes alloy steels containing a considerable number of elements constricting the zone of γ-solid solution. At low carbon content (which enlarges the γ-zone), allotropic transformations will be absent in these steels,

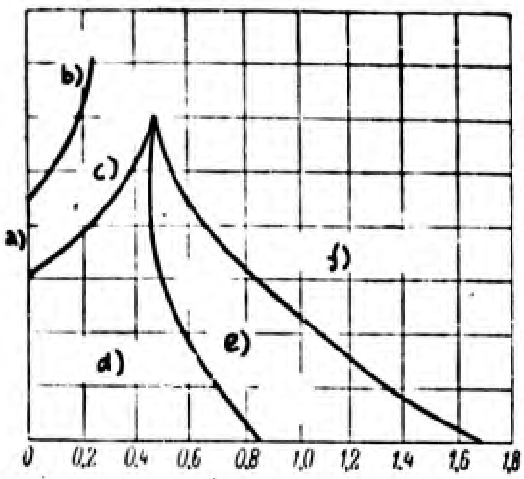

Fig.1 - Regions of Existence of Various Classes in Ternary Systems "Iron-Carbon-Alloying Element" for Elements Constricting the γ-Zone

a) Content of alloying element; b) Ferritic; c) Semiferritic; d) Hypoeutectoid; e) Hypereutectoid; f) Ledeburitic; g) Carbon content, %

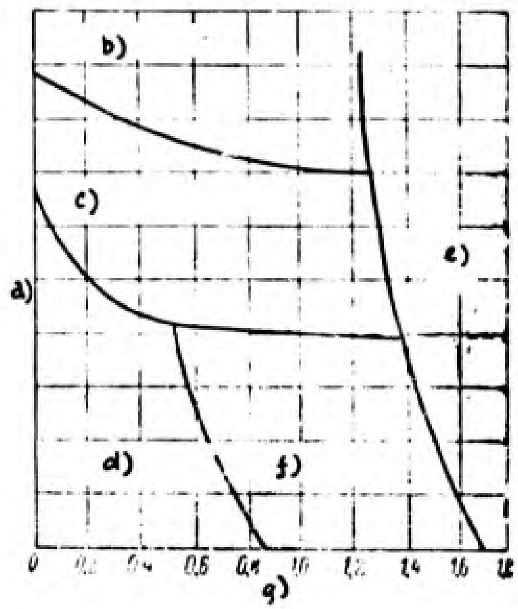

Fig.2 - Regions of Existence of Various Classes in Ternary Systems "Iron-Carbon-Alloying Element" for Elements Expanding the γ-Zone

a) Content of alloying element; b) Austenitic; c) Semiaustenitic; d) Hypoeutectoid; e) Ledeburitic; f) Hypereutectoid; g) Carbon content, %

which will, at all temperatures up to fusion, be in the state of α-solution, i.e., they will constitute alloyed ferrite.

Under the second heading, alloy steels are subdivided into hypoeutectoid, hypereutectoid, and ledeburite classes. The structure of hypoeutectoid steels contains excess (hypoeutectoid) ferrite, the structure of hypereutectoid steels contains excess carbides (secondary; precipitated from the austenite), while the structure of ledeburitic steels contains primary carbides (as eutectoids of the ledeburite type in the cast condition, and in the form of isolated inclusions in the forged and rolled condition).

The carbon steels fall into the following categories, depending upon the "iron-carbon" diagram: at a carbon content below 0.83%, into the hypoeutectoid class; at a carbon content above 0.83% (in practice, 1.0 - 1.7% C), into the hypereutectoid class; at a carbon content above 1.7% - to the ledeburite class. The majority of alloying elements shift the S point (corresponding to 0.83% C) and the E point (corresponding to 1.7% C), and consequently the boundaries between these classes, to the left, in the direction of a carbon content lower than that of carbon steels.

In steels having a high content of the alloying elements which narrow the γ-zone (Cr, Mo, Si, W, Ti, and others) and a low carbon content, $\alpha \rightleftharpoons \gamma$ changes do not occur upon heating (cooling), or occur only in part. Steel that has a stable γ-phase at all temperatures up to that of fusion is termed ferritic, and that which undergoes partial $\alpha \rightleftharpoons \gamma$ transformation is termed semiferritic.

Thus, in the case of steels alloyed by elements narrowing the γ-region, the following five classes are possible: hypoeutectoid, hypereutectoid, ledeburitic, ferritic and semiferritic.

In steels having a high content of alloying elements tending to enlarge the γ-region (Ni, Mn), $\alpha \rightleftharpoons \gamma$ transformations may not occur at all temperatures at which the alloy is in the solid state. In such steels the γ-phase is stable. They are termed austenitic, or semiaustenitic in the case of partial $\alpha \rightleftharpoons \gamma$ transformation.

Consequently, in the case of steels alloyed by elements tending to expand the γ-region, the following five classes are possible: hypoeutectoid, hypereutectoid, ledeburitic, austenitic, and semiaustenitic.

Figure 1 presents a general diagram of the regions in which the different classes exist in the iron-carbon-alloying element system for an element that narrows the γ-region, while Fig.2 shows the same for an element expanding the γ-region.

Alloy steels may be classified into three groups, by end use:

1) Structural steels (machine-building) employed in the making of parts for

machines and mechanisms;

2) Tool steels, from which various types of tools are manufactured;

3) Steels with special properties: stainless, acid-resistant, heat-resistant, etc. Structural steels fall chiefly into the pearlitic class, tool steels into the carbidic, steels with special properties into the austenitic or ferritic.

Structural alloy steels are classified as follows:

1) Low-alloy steels, in which the total content of alloying elements does not exceed 2%;

2) Medium-alloy steels, in which the total content of alloying elements is between 2 and 5%;

3) High-alloy steels, in which the total content of alloying elements exceeds 5%.

2. Structural Alloy Steels

General Data

Structural steels are usually subjected to tensile and impact testing (of notched specimens on the Charpy machine). The results of these tests provide a general idea of the mechanical properties of the given steel and make it possible to estimate its quality, as well as the heat treatment it has undergone. However, they are inadequate for judging the behavior of steel under real service conditions, since steel parts function under considerably more complex conditions of loading than is the case in the usual tensile and impact tests.

Moreover, the nature of the loading and the type of the resultant stressed state in the steel have a great influence upon its mechanical properties. For example, the indices of the resistance of steel to deformation (σ_t, σ_T), ductility (δ, ψ), and particularly notcn toughness (a_k) change over a wide range in accordance with temperature, the presence of notches in the test specimen, rate of loading, dimensions of the specimen, etc.

In order to make it possible to judge more completely the properties of structural steels under various conditions, they are subjected not only to the usual tensile and impact tests, but to fatigue, wear, offset, or notch tensile testing, etc. These special mechanical tests are widely utilized in research.

A very important property of steels is the tendency to brittle failure. This property is determined by a series of impact tests according to N.N.Davidenkov. The toughness of common structural steels usually drops with any drop in temperature. Therefore, a steel that is ductile at room temperature may be brought to a brittle state by cooling to below $0^{o}C$. Impact tests of steel at gradually declining temperatures may be used to determine the temperature at which this steel begins to change over (or completely changes over) into a brittle state. These temperatures may serve as a criterion for the tendency of a steel toward embrittlement. When measured against the temperature at which the steel is worked (usually atmospheric temperature), they constitute indices of the residual ductility of the steel.

Purpose of Alloying

The major purpose of alloying structural steels is to improve their mechanical qualities. Optimum ratios of mechanical properties are achieved by proper selection of the type of heat treatment of the steel. By way of example, Table 1 presents indices of mechanical properties depending upon the type of heat treatment for 40Kh steel, which is widely employed in machine-building.

The Table shows that the best indices of mechanical properties are achieved in combined heat treatment: hardening, followed by high or low tempering.

Characteristic of low tempering are exceedingly high indices of resistance to deformation σ_T and σ_t at satisfactory ductility; whereas high tempering is characterized by medium values of σ_T and σ_t at elevated toughness a_k and little tendency to brittle failure.

After a single heat treatment (annealing or normalization), the overall complex of mechanical properties of steel will be lower.

Table 1

Mechanical Properties of 40Kh Steel Relative to Various Heat Treatments

Heat Treatment	σ_T in kg/mm²	σ_{pr} in kg/mm	δ in %	ψ in %	a_K in kg-m/cm²	Temperature of Embrittlement in °C, Determined by Impact Test
Annealing at 850 - 860°C	29,5	58,5	22,0	53,4	6,2	— 60
Normalization from 850 - 860°C (rods 15 mm in diam)	39,6	69,2	19,3	57,3	8,7	— 75
Hardening from 850 - 860°C, tempering at 180 - 200°C	162,3	189,4	8,3	33,7	5,6	— 90
Hardening from 850 - - 860°C, tempering at 600 - 610°C	78,2	95,2	21,2	63,1	14,3	— 125

In the case of other types of structural steels, the effect of heat treatment upon changes in their mechanical properties is in general of the same nature as for 40Kh steel. Therefore, structural alloy steels are most frequently subjected to hardening followed by high or low-temperature tempering.

An important purpose in the alloying of structural steels is that of increasing their hardenability* to a point that will produce optimum mechanical properties as the result of heat treatment.

Alloying of structural steels also has the purpose of reducing their tendency to brittle failure. The data in Table 2 show that the tendency of structural steel to brittle failure is related to the alloying elements it contains. The two steels differ only little in terms of σ_T, σ_t, δ, ψ, and a_k at room temperature. At the

*The hardenability of steel is determined by the depth from its surface to which a heat-treated steel may be hardened to martensite.

same time, the first steel (medium-alloy) changes to a brittle state more rapidly with a reduction in temperature than does the second (high-alloy). The first steel has a considerably smaller reserve of ductility than the second and a greater tendency to brittle failure under actual service conditions.

The various alloying elements have different effects upon the reserve ductility of structural steel. Nickel has the most favorable effect in this respect, and copper and silicon act to some degree in this manner (in low-tempered steels). Chromium, tungsten, and molybdenum have a positive but very slight effect, whereas large amounts of manganese act negatively.

Table 2

Mechanical Properties of Chromium-Manganese-Molybdenum and Chromium-Nickel-Molybdenum Steels in the Improved State

Chemical Composition of the Steel in %	Heat Treatment	σ_T in kg/mm²	σ_{pr} in kg/mm²	δ in %	ψ in %	a_k in kg-m/cm² at the Temperatures				
						+20°	−75°	−12[illegible]°	−150°	−1[illegible]°
0,28 C; 1,45 Mn; 1,40 Cr; 0,30 Mo	Hardening and Tempering at 640 – – 660°C	70,8	86,3	17,9	63,8	15,6	8,1	1,8	0,4	0,4
0,26 C; 1,58 Cr; 4,01 Ni; 0,39 Mo		73,2	93,4	16,3	58,4	[illegible]3,6	12,6	10,5	8,6	7,0

Mechanical Properties and Brittleness in Tempering of Alloy Steels

Unlike straight carbon steels, structural alloy steels display two types of temper brittleness.

First Type of Temper Brittleness. Figure 3 gives a typical diagram of the changes in the mechanical properties of structural alloy steel relative to the tempering temperature. As indicated in the diagram, starting at temperatures of the order of 200°C, corresponding to the intensive decomposition of martensite on tempering, this steel displays a gradual diminution in σ_t and σ_T with a simultaneous rise in δ and ψ. When the tempering temperatures are 550 - 600°C, the steel retains significant strength.

The toughness varies in accordance with a different regularity. Unlike in

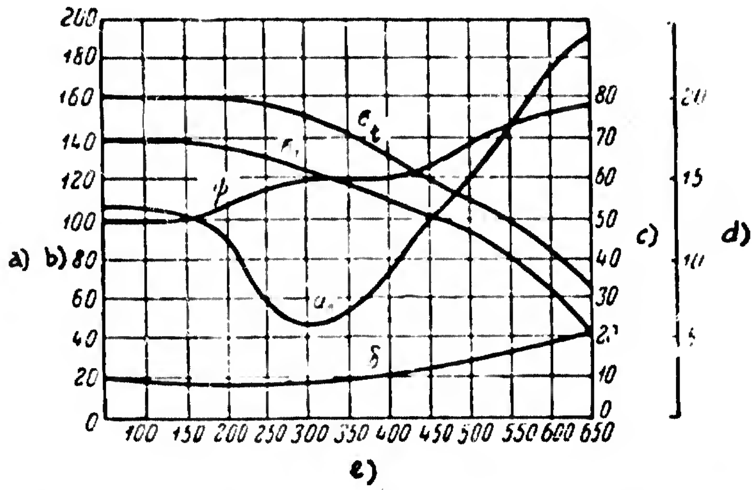

Fig.3 - Change in the Mechanical Properties of Alloy Steel (0.26% C, 1.25% Cr, 0.24% Mo) Upon Tempering

a) Tensile strength σ_t, kg/mm^2; b) Yield point, σ_T, kg/mm^2; c) Elongation δ, Necking ψ, %; d) Toughness a_k, kg-m/cm^2; e) Tempering temperature, °C

structural straight carbon steels, in which the malleability rises continually with temperature, a break occurs here in the ductility curve, i.e., a sharp reduction in the value of a_k after tempering in a given temperature interval (in the given instance, the 250 - 400°C interval causes embrittlement of the steel).

This brittleness, depending solely upon the temperature of tempering, is permanently retained in the steel if the temperature corresponds to the region of the "dip" in the a_k curve. Therefore, this type is called irreversible temper brittleness.

Depending upon the composition of the structural alloy steel, the irreversible temper brittleness may vary in degree. Sometimes, and in certain steels, two intervals of brittleness appear: one at 250 - 400°C and one at 500 - 550°C. The appearance of brittleness in the first interval is not accompanied by any significant increase in hardness. In the second interval, it frequently denotes some rise in hardness.

The appearance of irreversible brittleness on tempering is prevented by avoiding the tempering of structural alloy steels in the 250 - 400°C temperature interval. However, if the steel is also subject to brittleness on tempering in the 500 - 550°C interval, tempering in this temperature interval is also avoided.

Second Type of Temper Brittleness. Many structural alloy steels reveal another type of brittleness upon tempering, but only at high temperatures (above 450°C).

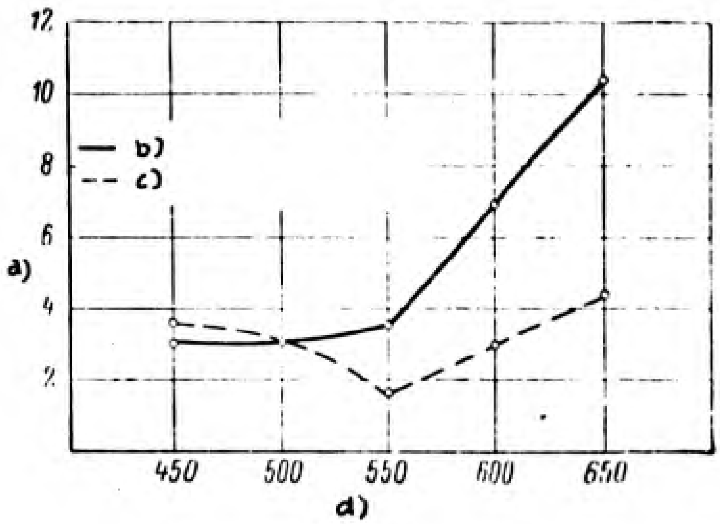

Fig.4 - Effect of Cooling Rate after High-Temperature Tempering upon the Toughness of Steel (0.43% C, 1.48% Cr, 3.10% Ni)

a) Toughness, a_k, kg-m/cm^2; b) Quenching in oil; c) Cooling in the furnace; d) Tempering temperature, °C

This type of brittleness is related to the rate of cooling after the reheating for tempering (Fig.4). If cooling is slow, the toughness diminishes and brittleness appears. If cooling is rapid, the toughness remains at a high level.

A characteristic of this type of brittleness is its reversibility. The brit-

Table 3

Classification of Constructional Alloy Steels Under GOST 4543-48

Group No.	Group of Steels	Limits of Carbon and Alloying Elements (in the Various Grades)
1	Chromium	0,12—0,55% C; 0,7—1,1% Cr
2	Chrome-vanadium	0,12—0,54% C; 0,8—1,1% Cr; 0,10—0,20% V
3	Molybdenum	0,10—0,34% C; 0,40—0,55% Mo
4	Chromium-molybdenum	0,1—0,4% C; 0,8—1,9% Cr; 0,15—0,55% Mo
5	Chromium-silicon	0,29—0,45% C; 1,3—1,6% Cr; 1,0—1,6% Si
6	Chromium-manganese	0,12—0,45% C; 0,4—1,2% Cr; 0,9—1,9% Mn
7	Chromium-manganese-titanium	0,16—0,24% C; 1,0—1,3% Cr; 0,8—1,1% Mn; 0,08—0,15% Ti
8	Chromium-manganese-molybdenum	0,16—0,45% C; 0,9—1,2% Cr; 0,9—1,2% Mn; 0,2—0,3% Mo
9	Silicon-manganese	0,22—0,40% C; 1,1—1,4% Si; 1,1—1,4% Mn
10	Chromium-silicon-manganese	0,15—0,40% C; 0,8—1,4% Cr; 0,9—1,4% Si; 0,8—1,1% Mn
11	Chromium-aluminum and chromium-molybdenum-aluminum	0,31—0,42% C; 1,35—1,65% Cr; 0,15—0,25% Mo; 0,7—1,2% Al
12	Chromium-molybdenum-vanadium	0,22—0,38% C; 1,0—1,8% Cr; 0,2—0,3% Mo; 0,1—0,3% V
13	Nickel	0,20—0,35% C; 0,5—1,2% Ni
14	Nickel-molybdenum	0,10—0,45% C; 1,5—2,0% Ni; 0,2—0,3% Mo
15	Chromium-nickel	0,11—0,45% C; 0,45—1,75% Cr; 1,00—3,75% Ni
16	Chromium-nickel-vanadium	0,16—0,24% C; 0,7—1,1% Cr; 3,75—4,25% Ni; 0,15—0,30% V
17	Chromium-nickel-tungsten	0,14—0,28% C; 1,35—1,65% Cr; 4,0—4,5% Ni; 0,8—1,2% W
18	Chromium-nickel-molybdenum	0,10—0,44% C; 0,60—1,75% Cr; 1,25—3,75% Ni; 0,15—0,30% Mo
19	Chromium-nickel-molybdenum-vanadium	0,26—0,50% C; 0,6—1,1% Cr; 1,3—2,5% Ni; 0,2—0,3% Mo; 0,1—0,3% V

tleness arising in the process of slow cooling of steel may be eliminated by rapid cooling when the steel is again tempered. Brittleness may again appear in this steel if it is heated once more, followed by slow cooling.

This type of brittleness is sometimes observed upon slow cooling after the heating of normalized and even of tempered steel to 500 - 700°C. However, it usually appears upon the tempering of hardened steels. Therefore, this type is termed temper brittleness or reversible brittleness upon tempering.

Alloying elements have differing effects upon the tendency of steels toward temper brittleness. Manganese and chromium sharply increase the sensitivity of steel to this form of brittleness. Other elements act in the same direction, but less strongly. Only molybdenum and tungsten significantly reduce the sensitivity of steel to temper brittleness, and may even eliminate this completely.

In industrial practice, two methods of counteracting the appearance of temper brittleness are employed:

1) Addition of molybdenum (0.25 - 0.45%) or tungsten (0.6 - 1.2%) to the steel;

2) Rapid cooling of the steel after high-temperature tempering by quenching in water or oil, when stretcher strains do not constitute a limiting factor.

Simultaneous use of both methods permits a complete elimination of temper brittleness in properly alloyed steels.

Influence of Alloying Elements Upon the Hardenability of Steel

All alloying elements other than cobalt reduce the critical speed of steel hardening and increase the hardenability. The most important alloying elements may be arranged in the following series of diminishing influence upon the hardenability of steels: Mo, Mn, Cr, Ni, Cu, Si.

The carbide-forming elements result in an increase in the hardenability of steel only if they are dissolved in the austenite. When these elements are enclosed in carbides, they do not increase the hardenability but merely facilitate an accelerated decomposition of austenite on cooling of the steel.

If the steel contains a number of alloying elements, the quantitative influence of each of the elements upon the hardenability of the steel will rise.

Alloying makes it possible, at a comparatively small total content of these elements, to achieve a hardenability of steel in water attaining a critical diameter of hundreds of millimeters. In carbon steel, however, the critical diameter is about 25 mm.

Government Standards for Structural Alloy Steels

The classification of the structural alloy steels manufactured in the USSR, as well as of their specifications, are standardized by GOST 4543-48. This Standard covers the 19 groups of steels presented in Table 3.

The system of designation of structural alloy steels, adopted by the Government Standards of the USSR, permits a ready identification of the chemical composition of any given steel. In this system, the alloying elements in the steel are denoted by the (Russian) initials of these elements: Kh - chromium (Cr), N - nickel (Ni), M - molybdenum (Mo), T - titanium (Ti), K - cobalt (Co), V - tungsten (W).

The following arbitrary designations constitute exceptions to the foregoing: G - manganese (Mn), S - silicon (Si), F - vanadium (V), Yu - aluminum (Al), D - copper (Cu).

The quantitative content of alloying elements and carbon is denoted by digits. The first two digits in the grading of a steel represent average carbon content in hundredths of one percent. The digits after the letters indicate the percentage content of the given element in whole numbers, if it exceeds 1.5%. If the content of the given element is less than 1.5%, no digit is provided.

At the end of the grading, the letter A is added to denote high-quality steel, purer than quality steel in terms of sulfur and phosphorus, and having better mechanical properties.

3. Effect of Alloying Elements on the Mechanical Properties of Structural Steels when Tempered at High Temperature

The sorbite state of steel after thermal improvement (hardening to martensite), followed by high-temperature tempering) is characterized by an optimum combination of mechanical properties for the majority of cases of steel utilization: high tensile strength (σ_t = 75 - 110 kg/mm^2) and high ductility (a_k = 14 to 7 kg-m/cm^2). Therefore, thermal improvement is widely employed in structural steels.

In order to achieve the required mechanical properties of steel in the sorbitic state, it is necessary to develop the required volume of carbides having the optimum degree of dispersion while maintaining the specific properties of the ferritic base. The strength of this steel is related chiefly to the quantity and degree of dispersion of the carbides, and the toughness is also dependent upon the ferritic base.

The relative quantity of carbides in alloy steel is determined chiefly by carbon content. Theoretically, this depends upon the content of alloying elements as well, but the latter factor is of subordinate significance. We learn from practical experience that the maximum permissible quantity of carbides in medium-alloy structural steel tempered at high temperature is limited to a carbon content of the order of 0.45 - 0.50%. A further increase in the carbide phase and the carbon content to over 0.45 - 0.50% causes the ductility to drop to a level impermissible for structural steels (a_k ≈ 3 kg-m/cm^2). At the same time, any excessive reduction in the carbon content of the steel (to less than 0.2%) will result in a sharp reduction in its strength. Therefore, the structural alloy steels, employed in the sorbitic state, most often contain 0.25 - 0.45% carbon.

In order to prevent carbides from coagulate to dimensions that would sharply reduce σ_t and σ_T, alloying elements are introduced to form carbides that coagulate with difficulty upon tempering in the 550 - 650°C temperature interval. The alloying element most frequently introduced is 0.8 - 1.7% chromium. Chromium steels

(15Kh, 20Kh ... 50Kh) have come into wide use in the machine manufacture.

However, chromium steels do not possess high hardenability or a high ductility reserve. The hardenability of these steels is improved by additional alloying with molybdenum and manganese. Vanadium is sometimes introduced to provide a fine-grain structure. These steels are represented in GOST 4543-48 by grades 30KhM, 40KhG, 40KhFA, and others.

Chromium-nickel-molybdenum and chromium-nickel-tungsten steels are the best structural steels presently available. At a high nickel content, these steels harden to depths of 200 mm and more. Moreover, they are little subject to brittle failure, and as a result, parts made of such steels behave well under impact.

Table 4

Structural Alloy Steels Employed in the Sorbitic (High-Tempered) State

Grade	Chemical Composition, %				Other elements	Guaranteed Mechanical Properties (per GOST)				
	C	Cr	Ni	Mo		σ_T in kg/mm²	σ_b in kg/mm²	δ in %	ψ in %	a_k in kg-m/cm²
40Kh	0,35—0,45	0,8—1,1	⩽ 0,4	—	0,5—0,8 Mn	80	100	9	15	6
40KhNMA	0,36—0,44	0,6—0,9	1,25—1,75	0,15—0,25	0,5—0,8 Mn	85	100	12	55	10
37KhN3A	0,33—0,41	1,2—1,6	3,0—3,5	—	0,25—0,55 Mn	100	115	10	50	6
40KhGM	0,37—0,45	0,9—1,2	⩽ 0,4	0.2—0,3	0,9—1,2 Mn	80	100	10	45	9
38KhNYuA (nitrided)	0,35—0,42	1,35—1,65	⩽ 0,4	0,15—0,25	0,7—1,1 Al	85	100	15	50	9

The high cost of these steels, due to the presence of nickel, molybdenum, and tungsten, has resulted in the development of substitutes. In some cases, a certain portion of the nickel is supplanted by copper or manganese. Introduction of vanadium, or an increase in the content of chromium in these steels (to 2.8%) sometimes permits reducing the molybdenum and tungsten content. The resultant steel is just as good, in terms of tensile strength, after tempering at high temperature.

Table 4 presents typical grades of modern structural alloy steels that have undergone heat treatment. The mechanical properties indicated in the Table are those prescribed by GOST. In this list, 40KhGM steel is an example of a substitute for a chromium-nickel-molybdenum steel.

It is evident that all these grades of steel have high strength and considerable ductility. Despite the great difference in the chemical composition of these steels and, particularly, in the nickel content ratio, their mechanical properties differ but little. From this it follows that nickel has no serious effect upon the mechanical properties of steel tempered at high temperature, and its function consists chiefly of ensuring the required hardenability of steel of a given cross section.

4. Effect of Alloying Elements upon the Mechanical Properties of Structural Steels in the Low-Tempered (Hardened) State

The martensitic state of structural steels is distinguished by very high hardness and tensile strength (σ_t = 120 - 210 kg/mm^2), but diminished toughness (a_k = = 8 - 3 kg-m/cm^2).

Heat treatment of alloy steels to achieve the martensitic state has the purpose of providing high hardness and tensile strength. In actual practice, these steels are then tempered at low temperature, so as to avoid any significant changes in hardness and tensile strength but improve somewhat the toughness and diminish the residual strains of the hardening process. Steels so treated have come to be called "hardened". In reality, these are steels that have been subjected to hardening and subsequent tempering at low temperature.

The content of alloying elements in a given steel should result in complete hardenability to martensite. However, excessive alloying may even have a negative effect, since the considerable amount of retained austenite leads to a reduction in hardness of the hardened steel. The mechanical properties of hardened alloy steels are determined primarily by their carbon content.

Influence of Carbon

Table 5, compiled for medium-alloy hardened steels, confirms the strong influence of carbon content upon the mechanical properties of steel. A carbon content of about 0.45% produces approximately the maximum tensile strength in steel. Any further increase in carbon content results in an insignificant increase in tensile strength, but in a greater reduction in ductility. When the carbon content is 0.18% or less, hardened steel does not possess high tensile strength and hardness.

Table 5

Effect of Carbon upon Mechanical Properties of Hardened Structural Steels

Carbon Content of Steel, in %	Tensile Strength, in kg/mm^2	Toughness, in $kg\text{-}m/cm^2$
0,18	120	8,0
0,35	175	5,0
0,45	200	3,0
0,60	210	1,5

The structural alloy steels employed in the hardened state contain 0.2 - 0.4% carbon. The carbon content is reduced to 0.12 - 0.25% in carburized steels with a ductile core.

General Nature of the Influence of Alloying Elements

The effect of alloying elements upon the tensile strength and the yield point of a hardened steel is negligible. These characteristics are determined chiefly by the carbon content of the steel, and not by the quantity of alloying elements therein. The latter have an important influence upon the notch toughness and the ductility reserve of a steel.

Table 6 presents the mechanical properties of variously alloyed hardened steels of identical carbon content. It will be seen that, despite the considerable quantitative and qualitative difference in the content of the alloying elements, the yield points and tensile strengths of these steels are approximately equal. Nor is there any great difference in the influence of the alloying elements upon elongation per unit length. Only with respect to notch toughness is there any great difference between manganese and other steels.

The nature of the influence of various alloying elements upon the mechanical

Table 6

Mechanical Properties of Hardened Constructional Steels Alloyed by Various Elements

Steel	Total Alloying Elements, in %	Chemical Composition, in %							σ_T, in kg/mm²	σ_B, in kg/mm²	δ, in %	a_k, in kg-m/cm²
		C	Si	Mn	Cr	Ni	Mo	Cu				
Mn	2,40	0,34	0,30	2,10	--	-	--	-	140	169	12,0	2,5
Cr—Mo	2,54	0,32	0,40	0,42	1,42	-	0,30	--	141	172	12,5	5,2
Si—Cr—Mo	3,70	0,31	1,42	0,33	1,60	--	0,35	--	152	180	15,2	6,0
Mn—Cr—Ni—Mo—Cu	7,17	0,34	0,32	1,81	1,41	2,43	0,28	0,89	146	178	16,4	5,5

properties of alloy steels is retained to some degree in multiple-component steels. Alloying elements have little influence upon the strength and hardness of hardened steels. Some elements have a noticeable influence upon the notch toughness and ductility reserve of steels.

Carbon is decisive in determining the mechanical properties of hardened structural steels. Despite this fact, structural carbon steels with 0.2 - 0.4% C are not employed in the hardened condition. This is explained by the superiority of structural alloy steels.

The major advantage lies in the fact that the critical hardening rate of alloy steels is lower, and therefore both hardenability at the surface and depth of hardening are better. Low-carbon unalloyed steel, particularly of large section, cannot be hardened to martensite. Moreover, alloy steels have less of a tendency to grain growth, i.e., to overheat, than do unalloyed steels.

Another major advantage of alloy steels over unalloyed steels is the possibility of achieving a substantial degree of toughness in the hardened (low-tempered) state. Hardened carbon steels are brittle.

Let us examine the alloying elements employed in hardened structural steels.

Silicon. Silicon is added to constitute 1.0 - 1.8% of the steel. This element has a positive influence upon the notch toughness and the ductility reserve of the steel, reduces its sensitivity to overheating, and considerably increases the temperature at which martensite converts to troostite in the tempering of steel. This makes it possible to raise the temperature at which low-temperature tempering is performed and to reduce temper strains.

However, silicon has little effect upon the hardenability of steel. In hardenability, silicon steels differ little from ordinary straight carbon steels. Therefore structural steels are alloyed not only with silicon but with also other elements.

Chromium. Chromium is usually added to constitute 1.0 - 1.8% of the steel. Chromium-silicon steels have high mechanical properties and little tendency to overheat, but are low in hardenability.

Manganese. Manganese is added to chromium-silicon steels for hardenability, and constitutes 0.8 - 1.4% of the product. The presence of manganese in a steel results in some reduction in notch toughness and ductility reserve, but the hardenability rises sharply and the mechanical properties remain at a fairly high level.

Steels containing approximately the same amount of chromium, silicon, and manganese (1.0 - 1.5%) are called chromansils. They have acquired wide popularity as structural alloy steels hardenable up to martensite.

Sometimes 0.15 - 0.40% molybdenum is added to chromansil and chromium-silicon steels to increase the hardenability and reduce the tendency to grain growth upon heating.

Nickel. The addition of nickel markedly increases the hardenability of chromium-silicon steels and chromansils. The resultant steels are widely employed in the making of large-diameter parts. Chromium-nickel-molybdenum steels are employed for the same purposes. However, the field of application is being narrowed down in favor of silicon steels. Steel for parts subject to carburization constitutes an exception. Chromium, nickel, chromium-nickel, and chromium-nickel-molybdenum steels are the types most widely used for this purpose.

Table 7

Typical Structural Alloy Steels Employed in the Hardened State

Steel	Chemical Composition, %					Approximate Mechanical Properties					
	C	Mn	Si	Cr	Ni	σ_T in kg/mm²	σ_b in kg/mm²	δ in %	ψ in %	a_k in kg-m/cm²	H_{Rc}
15KhA, carburizable	0,12—0,18	0,3—0,6	—	0,7—1,0	⩽ 0,4	50	70	11	50	8	—
12KhN2A, carburizable	0,11—0,17	0,3—0,6	—	0,6—0,9	1,5—2,0	60	80	12	50	9	—
30KhGSA, non-carburizable	0,28—0,35	0,8—1,1	0,9—1,2	0,8—1,1	⩽ 0,4	130	155	7	40	4	—
ShKh15, ball-bearing	0,95—1,0	—	—	1,3—1,5	—	—	—	—	—	—	⩾62

Special note should be taken of the high-carbon chromium steel ShKh15* (0.95 - 1.0% C, 1.3 - 1.5% Cr) which is employed in the hardened (martensitic) state. This steel is used in making parts for ball and roller bearings, which operate under service conditions requiring high resistance to abrasion. Thanks to the high carbon content (which is typical of tool rather than structural steels), ShKh15 steel acquired a hardness of $H_{R_C} \geq 62$ after hardening and tempering at low

*This is not a GOST but an industrial designation. However, it has become firmly entrenched.

temperature.

Table 7 presents carburizable and non-carburizable grades of alloy steels employed in the low-tempered (martensitic) state. As may be seen, carburizable steels are distinguished by high notch toughness in the hardened state. This is explained by their low carbon content.

Noncarburizable steel 30KhGSA has come into wide use. Thanks to its high mechanical properties and the absence of expensive alloying elements, this steel has gradually come to replace more expensive chromium-nickel and chromium-nickel-molybdenum steels that had previously been employed in the hardened state. Due to its comparatively low hardenability (critical diameter 60 - 80 mm upon quenching in water), this steel is not used for large sections. Under these conditions, more nickel is usually added.

5. Present Concepts on the Mechanical Properties of Hardened Steels

Until recently, the mechanical properties of hardened steels had been characterized by hardness H_B(B.H.N. or H_{RC}) and tensile strength σ_t (both being indexes of resistance to deformation), elongation per unit length δ, or necking ψ (indexes of ductility), and notch toughness a_k (index of toughness). The ductility and toughness indexes are so low in the case of high-hardness hardened steels (close to zero) that such steels are usually regarded as completely brittle materials.

Ya.B.Fridman (Bibl.4) holds the view that brittleness is characteristic of hardened steels only in particular states of stress (tension, bending) at which the percentage of tensile stresses is sufficiently high. However, torsion testing, which is almost never used, makes it possible to discover new properties in hardened steels, not discoverable or not subject to quantitative measurement in tensile testing.

In the opinion of Ya.B.Fridman, the very possibility of measuring Brinell hardness shows that unlike still more brittle materials (for example, many glasses and silicates), hardened steels are capable, under particular conditions of stress, of undergoing quite considerable plastic deformations.

The ratio of the maximum tensile stresses to the maximum tangential stresses in torsion is only one half as great as in tension. Many hardened steels that are entirely brittle in tension display significant plastic strains in torsion.

By way of example, Ya.B.Fridman cites chromansil (0.38% C, 1.06% Cr, 0.89% Mn, and 1.06% Si), oil-quenched from 880°C without subsequent tempering. Whereas this steel is entirely brittle in tension (elongation being virtually equal to zero), it reveals substantial ductility to torsion (actual elongation per unit length e = 20%).

Ya.B.Fridman holds that the ductility of hardened steels of high hardness, which are wholly brittle to tension, may be determined easily and with sufficient dependability, by torsion testing.

B.D.Grozin (Bibl.5) has determined, by investigations of the mechanical properties of hardened steels, that when hardened steels and brittle materials in general are subjected to unequal compression from all sides, they will undergo plastic deformation.

The mechanical properties of hardened steels are characterized chiefly by hardness, which is determined by impressing a penetrator into the test material (the penetrator being a ball, a cone, or a pyramid). This causes some degree of plastic deformation in the metal. The deformed metal is in a stressed state of all-round uneven compression.

B.D.Grozin has developed a method of testing the mechanical properties of hardened steels, based on the idea that the deformable portion of the test specimen is in a stressed state throughout, similar to that of a metal subjected to denting by a penetrator during hardness testing.

A cylindrical test specimen is squeezed into a cylindrical ring of a ductile material (No.20 steel), whose diameter is 3.6 times as large as the diameter of the specimen. The faces of the sample and ring are then ground.

silicates), hardened steels are capable, under particular conditions of stress, of undergoing quite considerable plastic deformations.

The ratio of the maximum tensile stresses to the maximum tangential stresses in torsion is only one half as great as in tension. Many hardened steels that are entirely brittle in tension display significant plastic strains in torsion.

By way of example, Ya.B.Fridman cites chromansil (0.38% C, 1.06% Cr, 0.89% Mn, and 1.06% Si), oil-quenched from 880°C without subsequent tempering. Whereas this steel is entirely brittle in tension (elongation being virtually equal to zero), it reveals substantial ductility to torsion (actual elongation per unit length e = 20%).

Ya.B.Fridman holds that the ductility of hardened steels of high hardness, which are wholly brittle to tension, may be determined easily and with sufficient dependability, by torsion testing.

B.D.Grozin (Bibl.5) has determined, by investigations of the mechanical properties of hardened steels, that when hardened steels and brittle materials in general are subjected to unequal compression from all sides, they will undergo plastic deformation.

The mechanical properties of hardened steels are characterized chiefly by hardness, which is determined by impressing a penetrator into the test material (the penetrator being a ball, a cone, or a pyramid). This causes some degree of plastic deformation in the metal. The deformed metal is in a stressed state of all-round uneven compression.

B.D.Grozin has developed a method of testing the mechanical properties of hardened steels, based on the idea that the deformable portion of the test specimen is in a stressed state throughout, similar to that of a metal subjected to denting by a penetrator during hardness testing.

A cylindrical test specimen is squeezed into a cylindrical ring of a ductile material (No.20 steel), whose diameter is 3.6 times as large as the diameter of the specimen. The faces of the sample and ring are then ground.

The composite cylindrical specimen is then subjected to axial compression up to various levels of plastic deformation: from very slight to very great. This subjects the specimen of the steel being tested to uniform and omnilateral compression.

Experiments have shown that when an axial compressive stress of 500 to 700 kg/mm^2 is applied, the plastic deformation of hardened steel is 8 - 12%. Brittleness, i.e., failure under very low deformation, disappears at lateral pressures as low as 1000 atm.

Diagrams for unequal omnilateral compression of hardened steels, obtained in this investigation, make it possible to determine the major indices of their mechanical properties.

B.D.Grozin holds that in the case of parts, operating with contact load application and universal stress, indices for the mechanical properties of the hardened steel of which the part is made, derived in the manner developed by him, correspond more fully to their real operating conditions than do any other indices obtained in two-dimensional stressing, or the conventional hardness indices.

These data confirm the great potentialities inherent in the utilization of the mechanical properties of high-hardness steels in machine manufacture.

CHAPTER II

CERMETS, HARD ALLOYS, AND MINERAL CERAMICS

6. General Data

Modern achievements in the field of metal machining have been among the factors responsible for the development and constant improvement of cermets used for cutting tools.

The great superiority of hard alloys (in the sense of their cutting properties) over other tool materials has contributed to the development and extensive expansion in high-speed machining, as well as the possibility of machining (by turning, thread cutting, milling, drilling, reaming, and broaching) of steels brought to high hardness and of other difficultly machinable steels.

The present Chapter gives fundamental data on cermets of Soviet and foreign origin. Data are also presented on a new tool material - mineral ceramics - which offers prospects of large-scale industrial use. Mineral ceramics are beginning to be employed in the machining of hard steels.

The output capacity of a cutting tool is largely dependent upon the ability of its material to retain the cutting properties for an extended period of time. The cutting properties of a tool material are dependent chiefly upon hardness, resistance to wear, ductility, heat conductivity, impact toughness, and transverse rupture strength.

For proper execution of the machining process, the cutting tool must be harder than the material being machined. In the cutting process, the working edges of the tool are subject to wear (abraded). The wear occurs continually, during the entire cutting process, at all thicknesses of removed chip, at all machining speeds, and at any physical and mechanical properties of the materiel of the tool and of the part being machined. The greater the resistance of the tool material to wear, i.e., the greater its wear resistance, the higher will be its cutting properties.

The cutting process is accompanied by an emission of heat, which causes the

Table 8

Properties of Some Refractory Metals and Carbides Employed in Hard Alloys (Cemented Carbides)

Metals

Type	Chemical Base	Spec.Grav. γ, in gm/cm³	Melting Point in °C	Mohs Hardness
Refractory group				
Tungsten	W	19,5	3360	7
Titanium	Ti	4,5	1730	4
Tantalum	Ta	16,6	3030	7
Columbium	Nb	7,4	2500	—
Vanadium	V	5,8	1720	—
Zirconium	Zr	6,5	1860	6,5
Molybdenum	Mo	10,3	2620	6
Chromium	Cr	6,7	1920	9
Iron group				
Cobalt	Co	8,7	1480	5
Nickel	Ni	8,9	1450	5

Carbides

Type	Chemical Formula	Spec.Grav. γ, in gm/cm³	Carbon Content, in %	Melting Point in °C	Mohs Hardness
Tungsten carbide	WC	15,7	6,12	2870	9
Same	W_2C	17,2	3,16	2700	>9
Titanium carbide	TiC	4,5	20,00	3140	8—9
Tantalum carbide	TaC	14,0	6,21	3880	9
Columbium carbide	NbC	7,5	11,42	3500	9
Vanadium carbide	VC	5,3	19,05	2830	>9
Zirconium carbide	ZrC	7,9	11,65	3530	8—9
Molybdenum carbide	Mo_2C	8,9	5,88	2690	7—9
Chromium carbide	Cr_4C	7,2	5,45	1780	7
Same	Cr_7C_3	6,5	9,00	1700	7

layer of metal being removed and forming the chip, as well as the cutting instrument itself, to become heated in the cutting area. When the work is performed at the high cutting speeds typical of modern machining, the cutting edges of the tool are heated to 800°C and more.

The capacity of the tool material to retain its cutting properties, chiefly hardness and wear resistance at high temperatures, is termed hot-hardness.

The output of a cutting tool is higher, the greater its hardness, resistance to wear, hot-hardness, toughness, mechanical strength, and thermal conductivity and the lower the brittleness of the tool material of which the cutting edge is made.

Good cutting properties are achieved with hard alloys by the fact that they are mostly carbides of refractory metals, characterized by high hardness, wear resistance, and melting point. In hard alloys, a comparatively small number of metals can be used. Only three metals are employed in the industrial grades of Soviet hard alloys: tungsten, titanium, and cobalt. Table 8 presents data on some properties of the metals and carbides utilized in the production of hard alloys. The high hardness and melting point of the carbides of the refractory metals becomes obvious on a comparison with that of iron carbide - cementite (Fe_3C) whose hardness reaches 7 on the Mohs scale, and whose melting point is 1560°C.

As indicated, the carbides of the refractory metals constitute those components of hard alloys that give them their high hardness, resistance to wear, and hot hardness. However, it is impossible to produce hard alloys exclusively from carbides, since the product would be excessively brittle and weak. In order to give hard alloys the necessary strength, metal is added so as to cement the carbide particles into a solid body. Cobalt is the metal normally employed for such cementing purposes.

7. Soviet Hard Alloys (Cemented Carbides)

Classification of Cemented Carbides

Contemporary Soviet cemented carbides are divided into two major groups by chemical composition:

1) Cemented tungsten single carbides consisting of grains of tungsten car-

bide (WC) cemented by cobalt (Co);

2) Cemented titanium-tungsten double carbides consisting of grains of a solid solution of tungsten carbide in titanium carbide (TiC) and excess grains of tungsten carbide cemented by cobalt, or only of grains of a solid solution of tungsten carbide in titanium carbide, cemented by cobalt.

The USSR has standardized the grades of cemented carbides, the shapes and assortment of the blanks, and the technical specifications for cemented carbides. Government Standards GOST 3882-53, replacing GOST 3882-47 and 2209-45, and OST TsM-201-39 have set up thirty standard grades of cemented carbides (Table 9). The shape and size of cemented carbide blanks have been standardized by GOST 2209-55. Table 10 presents the classification of bar shapes.

Formerly, cemented carbides were designated under OST TsM-201-39 as indicated in Table 9: the cemented tungsten carbides as RE, and the titanium-tungsten as α. The present system of designation is based on the following considerations:

1) VK denotes cemented cobalt tungsten carbides. Digits to the right of the K indicate the percentage content of cobalt. Thus, VK3 means a cemented tungsten carbide with 3% cobalt;

2) TK denotes cemented titanium-tungsten cobalt carbides. Digits after the T indicate the percentage content of titanium carbide (TiC). Digits after the K indicate the percentage content of cobalt. Thus, T15K6 means: cemented titanium-tungsten carbide with 15% TiC and 6% cobalt, with the remainder tungsten carbide.

GOST 4872-52 regulates the specifications for cemented carbide blanks for cutting tools, the rules for employment of and methods of testing the blanks, as well as marking, packaging, and documentation.

Cemented-carbide blanks have to be tested for transverse rupture strength and hardness, as well as for machinability. In addition, the specific gravity must be checked (to an accuracy of 0.05%), as must gross structure, and linear and angular

Table 9

Composition and Major Properties of Soviet Cemented Carbides

Group of cemented carbides	Grade designations: OST TsM-201-39	GOST 2209-45	GOST 3882-47	GOST 3882-53	Approximate chemical composition, %: Tungsten carbide, WC	Titanium carbide TiC	Cobalt, Co	Physical and Mechanical Properties: Transverse rupture strength σ_r in kg/mm^2 not less than	Spec. Grav. γ, in gm/cm^3 not less than	Rockwell hardness H_{R_A} not less than	Heat conductivity in cal/cm·sec·°C
Tungsten single carbides	—	—	—	VK2	98	—	2	100	15,0—15,4	90,0	—
	RE3	VK3	VK3	VK3	97	—	3	100	14,9—15,8	89,0	0,169
	—	—	VK3a	—	97	—	3	100	14,9	89,0	—
	RE6	VK6	VK6	VK6	94	—	6	120	14,6—15,0	88,0	0,145
	—	—	VK6a	—	94	—	6	110	14,6	88,5	—
	RE8	VK8	VK8	VK8	92	—	8	130	14,4—14,8	87,5	0,141
	—	—	VK8a	—	92	—	8	130	14,35	87,5	—
	—	—	VK10	VK10	90	—	10	135	14,2—14,6	87,0	—
	—	—	VK10a	—	90	—	10	135	14,2	87,0	—
	—	—	—	VK11	89	—	11	150	14,0—14,4	86,0	—
	RE12	VK12	—	—	88	—	12	150	14,1	87,5	—
	—	—	VK15	VK15	85	—	15	160	13,9—14,1	86,0	0,108
Titanium-tungsten double carbides	α—5	T5K6	—	—	89	5	6	80	12,1	88,0	—
	α—10	T5K10	T5K10	T5K10	85	6	9	115	12,3—13,2	88,5	0,073
	—	—	—	T14K8	78	14	8	115	11,2—12,0	89,5	—
	α—15	T15K6	T15K6	T15K6	79	15	6	110	11,0—11,7	90,0	0,065
	—	—	T15K6a	T15K6T	79	15	6	110	11,0—11,7	91,0	—
	α—21	T21K8	—	—	71	21	8	100	10,0	88,0	—
	—	—	T30K4	T30K4	66	30	4	90	9,5—9,8	92,0	—
	—	—	—	T60K6	34	60	6	75	6,5—7,0	90,0	—

Table 10

Classification of Shapes of Cemented Carbide Bars Under GOST 2209-55

Conventional Number	Diagram	Purpose (Approximate)
01	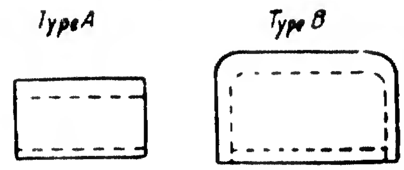	For turning tools (straight and bent shank), for wide-finishing, boring, and slotting.
02	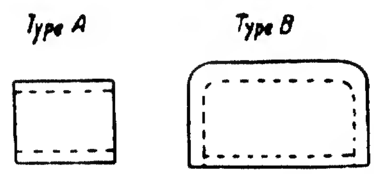	For punching (straight and bent shank), broad-finishing, boring, and slotting cutters on which the greatest wear is at the flank
03	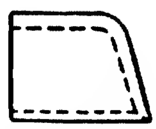	For bent shank turning tools under heavy loads
01		For straight shank turning tools
06	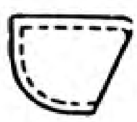	For facing and boring tools in the boring of blind holes
07		For facing and turning tools
08	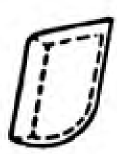	For boring and turning tools in which $\varphi = 60^{\circ}$, and also for the tools of milling heads

Table 10 (cont'd)

Conventional Number	Diagram	Purpose (Approximate)
09	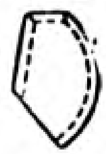	For automatic cutters
10	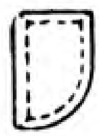	For turning and boring tools, and the teeth of end mills and facing tools
11	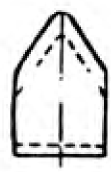	For finishing and threading cutters
12	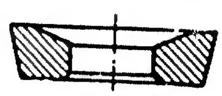	For cup-shaped cutters (fillets and tires)
13	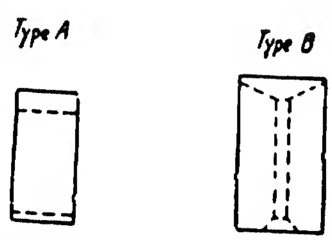	For cutting-off and necking tools
14	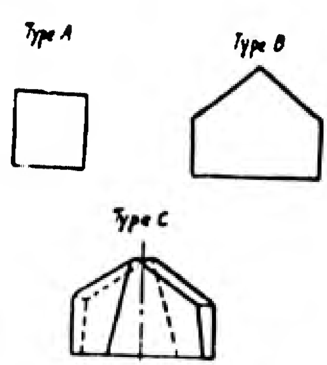	For twist and straight-fluted drills

Table 10 (cont'd)

Conventional Number	Diagram	Purpose (Approximate)
15	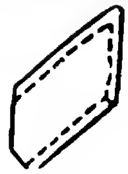	For bevel cutters and dovetail slotters
16	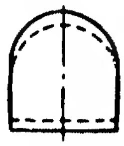	For fillet and tire cutters
17	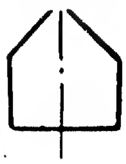	For drilling of nonmetals
18	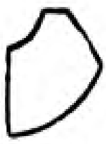	For round chamfer cutters
20	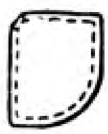	For end mills and countersinking
21		For end and spline mills, for rose reamers to make blind holes, and for countersinkers
24		For end and side mills and T-slot cutters, and also for shell end mills on multistation machines
25	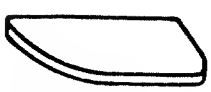	For rose reamers making through holes

Table 10 (cont'd)

Conventional Number	Diagram	Purpose (Approximate)
26		For flute reamers
27	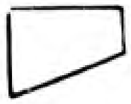	For rose facing reamers
30	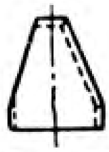	For hobs
31		For angular cutters
32	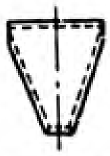	For slotting pulley grooves for belting of triangular cross section
33	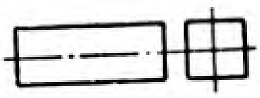	For turning cutters in holders used on multiple-tool lathes
34	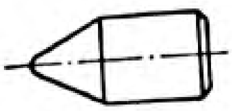	For centers of lathes and cylindrical grinders
35	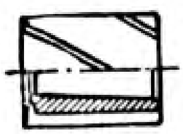	For spiral-toothed end mill arbor cutters of 10 to 22 mm

Table 10 (cont'd)

Conven- tional Number	Diagram	Purpose (Approximate)
36		For spiral-toothed end arbor and face mills of 10 to 120 mm diameter
37	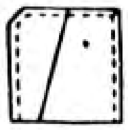	For coarse-feed turning tools
38	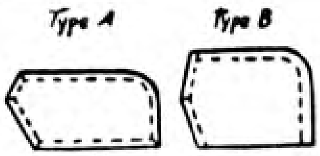	For deep-hole drills
39		For flute lengths of deep-hole drills
40	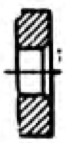	For end mills
41	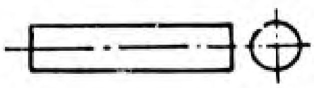	For borers when taking fine cuts
42	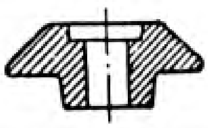	For chip-curlers with parts of type 12
43	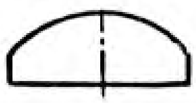	For fluted cutters
44	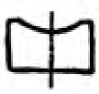	For bevel cutters

dimensions.

The transverse rupture strength of the bar is determined by means of a special lever apparatus for specimens of square cross section measuring 5 × 5 × 35 mm, made of a mixture prepared at the same time as the bars in the given lot.

The Rockwell scale A hardness of the bars has to be checked on its broad edge, protected to a depth of 0.2 mm, by a grinding wheel of green silicon carbide (ceramic binder, 80-mesh grain, hardness SM2). The hardness of the bar has to be checked at three points at equal distances from one another along a diagonal, and from the vertices of the angles.

The manufacturing plants must indicate the grade of the cemented carbide by stamp or roller on the top of each blank (or on any other surface, except that on which it rests). Blanks may also be identified by a single colored strip not more than 5 mm wide. The following color identifications have been assigned to the various grades of cemented carbides:

VK3a	black
VK6	blue
VK6a	violet
VK8	red
T5K10	yellow
T15K6	green
T30K4	light blue

Blanks of 0.5 cm^2 or smaller surface area do not have to be identified individually. Their identification is shown on the crate.

The identification of cemented carbide blanks is of major practical importance. It should be remarked that this important rule is not always followed by the manufacturing plants. Therefore, it is not uncommon for the enterprises utilizing them to mix up the blanks of various grades, leading to improper utilization of cemented

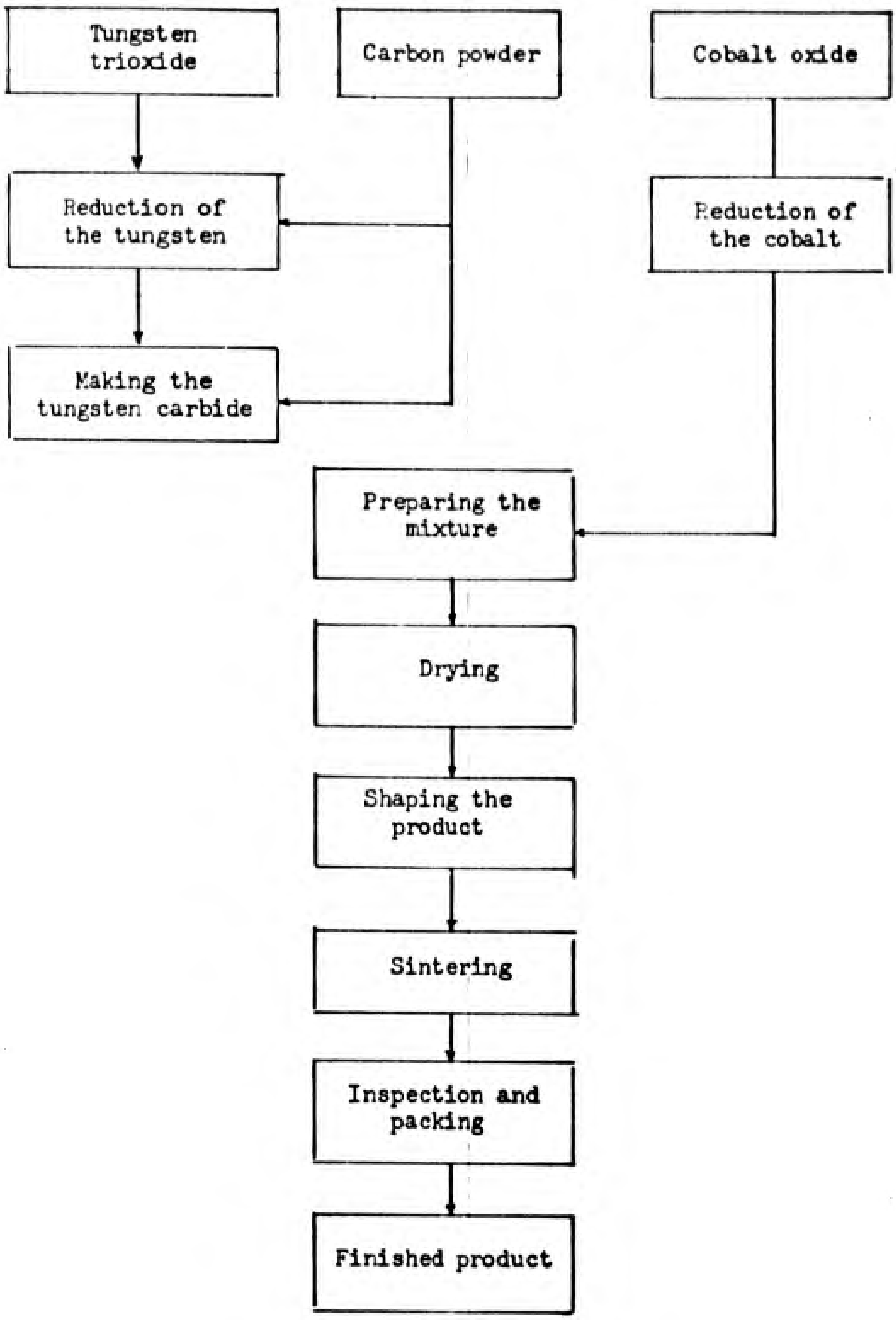

Fig.5 - Flow Sheet for Manufacture of Cemented Tungsten Carbides

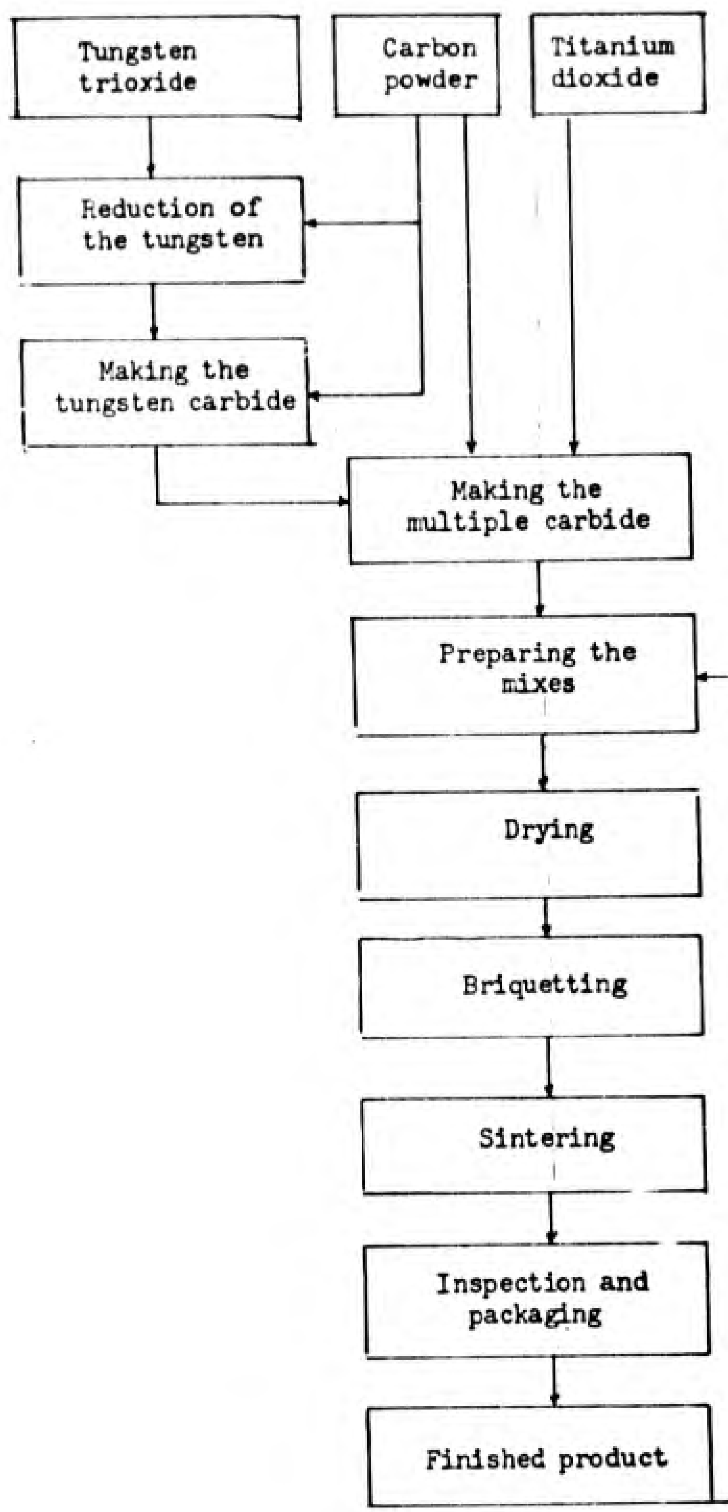

Fig.6 - Flow Sheet for Making Cemented Titanium-Tungsten Carbides

carbide tools.

Summary of the Process of Manufacturing Cemented Carbides

Cemented carbides cannot be called alloys in the usual meaning of the term. Their manufacture differs fundamentally from that of the production of straight carbon, alloy, and high-speed steels, which consists of melting in furnaces, followed by rolling. The manufacture of cemented carbides falls into the category of powder metallurgy. Cemented carbides are produced by sintering, because fusion, due to the decomposition of tungsten carbide, does not yield satisfactory results.

Figures 5 and 6 present flow sheets of the processes of manufacture of cemented carbides from raw material to the finished product. The most important starting materials for the manufacture of cemented carbides are tungsten trioxide (or tungstic acid, ammonium paratungstate), tungsten powder, titanium dioxide, cobalt oxide (or cobalt powder) and carbon powder.

The carbides are made either directly from the metal oxides or from the metal powder obtained as an intermediate. The individual carbides or the ready combined carbide are mixed with the cobalt powder and milled wet until a completely homogeneous fine carbon mixture results. The wet mixture is dried, reduced if necessary, and then pressed into rods, finished bars, or articles of any desired shape.

Certain products are made as follows:

Large blanks are first sintered at 800 - 1000°C and then cut into the required shapes.

The shapes produced in this - or some other - manner are then sintered in a protective atmosphere in electric furnaces.

Cemented carbides do not require any further heat treatment such as hardening, tempering, etc.

Major Properties of Cemented Carbides

Hardness. The most characteristic and valuable property of cemented carbides--

is their high natural hardness, due to the fact that they contain a large volume of carbides of the refractory metals. The chemical composition of the cemented carbide, its grain size and structure influence its hardness. The hardness of the cemented carbide is proportional to total carbide content, the degree of dispersion of the crystals and the carbide content of the solid solution. The hardness of cemented titanium tungsten carbides is as a rule greater than that of cemented tungsten carbides, due to the formation of a denser carbide shell and the fact that the complex carbide is harder than tungsten carbide.

The hardness of the cemented carbide today in use for tipping cutting tools reaches $H_{R_A} = 93$ (T30K4 alloy). Table 9 presents the minimum hardnesses of the cemented carbides now being manufactured. Their actual hardness usually exceeds the indicated limits by 1.0 - 1.5 units.

When compared to high-speed steel, the cemented carbides show 10 Rockwell units more hardness on the C scale (at room temperature). It is obvious that the machining of steels of high hardness (hardened steels) is possible only with cemented carbide tools (and thanks to powder metallurgy).

There is an intimate relation between the cobalt content and the H_{R_A} hardness of cemented tungsten carbides, made under identical conditions. The hardness diminishes with rise in the cobalt content. Thus, VK2, containing 2% cobalt, has an H_{R_A} hardness of 90, whereas the H_{R_A} of VK15 with 15% cobalt content is $H_{R_A} = 86$.

The hardness of cemented titanium tungsten carbides rises with the titanium carbide content. In these cemented carbides, as in the tungsten ones, hardness diminishes as cobalt content rises.

Transverse Rupture Strength. Transverse rupture strength, σ_r is one of the most important mechanical properties of cemented carbides. This property makes it possible to judge the ductility of the cemented carbide. The transverse rupture strength of cemented tungsten carbides rises with the cobalt content, whereas in cemented titanium-tungsten carbides it diminishes as the titanium carbide content rises. Table 9 shows that when the cobalt content of cemented tungsten carbides rises from 2% (VK2) to 15% (VK15), the transverse rupture strength σ_r rises by 60% (from 100 to 160 kg/mm^2). In cemented titanium-tungsten carbides, an increase in titanium carbide content from 5% (T5K10) to 60% (T60K6) causes the transverse rupture strength σ_r to diminish from 115 to 75 kg/mm^2.

Cemented titanium-tungsten carbides are weaker and less ductile than tungsten. In practice, the average values of σ_r are 10 - 15% higher than indicated in Table 9. In general, cemented carbides are considerably inferior to high-speed steel in terms of transverse rupture strength, which is σ_r = 370 kg/mm^2 for that steel.

It has been found (Bibl.6) that, in cemented carbides containing less than 10% cobalt, bending reveals no residual deformation prior to rupture. Deformation of this type becomes detectable only when the cobalt content exceeds 20%.

Compressive Strength. The compressive strength of cemented tungsten carbides σ_c is greatest at a cobalt content of 3 - 5%. With a further increase in the cobalt content, σ_c declines sharply. This value also drops with increasing titanium carbide content in the cemented titanium tungsten carbides.

Today's cemented carbides are distinguished by high compressive strength. In the case of T15K6, $\sigma_c \approx$ 440 kg/mm^2 (whereas for R18 high-speed steel, $\sigma_c \approx$ 380 kg/mm^2).

Tensile Strength and Elongation per Unit Length. Due to the brittleness of cemented carbides, it is very difficult to determine their tensile strength. Experiments (Bibl.6) have established that rupture without plastic yielding occurs in cemented tungsten carbides with less than 10% cobalt after negligible elastic deformation. In the case of a cemented tungsten carbide whose bending strength was σ_r = 144 - 165 kg/mm^2, the tensile strength proved to be 36 - 62 kg/mm^2.

In the case of cemented tungsten carbides, the ratio of σ_t to σ_c is about 0.3 (whereas it is 0.7 for high-speed steel) while the ratio of σ_t to σ_r is about 0.5. In industrial grades of cemented carbides the elongation per unit length on tension is $\delta = 0$.

Impact Strength. The brittleness of cemented carbides is responsible for their low resistance to impact loadings and vibration during the cutting process. This causes crumbling-out of the cemented-carbide bar and shortens the service life of the cutting tool.

The relative impact strength of notched specimens a_k, which is termed impact strength for short, may be employed to characterize the resistance of cemented carbides to shock loads.

Generally, a_k is not determined in the mechanical testing of cemented carbides.

Table 11

Percentage Reduction of Cemented Carbides at a 1000 kg/cm^2 Load

Cemented Carbide	Percentage Reduction at Temperatures, in °C			
	600	900	1000	1100
VK6	0	0	0,3	1,5
VK15	0	0,12	0,65	2,5—3,0
T15K6	0	0	0,1	0,8
High-speed steel, σ_t = 60 kg/mm^2	7	50	60	80

Nevertheless, the results of investigations made by I.S.Brokhin are of considerable interest (Bibl.7). He found the impact strength of cemented tungsten carbides to be higher than that of titanium-tungsten: a_k = 0.3 - 0.4 kg-m/cm^2 for VK8, whereas a_k = 0.20 - 0.25 kg-m/cm^2 in the case of T21K8. When a cemented tungsten carbide is heated to 300°C and a cemented titanium-tungsten carbide is brought to 400°C, a pronounced rise in a_k is observable: In the former instance it doubles, and in the latter it more than trebles. With a further increase in the temperature to 600°C, the impact strength of both cemented carbides drops to a level corresponding to that at room temperature. In the case of a cemented tungsten carbide, the impact strength remains at the same level until 800°C is reached. In the case of a cemented titanium-tungsten carbide, a further slight rise in a_k is observable in the 600 - 800°C interval.

By way of comparison, it is of interest that the impact strengths of carbon and high-speed steels are higher than of cemented carbides, being a_k = 0.89 kg-m/cm^2.

Ductility. Cemented carbides are characterized by very low ductility. This is evident from Table 11 which presents comparative data on cemented carbides and high-speed steels.

Resistance to Wear. The problem of the wear resistance of cemented carbides has had little study despite its great importance. All the more interesting, then, is the detailed study made by G.I.Granovskiy (Bibl.8) of the wear resistance of various tool materials. The fundamental conclusions resulting from this study are presented below.

Special equipment was used in these experiments. This made it possible, under conditions approximating real conditions of friction and wear in the cutting process, to determine the wear resistance of specimens made of various tool materials, under friction with various machined materials.

The wear resistance B is characterized by the work required to abrade 1 mg of material:

$$B = \frac{TL}{\Delta M} \text{ kg-m/mg},$$

where T is the force of friction, in kg;

L is the length of the friction track, in m;

ΔM is the mass of abraded material, in mg.

The investigation determined that wear resistance is not a definite and constant property of tool material. For one and the same material, the wear resistance B will be dependent, at changes in the conditions of friction and wear, upon the velocity of friction v. Figure 7 presents the experimentally-determined relationship between resistance to wear and velocity of friction for various grades of hard alloys and R18 high-speed steel. Friction and wear of specimens was determined against No.45 carbon steel. The friction path L for all specimens, at all speeds of friction, was 2000 m.

Figure 7 shows that all the tool materials studied have a common relationship between change in resistance to wear B with change in velocity of friction v. In

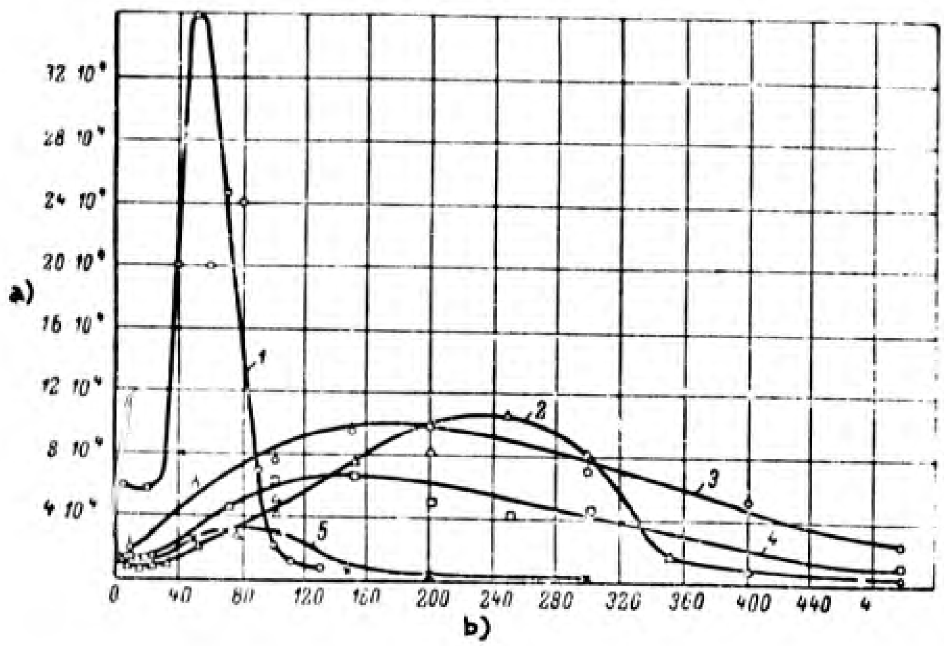

Fig.7 - Ratio of the Wear Resistance B of the Tool Material to the Velocity of Friction v in Dry Friction and Wear of No.45 Steel. Normal stress p = 10 kg/mm^2. Friction zone: 0.75 to 3.0 mm^2.

1 - Steel R18; 2 - Cemented carbide T15K6; 3 - Alloy T60K6; 4 - Alloy T30K4; 5 - Alloy VK8

a) Wear resistance B, kg-m/mg; b) Velocity of friction v, m/min

the interval of low velocities of friction (not over 10 m/min), there is some diminution of the wear resistance B of all materials with an increase in v. The lowest B corresponds to a velocity of friction v = 10 - 20 m/min. As v rises to over 20 m/min, the wear resistance rises, and at some definite velocity, which differs among the various tool materials, it attains its maximum. With further rise in v, wear resistance again diminishes, and the curves always reveal a tendency to approach asymptotically the abscissa axis.

Although a general regularity for the various tests of tool materials does exist, there is a considerable scatter both of the maximum values for wear resistance B and for the velocity of friction at which maximum wear resistance is achieved, as well as of the nature of the further behavior of the curves.

The curve of wear resistance for high-speed steel differs sharply from those for cemented carbides. At velocities of friction up to 90 m/min, the wear resistance of high-speed steel is higher than that of all the grades of cemented carbides investigated. At $v > 100$ m/min, the relationship changes in favor of the latter. The maximum value of wear resistance of high-speed steel exceeds that of the cemented carbides severalfold.

Of the grades of cemented carbides tested, T15K6 steel shows the highest wear resistance, when its velocity of friction is about 250 m/min. Cemented carbides of other grades can be arranged in an order of declining maximum wear resistance as follows: T60K6 (at $v \approx 180$ m/min), T30K4 (at $v \approx 150$ m/min), and VK8 (at $v \approx$ ≈ 80 m/min). In the interval of rates of friction v ranging from 190 to about 310 m/min, T15K6 alloy has a higher wear resistance than T30K4 and T60K6.

A different picture is obtained for cemented titanium-tungsten carbides when the velocity of friction exceeds 350 m/min. In this zone of velocity of friction, the most wear-resistant alloy is T60K6. In wear resistance, the alloy T15K6 is inferior to the alloy T30K4, their wear resistance becoming virtually identical only at $v > 500$ m/min.

Based on the experimental data obtained (Fig.7), G.I.Granovskiy came to the conclusion that the principal initial physical property of resistance of a cutting tool is the wear resistance of the tool material of which its cutting elements are manufactured. He bases his conclusion on a comparison of the curves in Fig.7 with the curve in Fig.8, reflecting the general regularity of change in the service lives of hard-alloy cutters with changes in cutting speed, as found by a number of investigators.

There is complete identity between the nature of the change in wear resistance B due to the velocity of friction and change in the service life of the cutter T due to cutting speed. The service life T, reflecting the rate of increase in the wear of the cutting elements of the cutter indirectly expresses the wear resistance of the tool material used for the cutting edge. Variations in cutting speed bring about a corresponding change in the velocity of friction at the contact areas of the cutting elements of the cutter subject to wear. From this it follows that the general law of change in the service life of a cutter with changes in cutting speed, illustrated in Fig.8, has to be in direct ratio to the law of change in the wear resistance of the cutting portion of the cutter relative to the velocity of friction.

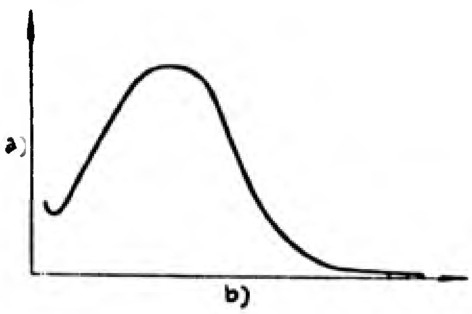

Fig.8 - Ratio of Cutting Speed to Service Life of a Cemented-Carbide Cutter

a) Service life of cutter I, min; b) Cutting speed v, m/min

The work of G.I.Granovskiy provides a theoretical confirmation of practical procedures in the employment of cemented carbide tools and of the results of various investigations on the service life relationships. We know that the VK8 cemented tungsten carbide cannot be efficiently used to machine steels of low and medium hardness, and that high-speed tools are successfully employed for the machining of steels at cutting speeds v = 30 - 80 m/min. Cemented titanium-tungsten carbides can be efficiently employed in the machining of steels only in a specific range of cutting speeds: 150 - 350 m/min for T15K6, 300 - 600 m/min for T30K4, 300 - 1200 m/min for T60K6. However, in the machining of steels for which $\sigma_t < 100$ kg/mm^2, cemented titanium-tungsten carbides do not yield the desired results at v < 50 m/min, because of their high rate of wear.

Experimental data (Bibl.8) show that the wear resistance of tool materials also depends upon the strength of the steel relative to friction and wear. Conditions of abrasion being equal, the wear resistance rises with any decrease in the strength of the steel being machined.

Let us further consider the question of the coefficient of friction, which has

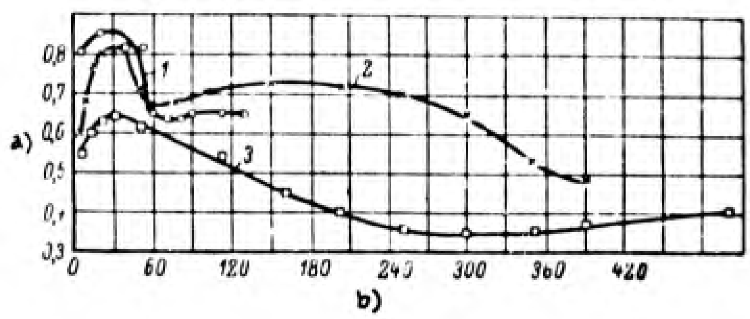

Fig.9 - Effect of Velocity of Friction v on the Coefficient of Friction μ in Dry Friction with No.45 Steel. Normal stress p = 10 kg/mm^2. Friction zone from 0.75 to 3.0 mm^2

1 - Steel R18; 2 - Cemented carbide VK8; 3 - Alloys T15K6, T30K4, T60K6

a) Coefficient of friction μ; b) Velocity of friction v, m/min

been investigated by G.I.Granovskiy (Bibl.8). Figure 9 gives curves for the relationship between the coefficient of friction μ ($\mu = \frac{T}{P}$) where P is the normal force, and the velocity of friction for high-speed steel R18 and the cemented carbides VK8, T15K6, T30K4, and T60K6 in friction with No.45 carbon steel. It will be seen that the coefficients of friction of the high-speed steel R18 and the cemented carbide VK8 are almost identical. The coefficients of friction of all the cemented titanium-tungsten carbides investigated were identical but were considerably lower than that of VK8.

Whereas the coefficient of friction μ first rises, then declines, and then rises again with an increase in the velocity of friction (Fig.9), the experimental data (Bibl.8) show that it is in a simpler relationship to changes in normal stress p. Other conditions being equal, the coefficient μ diminishes with increase in the stress p from 5 to 40 kg/mm^2.

Figure 10 presents curves expressing the regularities of change in the wear resistance B, coefficient of friction μ, and temperature θ in accordance with the velocity of friction. The curves are plotted on the basis of data of experiments (Bibl.8) performed under identical conditions of friction and wear, with specimens made of T15K6 and T30K4 alloys.

There is no direct and unique functional relationship between the wear resist-

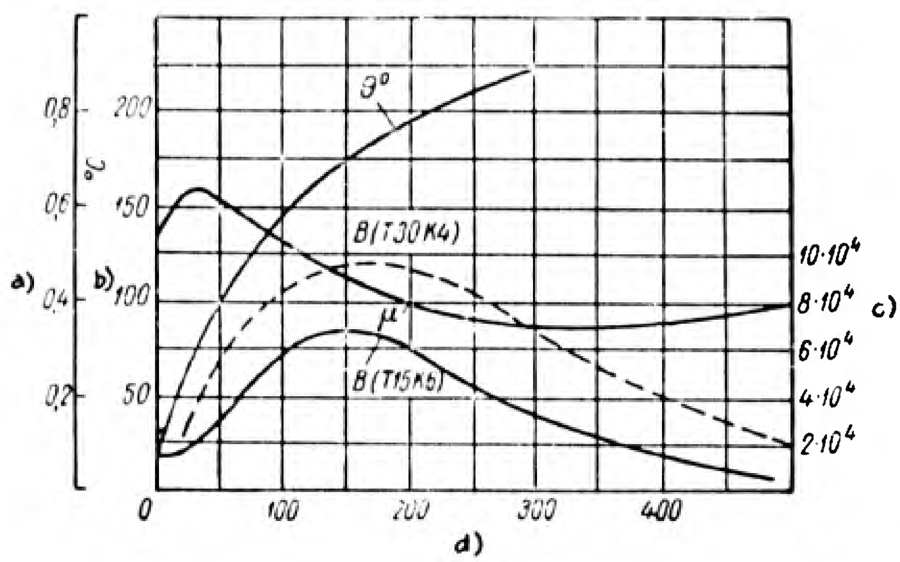

Fig.10 - Effect of Velocity of Friction v on the Coefficient of Friction μ, Temperature θ, and Wear Resistance B

a) Coefficient of friction μ; b) Temperature θ, °C; c) Wear resistance B, $kg\text{-}m/m^2$; d) Velocity of friction v, m/min

ance B and the coefficient of friction μ, or between the wear resistance B and the temperature of the specimen subject to wear on the one hand, and between the coefficient of friction μ and the temperature θ on the other hand.

Hot-Hardness. Hot-hardness is one of the most important properties of tool materials. This property has acquired decisive importance in very recent times, when high cutting speeds have resulted in temperatures in the cutting interval of 800°C and more. The high hot-hardness of cemented carbides, which substantially exceeds that of high-speed steel, is one of the principal factors that has caused this tool material to become so popular in machining.

A study of the effect of the temperature to which they are heated upon the hardness of carbides has been the subject matter of a number of investigations.

Table 12

Hardness of Cermets (Cemented Carbides) and Mineral Ceramics when Heated to Various Temperatures (Data due to A.I.Betaneli)

Tool Material		Temperature to which Heated, in °C					
		20	200	400	600	800	1000
		Hardness H_{136}					
Cemented carbides	VK2	1370	1210	1050	900	700	500
	VK6	1160	1010	860	700	500	300
	VK8	1130	1000	820	650	460	260
	T5K10	1200	1030	830	640	420	250
	T14K8	1250	1080	880	680	500	300
	T15K6	1280	1120	910	720	540	370
	T30K4	1370	1200	1000	800	620	440
	T60K6	1300	1230	1050	820	570	380
Mineral ceramic TsM-332		1370	1250	1130	1010	900	7[illegible]0

V.Ya.Riskin (Bibl.9) found a relationship between the hardness of cemented carbides and the temperatures to which they heat, and determined that the hardness remains unaffected even at temperatures of 900 - 1200°C. Other conclusions were arrived at by A.I.Betaneli (Bibl.10) and N.F.Kazakov (Bibl.11), who made detailed studies of this question. The results of their work are presented in Table 12 and Fig.11.

A.I.Betaneli ran his tests on a special device. The specimens under study were heated to the required temperature in an electric furnace mounted on the head of the lift screw of a Brinell hardness-testing machine. For protection against oxidation when being heated, the carbides were subjected to a protective treatment by chemicals and heat. The carbide tips were made in the form of rectangular pyramids with a vertex angle of 136°. Since the temperature of the tips was lower than that of the specimens, some temperature drop occurred in the process of measuring the impressions, which distorted the results of the tests. This distortion was taken

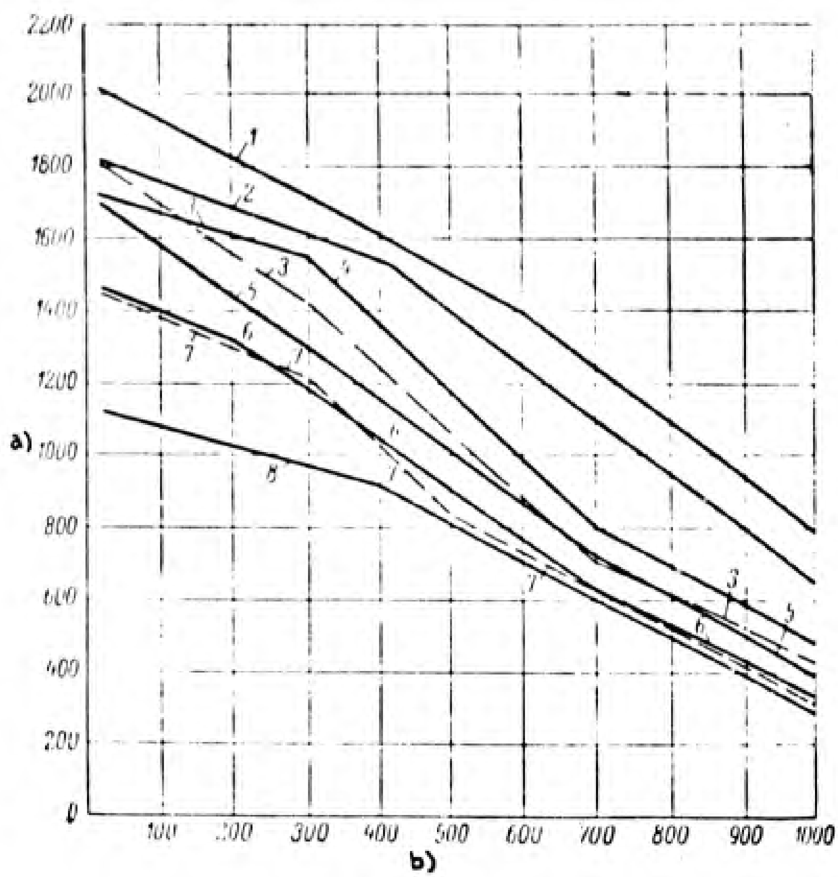

Fig.11 - Variation in Hardness of Specimens of Cermets and Mineraloceramics Heated in Vacuum:

1 - Mineraloceramic TsM-332; 2 - Cemented carbide VK2; 3 - Alloy T60K6; 4 - Alloy T30K4; 5 - Alloy T15K6; 6 - Alloy VK8; 7 - Alloy T5K10; 8 - Alloy VK15

a) Pyramid hardness H_n; b) Temperature to which specimens were heated, °C

into consideration by a correction factor. The H_{136} hardness was determined by dividing the load of 375 kg by the area of the impression remaining in the test specimen after it was cooled.

The hardness of the mineraloceramics was tested on tips made of the same material under a load of 250 kg.

N.F.Kazakov ran his tests on a special instrument permitting measurement of the hardness of various alloys when heated in vacuum to a temperature of 1100°C. The diamond tips employed were in the form of a square-based pyramid with a vertex angle of 136°. The hardness number H_n of the pyramid was determined by means of the usual formula for a 1 kg load.

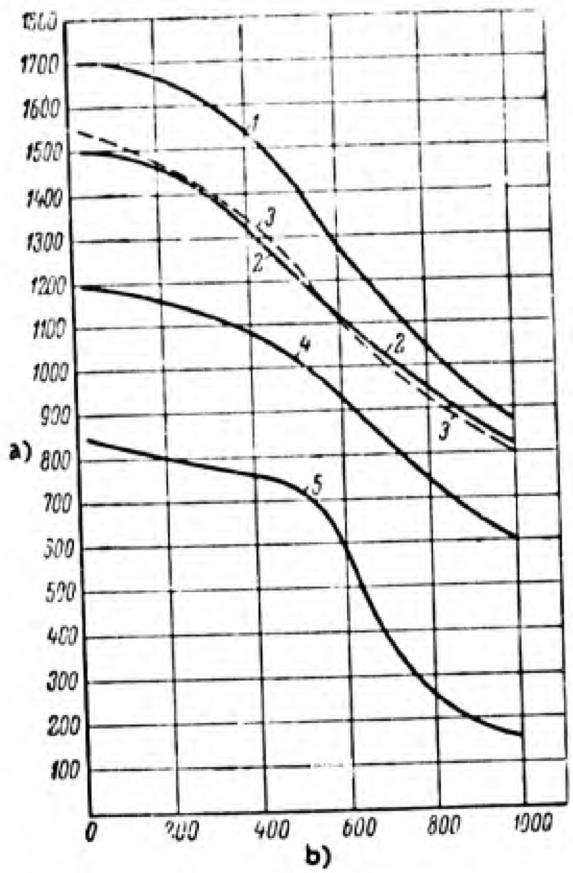

Fig.12 - Changes in Hardness of Cemented Carbides upon Heating:

1 - Alloy T15K6; 2 - Alloy VK6; 3 - Alloy T5K10; 4 - Alloy VK15; 5 - High-speed steel

a) Pyramid hardness H_n; b) Temperature to which specimen is heated, °C

Table 12 and Fig.11 show that at room temperature (20°C), the sequence of the various grades of hard steels, obtained by N.F.Kazakov proved to be the same as that obtained by A.I.Betaneli. However, as is more obvious from Table 13, their data for cemented titanium-tungsten carbides, particularly at high temperatures, differ substantially with respect to the degree of influence exercised by the temperature of heating upon reduction in the hardness of cemented carbides.

It follows from these data that the hardness of carbides diminishes sharply with rising temperature. The lower the cobalt content of the carbide, the higher its hardness at the given temperature, and vice versa. At temperatures below 300°C, the cemented titanium-tungsten carbide T60K6 is harder than T15K6, whereas at temperatures above 900°C the hardness of the two alloys is approximately equal. A.I.Betaneli offers the explanation that, at temperatures below 900°C, the titanium carbide content affects the hardness of the product, whereas at higher temperatures, when the cobalt binder has softened, the hardness of the product depends only upon the cobalt content, which was identical - 6% - for the two alloys.

VK8 and T5K10 are characterized by virtually identical hardness in the heated condition. The T15K6 and T30K4 cemented titanium-tungsten carbides are harder at all temperatures than the tungsten carbides VK6 and VK8. At the same time, tungsten carbide VK2, which contains little cobalt (2%), has a higher hardness at all temperatures than T30K4 and T15K6. The mineraloceramic TsM-332 is of even higher hardness.

Figure 12 presents the data by R.Kieffer and P.Schwarzkopf (Bibl.6). They differ from those by A.I.Betaneli and N.F.Kazakov. According to Kieffer and Schwarzkopf, the hardness of both tungsten and cemented titanium-tungsten carbides diminishes at a slower rate with increase in temperature than is indicated by the other investigators. Table 13 show that, if the hardness of the cemented carbides at room temperature is taken at 100%, the hardness of, for example, the alloy VK6 at a temperature of 1000°C will be as follows: 55%, according to Kieffer and Schwarzkopf, but only 26% according to Betaneli. Likewise, for the alloy T15K6, the figure is 51% according to Kieffer and Schwarzkopf, 29% according to Betaneli, and 21% according to Kazakov.

These data indicate that there is as yet no basis for believing that a solution has been found for the question of the influence of the temperature of heating upon the hardness of cemented carbides. To achieve more precise definition of this most important question it will be necessary to perfect further the methods of determining the hardness of cermets and mineraloceramics at high temperatures.

Table 13

Comparative Data on the Hardness of Cermets (Cemented Carbides) and Mineraloceramics when Heated to Various Temperatures

Tool Material	Data of A.I.Betaneli						Data of N.F.Kazakov						Data of Kieffer and Schwarzkopf*					
	Temperature to which Specimen is Heated, in °C																	
	20	200	400	600	800	1000	20	200	400	600	800	1000	20	200	400	600	800	1000
	Relative Hardness, in % (Hardness of Material at 20°C Taken as 100%)																	
VK2	100	88	77	66	51	37	100	93	85	66	52	35	—	—	—	—	—	—
VK6	100	87	74	60	43	26	—	—	—	—	—	—	100	97	88	75	64	55
VK8	100	88	73	58	41	23	100	92	72	54	39	26	—	—	—	—	—	—
VK15	—	—	—	—	—	—	100	91	85	63	45	27	100	97	90	78	62	50
T5K10	100	86	69	53	35	21	100	86	66	47	34	20	100	95	86	71	69	55
T14K8	100	87	70	54	39	24	—	—	—	—	—	—	—	—	—	—	—	—
T15K6	100	88	71	56	42	29	100	85	66	48	33	21	100	98	91	75	62	51
T30K4	100	88	73	58	45	32	100	91	71	54	37	26	—	—	—	—	—	—
T60K6	100	94	81	63	44	29	100	86	69	50	34	21	—	—	—	—	—	—
TsM-332	100	91	82	74	66	58	100	91	80	70	55	40	—	—	—	—	—	—

*German grades of cemented carbides have been arbitrarily reduced to Soviet grades, with which they are in very close correspondence in terms of chemical composition. The 16% TiC alloy constitutes an exception. It has been matched with T15K6, which has 15% TiC.

Thermal Conductivity. The high thermal conductivity of a cemented carbide is a factor favorable to the cutting process. Any reduction in thermal conductivity impairs the heat dissipation from the chip and from the cutting portion of the tool, causing thermal stresses to develop in the cemented carbide bar, which not infrequently results in cracks.

The data in Table 9 show that the heat conductivity of cemented tungsten carbides is not dependent upon their cobalt content. The heat conductivity of cemented titanium-tungsten carbides is considerably lower than that of tungsten carbides, and diminishes with increase in TiC content.

The lower heat conductivity of cemented titanium-tungsten carbides than of the tungsten alloy is due to the fact that the TiC + WC hard solution has a lower heat conductivity than the WC.

The heat conductivity of cemented titanium-tungsten carbides approximates that of high-speed steel R18, which is 0.06 cal/cm·sec·°C.

Sticking. The term "sticking" defines the ability of the tool material to bond (weld) with the machined material (or chip) during the cutting process. A high resistance to adhesion (low sticking) is a positive property of hard carbides. They are highly superior to high-speed steel in this respect.

The resistance of a hard carbide to wear depends to a significant degree upon the temperature at which it adheres to the material being machined. The higher this temperature, the higher the resistance of a carbide to wear.

The temperature at which sticking occurs diminishes with increase in the cobalt content of the tungsten carbides:

Cobalt content, in %:	0	1	5	20
Temperature of adhesion, in °C:	1000	775	685	625

The carbides of the refractory metals have a higher temperature of adhesion than the cemented carbides based on them:

Tungsten carbide (WC) . . . . 1000°C

Titanium carbide (TiC) . . . . 1125°C

Tantalum carbide (TaC) . . . . 1200°C

Niobium carbide (NbC) . . . . 1250°C

A significant point of superiority of cemented titanium-tungsten carbides over the tungsten products is their higher resistance to sticking. This is seen as the reason for the longer life of cemented titanium-tungsten carbides than of tungsten alloys in the machining of steel. It is held that the heating in the course of the cutting process results in the formation of a thin oxide film on the surface of the cutting portion of the tool, and that this protects the leading edge of the tool against direct contact with the chip. Moreover, titanium oxide has the same crystal lattice as titanium carbide itself, or the TiC + WC solid solution, and therefore the oxide film adheres tightly to the tool, protecting it from contact with the chip. In the case of single tungsten carbides, the tungsten oxide formed drops off readily, since crystal lattice differs from that of the tungsten carbide.

Specific Gravity. Specific gravity, or density, is an important characteristic of the quality of cemented carbides. The density of a carbide depends upon its chemical composition and sintering property. In practice, the density of an alloy is lower than the theoretical value because of the pores that are always present. Pores occupy up to 3% of the entire volume of the alloy. The density of an alloy diminishes with increasing cobalt content and porosity. The values for the specific gravity of various grades of cemented carbides, shown in Table 9, represent the lower limits of this property. In practice, the specific gravity is 0.1 - 0.2 above these limits. The higher the specific gravity of a hard carbide, the better its resistance to impact.

New Grades of Hard Carbides

The All-Union Institute for Hard-Alloy Research has developed new grades of

Table 14

Comparative Usefulness of Cemented Carbides

Grade of Hard Carbide	Useful Properties	Comparative Cutting Properties (Cutting Speed)
	Cemented Tungsten Carbides	
VK2 and VK3	High hardness and wear resistance. Limited cutting strength. Sensitive to shock and vibration. Permits higher cutting speeds than other grades of cemented tungsten carbides and yields higher output.	1.2 - 1.3
VK6	Adequate hardness and wear resistance, but lower than that of VK2 and VK3. Cutting density higher than that of these alloys. Less sensitive to shock and vibration. Cutting speeds must be lower than with VK2 and VK3, but may be higher than with VK8.	1.08 - - 1.12
VK8	Hardness and wear resistance lower than with VK6 but higher than with VK11. High strength in cutting metals. Good resistance to impact loading. Resistance to vibrations higher than that of the alloys VK2, VK3, and VK6. Requires lower cutting speeds than VK2, VK3, and VK6. Considerable toughness permits use of VK8 for heavy roughing of steels, whereas the use of cemented titanium-tungsten carbides results in crumbling of the cutting edge of the tool.	1.0
VK11	Hardness and wear resistance lower than with VK8. Substantial cutting strength - - higher than that of any of the cemented tungsten carbides. High resistance to shock and vibration. Requires lower cutting speed than the alloy VK8.	0.75 - - 0.80
	Cemented Titanium-Tungsten Carbides	
T5K10	Greater cutting strength than that of other grades of cemented titanium-tungsten carbides in cutting metals; highest resistance to shock, vibration and crumbling out, but less hardness and wear resistance than others. Permits cutting speeds 15 - 20% higher than that of VK8.	0.6 - 0.7

Table 14 (cont'd)

Grade of Hard Carbide	Useful Properties	Comparative Cutting Properties (Cutting Speed)
T14K8	Hardness and wear resistance higher than T5K10. High strength in cutting metals and high resistance to shock and vibration, but lower than that of T5K10. Permits higher cutting speeds than T5K10.	0.7 - 0.8
T15K6	Hardness and wear resistance higher than T5K10 and T14K8. Moderate resistance to shocks and vibration. Cutting strength higher than that of T30K4 and T60K6. The tool shows good resistance to crumbling if the system machine tool - workpiece - cutting tool is highly rigid. Permits higher cutting speed than T14K8.	1.0
T15K6T	Due to size difference of the carbide grains, hardness and wear resistance are higher, and cutting strength is somewhat lower than with T15K6. Moderate resistance to shock and vibration. Cutting strength higher than that of T30K4 and T60K6. Permits higher cutting speed than T15K6.	1.15 - - 1.20
T30K4	High hardness and wear resistance. More sensitive to shocks and vibrations than T15K6 and T15K6T. Low strength in cutting metals, but higher than that of T60K6. Permits higher cutting speeds than T15K6 and T15K6T.	1.4 - 1.5
T60K6	Has the highest resistance to wear of all the cemented titanium-tungsten carbides. Particularly sensitive to shocks and vibrations. Strength in cutting lower than that of T30K4. Permits considerably higher cutting speeds than T30K4.	1.7 - 1.8

cemented carbides with cutting properties improved over those of the now available grades. These include the cemented tungsten carbide VK4 which is successfully used in place of VK8 in heavy roughing of cast iron (Bibl.12). The new VN3K3 carbide has demonstrated its superiority over VK6 in the semifinishing of cast iron (Bibl.13). A number of experimental grades of cemented titanium-tungsten carbides developed for

Table 15

Cemented Carbides Recommended for the Machining of Hardened Steels

Type of Machining, and Conditions	Rigidity of System Machine Tool - Workpiece - Cutting Tool	Comparative Evaluation of Cemented Carbides as to Output	Recommended Grade of Cemented Carbide
Semifinish- and finish-turning, interrupted cutting process	High Normal Subnormal	Best Average Below average	T14K8 T5K10 VK8
Semifinish- and finish-turning, uninterrupted cutting process	High Normal Subnormal	Best Average Below average	T15K6, VK2, VK3 T14K8 T5K10
Fine turning	High Normal Subnormal	Best Average Below average	T30K4 T15K6T T15K6
Finishing in milling	High Normal Subnormal	Best Average Below average	T30K4 T15K6 T14K8
Drilling through holes	High Normal Subnormal	Best Average Below average	VK6 VK8 VK8
Hole enlargement by drilling	High Normal Subnormal	Best Average Below average	VK2, VK3 VK6 VK8
Final rose reaming	High Normal Subnormal	Best Average Below average	T15K6 T14K8 T14K8
Flute reaming	High Normal Subnormal	Best Average Below average	T30K4 T15K6T T15K6

making heavy cuts, are now being tested for their cutting properties (Bibl.14).

Comparative Usefulness of Hard Carbides and Grades Recommended for Machining of Hardened Steels

In practice, cemented titanium-tungsten carbides are employed to machine steels, and cemented tungsten carbides to machine iron, nonferrous metals, and nonmetals. The major shortcoming of titanium-tungsten carbides – high brittleness – somewhat limits the field of application of the good machining grades of these carbides, even in the machining of steels. The alloy T15K6 is rarely employed in impact roughing. In these uses, T5K10 which is not as good in output is to be preferred (the cutting properties of the alloy T5K10 are inferior to those of the alloy T15K6).

All grades of cemented titanium-tungsten carbides listed in Table 9 are manufactured solely for cutting tools to be used in the machining of steel. The alloys VK3, VK6, and VK8 are used, in addition, to make drawing dies, to drill various types of rock, to make machine parts subject to rapid wear, etc. The alloys VK10 and VK15 are not used in metal-cutting tools. VK11 may be used for machining special difficultly-machinable steels. VK2 is used only to tip cutting tools.

Table 14 presents data on the useful properties of various grades of cemented carbides employed in tipping cutting tools. Table 15 gives recommendations on the selection of the grade of cemented carbide for various types of machining of hardened steels.

8. Cemented Carbides in Other Countries

The major centers of production of cemented carbides for machining are West Germany, Austria, and the USA. As before the war, the owner of the most important patents for the manufacture of cemented tungsten carbides is the Krupp Co. in Essen, whereas the major patents for cemented titanium-tungsten carbides are held by the Deutsche Edelstahlwerke (DEW, Krefeld). Certain less important patents for the production of cemented carbides employing other components are held by the Austrian firm of Boehler. All the other West German and Austrian firms manufacture cemented carbides under license from the Krupp and DEW Cos.

In 1936, all German plants manufacturing cemented carbides were combined into a hard-carbide cartel. Austrian firms were also attached to it. This cartel standardized the composition of the various cemented carbides, as the result of which all grades were of identical quality regardless of the manufacture. This standardization was carried further by the fact that all the smaller firms used mixtures of starting powders provided by Krupp and DEW. They were thus essentially enterprises for shaping and sintering of hard carbides. The sintering processes were standardized and differed only as to the size and system of sintering equipment used.

The same system of organization continues to exist, essentially, to the present day. For example, the Austrian plants, and particularly the largest of them - the Planseewerke of Tyrol produces German hard carbides to German specifications.

The carbides manufactured in West Germany and Austria for machining have both standard designations and their own company symbols, such as Widia, produced by Krupp at Essen, or Titanite produced by DEW and its virtual subsidiary in Reuthe, the Planseewerke.

European Cemented Carbides

Table 16 presents the characteristics of cemented carbides produced in West Germany, Austria, and Sweden. Let us compare these with the data in Table 9 on cemented carbides currently manufactured in the USSR. To begin with, it should be noted that Austrian, German, and Swedish cemented carbides, like the Soviet products, encompass both single carbides (WC - Co) and double carbides (WC - TiC - Co). The list of Soviet carbides, particularly in the tungsten group, is somewhat larger than the German (we include the Austrian) and the Swedish lists. Grades G1, G2, and G3, which correspond approximately to the Russian VK6, VK11, and VK15, exhaust

Table 16

West German, Austrian and Swedish Cemented Carbides

Country	Grade	Chemical Composition in %			Physical and Mechanical Properties				
		WC	TiC	Co	Pyramid Hardness H_n	Rockwell Hardness HR_A	Specific Gravity γ	Transverse Rupture Strength σ_r, in kg/mm²	Compressive Strength σ_c, in kg/mm²
		Cemented Tungsten Carbides							
West Germany and Austria	G1	94,3	—	5,7	1500	90,0	14,8	160	580
	G2	89,3	—	10,7	1300	88,5	14,2	210	465
	G3	85,5	—	14,5	1200	87,0	13,7	240	415
	G4	80,0	—	20,0	1100	86,0	13,4	260	370
	G5	75,0	—	25,0	1050	85,0	13,1	270	330
	G6	70,0	—	30,0	950	83,5	12,7	280	—
Sweden	Ceko-1	94,0	—	6,0	—	91,0	14,5	150	—
	Ceko-3	94,0	—	6,0	—	90,5	14,6	130	—
		Cemented Titanium-Tungsten Carbides							
West Germany and Austria	S3	88,0	5,0	7,0	1550	90,5	13,3	150	500
	S2	77,3	14,7	8,0	1600	91,0	11,3	140	—
	S1	77,2	17,1	5,7	1700	92,0	11,2	110	460
	F1	70,5	24,0	5,5	1750	92,0	9,9	80	—
	F2	34,5	60,0	5,5	1850	93,0	6,8	60	—
Sweden	Ceko-5	85,0	6,0	9,0	—	89,5	12,6	140	—
	Ceko-6	81,0	8,0	11,0	—	90,0	11,6	135	—
	Ceko-2	79,0	15,0	6,0	—	90,5	14,6	120	—

the list of German cemented carbides in the tungsten group. The alloys G4, G5, and G6 are designed for a special purpose: the machining of graphite electrodes. The Swedish Ceko-1 and Ceko-3 correspond to the Russian VK6. In addition, GOST 3882-53 provides for the wide use of VK8 alloy which has been highly satisfactory particularly in the machining of iron, as well as VK2 and VK3 which have particularly high cutting properties and which have shown good results in the turning of hardened steels.

The numbers of different grades of cemented titanium-tungsten carbides, made in Germany and in the Soviet Union, coincide. There is approximate coincidence between the following grades: S3 and T5K10, S2 and T14K8, S1 and T15K6, F1 and T30K4, F2 and T60K6. However, whereas the tungsten carbide content of the T30K4 alloy is 66%, the WC content of F1 is 70.5%. There is also a slight difference in the chemical composition of the other pairs of hard carbides listed above.

The Swedish grades Ceko-2 and Ceko-5 correspond very closely to the Soviet grades T15K6 and T5K10. The grade Ceko-6 has no counterpart either among the German or the Soviet grades.

Let us turn to the important mechanical property of carbides of transverse rupture strength, σ_r. It should be noted at the outset that the established method of testing for transverse rupture strength shows the values of σ_r to be comparable in Soviet and West European hard carbides.

The situation is different with respect to the American cemented carbides. The σ_r of these and the Soviet carbides are not always comparable.

Moreover, it must be borne in mind that GOST 3882-53 specifies a minimum σ_r, whereas foreign Standards give average values.

It will be seen that the transverse rupture strength of German cemented tungsten carbides is higher than that of the corresponding Soviet carbides. For example, the German G1 has a transverse rupture strength of σ_r = 160 kg/mm^2, whereas that of the corresponding Soviet product VK6 is 120 kg/mm^2. The Swedish Ceko-1 also exceeds the VK6, which corresponds thereto, in σ_r.

The same is true for the cemented titanium-tungsten carbides T5K10 and T14K8, which correspond to the German S3 and S2 and the Swedish Ceko-5.

However, the Soviet grades T15K6, T30K4, and T60K6 are typified by an equal or

Table 17

American Cemented Tantalum-Tungsten Carbides

Chemical Composition, %			Physical and Mechanical Properties			
WC	TaC (NbC)	Co	Hardness, H_n	Hardness, H_{R_A}	Specific Gravity γ, in gm/cm^2	Transverse Rupture Strength, σ_r, in kg/mm^2
93	0,7 + (0,3 VC)	6	1600—1700	91—91,5	14,6—14,8	140—160
91,5	1 + (0,5 VC)	7	1650—1750	91,5—92	14,5—14,7	135—150
92	2,5	5,5	1600—1700	91—92	14,8—15,0	140—160
75	5	20	1100—1200	84—86	13,1—13,3	210—240
70	5	25	950—1050	82—84	12,8—13,0	200—230
84	10	6	1500—1600	89—90	14,5—14,7	140—160
81	10	9	1400—1500	88—90	14,3—14,5	160—180
74	20	6	1450—1550	88—89	14,4—14,6	150—170
60	27	13	1200—1300	86—88	13,7—13,9	180—210

Table 18

American Cemented Tantalo-Titano-Tungsten Carbides

Chemical Composition, %				Physical and Mechanical Properties					
WC	TiC	TaC (NbC)	Co	Hardness, H_n	Hardness, H_{R_A}	Spec. Grav. γ, in gm/cm^3	Transverse Rupture Strength σ_r, in kg/mm^2	Compressive Strength σ_c, in kg/mm^2	Heat Conductivity λ, in cal/cm • sec • °C
85	4	1	10	1350—1450	89—90	13,2—13,4	170—190	—	0,134
80,5	5	5,5	9	1400—1500	90—91	13,1—13,3	170—200	—	—
77	6,5	9	7,5	1550—1650	91—92	12,5—12,7	140—160	—	0,127
59	7	22	12	1300—1400	89—90	12,3—12,5	160—180	—	—
76	7,5	6,5	10	1350—1450	89—90	12,0—12,2	170—200	450	0,113
73,5	10	8	8,5	1450—1550	90,5—91,5	11,8—12,0	140—160	—	—
72,5	10	8	9,5	1400—1500	90—91	11,7—11,9	150—175	—	—
71,5	10	8	10,5	1350—1450	89—90	11,7—11,8	160—190	—	—
62	12	18	8	1600—1700	91—92	11,7—11,9	120—140	510	—
59	12	18	11	1400—1500	90—91	11,4—11,6	130—150	400	—
69,5	12,5	8	10	1450—1550	90,5—91,5	11,2—11,4	140—170	—	—
70,5	13,5	7,5	8,5	1500—1600	91—92	11,1—11,3	130—150	470	0,068

given in Table 17.

The addition of tantalum carbide acts, as does titanium carbide, to increase the wear resistance of cemented tungsten carbides and their resistance to sticking in the machining of steels. Since TaC* is considerably inferior to TiC in hardness [under a 50 gm load, the microhardness of TiC is 3200 kg/mm^2, while that of TaC is 1800 kg/mm^2 (Bibl.6)], the life of WC - TaC (NbC) - Co hard carbides is inferior to the life of WC - TiC - Co and WC - TiC - TaC (NbC) - Co carbides. This explains the failure of any efforts to introduce pure alloys of tantalum with cobalt or nickel, manufactured in the USA under the name "Ramet".

Cemented tantalum-tungsten carbides containing 0.75 - 3.5% TaC and 0.1 - 0.8% VC have been found satisfactory in the machining of high-hardness iron. At contents of 5 - 10% TaC and 6% Co, they are useful as universal alloys for the machining of iron and steel. However, tantalum-tungsten carbides containing 9% Co, and these same carbides with a content of 20 - 30% TaC, are employed only in the machining of low- and medium-hardness steels.

The cemented tantalum-titanium-tungsten carbides (Table 18) have gained wide popularity in the USA and have virtually driven the tantalum-tungsten carbides out of the market. It should be observed that the WC - TiC - TaC (NbC) - Co carbides, are somewhat more costly, particularly those with a high TaC content, than the WC - TiC - Co products.

Table 19 presents data making it possible to come to a judgment with respect to the influence of tantalum carbide (columbium carbide) upon the hardness and transverse rupture strength of cemented titanium-tungsten carbides. As we see, although their hardness is about the same, cemented carbides containing TaC are superior, in transverse rupture strength, to the same products without TaC. An addi-

---

*Technical tantalum carbide usually contains a considerable amount of columbium carbide which, all other properties being equal, is somewhat harder than pure tantalum carbide. Therefore, for the sake of clarity, we write TaC (NbC) instead of TaC.

greater transverse rupture strength than the corresponding German alloys S1, F1, and F2.

The German, Austrian, and Swedish hard carbides are applied in the same fields as the corresponding Soviet grades: the tungsten carbides for the machining of iron, nonferrous metals and alloys, and nonmetals; the titanium-tungsten products for the machining of steels.

American Cemented Carbides

In the USA, with the exception of the tungsten Carboloy A-55 (87% WC and 13% Co) used for rough machining of iron, the cemented carbides differ fundamentally in

Table 19

Effect of Addition of TaC (NbC) Upon the Properties of Cemented Titanium-Tungsten Carbides

Chemical Composition of the Alloy, in %				Hardness, H_{R_A}	Transverse Rupture Strength, σ_r, in kg/mm²
TiC	TaC (NbC)	WC	Co		
40,5	0	53	6,5	92—93	80—90
38	5	50,5	6,5	92	95—105
20,5	0	72	7,5	91,5	115—125
18	5	69,5	7,5	91	130—140
15	0	76,5	8,5	90	130—145
13	4	74,5	8,5	90	155—165
7,5	0	83,5	9	89	150—160
5	5	81	9	89	175—190
7	0	86,5	6,5	91	130—140
4	6	83,5	6,5	91,5	150—170

chemical composition from the European grades. They are based on WC - TaC (NbC) - Co or WC - TiC - TaC (NbC) - Co. The characteristics of the former group are tion of 4 - 6% TaC raises the transverse rupture strength by 12 - 18%.

Cemented tantalum-titanium-tungsten carbides have recently been employed with success in European countries in place of titanium-tungsten products. They are less brittle and more dependable.

New Experimental Grades of Cemented Carbides

Among the scientific investigations conducted abroad in the field of cemented carbides for the machining of metals, those dealing with the possibility of replacing cobalt by other binders, and also those seeking to eliminate the use of tungsten, are of interest.

Efforts have been made to replace cobalt in tungsten carbides (cobalt being the

Table 20

Cemented Titanium-Molybdenum Carbides

No.	Chemical Composition, in %			Physical and Mechanical Properties		
	Molybdenum Carbide Mo_2C	Titanium Carbide, TiC	Binder Metals	Spec.Grav. γ, in gm/cm^3	Hardness H_{R_A}	Transverse Rupture Strength σ_r, kg/mm^2
1	42,5	42,5	15Ni	6,9	91	90
2	30	55	15Ni	6,4	91,5	85
3	20	65	15Ni	6,2	92	80
4	12	73	15Ni	6,1	92	70
5	8	77	15Ni	6,0	92,5	70
6	3	82	15Ni	5,2	92	70
7	35	35	28Ni + 2Cr	7,1	86	110
8	15	58	25Ni + 2Cr	6,1	87	100
9	15	63	20Ni + 2Cr	5,9	87,5	100
10	17,6	70,4	12Ni	5,8	90,5	98—108
11	17,2	68,8	14Ni	5,9	90	102—112
12	44	44	12Ni	6,9	89,5	98—106
13	43	43	14Ni	7,0	89,5	102—110

Table 21

Cemented Titanium-Vanadium Carbides

Chemical Composition, in %			Physical-Mechanical Properties		
Vanadium Carbide, VC	Titanium Carbide, TiC	Nickel Ni	Spec. Grav. γ, in gm/cm^3	Hardness, H_{R_A}	Transverse Rupture Strength σ_r, kg/mm^2
25	65	10	5,05	93,5	90—100
45	45	10	5,15	92,5	90—100
65	25	10	5,25	92	70—80.

most expensive component) by other binder metals and alloys: iron, nickel or nickel-copper, nickel-chromium, nickel-molybdenum, cobalt-tungsten alloys, etc. None of these efforts have yielded positive results. For example, the use of nickel and

Table 22

Non-Tungsten Cemented Double Carbides

Chemical Composition, in %						Physical and Mechanical Properties		
Titanium Carbide TiC	Zirconium Carbide ZrC	Columbium Carbide NbC	Tantalum Carbide TaC	Molybdenum Carbide Mo_2C	Binder Metals	Spec. Grav. γ, in gm/cm^3	Hardness H_{R_A}	Transverse Rupture Strength σ_r, in kg/mm^2
68,8	17,2	—	—	—	14Co	5,5	92,5	75—80
51,6	34,4	—	—	—	14Co	6,7	88,5	65—70
69,6	—	17,4	—	—	12Ni + 1Cr	5,6	89	85—90
72,0	—	18,0	—	—	10Co	5,6	91	70—80
36,0	—	54,0	—	—	10Co	6,1	90	70—80
18,0	—	72,0	—	—	10Co	7,2	90	75—85
42,5	—	—	42,5	—	15Ni	8,7	89	80—90
—	—	—	42,5	42,5	15Ni	10,6	87	60—70

iron instead of cobalt causes a sharp decline in the transverse rupture strength

(40%). The extensive patent literature contains references to various binder metals and alloys. However, none of these is capable of serving as an adequate substitute for cobalt. However, many new experimental grades of cemented carbides make use of nickel and nickel-chromium, iron-nickel, or iron-nickel-chromium as substitutes for cobalt.

Economic factors and, to some degree, a shortage of tungsten, have led to numerous efforts at complete or partial substitution of other carbides or other hard substances for tungsten carbide. These investigations are proceeding in two directions:

1) Substitution of WC by other non-carbide hard substances, such as nitrides, borides, silicides, oxides (corundum) and nonmetallic carbides (silicon carbide, boron carbide);

2) Substitution of WC by carbides of other refractory metals and solid solutions thereof.

Thus far, only the second category has yielded promising results.

Table 20 presents the characteristics of cemented carbides based on Mo_2C - TiC. In view of the fact that molybdenum is presently not in short supply, these carbides today represent the fastest non-tungsten cemented carbides and offer the best prospects.

The Table shows that all the carbides but three are of high hardness. Low transverse rupture strength is characteristic of the carbides Nos.3 - 6, for which this property is at the level of the Soviet T60K6 - the most brittle of the modern cemented carbides of the titanium-tungsten group. In terms of strength, the alloys Nos.1 and 2 approximate the alloy T30K4, and Nos.7 - 13 approximate the alloys VK2, VK3 and T15K6. In all of these, nickel or nickel-chromium is used instead of cobalt.

Table 21 describes non-tungsten cemented carbides based on VC - TiC. Cutting tests have shown that the first two alloys are not inferior to T15K6 in speed, for

Table 23

Non-Tungsten Cemented Triple Carbides

No.	Chemical Composition, in %					Physical and Mechanical Properties		
	Titanium Carbide TiC	Vanadium Carbide VC	Columbium Carbide NbC	Tantalum Carbide TaC	Binder Metals	Spec.Grav. γ, in gm/cm^3	Hardness H_{R_A}	Transverse Rupture Strength σ_r, in kg/mm^2
1	72	—	6	12	10Co	5,7	91,5	85—100
2	45	—	15	30	10Co	6,6	90,5	80—90
3	18	—	24	48	10Co	7,7	90	75—85
4	61,6	17,6	8,8	—	9Fe + 3Ni	6,3	92,5	80—90
5	59,5	17	3,5	—	11Fe + 4Ni	6,3	92	80—90
6	61,6	17,6	8,8	—	12Co	6,3	93	70—80
7	60,9	8,7	17,4	—	9Fe + 3Ni + 1Cr	5,6	90,5	60—70

roughing and finishing. The third alloy also permits, in the finish-machining of steels, achievement of the speeds characteristic of T15K6.

Of the other cemented double carbides, those based on the following combinations are of some practical value in the finish-machining of steels: TiC - ZrC, TiC - NbC, TiC - TaC, and TaC - Mo_2C (Table 22).

In terms of strength, these non-tungsten carbides are, generally speaking, considerably inferior to those based on Mo_2C - TiC and VC - TiC. The transverse rupture strength of the cemented tantalum-molybdenum carbide is even less than that of T60K6 alloy.

Table 23 presents the properties of triple carbides whose practical usefulness has been experimentally proved. As we see, the hardness of these cemented carbides is quite high. In transverse rupture strength, Nos.1, 2, 4, and 5 correspond approximately to T30K4, and Nos.3 and 6 to T60K6. No.7 is not as strong as T60K6.

Cemented non-tungsten quadruple carbides have also been investigated. Those based on TiC - VC - NbC - Mo_2C are of practical significance. The carbide containing 53% TiC, 20% VC, 10% NbC, 5% Mo_2C and 12% binder metal in the iron group approximates the alloy T15K6 in wear resistance. Having high hardness (H_{R_A} = 91 - 92), this alloy is superior to T30K4 in transverse rupture strength (σ_r = 90 - - 105 kg/mm^2).

Attempts have recently been made in other countries to create new hard alloys which, in transverse rupture strength, would be midway between the present hard alloys ($\sigma_r \leq$ 160 kg/mm^2) and high-speed steel (σ_r = 300 kg/mm^2 or more) and would at the same time have a hardness and a wear resistance characteristic of the present cemented carbides.

These include: TT4 alloy (West Germany), the Austrian alloy S4T, the Swedish S5 and S4H and S6HL alloys (German Democratic Republic).

9. Mineral Ceramics

General Data

The cutting properties of the best modern tool materials - the cemented carbides - may be deemed to have reached their limits under conditions of high-speed machining in which the temperature in the cutting zone attains 800 - 900°C.

Further progress in the field of machining requires a search for tool materials superior to the cemented carbides in cutting properties, particularly in terms of heat resistance, and at the same time not containing the expensive alloying elements found in the carbides (tungsten, cobalt, etc.).

In 1951-52, many of our machine-building enterprises actively undertook the production of new tool materials - mineral ceramics - which are very high in heat resistance and at the same time contain no components that are expensive or in short supply. Large-scale industrial testing of the following mineral ceramics was undertaken with this purpose:

a) TsM-332 (microlite), produced by the Moscow Hard-Alloy Combinate; and

b) TV-48 (thermocorundum) manufactured by the Leningrad Experimental Abrasives Works of the All-Union Abrasives and Grinding Research Institute (VNIIASh).

The tests showed TsM-332 to be considerably superior to thermocorundum TV-48 and all other grades of the latter [TV-13 (TsV-13), TV-14 (TsV-14), TsV-18 and TV-44], formerly manufactured by the VNIIASh Abrasives Works and taken out of production as being inferior to TV-48.

Despite the satisfactory results of laboratory tests of bars made under laboratory conditions, these industrial tests yielded negative results in the majority of cases. The mineral-ceramic billets were found to be short-lived; their cutting properties varied even within single batches, and cleavage and breakage of the bars during the cutting process was quite common. As a result, the production managers lost confidence in this new tool material.

In 1953 and 1954, steps were taken to improve the strength of "mineroceramics", and also to perfect the design and technology of mineroceramic cutter manufacture. As a result, the introduction into industrial practice of cutting tools tipped with TsM-332 mineroceramics has been successfully resumed in the last few years.

Mineroceramics also find application in machining abroad. Despite the fact that tool ceramics is not a very recent development, it has been applied in practice due to unsuccessful experiments of the war years in Germany and England.

Recent investigations in this field have been successful, and the newer foreign literature contains numerous papers on the positive results of utilizing mineroceramics for the machining of steel and cast iron, and on its considerable advantages over high-speed and cermet tools in terms of permissible cutting speeds and tool life.

Cheap bauxites are the point of departure for the production of mineroceramics. The processing of bauxite yields aluminum oxide (Al_2O_3). Mineroceramic bars are made from a mixture of finely-ground white corundum (one of the modifications of Al_2O_3) and a very small amount of chromium oxide (Cr_2O_3). The pulverized mixture is shaped and briquetted under high pressure in special steel dies of suitable size and shape. The process of bar manufacture is completed with sintering at 1800°C.

Shape of Mineroceramic Bars

The Moscow Hard-Alloy Combinate makes about 40 shapes and sizes of mineroceramic bars for machining use. The majority correspond to the cermet bars defined in GOST 2209-55, designed for turning, boring, slotting, and cutting-off tools. The Combinate makes cermet bars of other shapes on special order, the customer being required to provide the dies.

Physical and Mechanical Properties of Mineroceramics

Experiments have established that variation in the specific gravities of mineroceramics in the range of γ = 3.80 - 3.91 have no great effect upon the wear resistance under conditions of continuous turning. An increase in γ causes an insignificant rise in the wear resistance of the tool material. In batch turning, with frequent insertion and withdrawal of the cutter, the specific gravity of a mineroceramic exerts a significant influence upon the strength of the cutting edge of the tool, this strength rising sharply with specific gravity.

The specifications of the Hard-Alloy Combinate stipulate a specific gravity of mineroceramics of not less than γ = 3.83 gm/cm^3.

Hardness. The hardness of a mineroceramic influences its cutting properties. Experiments show that a reduction in the H_{R_A} hardness of a mineroceramic from 88 to 82 reduces the life of the cutter by five-sixths. Under the specifications of the Hard-Alloy Combinate, the hardness of mineroceramic bars for cutting tools must be not less than H_{R_A} = 90.

Transverse Rupture Strength. Mineroceramics are greatly inferior to other tool materials in terms of transverse rupture strength. The transverse rupture strength σ_r of mineroceramics is two-thirds to four-fifths lower than that of cermets. Moreover, the σ_r of mineroceramics fluctuates widely from lot to lot and even within a single lot. Under the specifications of the Hard-Alloy Combinate, mineroceramic bar with $\sigma_r > 30$ kg/mm^2 are deemed acceptable.

Experiments have shown that in continuous turning, a range of σ_r = 19.6 - - 44.1 kg/mm^2 has no significant effect upon the wear resistance of the tool. However, in periodic turning, an increase in the transverse rupture strength σ_r of the mineroceramic bar will mean greater strength of the cutting edge of the tool and greater wear resistance.

Hot-Hardness. The most valuable property of a mineroceramic is its hot-hardness, which substantially exceeds that of cermets. Tables 12 and Fig.11 show that, at room temperature, the hardness of a mineroceramic differs insignificantly from that of the cermets VK2, T60K6, and T30K4. However, as the temperature rises, the difference in hardness widens in favor of the mineroceramic (Table 13). Whereas at 800°C, the hardness of the T60K6 cermet is 44% of its hardness at 20°C, a mineroceramic maintains 66% of its original hardness (according to A.I.Betaneli). N.F.Kazakov gives the respective figures as 55% against 34%.

Wear Resistance. In order to compare the wear resistance of the mineroceramic TsM-332 and of various grades of cermets, experiments were run (Bibl.18) by the method discussed earlier in the text. The steel 60 with σ_t = 80 kg/mm^2 was tested at a constant specific pressure of 10 kg/mm^2. The mineroceramic bars tested had a specific gravity of γ = 3.89 gm/cm^3, a hardness H_{R_A} of 91, and a transverse rupture strength σ_r of 35 kg/mm^2. The velocity of friction varied in the range of v = 5 to 600 m/min. The ratio of wear resistance B to velocity of friction v, for all tested tool materials, was similar in nature to that obtained in the investigations whose results are given in Fig.7.

Experimental data show that the maximum wear resistance of a mineroceramic corresponds to a velocity of friction of the order of 300 m/min, while for cemented titanium-tungsten carbides it corresponds to velocities of the order of 200 m/min. The cermet T60K6 exhibited the highest wear resistance maximum. This was followed by the cermet T30K4, the mineroceramic TsM-332, and the alloys T15K6, T14K8, and T5K10. Cemented tungsten carbides show a maximum wear resistance only 1/2 to 1/8 as great as that of cemented titanium-tungsten carbides and mineroceramics.

At velocities of friction in the range of $v = 300 - 600$ m/min, the wear resistance of mineroceramic TsM-332 was higher than that of the cemented titanium-tungsten carbides. The following declining order of wear resistance was observed: T60K6, T30K4, T15K6, T14K8, T5K10.

The data presented here show that, at high cutting speeds, the minerocermet TsM - 332 has a higher resistance to wear that the cermets of the titanium-tungsten group, for which a very high wear resistance in the machining of steels is characteristic.

Wear of Mineroceramic Tools

Because of the high brittleness of mineroceramics, a characteristic of the wear of such cutters is fine crumbling out of the cutting edge at the beginning of the machining process and, as a result, fairly extensive rounding of the edge and considerable initial wear on the flank (~ 0.1 mm). Therefore, the use of mineroceramics for fine-turning is not recommended.

In the machining of steels, the wear of tools tipped with mineroceramics proceeds both at the flank and the face, with crater formation. The wear is accompanied by the appearance of characteristic cracks on the contact areas of the working faces of the cutter, the workpiece, and the chip.

The intensity of cutter wear increases with increase in the hardness of the workpiece.

It should also be noted that the nature of the wear of mineroceramic-tipped tools has been little studied.

Grinding and Lapping of Mineroceramic Cutters

Proper grinding is the prime requisite for rational employment of a mineroceramic tool. Grinding is done with green silicon carbide ceramic-bonded abrasive wheels, grain size 46 - 80, hardness SM1-M1. Wheels of 46 grain are used for rough-grinding, and wheels of large grain size for finish-grinding. After grinding, the working faces of the tool are lapped.

There is wide disagreement on the subject of peripheral grinding-wheel speeds, as established in practice. Speeds of 8 - 15 m/sec are widely employed. However, there are some plants at which grinding is run at considerably lower speeds: 2.5 - - 5 m/sec. An investigation of this question (Bibl.18) has confirmed the desirability of low speeds. The following optimum grinding conditions have been established: peripheral speed of grinding wheel 2 m/sec, pressure approximately 75 kg/mm^2, longitudinal feed, and cooling.

Under these conditions, complete self-sharpening of the wheel occurs, good grinding is obtained, and a cutting edge without crumbling-out or cratering is maintained. In all studies of ceramic-bonded green silicon carbide wheels of 46 - 120 grain and M3 - SM2 hardness, the surface quality of the ground tool faces was in class 7 or 8. Depending upon the properties of the wheel, the grinding rate is 450 - 750 mm^3/min, which is 30 - 40 times as great as the grinding rate of a grinding wheel at high speed.

Inasmuch as, under the given conditions of grinding, a grinding wheel works under conditions of complete self-sharpening, the consumption of abrasives is high and constitutes, depending upon the nature of the wheel, 900 to 1500% of the volume of mineroceramic removed. However, the high abrasive consumption is compensated by the high output and quality of grinding. Moreover, the wheel is more fully utilized due to the low peripheral speeds and the fact that the wheel is trued only when necessary for correction of its geometry.

Experiments have shown that the lapping of mineroceramic tools must be done in the direction of rotation of the cast iron disk, opposite to the direction employed in lapping cermet cutters, i.e., from the cutting edge to the base of the blank. In the opposite case, chipping of the cutting edge occurs.

After grinding, mineroceramic cutters should be finished with a boron carbide powder of M28 grain (20 - 28 microns) for finish-grinding and M14 and M10 (17 and 7 microns) for highly precise work.

Geometry of the Cutting Portion of Tools with Mineroceramic Tips

Experience in the practical use of mineroceramic cutters makes it possible to recommend the following geometric parameters for finish and semifinish turning of carbon and light structural steels:

a) A positive rake angle ($\gamma = 5 - 10^o$) to reduce vibrations and cutting forces;

b) A bevel on the face 0.1 - 0.3 mm wide, with an angle of 20^o;

c) Angle of inclination of main cutting edge: $\lambda = 4^o$ in interrupted cutting; $\lambda = 8^o$ in continuous cutting;

d) Other parameters of the same magnitude as those employed in finish-turning with T30K4 cutters: $\alpha = \alpha_1 = 6^o$; $\varphi_1 = 10 - 15^o$; r = 1 mm.

Comparison of Lives of Cermet and Mineroceramic and Cermet Cutters

According to experimental data (Bibl.18), a comparison of the lives of cutters tipped with the mineroceramic TsM-332 and with the cermet T30K4 in turning steels with $\sigma_t = 80$ kg/mm^2, and in cast iron of hardness $H_B = 140 - 160$, yielded the following results:

a) In machining steel with a cutting speed of v = 100 m/min, the lives were identical; at v = 200 - 400 m/min, the life of the mineroceramic cutters was 75% higher than that of cutters made of T30K4; at v = 500 - 600 m/min, T30K4 cutters had hardly any useful life, whereas that of mineroceramics was T = 20 - 30 min.

b) In the finish-turning of cast iron, cutters tipped with mineroceramics showed an adequate life of T = 170 - 20 min at cutting speeds in the v = 100 - 1000 m/min range (wear of cutter flank h = 0.4 mm). Tools tipped with the considerably less brittle cermet T30K4, revealed a life of T = 4 min at v = 300 m/min and T = 2 min at v = 600 m/min (h = 0.7 to 0.8 mm).

The TsM-332 mineroceramic must be rated as the only present-day tool material permitting the machining of cast iron at cutting speeds of v > 200 - 300 m/min.

Studies of semifinish turning of steels for which σ_t = 60 to 90 kg/mm^2, performed at the NIAT have determined that mineroceramics make it possible to work at considerably higher cutting speeds than do the cermets T15K6 and T60K6, in addition to which the superiority of mineroceramics over the cermets rises with increasing cutting speed. This can be explained by the higher hot-hardness of the mineroceramic and its lower adherability. If the cutting speed of T15K6 is taken as unity, the cutting speed of the cermet T60K6 would be 1.50 and that of mineroceramic TsM-332 would be 1.75.

Cutting Force and Power

Experiments (Bibl.18) have shown that when steels are turned by cutters tipped with the mineroceramic TsM-332 and the cermet T15K6, the cutting forces are approximately identical.

Complete utilization of the cutting properties of mineroceramics require that the lathes have high rigidity, high speed (spindle speed up to 3000 rpm), and high power (10 - 50 kw).

Surface Quality Obtainable with the Mineroceramic TsM-332, and Condition of the Surface Layer of the Parts

Given equal conditions of cutter operation, the mineroceramic TsM-332 makes for a somewhat high surface quality than the cermet T15K6.

Experiments with steels Nos.35, 45, 40Kh, and 45Kh (Bibl.19) have shown that machining with mineroceramic cutters causes work-hardening of the surface layer of the metal to a depth of 20 - 30 microns. This results in a 25 - 30% rise in the microhardness of the surface layer relative to that of the base metal. Within the fine surface layer, residual tensile stresses appear, and at v = 350 m/min cutting speed, these attain considerably greater magnitude than in machining with cemented carbide cutters.

An increase in the cutting speed from 100 to 500 m/min results in a rise in residual stresses, which is more intensive at a depth of 0.005 - 0.006 mm. When the wear of the cutter flank changes to h = 0.6 mm, the residual tensile stresses in the fine surface layer increase. At h = 0.7 mm, the residual stresses change in nature from tensile to compressive.

Area and Prospects for Application of Mineroceramics in the Machining of Metals

The mineroceramic TsM-332 may be recommended for the final and penultimate turning of steels, cast iron, nonferrous metals, their alloys, and of nonmetallic materials, as well as for the finish-turning of hardened steels under conditions of shock-free loading and adequate rigidity of the machine tool - workpiece - system. In the turning of steels, the attainable finish of the machined surface falls into classes 6 and 7, while with cast iron, class 7 and 8 finishes are attainable. The precision of machining corresponds to the standards for classes 4 and 3.

Under both laboratory and industrial conditions, positive results have been achieved in the end milling of cast iron and steel by mineroceramic-tipped tools.

Further improvement of mineroceramics, primarily in the direction of increase in strength, will permit a considerable expansion of the field of application of this new tool material.

Mineroceramics are less sensitive to rise in cutting speed than are cermets. As a result, it is desirable to use mineroceramic tools at high cutting speeds with expectation of short life.

For high-speed cutting, preference should be given to cutters with mechanically-fastened mineroceramic bars since the replacement of a worn bar takes little time under these circumstances.

The development of a rational configuration of the mineroceramic blank for repeated use, combined with the reduction in price of this new tool material, will make it possible to use cutters with mechanical fastening of new bars without regrinding. This opens new possibilities for the further development of high-speed methods of machining and for increasing the output capacity of machining equipment.

CHAPTER III

TURNING OF HARDENED STEELS

10. Description of the Experimental Conditions Used by the Author

Working Materials

This Section will present the results of studies by the author of the machining of hardened structural alloy steels. Three steels were investigated: medium-alloy chromium-nickel-molybdenum, high-alloy chromium-nickel-molybdenum-silicon, and high-alloy chromium-nickel. The first steel (OKhN3M) had the following chemical composition: C = 0.29 - 0.30%; Cr = 0.82 - 0.92%; Ni = 2.84 - 2.94%; Mo = 0.34 - - 0.47%; Si = 0.17 - 0.27%; Mn = 0.36 - 0.42%; P = 0.023 - 0.030%; S = 0.017 - - 0.019%. The second steel differs from OKhN3M by a higher silicon and molybdenum content, and the third steel by a higher carbon and chromium content.

For convenience in presentation of the data, these steels are identified as A (OKhN3M steel), B, and C.

The steels were hardened and tempered, the latter at low temperature.

Shape and Dimensions of the Steel Ingots: Steel A: hollow cylindrical ingots with outside diameter D_o = 270 mm, inside diameter D_i = 150 mm and length L = 1700 mm. Steel B: solid cylindrical ingots, D = 250 mm and L = 1600 mm. Steel C: solid cylindrical ingots D = 200 mm and L = 1150 mm.

To begin with, the ingots were descaled and the rough outside layer removed, resulting in a uniform load on the tool and the absence of shock in the tests.

Table 24

Hardness Data on Steels A and B

Steel A				Steel B			
Ingot No.	Ingot Diameter, in mm	Rockwell Hardness, H_{R_C}	Average Data H_{R_C}	Ingot No.	Ingot Diameter, in mm	Rockwell Hardness H_{R_C}	Average Data H_{R_C}
1	250	41,0	40,0	6	249,6	50,0	49,0
	233	39,0			234,4	49,0	
2	256	45,0	41,0		220,2	49,0	
	229	41,0			205,7	49,0	
	209	38,0			197,4	48,5	
3	255	47,5	47,0		175,0	48,5	
	236	47,0		7	236,0	54,5	56,0
	212	47,0			220,4	55,5	
	193	46,5			201,2	56,5	
4	258	40,5	41,0		195,9	57,0	
	239	41,5		8	246,5	58,5	59,0
	232	41,0			232,5	60,0	
	212	41,0			213,2	59,0	
5	255	50,0	49,5		157,0	58,0	
	244	49,0		9	246,2	60,5	60,5
	230	49,0					
	217	50,0					
	186	50,0					

Five ingots of steel A, four of steel B, and one of steel C were tested. All the steels were subjected to metallographic analysis. Figure 13 presents a microsection of steel A, with a martensitic structure. Microsections of steels B and C also displayed martensitic structures. A small number of nonmetal inclusions were discovered in all the specimens prior to etching.

Hardness. The need for a systematic verification of the hardness of the material under investigation without removing the ingot from the lathe, and the large dimensions of the ingots made the author select the Pol'di testing machine for hardness determination. As the turning of the ingots proceeded, the hardness of the steel was tested at 7 - 10 points along their length. Table 24 presents the results of the hardness tests of ingots of steels A and B. The hardness number of an ingot of given diameter is the arithmetic mean of 7 to 10 readings obtained along its length. Conversion of the Pol'di hardness to the Rockwell hardness (C scale) was done on the basis of experimental relationships derived for steels A and B.

The data in Table 24 reveal that:

1) Ingots of steels of identical chemical composition differ in hardness despite identical heat treatment;

2) The ingots displayed different degrees of hardening. The ingots Nos.1, 2, and 3 of steel A showed diminishing hardness with depth, whereas in the ingot No.4 the outer surface was softer. This may be explained by the occurrence of decarburization. The ingot No.5 was characterized by constant hardness throughout its cross section, indicating through-hardenability.

The ingots of steel B exhibited an essentially constant hardness within the limits of the diameters investigated.

All the ingots without exception showed variations in hardness with length. The greatest hardness was acquired by the ends. The minimum hardness was observed in the midsections.

An ingot of steel C exhibited constant hardness in cross section. A disk 55 mm in thickness was cut from this ingot. The "inside" face of the disk (the face adjacent to the remainder of the ingot) had a Rockwell hardness of H_{R_C} = 65 at four points 30, 44, 79, and 88 mm from the center of the disk respectively (the disk diameter being 198 mm).

In conclusion, it should be noted that the determination of the hardness of hardened steels by means of the Pol'di machine yielded data that were far from accurate. The Pol'di hardness numbers differ from the Rockwell hardness, and the difference increases with increasing the difference between the hardness of the standard and the hardened test steel. The difference is due to the fact that the high-

GRAPHIC NOT REPRODUCIBLE

Fig.13 - Microstructure of Steel A

hardness hardened steel is tested by a ball (in the Pol'di machine) rather than by a diamond tip (in the Rockwell tester). The ball is subject to deformation which distorts the indentation left on the reference material and on the test material. However, if formulas compiled in advance are employed, which take into consideration the spread between the Pol'di and Rock   hardness numbers for the given hardened steels, it becomes possible to employ the Pol'di machine.

Gagarin specimens taken from ingot No.3 (steel A) and Nos.6 and 8 (steel B) were subjected to tensile testing. The resultant values for tensile strength are in good agreement with the literature data for these steels.

Lathe

The experiments with steels A and B were run on a DIP-400 lathe with a swing H = 400 mm and a distance between centers of L = 3000 mm. The lathe was equipped with 9.5 hp DC motors and a transmission chain for transferring motion from the motor shaft to the lathe, and two rheostats for fine and coarse adjustment of the cutting speed.

The experiments with C steel were run on a DIP-300 lathe of H = 300 mm and L = 3000 mm. The lathe was otherwise the same as the DIP-400.

Cutting Tool

The investigation was run with straight and right-hand bent-shank turning tools, with the shank diameter being 20 × 30 mm. Cemented carbide bars measuring 20 × 20 × 7 mm were brazed to the cutter shanks. An exception were the cutters tipped with VK3 alloy, whose bars measured 16 × 16 × 5 mm (shank section 16 × 25 mm). The bars were brazed to the shank with copper and brass. Both filler metals gave satisfactory results.

The cutters were dry-ground in two steps:

1) Rough-grinding on 36-grain green silicon carbon wheels;

2) Finish-grinding on the same type of wheels, but 80 grain.

The cutters were finished on their faces and flanks, and also on the nose radius. The finishing material was a boron carbide flour No.3 of 28 - 21 grain size (here grain size represents the grains in microns).

11. Chip Formation

The chip formed in the machining of metals is classified as follows:

1. Elementary chip, in which the weakly-differentiable elements are displaced with respect to each other, but are firmly coherent. On the side adjacent to the cutter, the chip has a mirrorlike surface. On the opposite side, if a heavy cut is taken, slight serrations may be seen. Continuous chip is formed in high-speed machining.

2. Sectional chip, in which all the elements are clearly defined but remain coherent. The side of the chip facing the cutter presents a smooth surface. On the other side, serrations are readily seen with the naked eye. Discon-

tinuous chip results when ductile metals are machined at low speeds.

3. Discontinuous chip, in which the individual sections are not coherent. As distinct from elementary and sectional chip, discontinuous chip has an uneven surface on the side facing the cutter. This type of chip results from the machining of metals of low ductility such as cast iron.

The chip formed in the machining of the hardened steels investigated by the author was elementary. The appearance of the chip coming off the work depends substantially upon the type of hard alloy used as the tip. In work with cutters tipped with cemented tungsten carbides (VK6, VK8, and others), the chip comes off in a long spiral because of the large craters on the face of the cutter. At the start of cutting, when no crater has yet formed on the cutter face, the chip looks like ribbon in spirals with a large radius of curvature. As a cutter with a tungsten bar becomes dulled, the radius of curvature of the coils of chip becomes smaller, and when the cutter is quite dull the chip comes off in short spirals and individual pieces.

Figure 14 shows four chips obtained at different stages of dulling of a VK8 cutter in the process of turning steel B whose H_{R_C} hardness was 59. The upper chip was produced with a sharp cutting edge of the cutter when no craters had yet appeared on its face (at the onset of cutting). With the formation of craters, the chip takes on a spiral form. As the cutter becomes dulled, the radius of each coil of chip becomes smaller.

Figure 15 shows three chips representing various stages of dulling of a VK8 cutter. The workpiece was steel B for which H_{R_C} = 59. The upper chip, produced at the start of the cutting when no craters had yet formed on the cutter face, appears as a long, tangled ribbon. When the tool became quite dull, the chip crumbled off in separate pieces (bottom chip in Fig.15).

The four chips illustrated in Fig.16 were obtained by machining steel C of H_{R_C} = 65, with a VK3 tool. The upper chip was produced after the cutter had been

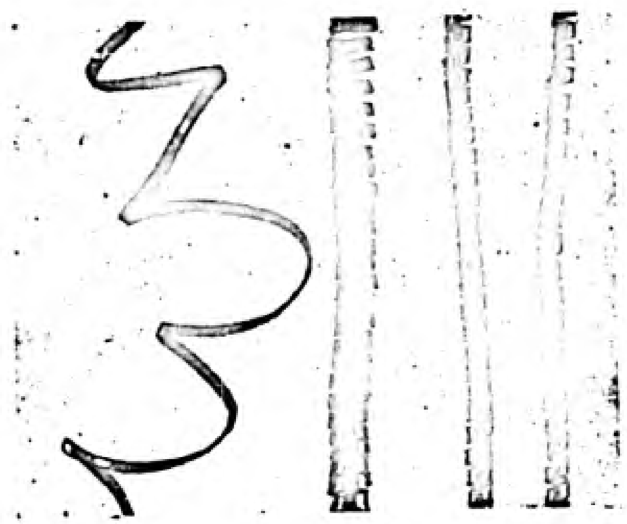

Fig.14 - Appearance of Chip, as Affected by the Degree of Dulling of Tool Tipped with Cemented Tungsten Carbide VK8. Turning of steel B; H_{R_C} = 59, t = 2.4 mm, s = 0.155 mm/rev., v = 20 m/min

Fig.15 - Appearance of Chip, as Affected by the Degree of Dulling of Tool Tipped with Cemented Tungsten Carbide VK8. Turning of steel B; H_{R_C} = 59, t = 2.4 mm, s = 0.395 mm/rev., v = 12 m/min

used for 10 min, the next after 20 and 30 min, respectively, and the bottom one represents normal dulling of the cutter (after 37 min). The photograph shows that reduction in chip coil radius as dulling of the tool proceeds is also typical of the hard alloy VK3.

In work with cemented titanium-tungsten carbides (T15K6 and others), a charac-

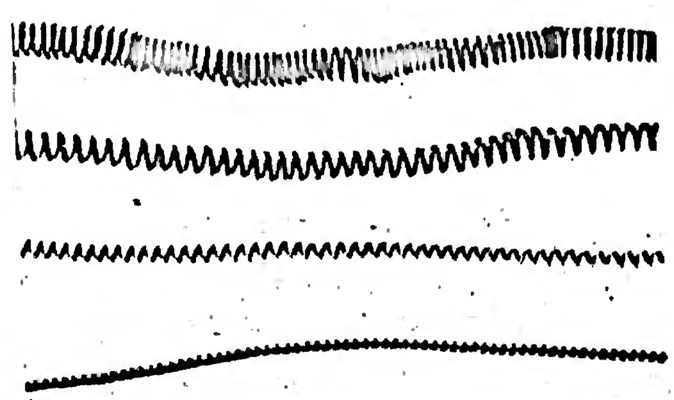

Fig.16 - Appearance of Chip, as Affected by the Degree of Dulling of Tool Tipped with VK3. Turning of steel C; $H_{R_C} = 65$, $t = 0.75$ mm, $s = 0.14$ mm/rev., $v = 10$ m/min

teristic sign of complete dulling of the cutter is the appearance of a goffered type of chip.

Figure 17 presents four chips produced in the turning of steel B, of $H_{R_C} = 59$, with a titanium-tungsten cutter. The bottom chip, goffered in appearance, was produced at the instant of normal dulling of the tool.

The six chips illustrated in Fig.18 were produced in the machining of steel C with a T15K6 cutter, the steel having a hardness of $H_{R_C} = 65$.

We see from Fig.18 that, when such a steel is turned with a comparatively heavy cut and feed, the process of dulling of the tool is not accompanied by the normal change in chip appearance. At the outset of machining, when the cutter shows little dulling, the chip flows smoothly in the form of a true spiral ribbon with absolutely smooth outside surface (contact area between chip and tool face). Then, as the

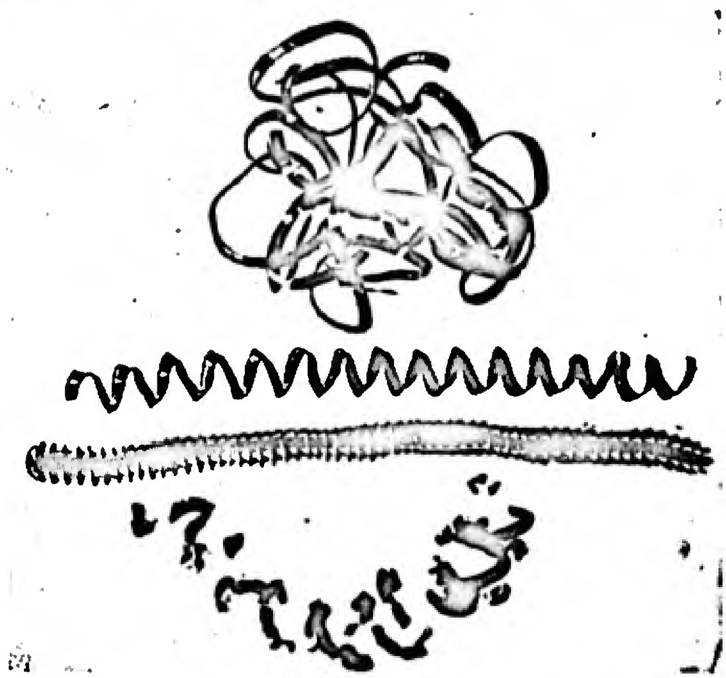

Fig.17 - Appearance of Chip, as Affected by the Degree of Dulling of the Titanium-Tungsten Tool. Turning of steel B; H_{R_C} = 59; t = 2.4 mm, s = 0.155 mm/rev., v = 25 m/min

cutter dulls, the chip loses the shape of a true spiral.

A different picture is observed when cut and feed are not as heavy (t = 0.25 mm, s = 0.053 mm/rev: Fig.19).

At the onset of machining, the chip also comes off in the form of a true spiral ribbon, but this shape is retained over virtually the entire period of machining. Only shortly before the cutter is dulled does the chip lose its spiral shape, coming off in the form of a tangled cluster, with the outer surface taking on the characteristic goffered appearance.

Consequently, in the case under examination, where t and s are low, the criterion for dulling of a T15K6 cutter may be taken to be the acquisition of a goffered

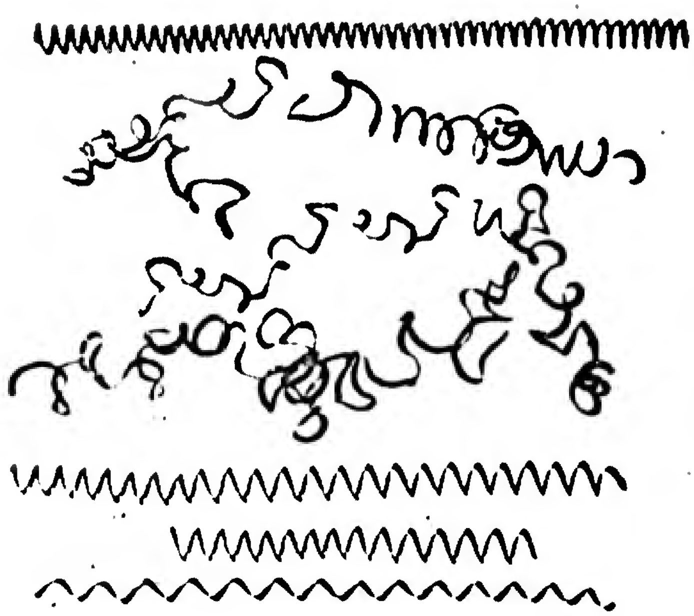

Fig.18 - Appearance of Chip, as Affected by the Degree of Dulling of the T15K6 Tool. Turning of steel C; H_{R_C} = 65, t = 0.75 mm, s = 0.14 mm/rev., v = 10 m/min

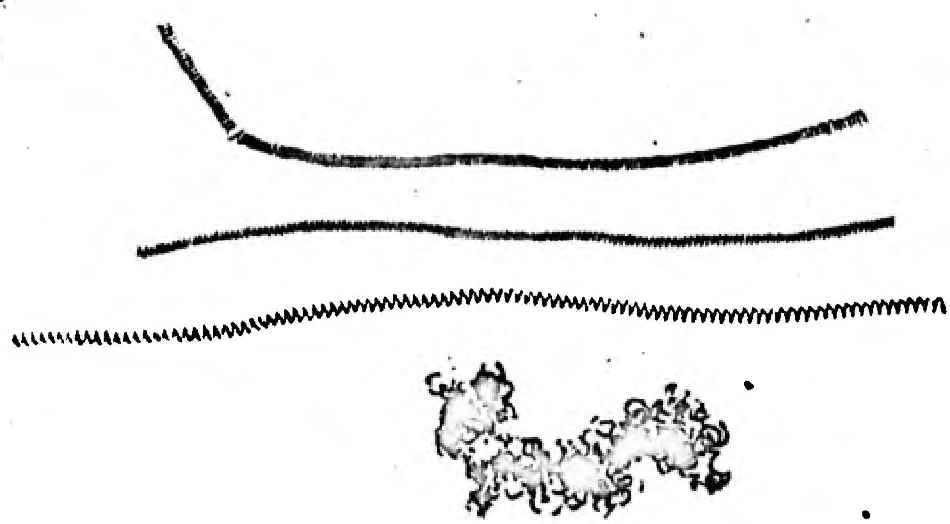

Fig.19 - Appearance of Chip, as Affected by the Degree of Dulling of the T15K6 Tool. Turning of steel C; H_{R_C} = 65, t = 0.25 mm, s = 0.053 mm/rev., v = 22 m/min

appearance by the chip. It would, however, be wrong to believe that, when hardened steel is turned with T15K6 cutters, the dulling of the cutter is accompanied by a characteristic change in the appearance of the chip only at low t and s. The author

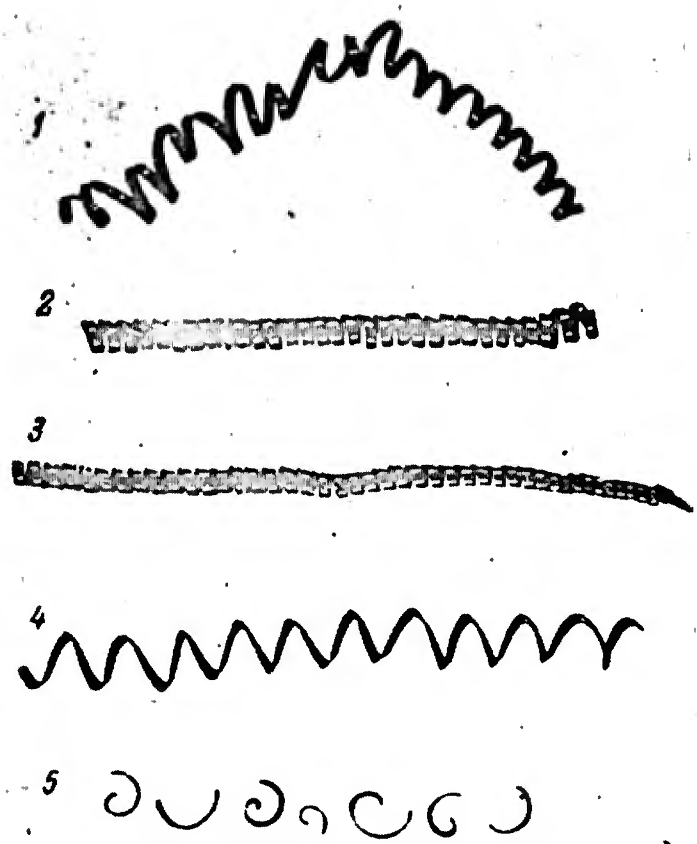

Fig.20 - Appearance of Chip, as Affected by the Cutting Speed in Turning of Steel A, H_{R_C} = 41. t = 1.2 mm and s = 0.225 mm/rev.

1 - v = 80 m/min; 2 - v = 55 m/min; 3 - v = 30 m/min; 4 - v = 15 m/min; 5 - v = 5 m/min

has also observed different results: chip that took on a goffered appearance at high t and s, but that did not look this way at low values thereof.

The sign of tool dulling we have examined - the acquisition of a goffered appearance by the chip - is highly graphic, and therefore valuable under industrial conditions, although it is, unfortunately, not always seen. This "symptom" can be used as a criterion for the dulling of tools tipped with cemented titanium-tungsten carbides.

In the case of cutters tipped with cemented tungsten carbides (VK8, VK6, and others), the change in appearance of the chip is a less distinct criterion of dulling. Nevertheless, also in these tools, a careful observation of the machining process makes it easy to spot any reduction in the radius of curvature of the chip coil.

These photos of chip show that the wear on the face of tools tipped with cemented tungsten carbides increases continually, whereas in the case of tools tipped with cemented titanium-tungsten carbides, it undergoes little change after a small crater has been formed on the face of the cutter at the start of machining. This is clear from the fact that, as the crater on the face of tungsten tools deepens, there is a continuous reduction in the radius of the coils of chip. In the case of tools tipped with titanium-tungsten carbide, a crater forms on the face of the tool at the onset of cutting, causing the chip to become spiral in form, but thereafter, until the tool has completely dulled, the depth of the crater remains virtually constant as does the radius of curvature of the chip coil.

Figure 20 shows five chips resulting from the turning of steel A of $H_{R_C} = 41$ by cutters of VK8. The cutting speed range was $v = 5 - 80$ m/min. As we see, elementary chip was formed at all cutting speeds. Consequently, the turning of hardened steels is characterized by the formation of elementary chip at various cutting speeds, including low speeds.

As we know, the following factors influence the nature of the chip formed: the true rake angle of the cutting tool γ, the cutting speed v, the thickness of the cut a, and the mechanical properties of the material being machined.

The machining of hardened steels is done by cutters of negative true rake ($\gamma < 0^o$) at relative low cutting speeds* and at fine cuts, i.e., under conditions favoring the production of sectional chip. At the same time, elementary chip was

* For footnote, see next page.

obtained in all the author's experiments in the turning of steels hardened to H_{R_C} = 41 - 65. Elementary chip was obtained in the machining of steel A (the least hard of the steels investigated) at relatively high cutting speeds and low feeds. The same kind of chip was obtained in the machining of steel B, of H_{R_C} = 59 at v = 12 m/min, t = 2.4 mm and s = 0.395 mm/rev (Fig.15), and of steel C of H_{R_C} = 65, at v = 10 m/min, t = 0.75 mm and s = 0.14 mm/rev (Fig.18).

The production of elementary chip in the machining of hardened steels, despite the fact that the cutting conditions favor the formation of elementary chip, is explained by the mechanical properties of the steels: high hardness and tensile strength, and low elongation per unit length.

12. Criteria for the Dulling of Cutters

Cutter Wear as a Criterion of Dulling

Here, a description is given of a test on cutters tipped with cemented tungsten and titanium-tungsten carbide, used in turning steel B of H_{R_C} = 59. The cutter was removed from the machine tool repeatedly as long as it remained serviceable, to determine the wear of both face and flank. The abrasion of the cutter flank (Fig.21 illustrates the thickness of the worn area) was measured with the aid of a tool microscope.

Below, we describe the picture of successive wear of a tungsten cutter, working under the following cutting conditions: t = 1.2 mm, s = 0.225 mm/rev. and v = 35 m/min. The cutter functioned for 40 min until a state of normal dulling was reached. Wear of the cutter occurred as follows:

1. At the start of cutting: finest crumbling out of the working portion of the

---

*(Footnote from preceding page). Below it will be shown that the cutting speeds employed by the author and other investigators in experiments in the cutting of other high-hardness tempered steels are actually the speeds that correspond to what is termed "high-speed" machining of metals. However, when compared to the speeds currently being employed in the machining of steels of ordinary hardness, these are low.

cutting edge, invisible to the naked eye but clearly definable under the microscope; definition of the contours of an incipient crater on the cutter face in the form of a brightly-gleaming area; appearance of slight abrasion on the flank, along the line of contact between cutting edge and workpiece; the chip came off in the form of a tangled ribbon with a high radius of curvature, and did not curl into a spiral due to the absence of a crater on the face. Heating of the chip was low.

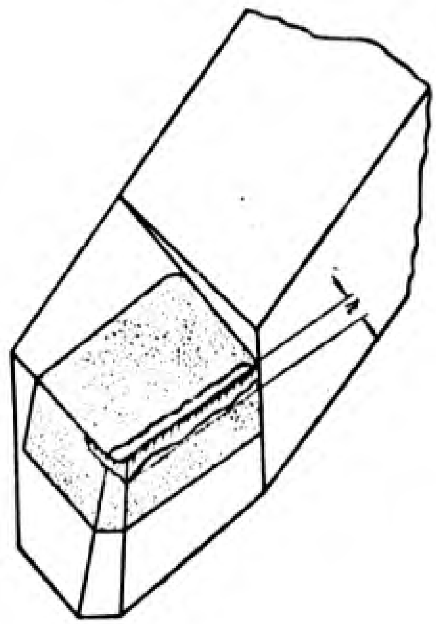

Fig.21 - Diagram of Wear of Carbide Cutter. h - Height of area of cutter wear along flank

2. As the cutter became duller, the following was observed: increase in the crumbling out of the working portion of the cutting edge; appearance of gradual deepening and expansion of the crater on the face; increase in abrasion on the flank, as well as of the radius of curvature of the cutter tip; noticeable increase in the heating of the chip and the material being machined; increase in the axial and radial forces P_x and P_y, recorded by dynamometer; some increase in power consumption; chip in the form of a long spiral; onset of impairment of finish of machined surface; and appearance of bands of variable (differing) diameters.

3. At the end of the cutting period, further deepening and widening of the crater on the cutter face and merging of the extreme points of the crater with the cutting edge; considerable increase in serrations on the working portion of the cutting edge, now visible with the naked eye; increase in abrasion of the flank to h = 1.08 mm; pronounced bouncing of cutter off work; appearance of a distinctive sound - buzzing and whistling; pronounced heating of the chip and the machined sur-

Fig.22 - Tungsten Cutter Used to Normal Dulling in Turning of Steel B; H_{R_C} = 59, t = 1.2 mm, s = 0.225 mm/rev and v = 35 m/min. Wear of cutter flank: h = 1.08 mm

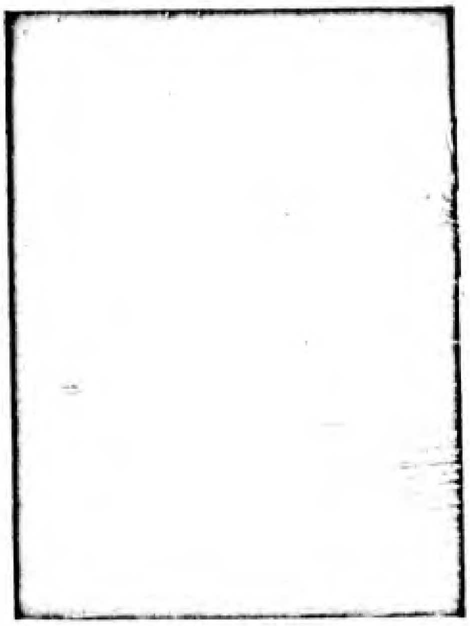

Fig.23 - VK8 Cutter Used to Normal Dulling in Turning of Steel B; H_{R_C} = 59 and t = 0.3 mm. s = 0.112 mm/rev and v = 41 m/min. Wear of cutter flank: h = 0.78 mm

Fig.24 - T15K6 Cutter Used to Normal Dulling. Turned steel B; H_{R_C} = 59, at t = 0.3 mm, s = 0.112 mm/rev and v = 64 m/min. Top view

face (hand in contact with the machined surface will receive burns); change in the appearance of the chip from long spirals to short ones and small pieces; sharp jump in the P_x and P_y forces; 10 - 15% rise in power consumption over the initial cutting period; sharp decline in the quality of the machined surface and appearance of coarse scratches.

4. When the cutter was retained too long (not removed from the machino tool at the end of 40 min of operation, i.e., kept after dulling), pronounced vibration of

GRAPHIC NOT REPRODUCIBLE

Fig.25 - T15K6 Cutter Seen in Fig.24; Side View

the machine tool and interruption in feed was observed: cutting proceeded unevenly and in jumps, resulting in failure of the carbide bar.

Figure 22 shows the cutter used in the described test. The photograph clearly shows the area of flank wear of the cutter at the instant of normal dulling, after 40 min of work.

A test of a cutter tipped with VK8 in the machining of the same steel B of H_{R_C} = 59, but with less depth of cut and lower feed, showed (Fig.23) that the process of dulling of the cutter proceeded in the same manner as in the case described and was accompanied by the same phenomena, but less clearly defined. After working for 60 min, the cutter was normally dulled; the abrasion of the flank came to h = 0.78 mm. The cutter also underwent pronounced wear of its face. The photograph clearly shows the crater.

Similar tests were run on cutters tipped with cemented titanium-tungsten carbide. The dulling process was of essentially the same nature as in the preceding instances, except for the fact that the crater on the face and the abrasion of the flank at the instant of normal dulling of the cutter were considerably less pro-

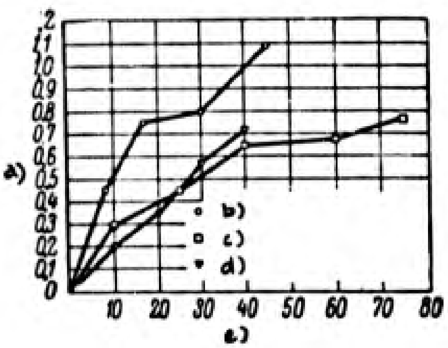

Fig.26 - Ratio of Cutter Flank Wear to Length of Use, for Various Hard Alloys. Turning of steel B; H_{R_C} = 59, t = 1.2 mm, s = 0.225 mm/rev

a) Wear of cutter flank h, mm;
b) VK8 cutter; v = 35 m/min;
c) T21K8 cutter; v = 40 m/min;
d) T15K6 cutter; v = 44 m/min;
e) Cutter working time T, min

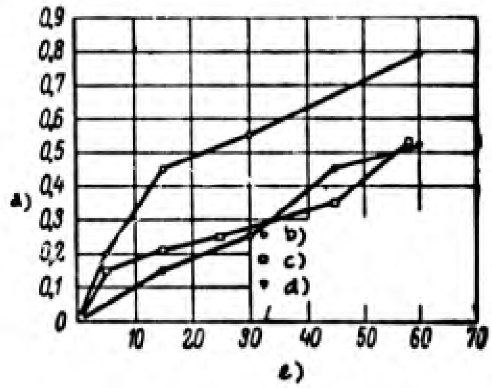

Fig.27 - Ratio of Cutter Flank Wear to Length of Use, for Various Hard Alloys. Turning of steel B; H_{R_C} = 59, t = 0.3 mm, s = 0.112 mm/rev

a) Wear of cutter flank h, mm;
b) VK8 cutter; v = 41 m/min;
c) T21K8 cutter; v = 56 m/min;
d) T15K6 cutter; v = 64 m/min;
e) Cutter working time T, min

nounced, and the chip had a goffered appearance. Figures 24 and 25 illustrate a T15K6 cutter at the instant of normal dulling. The cutter was tested in turning of the same steel as that used for the VK8 cutter, but at a higher cutting speed: v = 64 m/min. Here the abrasion of the flank was h = 0.53 mm, whereas for the VK8 cutter it was 0.78 mm.

It is evident from the data adduced that cermet cutters - both tungsten and titanium-tungsten - undergo wear on face and flank in the machining of hardened steels, and that this wear starts at the very outset of cutting, increasing constantly during the entire cutting period.

It should be mentioned that it is much easier to define the amount of wear of the flank than of the face of a cutter. Wear on the face of cutters of cemented titanium-tungsten carbide is so insignificant that it cannot always be measured. Therefore, all the reasoning and conclusions on cutter wear, given below, refer to their flanks.

Further, graphs are appended descriptive of the relationship of the wear of the flanks of carbide cutters to the length of time they are used in the turning of hardened steels.

Figures 26 and 27 present curves of the wear for cutters tipped with various grades of cemented carbides and used in turning steel B of H_{R_C} = 59. The cutters were operated to the instant of normal dulling. It will be seen that the VK8 cutters underwent considerably greater wear than the T15K6 and the T21K8. Furthermore, if it is considered that the VK8 cutters functioned at lower cutting speeds than the T15K6 and the T21K8 cutters, the superiority of cemented titanium-tungsten over tungsten carbides for the turning of hardened steels becomes obvious. Thus, a T15K6 cutter operating at a cutting speed v of 44 m/min, showed a wear of h = 0.55 mm in 30 min (Fig.26); the wear of a VK8 cutter operated for the same length of time at considerably lower cutting speed (v = 35 m/min) was greater (h = 0.8 mm).

The wear curves for T21K8 and T15K6 cutters virtually coincide, but this does not mean that their wear resistance is identical. The point is that the T15K6 cutters functioned at higher cutting speeds: v = 56 m/min for a T21K8 cutter, and v = 64 m/min for a T15K6 cutter (Fig.27). The fact that the T15K6 cutters showed the same amount of wear, but at higher cutter speeds, than the T21K8 cutters, signifies that the resistance of the T15K6 alloy is higher than that of the T21K8 alloy.

N.S.Logak (Bibl.21) made a study of the fine-turning of several grades of hardened steels. Figure 28 presents his curves for the wear of cutters tipped with the cermet T30K4.

We see that the normal flank wear of T30K4 cutters in the turning of 40KhS and ShKh15 hardened steels (H_{R_C} = 50 to 63) is approximately h = 0.5 mm. The same amount of normal wear is characteristic of T15K6 cutters in the machining of

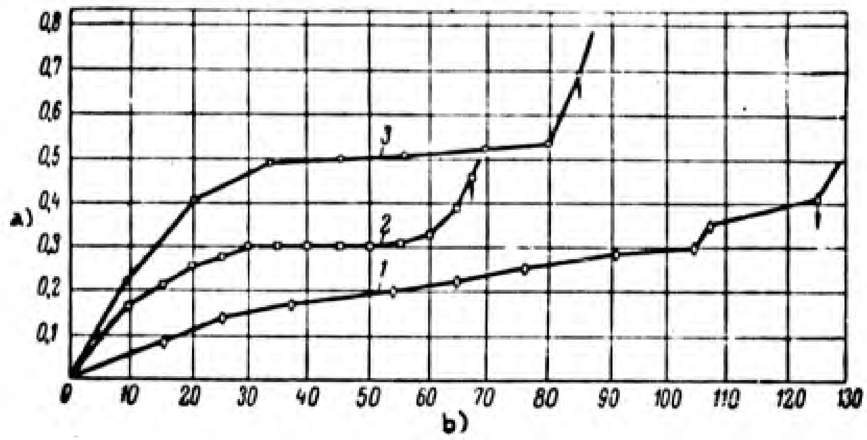

Fig.28 - Ratio of T30K4 Cutter Flank Wear to Service Time in the Fine-Turning of Hardened Steels, t = 0.2 mm and s = 0.1 mm/rev

1 - Machining of 40KhS steel, H_{R_C} = 50 - 52 at v = 80 m/min;

2 - Machining of 40KhS steel, H_{R_C} = 50 - 52, at v = 100 m/min;

3 - Machining of ShKh15 steel, H_{R_C} = 61 - 63, at v = 37 m/min

The arrow indicates onset of crumbling-out of the carbide bar.

a) Wear of cutter flank h, mm; b) Cutter working time T, min

steel B of H_{R_C} = 59 and t = 0.3 mm, s = 0.112 mm/rev (Fig.27).

In turning hardened steels, it is necessary to work until the cutter is normally dull. Further use of the cutter, in the majority of cases, will result in crumbling out or destruction of its working edge. This occurs most frequently in cutters tipped with cemented titanium-tungsten carbide, for which a brittleness higher than that of tungsten carbides is typical.

The grinding must not be continued until complete destruction of the cutting edge of the cutter, since this makes dressing more difficult, reduces the service life of the carbide bar (reducing the number of dressings possible) and also causes scratches, fissures, and the like, to appear on the machined surface. The cutter should be used to normal dullness, determined by the permissible wear of the flank. For example, in the case of a T15K6 cutter (Fig.25), the maximum wear and criterion of dullness under those conditions of work should be taken to be as h = 0.53 mm.

The maximum wear of a cutter is also dependent upon the nature of the machining. For rough machining, this may be greater than for finishing. In final operations, the maximum permissible cutter wear is specified on the basis of the requirements with respect to tolerance and surface finish. It must be borne in mind that fine-turning of hardened steels requires tolerances of classes 2 and 3, and surface finish of class 7.

Cutter wear is a highly dependable criterion of dulling and is employed under laboratory conditions for investigations of the cutting process. However, the use of this criterion under production conditions is complicated by the fact that the turner would have to stop his work, remove the cutter, and measure the amount of wear. It is therefore desirable to find other, simpler and more visual criteria of cutter dulling, capable of being employed under production conditions.

Change in the Appearance of Chip and Impairment of Surface Finish as Criteria for Cutter Dulling

In Section 11, we examined the problem of changes in the appearance of the chip as the cutter is dulled. In work with titanium-tungsten cutters (T15K6 and others), the criterion for dulling may be the formation of chip of the characteristic goffered appearance. Although this characteristic is not observed in all instances, it is suitable for use in hardened-steel-machining practice.

In the fine-turning of hardened steels by T30K4 cutters, changes in the direction of chip emergence may be used as the criterion: Instead of coming off in spiral form from the face of the cutter, the chip suddenly changes direction at the instant of dulling, and rises straight up.

In the case of tungsten carbide cutters (VK8 and others), the sharp change in the radius of a coil of chip relative to that at the onset of cutting, accompanied by a impairment of the surface finish, distinguishable by the naked eye, may be taken as a graphic criterion of dulling under plant conditions.

It should be remarked that surface finish is less acceptable as a criterion of

Table 25

Wear of Cutter Flank, Employed as the Dulling Criterion

Tungsten Carbide Cutters (VK8 and Others)			Titanium-Tungsten Cutters (T15K6 and Others)		
Cutting Depth t, in mm	Feed s, in mm/rev	Cutter Flank Wear h, in mm	Cutting Depth t, in mm	Feed s, in mm/rev	Cutter Flank Wear h, in mm
1,0—1,5	0,2—0,5	0,7—1,0	0,1—0,3	0,05—0,15	0,2—0,4
1,5—3,0	0,5—0,8	До 1,5	0,3—0,7	0,15—0,35	До 0,6
			0,7—1,5	0,35—0,50	До 0,8

dulling for cutters tipped with cemented titanium-tungsten carbides. Generally speaking, it is also true here the surface finish is impaired as the cutter becomes duller, but this is difficult to detect with the naked eye. Moreover, it must be taken into consideration that, as the hardness of hardened steel increases, this criterion loses its overall distinctiveness.

Dulling of the cutter is accompanied by an increase in power consumption as well as by a rise in the longitudinal and radial forces P_x and P_y. These signs of dulling are employed under laboratory conditions.

Conclusions

1. In turning steels with high-speed cutters, the appearance of a bright band on the machined surface may serve as the criterion for dulling of the cutter. In turning hardened steels, this sign is not useful since the surface of hardened

steel, freed of scale and skin is distinguished by a bright gleam both before and after machining.

2. The most objective and dependable criterion for the dulling of carbide cutters in the turning of hardened steels is the degree of flank wear. Cutters tipped with tungsten carbides will take larger wear than titanium-tungsten tipped cutters. Therefore, the criterion for the dulling of cutters in the former group must be a higher level of wear than in the latter case. Moreover, the degree of permissible cutter wear depends upon the nature of machining. For roughing, the permissible wear is greater than for finish-grinding.

Table 25 presents the amount of flank wear h suggested by the author as the dulling criterion in the turning of alloy steels, hardened to $H_{RC} = 41 - 65$.

The lower h values correspond to lower cutting depths t and feeds s; the higher h values correspond to higher t and s.

3. Under plant conditions, the change in the form of the chip is a valuable criterion for cutter dulling. In work with titanium-tungsten cutters, the formation of chip of a characteristic goffered appearance may serve as the dulling criterion. For tungsten-carbide cutters, a combination of the following two signs may serve as a graphic criterion of dulling:

a) Pronounced reduction in the radius of curvature of a coil of chip, relative to the initial cutting period;

b) Impairment of the surface finish, detectable with the naked eye.

12. Choice of Cermets

Certain investigators hold the opinion that high-hardness tempered steels must be machined with cutters tipped with tungsten carbides, and that titanium-tungsten carbides are not suited to this purpose because of their high brittleness.

The author has run experiments in the turning of steels tempered to very high hardness, in which he used cutters tipped with various cemented carbides. Data were obtained that permit comparisons of the cutting properties of these alloys. The usefulness of these data has not been impaired to this day, despite the fact that certain of the carbides used in the tests (T21K8 and VK12) are no longer in use.

The tests show that in the turning of hardened steels, titanium-tungsten car-

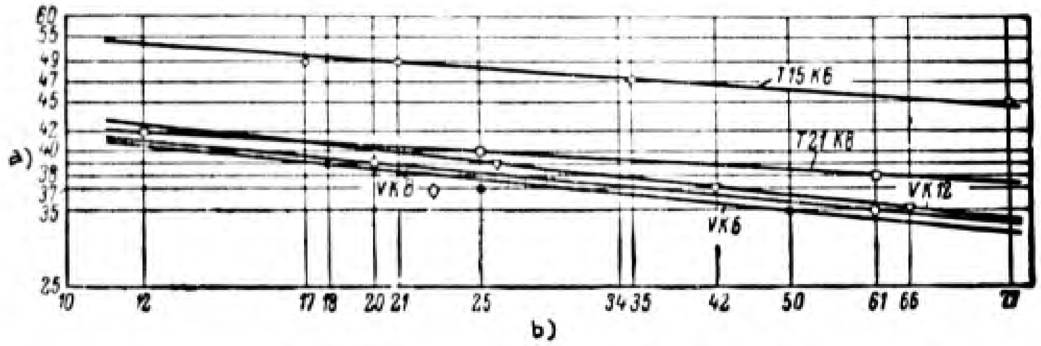

Fig.29 - Relationship Between Cutting Speed v and Life of Cutter T; Various Cermets. Turning of steel B, H_{R_C} = 56 at t = 1.2 mm and s = 0.225 mm/rev

a) Cutting speed v, m/min; b) Cutter life T, min

bides will function at considerably higher cutting speeds than tungsten carbides, and that this superiority rises with reduction in cut and increase in hardness of the metal machined.

Curves (Figs.29 and 30) show the results of tests with steel B of hardness H_{R_C} = 56. Two cuts were taken: a) t = 1.2 mm, s = 0.225 mm/rev; b) t = 0.3 mm and s = 0.112 mm/rev. The cutters were ground with boron carbide flour and used until normal dulling occurred.

The graphs show that titanium-tungsten carbides have considerably better cutting properties than tungsten carbides. In fact, at t = 1.2 mm and s = 0.225 mm/rev, a VK8 cutter displayed a life of T = 18 min at a cutting speed of v = 39 m/min, whereas the T15K6 cutter showed approximately the same life (T = 17 min) at a considerably higher cutting speed: v = 49 m/min. Experiments at t = 0.3 mm and s = 0.112 mm/rev are even more revealing. The VK6 cutter displayed a life T of 40 min at v = 43 m/min, whereas a T15K6 cutter had the same life at v = 70 m/min.

Table 26, containing data on cutting speeds for a 60-minute tool life, shows that the superiority of titanium-tungsten over tungsten carbides rises as the size

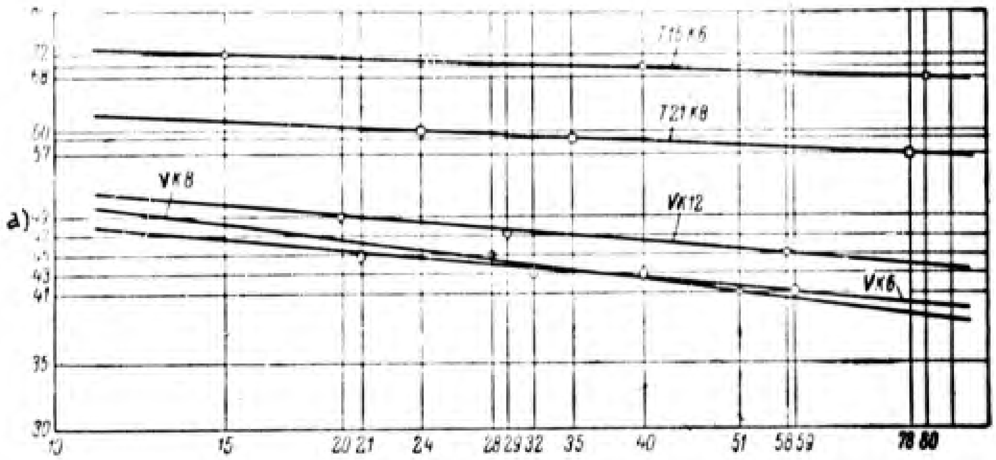

Fig.30 - Relationship Between Cutting Speed v and Cutter Life T for Various Cermets. Turning of steel B, H_{R_C} = 56 at t = 0.3 mm, s = 0.112 mm/rev

a) Cutting speed, v m/min; b) Cutter life T, min

of the cut diminishes. If the v_{60} cutting speed of T15K6 at t = 1.2 mm and s = 0.225 mm/rev is taken as unity, the v_{60} cutting speed of VK8 alloy will be 0.74.

Table 26

Values of v_{60} and Relative Life Indices m for Various Cermets

Turning of steel B with Hardness H_{R_C} = 56

Grade of Cermet	t = 1.2 mm; s = 0.225 mm/rev			t = 0.3 mm; s = 0.112 mm/rev		
	v_{60}, in m/min			v_{60}, in m/min		
	Absolute Value	Relative Value	Index, m	Absolute Value	Relative Value	Index, m
T15K6	45,7	1,00	0,063	69,0	1,00	0,039
T21K8	38,3	0,84	0,069	57,5	0,83	0,045
VK12	35,3	0,77	0,119	44,8	0,65	0,083
VK8	34,0	0,74	0,106	40,0	0,58	0,150
VK6	33,3	0,73	0,103	41,2	0,60	0,097

At t = 0.3 mm and s = 0.112 mm/rev, the relationship between the cutting properties of these cemented carbides changes still further in favor of T15K6 (1.0 : 0.58). Consequently, for purposes of turning high-hardness tempered steel at fine cuts, the

Table 27

Values of v_{60} and Indices m for Various Cermets

Turning of Steel C, H_{R_C} = 65 at t = 0.5 mm and s = 0.14 mm/rev

Grade of Cermet	v_{60}, in m/min		Index, m
	Absolute Value	Relative Value	
T21K8	11,7	1,01	0,150
T15K6	11,6	1,00	0,137
VK3	11,3	0,97	0,216
VK12	9,3	0,80	0,175
VK6	8,1	0,70	0,285
VK8	7,4	0,64	0,293

alloy T15K6 makes it possible to work at almost twice the cutting speed of the al-[illegible]. The cutting speeds of the alloys VK12, VK8, and VK6 are approximately the same.

The results of these tests provide convincing proof of the fact that cemented titanium-tungsten carbides should be employed in the machining of hardened steels, particularly in work at low cutting depths and feeds.

In order to arrive at an overall view of the cutting properties of various grades of cermets, the author ran tests on steel C hardened to H_{R_C} = 65. Table 27 presents the results of these tests. The experiments were run at a cutting depth of t = 0.5 mm and a feed of s = 0.14 mm/rev.

The cutters were dressed with boron carbide flour.

The data in Table 27 confirm the previous conclusions to the effect that cemented titanium-tungsten carbides have higher cutting properties than do tungsten carbides.

It must be noted that the alloy VK3, which is in the tungsten carbide group, approximates the alloy T15K6 in cutting properties. This cermet may be used successfully in the turning of hardened steels. The same holds for VK2, a new tungsten alloy.

For fine-turning of hardened steels, the T30K4 titanium-tungsten alloy should

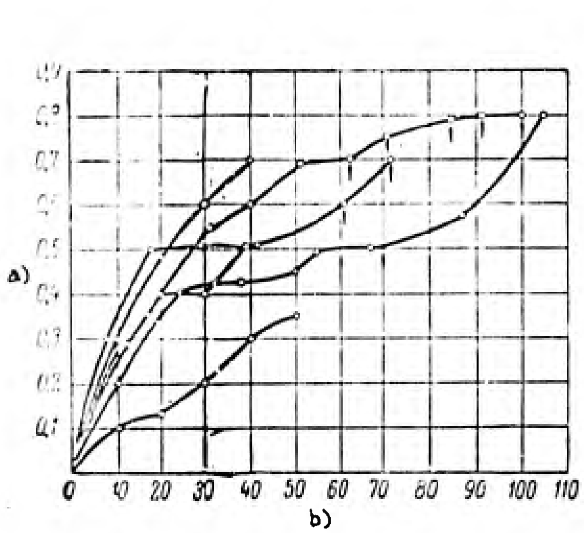

Fig.31 - Relationship of Flank Wear of T30K4 Cutters to Use Time. Turning of 40KhS steel, H_{R_C} = 50 - 52 at v = 40 m/min, t = 0.2 mm, s = 0.1 mm/rev. Cutter geometry: $\alpha = 5^{o}$, $\gamma = -5^{o}$, $\lambda = 5^{o}$, $\varphi = 45^{o}$, $\varphi_1 = 10^{o}$, r = 0.5 mm. Arrows represent crumbling out of hard-alloy cutters

a) Cutter flank wear h, mm; b) Cutter life T, min

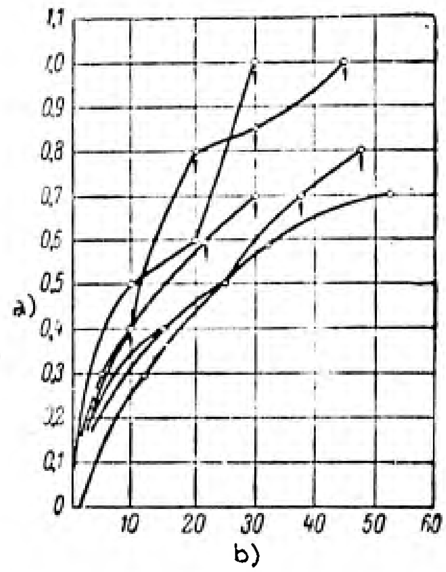

Fig.32 - Relation of Flank Wear of T15K6 Cutter to Use Time. Turning of 40KhS steel, H_{R_C} = 50 - 52, v = 40 m/min, t = 0.2 mm, s = 0.1 mm/rev. Cutter geometry: $\alpha = 5^{o}$, $\gamma = -5^{o}$, $\lambda = 5^{o}$, $\varphi = 45^{o}$, $\varphi_1 = 10^{o}$, r = 0.5 mm. Arrows represent crumbling out of hard-alloy bars.

a) Cutter flank wear h, mm; b) Cutter life T, min

be used (Bibl.21). This alloy has demonstrated significant superiority not only over the alloy VK8 but also over T15K6. This conclusion is confirmed by the results of comparative tests with T30K4 and T15K6 in the turning of 40KhS steel (H_{R_C} = 50 to 52) with t = 0.2 mm and s = 0.1 mm/rev (Figs.31 - 33).

After 40 min of use, the T30K4 cutters showed flank wear in the h = 0.3 to 0.7 mm range (Fig.31), while the T15K6 cutters revealed h = 0.65 to 0.95 mm wear (Fig.32). Of the six T30K4 cutters tested, only two revealed crumbling-out of the

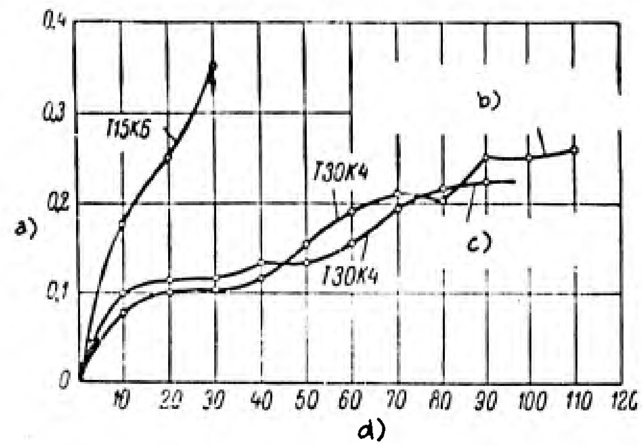

Fig.33 - Results of Comparative Tests of Cutters Tipped with Cermets T30K4 and T15K6, Having Identical Geometry. Turning of 40KhS steel, H_{R_C} = 50 - 52

at v = 60 m/min, t = 0.2 mm and s = 0.1 mm/rev

Arrows indicate crumbling-out of the cemented carbide bar.

a) Cutter flank wear h, mm; b) Test ended by crumbling-out during a plunge cut; c) Test terminated; d) Cutter life T, min

carbide bars, whereas of the six T15K6 cutters, five crumbled out, beginning after 20 - 30 min of use.

Figure 33 shows that a T15K6 cutter, used for 30 min, underwent h = 0.35 mm flank wear and crumbled out, whereas T30K4 cutters displayed considerably less wear after 90 minutes of use (h = 0.25 mm).

Thus, for the turning of a large group of alloy steels tempered to high hardness, the cemented titanium-tungsten carbides T15K6 and T30K4 proved best, particularly when fine cuts were taken. The results are entirely in line with the theory and practice of cemented carbide applications: tungsten carbides being preferable for the machining of cast iron and nonmetallic materials that produce discontinuous chip, and titanium-tungsten carbides being best for steels producing elementary or sectional chip. It was brought out in Section 11 that elementary chip is produced by the turning of chromium-nickel-molybdenum-silicon and chromium-nickel steels B and C, despite their very considerable hardness (H_{R_C} = 59 and 65).

A.Ya.Malkin (Bibl.23) bases his recommendation of the alloy VK8 for turning hardened steels of H_{R_C} = 62 to 65 on the idea that this alloy is considerably harder than the alloy T15K6.

We cannot agree with A.Ya.Malkin's point of view with regard to fine-turning and, in general, finish-turning of hardened steels. One of the fundamental requirements of this process - high quality of machined surface finish - can be satisfied only by the cemented titanium-tungsten carbides T15K6 and T30K4. As we have pointed out, the cemented tungsten carbides VK2 and VK3 constitute an exception in this respect.

It is possible that in rough work in which heavy cuts are taken and the system workpiece - machine tool - cutter is of inadequate rigidity, it would be desirable to employ VK8 alloy, in view of the high brittleness of the alloy T15K6 and particularly of the alloy T30K4. However, in these cases as well, steps have to be taken to improve the rigidity of the system and to use cemented titanium-tungsten carbides which make it possible to work at considerably higher cutting speeds.

Conclusions

1. Hardened steels machine well with all the present grades of cemented carbides, but those in the titanium-tungsten group have major advantages in terms of cutting properties, when compared with the tungsten carbides. The superiority of the titanium-tungsten over the tungsten carbides is more pronounced at fine cuts t and feeds s.

Careful dressing of the cutters is an important measure for counteracting the brittleness of titanium-tungsten carbides.

2. The tungsten carbides VK8 and VK6 and the titanium-tungsten carbide T5K10 are characterized by approximately the same cutting properties.

3. The tungsten carbides VK2 and VK3 have very fine cutting properties, and approach T15K6 in that respect.

4. The hard alloy T30K4 for fine-turning of hardened steels permit machining with cutting speeds up to 20% higher than that of the alloy T15K6.

5. The following carbides should be used for turning hardened steels without impact shock: T30K4, T15K6, VK2, and VK3, whereas VK8, VK6, and T5K10 should be used for turning where impact shock is involved.

14. Influence of Various Factors on Cutting Force

This Section will present the results of investigations to determine the relationships between cutting forces and various factors in the turning of hardened steels.

Effect of Cutting Speed Upon Cutting Force

In the literature on the machining of unhardened steels, the idea that cutting forces diminish with rise in cutting speed holds dominance.

The influence of cutting speed upon the cutting force in the turning of hardened steels has been investigated by the author with steel B, $H_{R_C} = 49$. The tests were run with titanium-tungsten cutters. Figures 34 and 35 present the results of these tests. Figure 34 gives the results of tests at a cutting depth of t = 2.41 mm and a feed of s = 0.395 mm/rev, with cutting speeds varied in the interval of v = 5 - 40 m/min. Figure 35 presents the results of tests with t = 1.19 mm and s = 0.225 mm/rev, with the cutting speeds varied in the interval from 5 to 60 m/min.

As may be seen from the curves, the tangential force P_z diminishes with increasing cutting speed. At the same time, a change in the cutting speed exercises so negligible an effect upon the radial force P_y that one may assume, without much error, that this force is not governed by the cutting speed. The longitudinal force P_x is also independent of the cutting speed.

M.N.Larev (Bibl.22) points out that, in cases of minor flank wear, all three forces diminish as the cutting speed increases. When the cutter wear is high, an

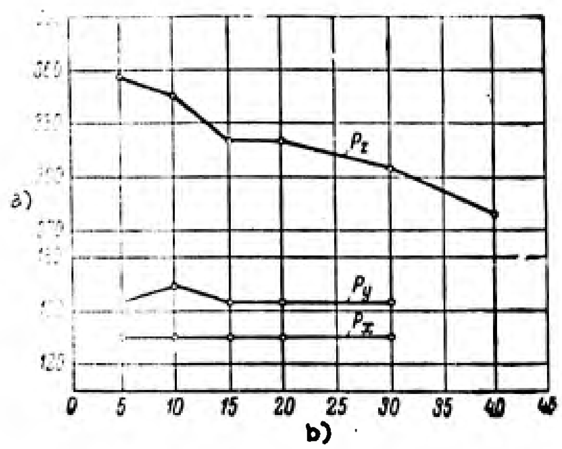

Fig.34 - Influence of Cutting Speed v upon the Forces P_x, P_y, and P_z. Turning of steel B, of H_{RC} = 49, at t = 2.41 mm and s = 0.225 mm/rev. Cutter geometry: $\alpha = 6^o$, $\gamma = -5^o$, $\lambda = 0^o$, $\varphi = 45^o$, $\varphi_1 = 15^o$; r = 1.15 mm

a) Forces P_x, P_y, and P_z, kg; b) Cutting speed v, m/min

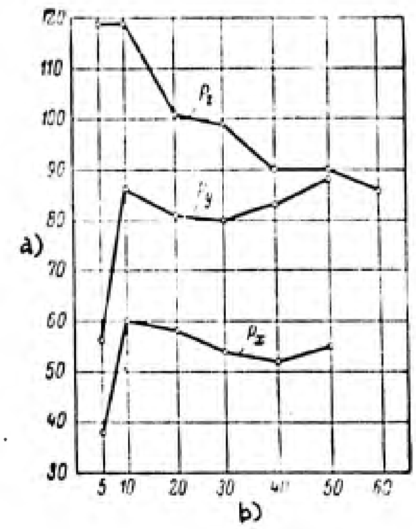

Fig.35 - Influence of Cutting Speed v upon the Forces P_x, P_y, and P_z. Turning of steel B, of H_{RC} = 49, at t = 1.19 mm and s = 0.225 mm/rev ($\alpha = 6^o$, $\gamma = -5^o$, $\lambda = 0^o$, $\varphi = 45^o$, $\varphi_1 = 15^o$, r = 1.15 mm)

a) Forces P_x, P_y, and P_z, kg; b) Cutting speed v, m/min

increase in the P_x and P_y forces with cutting speed is possible.

A.D.Makarov has come to the opposite conclusions (Bibl.24). In the investigation of Khl2M steel with H_{RC} = 61 - 62, he found that, at a cutting depth of t = 0.45 mm and a feed of s = 0.2 mm/rev, the variation in the cutting speed v from 9 to 23 m/min led to a reduction in P_z and a rise in P_x and P_y.

The discrepancy between the data of A.D.Makarov and those of the present author may be explained by the fact that the former apparently ran his tests with cutters that had undergone considerable dulling of their flanks, whereas the author conducted his with freshly-ground cutters.

Consequently, in the turning of hardened steels, the cutting speed exercises a significant influence upon the cutting force P_z. For hardened steels of medium hardness (H_{R_C} = 49), this influence was clearly manifested in the range of cutting speeds v from [illegible] to 60 m/min. For steels of high hardness (H_{R_C} = 61 - 62), this is manifested in a considerably narrower range: from 9 to 23 m/min.

A comparison of the data by A.M.Vul'f (Bibl.25) for unhardened steel with those by the present author for hardened steel of H_{R_C} = 49 revealed that, at an equal increase in cutting speed v, the force P_z also diminished to an identical degree. This refutes N.N.Zorev's claim that the cutting force is less dependent upon the speed in the turning of hardened steels than in the machining of unhardened steels.

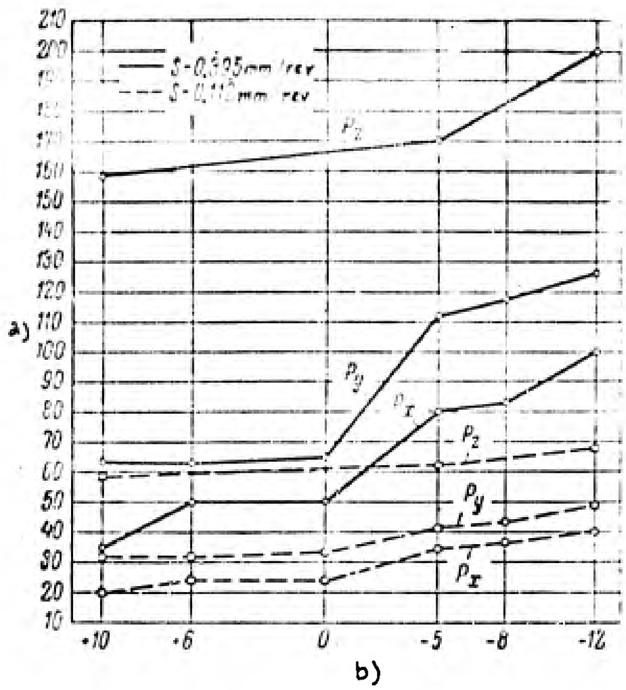

Fig.36 - Effect of True Rake Angle γ on the Forces P_x, P_y, and P_z at Various Values of the Feed s. Turning of steel B, of H_{R_C} = 49, at s = 1.2 mm,

s = 0.112 and 0.395 mm/rev, and
v = 20 m/min. Cutter geometry:
α = 6°, λ = 0°, φ = 45°, $φ_1$ = 15°,
r = 1.15 mm

a) Forces P_x, P_y, and P_z, kg;
b) True rake angle γ°

Influence of Cutter Geometry upon the Cutting Force

True Rake Angle. Experiments to determine the nature of the influence exercised by the true rake angle upon cutting force were run by the author with B steel, H_{R_C} = 49. Machining was with titanium-tungsten cutters at constant cutting speed (v = 20 m/min) and depth of cut (t = 1.2 mm), and various feeds s. The true rake angle γ was varied from +10 to -12°. The results of the tests run for feeds s = 0.112 and 0.395 mm/rev are presented in Fig.36.

As we see, a reduction in the true rake angle is accompanied by a rise in the forces P_x, P_y, and P_z, where the effect of the γ angle upon the cutting forces is manifested more sharply in the interval of negative rake angles ($\gamma < 0°$) than in the positive interval ($\gamma > 0°$).

The true rake angle γ affects the forces P_x and P_y more strongly than the

Table 28

Ratios $\frac{P_x}{P_z}$ and $\frac{P_y}{P_z}$ for Various True Rake Angles γ in the Turning of Steel B, of H_{RC} = 49 at Various Feeds, Cut t = 1.2 mm, and Cutting Speed v = 20 m/min

Feed s, in mm/rev	γ = +10°		γ = 0°		γ = −5°		γ = −12°	
	$\frac{P_x}{P_z}$	$\frac{P_y}{P_z}$	$\frac{P_x}{P_z}$	$\frac{P_y}{P_z}$	$\frac{P_x}{P_z}$	$\frac{P_y}{P_z}$	$\frac{P_x}{P_z}$	$\frac{P_y}{P_z}$
0,112	0,42	0,75	0,51	0,82	0,68	0,90	0,70	0,92
0,155	0,35	0,63	0,41	0,64	0,62	0,83	0,68	0,87
0,225	0,31	0,54	0,38	0,63	0,54	0,73	0,61	0,79
0,307	0,27	0,49	0,36	0,58	0,48	0,66	0,57	0,78
0,395	0,24	0,48	0,34	0,49	0,46	0,63	0,52	0,69

force P_z. For example, on varying the true rake angle between +10 and -12° (s = 0.395 mm/rev), the longitudinal force P_x increased from 34 to 99 kg, i.e., by a factor of 2.9, while the radial force P_y increased from 63 to 126 kg, i.e., by a factor of 1. At the same time, the tangential force P_z increased only by a factor of 1.27 (from 157 to 200 kg).

In the interval of negative values of the true rake angle γ, the $\frac{P_x}{P_z}$ and $\frac{P_y}{P_z}$ ratios are higher than at positive values thereof, with these ratios increasing with a decrease in the true rake angle γ (Table 28). The data in this Table also demonstrate that $\frac{P_x}{P_z}$ and $\frac{P_y}{P_z}$ diminish as the feed increases.

The results obtained by the present author are confirmed by other investigations of the process of machining hardened steels (Bibl.22, 23).

The conclusion may be drawn that the effect of the true rake angle upon the cutting force in the turning of hardened steels is of the same nature as in the machining of ordinary (unhardened) steels.

End-Cutting-Edge Angle. In the turning of hardened steels, reduction of the end-cutting-edge angle causes an increase in the longitudinal force P_x and the radial force P_y, with a change in the angle φ having a greater effect upon P_x than upon P_y. In accordance with the experimental data (Bibl.22), each 10° reduction in the angle φ results in a 7.5% rise in the force P_y, and a 30% rise in the force P_x. The influence of the angle φ on the tangential force P_z is negligible.

Complement of Back Rake Angle. An investigation by A.A.Maslov (Bibl.26) showed that, in the turning of hardened steels, an increase in the complement of the back rake angle λ from -30 to +45° results in an increase in the radial force P_y, whereas the axial force P_x declines.

According to the data of N.N.Zorev (Bibl.22), each 10° increase in the angle λ causes the force P_y to rise by 15% and the force P_x to diminish by 5%. These data are valid at an end-cutting-edge angle of φ = 20°, a depth of cut of a = 0.1 mm, and a flank wear of h = 0.2 mm. As the angle φ rises, the effect of the angle λ upon the force P_y diminishes, whereas its effect upon the force P_x increases. The influence of the angle λ upon the forces P_x and P_y also diminishes with increase in cutter wear. This is more pronounced, the greater the hardness to which the steel has been brought and the less the depth of cut.

The tangential force P_z undergoes virtually no change with a variation in the angle λ.

Effect of Depth of Cut and of Feed upon the Cutting Force

In order to determine the relationships of the forces P_x, P_y, and P_z to the depth of cut t and the feed s in the turning of hardened steels, the author ran a series of experiments. The results of four series of experiments are presented: three for steel B of H_{R_C} = 49 and one for the same steel of H_{R_C} = 59. The dynamic tests were run with titanium-tungsten cutters with the following geometry: $\alpha = 6^\circ$, $\gamma = -5^\circ$, $\lambda = 0^\circ$, $\varphi = 45^\circ$, $\varphi_1 = 15^\circ$, and r = 1.15 mm.

Figures 37 - 42 present, in log-log scale, curves for the relationships between the forces P_x, P_y, and P_z and the depth of cut t and the feed s for hardened steel B, of H_{R_C} = 49. For the same steel, Figs.43 and 44 present, in Cartesian coordinates, the ratios $\frac{P_x}{P_z}$ and $\frac{P_y}{P_z}$ for various values of the feed s.

Figure 43 shows that the ratio $\frac{P_x}{P_z}$ increases with a reduction in the feed and an increase in the depth of cut (considerably more weakly in the latter case). The ratio of the radial force P_y to the tangential force P_z increases with any reduction in feed and depth of cut (Fig.44).

The ratio of the longitudinal force P_x, the radial force P_y, and the tangential force P_z to the depth of cut and the feed in the turning of hardened steels may be presented in the following form:

$$P_x = C_{P_x} \cdot t^{x_{P_x}} \cdot s^{y_{P_x}} \; kg;$$

$$P_y = C_{P_y} \cdot t^{x_{P_y}} \cdot s^{y_{P_y}} \; kg;$$

$$P_z = C_{P_z} \cdot t^{x_{P_z}} \cdot s^{y_{P_z}} \; kg;$$

where C_{P_x}, C_{P_y}, and C_{P_z} are constants depending upon the work and other cutting conditions;

t is the depth of cut in mm;

s is feed in mm/rev.

The experiments show that the exponents x_{P_x} and x_{P_y} depend on the feed s, and the exponents y_{P_x} and y_{P_y} on the depth of cut t: x_{P_x} and x_{P_y} diminish with increasing depth of the cut t. However, it is obvious that the fluctuations in the values of the

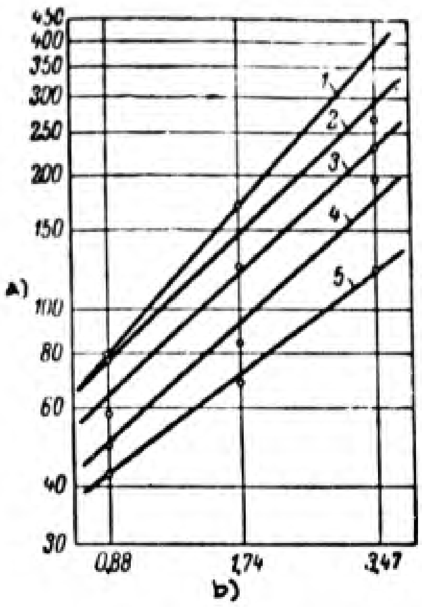

Fig.37 - Effect of Depth of Cut t upon the Force P_x at Various Feeds s. Turning of steel B, of H_{R_C} = 49 at a cutting speed v = 20 m/min. Cutter geometry: $\alpha = 6^o$, $\gamma = -5^o$, $\lambda = 0^o$, $\varphi = 45^o$, $\varphi_1 = 15^o$, r = 1.15 mm

1 - s = 0.505 mm/rev;
2 - s = 0.395 mm/rev;
3 - s = 0.286 mm/rev;
4 - s = 0.197 mm/rev;
5 - s = 0.122 mm/rev

a) Force P_x, kg; b) Depth of cut t, mm

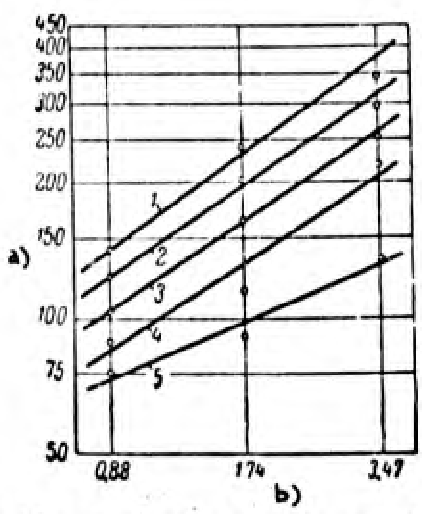

Fig.38 - Influence of Depth of Cut t upon the Force P_y at Various Feeds s. Test conditions as in Fig.37

a) Force P_y, kg; b) Depth of cut t, mm

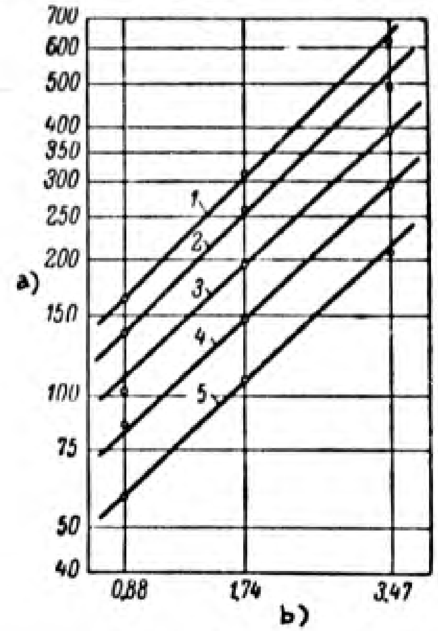

Fig.39 - Influence of Depth of Cut t upon the Force P_z at Various Feeds s. Test conditions as in Fig.37

a) Force P_z, kg; b) Depth of cut t, mm

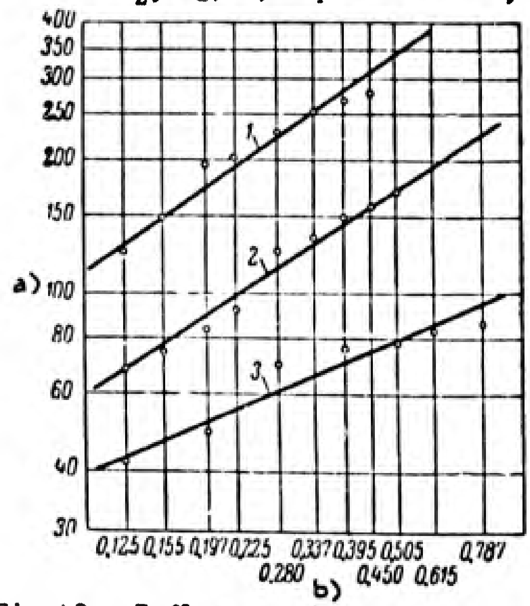

Fig.40 - Influence of Feed s upon the Force P_x at Various Cutting Depths t. Turning of steel B, of H_{R_C} = 49 at v = 20 m/min cutting speed. Geometry of cutter: $\alpha = 6^o$, $\gamma = -5^o$, $\lambda = 0^o$, $\varphi = 45^o$, $\varphi_1 = 15^o$, r = 1.15 mm

1 - t = 3.47 mm; 2 - t = 1.74 mm; 3 - t = 0.88 mm

a) Force P_x, kg; b) Feed s, mm/rev

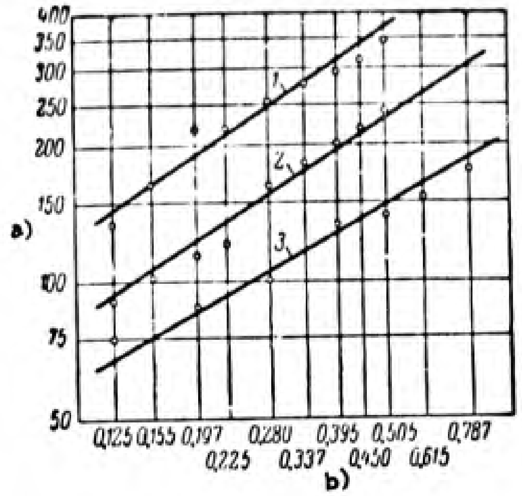

Fig.41 - Influence of Feed s upon the Force P_y at Various Depths of Cut t. Test conditions as in Fig.40

a) Force P_y, kg; b) Feed s, mm/rev

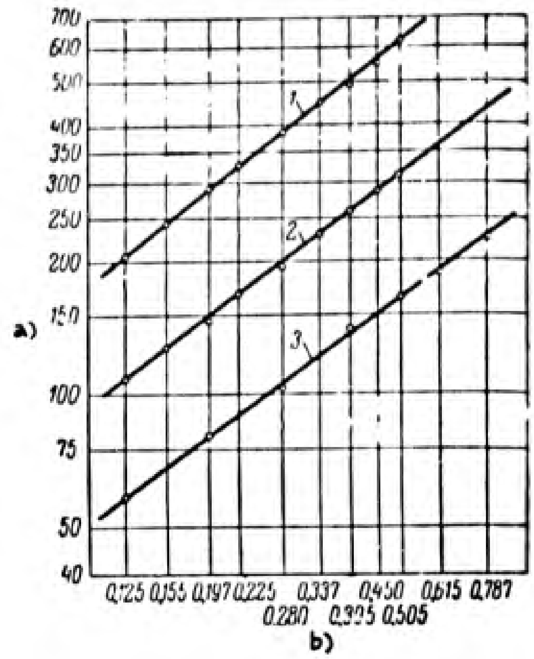

Fig.42 - Influence of Feed s upon the Force P_z at Various Depths of Cut t. Test conditions as in Fig.40

a) Cutting force P_z, kg; b) Feed s, mm/rev

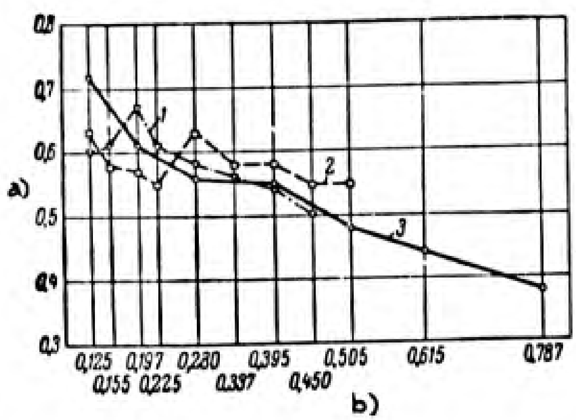

Fig.43 - Effect of Depth of Cut t and Feed s upon the Ratio $\frac{P_x}{P_z}$. Test conditions as in Fig.40

a) Ratio $\frac{P_x}{P_z}$; b) Feed s, mm/rev

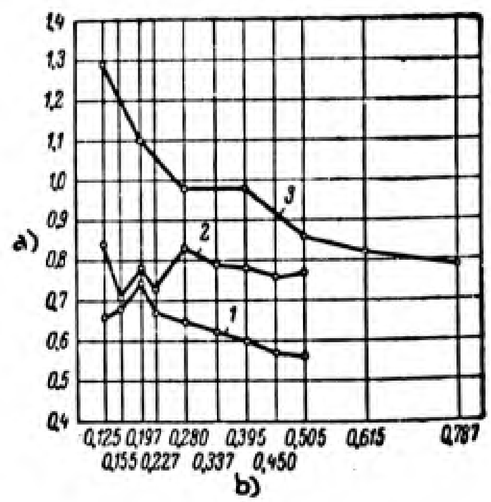

Fig.44 - Effect of Depth of Cut t and Feed s upon the Ratio $\frac{P_y}{P_z}$. Test conditions as in Fig.40

a) Ratio $\frac{P_y}{P_z}$; b) Feed s, mm/rev exponents x_{P_x} and x_{P_y} as well as the exponents y_{P_x} and y_{P_y} upon any change in the feed and depth of cut are negligible in their influence upon the forces P_x and P_y. Therefore, there is no point to complicating the equations $P_x = f_1$ (t and s) and $P_y = f_2$ (t and s) by introducing additional terms for the exponents x_{P_x} and x_{P_y}, as

Table 29

Values of Exponents of t and s in the Expressions: $P_x = f_1$ (t and s), $P_y = f_2$ (t and s), and $P_z = f_3$ (t and s)

Cutting Force	Exponents for t and s	Steel B, Hardness $H_{R_C} = 49$				Steel B, Hardness $H_{R_C} = 59$
		Series of Tests				
		I	II	III	Average Data	IV
P_x	x_{P_x}	0,94	0,95	0,98	0,96	0,72
	y_{P_x}	0,58	0,62	0,51	0,57	0,86
P_y	x_{P_y}	0,61	0,66	0,64	0,63	0,31
	y_{P_y}	0,60	0,78	0,49	0,62	1,08
P_z	x_{P_z}	0,95	0,96	0,99	0,97	0,83
	y_{P_z}	0,76	0,83	0,87	0,82	0,80

well as y_{P_x} and y_{P_y} relative to the feed s and the depth of cut t. With a degree of accuracy sufficient for practical purposes, these exponents may be based on the average values obtained from the results of four series of tests (Table 29).

The feed and depth of cut have a negligible influence upon the magnitudes of x_{P_z} and y_{P_z}. In the expression $P_z = f_3$ (t and s) it may be taken that the exponents x_{P_z} and y_{P_z} are not dependent upon the feed s and the depth of cut t.

These regularities are characteristic of steels of both hardnesses ($H_{R_C} = 49$ and 59).

The data in Table 29 permit a conclusion as to the nature of the influence of the hardness of tempered steel upon the exponents of t and s in expressions relating P_x, P_y, and P_z to t and s. As we see, in the equations $P_x = f_1$ (t and s) and $P_y = f_2$ (t and s), the exponents for the depth of cut diminish as H_{R_C} rises from 49 to 59: x_{P_x} falls from 0.96 to 0.72, and x_{P_y} from 0.63 to 0.31. The feed exponents, on the other hand, show a rise: y_{P_x} from 0.57 to 0.86, and y_{P_y} from 0.62 to 1.08. In the equation $P_z = f_3$ (t and s), the exponent for depth of cut x_{P_z} also diminishes with increase in the hardness of the steel (from 0.97 to 0.83). The exponent for feed y_{P_z} shows a negligible change.

From this it follows that, as the hardness of tempered steel rises, there is a pronounced increase in the influence of the feed s upon the values of P_x and P_y.

According to the author's experimental data, the equation for cutting force of hardened steels has the following form:

For steel of $H_{R_C} = 49$:

$$P_x = 129 \cdot t^{0{,}96} \cdot s^{0{,}57} \ \text{kg};$$
$$P_y = 227 \cdot t^{0{,}63} \cdot s^{0{,}62} \ \text{kg};$$
$$P_z = 330 \cdot t^{0{,}97} \cdot s^{0{,}82} \ \text{kg};$$

and for steel of $H_{R_C} = 59$:

$$P_x = 243 \cdot t^{0{,}72} \cdot s^{0{,}86} \ \text{kg};$$
$$P_y = 670 \cdot t^{0{,}31} \cdot s^{1{,}08} \ \text{kg};$$
$$P_z = 400 \cdot t^{0{,}83} \cdot s^{0{,}80} \ \text{kg}.$$

An influence upon the magnitude of the exponents of t and s in equations for P_x, P_y, and P_z is also exerted by the flank wear h (Bibl.22). As h increases, the exponents y_{P_x}, y_{P_y}, and y_{P_z} diminish, this diminution being greater the harder the tempered steel. Moreover, the exponents x_{P_x}, x_{P_y}, and x_{P_z} also diminish, but to a lesser degree than do the exponents y_{P_x}, y_{P_y}, and y_{P_z}.

These equations are valid for cutters with the following tip geometry: $\alpha = 6°$, $\gamma = -5°$, $\lambda = 0°$, $\varphi = 45°$, $\varphi_1 = 15°$, r = 1.15 mm.

For purposes of calculating the cutting regimes (see Appendix I), the author employed the following formula for the tangential force P_z:

$$P_z = C_{P_z} \cdot t^{0,9} \cdot s^{0,8} K_q, \qquad (1)$$

where C_{P_z} = 250, for steel of H_{R_C} = 38.

Table 30 permits a comparison of the values of the exponents of t and s in the

Table 30

Values of the Exponents x_{P_x}, x_{P_y}, x_{P_z}, y_{P_x}, y_{P_y}, and y_{P_z}, on the Basis of Various Investigations

Data	Material Investigated	$P_x = C_{P_x} \times t^{x_{P_x}} \cdot s^{y_{P_x}}$		$P_y = C_{P_y} \times t^{x_{P_y}} \cdot s^{y_{P_y}}$		$P_z = C_{P_z} \times t^{x_{P_z}} \cdot s^{y_{P_z}}$	
		Exponents					
		x_{P_x}	y_{P_x}	x_{P_y}	y_{P_y}	x_{P_z}	y_{P_z}
Author	Hardened steel B, H_{R_C} = 49	0,96	0,57	0,63	0,62	0,97	0,82
	Hardened steel B, H_{R_C} = 59	0,72	0,86	0,31	1,08	0,83	0,80
N.N.Zorev (Bibl.22)	Hardened steels, H_{R_C} = 35 - 65	1,0	0,60	1,0	0,60	1,0	0,76
A.A.Maslov (Bibl.26)	Hardened steel Khl2M, H_{R_C} = 45	0,91	0,37	0,91	0,47	1,0	0,77
A.D.Makarov (Bibl.24)	Hardened steel Khl2M H_{R_C} = 61 - 62	1,03	0,98	0,87	0,95	0,70	0,58
Handbook on high-speed machining procedures (Bibl.27)	Unhardened structural steel, σ_t = 75 kg/mm^2	1,20	0,55	0,90	0,75	1,0	0,75

equations for P_x, P_y, and P_z for hardened steels, based on various sources. It follows from the presented data that, in the turning of hardened steel, as in the turning of unhardened steel, the feed s has less effect upon the force P_z than the

Table 31

Cutting Force P_z for Hardened and Unhardened Steels, on the Basis of Various Investigations

Material Studied	Data by	Depth of Cut: t × s — 2.0×0.8	1.0×0.4	0.5×0.1
		Cutting Force P_z, in kg		
Hardened steels H_{RC} = 45	Author	465	142	22
H_{RC} = 50		520	158	29
H_{RC} = 60		620	190	34
Hardened steels H_{RC} = 45	N.N.Zorev (Bibl.22)	450	125	28
H_{RC} = 50		440	130	31
H_{RC} = 60		—	150	33
Hardened steel Khl2M H_{RC} = 45	A.A.Maslov (Bibl.22)	595	174	30
Hardened steel Khl2M H_{RC} = 61 - 62	A.D.Makarov (Bibl.24)	360	148	40
Unhardened steel, σ_t = 75 kg/mm^2 (H_B = 207 - 241)	Machining procedures handbook (Bibl.27)	320	96	17

depth of cut t (in all studies, $x_{P_z} > y_{P_z}$). It is not possible to develop generalized conclusions on the nature of the influence of t and s upon the forces P_x and P_y since the data differ greatly.

Let us compare the cutting force P_z in the turning of hardened steels, as derived from various sources (Table 31). The Table also presents an unhardened steel, $\sigma_t = 75$ kg/mm^2.

The data of A.D.Makarov, calculated on his suggested formula, are corrected for the large negative true rake angle ($\gamma = -24^\circ$) of the cutters he used in his investigation. The lack of uniformity in the P_z relationships for various depths of cut among the various investigators is explained by the different structures of the P_z formulas (different values of exponents for depth of cut t and feed s).

As we see, the values of the force P_z for steels of identical hardness differ considerably from one investigator to the next: Those by A.D.Makarov are low, and those by A.A.Maslov are high. The present author's data occupy a position intermediate between those of Zorev and Maslov.

The Table also shows that the tangential force P_z is greater for hardened steels than for unhardened types; the difference between them increases with the hardness of the steel.

It should be borne in mind that the values presented for the cutting force pertain to cutters whose edges are not worn (freshly-ground cutters). As the cutter wears, the force P_z increases at a greater rate the harder the tempered steel and the less the thickness of the cut a. In accordance with the experimental data of N.N.Zorev (Bibl.22), for example, an increase in the flank wear h from 0.2 to 0.8 mm (depth of cut t = 1.0 mm and feed s = 0.4 mm/rev) leads to an increase in the force P_z for hardened steel of $H_{R_C} = 40$ by 50%, and for steel of $H_{R_C} = 65$ by 71%. For hardened steel of $H_{R_C} = 50$ (t = 1.5 mm), an increase in cutter wear from 0.2 to 0.8 mm causes an increase in the force P_z of 35% for a feed of s = 0.8 mm/rev, and of 106% for a feed of s = 0.1 mm/rev.

It is natural that the relative value of the forces P_y and P_x is much higher for hardened steels than for unhardened types. Whereas for the latter, the ratio $\frac{P_y}{P_z}$ varies in the 0.18 - 0.67 interval, and the ratio $\frac{P_x}{P_z}$ in the 0.17 - 0.46 interval, these relationships for hardened steels fluctuate in the intervals, respectively, of 0.75 - 1.81 and 0.51 - 0.96. According to data by A.D.Makarov (Bibl.24), the relative values of the forces P_y and P_x are still higher for steel of H_{R_C} = 61 - 62 (t = 2 mm, s = 0.4 mm/rev): $\frac{P_y}{P_z} = 2.80$; $\frac{P_x}{P_z} = 1.14$.

It must be borne in mind in this connection that, as the flank wear h increases, the radial force P_y and the longitudinal force P_x rise sharply, and more intensively than the tangential force P_z. According to data by N.N.Zorev (Bibl.22) for

Table 32

Values n_{p_z} on the Basis of Various Investigations

Data of	Hardness Range of Tempered Steel H_{R_C}	Value of the Exponent n_{p_z}
Author	49--59	1,05
N.N.Zorev (Bibl.22)	35—60	0,88
	>60	3,25
NIBTN (Bibl.27)	38—58	1,30

Table 33

Unit Cutting Forces of Hardened and Unhardened Steels

Work Material	Depth of Cut F = t·s mm²		
	2,0·0,8 = 1,6	1,0·0,4 = 0,4	0,5·0,1 = 0,05
	Unit Cutting Force p, in kg/mm²		
Hardened steels			
H_{R_C} = 38	246	300	440
H_{R_C} = 49	325	395	580
H_{R_C} = 59	395	480	705
Unhardened steel, σ_t = =75 kg/mm²	200	240	340

t = 1.0 mm and s = 0.4 mm/rev, an increase in flank wear h from 0.2 - 0.8 mm results in a 120% rise in the force P_y for steel of H_{R_C} = 40 and in a 181% rise for steel of H_{R_C} = 65, the corresponding increases in the force P_x being 94 and 187%. Let us note that under the same conditions, the force P_z rises by 50 and 71%.

Machinability of Hardened Steels

The machinability of metals (their ability to be machined by cutting tools) is governed by the following primary indicators:

1) Cutting speed for a 60-minute tool life, under given cutting conditions

(material and geometric parameters of the cutting portion of the tool, depth of cut, feed, etc.);

2) Quality of the machined surface;

3) Magnitude of the cutting forces.

The machinability of a metal is better (higher), the higher the possible cutting speed of a tool, the better the finish of the machined surface, and the lower the cutting force.

Here we shall examine the machinability of hardened steels in terms of cutting force.

Influence of Hardness of Tempered Steel upon the Machinability. It is obvious from the foregoing that an increase in the hardness of tempered steel is accompanied by a decline in machinability and an increase in cutting force P_z. This regularity may be expressed by the equation

$$D_{P_z} = A \cdot H_{RC}^{n_{P_z}}, \qquad (2)$$

where $A = C_{P_z}$ for steel of the given hardness.

Table 32 presents the values of the exponent n_{P_z} derived from various investigations.

In calculating the recommended cutting procedures (Appendix I), the author employed the following n_{P_z} values:

Hardness of hardened steel H_{RC}	Value of n_{P_z} exponent
38 - 60	1.0
> 60	3.0

Unit Cutting Force in Turning Hardened Steels. The concept of the so-called cutting constant K_z has been developed to permit a comparative estimate of the machinability of metals. The cutting constant is often confused with the unit cutting force p. Unlike the cutting constant K_z, which is a constant for a given metal, the unit cutting force p is a variable depending upon the dimensions of the layer of metal being removed, and upon other cutting conditions. However, the unit force p may be employed for a comparative estimate of the machinability of various metals, if the cutting force P_z is determined under identical conditions.

Table 33 presents the values of the specific cutting force p for hardened steels of various hardnesses and for unhardened steel whose tensile strength is $\sigma_t = 75$ kg/mm^2.

As we see, the unit cutting force characterizing the machinability of the metal rises with reduction in the cross-sectional area F of the layer being removed, and with rise in the hardness of the tempered steel. In the case of unhardened steel, this force is less than for hardened steel. The machinability of hardened steels is less than that of unhardened types.

Conclusions

1. The turning of hardened steels differs from the machining of unhardened steels in that all cutting forces, particularly the radial and longitudinal forces, P_y and P_x, are higher. This is explained by the high strength and hardness of tempered steels, and also by the fact that cutters of negative rake are employed to machine them.

2. Hardened steels are characterized by poorer machinability than unhardened. The unit cutting force p of hardened steels is considerably higher.

3. The turning of hardened steels is distinguished by the high relative values of the longitudinal and radial forces P_x and P_y. For unhardened steels, $P_y = 0.4\ P_z$ and $P_x = 0.3\ P_z$. Where hardened steels are concerned, the longitudinal force $P_x = 0.5 - 0.9\ P_z$, whereas the radial force P_y approximates the tangential force in magnitude, and considerably exceeds the latter at low depths of cut.

4. With increase in flank wear, there is an increase in all cutting forces,

particularly in the radial and longitudinal forces P_y and P_x.

5. The increase in cutting forces is accelerated as the hardness of the tempered steel rises.

6. In the turning of hardened steels, the cutting speed exercises a significant influence upon the tangential force P_z. The force P_z declines as the speed increases. Consequently, from the viewpoint of load on the cutter it is better to work at relatively high cutting speeds.

Practically speaking, in the turning of hardened steels, particularly those of high hardness, the influence of the cutting speed upon the cutting force is negligible, since the interval of speeds employed is quite narrow.

7. In the case of hardened steels, the influence of the true rake angle γ upon the cutting forces is of the same nature as in the machining of unhardened steels: All the forces rise with a reduction in the true rake, particularly in the radial and longitudinal forces P_y and P_x.

8. In turning hardened steels, a reduction in the end-cutting-edge angle φ results in an increase in the radial and longitudinal forces P_y and P_x. A change in the angle φ has less effect upon P_y than upon P_x. The effect of the angle φ upon the tangential force P_z is negligible.

9. With a rise in the complement of the back rake angle λ, the radial force P_y increases and the longitudinal force P_x diminishes. The tangential force P_z undergoes virtually no change.

10. In the case of hardened steels the relationships of the cutting forces to the depth t and feed s are identical in nature with those of unhardened steels.

In the case of unhardened steels, the exponent for the depth x_{P_z} is greater than the exponent for feed, i.e., the depth has a greater effect upon P_z than does the feed. This same proposition is valid for hardened steels. However, unlike unhardened steels, for which the x_{P_z} exponent is 1, hardened steels may show a lower exponent.

11. Many factors influence the machining tolerances attainable, the most important of these being the bouncing of the tool off the work under the influence of the radial force P_y. The action of this force results in a distortion of the geometric shape of the machined surface and the appearance of taper.

Since the process under examination is distinguished by a high relative value of the radial force P_y, particularly when the layer of metal being removed is thin, the machining of hardened steels should be performed on machine tools of high rigidity.

12. Despite the fact that the turning of hardened steels is characterized by considerably higher cutting forces than that of unhardened steels (at the same depths of cut t and feeds s), the absolute value of these forces is relatively low, since the turning of hardened steels is performed at low t and s. Moreover, as compared to unhardened steels, the machining of hardened steels proceeds at considerably lower cutting speeds. As a result, the power consumed in machining is comparatively low, in the cutting of hardened steels.

15. Geometry of Cutter Point

In this Section we present the results of investigations to determine the optimum values for the geometry of cutters to be used for the turning of hardened steels.

True Rake Angle

Table 34 presents the results of the author's experiments with hardened steel B, of H_{R_C} = 56. The machining was performed with T21K8 cutters, at a depth of t = 2.4 mm and a feed of s = 0.307 mm/rev. The cutter geometry was as follows: relief angle $\alpha = 6^\circ$, complement of back rake angle $\lambda = 0^\circ$, end-cutting-edge angle $\varphi = 45^\circ$; complement of side-cutting-edge angle $\varphi_1 = 15^\circ$; nose radius r = 1.15 mm. The true rake angle γ was varied from +10 to -12°. The cutters were dressed with boron carbide flour.

It is clear from the Table that the cutting process was impaired on reduction in the true rake angle. When cutters with $\gamma = +10^{\circ}$ and $+6^{\circ}$ were used, the cutting proceeded smoothly, with good flow-off of chip. At high negative true rake angles ($\gamma = -8$ and -12°), all the cutting forces increased sharply, particularly the radial

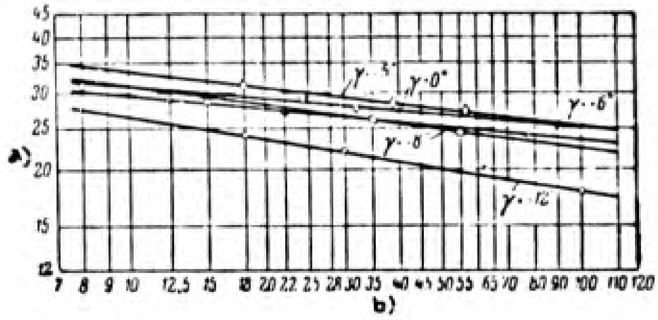

Fig.45 - Relationship Between Cutting Speed v and Tool Life T at Various True Rake Angles γ. Turning of steel B, of $H_{R_C} = 56$, at t = 2.4 mm and s = 0.307 mm/rev

a) Cutting speed v, m/min; b) Tool life T, min

force P_y, which resulted in the cutter bouncing away sharply from the part being machined, as well as in an increase in the deformation of the layer of metal being cut, and a sharp increase in the heating of the chip. However, at $\gamma = +10^{\circ}$, crumbling-out of the cutting edges was observed.

Figure 45 presents in logarithmic scale a graph of the relationship between cutting speed and tool life T. The curves are plotted on the data in Table 34. Cutting speeds, reduced to 60-minute tool life (v_{60}), and the index for relative life at the true rake angles γ investigated are presented in Table 35.

The influence of the true rake angle upon the cutting speed was also investigated for steel A of $H_{R_C} = 47$. The tests were run with T21K8 tools, having the same geometry as the cutters in tests of steel B of $H_{R_C} = 56$. The results of the tests are presented in Table 36.

Figure 46 offers the data of Tables 35 and 36 in graphic form. It is clear

Table 34

Influence of True Rake Angle γ upon Cutter Life and Cutting Speed

Turning of Steel B, of $H_{R_C} = 56$, $t = 2.4$ mm and $s = 0.307$ mm/rev

True Rake Angle γ^o	Cutting Speed, v in m/min	Cutter Life T, min	Nature of Cutter Dulling	Remarks
— 12	24	18	Normal dulling	Difficult cutting; chip heated severely from outset. Cutter bounced away strongly from machined part
	22	30	Same	
	18	100	Same	
— 8	28,5	15	Normal dulling	
	26	35	Same	
	24	55	Same	
— 5	31	18	Normal dulling	Cutting went easier; considerably less chip heating
	28,5	38	Same	
	28,5	40	Same	
	27	57	Same	
0	31	8	Normal dulling	
	31	8	Same	
	29	24	Same	
	28	24	Same	
	28	32	Same	
+ 6	29	12,5	Normal dulling	Cutting went easily, with good flow-off of chip, in the form of a long spiral; insignificant heating of chip, but large-scale crumbling-out of carbide bar at its nose and along the working portion of the cutting edge when dulling had not yet proceeded very far.
	27	22	Same	
	24	76	Same	
+ 10	26,5	1,5	Crumbling out of cutter	
	26	0,16	Same	
	26	3	Same	
	26	0,16	Same	
	26	0,16	Same	
	26	0,16	Same	
	24	37	Same	
	23,5	26	Same	

from these data that the highest cutting speed of both steels tested represents a true rake angle $\gamma = -5^{\circ}$. At the same time, the cutting speed v_{60} diminishes as the true rake angle is varied in either direction from the $\gamma = -5^{\circ}$ value. Whereas at $\gamma = -5^{\circ}$, the speed is $v_{60} = 26.8$ m/min, the speed at $\gamma = +6^{\circ}$ comes to 25.4 m/min, and at $\gamma = -12^{\circ}$, the cutting speed is v_{60} m/min (Table 35). Thus, at $\gamma = -12^{\circ}$, the

Table 35

Cutting Speeds v_{60} and Relative Life Index m for Various Values of the True Rake Angle γ

Machining of steel B, of $H_{R_C} = 56$, at t = 2.4 mm and s = 0.307 mm/rev

True Rake Angle γ°	Cutting Speed v_{60}, in m/min		Index m
	Absolute	Relative	
—12	19,6	0,80	0,169
— 8	24,1	0,98	0,096
— 5	26,8	1,09	0,122
0	25,6	1,04	0,096
+ 6	24,5	1,00	0,105

Table 36

Cutting Speeds v_{60} for Various True Rake Angles γ

Turning of steel A, of $H_{R_C} = 47$, at t = 1.2 mm and s = 0.305 mm/rev

True Rake Angle γ°	Cutting Speed v_{60}, in m/min	
	Absolute	Relative
—8	55,4	0,99
—5	58,2	1,04
0	58,0	1,04
+6	55,6	1,00

cutting speed is considerably less than at $\gamma = +6^{\circ}$. Moreover, the cutting speed for $\gamma = -5^{\circ}$ is only negligibly greater (9%) than the cutting speed for $\gamma = +6^{\circ}$. For the second grade of steel (Table 36), this difference is even smaller (4%).

Thus, for the purposes of turning high-alloy chromium-nickel-molybdenum-silicon and medium-alloy chromium-nickel-molybdenum steels of $H_{R_C} = 56$ and 47 hardness, a slight negative true rake angle ($\gamma = -5^{\circ}$) yields an insignificant gain in cutting speed relative to that afforded by a positive true rake ($\gamma = +6^{\circ}$), whereas, conversely, higher negative true rake angles ($\gamma = -12^{\circ}$) result in a considerable reduction in the cutting speed.

Table 37

True Rake Angles γ for Carbide-Tipped Cutters in Turning Hardened Steels

Investigator	Hardness of Hardened Steel H_{RC}	Carbide	Recommended True Rake γ^o	Other Cutter Angles	Cutting Procedure
N.I.Shchelkonogov (Bibl.28)	49 — 64	VK6 and VK8	fr. —5 to —7	$\varphi = 45 - 90°$; $\lambda = 4°$	$t = 0{,}25—0{,}50$ mm; $s = 0{,}25$ mm/rev
P.P.Grudov (Bibl.29)	44 — 49 50 — 54 55—58	T15K6 and T5K10 T15K6 and T5K10 T15K6 and T5K10	—10 and —5 —15 and —10 —20 and —15	$\varphi = 45 - 90°$; $\lambda = 4°$	$t = 0{,}20—2{,}0$ mm; $s = 0{,}05—0{,}30$ mm/rev
A.Ya.Malkin (Bibl.23)	41—50 51—60 61—65	VK8 and T5K10 VK8 and T5K10 VK8 and T5K10	—10 —10 fr. —15 to —20	$\varphi = 30°$; $\lambda = 45°$ $\varphi = 25°$; $\lambda = 45°$ $\varphi = 15—20°$; $\lambda = 45°$	$t = 0{,}5—2{,}5$ mm; $s = 0{,}15—0{,}32$ mm/rev
Ye.A.Belousov (Bibl.30)	49—57	VK3 and VK8 / T30K4	—12	$\varphi = 25°$; $\lambda = 10°$	$t = 0{,}5—1{,}5$ mm; $s = 0{,}1—0{,}84$ mm/rev / $t = 0{,}5$ mm, $s = 0{,}1—0{,}48$ mm/rev
	58—62	VK3 and VK8 / T30K4	—15	$\varphi = 20°$; $\lambda = 30—40°$	$t = 0{,}5—1{,}5$ mm, $s = 0{,}1—0{,}84$ mm/rev / $t = 0{,}5$ mm; $s = 0{,}1—0{,}48$ mm/rev
	63—65	VK3 and VK8 / T30K4	—20	$\varphi = 15°$; $\lambda = 40 — 45°$	$t = 0{,}5—1{,}5$ mm; $s = 0{,}1—0{,}84$ mm/rev / $t = 0{,}5$ mm; $s = 0{,}1—0{,}48$ mm/rev
M.N.Larin (Bibl.31)	45—64	—	—15	—	—
A.A.Maslov (Bibl.26)	45—65	VK6 and T15K6	fr. —15 to —20	$\varphi = 20—30°$; $\lambda = 10—15°$	$t = 2$ mm; $s = 0{,}3$ mm/rev

It must be emphasized that, at a large true rake angle, the cutting edge of the cutter crumbles out when high-hardness tempered steels are turned.

The optimum value of the true rake angle for the steels A and B investigated by the author lies in the interval from $\gamma = -5^{\circ}$ to $\gamma = 0^{\circ}$.

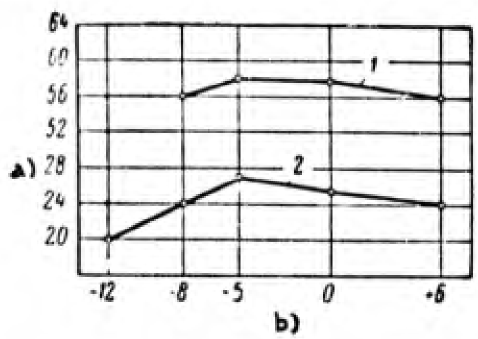

Fig.46 - Influence of True Rake Angle γ upon the Cutting Speed v_{60}. Cutter geometry: $\alpha = 6^{\circ}$, $\lambda = 0^{\circ}$, $\varphi = 45^{\circ}$, $\varphi_1 = 15^{\circ}$, r = 1.15 mm.

1 - Steel A, $H_{R_C} = 47$, t = 1.2 mm, s = 0.305 mm/rev; 2 - Steel B, $H_{R_C} = 56$, t = 2.4 mm, s = 0.307 mm/rev

a) Cutting speed v_{60}, m/min; b) True rake angle, γ°

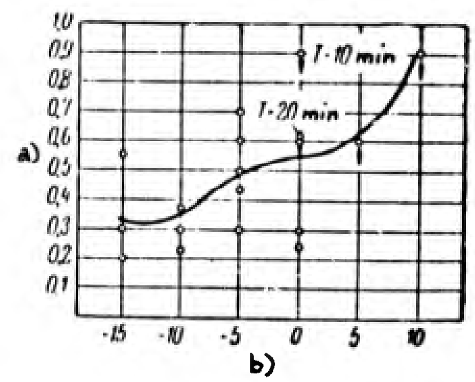

Fig.47 - Relationship of T30K4 Cutter Flank Wear upon True Rake Angle γ. Turning of 40KhS steel, of $H_{R_C} = 48$ to 50, at t = 0.2 mm, s = 0.1 mm/rev and v = 40 m/min ($\alpha = 5^{\circ}$, $\varphi = 45^{\circ}$, $\varphi_1 = 10^{\circ}$, $\lambda = 5^{\circ}$, r = 0.5 mm). Arrow indicates crumbling-out of carbide tip.

a) Flank wear h, mm; b) True rake angle γ°

Let us discuss next other studies of the turning of hardened steels. Table 37 presents the values for the true rake angle recommended by the authors of the respective studies.

The influence of the true rake angle upon the wear of T30K4 cutters in the finishing of 40KhS steel hardened to $H_{R_C} = 48 - 50$ (t = 0.2 mm, s = 0.1 mm/rev; v = 40 m/min) was investigated by N.S.Logak (Bibl.21). He ran tests with the following true rakes: $\gamma = 10, 5, 0, -10$, and -15°. In each experiment, the flank wear after 40 min was tested. The results of the tests are presented in Fig.47.

As we see, the cutters used in the tests with positive true rake γ crumbled out. No such phenomenon was noted when cutters with negative true rake were employed. At the same time, the flank wear h diminished as γ was reduced. The optimum value for the true rake proved to be in the -10 to -15° interval.

According to data published by V.A.Krivoukhov (Bibl.32), KBEK* cutters functioned quite successfully in the turning of hardened steels.

A distinctive feature of these cutters is their very low end-cutting-edge and complement of side-cutting-edge angles, φ and φ_1 and the absence of any nose curvature r. The following is the geometry of the KBEK cutter: relief angle $\alpha = 12^\circ$, true rake angle $\gamma = -5^\circ$, complement of back rake angle $\lambda = 0^\circ$, end-cutting-edge angle $\varphi = 10^\circ$, complement of side-cutting-edge angle $\varphi_1 = 10^\circ$.

The materials presented testify that cutters have to be given a negative true rake ($\gamma < 0^\circ$) for the turning of hardened steels. However, opinions differ on the degree of negative true rake. The dominant view is that hardened steels must be turned with cutters having large negative true rakes, attaining -20° to -25° in the case of high-hardness steels. However, N.I.Shchelkonogov, V.A.Krivoukhov, and the present author have found the optimum true rake to be $\gamma = -5^\circ$.

We believe it necessary to give some consideration here to the advantages of small negative true rakes for the machining of hardened steels.

It was noted above that negative true rake serves as a means of increasing the strength of the cutting edge of carbide cutters. When a cutter of positive true rake is employed, its cutting edge is subject to bending, i.e., a deformation to which hard alloys offer poor resistance. Whereas the transverse rupture strength of high-speed steel is $\sigma_r = 320$ kg/mm², the figure for T15K6 is 110 kg/mm², and that for T30K4 is only 90 kg/mm². At the same time, hard alloys are characterized by very high compressive strength, which rises as high as $\sigma_c = 450$ kg/mm². The cutting

*The cutter name is derived from the initials of its inventors: Krivoukhov, Brushteyn, Yegorov, and Kozlov.

edge of a cutter with negative true rake is primarily subjected to compression.

At the same time, a negative true rake causes a sharp rise in the radial force P_y and an increase in the cutter repulsion from the workpiece. If the system machine tool - workpiece - cutter is of inadequate rigidity, chatter will develop. According to the author's experimental data for steel B, of $H_{R_C} = 49$, tested at depths of cut t = 1.2 mm and feed s = 0.395 mm/rev, a reduction in the true rake angle γ from +10 to -12^o led to a doubling of the radial force P_y. However, the tangential force P_z increased by only a factor of 1.27.

Thus, the operation of cutters with negative true rake produces phenomena that are highly undesirable for finish-machining such as the turning of hardened steels. Therefore, one can well understand the effort to select the smallest possible negative true rakes, the more so as, according to the author, an increase in the negative true rake to over $\gamma = -5^o$ brought not an increase but a decline in cutting speed.

With the exception of P.P.Grudov and N.S.Logak, all investigators recommend large negative true rakes γ combined with small end-cutting-edge angles φ, and A.Ya.Malkin and Ye.A.Belousov also recommend large back rake complement angles λ.

With a reduction in the end-cutting-edge angle φ, the thickness of cut a diminishes, the width of cut b increases, and the cutter life T rises. According to the author, the cutting speed rises by 19% for hardened steel of $H_{R_C} = 41$ as the angle φ is changed from 60 to 20^o.

However, a reduction in the angle φ is accompanied by an increase in the relative value of the radial force P_y, and also in the intensity of vibrations, particularly in the case of cutting tools for which $\varphi < 30^o$. Consequently, a reduction in the end-cutting-edge angle here acts in the same sense as an increase in negative true rake. The difference lies in the fact that the tool life and the cutting speed rise with a reduction in the angle φ, whereas a reduction in the true rake angle γ is accompanied by an increase in the strength of the cutting edge of the tool, simultaneous with a reduction in its life.

One cannot agree with the recommendation that the turning of hardened steels be done by cutters having, at the same time, a large negative true rake γ (as much as -20°), a small end-cutting-edge angle φ ($10 - 30^{\circ}$), and a large back rake complement angle ($\lambda = 45^{\circ}$), the more so as we are here discussing hard alloys which are distinguished by relatively high strength and diminished brittleness (VK8, T5K10).

Industrial practice in the machining of hardened steels confirms the superiority of cutters with low negative true rake angle. At the Moscow Krasnyy Proletariy Plant (Bibl.33), steel ShKh15 hardened to $H_{R_C} = 60$ is machined by T30K4 cutters, the true rake being $\gamma = -5^{\circ}$. It should be noted that the T30K4 alloy is one of the most brittle of the cemented carbides.

At the Moscow Borets Plant (Bibl.34), the machining of hardened 40Kh steel of $H_{R_C} = 42 - 46$ is performed by T15K6 and VK8 cutters, true rake being $\gamma = -5^{\circ}$. The turning of hardened steel parts $H_{R_C} = 40$ to 48 is performed at the Gor'kiy Machine Tool Plant (Bibl.35) by T15K6 cutters, having a true rake angle of $\gamma = -5^{\circ}$.

Along with the foregoing, however, S.S.Nekrasov (Bibl.36) mentioned that at bearing plants, large-size ball and roller races made of ShKh15, ShKh15SG and 12KhN3 steels with $H_{R_C} = 60 - 65$, are machined on turret lathes by VK8 cutters with the following point geometry: $\alpha = 12^{\circ}$, $\gamma = -15$ to -20°, $\varphi = 20$ to 25°, $\varphi_1 = 12$ to 15°; $\lambda = 45^{\circ}$, $r = 0.5$ mm. In closing, we pause to consider two questions:

1) Influence of the hardness of tempered steel upon the true rake angle of the cutter;

2) Influence of the width of the flat upon the strength of the tool cutting edge.

In general, as the hardness of steel rises and the cutting forces increase in connection therewith, the true rake of the cutter should be reduced, i.e., its negative value should be increased. Thus, according to the data by N.N.Zorev (Bibl.22), the tangential cutting force P_z rises by 20% for a depth of cut of t = 2.0 mm and a feed of s = 0.3 mm/rev, as the hardness of the steel is increased from 45 to 55. A heavier load on the cutter requires greater reinforcement of its leading edge. However, as is evident from Fig.46, the optimum true rake γ changes from -2.5^o (average between $\gamma = 0^o$ and $\gamma = -5^o$) to -5^o as the hardness of the steel H_{R_C} increases from 47 to 56 (by approximately the same value and in about the same hardness interval).

Consequently, an increase in the hardness of tempered steel by 9 Rockwell units (scale C) led to the need of increasing the negative true rake by about 3^o. For hardened steel of $H_{R_C} = 65$, the optimum true rake will be, on this basis, -8^o, but not -20^o or -25^o. The author holds that, for purposes of turning hardened steels of $H_{R_C} = 38 - 65$, the true rake should be in the 0 to -10^o interval.

Research has established (Bibl.21) that the flat size used in the turning of unhardened steels (in cases in which a negative true rake is provided not on the entire face, but only on the flat) is not appropriate for hardened steels. In the turning of hardened steels by cutters tipped with T30K4, the flat of a point with negative true rake should be not less than 3 - 4 mm wide, i.e., many times larger than the feed s. In the case of cutters with a flat f = 2.5 - 3 mm, that had undergone flank wear in accordance with the dulling criterion adopted here, considerably less crumbling-out of the cutting edge occurred than in the case of cutters with a flat of f = 1.0 - 1.2 mm. Whereas the wear h = 0.7 - 0.9 mm in cutters with flats of f = 1.0 - 1.2 mm, was accompanied by crumbling (or cleavage) of the carbide bar not only over the entire width of the flat, but further along the face to a distance of 3 - 5 mm from the cutting edge, cutters with broader flats (f = 2.0 - 2.5 mm), undergoing the same flank wear, showed considerably less crumbling-out of the carbide bar and spread only 0.8 - 1.0 mm from the cutting edge.

Cutter Relief Angle

Figure 48 presents the results of tests run by the author to determine the influence of the relief angle α upon the cutter life T and upon the cutting speed v. The experiments were run with steel C, of H_{R_C} = 65, and the cutters were made of T15K6 alloy. The relief angle was varied in the range of α = 4 to 16°. Machining was performed at a depth of cut of t = 0.5 mm and a feed of s = 0.14 mm/rev.

As we see, higher cutting speeds v are permissible with no change in tool

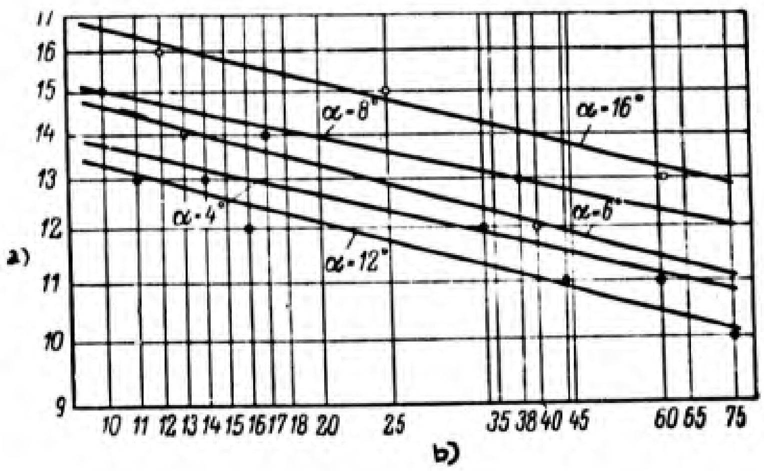

Fig.48 - Relationship Between Cutting Speed v and Life T of Cutter, for Various Values of the Cutter Relief Angle α. Turning of steel C, of H_{R_C} = 65, at t = 0.5 mm and s = 0.14 mm/rev (γ = -5°, λ = 0°, φ = 45°, φ_1 = 15°, r = 1.3 mm)

a) Cutting speed v, m/min; b) Cutter life T, min

life T if the relief angle α is increased, or else an increase in tool life T may take place at a given cutting speed. Thus, for α = 4° and a cutting speed of v = 13 m/min, the tool life is T = 16 min, whereas at α = 16° and at the same cutting speed as above, the tool life is T = 70 min. At α = 4°, the cutter revealed a life of T = 16 min for v = 13 m/min, whereas at α = 16°, the same tool life resulted for the higher cutting speed v = 16 m/min.

Table 38 and Fig.49 present cutting speeds v_{60} for various values of the angle α derived from the curves T - v (Fig.48).

These data show that an increase in the relief angle of the cutter results in an increase in the cutting speed: for $\alpha = 16^{\circ}$ it is 15% higher than for $\alpha = 4^{\circ}$. The diminished cutting speed for $\alpha = 12^{\circ}$ (which is 95% of the cutting speed for $\alpha = 4^{\circ}$) does not invalidate the general and clearly marked regularity.

Table 38

Effect of Relief Angle α Upon Cutting Speed v_{60} and Cutter Relative Life Index m

Relief Angle, α°	Cutting Speed v_{60} in m/min		Index m
	Absolute	Relative	
4	11,1	1,00	0,111
6	11,5	1,04	0,132
8	12,3	1.11	0,109
12	10,5	0,95	0,135
16	12,8	1,15	0,166

The results of another series of tests are presented in Table 39 for steel C of $H_{RC} = 65$ machined under constant conditions: t = 0.5 mm, s = 0.14 mm/rev, and v = 12 m/min. The relief angle was varied in the range of $\alpha = 6$ to 25°. The tests were run with T21K8 cutters having the following geometry: $\gamma = -5^{\circ}$, $\lambda = 0^{\circ}$, $\varphi = 45^{\circ}$, $\varphi_1 = 15^{\circ}$, r = 1.3 mm.

It will be seen that the tool life rises with an increase in relief angle. Where, for $\alpha = 6^{\circ}$, it was 1 - 2 min in seven tests, T = 28 to 50 min when $\alpha = 25^{\circ}$.

Some of the experiments, particularly with small relief angles, may seem open to doubt in the light of the short tool life (T under 10 min). It must be pointed out that the short cutter life here was due not to premature dulling or crumbling-out (the cutters which revealed a life of less than 10 min had been subjected to normal wear) but to the normal effect of the cutting speed and of the relief angle of the tool upon its life.

Except for the experiments in which the tool life proved to be less than 10 min, the data of Table 39 are presented in Table 40. As we see, an increase in the relief angle α from 10 to 25° was accompanied by a tool-life increase by a factor

Table 39

Effect of Relief Angle on Cutter Life

Turning of Steel C of H_{R_C} = 65, at t = 0.5 mm, s = 0.14 mm/rev, and v = 12 m/min

Relief Angle of Cutter α°	Tool Life T, in min	Relief Angle of Cutter α°	Tool Life T, in min
6	1	15	7
	1		32
	2		25
	2		46
	1		26
	1	20	2
	1		15
10	2		15
	8		22
	9		28
	5	25	4
	10		32
	14		42
	11		42
15	5		42
	2		28
	3		50
	5		

of 3.25. Whereas at α = 25°, the life was T = 39 min, at α = 10° it was only 12 min (at α = 6°, the tool life was T = 1 or 2 min).

These data are most interesting. It was established that in the turning, by titanium-tungsten tools, of steel hardened to virtually the maximum hardness for structural steels (H_{R_C} = 65), the life of the tool increases regularly with an increase in the relief angle. The possibility of machining this steel with tools having a relief angle α of 25° was demonstrated in practice.

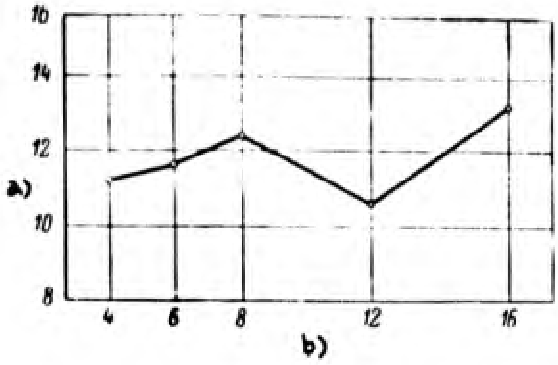

Fig.49 - Effect of Tool Relief Angle α upon the Cutting Speed v_{60}. Turning of steel C of H_{R_C} = 65 with T15K6 Cutters,

at t = 0.5 mm and s = 0.14 mm/rev

a) Cutting speed v_{60} m/min; b) Relief angle α°

Figure 50 demonstrates the results of an investigation of the relief angle (Bibl.21) in the turning by T30K4 cutters, of 40KhS steel hardened to H_{R_C} = = 48 - 50. The flank wear of the tools was measured after 40 min of use. As is evident, the optimum relief angle α lies between 10 and 12°. The nature of the h = f(α°) ratio is not known for large relief angles, since investigation was limited to α = 12°. In any case, the flank wear diminished with an increase in the relief angle.

The relation between the angles of a cutter: relief α, lip β, and true rake γ, is expressed by the following equality:

$$\beta = 90^\circ - (\alpha + \gamma).$$

Table 40

Effect of Relief Angle α upon Cutter Life

Turning of Steel C of H_{R_C} = 65 min, at t = 0.5 mm, s = 0.14 mm/rev, and v = 12 m/min

Relief Angle α°	Cutter Life T, in min	
	Absolute	Relative
10	12	1,00
15	32	2,67
20	20	1,67
25	39	3,25

At a given true rake angle γ, the lip angle β is larger, the smaller the relief angle. With an increase in the angle β, there is a rise in the mechanical strength of the cutting edge of the tool, and an improvement in its heat-emitting ability. A negative true rake angle means an increase in the lip angle, and in this connection an increase in the strength of the cutting edge of the cutter. However, the angle β also increases with any reduction in the relief angle α. From this point of view, it was to be expected that, in machining high-hardness steel by titanium-tungsten carbide-tipped tools, which are highly brittle, the best results in terms of tool life were demonstrated by cutters having a smaller relief angle α and consequently a larger lip angle β. Experiments run by the author yielded opposite results.

The data in Table 40 pertain to cutters whose true rake angle was $\gamma = 5^o$, but whose relief angles differed. For two relief angles (α = 10 and 25^o), we have the following: At $\alpha = 10^o$, the lip angle β is considerably larger than at $\alpha = 25^o$, and consequently the strength of the cutting edge is also higher. At the same time, the life of a tool with $\alpha = 10^o$ is considerably lower than that of a tool with $\alpha = 25^o$.

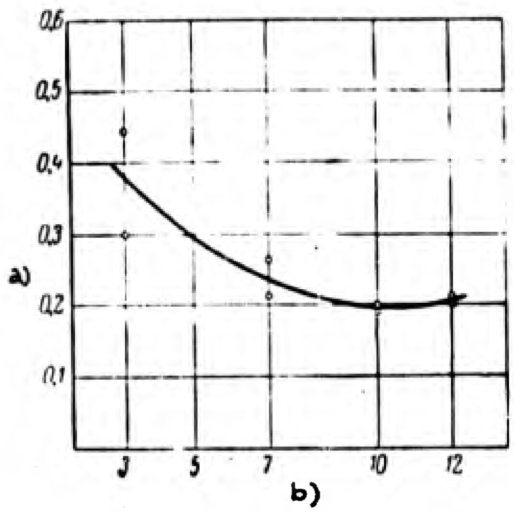

Fig.50 - Relationship Between Flank Wear of a T30K4 Cutter to Relief Angle. Turning of 40KhS steel of H_{RC} = 48 - 50, at t = 0.2 mm, s = 0.1 mm/rev, and v = 40 m/min

a) Wear of cutter flank h, mm; b) Relief angle α^o

The results of the investigation permit the conclusion that the true rake angle γ plays a more important role than the lip angle β in determining the strength of the cutting edge of hard-alloy tools. In fact, cutters with $\gamma = -5^o$, $\alpha = 25^o$, and $\beta = 70^o$ functioned without premature dulling and crumbling-out of their cutting edges. This cutter geometry ensured the necessary strength. At the same time, cutters with a somewhat larger lip angle ($\beta = 74^o$) proved completely useless at $\alpha = 6^o$ and $\gamma = +10^o$ (Table 34), due to premature crumbling-out of the cutting edge because of its inadequate strength.

Consequently, the relief angle of a cutter has to be regarded not only as a parameter permitting free movement of the cutter flank with respect to the cutting surface. It has been established that proper selection of relief angle, with due consideration for the process procedure, yields a considerable increase in cutter life.

End-Cutting-Edge Angle φ

Correct selection of the end-cutting-edge angle φ for the turning of hardened

Table 41

Average T and v_{60} for Various φ Values

End-Cutting-Edge Angle φ°	Tool Life T, in min	Cutting Speed v_{60}, in m/min	
		Absolute	Relative
30	80	81,7	1,07
45	36	76,5	1,00
60	22	73,2	0,96

steels is very important, in view of the high hardness of the material machined and the elecated brittleness of cemented titanium-tungsten carbides.

The author investigated the influence of the end-cutting-edge angle φ upon the life of the cutter in turning steel A of $H_{R_C} = 41$. The angle φ was varied from 30 to 60°. Machining was by T21K8 cutters to a depth of t = 1.2 mm, feed of s = 0.305 mm/rev, and constant cutting speed of v = 80 m/min. An analytic elaboration of the experimental data (Tables 41 and Fig.51) made it possible to express the relationship of cutting speed v_{60} to end-cutting-edge angle by

$$v_{60} = \frac{C_{\varphi}}{(\sin \varphi)^{0,2}} \ m/min . \qquad (3)$$

As we see, in turning hardened steel, the effect of the end-cutting-edge angle upon the cutting speed is of the same nature as in the case of unhardened steels: The cutting speed rises with a reduction in the angle φ.

When the angle φ was reduced in experiments with hardened steel, where cutters with φ = 30° were employed, the increase in cutting speed noted was accompanied by the appearance of vibration. These vibrations occurred despite the fact that the conditions of machining provided for adequate rigidity of the system consisting of the machine tool, the workpiece, and the cutter. These tests were run on a DIP-400 lathe, which has a carriage of high rigidity, and the ratio between the

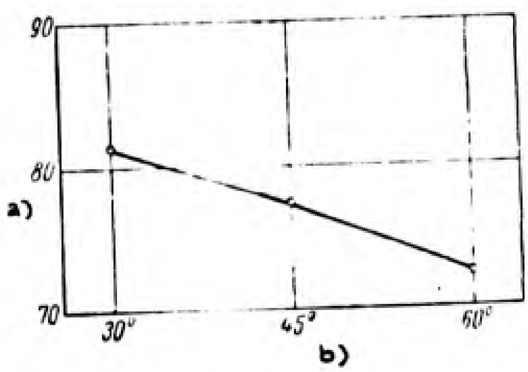

Fig.51 - Effect of End-Cutting-Edge Angle φ upon the Cutting Speed v_{60}. Turning of steel A of H_{R_C} = 41, at t = 1.2 mm and s = 0.305 mm/rev. Cutter Geometry: α = 6°, γ = -5°, λ = 0°, φ_1 = 15°, r = 1.15 mm

a) Cutting speed v_{60}, m/min;
b) End-cutting-edge angle, φ

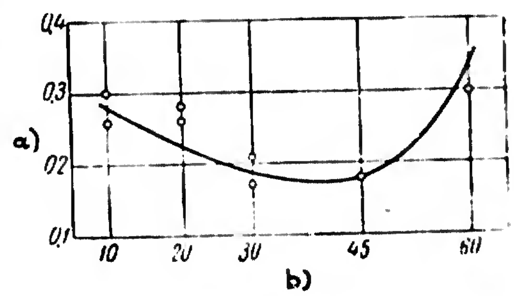

Fig.52 - Effect of End-Cutting-Edge Angle φ upon Flank Wear of the Cutter. Turning of 40KhS steel of H_{R_C} = 48 - 50 by T30K4 cutters, t = 0.2 mm, s = 0.1 mm/rev, and v = 40 m/min

a) Flank wear h, mm; b) End-cutting-edge angle, φ°

length of the part being machined to its diameter was 6.3 (ingot length L = 1700 mm, diameter D = 270 mm).

In view of the occurrence of vibrations when the work was conducted at φ = 30°, the author, in all his further experiments (not involving investigation of the angle φ) employed cutters with an angle of φ = 45°.

The relationship of the flank wear of T30K4 cutters to the end-cutting-edge angle φ was determined by turning 40KhS steel of H_{R_C} = 48 - 50 (Bibl.21). The following was the geometry of the cutters: $\gamma = -10^\circ$, $\alpha = 10^\circ$, $\varphi_1 = 10^\circ$, $\lambda = 5^\circ$, $r = 0.5$ mm. The end-cutting-edge angle was varied in the interval of $\varphi = 10 - 60^\circ$. Figure 52 presents the experimental data. The cutter wear depicted in the graphs represents a working time of T = 40 min.

It will be evident that the minimum cutter wear is that in the $\varphi = 30 - 45^\circ$ zone. N.S.Logak points out that vibration was noted and signs of chatter were seen on the machined surface when the angle φ was low. At $\varphi = 60^\circ$, the cutting edge of the tool crumbled out.

For the purpose of machining hardened steels, the optimum value of the end-cutting-edge angle should be deemed to be $\varphi = 45^\circ$.

Complement of Side-Cutting-Edge Angle, φ_1

The author made no investigation of the question of the influence of the complement of the side-cutting-edge angle φ_1 upon the tool life. However, the numerous tests he conducted with hardened steels revealed the optimum value of this angle to be $\varphi_1 = 15^\circ$. P.P.Grudov (Bibl.29) also recommends cutters for which $\varphi_1 = 15^\circ$.

It was established by investigation (Bibl.21) of hardened 40KhS steel $H_{R_C} = 48 - 50$) that the optimum value of the complement of the side-cutting-edge angle is $\varphi_1 = 10^\circ$. After 40 min of use of the T30K4 cutter, we see from Fig.53 that minimum wear of the flank resulted at $\varphi_1 = 10^\circ$, while at $\varphi_1 = 15^\circ$ the wear was less than when $\varphi_1 = 5$ and 20°. The tools tested had the following geometry: $\alpha = 10^\circ$, $\gamma = -10^\circ$, $\varphi = 30^\circ$, $r = 0.5$ mm.

Complement λ of the Back Rake Angle

In experiments with steels A, B, and C, hardened to different hardnesses $H_{R_C} = 41 - 65$), it appeared that the optimum value of the complement of the back rake angle came to $\lambda = 0^\circ$. This is the angle adopted in recommended cutting conditions.

An investigation of the process of turning 40KhS steel of H_{R_C} = 48 - 50 (Bibl.21) shows that the optimum value of the angle λ lies in the range from 0 to 5^o (Fig.54). Given uniform effect, $\lambda = 0^o$ is to be preferred, as it is much easier to grind cutters at this angle.

In another investigation of hardened steels (Bibl.29), the optimum value found was $\lambda = 4^o$.

The angle $\lambda = 0^o$ is satisfactory for work not involving shock loads. When

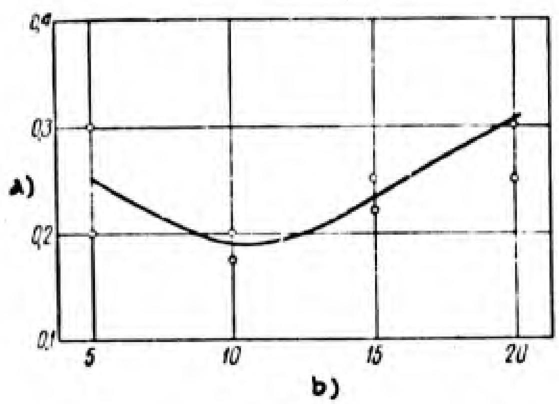

Fig.53 - Influence of Complement φ_1 of End-Cutting-Edge Angle upon Flank Wear of the Cutter. Turning of 40KhS steel of H_{R_C} = 48 - 50 by T30K4 cutters with t = 0.2 mm, s = 0.1 mm/rev, and v = 40 m/min

a) Flank wear h, mm; b) Complement φ_1^o of end-cutting-edge angle

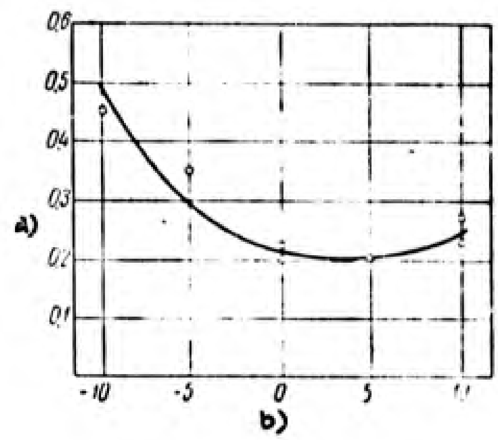

Fig.54 - Influence of Complement of Back Rake Angle upon Flank Wear. Turning of 40KhS steel of H_{R_C} = 48 - 50 by T30K4 cutters, with t = 0.2 mm, s = 0.1 mm/rev, and v = 40 m/min. Geometry of cutters tested: $\alpha = 10^o$, $\gamma = 10^o$, $\varphi = 30^o$, $\varphi_1 = 10^o$, r = 0.5 mm

a) Flank wear h, mm; b) Complement λ^o of back rake angle

hardened steels are machined under shock loads, higher complements of back rake angle are employed, attaining λ = 30 - 45^o (Bibl.26), so as to avoid crumbling-out of the tool at its most vulnerable point, the lip. Thus, when large ball and roller bearing races of ShKh15, ShKh15SG and 12KhN3 steels are machined on turret lathes (the steels having been hardened to H_{R_C} = 60 - 65), VK8 cutters were used in which the complement of the back rake angle was $\lambda = 45^o$ (Bibl.36).

Cutter Nose Radius r

As already noted, the machining of hardened steels, being a finishing process, must provide close dimensional tolerances and high-quality surface finish. The latter depends upon a number of factors, among which the cutter nose radius r plays an important role. With an increase in radius r, the surface finish rises. The use of cutters of large r is favored by the brittleness of the hard alloys, which manifests itself first at the cutter nose, as the most vulnerable portion of its cutting edge.

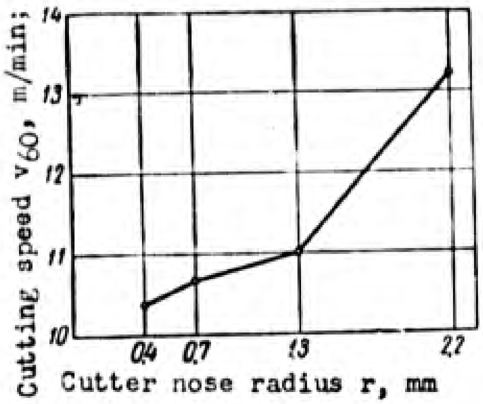

Fig.55 - Influence of Cutter Nose Radius r on the Cutting Speed v_{60}. Turning of steel C of H_{RC} = 65 by VK8 cutters, at t = 0.5 mm and s = 0.1 mm/rev

On the other hand, a large radius r causes vibrations, which are dangerous for brittle carbides and which lead to the appearance of waviness on the machined surface that reduces its quality.

Table 42

Influence of Cutter Nose Radius r upon Cutting Speed v_{60} and upon the Life Index m

Turning of Steel C of H_{RC} = 65 by VK8 cutters, at t = 0.5 mm and s = 0.1 mm/rev

Nose Radius r mm	Cutting Speed v_{60}, in m/min		Index m
	Absolute	Relative	
0,4	10,4	1,00	0,176
0,7	10,7	1,03	0,179
1,3	11,0	1,06	0,162
2,2	13,2	1,27	0,123

The author investigated the influence of the nose radius of the cutter upon its life and upon the cutting speed in the turning of steels C and B of H_{R_C} = 65 and 59.

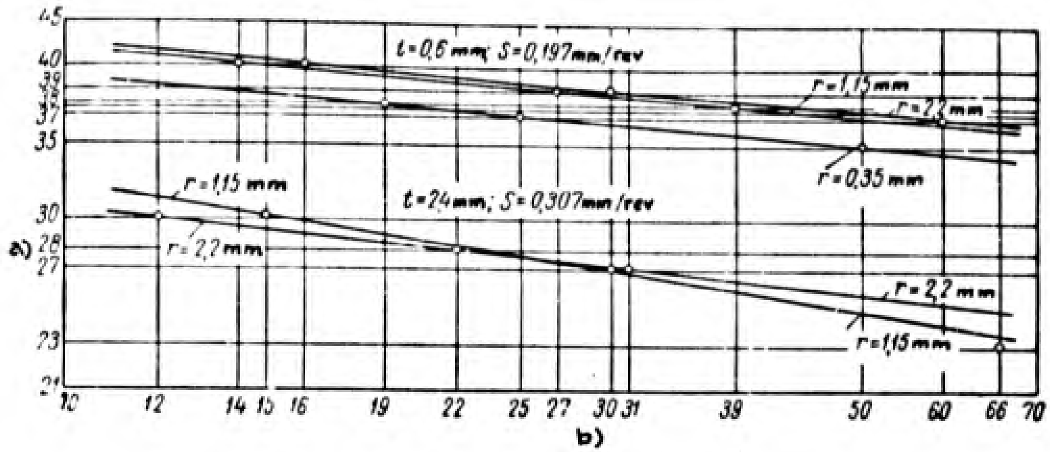

Fig.56 - Relationship Between Cutting Speed v and Cutter Life T for Various Values of the Nose Radius r. Turning of steel B of H_{R_C} = 59.

Cutter geometry T21K8: $\alpha = 6^\circ$, $\gamma = -5^\circ$, $\lambda = 0^\circ$, $\varphi = 45^\circ$, $\varphi_1 = 15^\circ$

a) Cutting speed v, m/min; b) Cutter life T, min

Table 42 and Fig.55 present the results of tests with steel C of H_{R_C} = 65. The tip radius varied in the interval from 0.4 to 2.2 mm.

Table 43

Influence of Nose Radius r upon Cutting Speed v_{60} and Magnitude of Relative Life Index m

Turning of Steel B of H_{R_C} = 59 by T21K8 Cutters

Nose Radius r, in mm	Depth of Cut t, in mm	Feed s, in mm/rev	Cutting Speed v_{60} m/min		Index m
			Absolute	Relative	
0,35	0,6	0,197	34,5	1,00	0,080
1,15			36,8	1,06	0,087
2,20			37,0	1,07	0,079
1,15	2,4	0,307	23,6	1,00	0,176
2,20			25,2	1,07	0,111

Experimental data show that, as the radius r rises at constant cutting speed, the cutter life T increases. Thus, cutters with r = 0.7 mm showed a life of T = 13 min at v = 14 m/min, whereas cutters with r = 2.2 mm showed a considerably longer life (T = 32 and 35 mm) at the same cutting speed. Cutters with r = 0.4 mm had a life of T = 25 - 29 min, with v = 12 m/min; virtually the same life (T = 25 - 26 min) was demonstrated by cutters for which r = 1.3 mm, but at a higher cutting speed (v = 13 m/min). However, vibrations were noted in the functioning of cutters for which r = 2.2 mm.

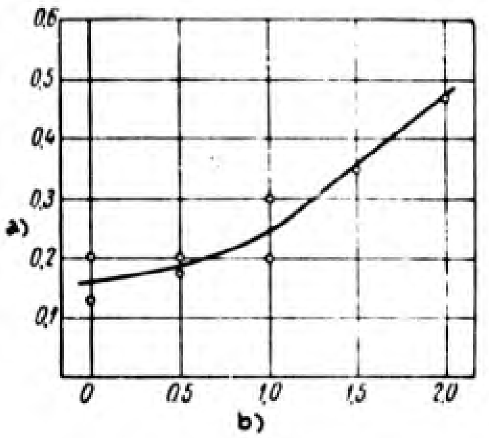

Fig.57 - Influence of Nose Radius upon Flank Wear. Turning of 40KhS Steel of H_{R_C} = 48 - 50 by T30K4

Cutters, at t = 0.2 mm, ε = = 0.1 mm/rev, and v = 40 m/min ($\alpha = 10^o$, $\gamma = -10^o$, $\lambda = 10^o$, $\varphi = 30^o$, $\varphi_1 = 10^o$)

a) Flank wear h, mm;
b) Nose radius r, mm

Table 43 and Fig.56 present the results of experiments with steel B of H_{R_C} = 59. The tests were run with T21K8 cutters under two sets of cutting conditions: t = 0.6 mm, s = 0.197 mm/rev; and t = 2.4 mm, s = 0.307 mm/rev. As we see, an increase in the radius r results in an increase in cutting speed, but one that is less marked than in the turning of steel C of H_{R_C} = 65. In these experiments, too, vibration was noted when using cutters with r = 2.2 mm.

This material makes it possible to draw the conslusion that, in the finish-turning by carbide tools of steels tempered to high hardness, the radius r has a significant influence upon the cutting speed, although this is less pronounced than in the turning of unhardened steels.

However, there is no basis for recommending cutters of large nose radius for the turning of hardened steel. On the other hand, cutters of low radius (r < 0.5 mm) also cannot be recommended, since the carbide bar would crumble right at the onset of cutting. The optimum nose radius for the turning of the hardened steels investigated by the author is r = 1.0 mm.

The same results were obtained in an investigation of 40KhS steel of H_{R_C} = = 48 - 50 (Bibl.21). After 40 min of work, the lowest flank wear occurred, as we see from Fig.57, in cutters with r = 1.0 and 0.5 mm. In working with cutters with r = 2.0 and 1.5 mm, vibrations were observed, although they occurred under conditions of adequate rigidity: The blank diameter was 80 - 85 mm and its length was 500 mm.

Effect of Lapping of Cutter upon its Life

Practical experience in the operation of carbide tools and research on the item

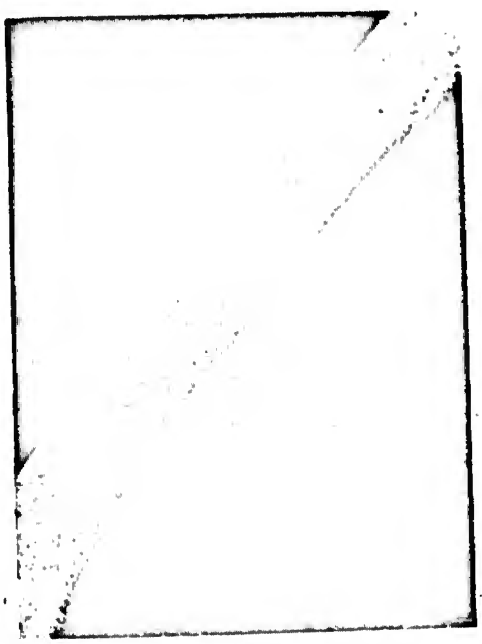

Fig.58 - Face of Titanium-Tungsten Cutter Lapped with Boron Carbide Flour

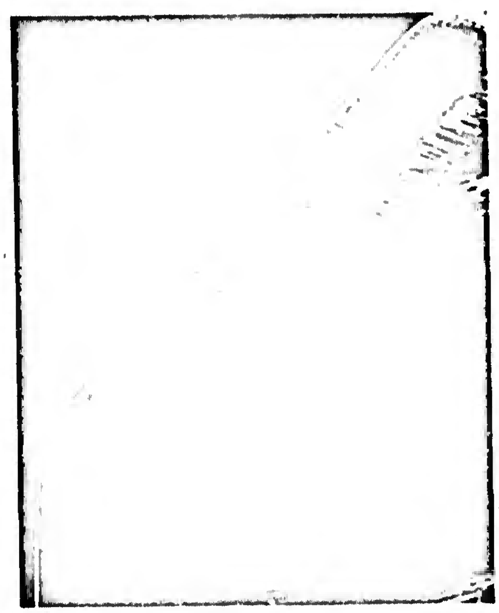

Fig.59 - Face of Titanium-Tungsten-Tipped Cutter Not Lapped

have established that the intensity of wear and consequently the life of the tool, as well as the finish of the machined surface, depend upon the quality of face and cutting edge finish.

Where carbide tools are concerned, no high-quality finish of the faces and the cutting edges is attained, even when two grinding operations are performed: roughing on green 36, 46, or 60 grain silicon carbide wheels and finishing on 80 or 100 grain wheels. Roughnesses and indentations remain. Moreover, the carbide bar retains a

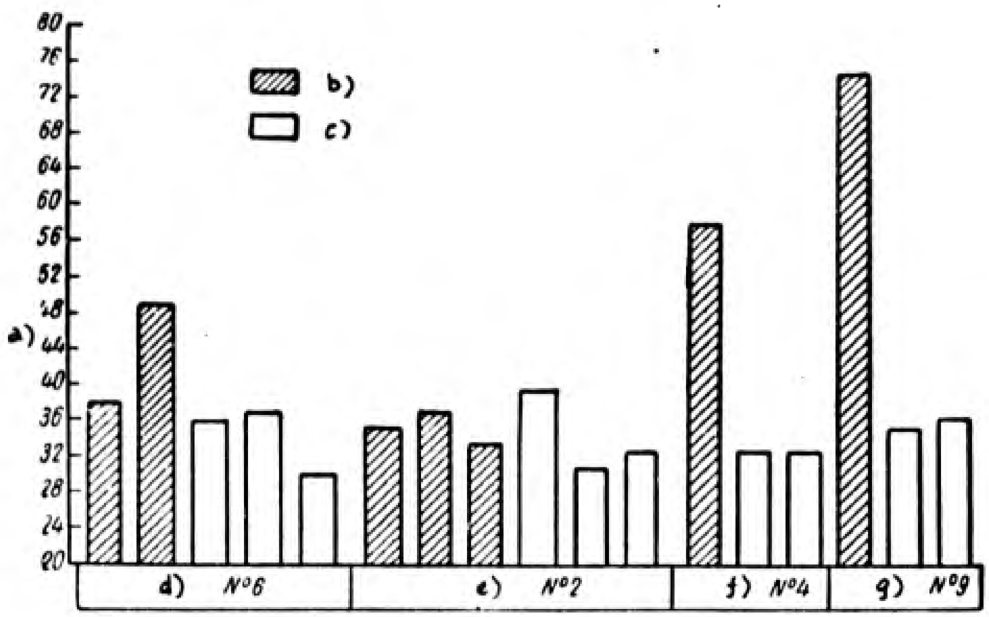

Fig.60 - Effect of Lapping upon Tool Life. Turning of steel B of H_{R_C} = 59 by T15K6 cutters, at t = 0.3 mm, s = 0.112 mm/rev, and v = 70 m/min ($\alpha = 6^\circ$, $\gamma = -5^\circ$, $\lambda = 0^\circ$, $\varphi = 45^\circ$, $\varphi_1 = 15^\circ$, r = 1.15 mm)

a) Cutter life T, min; b) Lapped cutters; c) Cutters, not lapped; d) Cutter No.6; e) Cutter No.2; f) Cutter No.4; g) Cutter No.9

damaged surface layer that acquires considerable stress under the high temperature developing during grinding.

Lapping has the purpose of reducing the roughnesses and indentations on the faces and cutting edges of cemented carbide cutters, of providing a smooth surface and proper geometric to the faces, and also of removing the surface layer of the carbide bar that has been damaged in the grinding process. The lapping process reduces the work of friction between the chip and the face, and that between the flank and the machined material, and the life of the cutter is increased.

At the present time, carbide cutters are lapped chiefly with a boron carbide flour (B_4C). This abrasive is second only to diamond in hardness. Practice has shown that the use of fine-grain green silicon carbide wheels for lapping is undesirable because of the slowness of the process. The extreme shortage and high cost of diamond wheels has also ruled them out as lapping media.

Boron carbide is made of technical boric acid and low-ash petroleum coke in electric furnaces, at a temperature of 2000 - 2300°C. The bars of boron carbide produced in the electric furnace are ground, screened, and separated by grain size. The boron carbide grain is 28 - 40 microns in size for ordinary work and 10 - 23 for finishing work. The abrasive capacity of boron carbide is very high. It is 75% of the abrasive capacity of diamond and 300% of that of silicon carbide.

The thick (pasty) compound with paraffin as binder for the boron carbide grains has gained preference for lapping purposes. The boron carbide compound is marketed in the form of cylinders 20 - 25 mm in diameter and 50 - 70 mm in length. Liquid compounds with oil as binder are not conveniently carried on a lapping wheel, since they splash off as it rotates. A briquetted solid compound is also carried poorly by the lapping wheel, which in this case must be generously greased with kerosene.

Two grades of boron carbide compound are made (under a VNIIASh formulation):

1) With 75 - 85% boron carbide content (remainder paraffin);

2) With 60 - 70% boron carbide content (remainder paraffin).

To improve the ability of the lapping wheel to carry the compound, 10 - 15% iron oxide by weight is added.

Figures 58 and 59 show the face of a lapped and an unlapped titanium-tungsten cutter. Lapping was done with boron carbide compound. The micrographs clearly show the effect of lapping.

The effect of lapping of carbide cutters upon their life in the turning of hardened steels is illustrated in Fig.60.

Four cutters were tested. Each was tested both with a lapped and an unlapped cutting portion. As we see, lapping failed to produce longer life in only one cutter of four (Cutter No.2). The lives of the other cutters were considerably lengthened thanks to lapping.

Table 44 presents the experimental data in systematized form. They convincingly demonstrate the positive effect of the lapping of a cutter upon its life. As a result of lapping, the life of cutters increased by 64 - 266%.

Table 44

Effect of Lapping of a Cutter upon its Life

Turning of Steel B of H_{R_C} = 59 by T15K6 Cutters, at t = 0.3 mm, s = 0.112 mm/rev, and v = 70 m/min

Cutter No.	Mean Tool Life T_{mean}, in min		Increase in Cutter Life, %
	Lapped Cutter	Unlapped Cutter	
6	23,5	14,3	164
2	15	14,3	105
4	38	12,0	317
9	55	15,0	366

It is not necessary to demonstrate the need for finishing carbide cutters. In order to employ them rationally in the machining of hardened steels, lapping must become absolutely obligatory.

It should be noted that lapping facilitates the detection, on carbide bars, of cracks formed in the process of grinding and not visible to the naked eye on the ground or polished surface.

<u>Conclusions</u>

1. The true rake angle γ of a cutter exercises a significant effect upon the

process of cutting hardened steels. With a reduction in true rake angle, there is an increase in the mechanical strength of the cutting edge, but the conditions for chip removal are impaired, heating of both chip and cutter increases, the radial cutting force P_y increases, and as a result the bouncing of the cutter away from the machined surface increases, and the precision of the machining operation is impaired.

To ease the chip removal and reduce the radial force P_y, it is more desirable to work with cutters having a positive true rake angle ($\gamma > 0^o$), but in this situation the cutting edge does not have the mechanical strength necessary for the machining of hardened steel. At $\gamma > 0^o$, crumbling-out of the carbide bar occurred, and this became more pronounced as the positive true rake angle γ increased.

The turning of hardened steels can be done only with carbide cutters having a negative true rake angle ($\gamma < 0^o$). The author's experiments have shown that, in the case of alloy steels tempered to high hardness, the most desirable value for the true rake angle γ is in the -5 to 0^o range. Changes in the angle γ toward the positive side resulted in crumbling-out of the cutting edge of the cutter, and a change toward larger negative values led to a reduction in the life of the cutter, although $\gamma = -5^o$ represented a slight gain in life over $\gamma = +6^o$.

Industrial experience in the turning of hardened steels confirmed the need to employ cutters with small negative true rake angles ($\gamma = -5^o$).

A difference of opinion exists with respect to the true rake angle. A considerable number of investigators hold the view that the turning of hardened steels should be done with cutters of high negative true rake angle γ: as much as -20 and -25^o for steels of high hardness. The author believes that the true rake angle γ for the machining of hardened steels of $H_{R_C} = 38 - 65$ should be in the 0 to -10^o range.

2. The optimum relief angle is determined by the level of the stresses occurring in the machined material past the line of cut. Deformation is greater, the thinner the layer of metal a removed (the less the feed s), the cutting speed v, and

the true rake angle γ. The thickness of cut a is the factor that affects the relief angle α most strongly. The author's experiments have established that when titanium-tungsten carbide tools are used to turn alloy steel hardened to $H_{R_C} = 65$, the life of the cutter rises as the relief angle α increases from 10 to 25°. It has been demonstrated in practice that this steel can be machined with a relief angle of $\alpha = 25°$.

It should, however, be borne in mind that the radial wear (for a given flank wear) and taper of the machined surface (if the cutter is not subject to radial readjustment) increase in relief angle and that, consequently, the precision of the machining on the given pass is diminished.

A relief angle of $\alpha = 15°$ is recommended for $s \leq 0.2$ mm/rev and $\alpha = 10°$ for $s > 0.2$ mm/rev.

3. The end-cutting-edge angle φ has a major influence upon the cutting speed. Any reduction in the angle φ, with no change in section of cut, results in a reduction in thickness of the cut a and an increase in its width b and, in connection therewith, in an increase in the length of the working portion of the cutting edge. Taken together, this results in an increase in cutter life and a reduction in the angle φ.

At the same time, the reduction in the angle φ causes a sharp increase in the radial force P_y and the appearance of vibrations which have a detrimental effect on the quality of the surface finish and also result in premature destruction of the cutting edge of the tool.

An end-cutting-angle φ of 45° should be employed to turn hardened steels. However, if the system workpiece - machine tool - cutter is highly rigid, cutters may be ground with an end-cutting-edge angle of $\varphi < 45°$. This makes it possible to increase the cutting speed.

4. In his experiments, the author found the optimum value for the complement of the side-cutting-edge angle to be $\lambda = 0°$. The optimum value of λ is between 0 and

5° according to N.S.Logak, and -4° according to P.P.Grudov.

When hardened steels are turned with the use of impact, the angle λ should be increased to 10 - 20°.

5. With an increase in lip radius, the life of the tool and the permissible cutting speed increase. There is also a reduction in the height of the residual projections on the machined surface. On the other hand, an increase in the radius r results in an increase in the radial force P_y and the appearance of vibration. This last factor requires the employment of carbide tools of small lip radius in the finish-machining of hardened steels. For the turning of hardened steels, r = 1 mm is to be recommended.

6. The machining properties of a carbide cutter are largely governed by the quality of finish of face, flanks, and cutting edge. The usual procedure of two-stage grinding (rough and finish) does not yield high-quality finish of face, flank, and cutting edge (unevenness and indentations remain).

The lapping of carbide tools has the object of reducing the roughness and depressions in the working surfaces, smoothing these surfaces and attainment of true geometric form thereof and, moreover, of eliminating the surface layer of the carbide bar damaged in the grinding process.

The best lapping compound is boron carbide. The experience accumulated in the utilization of carbide cutters has shown that their lives are considerably increased as a result of lapping. Lapping is absolutely essential for purposes of rational employment of carbide tips in the turning of hardened steels.

16. Effect of Various Factors upon Tool Life and Cutting Speed

Results of Tests of Tool Life

Tests of steel B of H_{R_C} = 49 - 59 and of steel C of H_{R_C} = 65 were run by the author to determine the relationship between cutting speed and tool life, depth of cut, and feed. Control experiments were also run on steel A of H_{R_C} = 49.5.

Figures 61 - 64 present the results of tool life tests of steel B of H_{R_C} = = 49 - 59. The tests were run with lapped titanium-tungsten cutters. The depth of cut was varied in the t = 0.3 - 2.4 mm interval, and the feed in the s = 0.07 to 0.61 mm/rev interval. The following was the geometry of the cutting portion of the

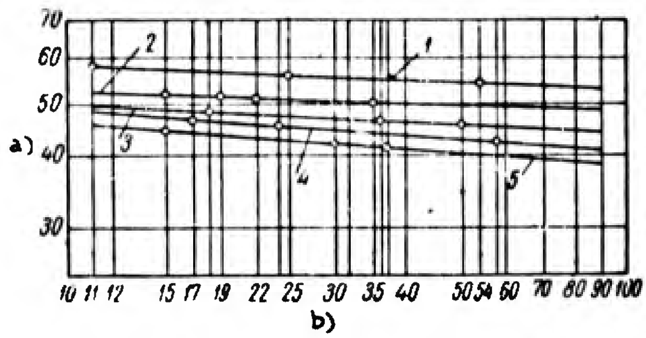

Fig.61 - Ratio Between Cutting Speed v and Tool Life T for Various Feeds s. Turning of steel B of H_{R_C} = 59, at t = 0.3 mm

1 - s = 0.07 mm/rev; 2 - s = 0.112 mm/rev; 3 - s = 0.155 mm/rev; 4 - s = 0.225 mm/rev; 5 - s = 0.307 mm/rev

a) Cutting speed v, m/min; b) Cutter life T, min

tools: $\alpha = 6^\circ$, $\gamma = -5^\circ$, $\lambda = 0^\circ$, $\varphi = 45^\circ$, $\varphi_1 = 15^\circ$, r = 1.15 mm.

Difficulties were encountered in these tests due to the different degrees of hardening of ingots of steel B both in cross section and (particularly) in length. The ingots hardened better from the ends than in the middle. Each ingot actually had three distinct areas of hardness and machinability.

In order to alleviate the lack of homogeneity of the steels investigated, a segment about 200 mm long was left untouched at each end of the ingot. Nevertheless, differences in the machinability of the steel along the length of a given ingot were often observed, which necessarily had to affect the results of the tests.

Tests of steel C of H_{R_C} = 65 were run with lapped T15K6 cutters having the following geometry of the cutting point: $\alpha = 6^\circ$, $\gamma = -5^\circ$, $\lambda = 0^\circ$, $\varphi = 45^\circ$, $\varphi_1 = 15^\circ$, r = 1.3 mm. The depth of cut was varied in the t = 0.1 to 1.0 mm interval, and the feed in the s = 0.05 to 0.28 mm/rev interval.

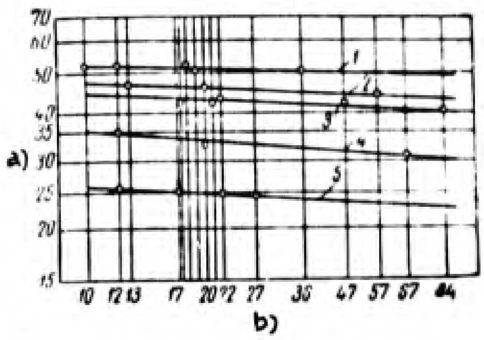

Fig.62 - Ratio of Cutting Speed v to Tool Life T for Various Feeds s. Turning of steel B of H_{R_C} = 59, at t = 0.6 mm

1 - s = 0.07 mm/rev; 2 - s = = 0.155 mm/rev; 3 - s = = 0.225 mm/rev; 4 - s = = 0.307 mm/rev; 5 - s = = 0.395 mm/rev

a) Cutting speed v, m/min; b) Tool life T, min

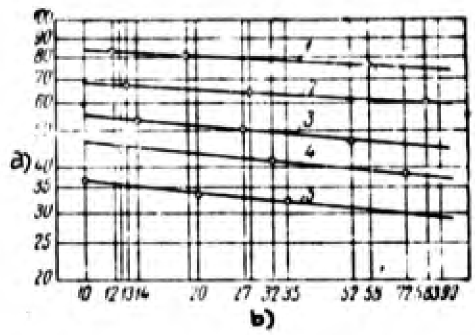

Fig.63 - Ratio of Cutting Speed v to Tool Life T for Various Feeds s. Turning of steel B of H_{R_C} = 49, at t = 1.2 mm

1 - s = 0.07 mm/rev; 2 - s = = 0.153 mm/rev; 3 - s = = 0.23 mm/rev; 4 - s = = 0.38 mm/rev; 5 - s = = 0.61 mm/rev

a) Cutting speed v, m/min; b) Tool life T, min

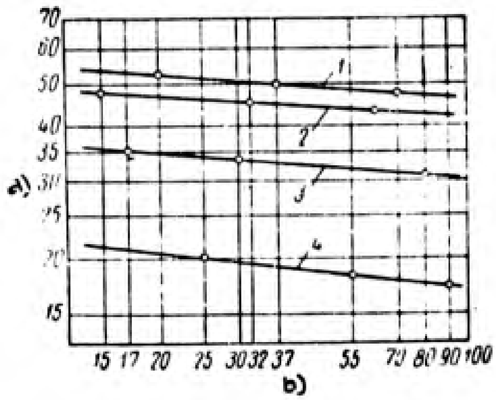

Fig.64 - Ratio of Cutting Speed v to Tool Life T for Various Feeds s. Turning of steel B of H_{R_C} = 59 at t = 2.4 mm

1 - s = 0.07 mm/rev; 2 - s = = 0.155 mm/rev; 3 - s = = 0.225 mm/rev; 4 - s = = 0.395 mm/rev

a) Cutting speed v, m/min; b) Cutter life T, min

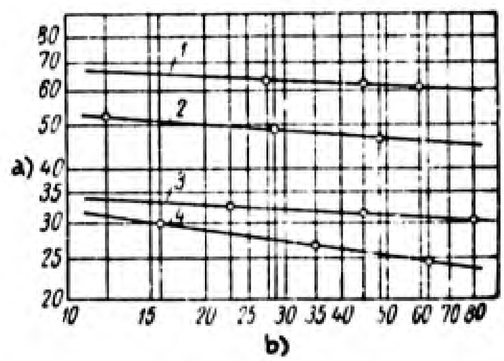

Fig.65 - Ratio of Cutting Speed v to Tool Life T for Various Feeds s. Turning of steel A of H_{R_C} = 49.5 at t = 1.5 mm ($\alpha = 6°$, $\gamma = -5°$, $\lambda = 0°$, $\varphi = 45°$, $\varphi_1 = 15°$, r = 1.15 mm)

1 - s = 0.153 mm/rev; 2 - s = = 0.305 mm/rev; 3 - s = 0.46 mm/rev; 4 - s = 0.61 mm/rev

a) Cutting speed v, m/min; b) Cutter life T, min

The ingot of steel C tested was characterized by identical hardenability throughout its length and cross section. However, foreign inclusions in the material resulted in premature dulling and crumbling-out of the cutters. This explains the considerable number of atypical (unsuccessful) experiments. It will be understood that the unsuccessful tests were not taken into consideration in the compilation of the analytical relationships. Control tests of steel A of $H_{R_C} = 49.5$ (Fig.65) were run with lapped cutters. The feed was varied in the s = 0.153 to 0.610 mm/rev interval, at constant cutting speed (t = 1.5 mm).

Ratio of Cutting Speed to Cutter Life

The ratio of the cutting speed to the cutter life has the same form for hardened steels as for unhardened:

$$v = \frac{C}{T^m}, \qquad (4)$$

where v is cutting speed in m/min;

T is tool life, or work in min until dulling;

C is a constant depending upon the physical and mechanical properties of the workpiece, cutting depth, feed and other conditions of cutting;

m is the relative life index.

The relative life index describes the rate of change in tool life with a change in the cutting speed. The lower the m index, the greater will be the effect of change in cutting speed upon tool life, and vice versa.

Numerous investigations have determined the relationship of the relative life index m to the factors influencing it, for unhardened steels. Let us examine this question as it pertains to hardened steels.

Table 45 presents data obtained by the author in tool-life tests of steel B of $H_{R_C} = 49 - 59$. The tests were conducted with cemented titanium-tungsten T21K8 cutters. Table 46 contains analogous data for steel C of $H_{R_C} = 65$ (T15K6 tools). Figures 66 and 67 present the ratio of m index to feed s for various cutting depths t.

Increasing the feed s results in a rise in m. A variation in depth of cut t has the same effect upon the index m. Figure 67 shows the t - m relationship very

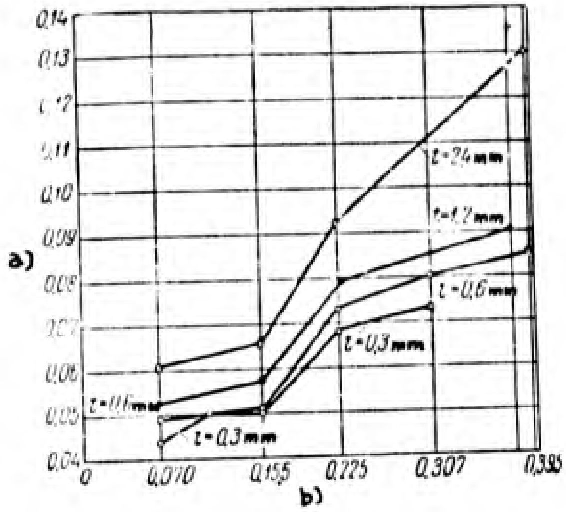

Fig.66 - Effect of Feed s and Depth of Cut t upon Relative Life Index m of Tool. Turning of steel B of $H_{R_C} = 59$, at

t = 0.3, 0.6 and 2.4 mm, and of steel B of $H_{R_C} = 49$, at

t = 1.2 mm

a) Relative life index m;
b) Feed s, mm/rev

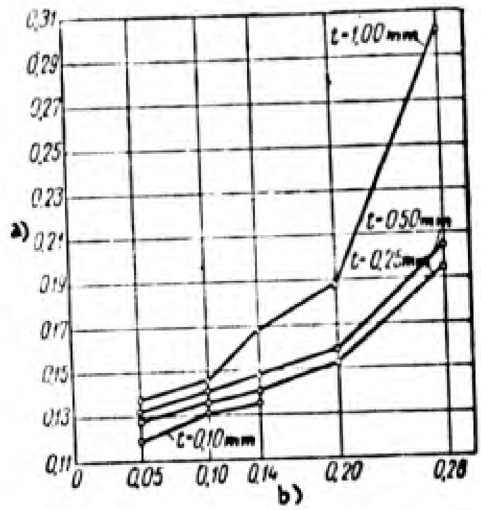

Fig.67 - Effect of Feed s and Depth of Cut t upon the Relative Tool Life Index m. Turning of steel C of $H_{R_C} = 65$

a) Relative life index m;
b) Feed s, mm/rev

clearly, whereas Fig.66 shows it, less clearly, for low cutting depths t and feeds s.

The index m is also affected by the ratio of depth of cut to feed, $\frac{t}{s}$. With a rise in $\frac{t}{s}$, there is a regular increase in m. For example, at s = 0.225 mm/rev, a fourfold rise in $\frac{t}{s}$ (due to a change in t from 0.3 to 2.4 mm) causes m to rise from 0.068 to 0.092. At s = 0.307 mm/rev, the index m rises, correspondingly, from 0.073 to 0.110.

The same regularity may be traced for steel C of H_{R_C} = 65. For example, at s = 0.14 mm/rev, a tenfold rise in $\frac{t}{s}$ (thanks to a change from 0.10 to 1.00 mm in t) results in an increase from 0.135 to 0.168 in the index m. When $\frac{t}{s}$ increases fourfold (t being changed from 0.25 to 1.00 mm), the relative life index m will increase from 0.195 to 0.302, for a feed of s = 0.28 mm/rev.

Consequently, in the turning of hardened steels, the relative tool life index m

Table 45

Influence of Depth of Cut t and Feed upon Relative Tool Life m and Cutting Speed v_{60}

Machining of Steel B of H_{R_C} = 49 - 59

Depth of Cut t, mm	Feed s in mm/rev	Index m	Cutting Speed v_{60} in m/min	Depth of Cut t, mm	Feed s in mm/rev	Index m	Cutting Speed v_{60} in m/min
0,3	0,070	0,044	54,0	1,2[1]	0,070	0,053	75,0
	0,112	0,050	48,8		0,153	0,057	61,0
	0,155	0,050	45,5		0,230	0,079	47,0
	0,225	0,068	42,0		0,380	0,090	38,7
	0,307	0,073	40,0		0,610	0,110	30,0
0,6	0,070	0,049	49,5	2,4	0,070	0,062	47,5
	0,155	0,051	43,9		0,155	0,066	43,1
	0,225	0,073	40,5		0,225	0,092	31,2
	0,307	0,080	31,3				
	0,395	0,085	22,3		0,395	0,130	17,9

*Tests at t = 1.2 mm were run on steel B of H_{R_C} = 49; all the other tests (t = 0.3, 0.6, and 2.4 mm) were run on steel B of H_{R_C} = 59.

is dependent upon the feed s, depth of cut t, and ratio of depth of cut to feed, $\frac{t}{s}$. The index m rises with an increase in s, t, and $\frac{t}{s}$.

The value of m also depends upon the true rake angle of the cutter γ, the relief angle α, the lip radius r, the particular carbide with which the cutter is tipped, and the hardness of the hardened steel.

As we see from Table 35, an increase in true rake angle γ from -12 to 6° results in a tendency of the index m to diminish. With increase in the relief angle

Table 46

Influence of Depth of Cut t and Feed s upon the Relative Tool Life m and the Cutting Speed v_{60}

Machining of Steel C of H_{R_C} = 65

Depth of Cut t, in mm	Feed s in mm/rev	Index m	Cutting Speed v_{60}, in m/min	Depth of Cut t, in mm	Feed s in mm/rev	Index m	Cutting Speed v_{60}, in m/min
0,10	0,05	0,119	23,4	0,50	0,05	0,132	19,6
	0,10	0,131	17,7		0,10	0,141	13,2
	0,14	0,135	14,4		0,14	0,148	11,5
0,25	0,05	0,128	20,5		0,20	0,159	9,0
	0,10	0,136	14,8		0,28	0,205	7,2
	0,14	0,141	12,0	1,00	0,05	0,138	16,5
	0,20	0,153	10,6		0,10	0,146	11,6
	0,28	0,195	8,4		0,14	0,168	9,0
					0,20	0,188	7,0
					0,28	0,302	5,4

of the cutter (Table 38), the value of m rises. This regularity is clearly pronounced despite the fact that the value of m for α = 8° constitutes an exception.

Let us now turn to the lip radius (Table 42 and 43). We see that in the machining of steel C with tungsten cutters, the hardness of the steel being H_{R_C} = = 65, an increase in the radius r results in a reduction in the index m. The same regularity applies when turning steel B of H_{R_C} = 59 with titanium-tungsten cutters. When the radius r increases from 1.15 to 2.20 mm, the relative life index diminishes from 0.176 to 0.111.

Let us examine the influence of the grade of carbide upon the value of the index m (Tables 26 and 27). The index m is considerably higher for single-carbides than for double. Whereas for carbides VK6, VK8, and VK12 (machining of steel B of H_{R_C} = 56 at t = 1.2 mm and s = 0.225 mm/rev), the index m = 0.103 - 0.119, it is m = 0.063 - 0.069 for the T15K6 and T21K8 alloys.

For smaller sections (t = 0.3 mm, s = 0.112 mm/rev), there was no change in the ratio of the index m to the carbide, when the same steel was machined.

In the machining of steel C of H_{R_C} = 65, the index m is of considerably higher value than for steel B of H_{R_C} = 56. The nature of the relationship did not change in this case either; the index m is lower for double carbides than for single.

The data presented for hardened steels confirm the familiar proposition that cemented titanium-tungsten carbides are more sensitive to changes in cutting speeds than are tungsten alloys.

Table 47 describes the influence of the hardness of a tempered steel upon the index m in fine-turning (Bibl.21).

Table 47

Influence of Hardness of Tempered Steel upon Relative Tool Life m and Cutting Speed v_{60}

Turning with T30K4 Tools at t = 0.2 mm and s = 0.1 mm/rev

Machined Material	Hardness H_{R_C}	Index m	Cutting Speed v_{60}, in m/min
40KhS steel	50—52	0.49	103
Same	57—59	0.266	37.1
ShKh15 steel	61—63	0.205	17.9

As we see, the relative life index m diminishes as the steel becomes harder. Note the fact that, in this case the index m proved considerably higher, particularly for steels of less hardness, than in the author's experiments.

We see that for the section of cut employed by N.S.Logak ($F = t \cdot s = 0.2 \cdot 0.1 = 0.02\ mm^2$), the present author found $m = 0.044$ at $H_{R_C} = 59$ (Table 45) and $m = 0.136$ at $H_{R_C} = 65$ (Table 46), whereas Logak found $m = 0.266 - 0.205$ for $H_{R_C} = 57 - 65$.

There is a more pronounced difference between the present author and N.S.Logak with respect to the nature of the effect of the hardness of tempered steel upon the index m. Contrary to Logak's conclusion, the author's data show that m rises with an increase in the hardness of the steel. Let us compare the data in Tables 45 and 46. At identical cross sections, the index m for steel B of $H_{R_C} = 49 - 59$ is considerably less than for steel C of $H_{R_C} = 65$. Whereas for steel B, at $F = 0.034\ mm^2$ ($t = 0.3$ mm, $s = 0.112$ mm/rev), the index is $m = 0.050$, for steel C ($F = 0.25 \times 0.14 = 0.035\ mm^2$) it comes to 0.141. At $F \approx 0.28\ mm^2$ for steel B ($t = 1.2$ mm and $s = 0.23$ mm/rev), the index is $m = 0.079$, whereas for steel C ($t = 1.0$ mm, $s = 0.28$ mm/rev), it is $m = 0.302$.

It must be borne in mind that the tests discussed here were run with cutters tipped with cemented titanium-tungsten carbides.

Thus, it was established that the hardness of a tempered steel affects the index m. However, investigators differ as to the nature of this influence.

It remains to analyze the problem of the relation between the relative life index m and the machinability of the steel, determined by the permissible cutting speed for a given tool life.

S.S.Rudnik (Bibl.37) and A.M.Vul'f (Bibl.25) state that, in the machining of unhardened steels, the index m rises with any increase in the mechanical properties of the steel and any reduction in the cutting speed. Of considerable interest is the conclusion arrived at by I.M.Besprozvannyi (Bibl.38) to the effect that the cutting speed has a negligible effect upon the index m if the variations are held within an interval of 20 to 25%. When the cutting speed is varied within broader limits than this, the value of m varies with any variation in the cutting speed.

These data for unhardened steels coincide with the results of investigations on the turning of hardened steels. An analysis of experimental data reveals the existence of a clearly defined relationship between the value of m and the level of the cutting speed used. As the machinability of the steel diminishes, there is an increase in the index m (Tables 45 and 46). In fact, whereas for steel B of H_{RC} = 59, a variation in machinability from v_{60} = 54 to 40 m/min (t = 0.3 mm, s = 0.07 to 0.307 mm/rev) causes the index m to change from 0.044 to 0.073, in the case of steel C of H_{RC} = 65, a variation in machinability from v_{60} = 20.5 to 8.4 m/min (t = = 0.25 mm, s = 0.05 to 0.28 mm/rev) causes the index m to vary from 0.128 to 0.195.

The relationship of the index m to the cutting speeds employed is also con-

Magnitum Table 48

Magnitude of the Index m

Cemented Carbide	t ≤ 0.5 mm s ≤ 0.15 mm/rev	t > 0.5 mm s > 0.15 mm/rev
	m	
VK2 VK3 VK6 VK8	0,12	0,20
T5K10 T15K6 T30K4	0,07	0,10

firmed by experimental data obtained by the author on the effect of the tip radius r and the type of carbide with which the cutter is tipped, upon the cutting speed.

The machinability of hardened steels in fine-turning (Bibl.21) drops with increasing hardness (Table 47). With an increase in H_{RC} from 50 - 52 to 61 - 63, i.e., by 11 units, the machinability of the steel dropped by a factor of approximately 5.7. At the same time, the index of relative life m did not increase but, on the contrary, decreased from 0.49 to 0.205. This result contradicts the author's conclusions with respect to hardened steels, as well as the data of numerous investigations of the ratio $v = \frac{C}{T^m}$ for unhardened steels.

A comparison of the results obtained by the author with the literature data (Bibl.37, 38, 39, 40, 41, 42, and 43) shows that the ratio of life to cutting speed [T = f(v)] for hardened steels is of the same nature as for unhardened steel. This confirms the conclusion that the turning of hardened steels must be regarded as a special case of the machining of metals.

Table 48 presents the values, adopted by the author, for the relative life index m in the turning of hardened steels of H_{R_C} = 38 - 65.

Relationship of Cutting Speed to Depth of Cut and to Feed

Table 49 presents the values for cutting speed based on 60-minute tool life (v_{60}) for various depths of cut and feed. The Table contains data from tool-life

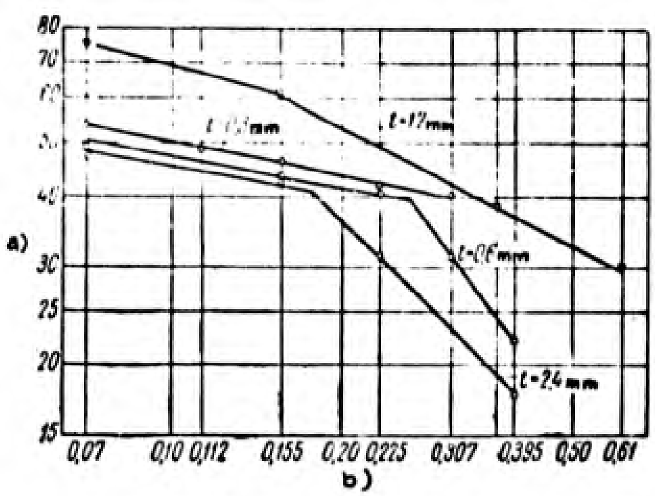

Fig.68 - Ratio of Cutting Speed v_{60} and Feed s at Various Depths of Cut t. Turning of steel B of H_{R_C} = 49 - 59 by T21K8 cutters having the following geometry: $\alpha = 6^o$, $\gamma = -5^o$, $\lambda = 0^o$, $\varphi = 45^o$, $\varphi_1 = 15^o$, r = 1.15 mm

a) Cutting speed v_{60}, m/min; b) Feed s, mm/rev

tests run by the author on steels A, B, and C of H_{R_C} = 49 - 65, as well as from tests for determining the effect of true rake and relief angles, lip radius and type

Table 49

Cutting Speeds v_{60} for Various Depths of Cut t and Feed s

Cutter geometry: $\alpha = 6^\circ$, $\gamma = -5^\circ$, $\lambda = 0^\circ$, $\varphi = 45^\circ$, $\varphi_1 = 15^\circ$, r = 1.15 – 1.3 mm

Machined Material	Carbide	Depth of Cut t, in mm	Feed s, in mm/rev																
			0,05	0,07	0,10	0,112	0,140	0,153	0,155	0,20	0,225	0,23	0,28	0,305	0,347	0,38	0,395	0,46	0,61
			Cutting Speed v_{60}, in m/min																
Steel C H_{RC} = 65	T15K6	0,10	23,4	—	17,7	—	14,4	—	—	—	—	—	—	—	—	—	—	—	—
		0,25	20,5	—	14,8	—	12,0	—	—	10,6	—	—	8,4	—	—	—	—	—	—
		0,50	19,5	—	13,2	—	11,5	—	—	9,0	—	—	7,2	—	—	—	—	—	—
		1,00	16,5	—	11,6	—	9,0	—	—	7,0	—	—	5,4	—	—	—	—	—	—
		1,50	—	—	—	—	—	—	—	5,9	—	—	—	—	—	—	—	—	—
Steel C H_{RC} = 65	VK8	0,50	—	—	11,0	—	—	—	—	—	—	—	—	—	—	—	—	—	—
Steel B H_{RC} = 59	T21K8	0,30	—	54,0	—	28,8	—	—	45,5	—	42,0	—	—	—	40,0	—	—	—	—
		0,60	—	49,5	—	—	—	—	43,9	—	40,5	—	—	—	31,3	—	22,5	—	—
		1,20	—	—	—	—	—	—	—	—	38,3	—	—	—	—	—	—	—	—
		2,40	—	47,5	—	—	—	—	43,1	—	31,2	—	—	—	—	—	17,9	—	—
Steel B H_{RC} = 56	T21K8	2,40	—	—	—	—	—	—	—	—	—	—	—	—	26,8	—	—	—	—
Steel A H_{RC} = 49.5	T21K8	1,50	—	—	—	—	—	60,0	—	—	—	—	—	45,0	—	—	—	51,0	24,0
		1,00	—	—	—	—	—	65,0	—	—	—	—	—	—	—	—	—	—	—
		0,30	—	—	—	—	—	—	—	—	—	—	—	60,1	—	—	—	—	—
Steel B H_{RC} = 49	T21K8	1,20	—	75,0	—	—	—	61,0	—	—	—	47,0	—	—	—	38,7	—	—	30,0
Steel A H_{RC} = 47	T21K8	1,20	—	—	—	—	—	—	—	—	—	—	—	58,2	—	—	—	—	—
Steel A H_{RC} = 41	T21K8	1,20	—	—	—	—	—	—	—	—	—	—	—	76,5	—	—	—	—	—

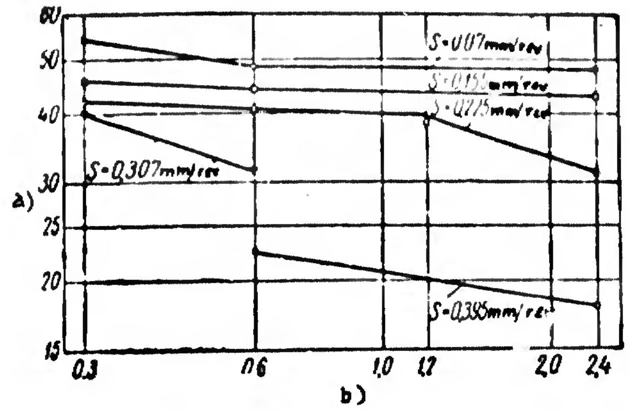

Fig.69 - Ratio of Cutting Speed v_{60} to Depth of Cut t, for Various Feeds s. Turning of steel B of H_{R_C} = 59. Tool description in Fig.68

a) Cutting speed v_{60}, m/min; b) Depth of cut t, mm

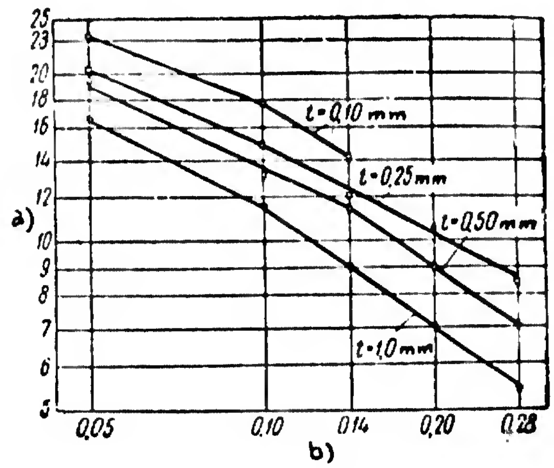

Fig.70 - Ratio of Cutting Speed v_{60} to Feed s, for Various Depths of Cut t. Turning of steel C of H_{R_C} = 65, T15K6 tools, geometry: $\alpha = 6^\circ$, $\gamma = -5^\circ$, $\lambda = 0^\circ$, $\varphi = 45^\circ$, $\varphi_1 = 15^\circ$, r = 1.3 mm

a) Cutting speed v_{60}, m/min; b) Feed s, mm/rev

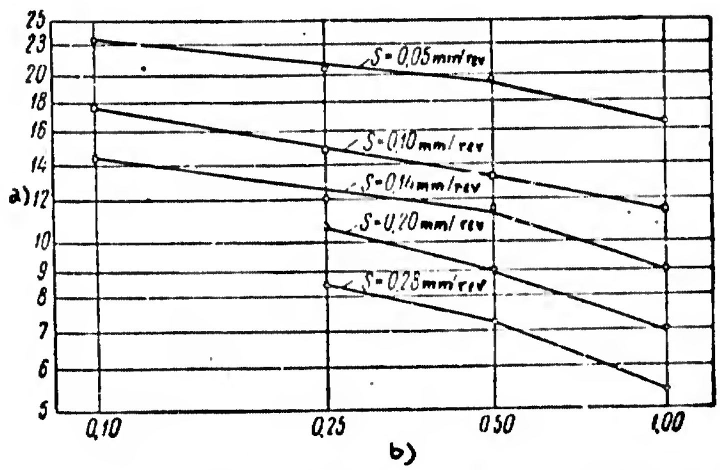

Fig.71 - Ratio of Cutting Speed v_{60} to Depth of Cut t, for Various Feed s. Turning of steel C of H_{R_C} = 65. Cutters described in Fig.70

a) Cutting speed v_{60}, m/min; b) Depth of cut t, mm of carbide, upon both cutting speed and tool life.

Figures 68 and 69 present the relationship of the cutting speed v_{60} to the feed s and depth of cut t for steel B of H_{R_C} = 49 – 59, whereas Figs.70 and 71 present the same relationships for steel C of H_{R_C} = 65, and Fig.72 gives the v_{60} versus s ratio for steel A of H_{R_C} = 49.5. The upper curve in Fig.68 pertains to steel B of H_{R_C} = 49, and the others to steel B of H_{R_C} = 59.

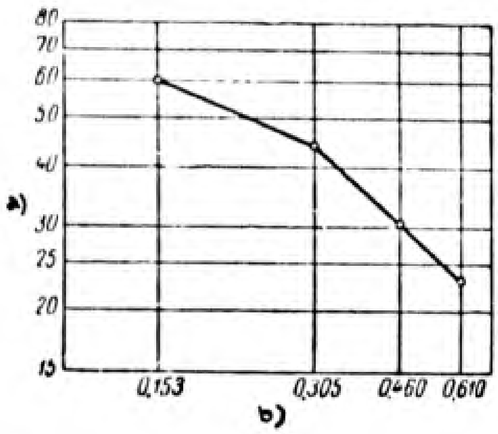

Fig.72 - Ratio of v_{60} Cutting Speed to Feed s, for Depth of Cut t = 1.5 mm. Turning of Steel A of H_{R_C} = 49.5

a) Cutting speed v_{60}, m/min; b) Feed s, mm/rev

These data make it possible to express the relationship of cutting speed to feed and depth of cut by the equations:

$$v_{60} = \frac{C_s}{s^{y_v}}, \qquad v_{60} = \frac{C_t}{t^{x_v}}.$$

Tables 50 and 51 and the graphs (Figs.68 - 72) show, above all else, the absence of a strict regularity in the dependence of v_{60} upon t and s for steel B. This is explained by the large fluctuations in the hardness of the ingots studied. Nevertheless, the nature of the relationships examined is expressed quite distinctly.

With respect to steel C, which is characterized by a higher uniformity of hardness both longitudinally and in ingot cross section (within the interval studied), the v_{60} - s and v_{60} - t relationships obtained are more dependable.

The exponent y_v for feed is considerably larger than the exponent x_v for depth of cut. For steel C of H_{R_C} = 65, the average value of y_v is 0.57, while that of x_v is 0.25. For steel B of H_{R_C} = 59, we have y_v = 0.52 and x_v = 0.14, respectively. From this it follows that feed has a greater influence upon the cutting speed than does the depth of cut and that, in turning hardened steels, it is more desirable, from the point of view of cutting speed v_{60}, to work with higher t and lower s.

Figures 68, 70, and 72 show that, for all the steels investigated, the v_{60} - s ratio is expressed, in logarithmic coordinates, by a broken line consisting

Table 50

Values of Exponent y_v in Equation $v_{60} = \frac{C_s}{s^{y_v}}$

Steel C, $H_{RC}=65$			Steel B, $H_{RC}=49 \div 59$*; Steel A, $H_{RC}=49,5$		
t in mm	s in mm/rev	y_v	t in mm	s in mm/rev	y_v
0,10	0,05 ÷ 0,10	0,40	0,3	0,07 ÷ 0,155	0,20
0,10	0,10 ÷ 0,14	0,66	0,3	0,155 ÷ 0,307	0,22
0,25	0,05 ÷ 0,10	0,45	0,6	0,07 ÷ 0,260	0,19
0,25	0,10 ÷ 0,28	0,53	0,6	0,26 ÷ 0,395	1,30
0,50	0,05 ÷ 0,14	0,50	1,2	0,07 ÷ 0,155	0,26
0,50	0,14 ÷ 0,28	0,72	1,2	0,155 ÷ 0,610	0,53
1,00	0,05 ÷ 0,10	0,52	1,5	0,153 ÷ 0,305	0,42
1,00	0,10 ÷ 0,28	0,72	1,5	0,305 ÷ 0,610	0,90
—	—	—	2,4	0,07 ÷ 0,175	0,18
—	—	—	2,4	0,175 ÷ 0,395	1,02

*The data for t = 1.2 mm pertain to steel B of H_{RC} = 49; those for t = 1.5 mm are for steel A of H_{RC} = 49.5; all other data are for steel C of H_{RC} = 59.

of two straight lines with a single point of inflection, to the left of which the effect of feed upon cutting speed is less pronounced than to the right. This indicates that the value of the exponent y_v in the equation $v_{60} = \frac{C_s}{s^{y_v}}$ depends upon the feed. This conclusion is confirmed by Figs.73 and 74. For all the steels investigated, the curve 2 lies higher than the curve 1.

The absence of parallelism between the broken lines expressing the v_{60} - s ratios at various depths of cut (Fig.68 and 70) indicate that the exponent y_v is also dependent upon the depth of cut. The existence of a y_v – t ratio is obvious from Figs.73 and 74, although for steel B of H_{R_C} = 59 it is expressed less clearly than for steel C of H_{R_C} = 65.

For steel B of H_{R_C} = 59 (Fig.68), the point of inflection of the broken line

Table 51

Values of x_v Exponent in Equation $v_{60} = \frac{C_t}{t^{x_v}}$

Steel C, H_{R_C} = 65			Steel B, H_{R_C} = 49 – 50		
s, in mm/rev	t, in mm	x_v	s, in mm/rev	t, in mm	x_v
0,05	0,10 ÷ 0,50	0,12	0,07	0,3 ÷ 0,6	0,17
0,05	0,50 ÷ 1,00	0,24	0,07	0,6 ÷ 2,4	0,02
0,10	0,10 ÷ 0,50	0,18	0,155	0,3 ÷ 0,6	0,07
0,10	0,50 ÷ 1,00	0,21	0,155	0,6 ÷ 2,4	0,02
0,14	0,10 ÷ 0,50	0,17	0,225	0,3 ÷ 1,2	0,06
0,14	0,50 ÷ 1,00	0,34	0,225	1,2 ÷ 2,4	0,31
0,20	0,25 ÷ 0,50	0,26	0,307	0,3 ÷ 0,6	0,33
0,20	0,50 ÷ 1,00	0,38	0,395	0,6 ÷ 2,4	0,16
0,28	0,25 ÷ 0,50	0,23			
0,28	0,50 ÷ 1,00	0,42			

for v_{60} – s occurs at the same feed (s = 0.17 mm/rev) at various values for t. The broken line for t = 0.6 mm is an exception. The point of inflection in this instance appears at s = 0.26 mm/rev. For steel C of H_{R_C} = 65 (Fig.70), the points of inflection at t = 0.10, 0.25, and 1.0 mm correspond to a feed of s = 0.10 mm/rev and, at t = 0.5 mm, represents s = 0.14 mm/rev. For steel A of H_{R_C} = 49.5 (Fig.72), the point of inflection is at s = 0.305 mm/rev. This shows that, in the turning of hardened steels, the point of inflection on the curves for the v_{60} – s ratios appears, in general, at s < 0.2 mm/rev and that, consequently, the general rule is that the feed has a negligible influence upon the cutting speed (low values of the index y_v) at small feed ($s < 0.2$ mm/rev). At $s > 0.2$ mm/rev, the feed has a greater effect upon the cutting speed.

As the hardness of tempered steel increases, the point of inflection on the

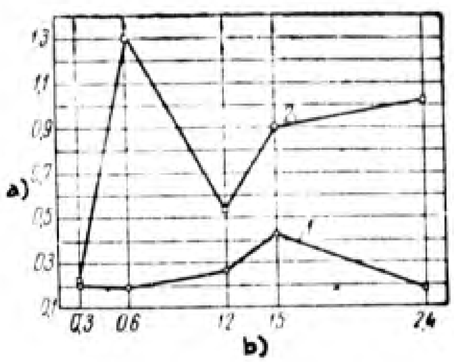

Fig.73 - Effect of Depth of Cut t and Feed s upon the Exponent y_v: 1 - Low interval s; 2 - High interval s. Turning of steels A and B of H_{R_C} = 49 - 59

a) Exponent y_v; b) Depth of cut t, mm

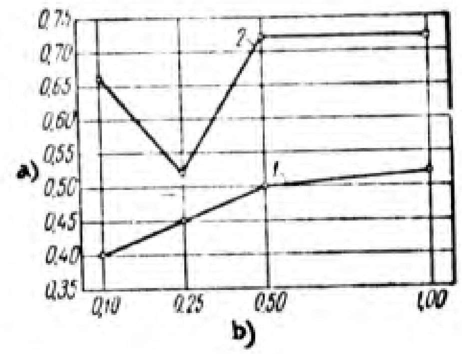

Fig.74 - Effect of Depth of Cut t and Feed s upon the Exponent y_v. 1 - Low interval s; 2 - High interval s. Turning of steel C of H_{R_C} = 65

a) Exponent y_v; b) Depth of cut t, mm

line v_{60} - s shifts leftward (toward smaller feeds). Whereas for steel C of H_{R_C} = = 65, the point of inflection is at s = 0.10 mm/rev, for steels A and B at H_{R_C} = = 49 - 59 it occurs at s = 0.305 and 0.175 mm/rev.

Let us proceed to the relationship between cutting speed and depth of cut (v_{60} - t). Figures 69 and 71 show that, in a logarithmic scale, the v_{60} - t ratio for the steels under study is expressed by a broken line consisting of two straight line segments with a single point of inflection. For steel C of H_{R_C} = 65, the influence of the depth of cut upon the cutting speed at all feeds is less pronounced to the left of the points of inflection than to the right thereof. For steel B of H_{R_C} = 59 (Fig.69), the lines describing the ratio v_{60} - t behave variously: At s = 0.07 mm/rev, the straight segment to the left of the point of inflection makes a larger angle with the abscissa than that to the right thereof. The line for s = 0.155 mm/rev is of the same nature. However, the line for s = 0.225 mm/rev is of the opposite nature. The nature of the v_{60} - t ratio obtained for steel C is more convincing.

The lack of parallelism between the broken lines representing the ratio v_{60} - t at various feeds indicates that the value of the exponent x_v at any given depth of cut depends upon the feed. This conclusion pertains equally to both steels, although the ratio x_v - s is more clearly marked for steel C (Fig.75). Moreover, Fig.75 demonstrates that the value of the exponent x_v is also dependent upon the depth of cut t (curve 2 is higher than curve 1).

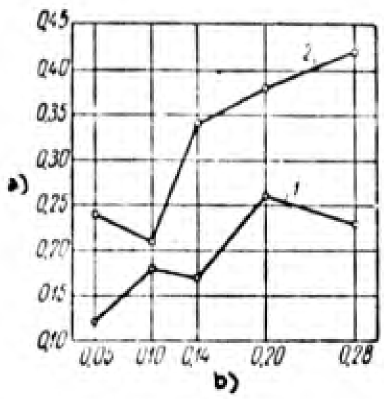

Fig.75 - Effect of Feed s and Depth of Cut t upon the Index x_v

1 - Low interval t; 2 - High interval t. Turning of steel C of H_{R_C} = 65

a) Exponent x_v; b) Feed s, mm/rev

In the case of steel C, (Fig.71), the point of inflection of the v_{60} - t lines at various feeds occurs at the same value for t = 0.50 mm. In the case of steel B (Fig.69), except for the line for s = = 0.225 mm/rev, the point of inflection of the lines expressing the relationship under examination occurs at t = 0.6 mm depth of cut.

Let us examine the data of other investigators. For hardened steels of H_{R_C} = = 47 - 56 (σ_t = 150 - 180 kg/mm^2), P.P.Grudov (Bibl.29) found that the feed exponent was dependent solely upon the depth of cut (and independent of the feed)

$$y_v = 0{,}47 \cdot t^{0{,}33}.$$

P.P.Grudov made use of the following values for the exponent with various depths of feed: x_v = 0.5 for $t < 1.25$ mm, x_v = 1.1 for t = 1.25 to 2.0 mm.

Let us employ P.P.Grudov's equation to determine the value of the exponent y_v for various depths of cut:

t, in mm	y_v
0.2	0.28
0.5	0.38
1.25	0.50
1.5	0.54
2.0	0.60

Consequently, according to P.P.Grudov, the exponent y_v for the feed is smaller than the exponent x_v for the depth of cut. An increase in the depth of cut will result in a rise in the exponents x_v and y_v.

N.S.Logak (Bibl.21) obtained the following values for the feed exponent for

Table 52

Values of the Exponents x_v and y_v

Material Machined	Limits of Intervals		Value of Exponents	
	Depth of Cut t, in mm	Feed s, in mm/rev	x_v	y_v
Hardened Kh12M steel, H_{R_C} = 45	0,25 ÷ 2,0	0,1 ÷ 0,3 0,3 ÷ 0,75	0,07	0,17 0,82
Hardened EI161 steel, H_{R_C} = 58 (hardened and oil quenched)	0,25 ÷ 0,5 0,5 ÷ 1,5 1,5 ÷ 2,0	0,09 ÷ 0,36	0,14 0,27 0,63	0,6

fine-turning of hardened steels (t = 0.2 mm): Steels of 50 - 52 H_{R_C} yielded y_v = = 1.21, whereas steels of H_{R_C} = 61 - 63 gave a value of y_v = 0.78. The exponent y_v diminishes as the hardness of tempered steel increases.

Table 52 presents the data by A.A.Maslov (Bibl.26). It will be seen that the feed exponent y_v is considerably larger than the depth-of-cut exponent x_v. An exception is the case of high t in the machining of steel of H_{R_C} = 58, where y_v = x_v. Moreover, the exponent x_v rises sharply with an increase in the hardness of the steel. So does the exponent y_v, but this regularity is not quite as clear.

Let us compare the ratio v = f(t and s) for hardened steels with the analogous expression for unhardened steels. First let us examine the index y_v.

Figure 76 depicts a curve for the ratio v_{60} - s plotted by A.A.Avakov (Bibl.39) for carbon steel of σ_t = 55 kg/mm^2, δ = 11.3%. He ran his experiments with high-speed cutters at a constant cutting depth (t = 2 mm) and a feed s varied in the interval from 0.015 to 3.06 mm/rev.

As we see, in the logarithmic scale, the v_{60} - s line has a point of inflection

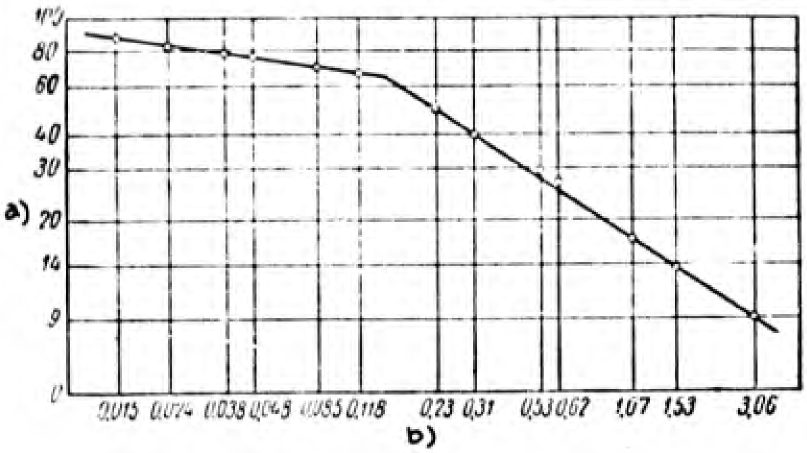

Fig.76 - Effect of Feed s upon Cutting Speed v_{60}; According to A.A.Avakov

a) Cutting speed v_{60}, m/min; b) Feed s, mm/rev

corresponding to a feed of approximately 0.12 mm/rev, the exponent being y_v = 0.146 to the left of the point of inflection, and y_v = 0.63 to the right thereof. Let us employ K_y to denote the relationship between the y_v exponents for the right and left segments of the v_{60} - s line, converging at the point of inflection. Then,

$$K_v = \frac{0,63}{0,146} = 4,3.$$

A break in the line for v = f(s) in the interval of low feeds has been found in many investigations of the machinability of unhardened steels. However, in these

Table 53

Characteristic Curves for the Ratio v = f(s) According to Various Sources

Source	Material Studied	Depth of Cut t, in mm	Range of Feed s, in mm/rev	Feed at Break in v = f(s) Line s, in mm/rev	Exponent y_v: To Right of Break	Exponent y_v: To Left of Break	Value of K_y
A.A.Avakov	Carbon steel, σ_t = 55 kg/mm^2; = 11.3 %	2,0	0,015÷3,06	0,12	0,63	0,146	4,3
I.M.Bes-prozvannyi	Carbon steel, σ_t = 57 kg/mm^2	0,5	0,1 ÷ 1,2	0,8	0,40	0,18	2,2
		1,0		0,2 0,4	0,22 0,44	0,18 0,22	1,2 2,0
		2,0		0,2 0,4	0,30 0,65	0,18 0,30	1,66 2,16
		4,0		0,2 0,4	0,30 0,65	0,18 0,30	1,66 2,16
Present Author	Hardened steel B, H_{R_C} = 59	0,3	0,07 ÷ 0,307	0,155	0,22	0,20	1,1
		0,6	0,07 ÷ 0,395	0,26	1,30	0,19	6.8
	Hardened steel B, H_{R_C} = 49	1,2	0,07 ÷ 0,610	0,155	0,53	0,26	2,04
	Hardened steel A, H_{R_C} = 49.5	1,5	0,153÷0,610	0,305	0,90	0,42	2,14
	Hardened steel B, H_{R_C} = 59	2,4	0,07 ÷ 0,395	0,175	1,02	0,18	5,65
	Hardened steel C, H_{R_C} = 65	0,10 0,25 0,50 1,00	0,05 ÷ 0,14 0,05 ÷ 0,28 0,05 ÷ 0,28 0,05 ÷ 0,28	0,10 0,10 0,14 0,10	0,66 0,53 0,72 0,72	0,40 0,45 0,50 0,52	1,65 1,18 1,44 1,39
A.A.Maslov	Hardened steel Khl2M, H_{R_C} = 45	0,25÷2,0	0,10 ÷ 0,75	0,30	0,82	0,17	4,8

investigations, the ratio K_y proved to be considerably smaller than that found by A.A.Avakov.

This problem was investigated in detail by I.M.Besprozvannyi (Bibl.38). Table 53 presents his data, together with the results of investigations of hardened steels pertaining to the index y_v. As we see, for all values of depth of cut except that for which t = 0.5 mm, I.M.Bresprozvannyi obtained two points of inflection, corresponding to s = 0.2 and 0.4 mm/rev, on each of his v - s curves. The ratio K_y at both points fluctuates from 1.2 to 2.16.

The data by the present author and by A.A.Maslov show that the line describing the v - s relationship is of the same nature for hardened steels as for unhardened types. For example, in the case of steel C, all depths of cut and feeds investigated show the jog in the v - s curve to be at the same point, representing a feed of s = 0.10 mm/rev (an exception is the line for t = 0.5 mm which has its point of inflection at s = 0.14 mm/rev). The K_y relationship here varies in approximately the same limits as those given by I.M.Besprozvannyi: from 1.18 to 1.65.

The K_y values for other grades of hardened steels investigated by the author and by A.A.Maslov are not very convincing. In any event, for these steels as well, the v - s line displays a point of inflection, and the exponent y_v on the right side of the bent line is larger than that on the left.

The agreement of the data by A.A.Avakov and I.M.Besprozvannyi with those by the author and by A.A.Maslov confirm that, contrary to the conclusion by P.P.Grudov, the influence of feed upon cutting speed in the turning of hardened steels is of the same nature as in the turning of unhardened steels.

Let us proceed to the index x_v. Table 54 presents data for the relation between cutting speed and depth of cut, for hardened and unhardened steels. As we see, the data by P.P.Grudov, A.A.Maslov, and the author for hardened steels coincide essentially. The v = f(t) lines reveal a point of inflection, to whose right the index x_v is larger than to the left. The ratios between the x_v indices for the right and left-hand segments of the v_{60} - t line (converging at the point of inflection), are denoted by K_x and approximate 2.0.

Consequently, the index x_v depends upon the depth of cut. The index x_v rises

Table 54

Characteristic Curves v = f(t) Ratio, According to Various Sources

Source	Material Studied	Feed s, in mm/rev	Depth of Cut t, in mm	Depth of Cut t, in mm, at Break in v = f(t) Line	Exponent x_v To Right of Break	Exponent x_v To Left of Break	Value of K_x
I.M.Besprozvannyi	Carbon steel, σ_t = 57 kg/mm²	0,4	0,5 ÷ 4,0	2,0	0,18	0,17	1,06
		0,8	0,5 ÷ 4,0	1,0 2,0	0,42 0,12	0,37 0,37	1,13 0,32
		1,2	0,5 ÷ 4,0	1,0 2,0	0,50 0,28	0,40 0,50	1,25 0,56
Present Author	Hardened steel C, H_{RC} = 65	0,05	0,10 ÷ 1,00	0,50	0,24	0,12	2,0
		0,10	0,10 ÷ 1,00	0,50	0,21	0,18	1,16
		0,14	0,10 ÷ 1,00	0,50	0,34	0,17	2,0
		0,20	0,25 ÷ 1,00	0,50	0,38	0,26	1,46
		0,28	0,25 ÷ 1,00	0,50	0,42	0,23	1,83
P.P.Grudov	Hardened steels, H_{RC} = 47 - 56	0,05 ÷ 0,30	0,2 ÷ 2,0	1,25	1,10	0,50	2,20
A.A.Maslov	Hardened steel, H_{RC} = 58	0,09 ÷ 0,36	0,25 ÷ 2,0	0,50	0.27	0,14	1,92
				1,50	0,63	0,27	2,33

with t. It also increases with the feed, as may be seen from the author's data for steel C (Fig.75).

According to the data by I.M.Besprozvannyi for unhardened steels, the relationship of the index x_v to feed is clearer than its relation to depth of cut. The index x_v rises with feed and depth of cut.

In any event, the effect of depth of cut upon cutting speed is of the same nature as in the case of unhardened steels. The effect of depth of cut upon cutting speed rises with any increase in depth of cut and feed.

The relationship between cutting speed, depth of cut, and feeds, for the hardened steels examined by the author in the H_{R_C} = 41 - 65 range is expressed by the equation

$$v_{60} = \frac{C_{v_{60}}}{t^{x_v} \cdot s^{y_v}}, \tag{5}$$

where v_{60} is the cutting speed in m/min to the 60-minute tool life;

$C_{v_{60}}$ is a constant;

t is depth of cut, in mm;

s is the feed, in mm/rev;

x_v is the exponent for depth of cut;

y_v is the exponent for feed.

The calculation of recommended cutting speeds (Appendix I) is based on x_v = = 0.25 and y_v = 0.45. The effective powers are determined by the formula

$$N_e = C_N \cdot t^{0,85} \cdot s^{0,35} \; Kw \; . \tag{6}$$

For constant $C_{v_{60}}$ and C_N, the following values are used:

Hardness of tempered steel, H_{R_C} .	38	41	44	47	50	52	54	56	58	60	62	65
$C_{v_{60}}$ . . .	50	40	31	27	22	19,5	17,5	16	14,5	12,5	7	2,8
C_N . . .	2,05	1,77	1,48	1,36	1,18	1,10	1,02	0,96	0,89	0,81	0,49	0,23

In determining the values of $C_{v_{60}}$, C_N, and the indices x_v and y_v, use was made not only of the author's experimental data but also of the work by N.S.Logak (Bibl.21), P.P.Grudov (Bibl.29), and by the NIBTN (Bibl.27).

Influence of the Mechanical Properties of Hardened Steels upon Cutting Speed

The machinability of steels, with consideration of the permissible cutting speeds, depends chiefly upon the chemical composition of the steels, their microstructure and mechanical properties. The effect of the chemical composition of steels upon their machinability, determining the cutting speed to permit a 60-minute tool life (v_{60}) are described as follows by the experimental data of E.I.Fel'dshteyn (Bibl.44):

Grade of steel being machined	Steel 15	Steel 40	У12	40Х	35ХГС	Р9	Р18
v_{60} in m/min	100	60	40	45	30	20	20
Coefficient	1,0	0,6	0,4	0,45	0,3	0,2	0,2

These data show that the machinability of steels is largely dependent upon their content of carbon and alloying elements.

It was established in the same study (Bibl.44) that the decisive factor in the machinability of steel of this composition is the structure resulting from heat treatment. The rate of dulling of the tool is intimately related to the form of pearlite in the machined steel. The best results are presented in cases of granular pearlite. With lamellar pearlite, the level of v_{60} speeds is considerably lower, particularly in the case of steels with a large content of carbon and alloying elements.

A comparison of the cutting speeds for steels of different structures investigated shows that the minimum wear of the cutting tool is observed in the machining of ferrite. In order of increasing wear, this is followed by: fine-granular pearlite, coarse-granular pearlite, lamellar pearlite, sorbitic pearlite, sorbite and troostite-sorbite.

Various investigators have made numerous attempts to find a direct relationship between cutting speed and mechanical properties of the material machined. For example, the NIBTN (Bibl.27) recommends the following formulas for unhardened steels (carbon and alloy):

$$v_{90} = \frac{C_\sigma}{\sigma_t^{n_\sigma}}\ m/min;$$

$$v_{90} = \frac{C_H}{H_B^{n_r}}\ m/min\ ,$$

where $n_v = 1.5$.

A relationship of the same nature was obtained by E.I.Fel'dshteyn (Bibl.44). The exponent of all steels tested by him was $n_v = 1.5$. A generalization of the results of all the steels investigated, including high-speed steels, for which poor machinability was characteristic, yielded $n_v = 2.2$. Only in the case of structural steels was a result of $n_v = 1.8$ obtained. An analysis of the experimental data led to the conclusion that the mechanical property characteristics σ_t and Hbn cannot serve as a foundation for a sufficiently accurate judgment as to the v_{60} cutting speed sought, since the errors in the determination of speeds with these formulas may attain 70%.

Let us now consider the hardened steels, The author's experimental data testify that the chemical composition of hardened steel has little effect upon its machinability. Steel A of $H_{R_C} = 49.5$ possesses approximately the same machinability as steel B of $H_{R_C} = 49$, although the alloying elements constitute 6.58 - - 7.66% in steel B, and 4.24 - 5.02% in steel A.

The fact that the composition of hardened steels does not affect their machinability was confirmed in the investigations by A.Ya.Malkin (Bibl.23) (for U10, U12, 40Kh, ShKh15, ShKh15G, OKhNM, OKhN3M and chromansil steels of $H_{R_C} > 49$) and by Ye.A.Belousova (Bibl.30) (for ShKh15, ShKh15G, 12KhN3, 9KhS, 40Kh and 45 steels of $H_{R_C} = 49 - 66$).

Figure 77 presents, in logarithmic scale, a curve of the relationship between the hardness of tempered steels of $H_{R_C} = 41 - 65$ and their machinability, expressed by the C_{v60} constant, for steels A, B, and C investigated by the present author. The curve shows that the effect of the hardness of tempered steel upon the cutting speed increases with increasing hardness. Thus, an increase by three Rockwell units in

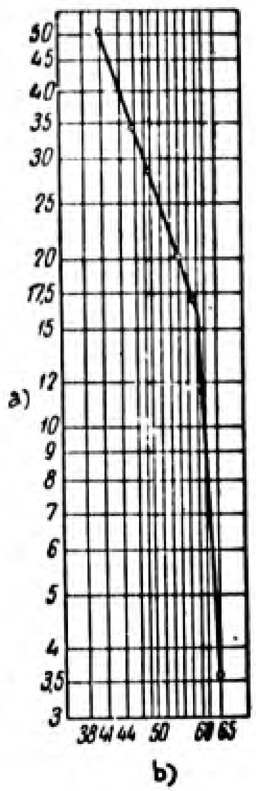

Fig.77 - Relationship Between the C_{v60} Constant and H_{RC} Hardness of Tempered Steels. Turning of steels A, B, and C of H_{RC} = = 41 - 65 by T15K6 cutters

a) Constant C_{v60}; b) Hardness of tempered steel H_{R_C}

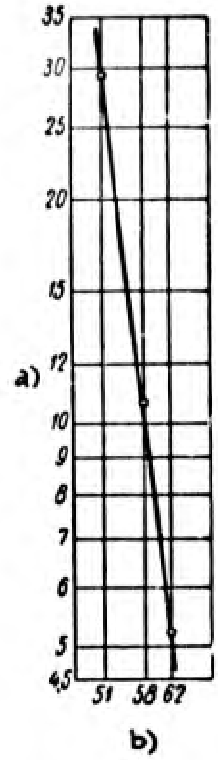

Fig.78 - Relationship Between the C_{v60} Constant and Hardness of Tempered Steels in the Interval H_{R_C} = 50 - 63. Data by N.S.Logak for T30K4 cutters

a) Constant C_{v60}; b) Hardness of tempered steel, H_{R_C}

steel hardness, from 41 to 44, results in a reduction from 51 to 40 in the C_{v60} constant, i.e., by approximately 22%, whereas a rise by three units from 62 to 65 results in a 60% drop in the C_{v60} constant (from 9.1 to 3.6).

The curve (Fig.77) shows a jog at the point representing H_{R_C} = 60. To the right of the jog the influence of the hardness of the steel upon its machinability is more pronounced than to the left thereof.

The $C_{v_{60}}$ - H_{R_C} relationship may be expressed by the equation

$$C_{v_{60}} = \frac{A'}{H_{R_C}^{n_v}}, \qquad (7)$$

where n_v = 3 for steels of $H_{R_C} \leq 60$, and n_v = 19 for steels of $H_{R_C} > 60$.

According to data by N.S.Logak (Bibl.21), the exponent for H_{R_C} is 9 for hardened steels of H_{R_C} = 50 - 63 (Fig.78).

These data for hardened steels permit the conclusion that the law of the effect of the mechanical properties of steel upon their machinability, which is known for unhardened steels, may be extended to all steels that are subject to machining. The effect of the hardness (or σ_t) of the machined steel upon the cutting speed increases progressively as one moves from one hardness interval (or σ_t interval) to the next higher. Whereas the exponent is $n_v < 2$ for unhardened steels, it becomes n_v = 3 for hardened steels of $H_{R_C} \leq 60$ and multiplies severalfold for $H_{R_C} > 60$.

The cutting conditions given in Appendix I are calculated for the n_v values obtained in the author's experiments.

Conclusions

1. The turning of hardened steels is governed by the basic law of the theory of the machining of metals, which is expressed by the equation

$$v = \frac{C}{T^m}.$$

The relative life index m describes the rate of change in the life of a tool with any change in cutting speed. The lower the index m, the greater will be the effect of change in cutting speed upon tool life, and vice versa.

2. In the machining of hardened steels, the relative tool life index m depends

upon the following factors: feed s, depth of cut t, ratio of depth of cut to feed $\frac{t}{s}$, true rake angle of cutter γ, working relief angle α, nose radius r, type of cemented carbide used to tip the cutter, and hardness of the tempered steel.

With an increase in s, t, and $\frac{t}{s}$, an increase in the index m is observed. The index diminishes with a rise in the true rake angle γ and in the nose radius r and with a diminution in the working relief angle α. For titanium-tungsten alloys the index m is lower than for the tungsten type, while it rises with an increase in the hardness of tempered steel.

The greatest influence upon the index m is that exerted by the hardness of the tempered steel, the feed, and the particular type of cemented carbide with which the cutter is tipped.

The relationship found between the relative tool life index m and the influencing factors was found to be of the same nature for hardened as for unhardened steels.

3. In the case of the hardened steels of H_{R_C} = 41 - 65 investigated by the author, the relationship between cutting speed, depth of cut, and feed may be expressed by the equation

$$v_{60} = \frac{C_{v_m}}{t^{x_v} \cdot s^{y_v}} \ m/min.$$

The exponent y_v is greater than the exponent x_v. This means that the feed affects the cutting speed more strongly than does the depth of cut. In the turning of hardened steels, as in that of the unhardened grades, it is more desirable to work at lower feeds and greater depths of cut.

The value of the indices x_v and y_v increases with an increase in the depth of cut t and the feed s. Inasmuch as the feed has a greater influence upon the cutting speed than does the depth of cut ($y_v > x_v$), it is more advantageous to work at higher $\frac{t}{s}$.

4. Hardened steels are machined at considerably lower cutting speeds than are

unhardened steels. The permissible cutting speed diminishes with an increase in the hardness of the tempered steel.

The cutting speeds employed in the studies of the machinability of hardened steels are the same as those at which machinists, who have introduced high-speed machining, run their equipment.

17. Surface Quality and Machining Tolerance

Hardened steels are now being turned in industry where rough grinding has normally been used, and there are particular conditions under which turning may even replace finish-grinding. Therefore, a knowledge of the nature of the influence of the machining of hardened steels upon surface quality and the condition of the surface layer of metal is of practical and scientific interest. Below we present the still limited experimental data available to shed light upon these questions.

Quality of the Machined Surface

Here we present the results of investigations on the degree of finish of the machined surface attained in the turning of hardened steels, as well as on the nature of the influence of various factors.

The author conducted this study with steel B of $H_{R_C} = 59$. The measurement of surface roughness was performed with an Abbott profilometer, presenting the rms deviation (H_{rm}) of the microscopic irregularities of the surface in micro-inches. The instrument gives readings in microns.

Rings were machined on the ingot tested. Hollow chamfers for the cutter were provided between each two rings.

All the tests except those devoted to determining the effect of the type of cemented carbide upon the surface finish were run with T15K6-tipped cutters. All the cutters were lapped.

The influence of the following factors upon the surface finish was investigated: speed v, feed s, nose radius r, true rake angle γ, type of carbide used for tipping the cutter, and lapping of the cutting portion of the tool.

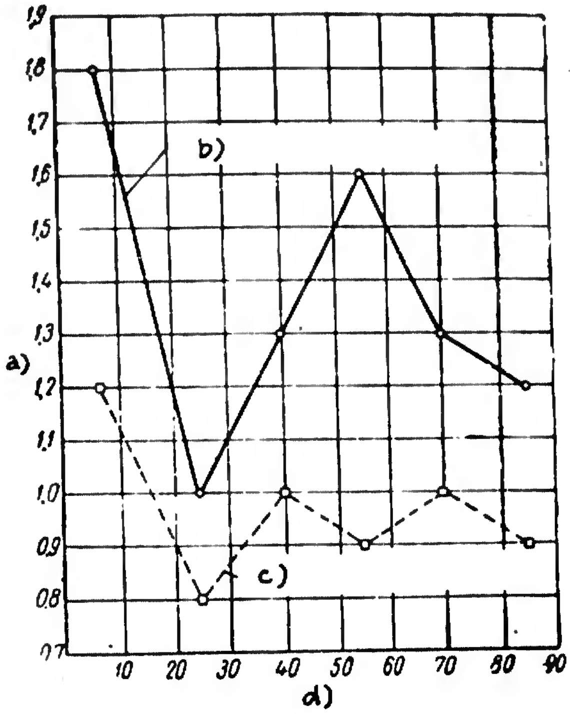

Fig.79 - Influence of the Cutting Speed upon the Finish of Machined Surfaces. Turning of steel B of H_{R_C} = 59, at t = 0.3 mm and s = 0.112 mm/rev. Cutter geometry: $\alpha = 6^o$, $\gamma = -5^o$, $\lambda = 0^o$, $\varphi = 45^o$, $\varphi_1 = 15^o$, r = 1.15 mm

a) Root-mean-square average irregularity, H_{rm}, microns;
b) Transverse roughness;
c) Longitudinal roughness;
d) Cutting speed v, m/min

Effect of Cutting Speed upon Surface Finish. The surface was machined at t = 0.3 mm and s = 0.112 mm/rev. The cutting speed was varied in the interval of v = 10 to 85 m/min. The experimental results (Table 55 and Fig.79) do not yield a clear picture, but do permit the conclusion that the cutting speed does not affect the surface finish.

This conclusion is confirmed by the study made by A.I.Isayev (Bibl.45). Figure 80 presents the results of his experiments on the turning of No.45 steel, heat-treated to various hardnesses. The range of cutting conditions employed (the lowest speed was v > 20 m/min) made it possible to work without producing a built-up edge. We see that the height of the fine irregularities diminished as harder material was machined. At cutting speeds of v > 140 m/min, the influence of the hardness of the machined material upon the roughness of the surface becomes negligible.

Experiments made with larger feeds yielded analogous results. It was found that, as the feed increased, the points on the curves at which a change occurs in the regularity of the effect of cutting speed upon the height of the irregularities of the surface move to the left (toward lower v).

The information of greatest interest in Fig.80 is the H_{mean} - v ratio for

Table 55

Influence of the Cutting Speed upon the Surface Finish

Cutting Speed v, m/min	Root-Mean-Square Average Irregularity H_{rm}, microns				
	Transverse Profile				Longi-tudinal Profile
	Measurement No.			Average Data	
	I	II	III		
10	1,7	1,8	1,8	1,8	1,2
25	1,0	1,0	0,9	1,0	0,8
40	1,6	1,2	1,1	1,3	1,0
55	2,0	1,4	1,4	1,6	0,9
70	1,5	1,3	1,2	1,3	1,0
85	1,3	1,1	1,1	1,2	0,9

No.45 steel heat-treated to a fairly high hardness of H_B = 500 (H_{R_C} = 51). Here, a change in the cutting speed has virtually no effect upon the size of the micro-roughnesses of the machined surface.

Influence of Feed upon Surface Finish. The surface was machined at t = 6 mm and v = 40 m/min. The feed was changed in the interval of s = 0.07 to 0.505 mm/rev. The results of the tests (Table 56) show that, as the feed is increased, there is a sharp rise in the roughnesses in the cross section. An impairment in surface finish is also noted in longitudinal section, but here it is considerably less pronounced.

Figure 81 presents two curves (Bibl.45) for cutting speeds v = 42.5 and 135 m/min for unhardened 40KhN steel. As we see, when the feed s is varied within the same range, the relation between the size of the roughnesses and the feed is of the same general nature for hardened steel (curve 3) as for unhardened steels.

The position of curve 3 below curve 1 and 2 (in experiments with both steels, the cutter nose radii were virtually identical, r = 1 mm) indicates that, in the

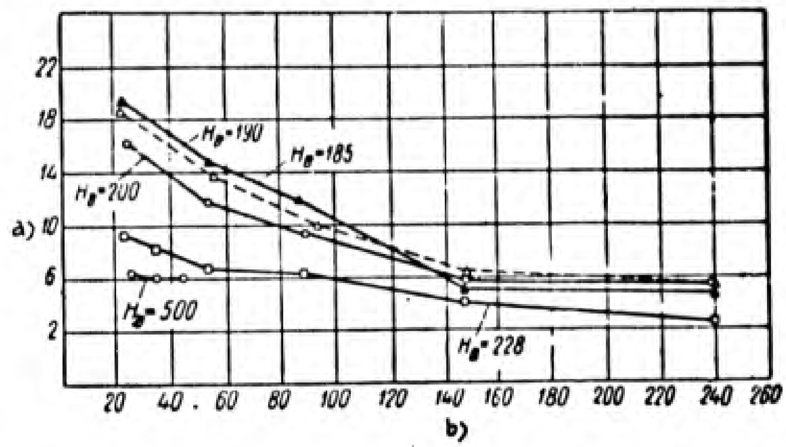

Fig.80 - Effect of Cutting Speed upon the Mean Height of Micro-Roughnesses of the Machined Surface

Turning of No.45 steel of various degrees of hardness, with t = 1 mm and s = 0.106 mm/rev. Geometry of the T15K6 cutters: $\alpha = 8^{\circ}$, $\gamma = 5^{\circ}$, $\lambda = 0^{\circ}$, $\varphi = 45^{\circ}$, $\varphi_1 = 15^{\circ}$, r = 1.5 mm. Data according to A.I.Isayev

a) Mean height of roughnesses, H_{mean}, microns;
b) Cutting speed v, m/min

machining of hardened steels, a higher surface finish is attained than with unhardened.

Table 56

Effect of Feed on Surface Finish

Feed s, in mm/rev	Root-Mean-Square Roughness H_{rm}, in Microns			
	Cross Section			Longitudinal Section
	Measurement No.		Average Data	
	I	II		
0,070	1,1	0,9	1,0	1,0
0,112	1,4	1,2	1,3	1,2
0,155	2,5	2,5	2,5	2,2
0,225	2,5	2,5	2,5	2,4
0,395	5,0	5,0	5,0	2,5
0,505	8,7	8,1	8,4	2,5

In steel B of H_{R_C} = 59, the lateral roughness may be related to the feed by the following expression:

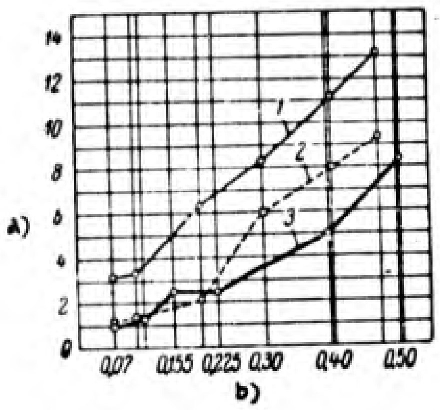

Fig.81 - Feed s versus Surface Finish in Turning of Hardened and Unhardened Steels (nose radius r = 1 mm)

1 - Unhardened 40KhN steel, v = 42.5 m/min; 2 - Same, v = 135 m/min; 3 - Steel hardened to H_{R_C} = 59 at v = 40 m/min (α = 6°, γ = -5°, λ = 0°, φ = 45°, φ_1 = 15°)

a) Root-Mean-square roughness H_{rm}, microns; b) Feed s, mm/rev

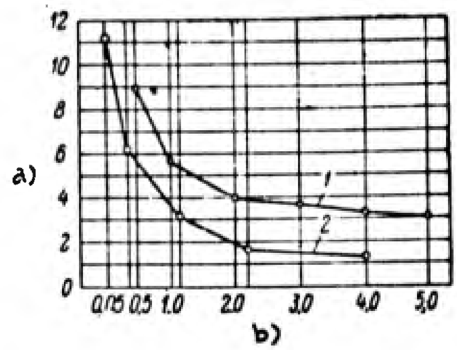

Fig.82 - Nose Radius r versus Surface Finish in Turning of Hardened and Unhardened Steels:

1 - Unhardened EI-107 steel (α = 8°, γ = 15°, φ = 45°, φ_1 = 15°, s = 0.35 mm/rev, v = 41.5 m/min; 2 - Hardened steel H_{R_C} = 59 (α = 6°, γ = 15°, λ = 0°, φ = 45°, φ_1 = 15°, s = 0.155 mm/rev, v = 38 m/min)

a) Root-mean-square roughness H_{rm}, microns; b) Nose radius r, mm

$$H_{rm} = 15{,}5 \cdot s^{1{,}07}. \qquad (8)$$

Effect of Nose Radius upon Surface Finish. The surface was machined under the following conditions: t = 0.6 mm, s = 0.155 mm/rev, v = 38 m/min. The nose radius r was varied from 0.05 to 4.0 mm. The tip of the cutter, for which r = 0.05 mm, had been lightly sharpened on a whetstone.

The results of the tests (Table 57) showed that an increase in the radius r leads to an increase in surface roughness both in cross section and longitudinal section.

Figure 82 shows that the nature of the influence of the radius r upon the

Table 57

Effect of Nose Radius upon Quality of Surface

Nose Radius r, mm	Root-Mean-Square Roughness H_{rm}, in Microns				
	Cross Section				Longitudinal Section
	Measurement No.			Average Data	
	I	II	III		
4,00	1,4	1,2	1,2	1,3	1,0
2,20	1,5	1,8	1,8	1,7	1,0
1,15	3,4	3,1	3,1	3,2	2,0
0,35	6,2	6,2	—	6,2	3,3
0,05	11,2	11,2	—	11,2	5,1

roughnesses of hardened and unhardened steels is essentially identical.

The relationship between lateral roughness and radius r for hardened steel B is

Table 58

Effect of True Rake Angle γ upon Surface Finish

True Rake Angle γ°	Root-Mean-Square Roughness in Cross Section H_{rm}, in Microns			
	Measurement No.			Average Data
	I	II	III	
+10	4,0	3,7	—	3,9
+6	4,5	4,7	4,2	4,5
0	5,0	5,0	5,0	5,0
−5	3,2	3,5	3,1	3,3
−8	3,7	4,5	3,6	3,9
−12	5,2	5,4	4,9	5,2

expressed by the equation

$$H_{rm}=\frac{2,8}{r^{0,63}}. \tag{9}$$

Effect of True Rake Angle upon Surface Finish. The surface was machined at $t = 0.6$ mm, $s = 0.307$ mm/rev, and $v = 30$ m/min. The true rake angle γ of the cut-

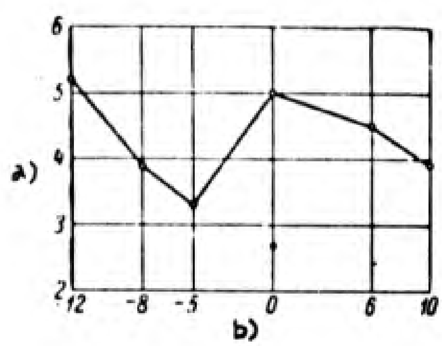

Fig.83 - True Rake Angle γ versus Surface Finish. Turning of steel B of $H_{R_C} = 59$ at $t = 0.6$ mm,

$s = 0.307$ mm/rev, and $v = 30$ m/min. Geometry of cutters: $\alpha = 6°$, $\lambda = 0°$, $\varphi = 45°$, $\varphi_1 = 15°$, $r = 1.15$ mm

a) Root-mean-square roughness H_{rm}, microns; b) True rake angle $\gamma°$

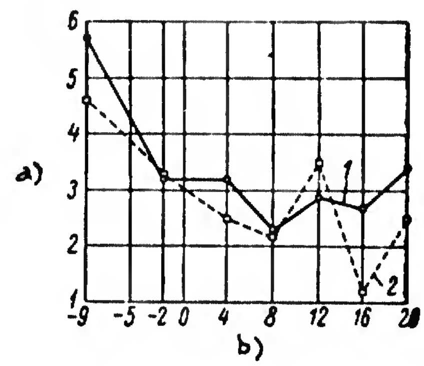

Fig.84 - True Rake Angle γ versus Surface Finish. Turning of unhardened EI-107 steel at $s = 0.2$ mm/rev. Geometry of cutters: $\alpha = 8°$, $\varphi = 45°$, $\varphi_1 = 12°$, $r = 1$ mm

1 - $v = 25.2$ m/min;
2 - $v = 141$ m/min

a) Root-mean-square roughness H_{rm}, microns; b) True rake angle $\gamma°$

ters was varied from +10 to -12°. The results of the tests are presented in Table 58 and Fig.83. The curve does not show any regular relation between true rake angle γ and the height of the roughnesses. In the specific condition of the given tests, the minimum H_{rm} was obtained at $\gamma = -5°$.

Analogous results were obtained by A.I.Isayev (Bibl.45) in an investigation of a number of grades of unhardened steels. The experimental data for EI-107 steel are presented in Fig.84. In the interval of negative γ values, the roughnesses become somewhat smaller as the true rake increases.

Influence of Type of Cemented Carbide Tip upon Surface Finish. The surface was machined under the following cutting conditions: $t = 0.6$ mm, $s = 0.155$ mm/rev, and v = 30 m/min. The following cemented carbides were tested: VK8, VK6, VK12, T15K6, and T21K8.

The experimental data (Table 59 and Fig.85) permit the conclusion that the

Table 59

Effect of Choice of Cemented Carbide upon Surface Finish

Cemented Carbide	Root-Mean-Square Roughness H_{rm}, in Microns				
	Cross Section				Longi-tudinal Section
	Measurement No.			Average Data	
	I	II	III		
VK6	2,7	2,7	—	2,7	2,0
VK8	2,5	2,5	—	2,5	1,9
VK12	3,5	3,7	3,6	3,6	2,2
T15K6	2,0	2,0	2,0	2,0	1,4
T21K8	2,5	2,2	—	2,3	1,7

titanium-tungsten carbides (T15K6 and T21K8) yield a surface of better finish than the tungsten carbides (VK6, VK8, and VK12). This may be explained by the fact that titanium-tungsten carbides are of higher hardness and wear resistance than tungsten carbides and have a lower tendency to pick up the chip. As a result, the cutting edge of a titanium-tungsten cutter retains for a longer period the shape obtained in the grinding and lapping process.

Effect of Lapping of Cutter upon Surface Finish. The tests were run with T15K6 cutters having the following tip geometry: $\alpha = 6^{\circ}$, $\gamma = -5^{\circ}$, $\lambda = 0^{\circ}$, $\varphi = 45^{\circ}$, $\varphi_1 = 15^{\circ}$, r = 1.15 mm. The surface was machined at t = 0.6 mm, s = 0.155 mm/rev, and v = 30 m/min. The results of the tests are presented in Table 60.

It will be seen that lapping of the cutter improves the finish of the machined surface.

Let us analyze the experimental data for hardened steel of $H_{R_C} = 59$. At t =

= 0.03 mm and s = 112 mm/rev, the mean H_{rm} for 18 readings was 1.3 microns. In some instances, the result was H_{rm} = 0.9 – – 1.1 micron; at t = 0.6 mm and s = = 0.07 mm/rev, H_{rm} = 1.1 and 0.9 micron. This level of roughness represents a Class 7 finish under GOST 2789-51, and approaches the upper limit near Class 8.

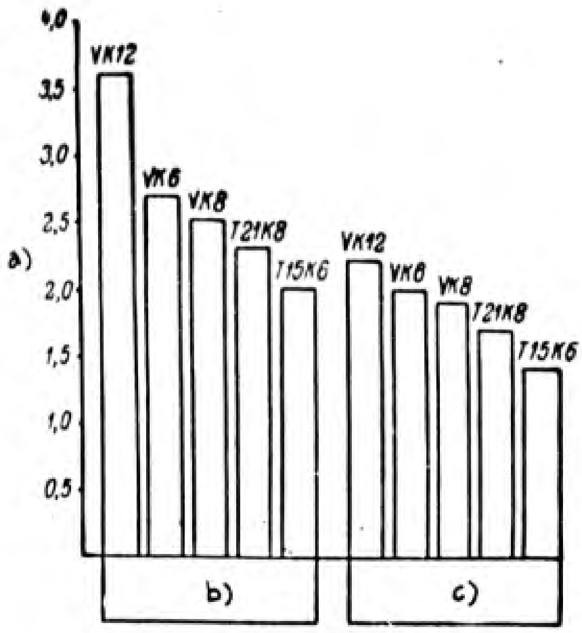

Fig.85 - Effect of Cemented Carbide upon Surface Finish. Turning of steel B of H_{R_C} = 59 at t = = 0.6 mm, s = 0.155 mm/rev, and v = 30 m/min. Cutter geometry: $\alpha = 6°$, $\gamma = -5°$, $\lambda = 0°$, $\varphi = 45°$, $\varphi_1 = 15°$, r = 1.15 mm

a) Root-mean-square roughness H_{rm}, microns; b) Lateral roughness; c) Longitudinal roughness

It is obvious that at feeds smaller than s = 0.07 mm/rev one can achieve H_{rm} < 0.8 microns, i.e., a surface of ▽▽▽8, or finish-ground. There is no difficulty in achieving surfaces of ▽▽5 and ▽▽6, since H_{rm} = 2 – 3 microns is obtained at relatively higher feeds s (to 0.3 mm/rev).

The following relationship exists between the height of the lateral roughnesses, the feed s, and the tip radius r for a steel of H_{R_C} = 59 (the feed varies in the interval of s = 0.07 to 0.505 mm/rev, and the nose radius of the cutter in the interval of r = 0.05 to 4.0 mm):

$$H_{rm} = \frac{19{,}1 \cdot s^{1{,}07}}{r^{0{,}63}} \text{ microns.} \quad (10)$$

The following formula is recommended by the Machining Committee (Bibl.46) for approximate determination of the height of the roughnesses in the turning of unhardened carbon and chromium steels with high-speed cutters

$$H_{max} = \frac{0,21 \cdot s^{1,07}}{r^{0,63}} \ mm. \qquad (11)$$

The H_{rm} is determined by means of eq.(10), and H_{max} by eq.(11). In order to

Table 60

Effect of Lapping of Cutter upon Surface Finish

Condition of Cutter	Root-Mean-Square Roughness H_{rm}, in Microns			
	Measurement No.			Average Data
	I	II	III	
Without lapping	7,7	5,0	5,0	5,7
With lapping	1,5	2,0	2,7	2,1
Without lapping	2,3	5,4	5,4	4,4
With lapping	2,7	4,2	—	3,4

compare the two equations, let us perform some transformations of eq.(10), taking $H_{max} = 4\ H_{rm}$. The equation then takes the form:

$$H_{max} = \frac{19,1 \cdot 4 \cdot s^{1,07}}{1000 \cdot r^{0,63}} = \frac{0,076 \cdot s^{1,07}}{r^{0,63}} \ mm. \qquad (12)$$

As we see, the constant for a steel hardened to $H_{R_C} = 59$ is about one-third that for unhardened steels.

The author's conclusions are confirmed by other investigations of the process of machining hardened steels. N.S.Logak (Bibl.21) produced a surface for which H_{rm} = 0.6 to 1.2 microns, i.e., Class 7 or 8 surface finish (close to Class 8) in the machining of high-hardness steel with cutters tipped with T30K4 and at cutting speeds allowing for a tool life of T = 60 min (t = 0.2 mm, s = 0.1 mm/rev). The superior results obtained by N.S.Logak at high feeds are explained by the fact that he employed T30K4 carbide, while the author ran his experiments with T15K6.

Ye.A.Belousova (Bibl.30), in turning high-hardness steels under average machining conditions (t = 1.0 to 2.0 mm; s = 0.15 mm/rev) achieved Class 7 surface finish. At lower feeds, surface finish was higher. It was found that, other conditions of machining being equal, an increase of 10 units on the Rockwell C hardness scale resulted in a 50% reduction in roughnesses.

In an investigation of the finish of the machined surface in turning hardened steels of H_{R_C} = 60 - 64 at high feeds (Kolesov's method), A.D.Makarov found (Bibl.24) that, when using cutters with a ratio of length of the side-cutting-edge to feed of $\frac{l}{s} > 5$ and feeds of s = 0.6 - 1.0 mm/rev, a Class 6 surface finish was always attained, whereas at smaller feeds (s = 0.1 to 0.4 mm/rev) and $\frac{l}{s}$ = 8 - 10 the resultant finish was not below Class 7.

In the turning of unhardened steels, the maximum effect upon the microgeometry of the machined surface is that exerted by the cutting speed v, the feed s, and the nose radius r. A distinctive characteristic of the machining of hardened steels is the fact that the cutting speed does not affect the size of the roughnesses. Otherwise, the major laws pertaining to unhardened steels, in terms of the microgeometry of the machined surface, may be applied to hardened steels.

Physical and Mechanical Properties of the Surface Layer of Metal

The question of the properties of the surface layer after the turning of hardened steels has attracted interest since the very first studies devoted to this problem. The experiments by N.I.Shchelkonogov (Bibl.28) showed that the turning of steel hardened to H_{R_C} = 61 did not change the structure of the surface layer of metal, but that its hardness increased somewhat. In his own tests, the author also noted an increase in the hardness of the surface layer of tempered steels after turning.

The data derived experimentally by Ye.A.Belousova (Bibl.30) in machining hardened steels of H_{R_C} = 50 to 65 are of considerable interest. It was found that the surface of hardened steel parts not only do not lose the hardness induced by heat treatment after turning on a lathe but becomes even harder as a result of work-hardening. The work-hardened layer is intimately bonded to the main bulk of the metal, and no metallographic transformations occur therein. The hardness of the work-hardened layer diminishes smoothly, from a maximum at the machined surface to the initial level acquired in hardening. The work-hardened layer is uniformly distributed throughout the work-hardened surface, and duplicates its profile. The depth of the work-hardening attains 100 microns, and the level of work-hardening comes to 1.1 - 1.4.

The hardness of the hardened steel has the maximum effect upon the depth and degree of work-hardening. A variation in the true rake angle γ from -5 to -30° causes the microhardness of the surface layer to be increased by as much as 10 - 15%, and this increase is the sharper, the lower the hardness of the material machined.

The feed s has little effect upon the depth and degree of work-hardening. In the entire range of feeds investigated (s = 0.15 - 0.84 mm/rev), the depth of work-hardening comes to 40 - 50 microns for steel hardened to H_{R_C} = 60 - 65, and 80 - 100 microns for steel hardened to H_{R_C} = 50. The degree of work-hardening fluctuates around 10%.

There is little difference in depth of work-hardening with changes in cutting speed v from 6 to 60 m/min. This depth is 80 - 100 microns for steel hardened to H_{R_C} = 50, and 30 - 40 microns for steel hardened to H_{R_C} = 60. Under these conditions, the degree of work-hardening changes by 10 - 30%.

The hardened layer is characterized by residual compressive stresses as high as 100 - 150 kg/mm². The upper layer of the machined surface is the most highly stressed. Deeper toward the axis of the part being machined, the residual stresses gradually diminish and disappear entirely at a depth of 100 to 150 microns.

A five-fold increase in feed s results in a rise in residual stresses by a factor of 2 - 2.5. The cutting speed has a significantly lower influence upon the magnitude of residual stresses. An increase in cutting speed v from 4 to 15 m/min results in reductions up to 20% in residual stresses. A further increase in cutting speed to 100 m/min has no effect in this direction.

The hardness of the material machined has a considerable influence upon the residual stresses. An increase of 10 points in the hardness of tempered steel (from H_{R_C} = 50 to H_{R_C} = 60) results in a doubling in residual stresses in the surface layer.

Residual compressive stresses in the surface layer take place at a true rake angle γ of -8 to -16°. At lower negative angles, tensile stresses may occur.

As shown in experiments by I.S.Shteynberg (Bibl.47), a change in the true rake angle affects not only the magnitude and sign of the residual stresses but, to a considerable degree, also the depth to which they are disseminated. When hardened 45KhNMFA steel is turned at a cutting speed of v = 75 m/min, a depth of cut t = = 0.5 mm, and a feed s = 0.5 mm/rev, an increase in the negative value of the true rake angle γ from -30 to -60° resulted in an increase in the depth of distribution of the residual stresses from 0.25 to 0.65 mm.

Let us adduce data from the literature on unhardened steels. As demonstrated by the experiments of P.Ye.D'yachenko (Bibl.48) (Fig.86), an increase by about a factor of 3.5 with feed s, from 0.23 to 0.76 mm/rev, caused an increase of 27% in the microhardness of the machined surface, in turning unhardened steel at cutting speeds of v = 50 and v = 100 m/min, 33% at speeds of v = 135 m/min, and 39% at v = = 170 m/min. Here we may trace the effect of cutting speed upon the degree of work-hardening of the top layer of metal. For example, for a feed of s = 0.6 mm/rev, an increase by about a factor of 3.5 in the cutting speed led to an increase of 25% in the microhardness of the machined surface.

Let us compare these data with the data presented previously for hardened steels of H_{R_C} = 50 - 65. For the latter, an increase of 5.6 times in the feed s yields a 10% increase in the degree of work-hardening, whereas for unhardened No.45 steel, an increase by a factor of 3.5 in the feed causes the work-hardening to rise by 27 - 39%.

A relationship of identical character is observed with respect to the effect of cutting speed upon degree of work-hardening. Whereas a 10-fold increase in cutting speed results in a 10 - 30% rise in the degree of work-hardening of tempered steels, an increase by only a factor of 3.5 in the cutting speed results in a 25% rise in degree of work-hardening of unhardened steel.

Consequently, the degree of work-hardening of the machined surface is considerably greater in the turning of unhardened steels than it is in the turning of hardened steels. This is also confirmed by the experimental data of I.S.Shteynberg (Bibl.47) with respect to the influence exerted by the true rake angle of a cutter upon the microhardness of the machined surface. Figure 87 shows that, in the case of unhardened steel, an increase in the negative true rake from -5 to -30° results in an increase in the microhardness of the machined surface from 450 to 560 kg/mm^2, or by 23%, whereas for hardened steels of H_{R_C} = 50 - 65, the same change in γ results in an increase of only 10 - 15% in microhardness (p.189).

It is interesting to compare the surface layer of turned hardened steel parts with that resulting from grinding. Studies by A.A.Matalin (Bibl.47) have shown that the grinding of hardened steels results in a considerable change in the structure of the surface layer of the steel. It is clear from the results of experiments with U8 steel that a layer of tempered metal, having a microhardness of 500 - - 700 kg/mm^2, is often found beneath the surface layer, 4 - 6 microns in thickness and of elevated hardness (800 - 1000 kg/mm^2).

Depending upon the grinding processes, the thickness of this layer may be anywhere from 0.02 - 0.20 mm. Under the tempered layer, the microhardness rises gradually to the initial hardness of the given steel, which is 800 - 850 kg/mm^2.

These experimental data permit the conclusion that, from the point of view of hardening of the machined surface, turning of hardened steels yields better results than grinding.

Let us turn to the question of residual stresses. Experiments (Bibl.47) have shown that in the turning of unhardened steels, the residual stresses fluctuate in

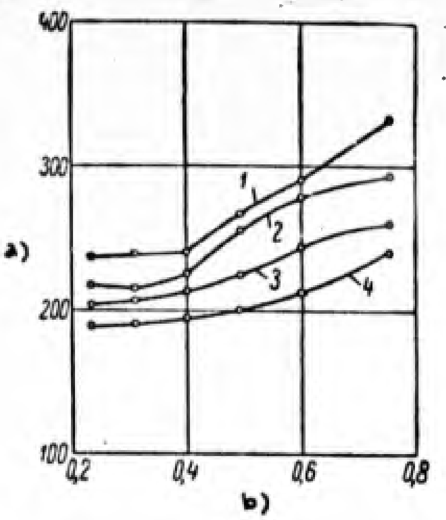

Fig.86 - Feed s and Cutting Speed v versus Microhardness of Machined Surface in Turning of No.45 Steel

1 - v = 170 m/min; 2 - v = 135 m/min; 3 - v = 100 m/min; 4 - v = 50 m/min

a) Microhardness H_d, kg/mm^2; b) Feed s, mm/rev

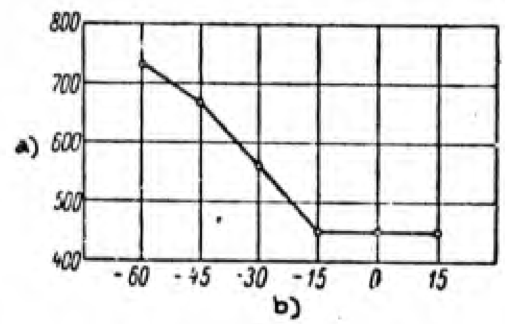

Fig.87 - Effect of True Rake Angle γ upon Microhardness of Machined Surface

a) Microhardness H_d, kg/mm^2; b) True rake angle γ^o

the 20 - 80 kg/mm^2 range, attaining 100 kg/mm^2 when a dulled cutter is employed.

The depth of residual stresses is 0.05 - 0.10 mm, although it may attain 0.65 mm when cutters of high negative true rake (of the order of -30^o) are used at high cutting speeds.

Experiments by P.Ye.D'yachenko and A.P.Dobychina (Bibl.47) have shown that, in the machining of 18KhNMA steel with a cutter of positive true rake and low cutting speeds (v = 6 to 20 m/min), residual tensile stresses are generated in the surface layer. However, with an increase in cutting speed, the magnitude of the tensile stresses diminishes, and at v = 200 to 250 m/min, the tensile stresses change to compressive stresses. Work at high cutting speeds (v = 500 - 800 m/min) results in the development of residual compressive stresses in the surface layer of 18KhNMA steel, whose magnitude rises with increasing cutting speed.

Analogous results were obtained in the experiments by P.Ye.D'yachenko and N.A.Podosenova (Bibl.47) in the boring of 30KhGS steel. An increase in cutting speed from 5 to 100 m/min results in a reduction in the residual tensile stresses. When the cutting speed is increased to 200 m/min, the residual tensile stresses become compressive stresses which increase with further increase in cutting speed.

The feed s and, in particular, the true rake angle γ play a particular role in determining the magnitude of the residual stresses in the surface layer of unhardened steels. The experiments by I.S.Shteynberg (Bibl.47) have shown that, in the turning of No.50 steel by cutters with $\gamma = -30^{\circ}$, depth of cut $t = 0.5$ mm, and cutting speed $v = 100$ m/min, a change in feed s from 0.1 to 0.5 mm/rev results in an increase in the residual compressive stresses from 10 to 25 kg/mm^2, and an increase in their depth from 0.17 to 0.35 mm.

We learn from the experiments by P.Ye.D'yachenko and A.P.Dobychina in the turning of 18KhNMA steel (Bibl.47) that, even at a cutting speed of $v = 150$ m/min, a negative true rake $\gamma = -30^{\circ}$ results in the appearance of residual compressive stresses; at $v = 750$ m/min and at a true rake γ of any negative value whatever, the surface layer develops compressive residual stresses, tensile stresses appearing only at high positive angles.

A comparison of hardened and unhardened steels shows that the effect of the feed s and the true rake γ upon the magnitude and sign of the residual stresses is identical in both. For these and other steels, a 5-fold increase in feed results in virtually the same degree of increase in residual stresses. In these and other steels, the appearance of residual compressive stresses in the surface layer is promoted by the use of tools with negative true rake angles.

However, hardened steels differ significantly from unhardened in that turning of the former is accompanied by the appearance of residual compressive stresses in the surface layer at speeds at which residual tensile stresses are caused in unhardened steels.

Effect of Cutter Wear upon Precision in Machining

One of the factors influencing the machining precision is dimensional wear of the cutter h_p, i.e., wear measured in a direction normal to the work surface. In the finish-turning of hardened steels, which is done at low feeds, the total error of machining is largely determined by tool wear.

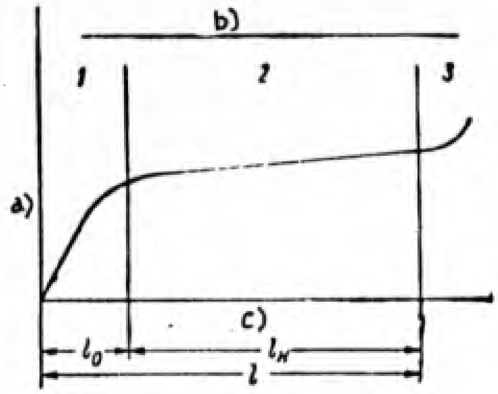

Fig.88 - Cutter Wear versus Cutting Path

a) Cutter wear, microns; b) Zone of wear; c) Cutting path, m

A distinction should be made between the zones of initial, normal and rapid tool wear (Fig.88). The laws governing wear differ significantly among these three zones. In zone 1, the wear proceeds considerably faster than in zone 2. The behavior of the tool in the wear zone 3 is less determinate. When rapid tool wear sets in, the finish of the work surface usually is sharply impaired.

The life of the tool in finish-machining is characterized by the length of the path traversed by the cutting edge in the metal (cutting path l).

The cutting path is calculated in accordance with the equation

$$l = v \cdot T \text{ m},$$

where v is the cutting speed in m/min;

T is the period of operation of the cutter, in min.

For turning on the lathe, the cutting path may also be determined from the equation

$$l = \frac{PD}{1000} \cdot \frac{L}{s} \text{ m},$$

where D and L are the diameter and the length of the machining work, in mm;

s is the feed in mm/rev.

In zone 2 (that of normal wear) the relationship between wear and cutting path

Table 61

Characteristics of Dimensional Cutter Wear

Test No.	Machined Diameter D, in mm	Cutting Speed v, in m/min	Cutting Time T, in min	Distance from Extreme Point of Cutter to Core Center, in mm		Dimensional Cutter Wear h_p, in μ	Cutting Path l, in m	Unit Cutter Wear h_o, in μ	Rate of Cutter Wear, in μ/min	Increase in Diam. of Part D, in μ/min
				Before Test	After Test					
1	174,2	10	110	3,805	3,769	36	1100	33	0,33	0,66
2	174,7	12	97	4,629	4,577	52	1160	45	0,54	1,08
3	176,5	14	73	5,000	4,950	50	1020	49	0,68	1.36
4	175,8	18	85	5,326	5,226	100	1530	65	1,18	2,36
5	173,55	22	30	4,285	4.233	52	660	79	1,73	3,46

is linear. This permits introduction of the concept of "Relative wear". Relative wear h_o is the term given to the dimensional wear of the tool in microns per 1000 m of cutting path:

$$h_o = \frac{1000 h_p}{l} \text{ microns.}$$

Table 61 contains the author's experimental data on the dimensional wear of a cutter in turning hardened steel C of H_{R_C} = 65 at a depth of cut t = 0.25 mm and a feed s = 0.053 mm/rev. The steel ingot was treated as a series of rings. Between each two adjacent rings, hollow chamfers were made for the cutter to run across. Before the tests, each ring was finish-turned at fine cut. The experiments were conducted with lapped T21K8 cutters having the following geometry: $\alpha = 12^\circ$, $\gamma = -5^\circ$, $\lambda = 0^\circ$, $\varphi = 45^\circ$, $\varphi_1 = 15^\circ$, r = 1.3 mm.

Let us compare the resultant data with the literature data on unhardened steels. Research (Bibl.49) has shown (Figs.89 and 90) that the relative cutter wear h_o is high when structural steels (No.45, ST5, 40Kh, and others) are finish-turned with a cemented carbide tool at low cutting speed. This wear declines as the

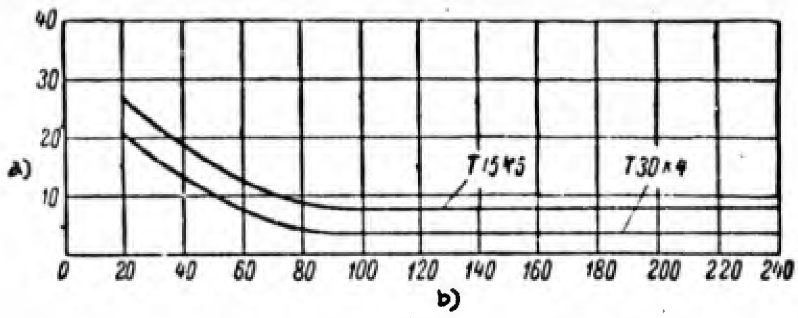

Fig.89 - Relative Cutter Wear versus Cutting Speed in Turning of Structural Steels in Annealed Condition

a) Relative wear h_o, microns; b) Cutting speed v, m/min

cutting speed rises and attains a minimum at some optimum value thereof. A further increase in the cutting speed results in an increase in relative wear.

When these steels are finish-turned in the annealed condition, the optimum cutting speeds lies in the range of v = 120 to 240 m/min (Fig.89). In this case, the optimum speeds for T15K6 are lower than for T30K4. The optimum speeds for the same steels are lower after they have been heat-treated: the range is v = 60 to 120 m/min. Here the cutting speed for T15K6 is also lower than for T30K4.

When these unhardened steels are machined in the annealed condition at optimum cutting speed (v = 120 tc 240 m/min) the relative wear of the cutter h_o is: 8 microns for T15K6 and 4 microns for T30K4. For the same steels in the heat-treated condition (range of optimum cutting speeds v = 60 to 120 m/min), the relative wear h_o for T15K6 changes as follows:

v, in m/min	h_o, in microns
60	16
110	8
220	18

It is evident from Table 61 that the relative wear h_o is high in the turning of hardened steels of H_{R_C} = 65. This wear is several times as great as in the case

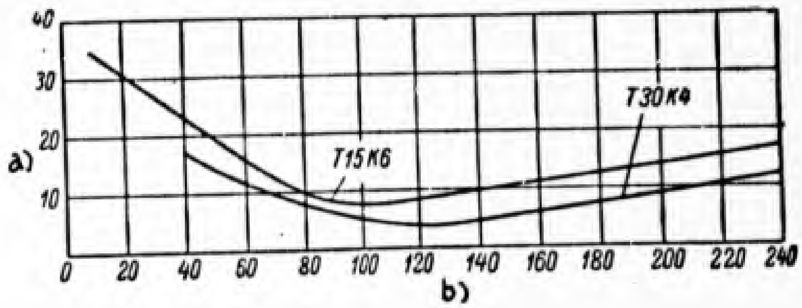

Fig.90 - Ratio of Relative Cutter Wear to Cutting Speed in Turning of Heat-Treated Structural Steels

a) Relative wear h_o, microns; b) Cutting speed v, m/min

of unhardened steels. In the range of cutting speeds investigated (v = 10 - - 22 m/min), the relative wear increases with increasing cutting speed.

The relative wear h_o is lower with reduced hardness of the tempered steel. Let us look at Fig.27. The flank wear of the T21K8 cutter h = 0.3 mm corresponds to a life of T = 35 min. This experiment was run with hardened steel of H_{R_C} = 59 (t = = 0.3 mm, s = 0.112 mm/rev, v = 56 m/min), using a cutter of working relief angle α = 6°. The dimensional wear of the cutter is approximately 31 microns:

$$h_p = h \cdot \text{tg}\,\alpha = 0{,}3 \cdot 0{,}105 \cdot 1000 = 31 \text{ microns.}$$

The cutting path was

$$l = v \cdot T = 56 \cdot 35 = 1960 \text{ m.}$$

The relative wear of the cutter was

$$h_o = \frac{1000 h_p}{l} = \frac{1000 \cdot 31}{1960} = 16 \text{ microns.}$$

The type of cemented carbide with which the cutter is tipped exerts a major influence upon the dimensional wear. In the machining of unhardened steels, the relative wear of T30K4 cutters is only one-half that of T15K6 (Figs.89 and 90).

According to data by A.D.Makarov (Bibl.24), T30K4 offers a small advantage over T15K6 in the turning of hardened steels. This superiority is expressed by a factor of 1.34. It should be noted that, according to the same source, the superiority of T30K4 over VK8 is 5.35.

When a given pass is to complete the finishing operation, one is faced with the problem of producing high finish and satisfactory tolerance simultaneously, not infrequently on surfaces of considerable size. In these conditions, the cutter must not be stopped, since otherwise steplike marks will show on the machined surface. Here, therefore, it is important to employ a carbide of high wear resistance, capable of machining surfaces of considerable size with minimum cutter wear, without stopping for adjustment to maintain the dimensions.

The maximum duration of the machining period for a workpiece within the required tolerance without adjusting the cutter is of practical interest. This time is determined by the formula

$$L = \frac{\delta D}{\Delta D} \cdot \frac{1000 \cdot v \cdot s}{\pi D} \ mm,$$

where δD is the specified tolerance in microns.

Let us determine the duration of work possible with hardened steels of $H_{R_C} = 65$, for a diameter D = 200 mm, cutting speed v = 14 m/min, and feed s = 0.1 mm/rev. Let us agree that we seek Class 2 and 3 tolerances. In the former instance, the tolerance (for D = 200 mm) comes to δD = 30 microns; in the latter case, to δD = 90 microns.

From Table 61 let us assume that ΔD = 1.36 micron. Then,

For the former case

$$L = \frac{30}{1{,}36} \cdot \frac{1000 \cdot 14 \cdot 0{,}1}{3{,}14 \cdot 200} \approx 50 \ mm;$$

For the latter case

$$L = \frac{90}{1{,}36} \cdot \frac{1000 \cdot 14 \cdot 0{,}1}{3{,}14 \cdot 200} \approx 150 \text{ mm}.$$

As we see, the duration of work that can be done without adjustment of the cutter is very short, due to the high dimensional wear. The calculation was made for T21K8. For T30K4, the relative wear will be less by at least a factor of 1.5 and, in this connection, the running length L of workpiece that can be machined will be, respectively, 75 and 225 mm.

The error in the shape of the cylindrical surface (taper) due to cutter wear consumes the entire Class 2 tolerance in the former case, and Class 3 in the latter. In reality, the precision of machining is influenced not only by tool wear but by other factors as well.

From this it follows that it is exceedingly difficult to ensure Class 2 precision in the turning of high-hardness tempered steels, and that this can be done only for a very small continuous running length of the workpiece. Class 3 tolerance is attainable over a longer length.

The reduction in the hardness of tempered steels is accompanied by a reduction in the relative tool wear, and by an increase in the possible running length of machining without stopping for adjustment of the cutter. According to experimental data, in the case of hardened steel of $H_{R_C} = 48 - 52$ (Bibl.21), the possible running length of a single pass for a diameter of D = 200 mm is L = 400 mm when a T30K4 cutter is used at a cutting speed of $v_{60} = 80$ m/min and a feed of s = 0.1 mm/rev. In this case, the dimensional wear of the cutter does not exceed one-half the tolerance for Class 2 precision.

Summary

1. A distinctive feature of the process of turning hardened steels is that it produces surfaces of high finish. When steels hardened to high hardness are ma-

chined at low feeds, the resultant surface is comparable to a finish-ground surface (Class 8 under GOST 2789-51). The production of a surface corresponding to rough-ground is achieved with relatively high feeds, attaining s = 0.3 mm/rev.

2. As the hardness of the tempered steel rises, the obtainable finish of the machined surface rises. It is easier to achieve this degree of surface finish for hardened than for unhardened steels.

3. In the case of hardened steels, turning may be used in place of rough-grinding if average feeds are employed (s = 0.15 to 0.3 mm/rev) and in place of finish-grinding in work with low feeds ($s \leq 0.1$ mm/rev).

Given cutters of specific geometry, rough-grinding may also be replaced by turning at high feeds, which simultaneously results in high output.

4. In the turning of hardened steels, changes in cutting speed do not affect the surface roughness.

The true rake angle γ has no significant influence upon the surface finish. A better finish is provided by cutters tipped with titanium-tungsten carbides. The carbide T30K4 is superior to T15K6 in this respect. Lapping of a cutter improves its finish. In the turning of hardened steels, the lateral roughness is higher than the longitudinal.

5. In the turning of hardened steels, the surface layer of the metal undergoes work-hardening. The work-hardened layer is firmly bonded to the main body of the metal and undergoes no structural transformation. The hardness of the work-hardened layer diminishes smoothly from a maximum on the machined surface to the initial hardness acquired by the metal in hardening. The major factors affecting the depth and degree of work-hardening are the true rake γ and the hardness of the material machined. The degree and depth of work-hardening rise with negative value of the top rake γ. The feed and cutting speed have little effect upon the depth and degree of work-hardening.

6. The degree of work-hardening of the machined surface is considerably less

in the machining of hardened steels than in that of unhardened steels.

7. The hardened layer is characterized by the formation of residual compressive stresses. The exterior layer of the metal is the most highly stressed. On moving toward the axis of the part, the residual stresses diminish steadily and disappear completely at a depth of 0.1 - 0.15 mm.

The residual stresses increase with an increase in the feed and hardness of the tempered steel. In contrast thereto, the cutting speed has a negligible effect upon the residual stresses.

8. A negative top rake results in compressive residual stresses in the surface layer.

9. In the turning of hardened steels, residual compressive stresses are obtained in the surface layer at fairly low cutting speeds, producing residual tensile stresses in unhardened steels.

10. In the machining of hardened steels, the relative wear of the cutter is high, greatly exceeding the wear in the machining of unhardened steels. As the hardness of the hardened steel is diminished, the relative wear of the cutter declines.

The cutting speed and the type of cemented carbide with which the cutter is tipped have a major influence upon the relative wear. The wear increases with an increase in cutting speed and is considerably lower for titanium-tungsten carbides than for the tungsten group. From the viewpoint of wear, T30K4 enjoys superiority over other carbides in the titanium-tungsten group.

11. The taper of the machined cylindrical surface, determined by the cutter wear, is quite considerable in the turning of hardened steels. For steel of H_{R_C} = = 65 and a machining diameter of 200 mm, the taper takes up the entire Class 2 tolerance over a running machining length of 75 mm (without intermediate adjustment of the cutter for dimensions) and Class 3 tolerance over a length of 225 mm.

With reduction in the hardness of the machined steel, the relative wear of the tool is reduced, making it easier to achieve high precision.

The closeness of tolerance is affected not only by tool wear but also by many other factors. Therefore, tolerances of Class 2 and 3 are achievable only over short running lengths (shorter in the case of Class 2) in the turning of steels brought to high hardness.

18. Lateral Forming on the Lathe

Great difficulties are involved in the lateral shaping of hardened steels by cemented carbide cutters. The removal of a wide and thin layer of metal is accompanied by excessive vibrations or chattering, resulting in a premature dulling of the cutter, crumbling-out of the cutting edge, and fissures in the carbide bar.

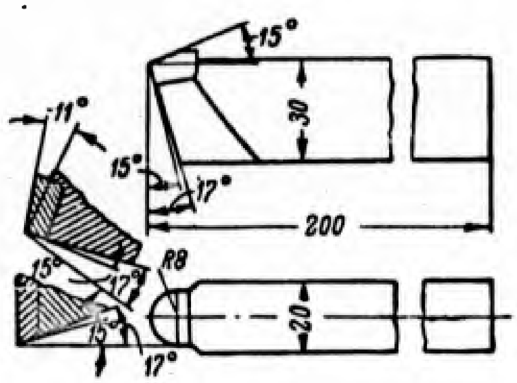

Fig.91 - Carbide-Tipped Shaping Tool for Use on Lathe

On the basis of a number of investigations of the process of turning of steels, it may be calculated that the conditions for the shaping of hardened steels on the lathe will be more dependable if electric current is introduced into the cutting zone.

A.V.Silant'yev (Bibl.50) has performed such a study of the lateral shaping of ShKh15 steel hardened to H_{R_C} = 60 to 62, with introduction of low-voltage electric current into the cutting zone.

The experiments were conducted with carbide cutters whose cutting edge was shaped in the form of a semicircle of radius 8 mm (Fig.91). The cutters were ground on a special fixture designed and made at the Il'yich Works for attachment to a universal tool grinder, the purpose of the fixture being to ensure a uniform working relief angle all along the cutter. The experiments were run on a modified lathe with a center height of H = 210 mm, driven by a DC motor with a power of N = 8 kw and n = 1560 rpm. The NDSh 1500/750 machine (N = 9 kw, n = 970 rpm, v = 6 - 12 v, I = 1500/750 amp) with a rheostat for adjustment of voltage, was used to introduce low-voltage current into the cutting zone.

A.V.Silant'yev came to the following conclusions:

1. Of the carbides tested, T5K10, T15K6, VK6 and VK8, used at a cutting speed of v = 25 m/min and a feed of s = 0.027 mm/rev, VK6 had the longest life and the highest resistance to crumbling-out of the cutting edge. The introduction of low-voltage current into the cutting zone reduced the number of cases of crumbling-out of the cutting edge of the cutter.

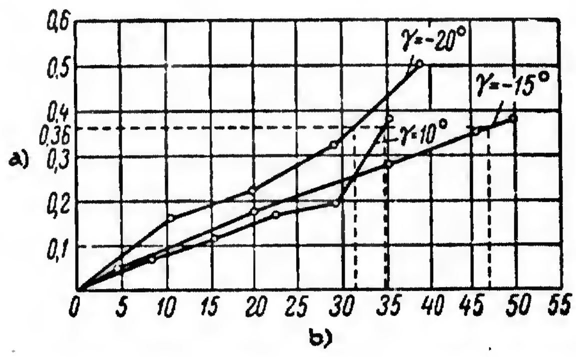

Fig.92 - Influence of Top Rake of Cutter Tipped with Hard Alloy VK6 upon Flank Wear. Shaping of Hardened ShKh15 steel of H_{R_C} = 60 to 62

a) Flank wear of cutter h, mm; b) Tool life T, min

2. At a cutting speed of v = = 18 to 19 m/min, a feed of s = = 0.03 mm/rev, a current of I = = 600 amp, and a flank wear of h = = 0.36 mm, the maximum life was displayed by cutters with a top rake of γ = -15° (Fig.92).

Work with cutters with γ = -10° proved impossible, due to the crumbling-out of the cemented carbides on the cutting edge.

If the working relief angle along the profile of the cutting portion has variable values, excessive chattering develops, and the cutter dulls prematurely.

3. For each cutting condition there is an optimum current, at which the tool life reaches a maximum (Fig.93).

4. The introduction of low-voltage current of optimum amperage into the cutting zone provides stability to the process. This increases the tool life by a factor

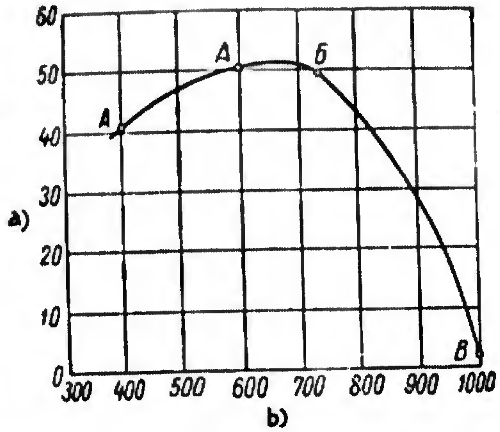

Fig.93 - Influence of Strength of Current Introduced into the Cutting Zone upon the Life of Cutters Tipped with Hard Alloy VK6, in Lateral Shaping of Hardened ShKhl5 Steel of H_{R_C} = 60 - 62, at v = 19 m/min, s = 0.027 mm/rev, and Cooling

A - Heavy vibration, work impossible, but cutting edge unimpaired; B - Cutter capable of further work; C - Fusion of cutting edge

a) Cutter life T, min; b) Current I, amps

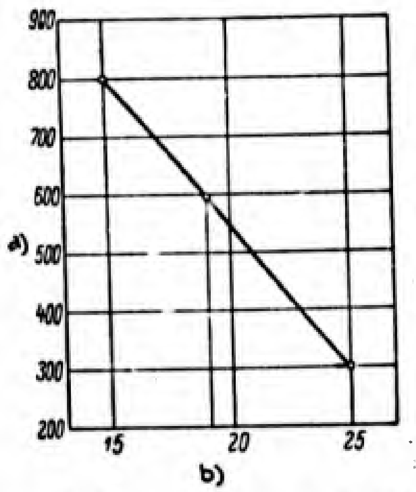

Fig.94 - Effect of Cutting Speed upon Optimum Current in Lateral Shaping of ShKhl5 Steel Hardened to H_{R_C} = 60 - 62, at a Feed s = 0.027 mm/rev, and Cooling

a) Optimum current I, amp; b) Cutting speed v, m/min

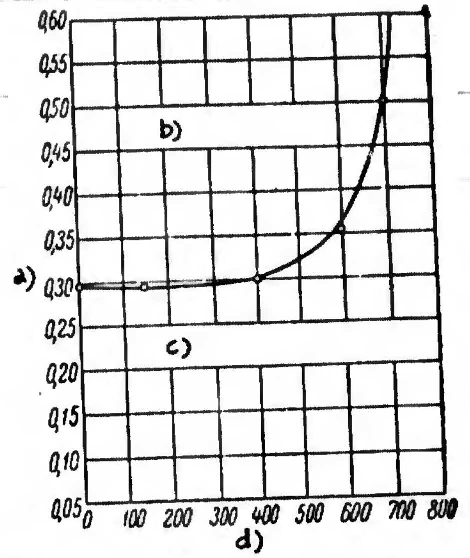

Fig.95 - Effect of Current upon Permissible Wear of Cutter Flank in Vibration-Free Work. Lateral forming of ShKhl5 steel hardened to H_{R_C} = 60 - 62 (v = 19 m/min, s = 0.027 mm/rev, α = 15°, γ = -15°)

a) Flank wear h of cutter, mm; b) Vibration zone; c) Zone of no vibration; d) Current I, amp

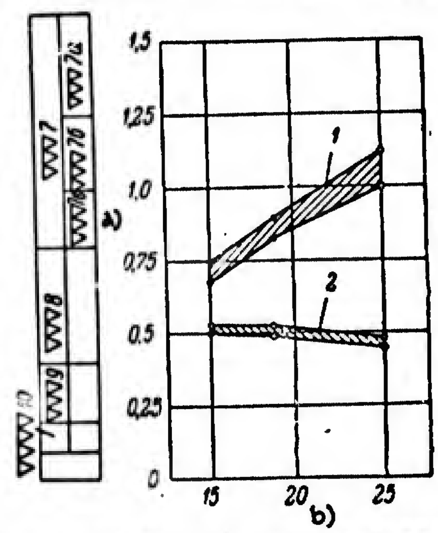

Fig.96 - Effect of Cutting Speed upon Finish of Machined Surface in Lateral Shaping of ShKhl5 Steel Hardened to H_{R_C} = 60 - 62

1 - Work without use of current;
2 - Work with introduction of optimum-strength low-voltage current into cutting zone

a) Root-mean-square roughness H_{rm}, microns; b) Cutting speed v, m/min of 1.5 - 2.5.

5. The optimum current diminishes as the cutting speed is increased (Fig.94).

6. Introduction of low-voltage current of optimum strength into the cutting zone extends the zone of chatter-free machining and makes it possible to raise the permissible flank wear, taking dulling as the criterion (Fig.95).

7. In form-turning of high-hardness tempered steel, the finish of the machined surface is raised one class (from Class 7 to Class 8) by the introduction of electric current of optimum strength into the cutting zone (Fig.96).

In work without current, an increase in the cutting speed v from 15 to 25 m/min results in a reduction of surface finish by one class. In work with the introduction of optimum current into the cutting zone, a change in the cutting speed within the same limits, will cause virtually no change in the surface finish, which remains in Class 8.

Work without current or with excessive current results in an extensive increase in flank wear, leading to a reduction in the finish of the machined surface.

8. In the forming of high-hardness steel on the lathe, any increase in the feed causes an increase in the ratio of radial to tangential force $\frac{P_y}{P_z}$ (Fig.97). As this ratio increases, an increase occurs in the instability of the process with respect to the probability of chatter.

The experimental data yield the following ratios of the forces P_z and P_y to the lateral feed s, for hardened ShKhl5 steel of H_{R_C} = 60 - 62:

$$P_z = C_z \cdot s^{0.5},$$
$$P_y = C_y \cdot s.$$

The lateral feed has a greater effect upon the force P_y than upon the force P_z.

According to data by G.N.Titov*, the relationships between these forces and the

*Titov,G.N. - Analysis of Profiles and Procedures for Use of Shaping Cutters. Mashgiz, 1941.

feed s for the same ShKhl5 steel, not subjected to hardening, have the following form:

$$P_z = C_z \cdot s^{0.75},$$
$$P_y = C_y \cdot s^{0.65}.$$

In the given instance, the feed has a virtually identical effect upon both forces.

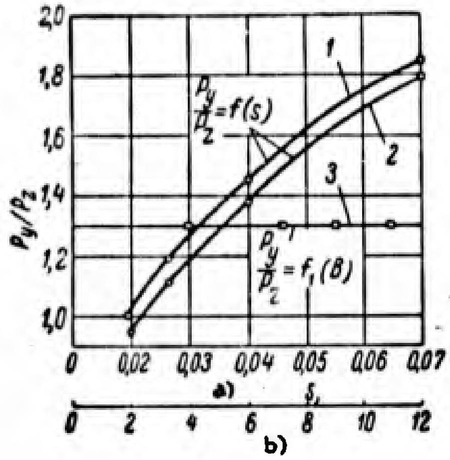

Fig.97 - Dependence of the $\frac{P_y}{P_z}$ Force Ratio on the Lateral Feed s and Width of Cut B

1 - v = 19 m/min, B = 11.2 mm;
2 - v = 25 m/min, B = 11.2 mm;
3 - v = 19 m/min, s = 0.027 mm/rev

a) Lateral feed s, mm/rev;
b) Width of cut, V mm

In the shaping of unhardened steels on a lathe, an increase in feed eliminates vibrations in the system machine tool - - workpiece - tool. Conversely, in the machining of hardened steel, an increase in feed results in a pronounced rise in chattering. Consequently, in contrast to the machining of unhardened steels, stability of the process in the shaping of hardened steel is achieved by reduction of the lateral feed to a given level.

An examination of the $\frac{P_y}{P_z} = \frac{C}{s^{0.1}}$ ratio of forces (for unhardened ShKhl5 steel) and the $\frac{P_y}{P_z} = C \cdot s^{0.5}$ (for hardened ShKhl5 steel of H_{R_C} = 60 - 62) demonstrates that, as the lateral feed increases there is somewhat of a reduction in the $\frac{P_y}{P_z}$ ratio in the machining of unhardened steel and a considerable increase in the cutting of hardened steel. The nature of the $\frac{P_y}{P_z} = f(s)$ relation may serve as a criterion for the stability of the process of lateral shaping of hardened steels on the lathe.

Investigations have shown that the introduction of electric current into the cutting zone facilitates a reduction in the amplitude of fluctuation of the forces P_y and P_z. Work at an optimum current of I = 600 to 800 amp makes it possible to reduce the amplitude of fluctuation of the force P_y by 33 - 44%. Moreover, some reduction in the average magnitude of this force is observed.

19. Turning with Cutters with Mineroceramic Tips

The highly satisfactory properties of the TsM-332 mineroceramic for cutting purposes and its superior resistance to heat over the best titanium-tungsten carbides is the justification for the use of this new tool material in the machining of hardened steels. Industry can already offer examples of the successful employment of mineroceramics in the turning of hardened steels. An investigation performed by V.I.Zhikharev (Bibl.51) provides the necessary understanding of the tool geometry, the tool life relationships, and certain other problems involved in the process of machining hardened steels by mineroceramics. Let us present the major conclusions from this investigation.

1. In the turning of steels brought to high hardness (H_{R_C} = 50 - 59), the wear of cutters tipped with TSM-332 mineroceramics is accompanied by cratering on the face and the appearance of zones of wear on the flank.

2. Curves for the wear of cutters tipped with mineroceramics are of the same nature as those for cermets (Fig.98). The curve for the mineroceramic reveals areas representing initial, normal, and rapid wear.

3. In turning hardened steel brought to H_{R_C} = 52 - 54, the maximum life was that revealed by cutters having a top rake of $\gamma = -5^\circ$ (Fig.99). Cutters with $\gamma = +5^\circ$ worked quietly, and flank wear was uniform. However, intensive crumbling-out of the cutting edge was observed. Vibrations arose at high negative top rakes.

4. With an increase in the relief angle α, the life of the cutter increases (Fig.100). It is recommended that relief angles not larger than $\alpha = 15^\circ$ be employed, since premature chipping of the cutting edge was noted at $\alpha = 18^\circ$.

5. The cutter life diminishes (Fig.101) as the complement of the side-cutting-

edge angle φ is raised from 20° to 60°. It is recommended that φ = 30° be used. At φ < 30° and at insufficient rigidity of the system machine tool - workpiece - - tool, vibrations arise that lead to a crumbling-out of the cutting edge of the cutter.

6. An increase in the nose radius r has a significant influence upon the life (Fig.102). At small r, the flank wear is uneven and is concentrated primarily at the cutter nose. The value that should be employed is r = 1.5 to 2.0 mm.

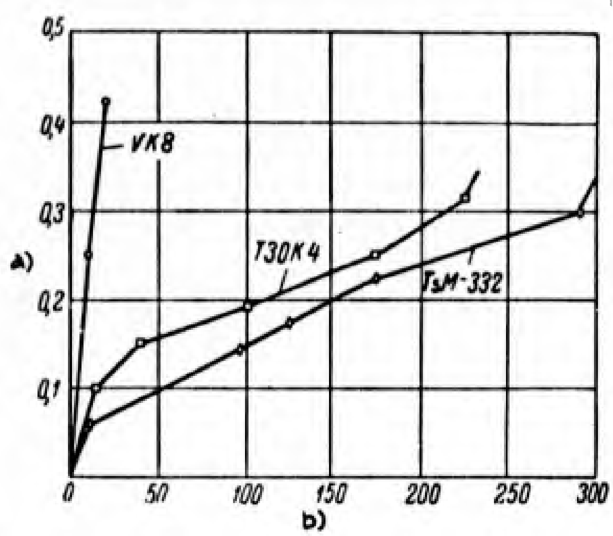

Fig.98 - Ratio of Flank Wear of Cutter to Duration of Use. Turning of steel hardened to H_{R_C} = 54 under following machining conditions: t = 0.75 mm, s = = 0.102 mm/rev, v = 50 m/min. Geometry of cutting edge of tool: α = 15°, γ = -5°, λ = 0°, φ = 30°, φ_1 = 15°, r = 1.5 mm

a) Flank wear h, mm; b) Cutter working time T, min

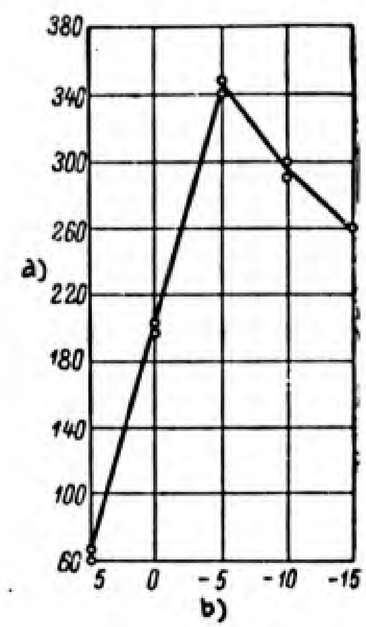

Fig.99 - Effect of Top Rake upon Life of Cutters Tipped with Mineroceramics. Turning of steel hardened to H_{R_C} = 52 - 54, at t = 0.75 mm, s = 0.102 mm/rev, and v = 70 m/min. Cutter geometry: α = 9°, φ = 45°, φ_1 = 15°, λ = 0°, r = 1.5 mm. Flank wear of cutters h = 0.4 mm

a) Cutter life T, min; b) True rake angle γ°

7. For cutters tipped with TsM-332 mineroceramic, there are optimum cutting speeds whose level depends upon the hardness of the tempered steel. For example, in

steels of H_{R_C} = 53 - 55, the optimum speeds lie in the v = 45 - 60 m/min range (Fig.103). Deviations from this range in the direction of decrease or increase in

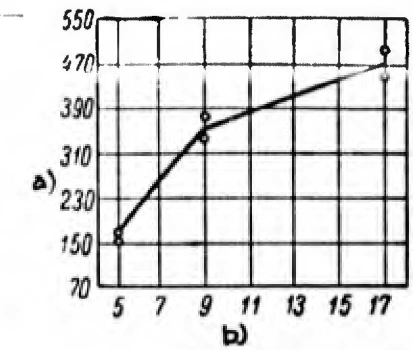

Fig.100 - Effect of Relief Angle upon Life of Cutters Tipped with Mineroceramics. Turning of steels hardened to H_{R_C} = 51 - 53,

t = 0.75 mm, s = 0.102 mm/rev and v = 70 m/min. Cutter geometry: $\gamma = -5^{\circ}$, $\lambda = 0^{\circ}$, $\varphi = 45^{\circ}$, $\varphi_1 = 15^{\circ}$, r = 1.5 mm. Flank wear of cutters h = 0.4 mm

a) Cutter life T, min; b) Relief angle of cutter α°

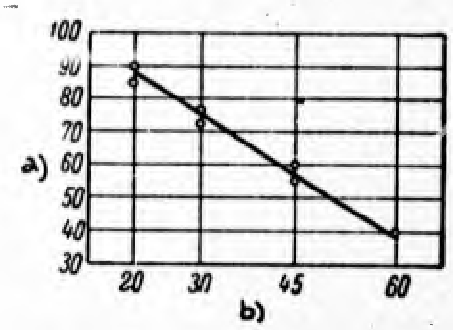

Fig.101 - Effect of End-Cutting-Edge Angle upon Life of Cutters Tipped with Mineroceramics. Turning of steels hardened to H_{R_C} = 51 - 53 under following cutting conditions: t = 0.75 mm, s = 102 mm/rev, v = 100 m/min. Geometry of cutting portion of tool: $\alpha = 15^{\circ}$, $\gamma = -5^{\circ}$, $\lambda = 0^{\circ}$, $\varphi_1 = 15^{\circ}$, r = 1.5 mm

a) Cutter life T, min; b) End-cutting-edge angle φ°

cutting speeds lead to a sharp reduction in tool life.

For hardened steels of H_{R_C} = 57 to 59, the optimum cutting speeds are in the range of v = 20 to 30 m/min (Fig.104).

8. The relationship of cutting speed to tool life may be expressed by the following equations:

For v = 25 to 40 m/min

$$v = \frac{C_v}{T^{0,64}},$$

For v = 40 to 50 m/min

$$v = \frac{C_v}{T^{0,10}}.$$

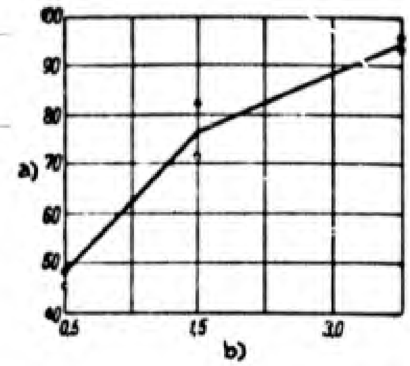

Fig.102 - Effect of Nose Radius upon Life of Cutter Tipped with Mineroceramics. Turning of steels hardened to H_{R_C} = 51 - 53, at t = = 0.75 mm, s = 0.102 mm/rev, and v = 100 m/min. Cutter geometry: $\alpha = 15^o$, $\gamma = -5^o$, $\lambda = 0^o$, $\varphi = 30^o$, $\varphi_1 = 15^o$

a) Cutter life T, min; b) Nose radius r, mm

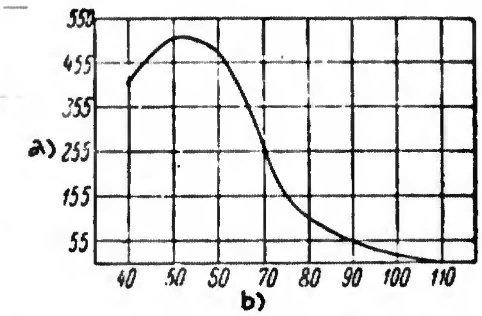

Fig.103 - Relation of Cutting Speed to Life of Cutters Tipped with Mineroceramics in Turning of Steels Hardened to H_{R_C} = 53 - 55, at t = 0.75 mm and s = = 0.102 mm/rev. Cutter geometry: $\alpha = 15^o$, $\gamma = -5^o$, $\varphi = 30^o$, $\varphi_1 = 15^o$, r = 1.5 mm. Flank wear h = 0.15 to 0.35 mm

a) Cutter life T, min; b) Cutting speed v, m/min

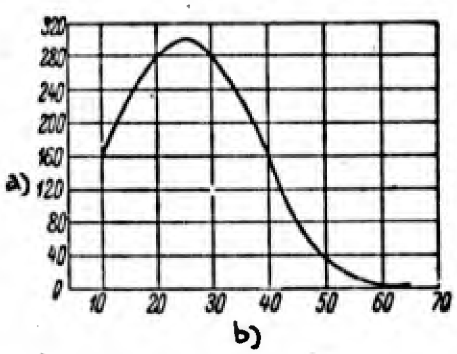

Fig.104 - Relation Between Cutting Speed and Life of Cutters Tipped with Mineroceramics in the Turning of Steels Hardened to H_{R_C} = 57 - 59, at t = 0.75 mm and s = 0.102 mm/rev. Cutter geometry: $\alpha = 15^o$, $\gamma = -5^o$, $\lambda = 5^o$, $\varphi = 30^o$, $\varphi_1 = 15^o$, r = = 1.5 mm. Cutter wear h = 0.2 mm

a) Cutter life T, min; b) Cutting speed v, m/min

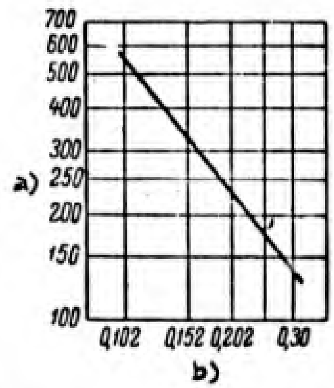

Fig.105 - Relation Between Life of Cutters Tipped with Mineroceramics and Feeds in the Turning of Steels Hardened to H_{R_C} = 53 - 55 at t = 0.75 mm and v = 50 m/min. Cutter geometry: $\alpha = 15^o$, $\gamma = -5^o$, $\lambda = 5^o$, $\varphi = 30^o$, $\varphi_1 = 1.5^o$, r = 1.5 mm. Cutter wear h = 0.3 mm

a) Cutter life T, min; b) Feed s, mm/rev

9. The feed has a significant effect upon the cutter life (Fig.105). The relationship between cutter life and feed is expressed by the equation

$$T=\frac{C_s}{s^{1,21}}.$$

10. The effect of depth of cut upon the cutter life is illustrated by the curve in Fig.106. The longest tool life is achievable at t = 0.75 mm. A reduction

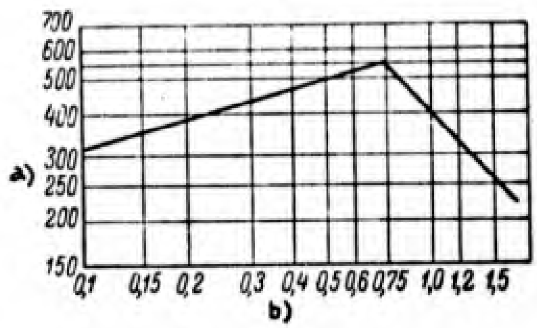

Fig.106 - Ratio of Life of Cutters Tipped with Mineroceramics to Cutting Depth in Turning of Steels Hardened to H_{RC} = 53 - 55,

at s = 0.102 mm/rev and v = 50 m/min. Cutter geometry: α = 15°, γ = -5°, λ = 5°, φ = 30°, φ_1 = 15°, r = 1.5 mm. Cutter wear h = 0.3 mm

a) Cutter life T, min; b) Depth of cut t, mm

in depth of cut below t = 0.75 mm or an increase above this value will lead, in the former variant, to a small, and in the latter variant, to a sharp reduction in cutter life.

The relationship between cutter life and depth of cut is expressed by the equations:

For t = 0.1 to 0.75 mm

$$T=C_t\cdot t^{1,31},$$

For t > 0.75 mm

$$T=\frac{C_t}{t^{1,14}}.$$

11. Hardened steels may be finish-turned by tools tipped with mineroceramic TsM-332 at cutting depths of $t < 0.75$ mm.

12. Of the tool materials tested to identical flank wear (TsM-332, T30K4, and VK8) ($h = 0.3$ mm), the longest life was demonstrated by the mineroceramic (Fig.98).

13. When steels brought to high hardness are turned with cutters equipped with the mineroceramic TsM-332, the closeness of tolerance and quality of machined surface attained are the same as when these steels are machined with cutters tipped with the cermet T30K4.

20. Some Problems of Turning Practice for Hardened Steels

Fitting Cutter Bars to Cutters, and Chip-Breaking

A special feature of the design of cutters for hardened steels is that the face is flat and has no bevel or else has a flat with a negative top rake, considerably wider (not less than 3 mm) than that of cutters designed for high-speed cutting of unhardened steels.

Tool-Holder Angle. When cutters of negative top rake were first used, the hard-alloy tip was mounted in the tool holder at an angle equal to the desired top rake γ. In other words, if a top rake $\gamma = -10^{\circ}$ was desired, the slot in the holder was machined at that same angle of -10° (Fig.107a). As a result, when a cutter was reground on its face, the entire surface of the alloy was ground to a thickness c.

Subsequently, cutters came into use that had a flat face with a bevel, the hard-alloy bar being mounted in the tool holder at an angle of 0° (Fig.107b) or at a positive top rake (Fig.107c), and the flat is ground at the required negative angle γ.

In the machining of steel, cemented carbide cutters undergo wear on face and flank. Therefore both are sharpened in regrinding. On each regrinding, a layer of carbide is removed, whose thickness is the combined depth of the crater and thickness of the layer removed in the lapping of the cutter. The layer removed from the flank is based on the surface wear suffered by the cutter, plus a layer for lapping.

Let us examine regrinding diagrams for a cutter in various positions within the holder (Fig.108). The diagrams are plotted for a cutter in a holder of 16 × 25 mm

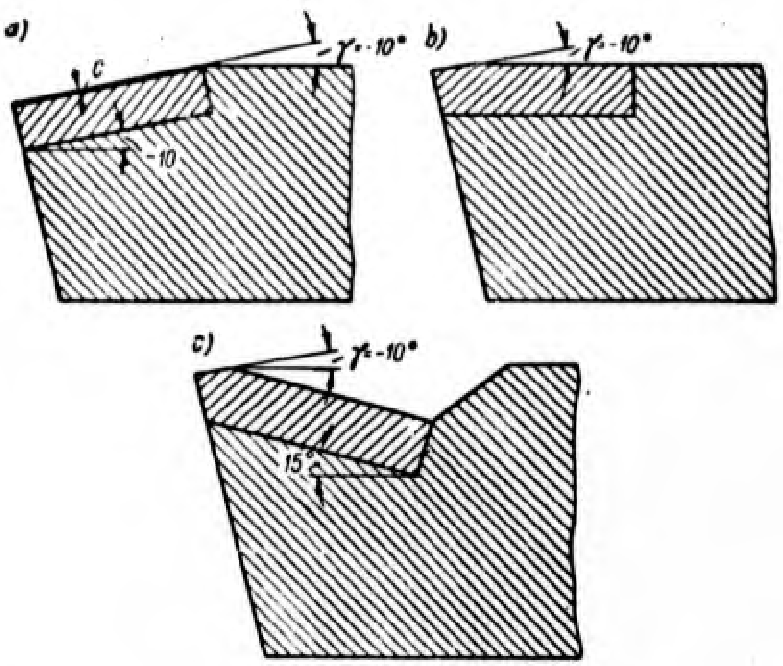

Fig.107 - Various Methods of Mounting the Carbide Bar in the Tool Holder: a) Flat face, no flat, top rake $\gamma = -10^{\circ}$; b) Flat face with flat ground at top rake $\gamma = -10^{\circ}$, the carbide bar being mounted in the tool holder at 0°; c) Flat face with flat ground at top rake $\gamma = -10^{\circ}$, the carbide bar being mounted in the tool holder at an angle of 15°

diameter and a carbide bar corresponding to this holder section, the assumption being that the cutter is brought to the same level of dulling before each regrinding.

Figure 108a presents a diagram for the regrinding of a cutter with a flat face, without flat, and a top rake $\gamma = -10^{\circ}$. The tool is mounted in the holder as illustrated in Fig.107a, i.e., at the same angle of -10°. As we see, the tool is capable of 13 regrindings. This number is the same, whether the grinding is performed so that the nose is on the straight line 1 or on the straight line 2, constituting a diagonal through the cross section of the bar. In the latter case, the regrinding causes a pronounced reduction in the length of the bar.

Figure 108b presents a regrinding diagram for a cutter with a flat face and a flat, the top rake being $\gamma = -10^{\circ}$. The bar is fitted into the holder horizontally (at an angle of 0°). The number of regrindings has here increased to 16. If grind-

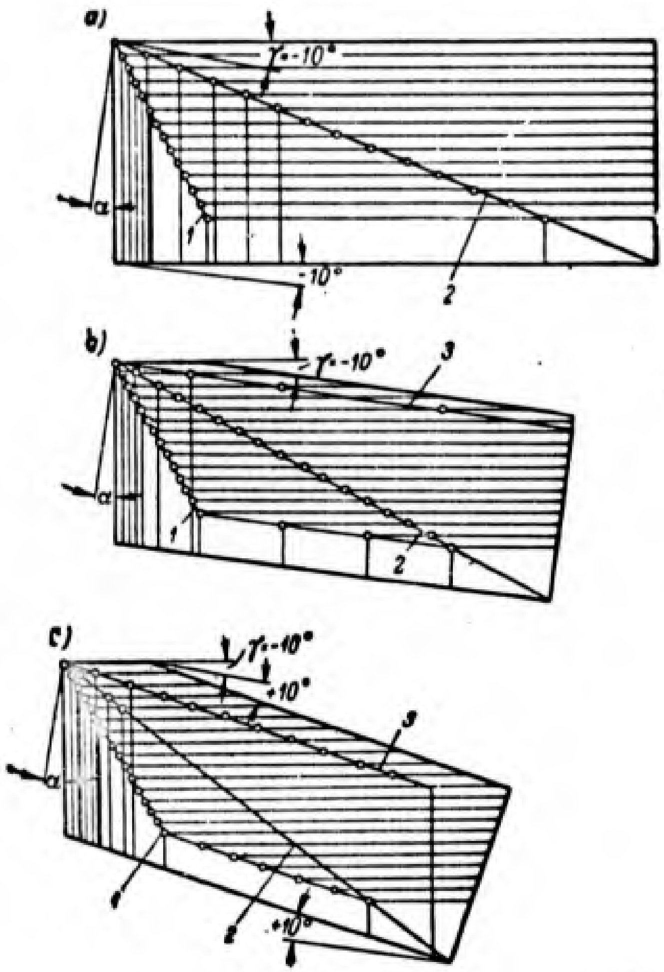

Fig.108 - Diagrams for the Regrinding of Cutters with Negative Top Rake

a) Carbide bar mounted in tool holder at same negative top rake;
b) Bar mounted in tool holder at 0° angle;
c) Bar mounted in holder at positive angle

ing is conducted so that the nose is along the straight line 3, this will result in a reduction in the permissible number of regrindings and, moreover, the regrinding will result in a pronounced reduction in bar length.

Figure 108c presents a diagram for regrinding a cutter with a flat face and a flat, the top rake being $\gamma = -10^{\circ}$. The bar is at a 10° positive tool-holder angle. The number of possible regrindings is now increased to 21.

Thus, from the point of view of saving carbides, the most advantageous shape for the face is that in Fig.107c, i.e., a flat face, with flat, ground at negative top rake (the bar being fitted into the tool holder at a positive angle). However, it must be borne in mind that the tool holder is weakened as this angle is increased. In turning stainless steels, every effort should be made to have the critical section of the holder as strong as possible. Therefore, the angle at which the carbide bar is fitted into the tool holder has to be reduced to 5°, not counting the fact that, when compared to a 10° angle, this leads to some reduction in the permissible number of regrindings of the carbide bar.

Chip Breakers. Under industrial conditions, hardened steels are machined at low t and s and at relatively high cutting speeds (exceeding v = 60 m/min). Therefore, the problem of breaking the chip is just as important in the machining of hardened steels as in the high-speed machining of unhardened steels. The considerations given in various handbooks with regard to the merits and shortcomings of various types and designs of chip breakers are applicable to the turning of hardened steels, since the chip formation is of the same nature here as for unhardened steels.

Dependable breaking of the chip is attainable without the use of a chip breaker, if the point of the cutter has the proper geometry (Fig.109). Such a cutter would have a flat face at a top rake of $\gamma = -5$ to -10°, the complement of the back rake angle being $\lambda = 10$ to 15°, and the end-cutting-edge angle being $\varphi = 70^{\circ}$.

However, this cutter shape involves the following very serious shortcomings, which render the advisability of its use quite dubious:

1) Necessity to remove a considerable layer of carbide in the regrinding process, due to the considerable depth of the crater formed in cutting. This

leads to cracks in the bars;

2) Greater consumption of cemented carbides because of the necessary regrinding of the face to a considerable depth along its entire length;

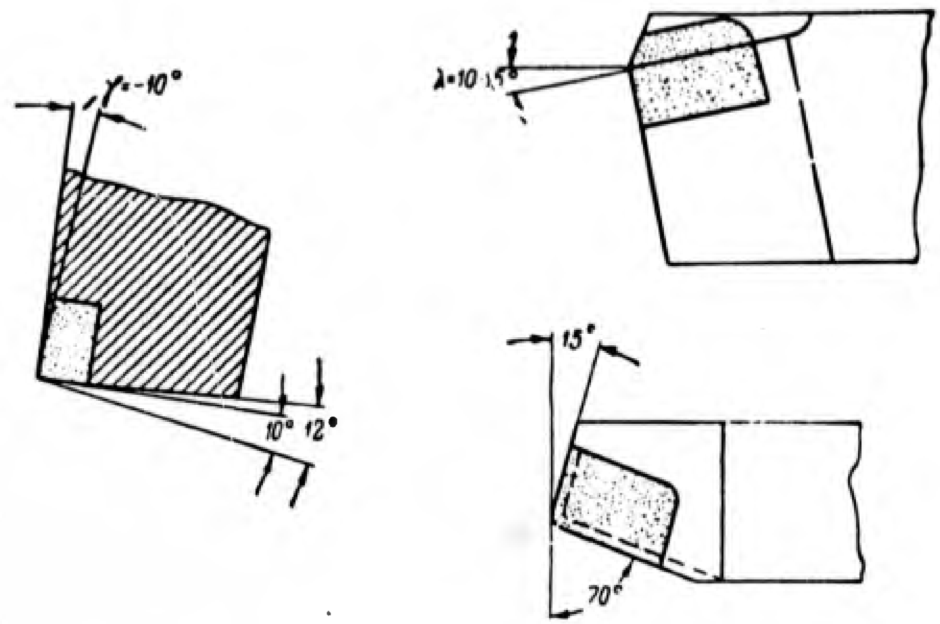

Fig.109 - Cutter Geometry Causing Chip Breakup

3) Complexity of grinding a cutter with a large angle λ, compared with the complexity for an angle of λ = 0° and the fact that the cutting edge is parallel to the major surface of the cutter;

4) Possibility of the chip ruining the machined surface; at positive angles λ, i.e., when the cutter nose is at the lowest point of its cutting edge, the chip will be removed in the direction of the machined surface;

5) Pronounced increase in radial force P_y, resulting in vibration if the system comprising the machine tool, the part, and the tool, is insufficiently rigid;

6) Unreliable crumbling of the chip unless the ratio of depth of cut to feed is $\frac{t}{s}$ = 5 to 10.

The all-purpose clamped-on chip breaker, designed by the Leningrad Metal Works

(Fig.110) and that designed by the Transport Machinery Design Institute (Fig.111), have proved satisfactory in practical work.

The chip breaker (Fig.110) consists of a base (1) (60S2 steel) of 1.5 - 3.0 mm thickness, and a block (2) (U7 steel). The carbide bar (6) is brazed to the block. The block is connected to the base by the bolt (3) which also forms the axis of the block. The block is capable of rotating about this axis.

A criss-cross pattern is knurled into the inner face of the block, adjacent to

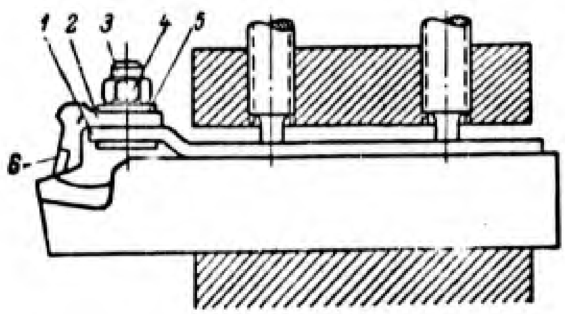

Fig.110 - Chip Breaker Designed by the Leningrad Metal Works

1 - Base; 2 - Block; 3 - Bolt; 4 - Nut; 5 - Elastic washer; 6 - Carbide bar

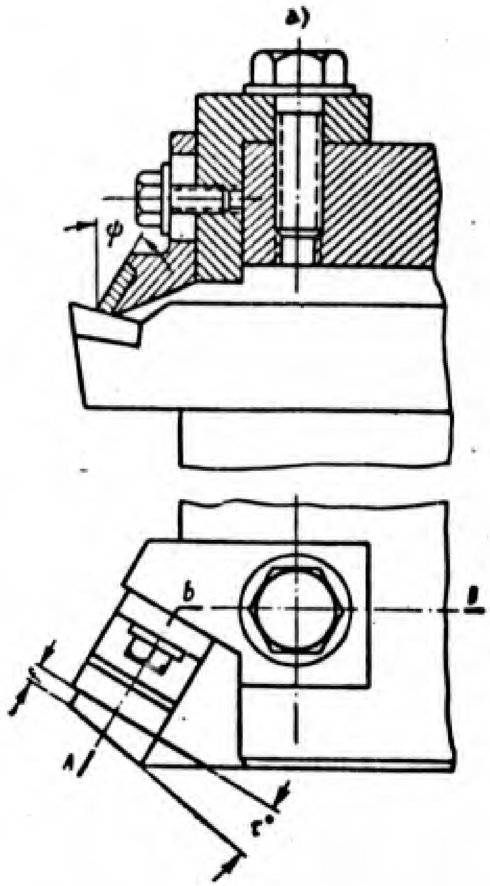

Fig.111 - Chip Breaker Designed by the Transport Machinery Design Institute

a) Section through AbB

the base, so as to create high friction. An elastic ring (5) is inserted between nut and block to prevent the nut (4), which holds the block to the base, from backing off in operation.

Thanks to the fact that the base of the chip breaker is made of a strip of thin

Table 62

Recommended Spacing between Cutting Edge of Tool and Working Surface of Chip-Breaker Block

Depth of Cut t, in mm	Feed s, in mm/rev				
	To 0,3	0,3—0,45	0,45—0,6	0,6—0,7	0,7—1,0
To 1,5	1,5	2,0	2,5	3,0	3,5
1,5—6,0	2,5	3,0	4,0	4,5	5,0

spring steel, the chip breaker, when mounted in the tool holder along with the cutter, can be deflected and thus forced against the cutter face, regardless of the top rake or the degree of wear of the carbide bar.

Table 63

Geometric Parameters for Installation of Chip Breaker

Machining	Dimensions of Cut		f, in mm	τ°	ψ°
	t, in mm	s, in mm/rev			
First finish	2—4	0,2 —0,4	4—5	0—5	120—130
Final finish	1,0	0,15—0,3	2—3	— 10	105—110

Since the chip breaker block is rotatable, it may be employed with cutters of various types.

The spacing between the cutting edge of the cutter and the working surface of the block is determined from Table 62.

The chip breaker illustrated in Fig.111 will provide reliable breakup of the chip when properly installed. The following are the parameters for chip breaker installation: f = distance between clamped-on unit and cutting edge of the tool; τ = angle of rotation; φ = angle between chip breaker and cutter face. Table 63 presents the recommended values for installation of the chip breaker.

Field of Application of the Process

The turning of hardened steels is to be preferred over grinding, from the viewpoint of the physical and mechanical properties of the surface layer of the metal. No difficulty is encountered in turning hardened steels to a finish comparable to that obtainable by rough grinding. Such a finish may be achieved at feeds ranging to $s = 0.3$ mm/rev, whereas in using the large-feed method with cutters of specific geometry, it is possible to work at $s = 0.6 - 1.0$ mm/rev.

At low feeds ($s \leq 0.1$ mm/rev), the surface finish corresponds to that of finish-ground material. With increasing hardness of the hardened steel, it becomes easier to obtain a high surface finish.

All the foregoing are determining factors for the major uses of the turning process for hardened steels. These may be widely employed in production to replace grinding, primarily rough grinding.

It should be pointed out that lathes are cheaper than grinders, and that it is cheaper and easier to regrind cemented carbide cutters than grinding wheels.

Let us list some examples of the rational application of the turning process to hardened steels.

1. In the manufacture of bearings, the turning is usually done parallel to rough grinding in the final machining of large high-alloy steel bearing races, hardened to $H_{R_C} = 65 - 60$. As a result of heat treatment, deformation of the races may attain 3 - 4 mm on the diameter. To avoid rejects, large allowances are left for finishing after heat treatment. The preliminary grinding of these races is a highly laborious operation that ties up a considerable number of face grinders which

are in short supply, and involves a substantial expenditure of grinding wheels.

The races are turned on turret lathes of up to 24 kw power. The tools employed are cutters tipped with VK8 carbide, having negative top rake.

Despite the fact that turret lathes are distinguished by the highest rigidity in the lathe category of machining equipment, the high cutting forces developed in the process of machining the races cause the cutter to bounce violently off the workpiece. As a result, the races develop a taper greater than permitted in the specifications, if the cutting depth is $t > 0.9$ mm. Therefore, the machining of races is divided into rough- and finish-machining, at a depth of cut for the roughing passes of 0.7 - 0.9 mm, whereas for the finishing passes it is 0.20 - 0.35 mm.

The allowance for finish-grinding is the same as that for races subjected to rough-grinding, and there are cases in which the finish-grinding is also replaced by turning.

At the First State Bearings Plant, the introduction of lathe turning instead of rough grinding for large 1-OK-33 bearing races made of ShKh15 steel and hardened to $H_{R_C} = 63 - 64$ caused a reduction in man-hour requirement for the job by 50 - 60% (Bibl.52).

As noted by S.S.Nekrasov (Bibl.36), the output in the turning of bearing races may be increased considerably by the development of more rigid machine tools, making it possible to work with a greater cutting depth per pass. A considerable increase in output is also attainable by using titanium-tungsten carbides instead of the VK8 alloy currently employed.

2. At the Novokramatorskiy Works, a batch of 9Kh steel rollers, 2090 - 2450 mm in length and 115 - 210 mm in diameter, was manufactured. After hardening, the bodies of these bearings, 1680 mm in length, were at $H_{R_C} = 67$. In view of the distortion during heat treatment, an allowance of 6 mm on the diameter was provided for machining of the barrel section of the rollers after hardening. Removal of this allowance by grinding took 100 machine-hours per roller.

Grinding was replaced by turning with VK8 tools at negative top rake. As a result, only 10 - 15 machine-hours were required for the machining of each roller.

3. At the Gor'kiy Machine Tool Works, bushings 300 mm in diameter and 200 mm in length are heat-treated to bring the hardness of the outer layer to H_{R_C} = 40 - 48. Grinding of these bushings has been replaced by turning on a DIP-300 lathe, using carbide cutters with negative top rake. The result was that the machining of these heat-treated bushings was cut in half as compared with grinding (Bibl.35).

4. As a result of the investigation conducted and of the analysis of the production experience in three machine-building plants, Ye.A.Belousova (Bibl.30) found it practicable to replace rough-grinding of hardened steels by turning and also found it possible to replace finish-grinding by turning, special cutters being used in these cases.

Depending upon the amount of rough allowance, and thanks to the replacement of rough-grinding of hardened steels by turning, machine-time is being cut by 2 - 5 times.

In the opinion of Ye.A.Belousova, replacement of the grinding of hardened steels by turning becomes profitable if the rough allowance exceeds 1 mm.

5. As pointed out by A.D.Makarov (Bibl.24), the turning of hardened steels at high feeds results in high surface finish and an output considerably greater than that of rough-grinding.

6. Lathe centers may serve as an example of hardened steel parts repaired by turning on a lathe.

The repair of a worn center usually requires the performance of a series of operations: annealing, turning, hardening, tempering, and grinding. All together, these operations take some dozens of hours. When a hardened center is turned with a carbide tool, it can be fixed in the space of a few minutes without the slightest difficulty.

7. The turning of hardened parts can be extensively used in repair shops in the

machining of equipment spare parts. Usually, a small allowance is left on spare parts for purposes of fitting in situ, which often proves inadequate. As a result, the part has to be discarded. In view of the possibility of machining hardened steels on a lathe, it is desirable to leave larger allowances on spare parts, since these are readily removed with little loss of time, when the parts are fitted in situ.

8. The turning of hardened steels is a method useful for the tool industry, for example, in resizing of calipers that are no longer within the specified tolerance. Calipers are usually reground to the next size or, in time, discarded. The grinding of calipers to the next size requires several hours, while the turning of a hardened caliper from, say, 47 mm diameter to 39 mm, takes 10 - 15 min in all.

These examples show that turning of hardened steels on the lathe can replace grinding, both in the production departments and in the repair and tool shops. The superiority of turning over rough-grinding, in terms of rate of output, is confirmed by investigation and by production experience.

Cutting Schedules

Appendix I presents cutting schedules for the turning of steels hardened to H_{R_C} = 38 - 65. In developing these schedules, the author also considered the literature data published after his schedules for chromium-nickel, chromium-nickel-molybdenum, and chromium-nickel-molybdenum silicon steels had appeared in print (Bibl.53, 54).

The differences in the chemical composition of these steels, and the insignificant effect of the chemical composition of structural alloy steels (Bibl.30) upon its machinability in the hardened condition, provided the foundation on which the author developed the schedules he recommends for all structural alloy steels.

Let us compare these schedules with the literature data. Table 64 presents a comparison of the author's data with those by P.P.Grudov (Bibl.29) and by the

NIBTN (Bibl.27) for steel hardened to H_{R_C} = 47. The cutting speeds are reduced to 60-minute tool life.

As we see, the author's data are midway between the others. The v_{60} cutting

Table 64

v_{60} Cutting Speed in the Turning of Steels Hardened to H_{R_C} = 47 by Cutters Tipped with T15K6

$t \cdot s$	Data of					
	P.P.Grudov	Author	NIBTN	P.P.Grudov	Author	NIBTN
	v_{60} Cutting Speed, m/min					
	Absolute			Relative		
0,2 · 0,05	115	155	173	0,75	1,00	1,12
1,2 · 0,15	58	63	84	0,92	1,00	1,33
2,0 · 0,30	25	38	56	0,66	1,00	1,47

speeds recommended by P.P.Grudov are very much lower than the NIBTN data (55% in the fast schedules). At low t and s, the NIBTN speeds differ little from the author's data, but as the schedules are speeded up, the difference increases.

There is agreement between the author's data and those by N.S.Logak (Bibl.21) for steel of H_{R_C} = 62. At t = 0.2 mm and s = 0.1 mm/rev, the v_{60} cutting speed comes to: 37.8 m/min for T30K4 according to N.S.Logak, and 30 m/min for T15K6 according to the author. It must be borne in mind that the superiority of the alloy T30K4 over T15K6 reaches 30% in terms of cutting properties.

The cutting speeds employed by Ye.A.Belousova are too low (Bibl.30).

For a steel of H_{R_C} = 53, at t = 0.45 mm and s = 0.45 mm/rev, the above author used v_{60} = 28 m/min (in the case of T30K4 carbide). For these conditions, the author found v_{60} = 41 m/min (47% more).

In conclusion, it should be noted that the cutting speeds recommended by the author should be regarded as minimal. Their level has to be raised as the machining of hardened steels is mastered on the job.

Here it is advisable to cite foreign experience (Bibl.55). The cutting speed for S1 carbide, which virtually corresponds to our alloy T15K6, is 60 - 70% higher according to German data than those recommended by the author.

21. Machining of Hardened Steels with Introduction of Electric Current into the Cutting Zone

Here we present the results of investigation and industrial introduction of a method of machining hardened steels, with the introduction of electric current into the cutting zone. The method was developed by M.N.Larin and his coworkers (Bibl.56).

Three hardened steels were investigated: high-speed R18 of H_{R_C} = 62 to 64, alloy tool steel KhVG of H_{R_C} = 45, and 45KhNMFA structural steel of H_{R_C} = 45. The tests were run on a DIP-300 lathe equipped with an 8 kw DC motor. Straight-shanked turning tools with holders measuring 25 × 30 mm in cross section, tipped with various carbides, were used.

Figure 112 presents the electric circuit used in these experiments to feed transformed current to the workpiece and the cutter. The lathe rest was insulated from its carriage by a textolite gasket of 5 mm thickness and by hard-rubber sleeves placed over the bolts connecting the rest to the carriage. Fiber washers were placed under the nuts securing these bolts. The low-voltage winding of the transformer was connected to the tool-to-workpiece electric circuit as follows: Two copper buses carried the current from the transformer either to the lathe housing or to brushes through which, by means of a slip ring, the current was fed to the spindle and then through the chuck to the workpiece. The other end of the low-voltage winding of the transformer was connected to the tool holder by cable.

Experiments showed that introduction of a given current into the cutting zone greatly increased the life of the carbide cutter. This current was termed optimum. The optimum current depends upon the cutting speed and the hardness of the tempered steel. The lower the machinability of the steel in standard working (without current), the more efficient will be the machining with introduction of current into the cutting zone.

Figure 113 presents the relationship between cutting speed and cutter life in

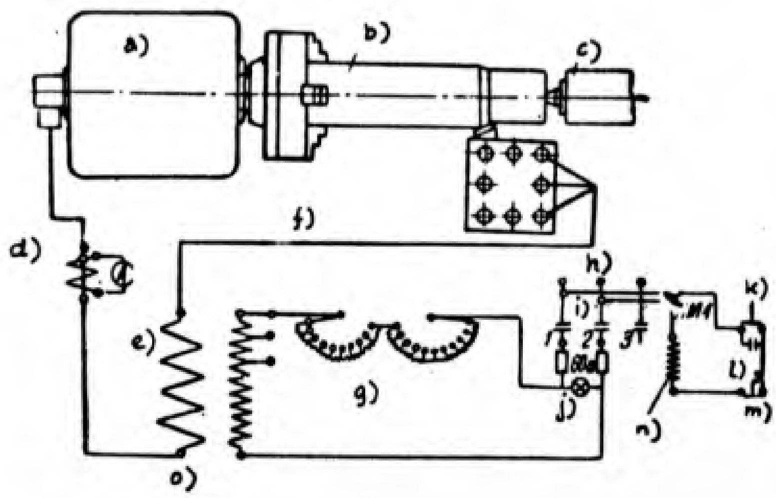

Fig.112 - Electric Circuit for Feeding Transformed Current to Workpiece and Cutter

a) Headstock; b) Workpiece; c) Tailstock; d) EN ammeter with 300/5 transformer; e) Transformer 12 kw 220/8-4-2v; f) SBS cable 3 × 150; g) Adjustment rheostat 5 amps 400 ohms (9 × 40 ohms and 10 × 4 ohms); h) 220-volt, 50-cycle network; i) Starter; j) Tube; k) Start; l) Block contact; m) Stop; n) Starter coil; o) Two (50 × 5) copper buses

the turning of R18 steel hardened to H_{RC} = 62 to 64 without current (curve 1) and with introduction of current into the cutting zone (curve 2). The machining was done at t = 2 mm and s = 0.21 mm/rev by tools tipped with VK6, having the following geometry: $\alpha = 10^\circ$, $\gamma = -15^\circ$, $\lambda = 10^\circ$, $\varphi = 20^\circ$, $\varphi_1 = 10^\circ$. Obviously, when the cutting speed was v = 15 m/min in working without current and the flank wear of the cutter was h = 0.32 mm, its life was T = 43 min, whereas in working with a current of I = 90 amp and a wear of h = 0.20 mm, the life was T = 253 min. Consequently, the result of introducing transformed current into the cutting zone caused the cutter life to increase almost six-fold. At this cutting speed, which is optimal, the cutting edge of the cutter did not crumble out.

Figure 114 illustrates the influence of the current strength in the cutting zone upon the life of a T15K6 cutter in the turning of 45KhNMFA steel hardened to $H_{R_C} = 45$. The experiments were run at t = 2 mm, s = 0.3 mm/rev, and v = 70 m/min.

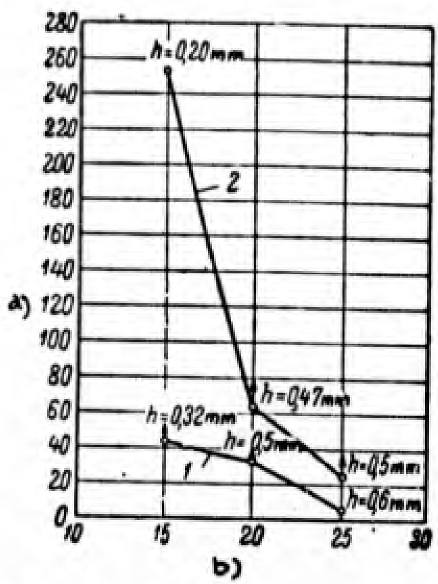

Fig.113 - Cutting Speed versus Tool Life in the Turning of Hardened R18 Steel (H_{R_C} = 62 - 64);

1 - Without current; 2 - With current fed to the cutting zone

δ - Cutting edge crumbled out.
h - Cutter could continue to be used

a) Cutter life T, min; b) Cutting speed v, m/min

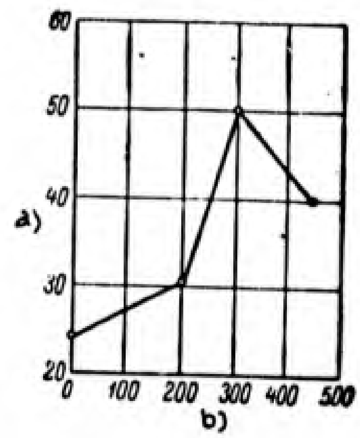

Fig.114 - Influence of Current Strength upon Tool Life in the Turning of 45KhNMFA Steel H_{R_C} = 45

a) Cutter life T, min; b) Current introduced I, amp

The following was the cutter geometry: $\alpha = 10^\circ$, $\gamma = -15^\circ$, $\lambda = 10^\circ$, $\varphi = 30^\circ$, $\varphi_1 = 10^\circ$. The flank wear of the cutters was h = 0.3 mm. The diagram shows that introduction of current of optimum value into the cutting zone (I = 300 amp), almost doubled the cutter life over that in working without current.

The investigation showed that, when optimum current was introduced into the cutting zone, the cutting forces P_x, P_y, and P_z did not differ from those in working without current. In the turning of hardened R18 steel (H_{R_C} = 62 - 64), the surface finish diminishes somewhat as the current strength is increased. The surface

Table 65

Comparison of Cutting Schedules in Machining Release Clutch

Cutting Parameters	Prior to New Method	With New Method, I = 100 amp
Cemented carbide	TA - Ferthite	VK6
Depth of cut t, mm	0.1 - 0.5	0.1 - 0.5
Feed s, mm/rev	0.05	0.16
Cutting speed v, m/min	37	36
Machine-time T_{mach}, min . . .	28	8.8

finish improves somewhat, conversely, in the machining of KhVG hardened steel (H_{R_C} = 45), and particularly of unhardened 20KhNZA and No.40 steels.

A new method of machining hardened steels has been introduced at the Chelyabinsk Tractor Works in the facing of grooves in the release clutch and the motor sleeve.

As indicated by Table 65, the machine time for machining the release clutch (carburized and hardened to H_{R_C} = 58 - 60) was reduced to less than a third as a result of the new method.

The finish-machining of the ends of the 38KhMYuA sleeve is done after nitriding to H_{R_C} = 54 - 64. This operation is performed on a grinder, and 5.5 min of machine-time is required to machine the two ends of a single sleeve. Replacement of grinding by turning, with introduction of the optimum current of I = 150 to 200 amp into the cutting zone, resulted in a doubling of labor productivity. The VK8 alloy proved best. The machining was performed at v = 28 - 20 m/min, t = 1.0 - 1.5 mm, and s = 0.2 mm/rev. Bent-shank facing tools of the following geometry were employed: $\alpha = 10^\circ$, $\gamma = -15^\circ$, $\lambda = 10^\circ$, $\varphi = 45^\circ$, $\varphi_1 = 10^\circ$, whereas the transitional cutting edge had $\varphi_0 = 20^\circ$ and $f_0 = 0.6$ mm. In working without current, the tool life was T = 5 min. In working with a current of I = 150 - 200 amp, the life was T = 18 min.

The reasoning of authors who investigated the physical nature of the process

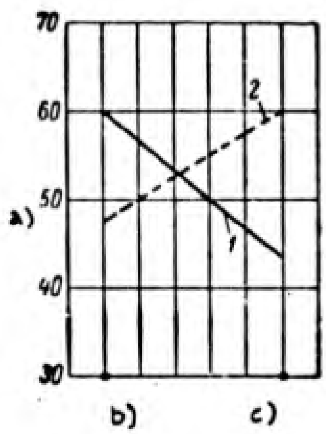

Fig.115 - Change in Hardness on Inside and Outside Surface of Chip

1 - Work with current;
2 - Work without current

a) Hardness H_{R_C}; b) Chip facing cutter; c) Outer surface of chip

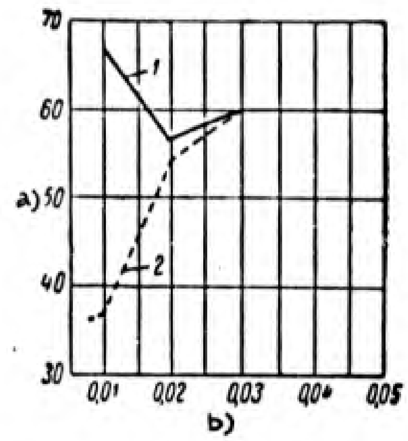

Fig.116 - Change in Hardness in Surface Layer of Workpiece

1 - Work with current;
2 - Work without current

a) Hardness H_{R_C}; b) Depth of surface layer, mm

of machining hardened steels are of interest. Their research was based on a metallographic analysis of the chip and the machined surface resulting from the turning of hardened R18 steel of H_{R_C} = 62 - 64, with and without current (I ≈ ≈ 100 amp). The experiments were run at t = 0.2 mm, s = 0.21 mm/rev, and v = = 15 m/min. The VK6 tool had the following geometry: $\alpha = 10^\circ$, $\gamma = -15^\circ$, $\lambda = 10^\circ$, $\varphi = 20^\circ$, $\varphi_1 = 10^\circ$. The work was conducted under extensive cooling with 5% emulsion solution. Specimens were taken of the chip cross section and the transverse section through the machined surface.

It was found that, in working without current, the chip is not uniform in hardness throughout its cross section (Fig.115). The surface facing the cutter has a hardness of H_{R_C} = 47. Moving away from this surface, the hardness increases and reaches 60 - 61 in the layers near the outer surface. A layer of metal, consisting of tempering products of hardened steel (of H_{R_C} = 37 - 58) and of carbides, forms on the machined surface. The hardness of this film increases with the distance from the outer surface: from H_{R_C} = 37 to H_{R_C} = 54 at a depth of 0.02 mm (Fig.116).

These data have made it possible to conclude that a temperature up to 600°C develops in the surface layer of the workpiece.

In working with a current of I = 100 amp, the chip layer facing the cutter reaches H_{R_C} = 60 at a depth of 0.01 mm, whereas the H_{R_C} of the outer surface is only 44 (Fig.115). A hardened layer forms on the surface of the workpiece. At a depth of 0.01 mm, the hardness reaches H_{R_C} = 67 (Fig.116). As we see, the hardness drops to H_{R_C} = 57 at a depth of 0.02 mm and then rises somewhat, until reaching a depth of 0.03 mm, and finally stabilizes.

The authors of this study assume that, thanks to the introduction of current into the cutting zone, the thin layer of chip adjacent to the cutter heats to a temperature of 900 - 1000°C. A hardened layer forms on the machined surface as the result of pronounced cooling of the metal when the temperature is that required for hardening; this layer is the result of the combined effects of work of deformation, work of friction, and heat caused by the flow of electric current through the layer of metal being removed. The reduction in hardness in the portion of the chip adjacent to the cutter, occurring in work without the use of current, is attributed by the authors to the tempering phenomenon. The hardness does not change in the outer layer of chip, since the temperature to which it is heated is lower than the tempering temperature.

M.N.Larin and A.A.Maslov have come to the conclusion that, in work with electric current of optimum strength, a temperature field is artificially created in the machining zone, of such nature as to facilitate the formation in the layer of chip facing the cutter of a thin plastic stratum acting, as it were, as a heavy natural lubricant which reduces the work of friction and the support pressure. The latter is understood to be the pressure per unit surface of true contact between the adjacent surfaces of chip and cutting tool.

CHAPTER IV

FACE MILLING OF HARDENED STEELS

22. Design of Milling Cutters

The milling of hardened steels is done with the same types of carbide-tipped end mills employed in high-speed milling of ordinary (unhardened) steels. These mills differ from the carbide mills used to machine cast iron by the fact that the point is machined to negative true rake and that the number of teeth is less. As compared to the analogous high-speed mills, the body and other parts of the given mills are stronger and more massive. The mills have to be mounted to the machine both rigidly and reliably. Mill design should provide for ready replacement of the individual teeth when they wear out and break.

It should be remarked that the superior life of carbide over high-speed mills is even more pronounced with increase in the hardness of the steel being machined.

There are three methods of joining the carbide bars to the body of the mill:

1) Brazing directly to the body;

2) Brazing to the inserted teeth;

3) Mechanical mounting in the body.

In industry, the inserted-tooth cemented-carbide end mill is the type which has achieved the greatest popularity. In some cases, milling cutters with mechanical fastening of the cemented carbide bar are employed. Mills having bars directly brazed to the body are used only rarely despite their high rigidity. The point is that, in grinding a crumbled tooth of such a mill, one has no choice but to remove a considerable layer of carbide from all the teeth. In addition to a waste of carbide, this involves considerable expenditure of time in grinding the tool. The need for secondary brazing of carbide bars, if the individual bars have been greatly damaged, limits the service life of the body of such mills.

Inserted-Tooth End Mills

VNII-designed inserted-tooth carbide end mills are the type in widest use (Fig.117 - 119). Mills up to 100 mm in diameter (Fig.117) have a tapered integral

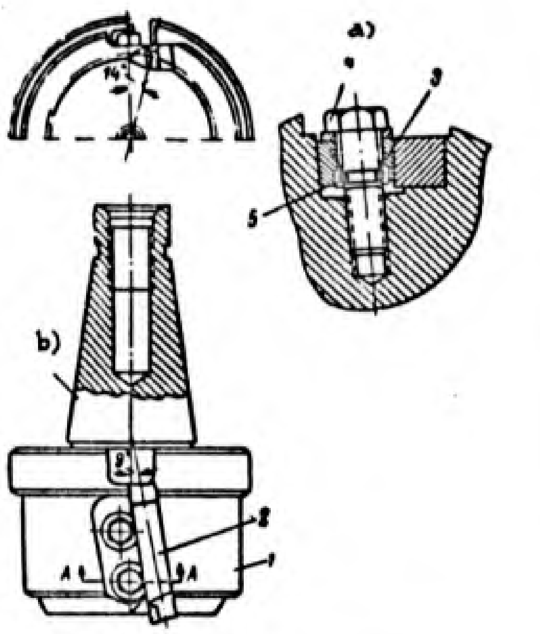

Fig.117 - Design of Inserted-Tooth End-Milling Cutter, Carbide-Tipped, up to 100 mm Diameter

a) Section through A-A; b) Taper 7:24

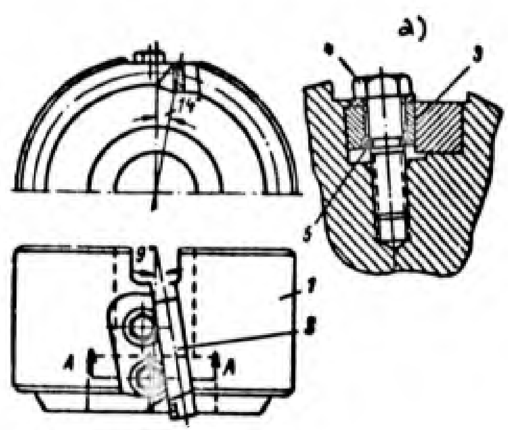

Fig.118 - Design of Carbide-Tipped, 110 - 150 mm Diameter Inserted Tooth End-Milling Cutter

a) Section through A-A

shank for direct seating in the spindle-nose taper of the milling machine. The rear end of the body (1) has a keyway for an end key, absorbing the spindle torque.

The body (1) of a mill 110 - 150 mm in diameter (Fig.118) has a cylindrical hole in its base to mount the cutter on an arbor, and a keyway in its face.

Milling cutters from 200 to 400 mm in diameter (Fig.119) are seated on the cylindrical flange of the milling-machine spindle, by means of a cylindrical groove on the rear face of the body (1). The keyway is also at this point. The cutter is mounted by four cap screws with internal hexagonal keyways.

The teeth (2) are prismatic in shape, square in cross section, and with smooth faces. The cross section is greater than that of teeth in cutters of high-speed steel.

Diameter of milling cutter D, in mm	Tooth cross-section dimensions, in mm
75 - 130	14 × 14
150 - 400	16 × 16

Because of the fact that carbides have a tendency to crumble out when vibration sets in during the machining process, the tooth depth is small: 5 mm for cutters of 75 - 200 mm diameter, and 8 mm for those more than 200 mm in diameter.

The teeth are mounted to the mill bodies (Figs.117 - 119) by cylindrical keyed bushings (3) with flat 5° chamfer. The bushings are tightened by bolts (4), using an ordinary monkey wrench. Springs (5) are fitted over the bolts to simplify disassembly of the mill. When the bolt is unscrewed, the spring enters a groove in the key, lifts it, and frees the inserted tooth.

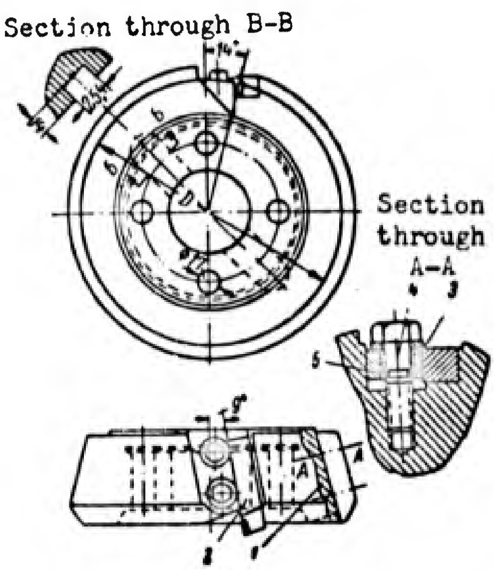

Fig.119 - Design of Carbide-Tipped, 200 - 400 mm Diameter Inserted-Tooth End-Milling Cutter

In determining the outer-circle diameter of milling cutters, consideration is given to the fact that the inserted teeth and their mounting elements must not project beyond the body.

Chip-removing grooves are provided at the tooth faces on the cutting end of the mill. The tapered chamfer on the cutting end is so selected that the back of the tooth (2), at the face cutting edge, is entirely outside the body of the mill. This on the rear face of the body (1). The keyway is also at this point. The cutter is mounted by four cap screws with internal hexagonal keyways.

The teeth (2) are prismatic in shape, square in cross section, and with smooth faces. The cross section is greater than that of teeth in cutters of high-speed steel.

Diameter of milling cutter D, in mm	Tooth cross-section dimensions, in mm
75 - 130	14 × 14
150 - 400	16 × 16

Because of the fact that carbides have a tendency to crumble out when vibration sets in during the machining process, the tooth depth is small: 5 mm for cutters of 75 - 200 mm diameter, and 8 mm for those more than 200 mm in diameter.

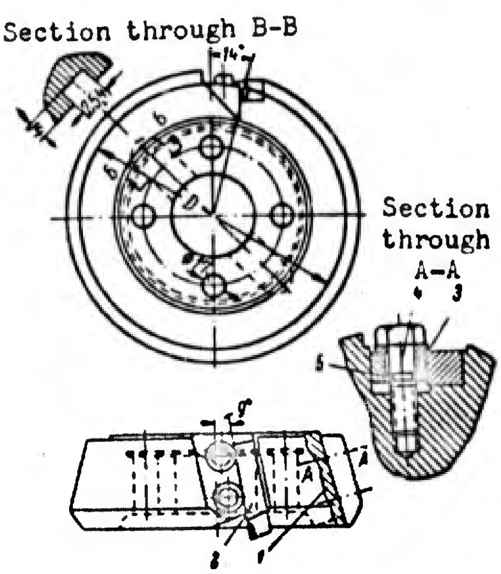

Fig.119 - Design of Carbide-Tipped, 200 - 400 mm Diameter Inserted-Tooth End-Milling Cutter

The teeth are mounted to the mill bodies (Figs.117 - 119) by cylindrical keyed bushings (3) with flat 5° chamfer. The bushings are tightened by bolts (4), using an ordinary monkey wrench. Springs (5) are fitted over the bolts to simplify disassembly of the mill. When the bolt is unscrewed, the spring enters a groove in the key, lifts it, and frees the inserted tooth.

In determining the outer-circle diameter of milling cutters, consideration is given to the fact that the inserted teeth and their mounting elements must not project beyond the body.

Chip-removing grooves are provided at the tooth faces on the cutting end of the mill. The tapered chamfer on the cutting end is so selected that the back of the tooth (2), at the face cutting edge, is entirely outside the body of the mill. This facilitates grinding of the teeth flanks with the milling cutter in assembled position.

Cutters over 200 mm in diameter have tapered bodies. The angle of the tooth slots to the cutter axis is set at about 15°. Therefore when teeth are ground and then moved outward, the nominal diameter of the cutters hardly changes.

In providing for identical mounting of all teeth in the body, with respect to the axis and the cutting end of the mill, this design makes it possible - provided that the teeth are carefully inserted - to avoid extra grinding and dressing of the cutting elements when they have been mounted on the cutter, or at most it requires that an insignificant oversize be left for that purpose.

Mounting of the teeth is facilitated by the use of a magnetic hold (Fig.120). When the projecting tooth is brought into contact with the micrometer screw of the hold (placed on the cutting end of the mill body), it is then fastened with the tie-in bolts (4) (Fig.117 - 119). The teeth are mounted to the cutter face with a tolerance of 0.04 mm. The following is the number of teeth employed with VNII end milling cutters:

Cutter diameter D, in mm ...	75	90	110	130	150	200	250	300	350	400
Number of teeth z	4	6	8	8	10	10	12	16	18	22

The principal dimensions of VNII end mills and those of their various parts are presented in the book by V.S.Rakovskiy and others, Cemented Carbides in Machine-Building (Bibl.16) and also in the VNII compendium, Design of Cemented Carbide Tools (Bibl.57).

A number of tool plants have organized series output of carbide-tipped end mills designed by the Kalinin Freezer Works for the machining of steels (Fig.121). In accordance with GOST 3789 - 52, these mills have the following prime dimensions:

Mill diameter D, in mm	150	200	250	320	400	500	600
Width of milling cutter B, in mm	56	72	72	72	97	97	97

Diameter of seating groove on end, d mm	69.83	88.88	128.57	128.57	128.57	128.57	128.57
Tooth depth h mm	6	7	7	7	17	17	17
Number of teeth z	6	8	8	10	12	14	16

The inserted teeth 2, 13 - 18 mm in thickness, are of trapezoidal cross section. They are fixed in slots in the body (1) by smooth wedges (3) with a taper of 5°. The support end of the cutter body is provided with screws (4), pressing against the teeth (2), for which special slots are provided. The screws (4) are to prevent the inserted teeth from moving axially when the milling cutter is being assembled and adjusted.

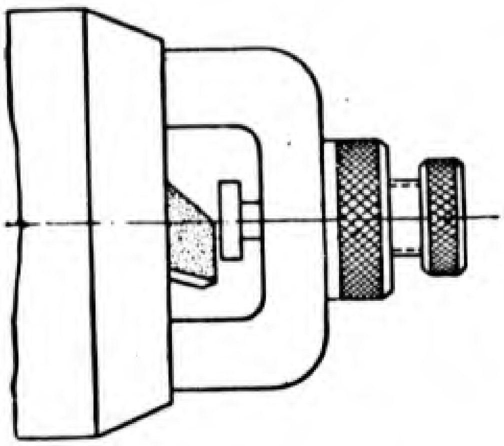

Fig.120 - Magnetic Hold for Inserting Teeth into Bodies of End Mills

This design is characterized by its simplicity and dependability in operation. The individual teeth are readily replaced, and moved outward in their slots with equal ease. However, there are many conditions under which these mills do not meet manufacturing needs. The major shortcomings limiting their use are the small number of teeth (considerably smaller than in the VNII cutters) as well as the fact that the cutter geometry presupposes very specific operating conditions. This complicates the use of the body of the milling cutter when the operating conditions are changed. The small number of teeth means that the output is low, often interfering with the smooth functioning of the milling machine and cutter. Moreover, difficulties are encountered in the grinding of assembled cutters of larger diameters ($D > 300$ mm).

<u>End Mills Providing Individual Grinding of Inserted Teeth (Grinding Outside Mill Body).</u> The effort to avoid the difficulties encountered in grinding end mills in the assembled form, complete with carbide tips, and to increase the operating efficiency, has led to the development of designs in which the teeth are ground out-

side the body of the mill. The following designs of end mills with separate tooth grinding are known:

1) Mills with adjustable tooth mounting;

2) Mills with free tooth mounting;

3) Mills with precision tooth mounting.

Individual installation of ground teeth to size in the first of these types of

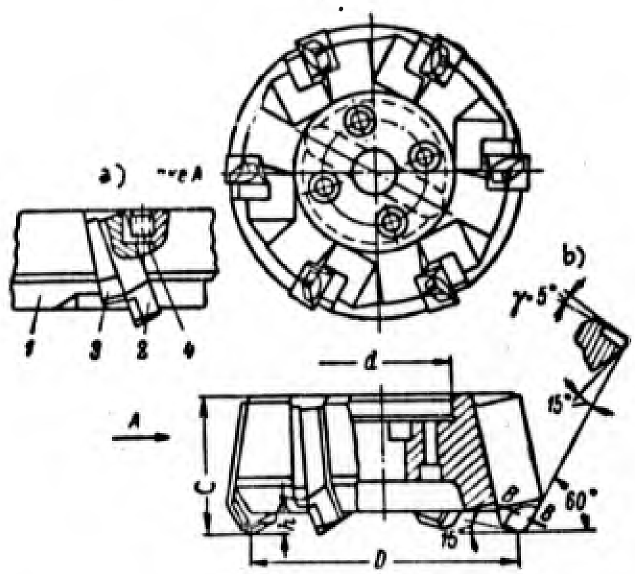

Fig.121 - End Milling Cutter, Carbide-Tipped, With Inserted Teeth, Designed by the Kalinin Freezer Works

a) View along arrow A; b) Section through B-B

milling cutters is performed by adjustment of the tooth position in two directions in the body by means of devices specially provided for this purpose. Figure 122 presents one such design (ENIMS). The teeth (1) are mounted to size with the aid of a special template or indexing device. Radial shifting of the tooth in the slot within the body (2) is performed by means of the wedge (3) actuated by the screw (4). This screw is fixed relative to the body, as it rests within a slot in the bottom ring (5). Axial movement of the tooth is by the screw (6) within the body of the toolholder. The screw (6) cannot move in axial direction. This is prevented by the L-shaped aligning strip (7) in the slot of the top ring (8). The spring (9) fixes the position of the tooth in the body before it is fastened down, this being done by the wedge (10) and the screw (11). The screws (11) have differential threading to facilitate disassembly of the milling cutter.

This design partially solves the problem of grinding inserted teeth outside the

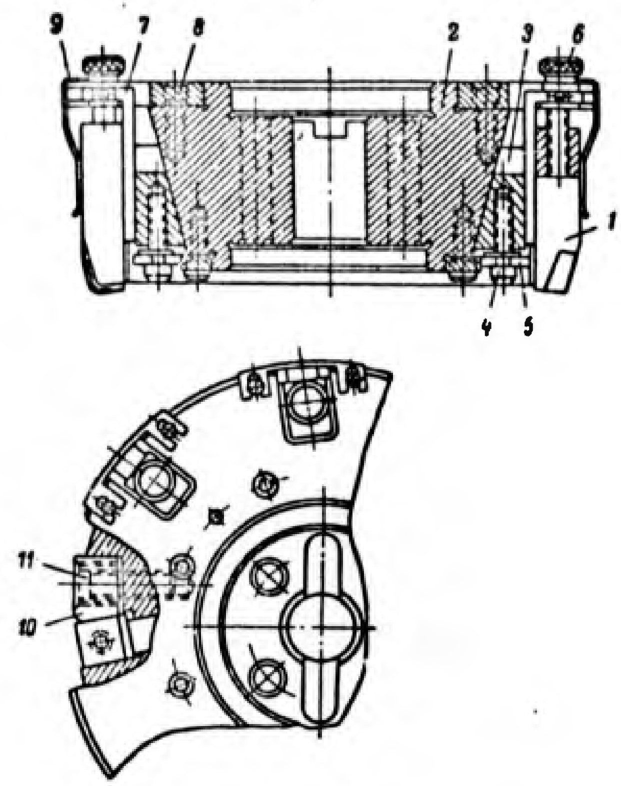

Fig.122 - ENIMS End Milling Cutter With Adjustable Inserted Teeth

cutter body. Serious inadequacies are inherent to this design, including the fact that the body is further complicated by special adjusting devices, the fact that the body has to be removed from the milling machine in order for the teeth to be mounted in the jig, and the large amount of time required to assemble the milling cutter. Moreover, the number of cutter bodies required to keep for proper working is not lower than when the more common designs are used.

Milling cutters with free tooth attachment are characterized by the absence of special adjustment devices. The teeth are installed by template in special jigs, or directly on the milling machine to line up with the mark made on the work by the first tooth alone. Milling cutters in this design category are employed at the Chelyabinsk Tractor Works* and have been introduced into the departmental standard for end mills.

The design with free tooth mounting enjoys advantages over the designs previously discussed. Assembly of the cutters is simplified and there is a reduction in the number of bodies simultaneously in use, inasmuch as tooth installation takes place without the need to remove the body from the milling machine. However, this design is not in wide use. The problem is that the degree of run-out of the teeth of milling cutters mounted by line-up depends upon the skill of the worker and the care with which the operation is performed. Moreover, assembly of large-diameter milling cutters consumes a lot of time. And when heavy cuts are taken, the tooth fastening is not dependable.

When compared to the above varieties of end mills with separate tooth grinding, cutters with precision tooth mounting enjoy a number of considerable advantages: universal application, reliable attachment for work with heavy cuts, reduction in the number of bodies to be kept on hand, and simplification of replacement of individual cutter teeth or sets of teeth right at the work station.

The Voskov Tool Mill has mastered the production of end mills of 200 - 350 mm diameter with precision mounting of teeth. Tests of these cutters in production have shown that the design provides the required precision in the mounting of individually ground teeth. However, significant drawbacks of design were found at the same time. Introduction of these cutters into industry is being delayed by the absence of designs for grinding the teeth and regulating their length.

At the present time, tool plants are making VNII-designed milling cutters of diameter $D > 320$ mm to special order (Fig.123). These cutters are distinguished by the presence of thrust washers and adjustment screws on the teeth, making it easier to assemble the cutters (without removing the body from the machine). This design

*This milling cutter is described elsewhere (Bibl.58).

provides for closer tolerance in the manufacture of the surfaces on which the teeth (2) rest in the body (1), and also of the teeth themselves. Each inserted tooth has three bearings in the body slot: a gage block (10) fastened to the bottom

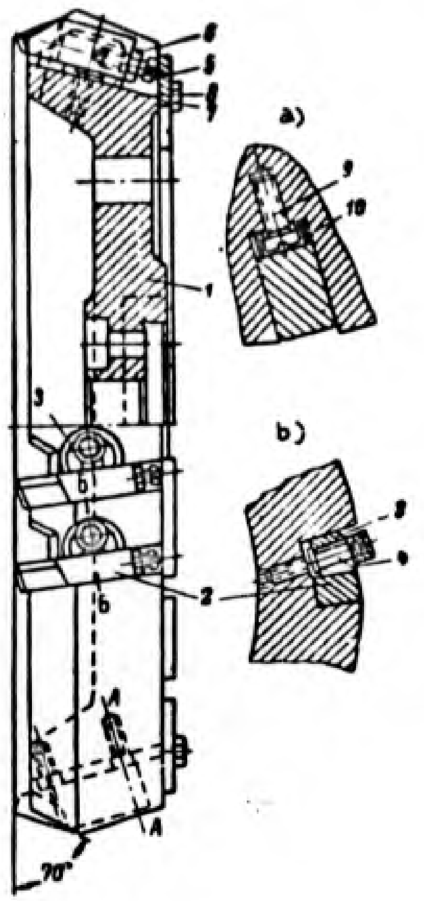

Fig.123 - End Milling Cutter Wtih Precision Setting of Teeth in the Body

a) Section through A-A
b) Section through B-B

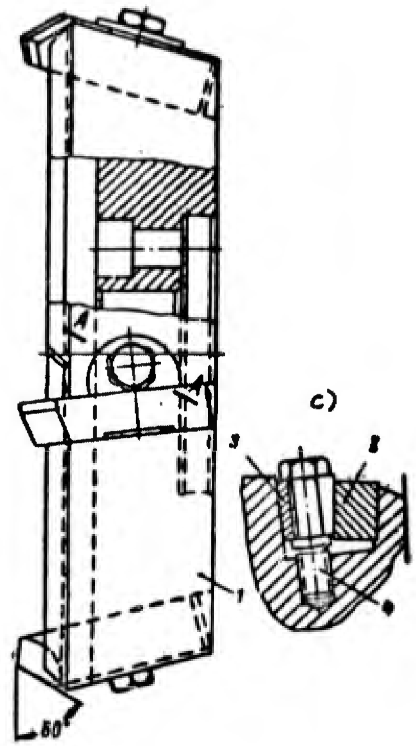

Fig.124 - End Milling Cutter With Precision Setting of Teeth in the Body by Lining-Up

1 - Body; 2 - Inserted tooth; 3 - Wedge; 4 - Bolt

a) Section through A-A

of the slot by screws (9) (bottom bearing); the side bearing surface of the body slot (side bearing); and a ground strip (7), held to the back of the body by a screw (8) (rear bearing).

The setting of the blocks (10) is monitored by an indicator, a single standard tooth being used for all slots in the body. The gage blocks are installed once and for all when the cutter is manufactured. Precise location of the third bearing base for the teeth in the body, relative to the axis of the cutter, is achieved by grinding the back of the body strictly normal to the axis of the cutter, and also by grinding the bearing surface of the strips (7).

Teeth are ground outside the body, in a special jig. On all teeth, identity of the positioning of the cutting edges relative to two base surfaces of the tooth is provided. The third base of the support is provided by a bolt (5) and a nut (6). After grinding, these are used to adjust the length of the teeth, in a special fixture. The support bases for the teeth in the jig reproduce those in the body of the cutter. In this connection, the point of support on the bolt (5), used in adjusting the length of the tooth, also serves as the point of support in mounting the tooth in the body of the mill.

The inserted tooth is fastened into the slot in the body by a single cylindrical keyed bushing (3), tightened by a fillet bolt (4).

When these parts are made to the necessary tolerance, the run-out of the cutter does not exceed the permissible limits.

The design of the devices referred to for grinding teeth outside the body and for adjusting tooth length is presented in the VNII pamphlet, Design of End Milling Cutters Having Teeth Ground Separately from the Body (Bibl.59).

It is not advisable to use this design (tooth installation on bearings) for milling cutters whose diameter is $D < 320$ mm. When teeth are mounted by lining up, this design is considerably simplified, and the use of milling cutters is considerably eased (there is no need for thrust strips and screws to regulate the length of the teeth). Figure 124 presents the VNII end milling cutter, providing for installation of teeth by lining up, which is recommended for milling cutters of diameter $D = 150 - 320$ mm. This may be employed for milling cutters to be ground in the assembled form and for cutters whose teeth are ground independently. In the latter case, the parts must be made to closer tolerances.

This design differs from the VNII designs for cutters in which teeth are ground in the assembled form (Fig.117 - 119) in that only one wedge is provided for fastening the tooth. Experiments run in the VNII have shown that the use of two wedges results in a greater error in tooth installation. Moreover, there is an increase in body dimensions and in the time required for assembling the cutter. Industrial practice has confirmed the fact that the use of a single wedge alone provides adequate reliability in tooth fastening.

Step Cutters. The use of face mills with the inserted teeth in "stepped" position relative to the work (Fig.125) is desirable in cases in which inadequate power in the milling machine and rigidity of the machine tool - workpiece - cutter system makes it impossible to remove the entire allowance in a single pass by a normal multiple-toothed mill. Step cutters may have two, three, four, or more steps. This is determined by the machining allowance, the dimensions of the cutter, the power of the motor driving the milling machine, the rigidity of the part being machined, etc.

It must be borne in mind that the cutter output, as defined by feed per minute, declines with increasing number of steps. This is clear from the following expression:

$$s_m = \frac{s_z \cdot z \cdot n}{i},$$

where s_m is feed per minute in mm/min;

s_z is feed per cutter tooth in mm;

z is the number of cutter teeth;

n is the cutter rpm;

i is the number of steps on the cutter.

Normal operating conditions for a step cutter are provided when the teeth of one step are in a specific state relative to those of another, in both axial and radial directions.

In the axial direction the teeth may be mounted either with even or uneven distribution of the allowance among the individual steps of the cutter (Fig.126). When the allowance is evenly divided (Fig.126a), the depth of cut for each step of the cutter can be defined as the quotient resulting from the division of the allowance

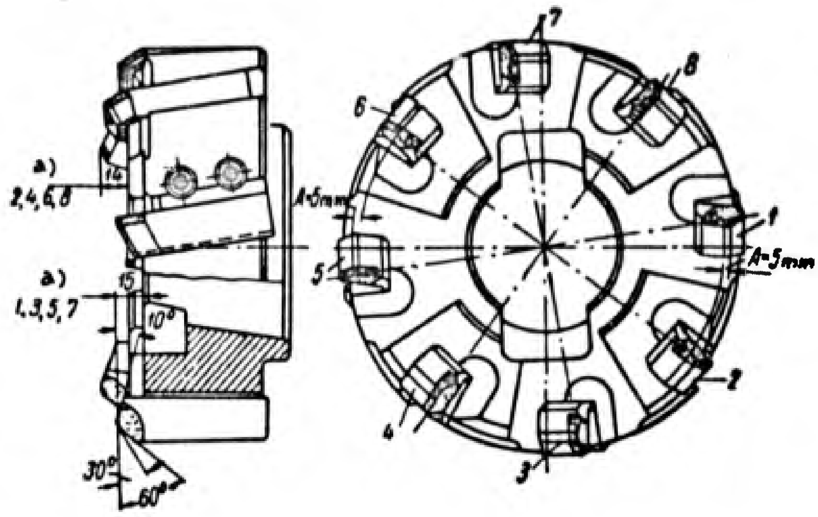

Fig.125 - Two-Step Clamped-On End Mill with Inserted Prismatic Teeth

1,3,5,7 - Teeth of first step; 2,4,6,8 - Teeth of second step

a) For teeth

by the number of steps. In uneven distribution of the allowance among the steps (Fig.126b), the depth of cut for the teeth farthest projecting in the axial direction

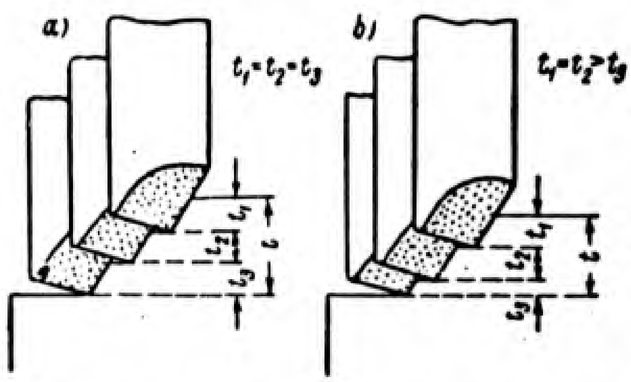

Fig.126 - Distribution of Allowance among Steps of a Three-Step End Milling Cutter

a - Even distribution; b - Uneven distribution

is taken as 1.5 - 2.0 mm. The rest of the allowance is divided uniformly among the remaining steps of the mill.

In the radial direction, the teeth of any given step must be at a specific distance from those in the adjacent step (Fig.125). This spacing A is determined by the formula

$$A = \frac{t}{\operatorname{tg} \varphi} + (s_z + 2) \text{ mm},$$

where t is the distance between the tooth addendums of adjacent steps in the axial direction, or depth of cut in mm;

φ is the face cutting edge angle of the mill;

s_z is the feed per cutter tooth in mm.

For a two-step milling cutter, A is 5 mm.

Face Mills With Mechanical Fastening of the Hard-Alloy Bars

Mechanical fastening of the cemented-carbide bars to the body of the cutter enjoys a number of advantages over brazing. The most important of these is the elimination of various defects arising in the bars during the brazing process and a reduction in tool cost, because of the fact that the operations involved in brazing and in the making of holders for inserted teeth are eliminated. However, mechanical fastening involves serious inherent drawbacks. The need to employ a portion of the hard-alloy bar for clamping purposes and the relatively small dimensions of standard bars mean that the cutter can be reground only a limited number of times. Together with a spalling of the bars which might occur upon mounting in the body, this results in an elevated consumption of hard alloys. The development of milling cutters of rational design with mechanical fastening of the cemented-carbide bars is facilitated by using bars with dimensions larger than standard (bars of this type are manufactured on special order).

Let us examine the characteristic designs of millers with mechanical fastening of prismatic bars, multiple-point tool inserts, and cemented carbide disks.

Figure 127 illustrates the Orgtransmash clamped-on end mill. The bars (2) are fastened in slots on the face of the body (1). Fastening is done by a cylindrical sleeve (3), with the aid of a screw (4). To facilitate disassembly of the cutter, the screws (4) are provided with differential threads. The teeth are adjusted by screws (5). These cutters are made in diameters of D = 150 - 250 mm.

This design is in limited use due to a number of shortcomings: the small number

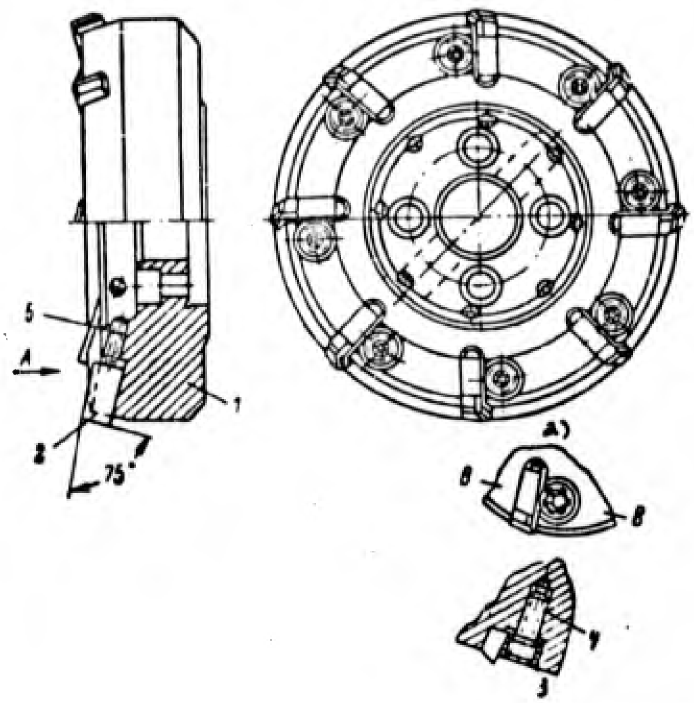

Fig.127 - Clamp-On End Mill With Mechanical Mounting of Cemented-Carbide Bars, Designed by Orgtransmash

a) View along arrow A; b) Section through B-B

of teeth (the same as in ordinary inserted-tooth cutters); the need to use carbide bars 9 - 10 mm instead of 3 - 4 mm thick, as is the case with brazed milling cutters; the complexities involved in making closed slots for the carbide bars; the higher tolerance needed in making the bushes 3 and the sockets for them in the body 1; and the fact that the cutter has to be ground in the assembled form.

The end mills designed by Orgavtoprom (Fig.128) employ multiple-point inserts of cemented carbide. Slit posts (2) are fastened into openings in the body (1) by means of blocks (3) and nuts (4). The bars (5) are inserted in the posts (2) and fastened therein by bolts (6). The screws (7), kept from rotating by set screws (8), have the purpose of adjusting the bars and preventing them from moving axially. When the mills are assembled, the position of the bars is adjusted on a special indexing device.

The advantages of this design are: the large number of grindings permissible

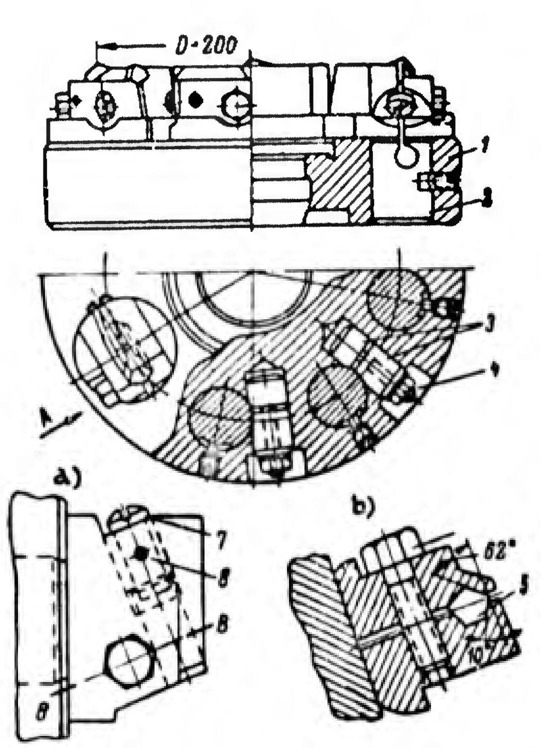

Fig.128 - Orgavtoprom End Mill With Mechanical Fastening of Multiple-Point Hard-Alloy Inserts

a) View along arrow A; b) Section through B-B

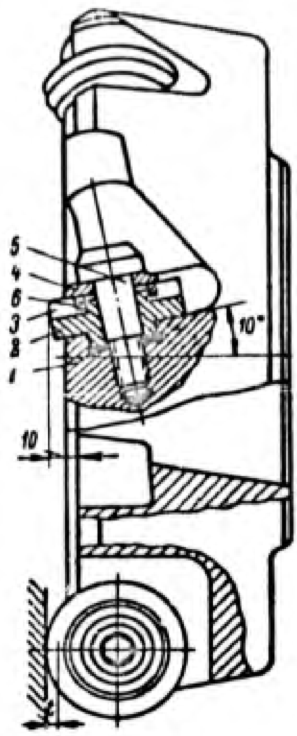

Fig.129 - End Mill With Mechanical Fastening of Cemented-Carbide Disks, Designed by NIAT

during the life of the set of bars, the long overall life of the cutter between grindings (by the artifice of rotating the bars), and the possibility of grinding each bar separately. However, this design is not to be recommended for general use. In addition to complexity, its major drawbacks are: the need to use a special jig for installing the bars in the body of the cutter (the body has to be removed from the milling machine for this purpose); the fact that this design is not suited to small-diameter cutters; the small number of teeth; and the fact that only open surfaces can be machined in this way.

The NIAT end mills (Fig.129) utilize carbide disks. The disks (3), seated in bushes (6), and the cutter holders (2), are mounted in the body (1) of the cutter. The disk is fastened by the screw (5) via the washer (4).

This design enjoys significant advantages: dependable fastening of the cemented-carbide disks, permitting a precise mounting in the body of the mill without the use of templates; elimination of a possible shifting of the disks during the fastening process or during operation of the cutter; easy shifting (rotating) of the disks when they are dulled, without removing the body from the milling machine; high over-all cutter life between grindings vs. the use of prismatic teeth (8 - 10 times as high when one side of the disk is used, 15 to 20 times when both are employed); and ease of individual grinding of the set of disks on a cylindrical grinder.

The shortcomings of the design include: the small number of teeth, the fact that only open surfaces can be machined, an increased tendency to vibrate due to the great length of the working portion of the cutting edge and the small angle of the face cutting edge, and the complex procedures involved in manufacturing the miller body to the required tolerance.

This design may be recommended for use in cases in which reduction of the time required to grind the cutters is the major problem.

23. Dulling Criteria and Service Life of Cutter

When steels are milled at high speed by face cutters tipped with titanium-tungsten carbides working at feeds not higher than s_z = 0.2 mm/tooth, wear of the cutter teeth occurs chiefly on the periphery. At higher feeds, wear occurs on both face and periphery. With an increase in feed s_z there is an increase in wear on the face and a reduction in wear on the back.

In the face-milling of hardened steels at low feeds s_z, the wear of the tool occurs on its periphery. In some cases the cemented-carbide bar will show a slight splitting on its face. Figure 130 illustrates experimentally-determined (Bibl.60)

a) b)

Fig.130 - Tooth Wear of End Mill in the Machining of Hardened Steel ($D = 110$ mm, $\gamma = -22^\circ$, $\varphi = 60^\circ$, $\varphi_o = 30^\circ$, $t = 2$ mm, $s_z = 0.095$ mm/tooth; $v = 112.6$ m/min, $B = 90$ mm):

a - Normal peripheral wear without splitting of the cemented-carbide bar;
b - Wear accompanied by splitting of bar on face

characteristic types of wear of a single-tooth end mill, tipped with T15K6T in the machining of steel hardened to $H_{R_C} = 51$.

Generalization of a number of investigations and of industrial practice has led P.A.Markelov to recommend the following degrees of peripheral tooth wear as criteria for the dulling of end mills in the machining of hardened steels:

Hardness of hardened steel H_{R_C}	Optimum peripheral mill tooth wear h, in mm
38 - 47	2.0 - 1.5
47 - 54	1.5 - 1.0

The NIBTN takes h = 1.5 mm for steels hardened to $H_{R_C} = 38 - 58$ (Bibl.27). The latter data are employed in the cutting schedules presented in Appendix II.

In Chapter III of this book, which was devoted to the turning of hardened steels, we showed that a visual criterion of the dulling of cutters in turning on the lathe is the acquisition of a "goffered" appearance by the chip. It should be noted that this criterion may also be employed in the end-milling of hardened steels.

A correct determination of the tool life of a cutting tool is quite important in determining the efficiency of the machining process. The literature data on the tool life of cemented-carbide end mills show major differences of opinion. M.N.Larin

(Bibl.61) defines the service life of end mills in terms of their diameter:

$$T = (1{,}25 \div 1{,}50)\, D \text{ min} \; ,$$

where D is the mill diameter in mm.

P.A.Markelov (Bibl.60) suggests to determine the end-mill life relative to the number of teeth, figuring 30 - 40 min per prismatic tooth:

Number of teeth in end mill, z	4	5	6	8	10	12
Service life T, in min	120-160	150-200	180-240	240-320	300-400	360-480

However, investigations of fast milling of chromium-molybdenum steel with end mills of a diameter of D = 265 mm and with tips of T15K6U (Bibl.62) showed that the life of a six-tooth mill differed insignificantly from that of a three-tooth or of a single-tooth mill.

The NIBTN (Bibl.27) mentions considerably longer lives for end milling cutters than obtained from the data by M.N.Larin and P.A.Markelov:

Diameter of end milling cutter, D, in mm	75	90	110	130-150	200	250
Service life T, in mm	150	240	300	360	480	600

The recommended cutting schedules (Appendix II) specify T = 300 mm. The author believes this service life to be justified by the degree of peripheral dulling of the cutter teeth (h = 1.5 mm).

24. Geometry of Milling Cutter

Here we present the currently employed nomenclature and terminology for the shape of end-mill teeth edges (Fig.131). The major geometric parameters are:

In Fig.131, the symbols used denote:

γ - true rake angle;

α - working relief angle;

α_o – nose working relief angle;

α_1 – working relief angle of face cutting edge;

λ – angle of rake of the main cutting edge;

φ – main angle in plan (angle in plan of main cutting edge);

φ_o – angle in plan of transition to cutting edge;

φ_1 – angle in plan of face cutting edge;

f_o – length of transition to cutting edge.

In addition, in the making and grinding of end mills it is necessary to know the following supplementary angles:

ω – longitudinal (axial) true rake angle;

γ_1 – lateral (radial) true rake angle.

The angles γ, ω, and γ_1 relate to the axial rake angle λ and the peripheral

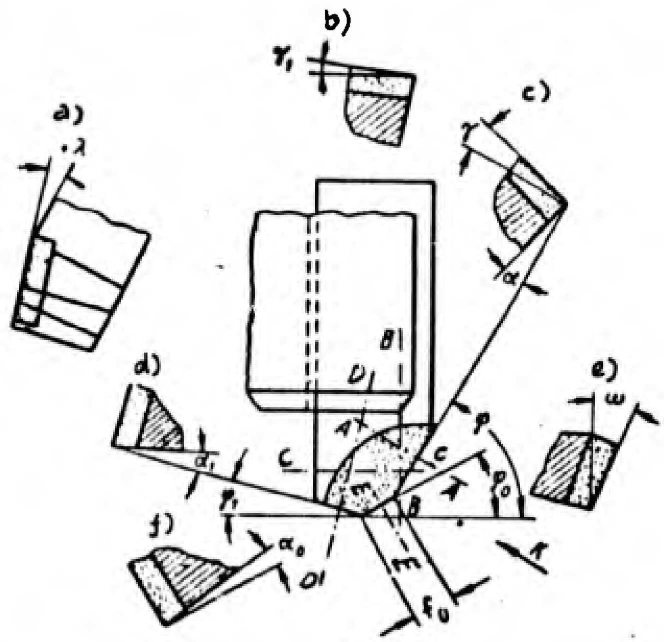

Fig.131 – Geometry of Cutting Part of End Mill

a) View along arrow K; b) Section through C–C; c) Section through A–A; d) Section through D–D; e) Section through B–B; f) Section through E–E cutting edge angle φ as follows:

$$\operatorname{tg} \gamma = \operatorname{tg} \gamma_1 \cdot \sin \varphi + \operatorname{tg} \omega \cdot \cos \varphi,$$
$$\operatorname{tg} \lambda = \operatorname{tg} \gamma_1 \cdot \cos \varphi - \operatorname{tg} \omega \cdot \sin \varphi,$$
$$\operatorname{tg} \omega = \operatorname{tg} \gamma \cdot \cos \varphi - \operatorname{tg} \lambda \cdot \sin \varphi,$$
$$\operatorname{tg} \gamma_1 = \operatorname{tg} \gamma \cdot \sin \varphi + \operatorname{tg} \lambda \cdot \cos \varphi.$$

True Rake Angle γ

Experiments have shown that in high-speed milling of steels, including hardened steels, with cemented-carbide face mills, the optimum true rake angle γ is governed chiefly by the physical and mechanical properties of the material machined (tensile strength σ_t, hardness, etc.). Each steel, with its particular physical and mechanical properties, has an optimum true rake angle at which cutter life is longest. The tool life is reduced by either increasing or reducing the true rake angle relative to this optimum value. This is demonstrated in Fig.132, where the relationship between the life of an end milling cutter and the true rake angle γ is plotted (Bibl.60). The test was run on 30KhGSA steel, hardened to H_{R_C} = 51 to 54, at a depth of the milling cut of t = 3 mm, a width of cut of B = 90 mm, a feed per tooth of s_z = 0.095 mm, and a cutting speed of v = 138 m/min. The mill was tipped with T15K6S hard alloy, its diameter was D = 110 mm, and the number of cutter teeth was z = 1. Dulling of the teeth flank

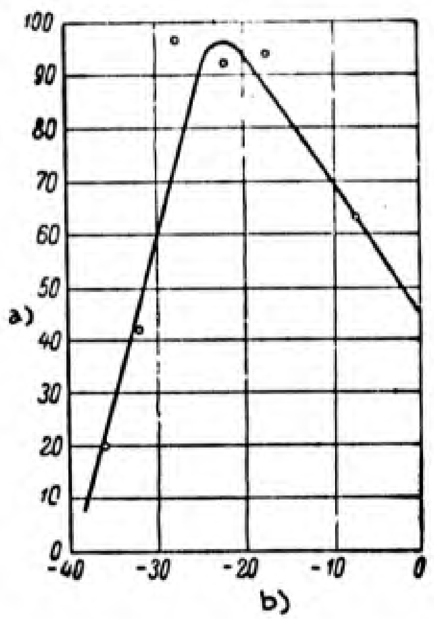

Fig.132 - True Rake of Teeth Versus Life of End Mill. Machining of 30KhGSA steel hardened to H_{R_C} = 51 to 54 by a mill tipped with T15K6S cemented carbide (α = 23°, λ = 6°, φ = 60°, φ_o = 30°, f_o = 2.0 - 2.5 mm)

a) Face milling cutter life T, min;
b) True rake angle of cutter γ°

was h = 1.2 mm. The true rake angle was varied in an interval of -7 to -37°.

The curve shows the optimum true rake angle for this steel to be approximately γ = -20°. The true rake angle becomes less negative on reduction in the hardness of the tempered steel.

The angle γ is considerably more negative for hardened than for unhardened steels. Test data (Bibl.60) for 30KhGSNA steel (σ_t = 80 kg/mm²) at t = 3 mm, B = 175 mm, s_z = 0.1 mm, v = 286 m/min, and h = 1.0 mm show the optimum true rake angle of a milling cutter tipped with T15K6 alloy to be γ = -5°.

Table 66 presents the recommendations by P.A.Markelov (Bibl.60) and M.N.Larin

Table 66

True Rake Angle γ

Source of Data	Hardness of work steel H_{R_C}			
	38–44	45–49	50–54	55–64
	True rake angle γ°			
P.A.Markelov	−11 ÷ −14	−14 ÷ −18	−18 ÷ −22	—
M.N.Larin	−5	−10	−10	−15

(Bibl.31) with respect to the true rake angle of face mills for machining hardened steels.

As we see, M.N.Larin employs considerably smaller negative true rake angles.

The standards for high-speed milling of ferrous metals, published by the Ministry of the Machine-tool Manufacturing Industry (Bibl.27), show the true rake angle to be γ = -10° for steels hardened to H_{R_C} = 38 - 58.

It should be noted that P.P.Grudov (Bibl.63) is in favor of large negative angles γ. In the high-speed milling of hardened steels he recommends γ = -20° for T15K6 and γ = -15° for T5K10.

The ideas advanced in Chapter III with respect to using the smallest possible negative true rake angles in the turning of hardened steels are believed by the present author to be equally valid for end-milling. However, end mills differ from turning cutters in that they work under impact loads. Therefore, the cutting edges of the teeth of face mills must be stronger than those of lathe cutters, which is accomplished by increasing the negative value of the true rake angle. In the author's opinion, the true rake angles recommended by M.N.Larin (Table 66) should be employed in the face milling of hardened steels by tools tipped with cemented carbides of the

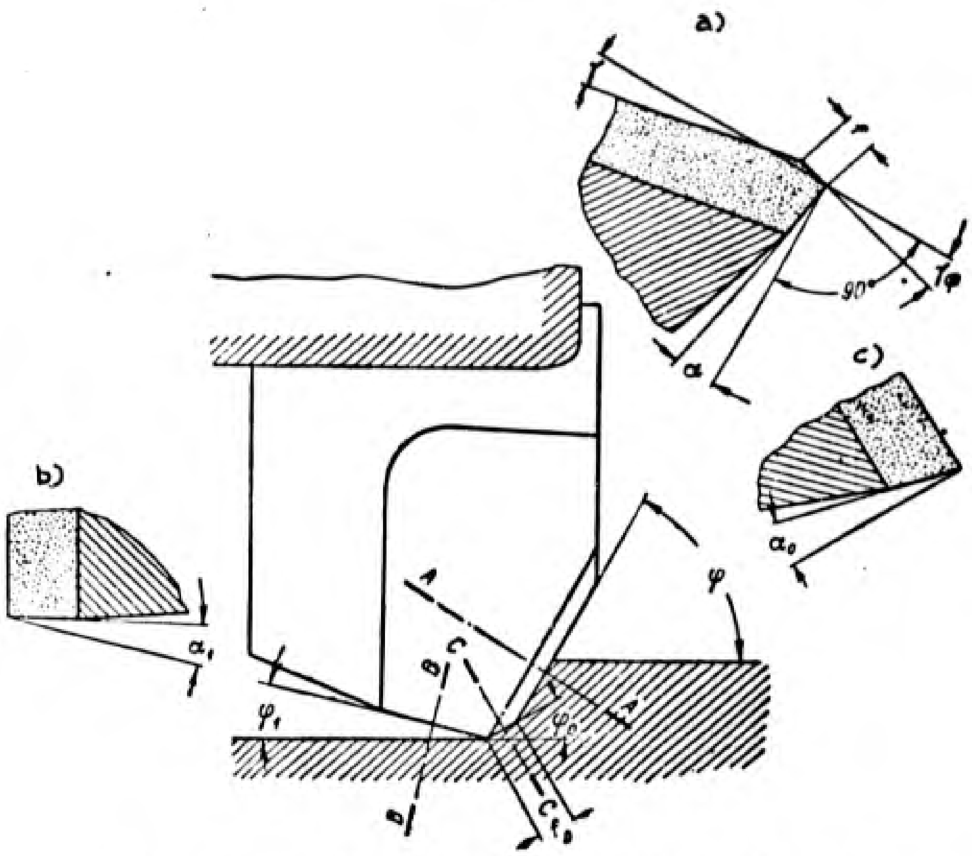

Fig.133 - Shape of Tooth of End Milling Cutter

a) Section through A-A; b) Section through B-B; c) Section through C-C

titanium-tungsten group (T15K6, T14K8, and T5K10). Only for T30K4 should the negative values of these angles be increased by 3 - 5°.

In conclusion, let us examine the problem of the two angles of grinding of end-mill teeth faces (Fig.133). The following was found in an investigation by

P.P.Grudov and S.I.Volkov (Bibl.63) into the milling of unhardened 18KhNMA steel, σ_t = 110 - 120 kg/mm^2 (the tests were run with a single-tooth end mill, 200 mm in diameter, of the following geometry: true rake angle $\gamma = 15^{\circ}$, true rake of flat $\gamma_f = -20^{\circ}$, $\alpha = 15^{\circ}$, $\lambda = 15^{\circ}$, $\varphi = 60^{\circ}$, $\varphi_1 = 4 - 5^{\circ}$, $\varphi_o = 30^{\circ}$, f_o = 0.1 - 0.3 mm; width of flat f varied from 0 to 3 mm; cutting conditions t = 3 mm, B = 100 mm, s_z = 0.089 mm/tooth, v = 180 m/min, surface per pass l = 300 mm).

1. When the flank wear was identical with a flat width of $f \leq 1.5$ mm, the life diminished with a reduction in flat width.

2. The width of the flat f greatly influences the conditions of chip flow and the degree of deformation thereof. As f rises from 0 to 0.5 mm, there is a pronounced increase in the deformation of the chip. If the flat is narrow ($f \leq 0.2$ mm), the chip rests on the portion of the face with positive true rake angle. Here, deformation of the chip occurs in the same manner as in a face that has a positive angle γ along the entire surface. In this situation, the presence of a flat has no effect upon the deformation of the chip.

In the case of a face with a width of $f > 0.5$ mm, the chip rests only on the portion of the face that has a negative true rake angle, and the chip is therefore subject to pronounced deformation.

3. To reduce the deformation of the chip, it is desirable to use a flat width for which the true rake angle will be between 0.1 and 0.3 mm. However, at such a flat width, premature chipping of the cutting edge occurs since, under these conditions, the cemented carbide is subject to bending and not to compression, which latter is the type of stress to which cemented carbides offer the best resistance.

4. The purpose of the double grinding of the face is not to reduce the chip deformation and cutting force, which are of secondary significance here, but to increase the tool life.

P.P.Grudov and S.I.Volkov have come to the conclusion that, in high-speed milling of steel by end mills tipped with cemented carbides, it is necessary to provide a negative true rake for the entire face. The use of a face ground at two angles with a positive main true rake angle and a negative true rake angle on a flat less than 1.5 mm wide results in a reduction of the cutter life.

It is obvious that the fact that cutters with the face cut at two angles are inefficient in fast face-milling of unhardened steels will manifest itself even more markedly in the machining of hardened steels.

We note that the NIBTN (Bibl.27) recommends that a face cut at two angles be employed in fast face-milling of steels, the first true rake angle being 5° larger than that on the flat. For hardened steels the angles are $\gamma = -5^{\circ}$ and $\gamma_f = -10^{\circ}$, the width of the flat being $f = 1.5$ mm. As indicated in Chapter III, a face having this shape results in some increase in the number of possible regrindings of the carbide bar, as compared to a flat face.

Axial Rake λ of the Cutting Edge

In the fast milling of steels by hard-alloy face mills, the main purpose of the axial rake λ is that of strengthening the edge. The angle λ influences the position of the point of impact of the mill tooth cutting edge at the moment that it bites into the workpiece (Fig.134). At $\lambda = 0^{\circ}$ and at any value of the true rake angle γ, the initial shock is distributed along the entire cutting edge or parallel thereto. At $\lambda < 0^{\circ}$, the leading edge of the tooth is the first part to touch the work, but at $\lambda > 0^{\circ}$, the impact occurs at a distance from the leading edge approximately equal to the depth of cut. Therefore, the working portion of the hard-alloy bar must be protected against premature chipping or crumbling-out at the leading edge of the tooth.

In fast milling of steels by face mills tipped with cemented carbides, only positive axial rakes λ should be employed, despite the fact that an increase in the positive angle λ increases the degree of chip deformation and the power consumption and introduces difficulties into the chip removal.

The magnitude of the angle λ is affected primarily by the machining conditions: whether the workpiece travels with or without impact. The angle λ also depends upon the physical and mechanical properties of the material machined and on the strength of the hard alloy. The angle λ must be increased with any increase in the strength of the material mechined and with any reduction in the strength of the hard alloy.

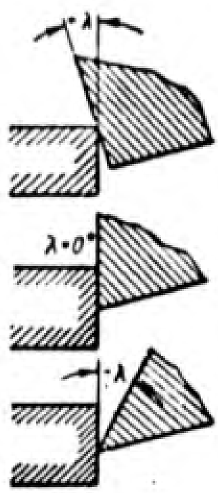

Fig.134 - Diagram Showing Site of Initial Impact of Cutting Edge of End Mill Tooth on Contact with the Workpiece, Varying with the Axial Rake λ.

Figure 135 presents the relationship between the life of a single-tooth face mill tipped with T15K6 alloy (D = 200 mm) and the axial rake λ, as plotted from experimental data (Bibl.63). Grade 18KhNMA steel (σ_t = 110 to 120 kg/mm^2) was tested at t = 3 mm, B = 100 mm, l = 100 mm, v = 81.6 m/min, and s_z = = 0.122 mm. The axial rake λ was varied from 0 to 39°. The experiments were conducted with symmetrical cutting and without coolant.

As will be seen, the optimum angle λ is in the 10 to 20° interval, and the maximum life is obtained at λ = 15 - 16°.

V.N.Mezhyuev (Bibl.61) came to approximately the same conclusions in investigating the T = f(λ°) relation while varying the axial rake λ from -10 to 45°. The experiments were run with single-tooth end mills (D = 240 mm), tipped with T15K6 alloy. Number 20 steel was machined at t = 4 mm, B = 110 mm, v = 305 m/min, and s_z = 0.14 mm.

The experiments showed (Fig.136) that the magnitude and sign of the true rake angle γ do not affect the optimum value of λ, which is +10° either for cutters with γ = +10° or for cutters with γ = -10°. At greater values of λ (> 30°), the life of the cutter diminishes sharply, because the wear of the tooth flank spreads to the face cutting edge.

With an increase in the angle λ, an increase occurs in the degree of deformation of the chip, which manifests itself in an increase in longitudinal contraction

(Bibl.63). An increase in the angle λ from 0 to 22° causes an increase in the shrinkage of the chip from 1.6 to 2.0, or by 25% (Fig.137). A further increase in the angle λ results in a sharp rise in the deformation of the chip: An increase from 22 to 37° in the angle λ represents an increase in chip contraction from 2.0 to 4.2, i.e., by more than twice its value.

This pronounced increase in chip shrinkage testifies to the fact that cutting

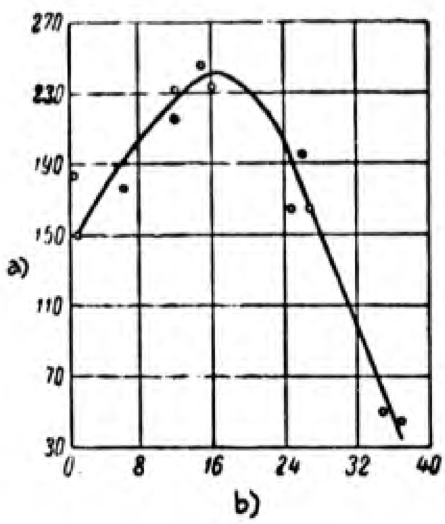

Fig.135 - Effect of Angle λ upon the Life of a Face Mill in Fast Milling of 18KhNMA Steel with Tensile Strength σ_t = 110 - 120 kg/mm². Mill dulling criterion, h = 1.75 - 1.90 mm (α = 4 - 5°, γ = -10°, φ = 90°, φ_0 = 45°, φ_1 = 3 - 5°, f_0 = 1.0 - 1.3 mm)

a) Cutter life T, min; b) Axial rake λ°

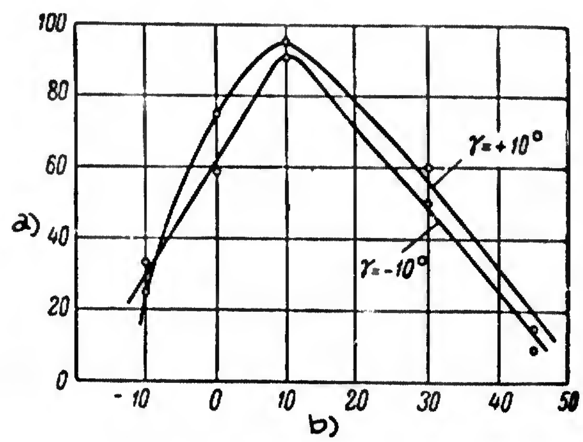

Fig.136 - Effect of Axial Rake of Face Mill Tipped with T15K6 Alloy, upon its Life (α = 15°, φ = 75°, φ_0 = 40°, f_0 = 1 mm, γ = +10 and -10°)

a) Cutter life T, min
b) Axial rake λ°

conditions become worse with an increase in axial rake. The degree of deformation of the chip increases, as does the cutting force and the power consumed for cutting.

P.P.Grudov and S.I.Volkov believe that the optimum axial rake λ = 15°, which they found to hold for steel with σ_t = 110 - 120 kg/mm², has to be employed for all steels. M.N.Larin (Bibl.64) and the NIBTN (Bibl.27) also accept λ = 15° for face-milling both of unhardened and of hardened steels. For asymmetrical milling, M.N.Larin suggests λ = 5°.

P.A.Markelov holds another view (Bibl.60). In his opinion, the angle λ has to be reduced with an increase in the strength of the steel being machined:

Tensile strength of the steel σ_t in kg/mm^2	Axial rake λ°
60 - 100	15
100 - 140	10
140 - 180	5

Strengthening of the cutting edge of face mills tipped with titanium-tungsten carbides is of even greater importance in the machining of hardened steels than in the milling of the unhardened types. The axial rake of face mills used in machining hardened steels should in any case not be less than the optimum λ found in studies of unhardened steels. The author maintains that, until special studies are made, the axial rake employed in the milling of hardened steels should be $\lambda = 15^{\circ}$. This is the λ value of the angle λ specified in the cutting schedules he recommends.

Working Relief Angle α

The working relief angle α exerts a significant influence upon the lives of cemented-carbide face mills. Investigations have determined that, in the milling of steels with hard-alloy face mills having low working relief angles, considerable friction occurs between the mill teeth flanks and the surface being cut as well as intensive cutter wear and vibrations which latter result in crumbling-out of the cemented-carbide bar. At high working relief angles, there is a reduction in the lip angle of the mill teeth, a reduction in the strength of the working portion of the cemented-carbide bar, premature crumbling and chipping of the cutting edge, and limited dulling of the teeth on their flanks.

A generalization of the results of numerous investigations has led M.N.Larin (Bibl.31) to the conclusion that the optimum working relief angle depends chiefly upon the maximum thickness of cut a_{max}. The smaller the thickness of cut (feed per tooth), the greater must be the working relief angle. Cutting speeds up to 350 m/min, mechanical properties of the machined steel within a range of σ_t = = 40 - 120 kg/mm^2, and a true rake angle γ ranging from +15 to -15° have so negligible an influence upon the optimum working relief angle as to make it possible to disregard them for all practical purposes.

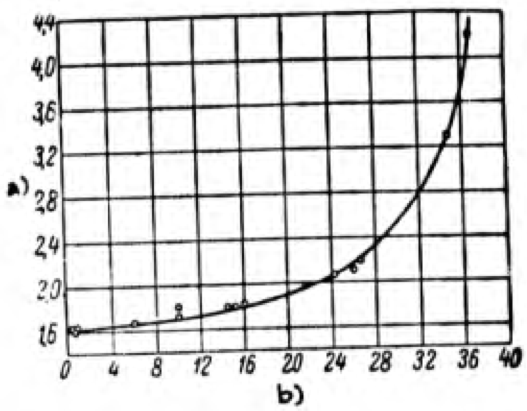

Fig.137 - Effect of Axial Rake of Face Mill (D = 200 mm) Tipped with T15K6 Alloy upon the Longitudinal Shrinkage of Chip in the Machining of 18KhNMA Steel. Cutting schedule: t = 3 mm, s_z = 0.122 mm/tooth, v = 81.6 m/min, B = 100 mm. Cutter shape: α = 4 to 6°, γ = -10°, φ = 90°, φ_o = 45°, φ_1 = 3 - - 5°, f_o = 1.0 - 1.3 mm.

a) Longitudinal shrinkage of chip
b) Axial rake λ^o

Let us next turn to experimental data. Figure 138 presents the relationship of the total length of the machined surface to the working relief angle α, as derived in a study by A.V.Shchegolev and V.I.Tkachevskiy (Bibl.62) in the fast milling of carbon steel No.40. The tests were run with face mills tipped with T15K6, diameter D = 250 mm, at a width of cut of B = 90 mm, a depth of cut of t = 5 mm, a feed of s_z = 0.095 mm/tooth, and a cutting speed of v = 200 m/min. As the curve shows, the optimum working relief angle is α_{opt} = 16 - 20°. The authors report that they obtained analogous results with the other steels tested.

In the fast face-milling of 18KhNMA steel (σ_t = 110 - 120 kg/mm^2), the optimum working relief angle of the cutter proved to be α_{opt} = 15° (Bibl.63).

Figure 139 presents curves describing the relationship of the total life of end mills tipped with titanium-tungsten carbides with the working relief angle α in the high-speed machining of hardened and unhardened steels (Bibl.60). The curves show that, for hardened 30KhGSA steel, the interval of optimum values of the working relief angle is α_{opt} = 23 - 28°, whereas for both grades of unhardened steels it is

$\alpha_{opt} = 12^{\circ}$.

Thus, the working relief angle is also influenced by the true rake angle γ. The higher the negative true rake, the higher will be the working relief angle. This explains the substantially higher value of the angle α for hardened steel than for unhardened steels. The former was machined by a cutter whose true rake angle was $\gamma = -22^{\circ}$, whereas unhardened steels were milled at $\gamma = -5^{\circ}$. The feed per tooth was approximately the same for all the steels tested.

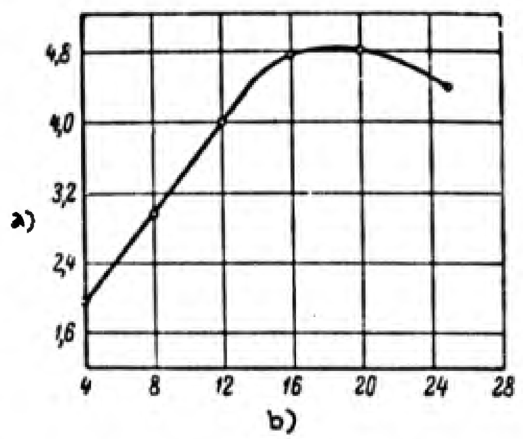

Fig.138 - Effect of Working Relief Angle of Face Mills Tipped with T15K6 Cutters upon the Total Length of Machined Surface in the Milling of No. 40 Steel, $\sigma_t = 57$ kg/mm^2. Data by A.V.Shchegolev and V.I.Tkachevskiy ($\gamma_1 = -10^{\circ}$, $\gamma_2 = -10^{\circ}$, $\varphi = 75^{\circ}$, $\varphi_1 = 15^{\circ}$, $\alpha_1 = 12^{\circ}$, $r = 1.5$ mm)

a) Total length of machined surface, m; b) Working relief angle α°

In view of the fact that the physical and mechanical properties of the workpiece influence the optimum thickness of cut a_{max} and the true rake angle γ in the fast milling of steels with face mills, P.A.Markelov has defined α as follows, in accordance with the tensile strength of hardened steel: $\alpha = 16^{\circ}$ for $\sigma_t = 120$ kg/mm^2, $\alpha = 20^{\circ}$ for $\sigma_t = 180$ kg/mm^2. NIBTN makes the same recommendations for the angle α (Bibl.27).

M.N.Larin (Bibl.31) suggests that the same working relief angle be employed for cemented-carbide face mills in the machining of both unhardened and hardened steels: $\alpha = 15^{\circ}$ at $a_{max} > 0.08$ mm and $\alpha = 20^{\circ}$ at $a_{max} < 0.08$ mm.

These data differ from the opinion of A.V.Shchegolev and V.I.Tkachevskiy (Bibl.62) who believe that the working relief angle of end mills has to be reduced with increasing strength of the work steel.

The author employs the following working relief angles for end milling of hardened steels: $\alpha = 15^{\circ}$ for steels of $H_{R_C} = 38 - 49$ and $\alpha = 20^{\circ}$ for steels of

$H_{R_C} > 49$.

Let us consider the influence of the working relief angle upon the radius of the cutting edge and the achievable tolerance which is related to dimensional stability of the tool.

The purpose of providing a working relief angle in face mills is, in part, to

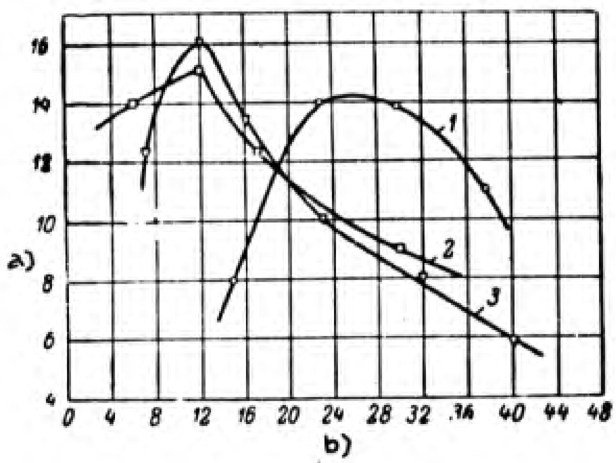

Fig.139 - Effect of Working Relief Angle of End Mill Upon Total Life

1 - Steel 30KhGSA hardened to H_{R_C} = 51 to 54, D = 110 mm, z = 1, T15K6, $\gamma = -22°$, $\alpha = 6°$, $\varphi = 60°$, $\varphi_o = 30°$, t = 2 mm, B = 90 mm, s_z = 0.095 mm/tooth, v = 138.2 m/min, h = 1.2 mm; 2 - Steel 40KhNMA (σ_t = 70 kg/mm^2), D = 90 mm, z = 1, T30K4, $\gamma = -5°$, $\lambda = 15°$, $\varphi = 60°$, $\varphi_o = 30°$, t = 3 mm, B = 70 mm, s_z = 0.1 mm/tooth, v = 450 m/min, h = 1.2 mm; 3 - Steel 30KhGSA (σ_t = = 80 kg/mm^2), D = 200 mm, z = 1, T15K6, $\gamma = -5°$, $\lambda = 15°$, $\varphi = 60°$, $\varphi_o = 30°$, t = 3 mm, B = 174 mm, s_z = 0.1 mm/tooth, v = 286 m/min, h = 1.0 mm.

a) Overall tool life, hrs; b) Working relief angle $\alpha°$

reduce the radius of the cutting edge so as to permit the cutter tooth to penetrate into the work metal with a minimum angle of slip. From this point of view, it is necessary, in the milling of hardened steels with thin chip, to seek to increase the working relief angle. On the other hand, an increase in the working relief angle results in an increase in dimensional wear of the cutter and in a reduction in the precision of machining on the given pass.

The working relief angle of the face cutting edge is taken to be $\alpha_1 = 8 - 10°$, regardless of the mechanical properties of the steel being machined. If the angle α_1

is excessive, a reduction in nose strength will occur and there is increased danger of crumbling-out at the junction of the cutting edges.

The nose working relief angle α_0 is taken to be the same or somewhat smaller than the first working relief angle α.

Complement of Peripheral Cutting Edge Angle φ

Given identical depth of cut t and feed per tooth s_z, a reduction in the complement of the peripheral cutting edge angle φ results in a reduction in thickness of the cut a, an increase in its width b, as well as in an increase in the nose angle. The result is a stronger edge, a reduction in thermal stress, and an increase in the life of the milling cutter.

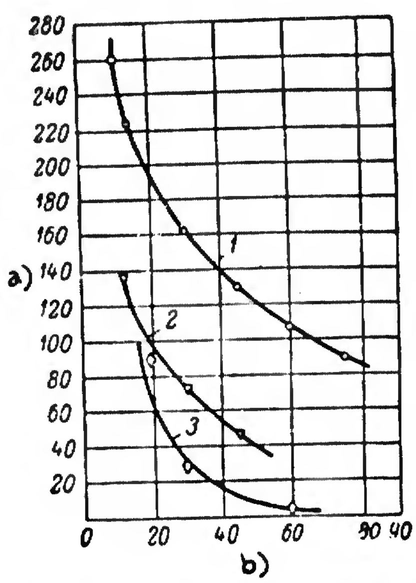

Fig.140 - Effect of Complement of Peripheral Cutting Edge Angle φ upon Life of End Mills:

1 - Steel OKhNM (σ_t = 87 kg/mm^2), D = = 250 mm, T15K6, γ = -10°, λ = 10°, t = 1.5 mm, s_z = 0.25 mm/tooth, B = = 100 mm (according to L.A.Rozhdestvenskiy). 2 - Steel 18KhNMA (σ_t = 110 to 120 kg/mm^2), D = 200 mm, T15K6, γ = = -20°, λ = 15°, t = 1.5 mm, s_z = = 0.244 mm/tooth, B = 100 mm, v = = 197.6 m/min (according to P.P.Grudov). 3 - Steel 30KhGSA (σ_t = 75 kg/mm^2), D = 150 mm, T15K6, γ = -5°, λ = 15°, t = 2 mm, s_z = 0.26 mm/tooth, B = = 110 mm, v = 297 m/min (according to P.A.Markelov)

a) Life of end mill T, min; b) Complement of peripheral cutting edge angle φ°

Figure 140 (Bibl.60) shows the effect of the complement of the peripheral cutting edge angle φ upon the life of end mills tipped with cemented carbides. A reduction in the angle φ results in an increase in cutter life.

According to data by P.A.Markelov, the relationship between the complement of the peripheral cutting edge angle φ, the life of the mill T, and the cutting speed v for thicknesses of cut $a \leq 0.11$ mm/tooth is expressed by the equations:

$$T = \frac{C_\varphi}{\sin\varphi} \; min.;$$

$$v = \frac{C'_\varphi}{(\sin\varphi)^{0.3}} \; m/min.$$

It follows from these formulas that, if the life of an end mill with a complement of peripheral cutting edge angle of $\varphi = 60°$ is taken as unity under given cutting conditions (v, s_z, t, etc.), then, under these same conditions, the life of a cutter for which $\varphi = 30°$ will be 1.7, and that of one in which $\varphi = 20°$ will be 2.5. At identical tool life, the cutting speed for an end mill with $\varphi = 20°$ may be increased 15% of that for a cutter the complement of whose peripheral cutting edge angle is $\varphi = 60°$.

However, when using end mills with low complements of peripheral cutting edge angle, the longitudinal cutting forces acquire higher values, and if the system comprising the milling machine, the workpiece, and the tool are of inadequate rigidity, vibration and bouncing of the workpiece sets in. In some cases, vibration and chatter are so great that milling ceases to be possible. Thus, in the fast milling of 30KhGSA steel (σ_t = 75 kg/mm^2) by an end mill (D = 150 mm, z = 8) at a cutting speed of v = 280 m/min, a feed of s_z = 0.15 mm/tooth, a depth of cut of t = 5 mm, and a width of cut of B = 110 mm, the longitudinal force will be: 800 kg at $\varphi = 60°$, 1550 kg at $\varphi = 30°$, and 2500 kg at $\varphi = 20°$ (Bibl.60).

Consequently, in connection with a reduction in the complement of the peripheral cutting edge angle from 60° to 30° and 20° the axial force rose two- and three-fold, respectively. Therefore, the use of end mills with low complement of peripheral cutting edge angle φ involves a considerable diminution of the allowance that can be removed at a single pass of the mill at $\varphi = 60°$.

It should also be borne in mind that a reduction in φ increases the power consumption. For example, in the case of an end mill for which the complement of the peripheral cutting edge angle is $\varphi = 30°$, this power is 25 - 30% higher than in the case of a mill for which $\varphi = 60^\circ$.

Low complements of the peripheral cutting edge angle φ may find application in two-step end mills, in the machining of hardened steels.

A.V.Shchegolev and V.I.Tkachevskiy (Bibl.62) found other results in their research.

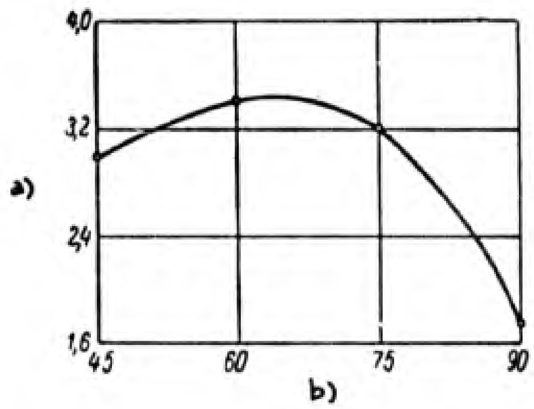

Fig.141 - Effect of Complement of Peripheral Cutting Edge Angle φ of End Mill (D = 250 mm), Tipped with T15K6 Alloy, Upon the Total Length of the Machined Surface ($\gamma_1 = -10^\circ$, $\gamma = -10^\circ$, $\varphi_1 = 15^\circ$, $\alpha = 12^\circ$, $\alpha_1 = 12^\circ$, r = 1.5 mm).

a) Total length of machined surface, m; b) Complement of peripheral cutting edge angle φ°

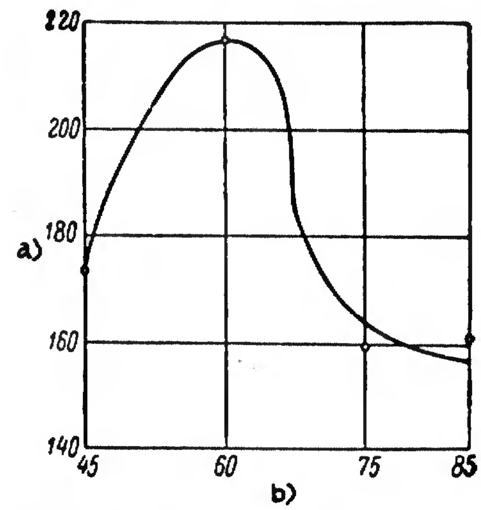

Fig.142 - Influence of Complement of Peripheral Cutting Edge Angle φ Upon the Life of an End Mill (D = 280 mm) Tipped with T15K6. Shape of mill point: $\gamma_1 = -10^\circ$, $\gamma_2 = -10^\circ$, $\alpha = 8^\circ$, $\alpha_1 = 4^\circ$, $\varphi_1 = 4^\circ$, $f = 1 \times 45^\circ$.

a) Life of end mill T, min; b) Complement of peripheral cutting edge angle φ°

Figure 141 depicts the relationship of total length of machined surface to the angle φ in the fast milling of No.40 carbon steel ($\sigma_t = 57$ kg/mm^2) at t = 5 mm, B = 90 mm, $s_z = 0.095$ mm/tooth, and v = 200 m/min. Obviously, the optimum complements of the peripheral cutting edge angles are in the $\varphi = 60 - 75^\circ$ interval. The mill life diminishes when the angles φ are above or below this range.

Figure 142 illustrates the effect of the angle φ upon the life of an end mill in the machining of chromium-nickel-molybdenum steel for which $\sigma_t = 90$ kg/mm^2. The following cutting conditions were used: t = 3 mm, B = 140 mm, $s_z = 0.105$ mm/tooth, v = 135 m/min. The curves show the optimum complement of the peripheral cutting edge angle to be $\varphi = 60^o$. When φ is either increased or decreased, the life of the mill drops sharply.

The difference in the nature of the $T = f(\varphi)$ relation found be various investigators can apparently be explained chiefly in terms of the differences in the rigidities of the machine tools on which the tests were run. It must be also borne in mind that the experiments by A.V.Shchegolev and V.I.Tkachevskiy were conducted at considerably lower feeds ($s_z = 0.095$ and 0.105 mm/tooth) than those by L.A.Rozhdestvenskiy, P.P.Grudov, and P.A.Markelov ($s_z = 0.25$, 0.244 and 0.26 mm/tooth). Low feed per tooth at low complements of peripheral cutting edge angle results in exceedingly fine chip, particularly at the instant when the mill bites into the metal. This accelerates the wear of the mill flanks due to the rounding of the cutting edges occurring as a result of the increase in the plastic deformation of the machined metal.

The data by A.V.Shchegolev and V.I.Tkachevskiy are of considerable interest for the milling of hardened steels which is, as we know, performed at low feeds per tooth.

Let us turn to practical recommendations for selecting the complement of the peripheral cutting edge angle φ of end millers. M.N.Larin (Bibl.61) takes $\varphi = 60^o$ for the milling of steels of $H_B = 200 - 500$. The same angle φ is chosen by P.P.Grudov and S.I.Volkov (Bibl.63) for steels of $H_B = 179 - 362$, and by NIBTN (Bibl.27) for unhardened and hardened steels. M.I.Klushin (Bibl.43) raises the complement of the peripheral cutting edge angle to $\varphi = 75^o$ for steels of $H_B = 200 - 350$.

A generalization of these data makes it possible to recommend that, in the milling of hardened steels, cemented-carbide face mills be used whose complement of peripheral cutting edge angle is $\varphi = 60^o$. Mills with an angle of $\varphi = 90^o$ should be used only under exceptional conditions, when this is a matter of necessity in terms of production desired: the milling of surfaces for beads or crimps.

All the sources cited recommend that the nose chamfer be $\varphi_o = \frac{\varphi}{2}$, and that the length of the chamfer be f_o = 1.0 to 2.0 mm.

Face Cutting Edge Angle φ_1

Reduction in the face cutting edge angle φ_1 results in an increase in the work of friction along the face flank, which leads to vibration. However, this increases the length of the face flank participating in the cutting, as well as the nose angle. As a result, the tip of the tooth becomes stronger, and the heat dissipation is improved due to the increase in the mass of metal between the peripheral and face cutting edges, the end result being an increase in cutter life. The reduction in the angle φ_1 causes a reduction in the residual cross section of the layer of metal removed, and improves the quality of the machined surface.

For face milling of hardened steels it is necessary to use cutters with a face edge angle φ_1 of the order of 5°.

An efficient means for improving the finish of the machined surface in the face milling of hardened steels is the use of cutters having a finishing edge with a face cutting edge angle of 0°, and a length of 1 - 3 mm (Fig.143).

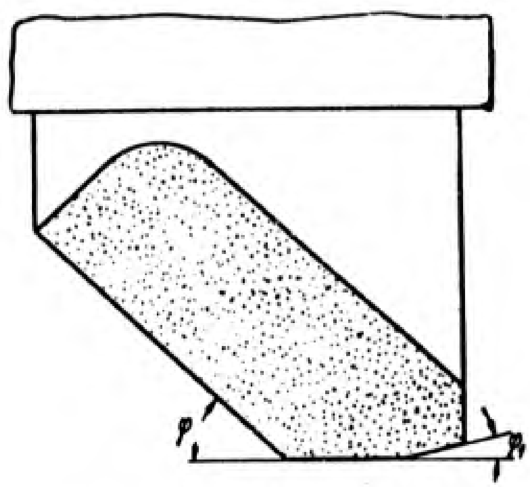

Fig.143 - End Mill Tooth With Finishing Edge

25. Effect of Various Factors on Mill Life and Cutting Speed

Ratio of Cutting Speed to Mill Life

The relationship between cutting speed and the life of hard-alloy end mills is of the same nature in the machining of hardened steels as in turning on the lathe:

$$v = \frac{C}{T^m}.$$

Experimental data show that in fast machining with hard-alloy face mills, the relative life index m for hardened steels is somewhat lower than for unhardened steels. The average data for a number of investigations yield m = 0.30 for unhardened alloy steels, and m = 0.25 for hardened steels. These data pertain to face mills tipped with cemented carbides of the titanium-tungsten group (T15K6, T30K4, etc.).

The relative life index in the milling of hardened steels is considerably higher than in turning on the lathe.

In the recommended cutting schedules (Appendix II), the relative life index m is taken to be 0.25.

Effect of Mechanical Properties of Hardened Steels Upon Cutting Speed

In the milling of steels with carbide tools, as in turning on the lathe, the effect of the mechanical properties of the workpiece on the cutting speed rises progressively with transition from one range of hardness (or tensile strength) to the next interval of higher hardnesses of the material.

The relation of cutting speed to the tensile strength of a machined steel is expressed by the equation

$$v = \frac{C_v}{\sigma_t^{n_v}}.$$

According to the data by P.A.Markelov (Bibl.60) and the NIBTN (Bibl.27), the n_v index describing the effect of the mechanical properties of the machined material upon the cutting speed will be

For steels with σ_t = 60 - 125 kg/mm^2, n_v = 1.0 - 1.1;

For steels with σ_t = 125 - 180 kg/mm^2, n_v = 2.0

As we see, the degree of influence of the mechanical properties of the machined material upon the cutting speed is considerably higher for hardened than for unhardened steels.

If, for hardened steel of σ_t = 120 kg/mm^2, we take the cutting speed under given conditions to be unity, the cutting speed under the same conditions will be 0.63 for a hardened steel with σ_t = 150 kg/mm^2 and 0.36 for a steel with σ_t = 200 kg/mm^2.

In our cutting schedules (Appendix II), the following are the values of the index n_v employed with respect to v - σ_t. For steels with σ_t = 120 - 210 kg/mm^2 (H_{R_C} = 38 - 60), we have n_v = 2.0. For steels with σ_t > 210 kg/mm^2 (H_{R_C} > 60), the value is n_v = 7.0.

Influence Upon Cutting Speed the Hard Alloy Used to Tip End Mill

The chemical composition of the hard alloy has a significant influence upon the cutting speed in the end milling of hardened steels. The cutting properties of the hard alloy increase with the titanium carbide content.

Of the titanium-tungsten carbides T30K4, T15K6, T14K8, and T5K10, the best cutting properties are displayed by T30K4, and the poorest by T5K10.

According to experimental data (Bibl.60), the T30K4 carbide permits a cutting speed higher by a factor of 1.7 than does T5K10.

Effect of Feed per Tooth Upon Cutter Life and Cutting Speed

The following relation exists between the life of an end mill and the feed per tooth

$$T = \frac{C_s}{s_z^{y_T}},$$

where T is cutter life, in min;

s_z is the feed per mill tooth, in mm.

Figure 144 presents this relation for 30KhGSNA steel with σ_t = 170 - 180 kg/mm^2 (Bibl.60). The milling was done with an end mill (D = 110 mm) tipped with T15K6 alloy, at t = 2 mm, B = 90 mm, and v = 112.6 m/min. As we see, the T = f(s_z) relationship is expressed in log-log form by a broken line consisting of two straight lines joined at a jog corresponding to a feed of s_z = 0.1 mm/tooth. To the right of this point of inflection, the influence of feed per tooth s_z upon cutter life is expressed more sharply than to the left thereof.

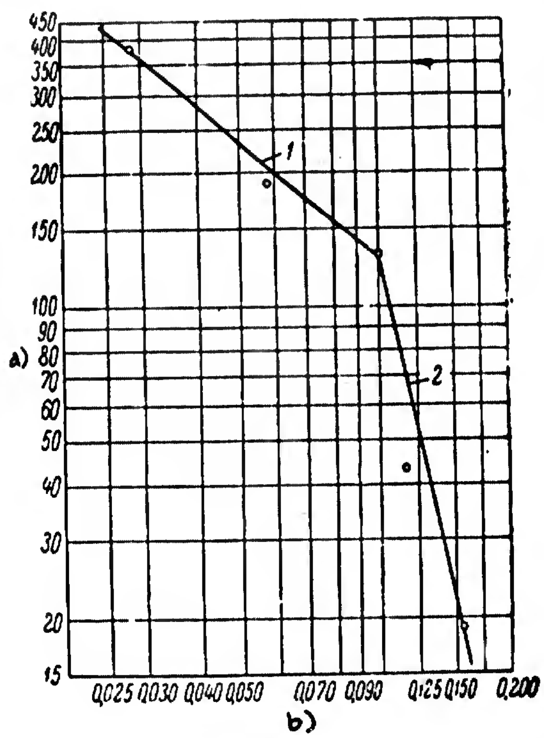

Fig.144 - Feed per Tooth s_z versus Life T of End Mill, Tipped with Hard Alloy T15K6 Used to Machine 30KhGSNA Steel, σ_t = 170 - 180 kg/mm^2. Data according to P.A.Markelov

a) Tool life T, min; b) Feed per mill tooth s_z, mm

In numerous investigations on the milling of steels of various hardness, ratios of T - s_z of an analogous character have been discovered. With further improvement in the mechanical properties of the work steel (σ_t, H_B) we get a reduction in the feed s_z at which the jog in the curve for the relation T = f(s_z) takes place.

In the milling of hardened steels, the interval of least feeds is of practical significance. According to Fig.144, the following relationships (the relative life factor being m = 0.3) are valid for this interval (segment 1):

$$T = \frac{C_v}{s_z^{0.93}} \ min.,$$

$$v = \frac{C'_v}{s_z^{0.28}} \ m/min.$$

For the second zone of feeds per tooth (segment 2), these relations take on the form:

$$T = \frac{C_v}{s_z^{4.1}} \ min.,$$

$$v = \frac{C'_v}{s_z^{1.23}} \ m/min.$$

Employment of the feeds in the second is desirable only on the condition that the exponent of s_z in the $T - s_z$ relation is less than the reciprocal of the relative life index m (less than $\frac{1}{m}$).

The following factors have the greatest effect upon the value of s_z:

1) Required finish of the machined surface;

2) Thickness of cut a_{max};

3) Grade of carbide used in tipping the cutting edge of the mill;

4) Mechanical properties of the machined steel;

5) Design and shape of the cutter;

6) Rigidity of the system machine tool-workpiece-mill.

The finish of the machined surface is improved with a reduction in feed per tooth s_z. A higher surface finish is achieved in the milling of hardened steels than in the machining of unhardened steels, with the same feed per tooth s_z.

The feed per tooth s_z and the thickness of cut a are related by the expression

$$s_z = \frac{a}{\sin \varphi},$$

where φ is the complement of the peripheral cutting edge angle of the face mill.

The major influence upon mill life is exerted not by the feed s_z but by the thickness of cut a, At the same feed s_z but at different thicknesses of cut a, the life of the cutter may show substantial differences which may reach a factor of tens in the second feed zone.

In selecting the thickness of cut it should be borne in mind that, in order for the milling process to proceed normally, it is necessary to guarantee that the thickness of cut a_x be larger than the radius of curvature ρ of the mill tooth cutting edge (Fig.145). If the thickness of the instantaneously removed layer is less than the radius of curvature of the cutting edge ($a_x < \rho$), the latter cannot penetrate the work metal and slides over an arc without removing a chip, and as a result undergoes more intensive wear. As the cutter dulls, the radius of curvature of the cutting edge ρ increases.

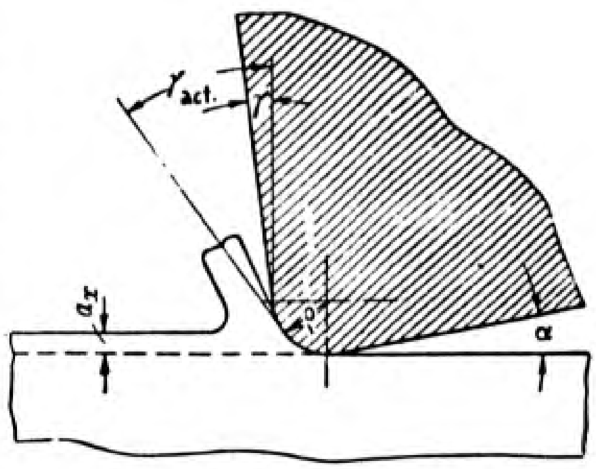

Fig.145 - Diagram of Bite of Cutting Edge of Face Mill at Small Thickness of Cut

In the end milling of steel, the thickness of cut, if the penetration process is to be normal, should not be less than a = 0.025 - 0.030 mm; at a complement of the peripheral cutting edge angle of φ = 60°, this represents a feed of s_z = 0.03 - 0.35 mm/tooth.

Figure 145 also shows that, at a small thickness of cut, the chip does not flow off over the face of the cutter tooth but over the cutting edge itself, which has a radius of curvature ρ. As a result, the actual true rake angle γ_{act} acquires a high negative value and the conditions of cutting become unfavorable.

The greater the bending strength of the cemented carbide with which the point of the mill is tipped (i.e., the higher the cobalt content), the higher will be the permissible feed per tooth. This diminishes with a further improvement in the mechanical properties of the machined steel.

Feed per tooth s_z may be increased with an increase in the rigidity of the cutter, the system miller-workpiece-fixture, and with a reduction in the complement of the peripheral cutting edge angle φ.

Data are presented in the literature with respect to the feed per tooth in the face milling of hardened steels. A.V.Shchegolev and V.I.Tkachevskiy (Bibl.62) recommend that s_z of up to 0.06 mm/tooth be employed, whereas NIBTN (Bibl.27) recommends a value of s_z = 0.03 to 0.09 mm/tooth. The use of T15K6 hard alloy is envisaged. According to data by P.P.Grudov and S.I.Volkov (Bibl.63), for mills tipped with this same carbide, the maximum chip thickness is a_{max} = 0.040 - 0.065 (for mills where φ = 60°, this corresponds to s_z = 0.45 - 0.75 mm/tooth). For T5K10 alloy this may be raised by 25 - 35%.

Table 67 presents the recommended values for the feed s_z when end milling cutters with a complement of peripheral cutting edge angle of φ = 60° are used on milling machine, models 615, A662, and the like, differentiated in accordance with the hardness of the hardened steel with which the cutter is tipped.

Table 67

Feed Per Cutter Tooth s_z in the Face-Milling of Hardened Steels

Grade of Cemented Carbide	Hardness of Tempered Steel H_{R_C}		
	38—46	47—54	55—62
	Feed s_z, in mm/tooth		
T15K6	0,09—0,07	0,08—0,06	0,06—0,04
T30K4	0,08—0,06	0,07—0,05	0,05—0,03

In working with less rigid milling machines (models 6B12, 6N12, and similar types), these feeds should be reduced by 15%. When using more rigid milling machines (model 6A54, A664, and the like) they should be raised by 15 - 20%. When T14K8 and T5K10 are used, the s_z feeds may be raised by 10 - 15%.

Effect of Depth of Cut Upon Mill Life and Cutting Speed

The depth of cut t, i.e., the thickness of the layer of metal cut away at a single pass, exerts considerably less influence upon the life of a cemented-carbide mill in face milling than do the cutting speed and feed per tooth.

The following relation exists between the life of a face mill T and the depth of cut t:

$$T = \frac{C_t}{t^{x_T}} \; min .$$

The magnitude of the exponent x_T for unhardened steels, reported by various investigators differs widely: from 0.20 to 0.68. According to data by P.A.Markelov, this exponent is 0.82 for 30KhGSA steel of H_{R_C} = 51 - 54.

The relation T - t for hardened steel has the following form:

$$T = \frac{C_t}{t^{0.82}} \; min .$$

If we take the relative life index m as 0.3, we get

$$v = \frac{C'_t}{t^{0.25}} \; m/min .$$

Consequently, in the face-milling of hardened steels, the depth of cut t exerts approximately the same effect upon the cutting speed as does the feed per tooth s_z. This is due to the fact that in the relations v - s_z (p.270) and v - t, the exponents of s_z and t are virtually equal. This pertains to the low feed interval ($s_z \leq 0.1$ mm/tooth). For the zone of higher feeds, the exponent of s_z is virtually five times as great as that of t (1.23 as compared to 0.25).

However, it is generally advantageous to use deeper cutting depths in the milling of hardened steels. In practice, the depth should not exceed t = 3 to 4 mm. When high precision is necessary, the machining should be performed in two passes. In milling steel forgings or castings through a thick layer of scale, the depth of cut should be set so that the mill teeth nowhere touch the surface of the workpiece underneath the layer of scale, as this will crumble the carbide bar.

Effect of Milling Width and Diameter of End Mill Upon Life and Cutting Speed

Upon increase in the milling width B, the life of the mill is reduced due to the increase in the path followed by its teeth in the metal. The life of the mill also diminishes if the diameter D is reduced and no change is made in the milling width.

It is common to consider the effect upon cutter life exerted by the ratio of milling width to mill diameter. The greater the ratio $\frac{B}{D}$, the lower the life of the end mill.

On the basis of experimental data, the relation between cutting speed and the ratio $\frac{B}{D}$ in the milling of steels by cemented-carbide end mills may be expressed as follows:

$$v = \frac{C}{\left(\frac{B}{D}\right)^{0,2}} \, m/min.$$

Investigations and industrial practice have determined that face milling of steels will occur under the most favorable conditions if, with the mill in symmetrical position, the width is B = 0.55 - 0.65)D. Proceeding from this basis, the diameter of a mill is, in practice, determined from the condition:

$$D = (1,5 \div 1,8)\, B \; mm.$$

P.A.Markelov recommends that the diameter of an end mill be based on the power of the milling machine:

Power of milling machine N, in kw	up to 3.5	over 3.5 to 5.5	over 5.5 to 7.5	over 7.5 to 12.0
Maximum diameter of end mill D, in mm ...	110	150	200	250 - 300

Influence of Number of Teeth Upon Mill Life and Cutting Speed

In studies of the high-speed milling of steels with cemented-carbide face mills, it is recommended that the cutting speed be calculated without consideration of the number of teeth in the mill. This is based on the fact that the number of teeth in the end mill has so negligible an effect upon the life that it may be neglected for all practical purpcses.

A.V.Shchegolev and V.I.Tkachevskiy (Bibl.62) investigated the influence of the cutting speed upon the lives of end mills with various numbers of teeth in the machining of chromium-molybdenum steel with σ_t = 70 kg/mm^2. The tests were run with a mill tipped with T15K6 alloy (D = 265 mm), at t = 3 mm, B = 90 mm, and s_z = = 0.13 mm/tooth. Experiments have shown that the life of a six-tooth mill differs very little from that of a three-tooth and one-tooth cutter.

Generalized Formulas for Cutting Speed

The following formulas exist for determining the cutting speeds in the face-milling of hardened steels:

Formula by P.A.Markelov:

$$v = \frac{C_v}{T^{0,3} \cdot t^{0,25} \cdot s_z^{0,36} \cdot \left(\frac{B}{D}\right)^{0,24}} \ m/min,$$

where C_v is a constant varying in the 319 to 170 interval with increase in the tensile strength of the machined steel σ_t from 120 to 180 kg/mm^2.

Formula by P.P.Grudov and S.I.Volkov:

$$v_{300} = \frac{C_{v_{300}} \cdot D^{0,2}}{t^{0,06} \cdot s_z^{y_v} \cdot B^{0,2}} \ m/min,$$

where C_{v300} = 650 and y_v = 0.1 for s_z = 0.04 - 0.08 mm/tooth; C_{v300} = 305 and y_v = 0.4 for s_z > 0.08 mm/tooth.

Formula by the NIBTN:

$$v_{300} = \frac{C_{v_{300}}}{t^{0,5} \cdot s_z^{0,3} \cdot \left(\frac{B}{D}\right)^{0,2}} \ m/min.$$

P.A.Markelov's formula pertains to the zone of low feeds ($s_z < 0.1$ mm/tooth). The difference in the value of the s_z exponent here ($y_v = 0.36$) and in the $v - s_z$ relation, presented above ($y_v = 0.28$) is explained by the various ranges of strength of hardened steels.

On the basis of an analysis of the literature data, the author has arrived at the following formula for the cutting speed:

$$v_{300} = \frac{C_{v300}}{t^{0,25} \cdot s_z^{0,30} \cdot \left(\frac{B}{D}\right)^{0,30}} \ m/min. \qquad (13)$$

The value of the constant $C_{v_{300}}$ are presented in Table 68.

Table 68

$C_{v_{300}}$ Coefficient

Characteristics of steel being machined	σ_t in kg/mm^2	120	130	140	150	160	170	180	190	200	210	220
	H_{R_C}	38	41	44	47	49	51	54	56	58	60	62
Values of $C_{v_{300}}$ constant		70	59,5	51	44	39	35	31,5	28	25	22,5	16

Calculating of the cutting speed corresponding to a 300-min cutter life for a steel with σ_t = 120 kg/mm^2 (H_{R_C} = 38), t = 3 mm, B = 90 mm, D = 150 mm, and two values of feed per tooth, yields the following results:

	s_z = 0.09 mm/tooth	s_z = 0.04 mm/tooth
As per formula of P.A.Markelov ...	v_{300} = 118 m/min	v_{300} = 154 m/min
As per formula of P.P.Grudov and S.I.Volkov	v_{300} = 150 m/min	v_{300} = 168 m/min

As per eq.(13) .... v_{300} = 121 m/min v_{300} = 157 m/min

As per formula of NIBTN (Bibl.27). v_{300} = 134 m/min v_{300} = 172 m/min

As we see, the formula derived by the author yields results corresponding to those of P.A.Markelov's equation. They differ only slightly (10% on the average) from the cutting speed values obtained by the equations of P.P.Grudov, S.I.Volkov, and NIBTN.

26. Cutting Speed and Effective Output

We give here the data by P.A.Markelov (Bibl.60), based on an investigation he made into cutting forces and output in high-speed milling with cemented-carbide face mills of unhardened steels 30KhGSNA and 30KhGSA (σ_t = 75 - 80 kg/mm^2). The author of the investigation suggests coefficients for determining, on the basis of the relationships he found for unhardened steels, the peripheral cutting force and effective output for the end milling of hardened steels of various hardnesses.

The experiments were run with a single-tooth end mill of D = 200 mm. The flank wear of the mill teeth was taken as h = 1.5 mm. In all experiments other than those for investigating individual factors of shape, the following was used as cutter geometry: $\alpha = 16^\circ$, $\gamma = -5^\circ$, $\lambda = 15^\circ$, $\varphi = 60^\circ$, $\varphi_1 = 15^\circ$, $\varphi_o = 30^\circ$, f = 1.5 mm. The maximum peripheral force $P_{z_{max}}$ was measured.

Let us list the results of the investigation.

1. With an increase in the number of teeth z in the mill and in the ratio of cutting width to mill diameter $\frac{B}{D}$, a reduction occurs in the difference between the maximum $P_{z_{max}}$ and the average P_z of the peripheral forces. Whereas, for a single-tooth mill and for $\frac{B}{D}$ = 0.15, the maximum peripheral force is 21 times as large as the average, the ratio of these forces becomes 1.2 at z = 10 (D = 200 mm) and $\frac{B}{D}$ = 0.7.

2. Within the interval from +10 to -5°, the true rake angle γ does not influence the value of the maximum peripheral force. The maximum $P_{z_{max}}$ increases as the true rake angle changes from -5 to -20°. For $\gamma = -20^\circ$, it is 20% larger than

for $\gamma = -5^o$.

3. A change in axial rake λ in the +30 to -10^o interval does not affect the force $P_{z_{max}}$.

4. The complement of the peripheral cutting edge angle seriously affects the value of $P_{z_{max}}$. At its smallest, this force is $\varphi = 60^o$. A change in the angle φ its 60^o value in either direction results in an increase in the force $P_{z_{max}}$.

5. With an increase in the wear of the cutter teeth, the force $P_{z_{max}}$ will rise. At a wear of h = 1.5 - 2.0 mm, the force will be 40 - 50% higher than at the outset of the cutter operation.

6. The cutting speed influences the value of the force $P_{z_{max}}$. An 11-fold increase in cutting speed (from 50 to 550 m/min) causes a reduction in this force by 20%.

7. When the feed per tooth s_z rises 5-fold (from 0.06 to 0.30 mm), the force $P_{z_{max}}$ will rise by a factor of 3.6.

8. The maximum peripheral force and the depth of cut (depth of cut varying within the limits of t = 1 - 10 mm) are in direct proportion to each other.

9. The most important influence upon the power consumed by the drive of the feed mechanism of a milling machine is its feed per tooth s_z.

The depth of cut t has a considerably smaller effect thereon, and the cutter diameter D as well as the cutting width B have very little effect.

10. The effective output N_e of the feed drive of milling machines is negligible compared with that of the main drive. The relative effective power of the feed drive may be characterized by the following data:

N_e of main drive, in kw ...	1	2	3	4	5	6	7	8	9	10	11	12
N_e of feed drive in % of N_e of main drive	12	10	8	6.5	5.5	4.5	4	4	4	3.5	3.5	3

11. The dulling of the teeth of an end mill has a pronounced influence upon the power consumed by the main drive of the milling machine. If we take as unity the

output of the main drive when a freshly-ground mill is used, the power at various levels of dulling of the teeth may be expressed by the following factors:

Wear h, in mm	1.5	2.0 - 2.3	5.3
Coefficient K	1.25	1.35	1.65

The author has employed the following equation, derived by P.A.Markelov, for determining the effective output in fast machining of steels by cemented-carbide end mills with prismatic teeth:

$$N_e = C_N \cdot v^{0,9} \cdot t \cdot s_z^{0,8} \cdot z \cdot \frac{B}{D} \text{ kw .} \qquad (14)$$

For stepped mills with prismatic teeth, the formula takes on the form:

$$N_e = \frac{C_N \cdot v^{0,9} \cdot a \cdot s_z^{0,8} \cdot z \cdot \frac{B}{D}}{i} \text{ Kw .}$$

where a is the allowance in mm, taken off the work per pass of cutter;

i is the number of steps of the cutter.

The author employs the following equation to determine the value of the constant C_N relative to the tensile strength of hardened steel;

$$C_N = 0,034 \cdot \frac{\sigma_t'}{\sigma_t},$$

where σ'_t is the tensile strength of the given steel, in kg/mm^2;

σ_t = 120 kg/mm^2 (H_{R_C} = 38 steel, for which C_N = 0.034).

The total output of the main drive of milling machines can be determined by means of the following approximate formulas:

1) In the absence of a special motor for the feed drive:

$$N = \frac{1.1 N_e}{\eta} \text{ kw ;}$$

2) In the presence of an electric motor on the feed drive of the milling machine

$$N = \frac{N_e}{\eta} \text{ kw,}$$

where η is the efficiency of the machine tool.

27. Surface Finish

The machining of steels with end mills tipped with cemented carbides results

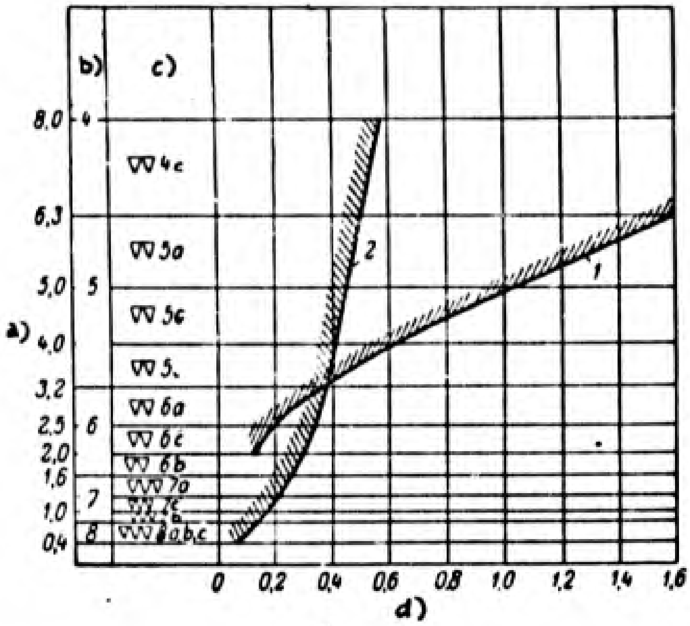

Fig.146 - Effect of Feed Upon Quality of Machined Surface in End Milling of Unhardened Steels

1 - Experimental data according to P.A.Markelov for 30KhGSA steel of σ_t = 60 - 70 kg/mm^2; 2 - NIBTN data for steel of σ_t = 70 kg/mm^2

a) Root-mean-square average roughness H_{rm}, microns; b) Class of finish; c) Grade of finish; d) Feed per rotation of cutter s_o, mm

in a better surface finish than does machining with cutters of high-speed steel. Higher cutting speeds promote an improvement in surface finish.

In addition to the cutting speed, the feed per cutter revolution s_o and the face cutting edge angle of the cutter φ_1 have a significant effect upon the surface roughness.

Figure 146 shows the relation between the height of the surface roughnesses and the feed s_o, in the end milling of unhardened steel by a tool tipped with titanium-tungsten carbides. Curve 1 presents the results of experiments (Bibl.60) performed with a cutter with D = 200 m, z = 8, and φ = 60° at t = 3 mm, B = 110 mm, and v = 315 m/min. The curve shows that, on increasing the feed s_o from 0.1 to 1.24 mm/rev, the finish of the machined surface drops by more than one class (from $\nabla\nabla$6b to $\nabla\nabla$5a).

P.A.Markelov has found that, on machining hardened steels in this fashion, the surface quality achieved is one to two classes higher than with unhardened steels. He recommends the following feeds per revolution of an end mill relative to the given surface finish:

Surface Finish Class or Subclass	Feed s_o
$\nabla\nabla$ 5	0.35 - 1.60
$\nabla\nabla$ 6a	0.20 - 0.35
$\nabla\nabla$ 6b	0.15 - 0.20

These feeds are calculated with respect to the machining of unhardened steels with end mills with z = 8, the run-out of the teeth in radial and axial directions being not greater than 0.03 - 0.04 mm.

The feeds s_o recommended by the NIBTN (Bibl.27) for unhardened and hardened steels (Table 69) are calculated for a face run-out of the cutter up to 0.02 mm, a flank wear of the teeth of h = 0.8 to 1.4 mm, and a face cutting edge angle of φ_1 = 5°. The relation between the feed s_o and the roughnesses of unhardened steel of σ_t = 70 kg/mm², according to NIBTN data, is shown by curve 2 in Fig.146. Obviously, the relation between the feed s_o and the surface finish, according to the NIBTN, corresponds to P.A.Markelov's data (curve 1) only in a small interval of feeds.

Despite the different nature of the relationships under examination, both data confirm the possibility of achieving a surface quality equal to that of class 8 by end milling of hardened steels with low feeds s_o.

The investigations have led to the following conclusions:

1. The quality of the machined surface increases with the strength of the steel

machined (Table 69). This surface quality is achieved by the machining of hardened steels at considerably higher feeds s_o than are employed for unhardened steels. Thus, at s_o = 0.22 - 0.35 mm/rev, the surface finish of hardened steels is of class 7, whereas for steels with σ_t = 70 kg/mm^2 it is only of class 6.

2. With a reduction in the face cutting edge angle φ_1, the roughnesses are smoothened. The feeds s_o presented in Table 69 may be doubled with cutters of $\varphi_1 = 2°$.

Table 69

Feeds s_o Recommended by the NIBTN Relative to Required Surface Finish, in End Milling of Steels

Surface finish class, GOST 2789 - 51		Unhardened steels			Hardened steels
		Tensile strength σ_t, in kg/mm^2			
Designation	H_{rm}, in microns	70	90	110	
		Feed s, in mm/rev			
∇∇ 5	Above 3,2 to 6,3	0,35—0,50	0,40—0,60	0,50—0,75	0,60—0,90
∇∇ 6	" 1,6 to 3,2	0,20—0,35	0,25—0,40	0,30—0,50	0,35—0,60
∇∇∇ 7	" 0,8 to 1,6	0,15—0,20	0,15—0,25	0,20—0,30	0,22—0,35
∇∇∇ 8	" 0,4 to 0,8	0,15	0,15	0,15—0,20	0,15—0,22

3. The true rake angle γ of end mill teeth and the axial rake λ do not affect the heights of the roughnesses so long as these angles are between 0 and 15°, but the heights do increase somewhat in work with cutters for which $\lambda > 15°$. In the range from 45 to 75°, the working relief angle α and the complement of the peripheral cutting edge angle φ have a negligible influence upon the surface finish.

4. In the initial period of operation of an end mill, when the tooth wear is still insignificant, the surface finish is considerably lower than in the subsequent period, when the cutter wear becomes greater.

In choosing a cutting schedule for the end milling of hardened steels, the data in Table 69 with respect to such steels should be employed.

CHAPTER V

THE DRILLING OF HARDENED STEELS*

<u>Drill Design.</u> Figure 147 presents the design of a straight-fluted drill tipped with cemented carbide. This type of drill has come into wide use for machining holes in hardened-steel parts. These drills have a number of advantages over twist drills. The shorter body length and the considerably larger cross section thereof increase the rigidity and the ability of the body to absorb vibrations generated during the cutting process, and protect the carbide bar against their effects. The straight flutes simplify manufacture. For the rest, the structural dimensions of drills with straight flutes are taken to be the same as those of twist drills. Drills with diameters of D < 10 mm are made with straight shanks, while those with D = 10 to 30 mm

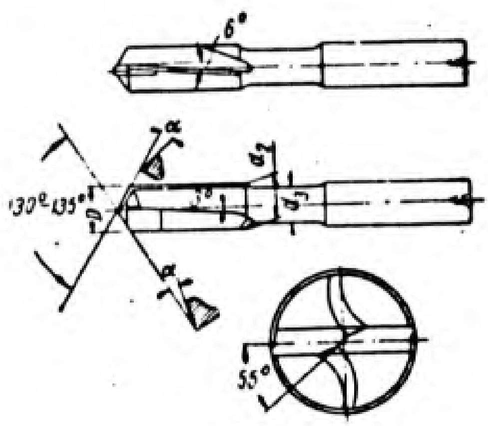

Fig.147 - Design of Straight-Fluted Drill, Carbide-Tipped

---

*The drilling of hardened steels with tools tipped with carbide first came into use simultaneously with the turning of hardened steels on lathes, and perhaps even earlier. However, unlike turning, drilling has had little coverage in the literature. Until recently, the data were limited to a study by B.G.Levin (Bibl.65) and to the exceedingly brief data on the selection of cutting speeds provided in the standards for high-speed machining of metals issued by the NIBTN of the Ministry of the Machine-Tool Industry (Bibl.66). However, drills tipped with cemented carbides have been designed (Bibl.16) that have proved satisfactory in the machining of hardened steels.

In 1956, the results of an investigation by B.A.Ignatov into the process of drilling hardened tool steels KhVG, 3KhV8, and R18 were published in condensed form (Bibl.67).

are made with taper shanks.

VNII-designed drills with oblique flutes and cemented-carbide tips (Figs.148 and 149) have been developed to drill hardened sheet steel (Bibl.16). Their flutes for chip removal are short. As a result, the design with oblique flutes is charac-

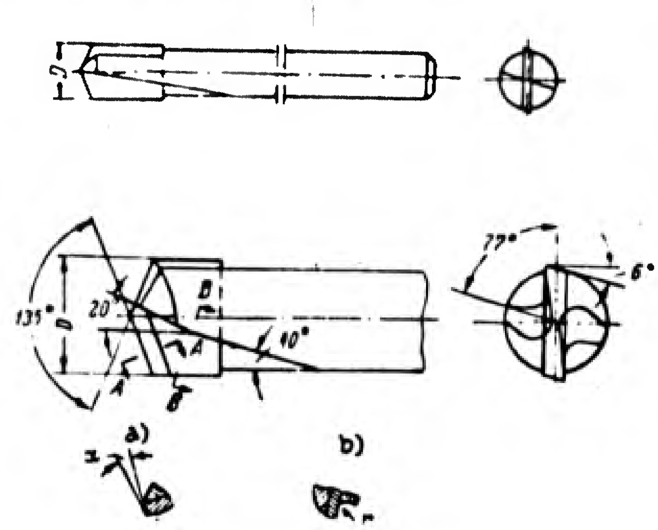

Fig.148 - Design of Oblique-Flute Carbide-Tipped Drills, D = 2.5 to 10.5 mm

a) Section through A-A; b) Section through B-B

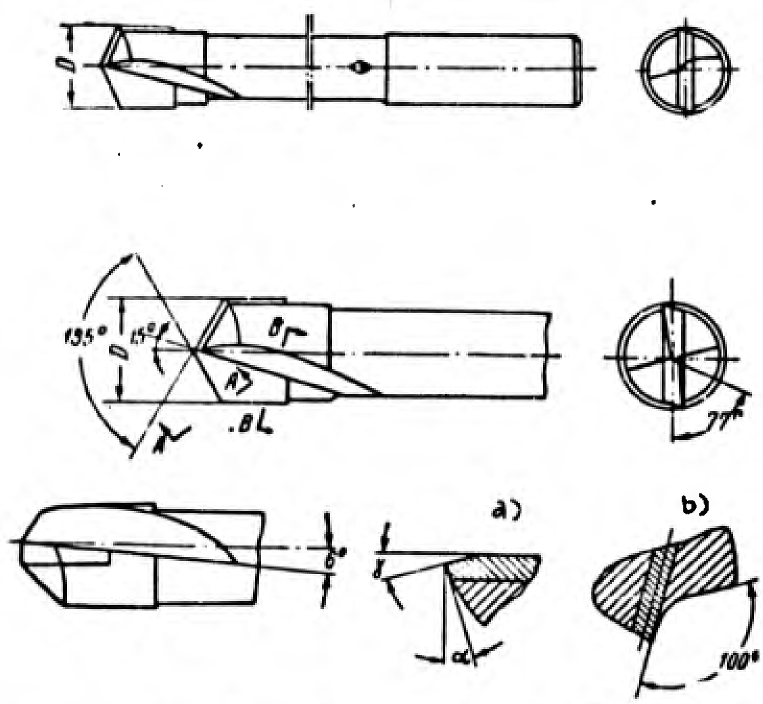

Fig.149 - Design of Oblique-Flute Carbide-Tipped Drills, D = 11 to 20 mm

a) Section through A-A; b) Section through B-B terized by massiveness and increased rigidity. Depending upon the drill diameter, the rake is between 10 and 20°. Grinding of the outside diameter is facilitated by the fact that the body diameter is smaller than the tip diameter.

The guidance data issued by the VNII (Bibl.16) list two types of designs: short and long drills. The latter type is about twice as long as the former.

Drills with triangular points and cemented-carbide inserts (Fig.150) are employed to drill hard-alloy steels of great hardness. The triangular drill has a straight shank and a point consisting of a triangular cemented-carbide insert. The cutting end of the insert has rounded sides converging at the center, while the other end is tapered and is inserted into the hole in the shank. The design is quite simple and presents no difficulties in drill manufacture. All that is necessary is to make sure that the triangular insert is properly seated in the body of the tool. Triangular drills with carbide inserts are used to machine holes of D = 3 - 20 mm.

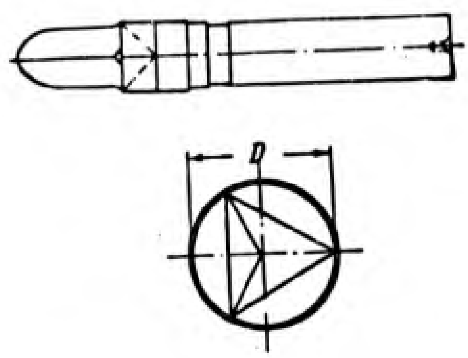

Fig.150 - Triangular-Point, Carbide-Insert Drill

In a paper by V.S.Rakovskiy and others, Carbides in the Manufacture of Machinery (Bibl.16), Tables 156, 158, 159, and 160 present the dimensions of the design elements of straight-flute drills (Fig.147), oblique-flute drills (Figs.148 and 149), and triangular-point, carbide-insert drills (Fig.150).

Cemented Carbide Grades. V.G.Levin (Bibl.65) has tested the following cemented carbides: VK3, VK8, VK12, VK15, and T21K8. Drills tipped with hard alloy T21K8 and VK3 crumbled out shortly after the start of cutting, due to the excessive brittleness of the carbides. The best results in terms of tool life were obtained with drills tipped with VK8.

Of the cemented carbides tested by V.A.Ignatov (T5K10, T15K6, VK6, and VK8), VK8 also proved best. The cutting schedules (Appendix III) are calculated for this hard alloy.

Geometry of Cutting Edge of Drill. B.G.Levin recommends that the true rake angle at the drill periphery be $\gamma = -15^\circ$. B.A.Ignatov takes $\gamma = -15^\circ$ for steel of $H_{R_C} = 62$; $\gamma = -10^\circ$ for steel of $H_{R_C} = 55$; $\gamma = -5^\circ$ for steel of $H_{R_C} = 50$, and $\gamma = 0^\circ$ for steel of $H_{R_C} \leq 40$. The VNII data (Bibl.16) for hardened steels specify an angle γ from 0 to -5°.

For steels of $H_{R_C} = 35 - 65$, the author employs a true rake angle γ from 0 to -10°. These cutting schedules are based on the indicated true rake angle.

In accordance with the VNII data, the working relief angle α is taken as 8°.

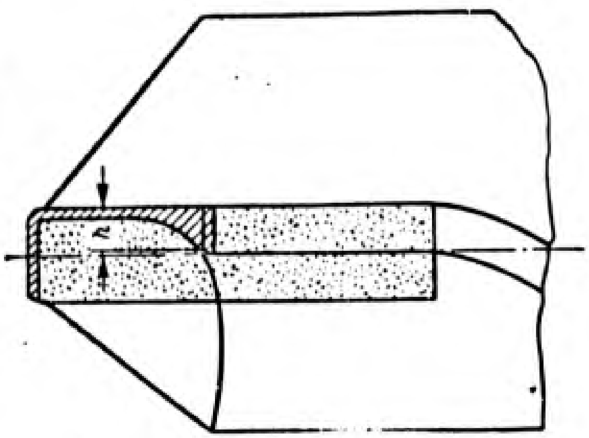

Fig.151 - Diagram of Drill Wear

Criteria of Drill Dulling. The machining of hardened steels with carbide-tipped drills results in the same type of wear as that resulting from the drilling of unhardened steels: Wear occurs along the radial edge and the flanks. The drill also wears along its faces, but this wear is insignificant. The author has taken the following values for the wear h as criterion for the dulling of drills tipped with VK8 alloy (Fig.151), which agree with the data by B.A.Ignatov:

Drill diameter D, in mm	Wear h, in mm
10 - 14	0.4
16 - 20	0.6
24 - 30	1.0

Feed. The feed s may be calculated from the formula

$$s = C_s \cdot D^{0.84} \text{ mm/rev,} \qquad (15)$$

where D is the drill diameter, in mm;

C_s is a constant coefficient.

The following are the values for the coefficient C_s employed (for the hard alloy VK8):

Hardness of machined steel H_{R_C}	Value of C_s
35 - 45	0.007
46 - 56	0.005
57 - 65	0.004

The feeds calculated in accordance with eq.(15) (rounded-off) are presented in Table 70.

The small feed s for small-diameter drills is of interest. Feeds of s = 0.03 - - 0.06 mm/rev are possible on the radial drills 2G53, and still lower feeds are obtainable by hand.

Cutting Speed. For hardened steel 3KhV8 brought to H_{R_C} = 50, B.A.Ignatov has drived the following formula for the cutting speed (in work with VK8 alloy):

$$v = \frac{C_v \cdot D^{0,2}}{T^{0,24} \cdot s^{0,5}} \ m/min .$$

Under this formula, cutting speed v = 32 m/min for drills of D = 10 to 30 mm diameter. According to the data of B.G.Levin, the cutting speed is v = 20 m/min for steels brought to the same hardness, when VK8 drill tips are used at a rate resulting in the same drill life.

The lower cutting speeds obtained by B.G.Levin compared to those by B.A.Ignatov can be explained by the improvement in the quality of VK8 (and other hard alloys), achieved since the days of B.G.Levin.

The author has taken the cutting speed at the level suggested by B.A.Ignatov and has used the above formula for steels hardened to H_{R_C} = 35 - 65.

The cutting speeds recommended in Appendix III are calculated from the formula

$$v_{30} = \frac{C_{v_{30}} \cdot D^{0.2}}{s^{0.5}} \; m/min. \quad (16)$$

The following values have been taken for the constant coefficient C_{v30}:

Hardness of machined steel H_{R_C}	Value of C_{v30}
35 - 45	7.9
46 - 56	4.2
57 - 65	2.7

Table 70

Feeds for Drills Tipped with VK8 Alloy in Machining Hardened Steels Brought to H_{R_C} = 35 - 65

Hardness of Hardened Steel H_{R_C}	Drill diameter D, in mm							
	10	12	14	16	20	24	28	30
	Feed s, in mm/rev							
35—45	0,050	0,055	0,065	0,070	0,085	0,100	0,110	0,120
46—56	0,035	0,040	0,045	0,055	0,065	0,075	0,085	0,090
57—65	0,030	0,035	0,040	0,045	0,050	0,060	0,065	0,070

Axial Force. In his determination of the axial force the author has employed, with insignificant amendments, the equation proposed by V.A.Ignatov for hardened steel R18 brought to H_{R_C} = 62:

$$P_o = C_P \cdot D \cdot S^{0,5} \; Kg. \quad (17)$$

The following are the values of the C_P coefficient:

Hardness of work steel H_{R_C}	Value of C_P
35 - 45	230
46 - 56	250
57 - 65	300

The values C_P employed are midway between those given by B.A.Ignatov and B.G.Levin. The ratio of the C_P to the hardness of the tempered steel is taken to agree with the data by B.G.Levin.

Torsional Moment. In order to determine the torque, the formula suggested by B.A.Ignatov for R18 steel hardened to H_{R_C} = 62 is employed, with negligible changes.

$$M_t = C_M \cdot D^{2.2} \cdot s^{0.7} \; Kg\text{-}m. \qquad (18)$$

The following are the values of the C_M coefficient:

Hardness of work steel H_{R_C}	Value C_M
35 - 45	0.038
46 - 56	0.044
57 - 65	0.051

The ratio of the value C_M to the hardness of the tempered steel is taken to agree with the data by B.G.Levin.

Interruptions in the Work. When drilling steels are hardened to more than H_{R_C} = 40, the drill must be lifted periodically from the hole being machined. Otherwise the red-hot chip, undergoing deformation in the drill flute, might weld to the flute walls. Withdrawal of the drill from the hole guarantees that its flutes will be freed from the chip. In drilling steels of a hardness below H_{R_C} = 40, no welding of the chip to the flute walls occurs and cutting proceeds without interruption.

This welding of the chip is observed more frequently, the higher the hardness of the material machined and the heating of the drilled metal. The number of times the drill has to be withdrawn from the machined hole increases with a reduction in tool diameter. Table 71 illustrates the number of withdrawals of the drill for every 10 mm of drilling depth. The cutting process is interrupted for 5 - 6 sec to withdraw the drill.

Drilling of Hardened Steels With Introduction of Electric Current Into the Cutting Zone. The following was determined as the result of an investigation of the process of drilling hardened steels, conducted by B.A.Ignatov.

1. In the machining of hardened steels of normal microstructure (absence of

large carbides or of carbide inhomogeneities with excessive concentration of carbides), the life of a drill tipped with hard alloys may be increased by introducing

Table 71

Number of Drill Withdrawals

Hardness of work steel H_{R_C}	Drill diameter D mm				
	10	16	20	24	30
	Number of drill withdrawals per each 10 mm of drilling depth				
45 - 60	3	3	2	2	2
above 60	6	6	4	4	4

low-voltage current of optimum amerage into the cutting zone.

2. The effect obtained from the use of current depends upon the hardness of the machined steel, its structure, the cutting proceedure, and other factors. Under given conditions, the effect may be quite considerable.

Whereas for steel of $H_{R_C} = 50$, an increase in drill life due to the introduction of optimum current into the cutting one is expressed by the coefficient 1.5, the coefficient for $H_{R_C} = 62$ steel will be 2.5.

The effectiveness of use of current rises with a reduction in the thickness of the cut. If the structure of the machined steel is unfavorable, the use of current will have a very insignificant effect.

3. With an increase in cutting speed v and feed s, the optimum current will diminish.

4. When hardened KhVG steel ($H_{R_C} = 62$) is drilled without current, a change in cutting speed in the range of v = 12.8 to 51.3 m/min will first result in some increase, but then in a substantial decrease in the forces P_o and M_t.

At v = 51.3 m/min, the force P_o will diminish by 75% and the torsional moment by 30% relative to their values at v = 12.8 m/min.

The introduction of current of optimum strength when $v = 12.8$ m/min reduces the P_o by 61.5%.

5. In the drilling of KhVG hardened steel ($H_{R_C} = 62$), the surface finish will be $\nabla\nabla\nabla 7$ and $\nabla\nabla\nabla 8$. By using current of optimum strength, the surface finish will be improved by one grade.

6. The drilling of hardened steels results in a shrinkage of the hole, i.e., the diameter of the hole will be smaller than that of the drill. The use of current reduces this effect.

CHAPTER VI

FINISH-REAMING OF HARDENED STEELS

28. Design of Flute Reamers and Fixtures Required

Design of Flute Reamers

Experimental studies* and industrial experience have demonstrated that, for purposes of machining hardened steels, flute reamers tipped with cemented carbides should be of a design differing somewhat from the reamers used in the machining of unhardened steels. Unlike the flute reamers designed by the VNII (Bibl.57, 58), the entering edge and finishing sections have to be separated by a second bevel with a taper of $\varphi_0 = 1°30'$ to $2°$, and length $l_0 = 1.0$ to 1.5 mm (Fig.152). This provides separation from the finishing section of the portion of the cutting edge that is subject to the most intensive wear.

The design has to provide for the use of guide bushings (if necessary, flute reamers may be employed without these). Centering in the guide bushing should not be effected by means of the working portion of the tool, but by its rear pilot. The diameter of the pilot must be larger than that of the flute. This prevents crumbling-out of the carbide cutting edges, a phenomenon not infrequently observed when a

*As indicated in the Introduction, the literature data on flute and rose reaming of hardened steels are limited (unlike those on turning and milling) and consist solely of the work by K.F.Romanov (Bibl.68) and the cutting conditions recommended by the NIBTN of the Ministry of Machine-Tool Manufacture (Bibl.66). The experimental data presented in this Chapter and in Chapter VI were obtained in K.F.Romanov's investigation.

reamer passes through a guide bushing (due to run-out of the reamer and failure of its axis to coincide with that of the bushing).

However, an increase in the diameter of the rear pilot makes it necessary for such a reamer to be longer than one in which guidance is performed by means of the flute. This reduces the rigidity of the system machine tool-workpiece-reamer and increases the danger of vibrations.

A successful solution is the use of an adapter (Fig.162) which enters the guide

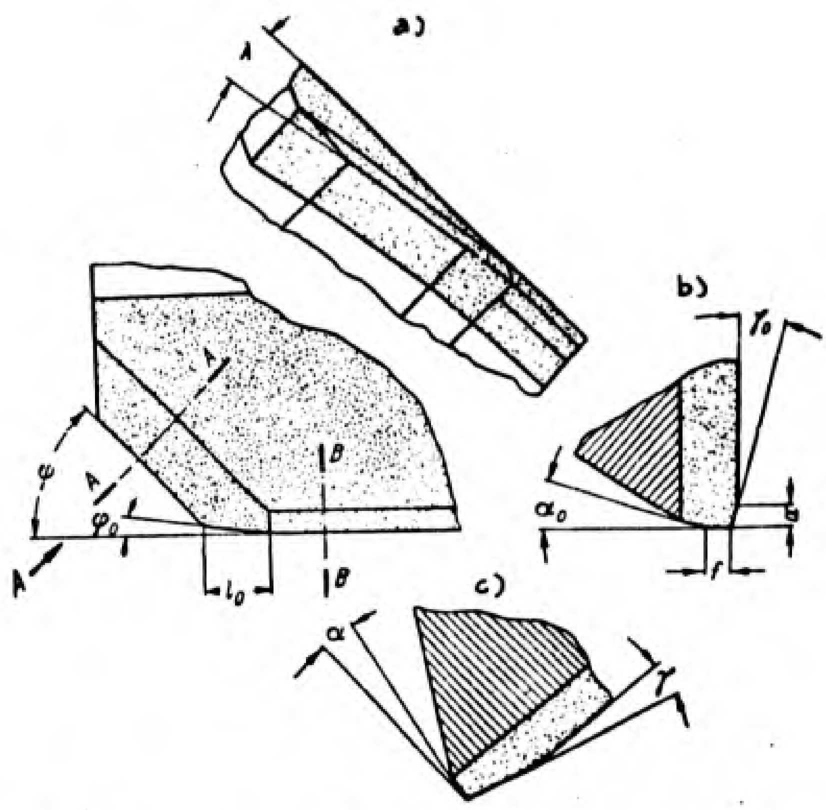

Fig.152 - Geometric Parameters of Reamer Flute

a) View along arrow A; b) Section through B-B; c) Section through A-A

bushing as the reamer is brought up to the workpiece and remains there so long as reaming continues.

Adapters are employed in the reaming of holes whose length is more than three times the tool diameter, if the flute diameter is larger than that of the rear pilot.

The diameter of the front pilot in these reamer designs is smaller than that of their flutes by a magnitude exceeding the combined reaming allowance and the possible deviation of the axis of the hole.

Figure 153 presents a 6-tooth reamer with two pilots and internal cooling. This design has proved satisfactory in the machining of hardened steels.

Investigations have shown that the appearance of longitudinal scratches on the machined surface, as the reamer is withdrawn from the hole, are due to shrinkage of the hole after reaming, i.e., to the fact that the diameter of the machined hole becomes smaller than that of the reamer.

The appearance of scratches is due to the fact that higher cutting speeds are used than those at which steels are machined with high-speed reamers. Protection of the machined holes against scratching can not be obtained by setting the cutting blades at a 3° axial rake, as is specified in the VNII design. This shortcoming is eliminated by changing the conventional pattern for reamer allowance fields.

Reamers with carbide tips brazed to their bodies are used for small diameters (to 30 mm), at which it is difficult to mount attached blades tipped with carbide.

Shell reamers, 40 mm diameter and larger, are of the assembled type. The major requirement to be met by the assembled type of reamer is provision for axial and radial adjustment of the blades. This is necessary because the reamer undergoes wear both on its entering and finishing edges. Moreover, the appearance of fine crumblings of the cutting edge along the finishing section as the reamer is dulled on its entering edges makes it necessary to grind the reamer along its guiding lands (to diameter) after every - or every second - regrinding on the entering edge. Grinding of the guiding lands should also be performed in cases when the reamer has not worn beyond its wear allowance on the diameter.

Several types of flute (and rose) reamers have been developed in which the carbide tips are mechanically fitted on. However, these designs have not yet passed the experimentation stage and are therefore not in industrial use.

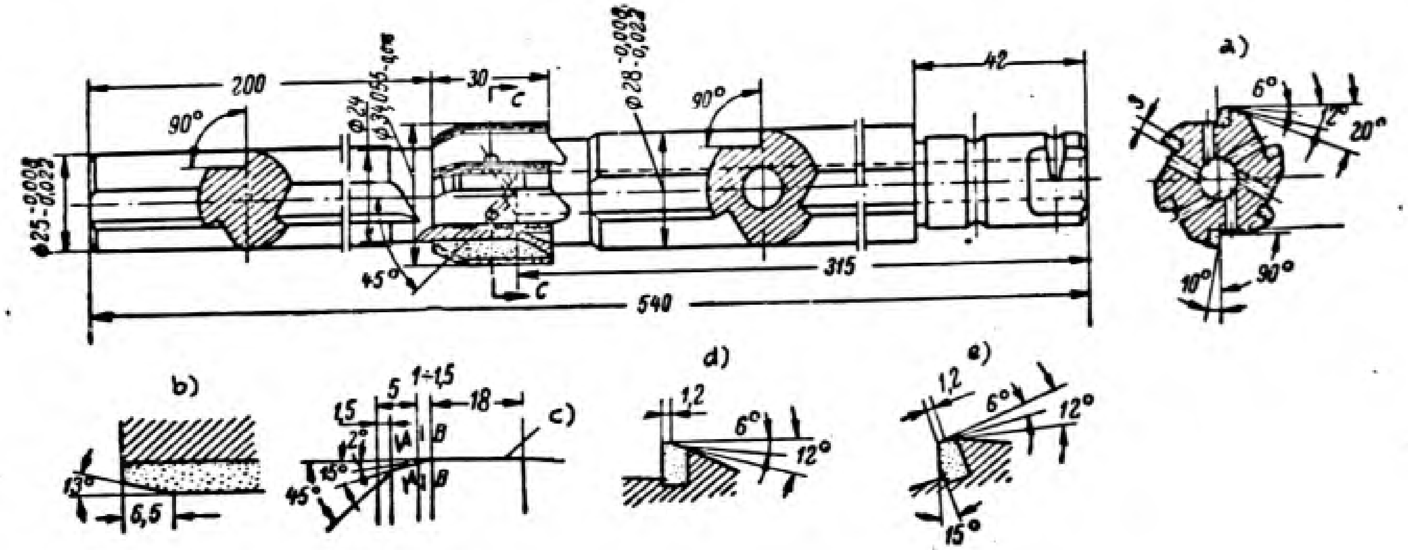

Fig.153 - Reamer, Tipped with T15K6 Alloy, with Front and Back Pilots and Internal Cooling

a) Section through C–C; b) Section through D–D; c) Back taper 0.1 mm; d) Section through B–B; e) Section through A–A

When the carbide tips are fitted mechanically to flute (and rose) reamers, the tool operating costs are substantially reduced, since the expenditures involved in

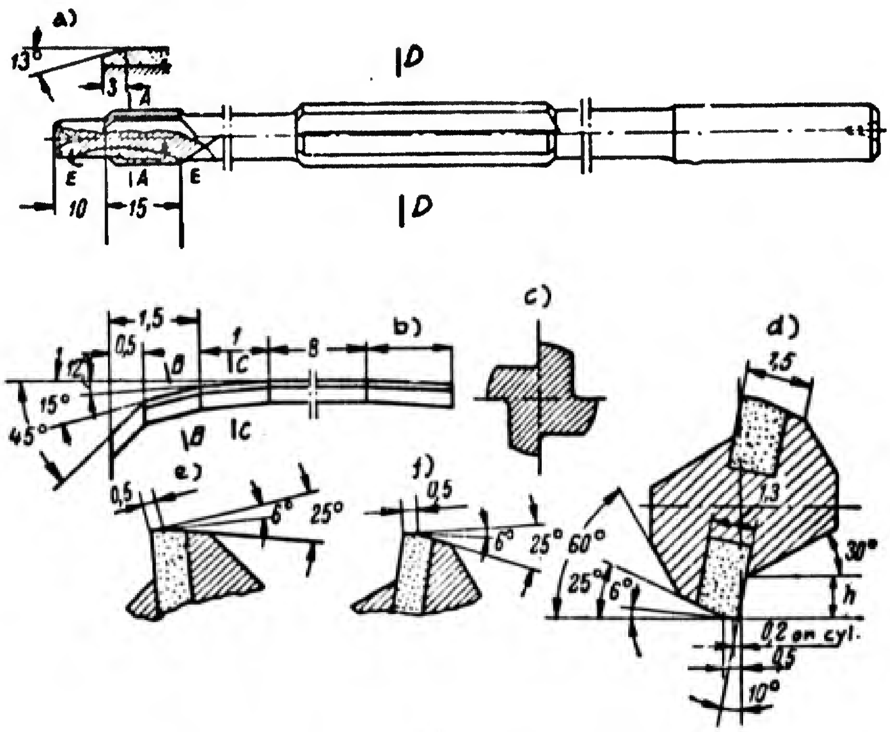

Fig.154 - Design of Carbide-Tipped, Straight-Shank Reamers of D = 6 - - 9 mm, With Rear Pilots

a) Section through E-E; b) Back taper; c) Section through D-D; d) Section through A-A; e) Section through B-B; f) Section through C-C

the making of inserted blades are eliminated. However, mechanical fastening results in uneconomical consumption of carbides, due to incomplete utilization of the carbide bars and cracking during assembly.

The experience accumulated in the reaming of hardened steels indicates that the use of mechanically fitted carbide tips is not practicable.

The carbide-tipped reamers illustrated in Figs.154 - 157 are recommended for the machining of hardened steels.

As shown by tests, the method of fastening inserted blades employed with assembled reamers does provide dependable clamping and precise adjustment to the de-

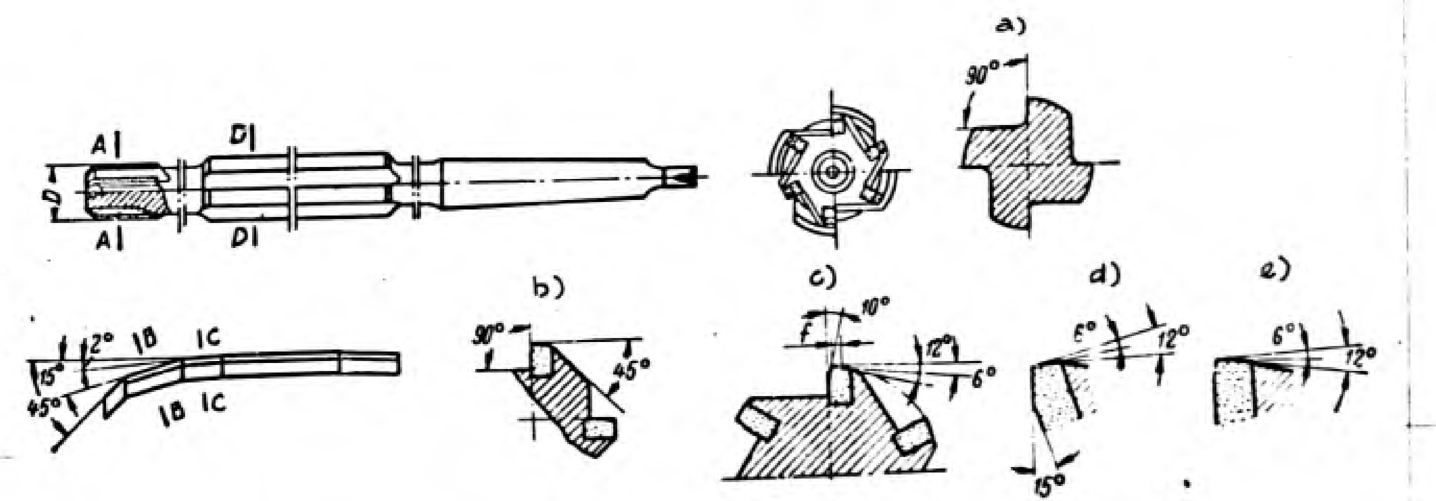

Fig.155 - Taper Shank Carbide-Tipped Reamers, D = 10 - 30 mm, With Rear Pilot

a) Section through D-D; b) Section through A-A for D up to 17 mm; c) Section through A-A for D over 17 mm; d) Section through B-B; e) Section through C-C sired diameter. Axial serrations are provided on the support side of the inserted blade (2) (Fig.156, 157). Identical longitudinal serrations are present on the rear

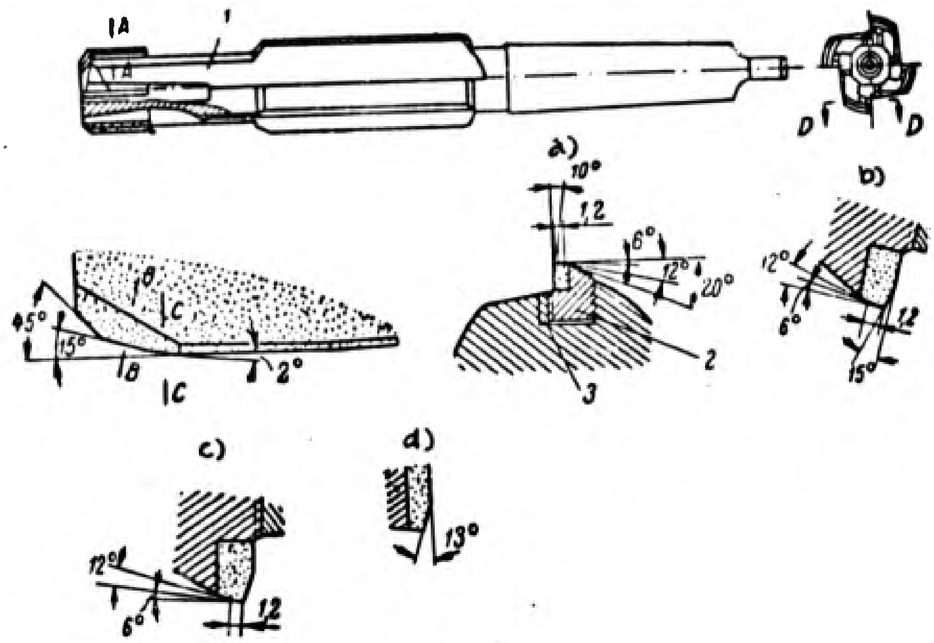

Fig.156 - Carbide-Tipped Inserted-Blade Flute Reamers of Diameter D = 25 - 50 mm, With Rear Pilots and Taper Shank

1 - Body; 2 - Inserted blade; 3 - Wedge

a) Section through A-A; b) Section through B-B; c) Section through C-C; d) Section through D-D

wall of the slot in the body (1). Contact between blade and slot on these serrations prevents radial movement of the blade. The radial serrations on the opposite side of the blade and on the adjacent surface of the wedge (3) attach the blade to the wedge, and thus prevent axial movement.

Adjustment of the blade to the required reamer diameter is achieved by moving the blade one serration in either direction, relative to the wedge. The blade and wedge are then inserted in the slot, which is axially angled into the reamer body. In the cutting process, the inserted blade and the wedge are firmly wedged into the slot under the effect of the force of feed.

This design ensures reliable fastening of the inserted teeth into the body of the reamer without the need for particularly precise fitting of the slots, blades, and wedges.

Tolerance System

In view of the fact that reaming of hardened alloy steels results not in ex-

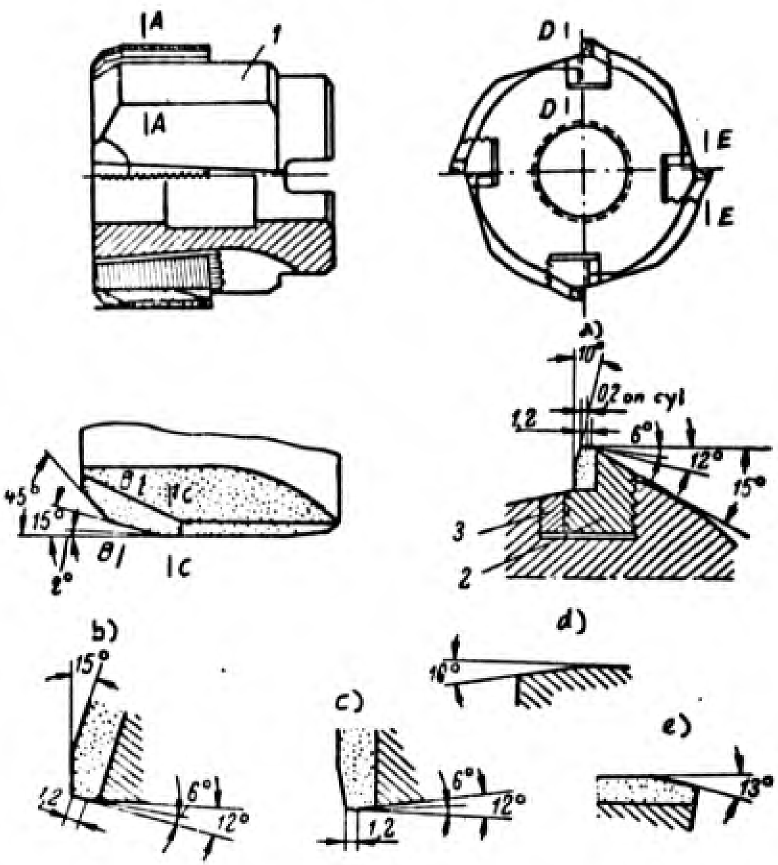

Fig.157 - Inserted Carbide-Tipped Shell Reamers, D = 40 - 80 mm

1 - Body; 2 - Inserted blade; 3 - Wedge

a) Section through A-A; b) Section through B-B; c) Section through C-C; d) Section through D-D; e) Section through E-E

pansion but in shrinkage of the holes, the system of tolerances for the reamer has to be fundamentally different than those for the holes machined. K.F.Romanov has suggested the system of tolerances presented in Fig.158b. Figure 158a shows the common system of tolerances for high-speed and cemented-carbide reamers.

The following is the notation employed in Fig.158:

Δ - tolerance on hole;

AB - maximum deviation of reamer diameter;

CD - minimum deviation of reamer diameter;

N+J - total reaming tolerance;

N - Tolerance for inaccurate manufacture of the reamer;

J - tolerance for reamer wear;

P_{max} - maximum expansion of hole;

P_{min} - minimum expansion of hole;

R_{max} - maximum shrinkage of hole;

R_{min} - minimum shrinkage of hole.

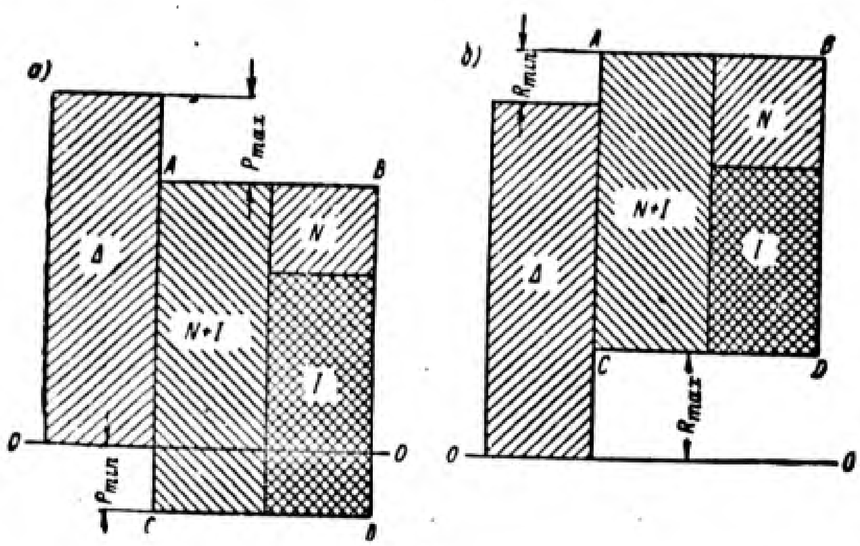

Fig.158 - Reaming Tolerance Systems

a - As generally accepted for high-speed and carbide tools;
b - Proposed by K.F.Romanov for carbide tools in reaming hardened alloy steels for which H_{R_C} = 49 - 54

Jigs and Fixtures

Guide Bushings. The reaming of hardened steels proceeds at cutting speeds higher than those at which unhardened steels are reamed by high-speed (HSS) tools. Experience in the reaming of hardened steels shows that the use of holding fixtures for a rear, or for a rear and front pilot of a tool with rigid guide bushings results in premature failure of both reamers and guide bushings. The slightest skewing results in seizing of the tool pilots in the bushings.

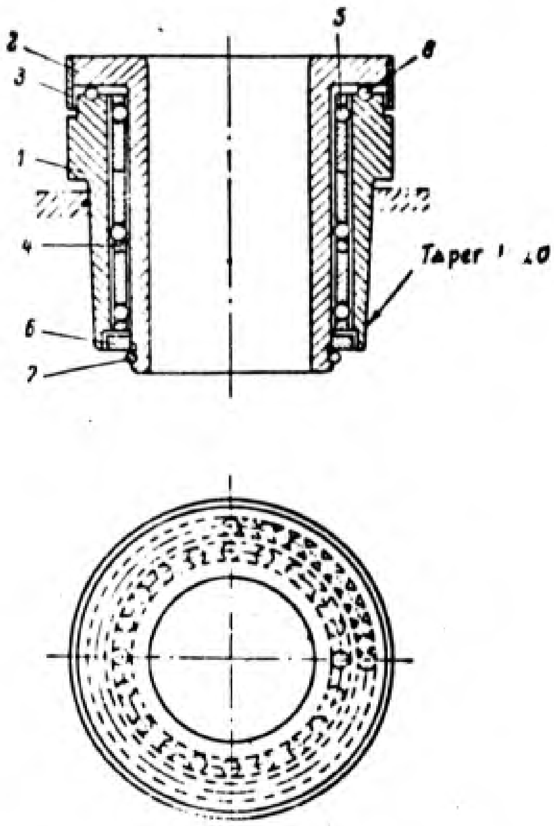

Fig.159 - Rotary Guide Bushing, Mounted on Ball Bearings

1 - Outer bushing; 2 - Inner bushing; 3 - Guard ring; 4 - Separator rings; 5 and 8 - Ball bearings; 6 - Washer; 7 - Annular spring

Rotary guide bushings are free of this shortcoming. A design found satisfactory is presented in Fig.159. The axial forces are absorbed by ball bearings (8), in a groove in the upper portion of the outer bearing (1). The inner bearing (2) is retained from below by a ring (6), which fits into a hollow in the outer bush (1), and by an annular spring (7). This creates a labyrinth packing that protects the ball bearings (5) from fouling. The same function with respect to the ball-bearings (8) is played by the ring (3) which is mounted to the bead of the inner bushing (2).

Coolant Supply. Figure 160 shows an arrangement for flute-reaming of holes of less than two diameters depth and of holes of small diameter, with the coolant fed through tubular rings. The rings are illustrated separately in Fig.161.

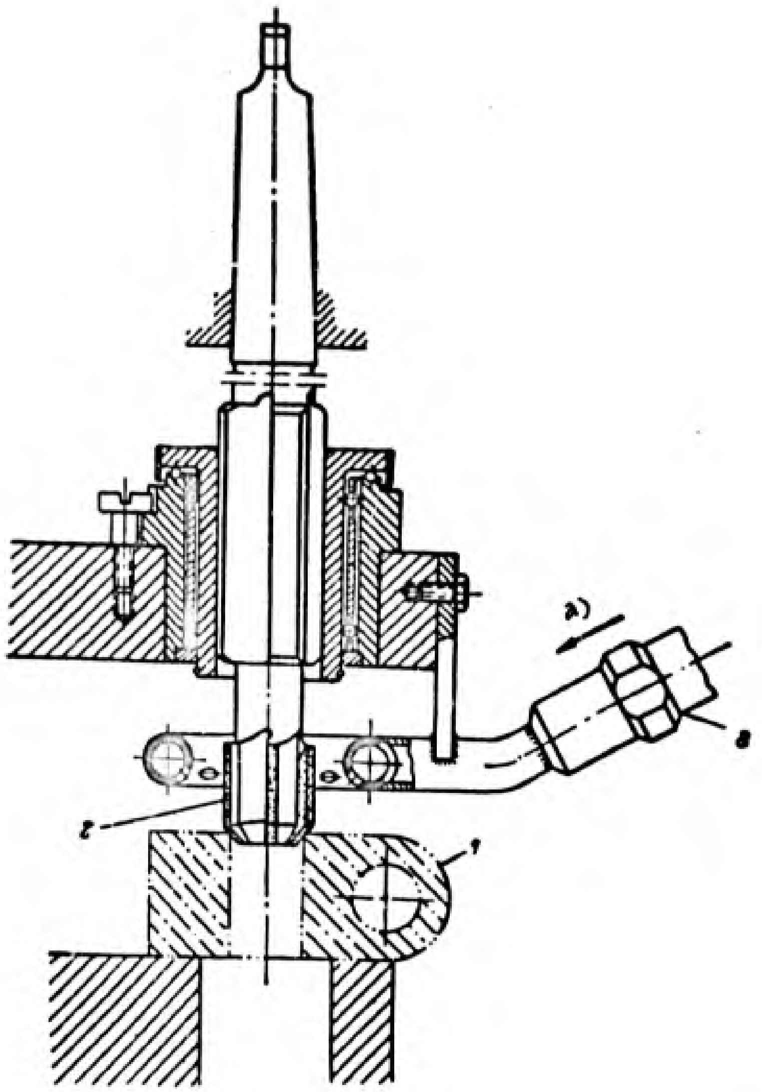

Fig.160 - Flute Reaming Setup With Coolant Introduced Through Special Rings

1 - Part being machined; 2 - Flute reamer; 3 - Tubular rings for coolant

a) Coolant

The arrangement illustrated in Fig.162 is employed for reaming with internal feeding of coolant to the cutting edge of the tool when the hole is to be over 25 mm in diameter and more than two diameters in depth. The reamer is clamped in a special

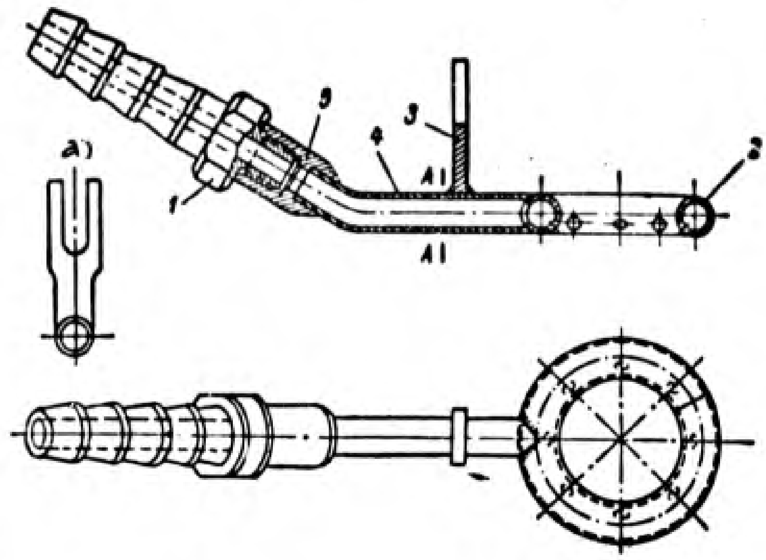

Fig.161 - Tubular Rings for Coolant Supply

1 - Union; 2 - Ring; 3 - Support; 4 - Pipe; 5 - Sleeve

a) Section through A-A

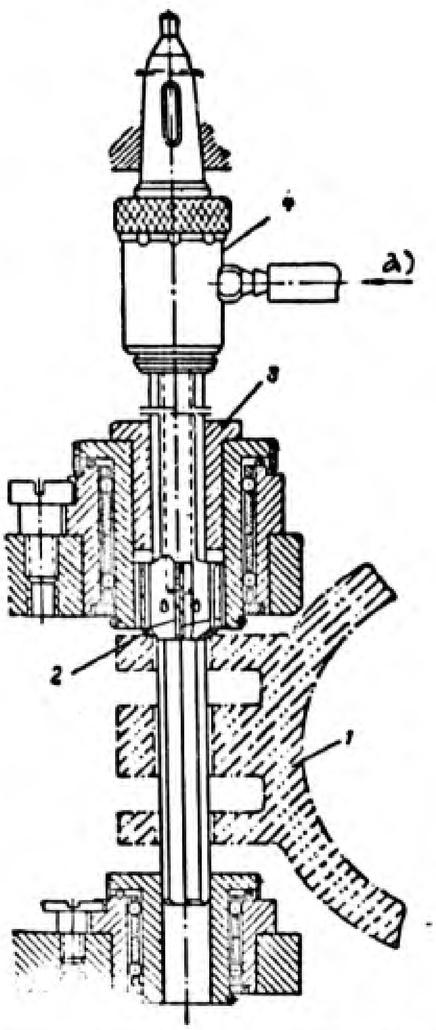

Fig.162 - Flute Reaming Setup with Internal Cooling

1 - Workpiece; 2 - Reamer; 3 - Adapter; 4 - Chuck

a) Coolant

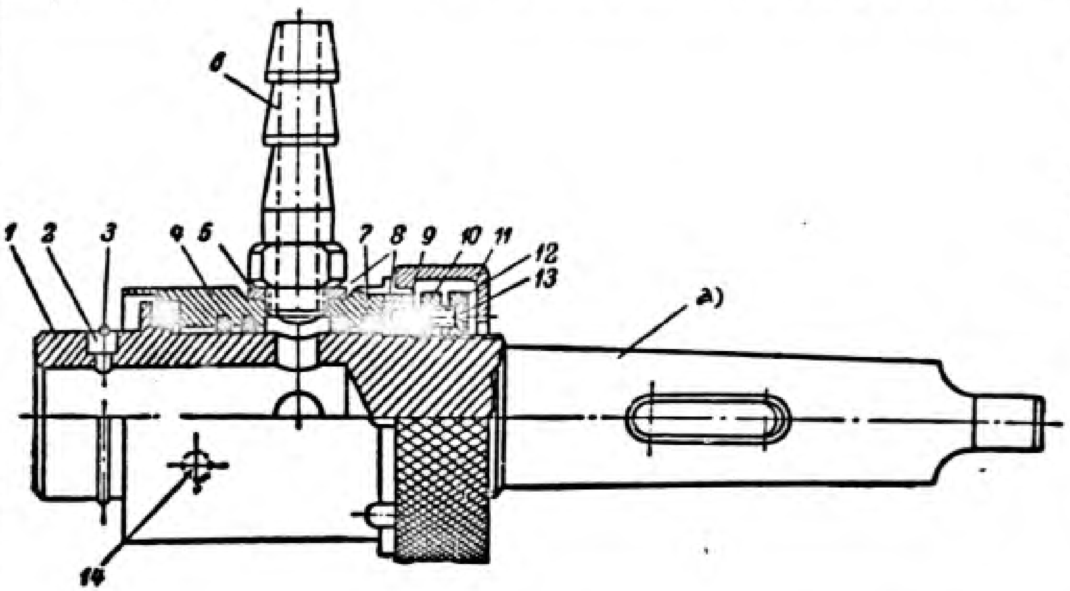

Fig.163 - Chuck for Holding Reamers with Internal Cooling

1 - Body; 2 - Pin; 3 - Annular ring; 4 - Bushing; 5 - Gasket; 6 - Union; 7 - Gland; 8 - Inside bushing; 9 - Ball bearing; 10 - Outside ring; 11 - Nut; 12 - Split nut; 13 - Screw; 14 - Pin

a) Morse taper No.4

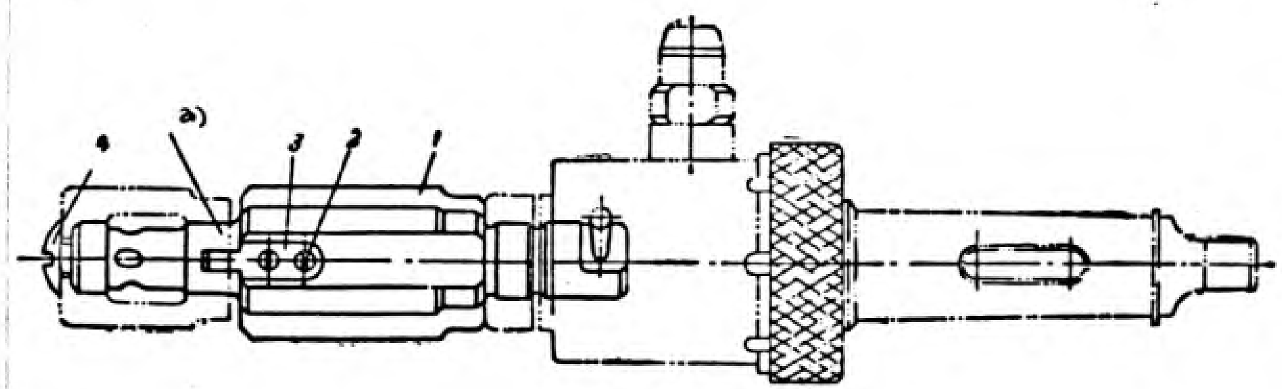

Fig.164 - Arbor for Shell Reamers with Internal Cooling

1 - Body; 2 and 4 - Screws; 3 - Tongue

a) Taper 1:30

chuck (Fig.163) through which the coolant is supplied. The fluid is fed through the stub pipe (6) held in the sleeve (4) to an internal chamber, through holes drilled in the body (1). From this chamber, the fluid goes to the inside duct of the reamer. The chamber also serves to clamp the tool.

For flute reaming with internal cooling where larger holes are desired, shell reamers are employed and the chuck is replaced by the arbor illustrated in Fig.164.

Appendix 5 of K.F.Romanov's book (Bibl.68) presents the dimensions of the design elements of flute reamers with D = 6 - 80 mm, illustrated here in Figs.154 -157. The same source presents the major dimensions of reamers tipped with T15K6 alloy for the machining of holes of various tolerance classifications, in alloy steel hardened to H_{R_C} = 49 - 54. The major dimensions are calculated in accordance with the tolerance system in Fig.158b. The minimum hole shrinkage is set at R_{min} = 5 microns, and the maximum shrinkage on the average, at R_{max} = 15 - 20 microns. It is assumed that rotary guide bushings will be used.

These effective dimensions may also be employed for flute reamers designed for the machining of hardened steels of reduced hardness ($H_{R_C} < 49$). The R_{min} and R_{max} of hardened steels of higher hardness ($H_{R_C} > 54$) machined at lower cutting speeds than steels of H_{R_C} = 49 - 54, should be established by experimental means.

Appendices 4 and 6 of the same paper by K.F.Romanov give the dimensions of the design elements of rotary guide bushings and of a chuck for interiorly-cooled reamers.

29. Geometry of the Flute Reamer Bit and the Cemented Carbide for Tipping

An investigation has been made as to the effect of the following geometric parameters of reamer bits upon their service life: true rake angle γ, working relief angle α, chamfer angle φ, and axial rake of cutting edge λ (Fig.152).

Tests were run on various titanium-tungsten carbides. The tests were conducted in the machining of alloy steels hardened to H_{R_C} = 49 - 54 (σ_t = 160 - 180 kg/mm^2).

Effect of True Rake Angle γ and Working Relief Angle α on Reamer Life

In the course of the experiments, the true rake angle γ was varied in the interval from 0 to -15°, and the working relief angle α from 6 to 15°. The depth of cut was $t = 0.2$ mm, the feed $s = 0.275$ mm/rev, and the cutting speed $v = 50$ m/min. Figure 165 shows that the optimum values of the true rake and working relief angles are $\gamma = -15^\circ$ and $\alpha = 6^\circ$. The service life of the reamer rises with a reduction in the working relief angle α from 15 to 6°. A further reduction in α angle leads to impairment of the cutting process: a noticeable increase in axial force and torque.

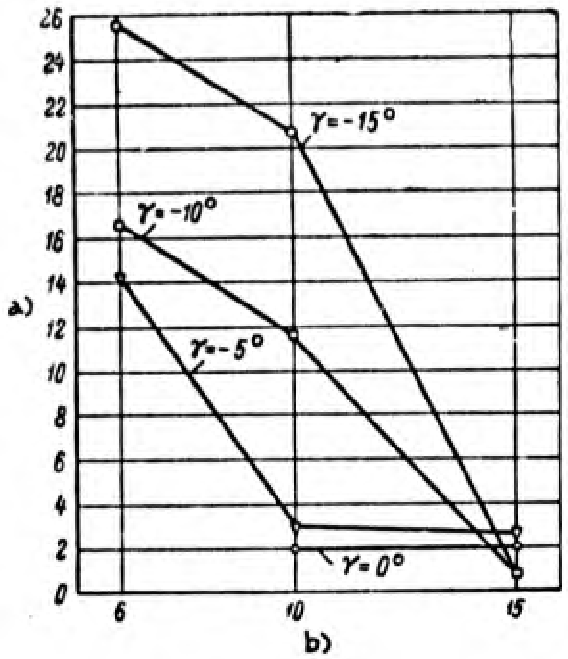

Fig.165 - Influence of True Rake γ and Working Relief α Angles upon Reamer Life. Machining of hardened steel, $R_{R_C} = 49 - 54$ by reamers tipped with T15K6 alloy

a) Tool life T, min; b) Working relief angle of reamer, α°

The life of a reamer rises with increasing negative value of the true rake angle γ (increase in lip angle β). The purpose of the true rake angle here is that of strengthening the cutting edge, and not of facilitating the process of chip formation.

The manufacture of flute reamers may be simplified by providing a negative true rake angle of $\gamma = -15^\circ$ only on the entering edge. The finishing portion of the reamer requires an angle γ of only -5 to -10°. This facilitates chip removal in the direction of the unmachined surface of the hole.

Influence of Chamfer Angle of the Entering Edges of the Teeth φ Upon Reamer Life.

The following chamfer angles on the entering edge were investigated: $\varphi = 5, 10$

and 45° (Fig.166a); φ = 15° and φ_o = 1°30' - 2° (Fig.166b). At φ = 5°, vibrations appear at the outset of operation of the reamer, when it bites into the metal. The

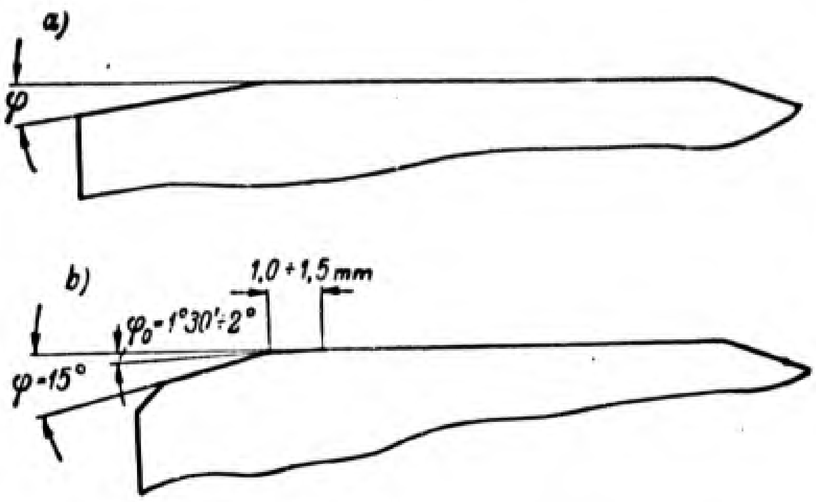

Fig.166 - Chamfer Angle of Reamer

chip is soon ground up, which makes its removal difficult. The life of the reamer is satisfactory: T = 19.3 min. At φ = 10°, the machined surface is not as well finished as at φ = 5°, and the life is considerably shorter: T = 7.2 - 0.6 min, and the cutting edges of the reamer blades crumble out. At φ = 45°, the finish of the machined surface is not higher than Class 7. The cutting edges crumble out soon after the onset of cutting. The best results are achieved at φ = 15° and φ_o = 1°30' - 2°. The finish of the machined surface is of Class 11, and the reamer life is high (T = 11.7 - 25.5 min).

For purposes of reaming hardened

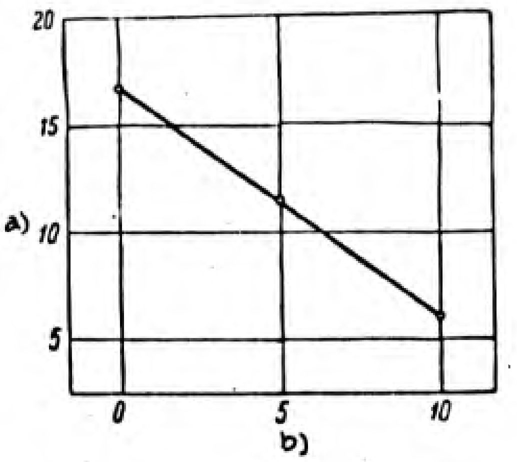

Fig.167 - Effect of Axial Rake γ upon Reamer Life. Geometry of reamer bit: α = 6 - 8°, γ = -5°, φ = 15°, φ_o = 1°30' to 2°, width of margin on finishing portion f = 0.15 to 0.20 mm

a) Reamer life T, min; b) Axial rake λ°

steel, the chamfer angle, and the second bevel recommended are as shown in Fig.166b.

Effect of Axial Rake λ Upon Reamer Life

Special sharpening of the blades along the entering edge of the reamer at an angle λ to its axis (Fig.152) assists the chip in flowing toward the unmachined surface of the hole. However, this weakens the cutting edges, and a positive true rake angle on the entering edge will then be variable.

Reamers tipped with T15K6 alloy have been tested with the following axial rakes: $\lambda = 0$, 5 and 10°. Machining was done at $t = 0.2$ mm, $s = 0.275$ mm/rev, and $v = 50$ m/min. It was found that special sharpening was unnecessary. The longest life was obtained at $\lambda = 0^{\circ}$ (Fig.167).

Influence of the Grade of Hard Alloy Upon Reamer Life

Experiments have shown that the titanium-tungsten carbides T15K6 and T15K6T should be used in the reaming of hardened steels. The alloy T15K6T permits operation at higher cutting speeds than does the T15K6. Reamers tipped with tungsten carbides have a considerably shorter life.

Efforts to use the alloys T30K4 and T60K6, which are particularly wear-resistant, in the reaming of hardened steels, have not been successful. These cemented carbides yield good results when employed in cutters and mills. Reamers are less rigid than single-point cutters and mills. Therefore, reaming is accompanied by vibrations, and the cutting edges of reamers tipped with highly brittle T30K4 and T60K6 tend to crumble out.

30. Reamer Wear and Dulling Criteria

Reamer Wear

Reamers tipped with carbides undergo wear on their entering and finishing edges. On its entering edge, a reamer undergoes wear particularly along the flanks of its blades (Fig.168). The use of a second bevel φ_o, considerably smaller than the chamfer angle φ, tends to remove the portion of the cutting edge that undergoes the

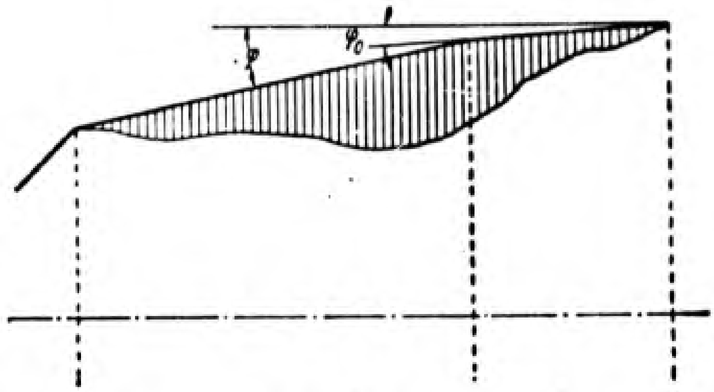

Fig.168 - Wear of Entering Edge of Reamer in the Machining of Hardened Steels

most wear (the portion where the edge changes sharply) from the machined surface.

The wear of the reamer along the diameter of the finishing portion is of importance since it determines its service life. Experiments have shown that the cutting speed is the most important factor in determining the wear of the finishing edge. Tests of reamers tipped with T15K6 (t = 0.2 mm and s = 0.275 mm/rev) showed that, as the cutting speed v was increased from 8.3 to 50 m/min, the wear of the finishing edge of the reamer diminished. The results of these tests are presented in Table 72.

Obviously, the unit wear diminishes as the cutting speed rises, although in the range of cutting speeds up to v = 20 m/min, the wear diminishes more sharply than for speeds in the v = 20 - 50 m/min range. At v = 19.9 m/min, the unit wear is higher by a factor of 1.82 than at v = 50 m/min, and is 13 times higher at v = 8.3 m/min. From the viewpoint of unit wear at the finishing edge it is most desirable to work at cutting speeds in excess of 20 m/min.

Criteria of Reamer Dulling

In determining the dulling criteria for a reamer, it must be considered that this tool is used to provide the finishing dimensions of the hole, while giving it the required surface finish. All the criteria employed for HSS reamers cannot be

Table 72

Wear of Cemented-Carbide Reamers in the Machining of Steels Hardened to H_{R_C} = 49 to 54

Cutting speed v, in m/min	Reamer wear on diameter of finishing edge during service life T, in microns	Number of machined holes	Unit wear h_y*, in microns	Ratio of unit wear to wear at v = 50 m/min
8,3	28	39	0,718	13,00
13,4	38	78	0,487	8,85
19,9	13	130	0,100	1,82
32	12	137	0,088	1,60
50	8	144	0,055	1,00

*Unit wear is the wear of a reamer per hole machined.

applied to carbide-tipped reamers. For example, the criterion for enlargement of the machined hole past the given tolerance is not applicable. High-speed machining of hardened steels with carbide reamers results not in enlargement but in shrinkage of the holes.

The quality of the machined surface is also useless as a criterion of dulling, Unlike HSS reamers, it is characteristic of carbide tools in this class that there is no impairment of surface quality as the wear reaches h = 0.7 - 0.8 mm.

In the reaming, as in the turning, of hardened steels, the acquisition of

GRAPHIC NOT REPRODUCIBLE

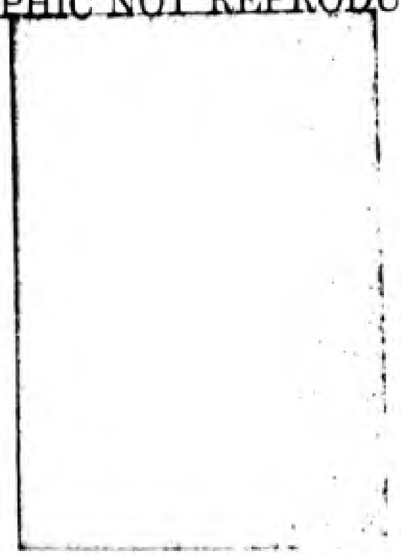

Fig.169 - Effect of Degree of Dulling of Reamer Tipped with T15K6 Upon the Appearance of Chip in the Machining of Alloy Steels Hardened to H_{R_C} = 49 - 54

a goffered shape by the chip may be taken as a visible criterion of the dulling of the tool. Figure 169 presents three chips resulting from different degrees of dulling of a carbide reamer (t = 0.2 mm, s = 0.275 mm/rev, v = 31.2 rpm). The topmost chip came from the first hole drilled, and the next from the 85^{th} hole when the tooth wear along the flank of the entering edge of the reamer was h = 0.15 - 0.2 mm. The lowest chip represents a wear of h = 0.30 - 0.35 mm and was obtained in the machining of the 120^{th} hole.

Since a reamer wear of h = 0.3 - 0.35 mm is accompanied by the formation of chip of a clearly visible goffered appearance, this criterion can be used widely under industrial conditions.

When employing this criterion, it must be remembered that the size of the machined hole must not be allowed to become smaller than the minimum tolerance.

An investigation was made on the ratio of shrinkage of the hole and surface finish to reaming time, at various cutting speeds. The experiments were run at t = 0.2 mm, s = 0.27 mm/rev, and v = 8.3 - 51.5 m/min. It was found that, at cutting speeds higher than 20 m/min, the shrinkage of the hole and the surface finish are practically independent of the reaming time. The hole shrinkage was about 0.02 mm. At cutting speeds below 20 m/min, the shrinkage rose in proportion to the time the tool was in use, while the surface finish varied greatly and was impaired as the reaming was continued.

These data confirm the desirability of high cutting speeds in the machining of hardened alloy steels with carbide reamers.

31. Service Life Relationships

Relation Between Cutting Speed and Reamer Life

Table 73 and Fig.170 present the results of experiments to determine the relationship between the cutting speed v and the reamer life T in the machining of alloy steels hardened to H_{R_C} = 49 - 54. Reamers with a diameter of 14 and 28 mm, tipped with T15K6 and T60K6 alloys, were tested with the following lubricants: 10% emulsol, 5% sulfofrezol, 0.2% sodium carbonate, and the remainder water.

The curves show that reamer life decreases with increasing cutting time, no

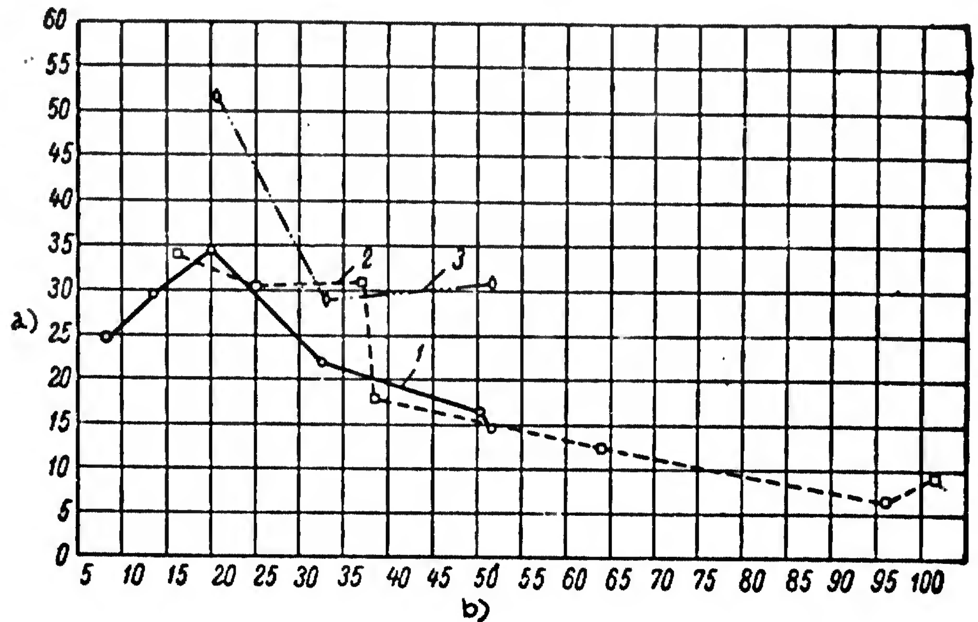

Fig.170 - Effect of Cutting Speed v Upon Life of Reamer T in the Machining of Hardened Alloy Steels, H_{R_C} = 49 - 54 (t = 0.2 mm, s = 0.275 mm/rev);

1 - Reamers of D = 14 mm, tipped with T15K6 alloy; 2 - Reamers of D = 28 mm, tipped with T15K6 alloy; 3 - Reamers of D = 14 mm, tipped with T60K6 alloy

a) Reamer life T, min; b) Cutting speed v, m/min

matter which of these carbides is employed. The range of cutting speeds v from 8.3 to 19.9 m/min for reamers 14 mm in diameter tipped with T15K6 alloy constitutes an exception. Here the tool life actually rises with the cutting speed.

Table 74 presents the values of the relative life indices m in the equation $v = \frac{C}{T^m}$.

A cutting speed of v > 20 m/min is of practical interest for reamers with D = = 14 mm. An increase in the cutting speed results in an increase in output by this process (Fig.171). This has been defined for the life of the reamers tested under conditions of identical wear of their teeth at the entering edge (h = 0.3 mm).

Work at lower speeds impairs the surface finish and causes an increase in the

Table 73

Effect of Cutting Speed Upon Tool Life in Flute Reaming of Hardened Steels, $H_{R_C} = 49 - 54$

Reamer diameter D, in mm	Cemented Carbide	Cutting Conditions			Reamer Life T, in min
		Cutting Depth t, in mm	Feed s, in mm/rev	Cutting Speed v, in m/min	
14	T15K6	0,2	0,275	8,3	24,5
				13,6	29,5
				19,9	34,5
				32,6	22
				50,2	12
				50,4	21,5
				51,4	14,5
	T60K6			20,6	51,5
				32,8	29
				51,6	31
28	T15K6	0,25		16,2	34
				24,9	30,5
				37,2	31
				38,4	17,5
				64,0	12,5
				96,0	6,5
				101,5	8,5

Table 74

Magnitude of Relative Life Index m in Flute Reaming of Steels Hardened to $H_{R_C} = 49 - 54$

Cemented Carbide	Reamer diameter D, mm	Conditions of Experiment	Index m
T15K6	14	At v > 20 m/min	0,85
		At v < 20 m/min	—2,55
	28	Excluding experiments where life is T < 10 min.	1,0
		Including all experiments	1,3

unit wear of the reamers along their finishing edge, as well as hole shrinkage.

It should be noted that the life of a reamer of 28 mm diameter, at equal cutting speeds, is somewhat greater than that of reamers with a diameter of 14 mm.

Cutting speeds for the reaming of hardened steels should be in excess of 20 m/min.

Effect of Feed Upon Reamer Life

Table 75 presents experimental data descriptive of the influence of feed upon the life of a reamer (14 or 28 mm diameter) tipped with T15K6 alloy, in the machining of alloy steels of H_{R_C} = 49 – 54. The experiments were run with 10% emulsol in soda solution, with the addition of 5% sulfofrezol.

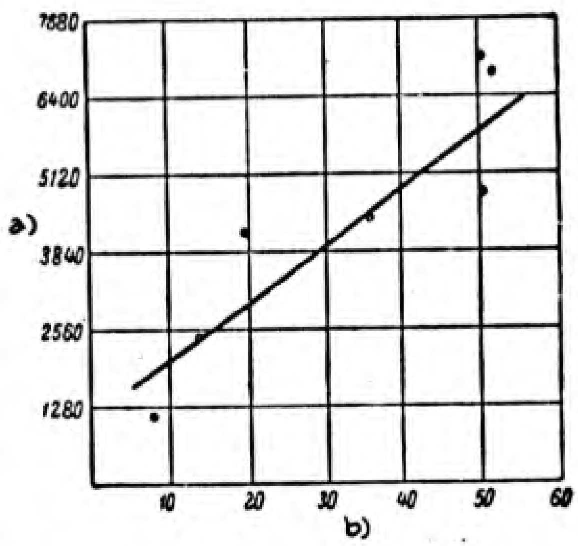

Fig.171 – Distance Reamed L versus Cutting Speed v. Machining of steels hardened to H_{R_C} = 49 – 54 by reamers 14 mm in diameter, tipped with T15K6 alloy

a) Length of machined surface, L, mm; b) Cutting speed v, m/min

Taper, out-of-round, shrinkage, and surface finish of all the holes machined in these tests were within the required tolerance.

Figure 172 presents the relations between the lives of reamer with diameters of 14 and 28 mm and the feed. As we see, life is reduced as the feed is increased.

The curves in Fig.173 describe the relation between cutting speed and the life of reamers at various feeds. Machine oil was the coolant used in these tests. As we see, the cutting speed declines as the feed increases. The curves also show that, for the feed values tested, an increase in the cutting speed results in a reduction in the reamer life, a law which holds for cutting speeds of v > 31.8 m/min at s = 0.1 mm/rev, and v = 30.8 m/min at

Table 75

Relation of Reamer Life T to Feed s in Machining Steels Hardened to H_{R_C} = = 49 ÷ 54

Reamer diameter D, in mm	Cutting Conditions				Reamer Life	
	t, in mm	s, in mm/rev	n, in rpm	v, in m/min	Number of holes machined	T, in min
14,62		0,100		52,5	46	13
14,84		0,100		53	118	33,5
14,72		0,195		53	124	18
15,20		0,195		54,5	85	12
14,34		0,275		51,5	144	14,5
14,10	0,20	0,275	1140	50	212	21,5
14,00		0,275		50	115	11,5
14,00		0,275		50	251	25,5
15,18		0,400		54,5	148	10
15,00		0,400		53,5	96	6,5
15,23		0,575		54,5	117	6
25,39		0,100		57,5	100	50
28,01	0,25	0,275	725	64	78	12,5
27,19		0,275		61,5	111	18
27,18		0,400		61,5	113	12,5

s = 0.3 mm/rev. The opposite law is valid for lower cutting speeds: The reamer life increases with a rise in cutting speed.

For reamers of 14 mm diameter, the folowing relationship may be established between the feed s and the reamer life T:

$$s = \frac{1{,}96}{T^{0{,}81}}.$$

Experiments have shown that stable results in terms of surface finish are ensured at feeds of s > 0.2 mm/rev. It is recommended that feeds up to 0.4 mm/rev be employed for reamers with D = 14 mm and s up to 0.6 to 0.7 mm/rev for reamers with D = 28 mm.

To prevent the outflowing chip from jamming the grooves between the reamer blades, as may occur at feeds of s ≥ 0.4 mm/rev (at which upward removal of chip becomes difficult), the reamer body must be subjected to heat treatment providing a hardness of H_{R_C} = 45 - 50, and the grooves between the blades must be polished.

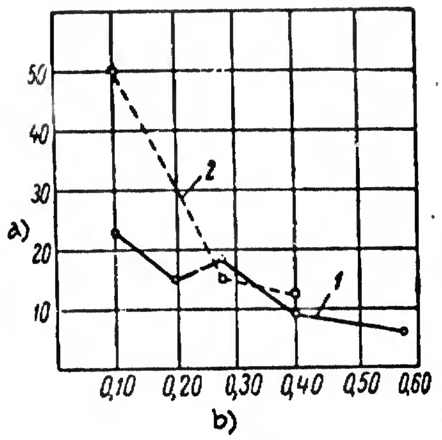

Fig.172 - Effect of Feed s Upon Reamer Life T in the Machining of Hardened Steels of H_{R_C} = 49 -54

1 - For reamer of 14 mm diameter (t = = 0.2 mm, v = 50 m/min); 2 - For reamers of 28 mm diameter (t = 0.25 mm, v = 60 m/min)

a) Reamer life T, min; b) Feed s, mm/rev

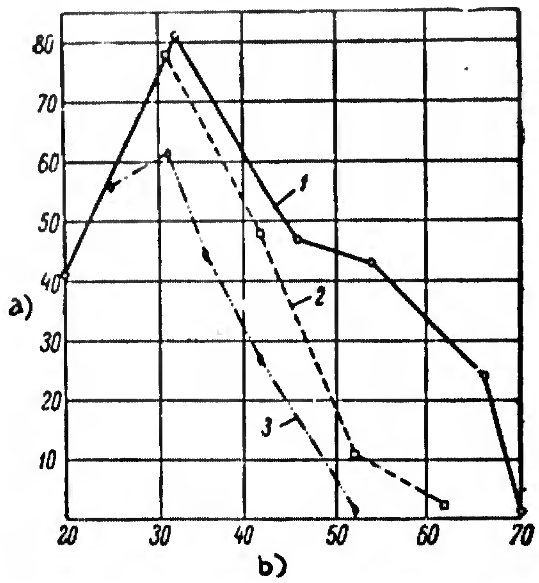

Fig.173 - Cutting Speed v versus Reamer Life T at Various Feeds s (t = = 0.2 mm) in the Machining of Hardened Steels of H_{R_C} = 49 - 54. Lubricant used, machine oil.

1 - s = 0.1 mm/rev; 2 - s = 0.2 mm/rev; 3 - s = 0.3 mm/rev

a) Reamer life T, min; b) Cutting speed v, m/min

Effect of Cutting Depth Upon Reamer Life

Table 76 and Fig.174 present experimental data for the influence of the depth of cut upon the life of reamers tipped with T15K6 alloy and employed to machine steels hardened to H_{R_C} = 49 - 54.

Obviously, the depth of cut t exerts a negligible influence upon the reamer life T (at t > 0.10 mm).

The relation between the depth of cut t and the reamer life T may be expressed by the equation

$$t = \frac{4{,}05}{T^{1{,}12}}.$$

The machining of hardened steels with carbide-tipped reamers differs significantly from the machining of unhardened steels with HSS reamers. In the latter case, an allowance is left for finish-reaming to provide the required surface finish, of such size that the cutting takes place in a layer work-hardened by the preceding operation. With respect to hardened steel, there is no need to strengthen the material in the course of prior machining. Therefore, it becomes possible to simplify the procedure for the machining of holes. Table 77 gives the procedure recommended by K.F.Romanov for machining holes into parts consisting of hard-alloy steels, including hole size and allowance for operations after drilling.

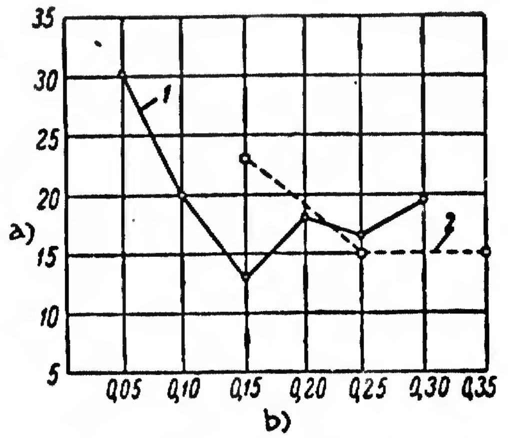

Fig.174 - Depth of Cut t Versus Reamer Life T in the Machining of Alloy Steels Hardened to H_{R_C} = 49 - 54

1 - For reamers with D = 14 mm;
2 - For reamers with D = 28 mm.

a) Reamer life, T min; b) Depth of cut t, mm

It will be seen that the maximum allowance for flute-reaming is 0.6 mm on diameter. Except for cases in which the intermediate operation of rose-reaming is required (welding of assemblies with holes, final assembly and assembled finish-machining of holes, etc.), the procedure in the machining of holes in hardened steel parts consists of the following operations: drilling with allowance for flute-reaming; heat treatment; finish flute-reaming.

The minimum allowance for flute-reaming with reamers having a chamfer angle of $\varphi = 15^{\circ}$ is 0.14 mm on the diameter. At lower allowances, the entering edges do not participate in the work, and cutting is performed by the taper, its bevel being $\varphi_0 = 1^{\circ}30' - 2^{\circ}$. This will create the danger of spalling (as the reamer enters the work hole).

Tests have shown that, in reaming holes into parts consisting of steels tempered to high hardness, the surface finish will be independent of the allowance in a range of 0.2 to 0.7 mm on the diameter.

Table 76

Reamer Life T Versus Depth of Cut t in the Machining of Steels Hardened to $H_{R_C} = 49 - 54$

Reamer diameter D, in mm	Cutting Conditions				Reamer Life	
	s, in mm/rev	n, in rpm	v, in m/min	t, in mm	Number of holes machined	T, in min
14,10	0,275	1140	50,5	0,05	300	30,5
15,00			54.	0,10	196	20
15,10			54	0,15	130	13
14,34			51,5	0,20	144	14,5
14,01			50	0,20	212	21,5
14,01			50,5	0,20	115	11,5
14,01			50,5	0,20	251	25,5
15,23			54,5	0,25	163	16,5
14,89			53	0,30	189	19,5
28,32	0,275	725	64,5	0,15	145	23
28,01			64	0,25	78	12,5
27,19			61,5	0,25	111	18
25,67			58,5	0,35	93	15

General Formula for Cutting Speed

An equation is presented below for determining the cutting speed in the reaming of holes into parts made of alloy steels hardened to $H_{R_C} = 49 - 54$:

$$v = \frac{14D^{0{,}4}}{T^{0{,}85} \cdot t^{0{,}75} \cdot s^{1{,}04}}, \qquad (19)$$

where v is the cutting speed, in m/min;

D is the reamer diameter, in mm;

T is the reamer life, in min;

t is the depth of cut equal to one-half the allowance, in mm;

s is the feed, in mm/rev.

Table 77

Machining Allowance After Drilling and Procedure for Reaming Holes in Alloy Steels Tempered to High Hardness

Hole diameter D, mm	Allowance on diameter after drilling, in mm	Sequence of Operations
To 18	0,3—0,6	1. Heat treatment 2. Finish flute-reaming
	0,6—2,0	1. Heat treatment 2. Rose-reaming with allowance of 0.3 - - 0.4 mm on diameter for flute reaming 3. Finish flute-reaming
	2,0—4,0	1. Heat treatment 2. Preliminary rose-reaming 3. Rose-reaming, leaving allowance of 0.3 - - 0.4 mm on diameter for flute reaming 4. Finish flute-reaming
Over 18	0,3—0,6	1. Heat treatment 2. Finish flute-reaming
	0,6—3,0	1. Heat treatment 2. Rose-reaming with 0.4 - 0.5 mm allowance on diameter for flute reaming 3. Finish flute-reaming
	3,0—6,0	1. Heat treatment 2. Preliminary rose-reaming 3. Rose-reaming with 0.4 - 0.5 mm allowance on diameter for flute-reaming 4. Finish flute-reaming

The increase in cutting speed with rising reamer diameter is based on experiments performed with a tool of 14 and 28 mm diam (Table 75 and 76). This regularity has also been confirmed by tests under production conditions, involving the use of reamers of 34, 55, and 61 mm diameter.

Machinability of Steels Hardened to $H_{R_C} = 35 - 38$

Experiments have shown that, in the reaming of hardened alloy steels tempered to H_{R_C} = 35 - 38, the relation T - v is of the same nature as for steels of H_{R_C} = = 49 - 54. The curve expressing this relation has a jog at the point representing a cutting speed of v = 70 m/min. To the right of the jog, the reamer life diminishes with further increase in cutting speed.

It is the interval of cutting speeds to the right of the jog that is of practical significance. At these speeds, as compared to the interval to the left of the jog, a high-quality surface finish is achieved, and the intensity of tool wear along the finishing edge is diminished.

Investigations have shown that, in the machining of hardened alloy steels of H_{R_C} = 35 - 38 at cutting speeds of v = 70 to 120 m/min and splash lubrication, shrinkage of the holes will result.

The general formula for determining the cutting speed in the reaming of steels hardened to H_{R_C} = 35 to 38 has the following form:

$$v = \frac{39D^{0,4}}{T^{0,4} \cdot l^{0,19} \cdot s^{0,43}} \ m/min. \qquad (20)$$

32. Influence of Various Factors on Dimensional Stability and Surface Quality After Reaming

Influence of Length of Finishing Edge of Reamer l and Width of Land f.

Table 78 and Fig.175 present experimental data on the effect of the length l of

Table 78

Effect of Length of Finishing Edge of Reamer Upon Dimensional Stability and Surface Finish of Holes

Length of finishing Edge of Reamer l, in mm	Out-of-True, in microns	Taper, in microns	Shrinkage, in microns	Surface Finish H_{rm}, in microns
2	3,8	5,1	19,2	0,60
5	5,2	5,4	5,4	0,74
9	2,4	5,1	18,5	0,44
12	3,3	7,3	12,1	0,50

the finishing edge of a flute reamer (14 mm diameter) tipped with T15K6 alloy upon its dimensional stability (shrinkage, out-of-true, and hole taper) and the surface

Table 79

Influence of Width of Reamer Land Upon Dimensional Stability and Surface Finish of Holes

Width of land f, in mm	Out-of-True, in microns	Taper, in microns	Shrinkage, in microns	Surface finish H_{rm}, in microns
0,05	3,5	4,7	14	0,50
0,10	3,4	3,7	14	0,49
0,20	3,9	5,3	13	0,30
0,30	3,7	8,5	12,6	0,42
0,40	6,2	9,9	21	0,80

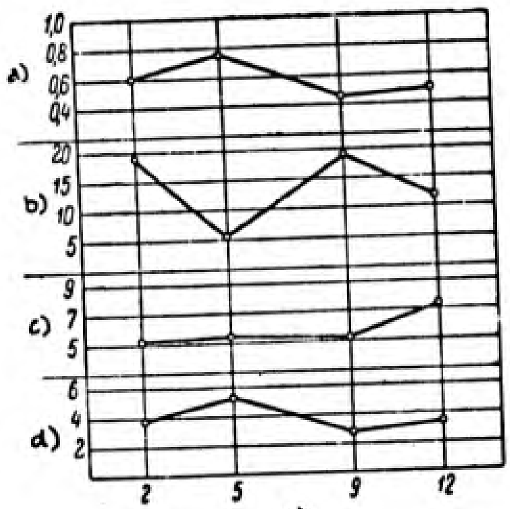

Fig.175 - Effect of Length of Finishing Edge of Reamers with D = 14 mm, Tipped with T15K6 Alloy, Upon Out-of-True, Taper, and Shrinkage, and also Upon Surface Finish of Flute-Reamed Holes. Machining of alloy steels tempered to H_{R_C} = 49 - 54

a) Average roughness H_{rm}, microns; b) Shrinkage, microns; c) Taper, microns; d) Out-of-true, microns; e) Length of finishing edge of reamer l, mm

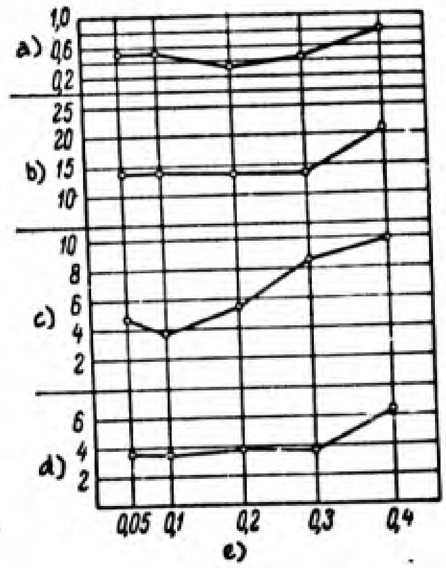

Fig.176 - Effect of Width of Land of T15K6-Tipped Reamer with D = 14 mm Upon Out-of-True, Taper, Shrinkage, and Surface Finish of Flute-Reamed Holes. Machining of alloy steels tempered to H_{R_C} = 49 - 54

a) Average roughness H_{rm}, microns; b) Shrinkage, microns; c) Taper, microns; d) Out-of-true, microns; e) Width of land f, mm finish of the machined holes. Steels tempered to H_{R_C} = 49 - 54 were tested. The width of the land on the reamers was f = 0.15 - 0.20 mm.

Obviously, the best results in terms of out-of-true, taper, and surface finish are obtained at a length of the finishing edge of 9 mm. A reamer with l = 5 mm showed minimum shrinkage. For reamers with D = 14 mm, the length of the finishing edge must be taken not less than 9 mm. Including regrindings, it is desirable to use l = 15 mm.

Table 79 and Fig.176 present the results of tests for establishing the nature of the effect of the land width f of flute reamers (14 mm diameter) tipped with T15K6 alloy on the dimensional stability and surface finish of machined holes.

Experimental data show that the best results in terms of out-of-true and taper are obtained with a land width of f = 0.1 mm. Minimum hole shrinkage and minimum

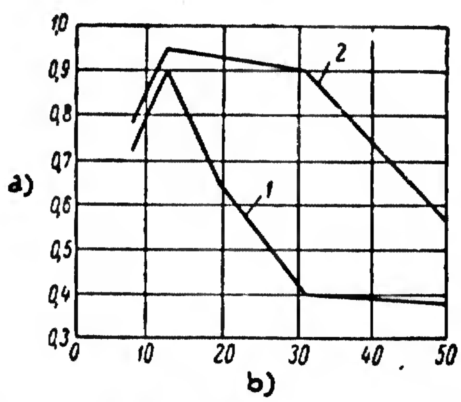

Fig.177 - Effect of Cooling Upon Hole Surface Finish in Reaming at Various Cutting Speeds. Machining of alloy steels tempered to H_{R_C} = 49 - 54 at t = 0.15 mm and s = 0.195 mm/rev. Flute reamers tipped with T15K6 alloy:

1 - Cooled with 10% aqueous emulsol solution +2% sulfofrezol; 2 - No coolant

a) Hole surface microroughness after reaming, H_{rm}, microns; b) Cutting speed v, m/min

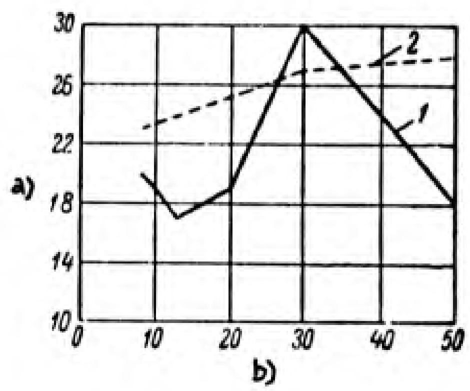

Fig.178 - Effect of Cooling Upon Enlargement after Reaming at Various Cutting Speeds. Reamers tipped with T15K6 alloy used in machining hardened alloy steels of H_{R_C} = 49 - 54 at t = 0.15 mm and s = 0.195 mm/rev:

1 - Cooling by 10% aqueous emulsol solution +2% sulfofrezol; 2 - No coolant

a) Hole expansion after reaming, microns; b) Cutting speed v, m/min

H_{rm} value are attained at f = 0.2 mm. On this basis, the land width to be recommended is f = 0.1 to 0.2 mm.

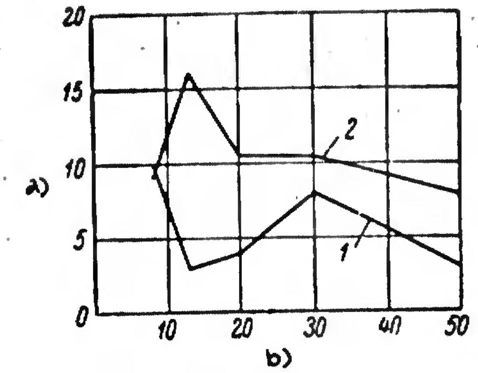

Fig.179 - Effect of Cooling Upon Hole Taper after Flute-Reaming at Various Cutting Speeds. Machining by T15K6-tipped flute reamers of alloy steels tempered to H_{R_C} = 49 - 54 at t = = 0.15 mm and s = 0.195 mm/rev

1 - Cooling by 10% aqueous emulsol +2% sulfofrezol; 2 - No coolant

a) Hole taper after reaming, microns; b) Cutting speed v, m/min

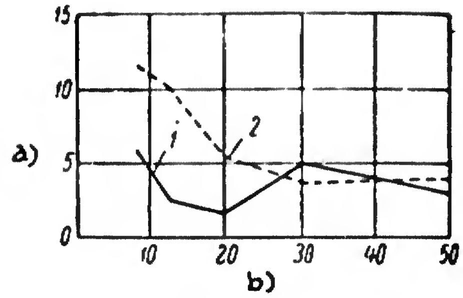

Fig.180 - Effect of Cooling Upon Out-of-True of Hole after Flute-Reaming at Various Cutting Speeds. Machining by T15K6-tipped flute reamers of alloy steels tempered to H_{R_C} = 49 - 54 at t = 0.15 mm and s = 0.195 mm/rev

1 - Cooling by 10% aqueous emulsol solution +2% sulfofrezol; 2 - No coolant

a) Hole out-of-true after reaming, microns; b) Cutting speed v, m/min

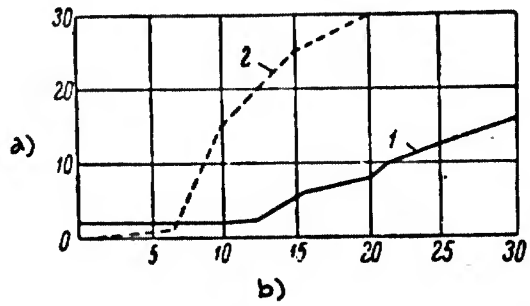

Fig.181 - Effect of Lubricant Upon Rate of Wear on Diameter of Finishing Edge of Reamer. Machining by T15K6-tipped reamers of alloy steels tempered to H_{R_C} = 49 - 54 at t = 0.2 mm, s = = 0.275 mm/rev, and v = 50 m/min:

1 - Cooling by 10% aqueous emulsol solution +5% sulfofrezol; 2 - Cooling by 10% aqueous emulsol solution +2% sulfofrezol

a) Wear of finishing edge of reamer, microns; b) Reamer operating time T, min

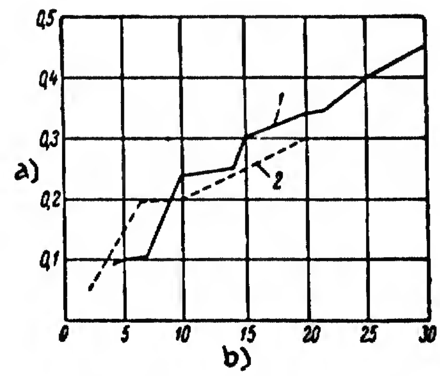

Fig.182 - Effect of Composition of Lubricant Upon Rate of Wear of Flank of Entering Edge of Reamer. Machining by T15K6-tipped reamers of alloy steels tempered to H_{R_C} = 49 - 54 at t = 0.2 mm, s = 0.275 mm/rev, and v = 50 m/min.

1 - Cooling by 10% aqueous emulsol solution +5% sulfofrezol; 2 - Cooling by 10% aqueous emulsol solution +2% sulfofrezol

a) Wear of flank of entering edge of reamer h, microns; b) Reamer operating time T, min

A back taper of 3 - 5 microns on the finishing edge of a carbide-tipped reamer is recommended to provide normal functioning. This taper reduces the axial force and the torque.

Influence of Lubricants

The following fluids were tested to determine the optimum lubricant-coolant for use in the flute-reaming of parts made of hardened alloy steels (H_{R_C} = 49 - 54):

1) 5% aqueous emulsol solution;

2) 10% aqueous emulsol solution;

3) sulfofrezol;

4) machine oil;

5) spindle oil;

6) 10% aqueous emulsol solution + 2% sulfofrezol.

The reamed holes were tested for expansion after reaming for dimensional stability, out-of-true, taper, and surface finish. Machining was performed at a cutting speed of v = 50 m/min, depth of cut of t = 0.2 mm, and feeds in the s = 0.2 to 1.1 mm/rev interval. The best results were obtained with spindle oil and with 10% aqueous emulsol solution +2% sulfofrezol as lubricants. The latter fluid is to be perferred in terms of safety at cutting speeds resulting in highly heated chip.

Comparative tests with and without the selected fluid were run to determine its effectiveness. A check was made of expansion beyond reaming dimensions, out-of-true, taper, and surface finish of the holes machined, as well as of the flank wear of the entering edges and on the wear on the diameter of the finishing edge. The results of these tests are plotted in Figs.177 - 182. The curves in Fig.177 demonstrate the effect of the cutting speed on the surface finish of the hole. The curves in Figs.178, 179, and 180 demonstrate the effect of the cutting speed on the expansion beyond reaming dimensions, the taper, and the out-of-true of the holes after reaming. It will be seen that surface finish is higher, while the elongation, taper, and out-of-true are less when a coolant is used.

In reaming without coolant at cutting speeds in excess of 20 m/min, the high temperature generated in the cutting zone may have a harmful influence upon the quality of the surface layer of metal. Moreover, excessive wear of the finishing edge of the reamers occurs under these circumstances.

Experiments have also shown that an increase from 2 to 5% in the sulfofrezol content of the fluid results in a lowered wear of the finishing edge of the reamer (Fig.181). Figure 182 shows that the percentage of sulfofrezol in the lubricant-coolant fluid has little effect upon the extent of wear on the flanks of the entering edge of a reamer.

In reaming holes in alloy-steel parts tempered to high hardness, the use of a lubricant may be deemed obligatory, and the best results are obtained with 10% soda-emulsol solution (0.2% soda) and of 5% activated sulfofrezol.

Effect of Cutting Conditions Upon Shrinkage of Holes After Reaming

The curves in Figs.183, 184, and 185 show the effect of the cutting speed v, feed s, and depth of cut t upon the shrinkage of holes after reaming. The experimental data pertain to reamers of 14 mm diameter tipped with T15K6 alloy, used in the machining of alloy steels hardened to $H_{R_C} = 49 - 54$. The center line ($\bar{X}$) of the graph gives the average deviations of the diameters of the flute-reamed holes. The broken lines represent the theoretical limits of the hole-dimension scatter. As we see, this closely approximates the real limits of the range of scatter.

An examination of these curves indicates that, unlike feed and depth of cut, the cutting speed has a significant influence upon the shrinkage of holes after reaming, and upon the area over which the experimental points are scattered. In the case of cutting speeds in excess of 20 m/min, the area of scatter is substantially narrowed when compared to cutting speeds of less than 20 m/min (Fig.183). The range of scatter of the hole dimensions is least at v = 33 m/min. However, at this speed,

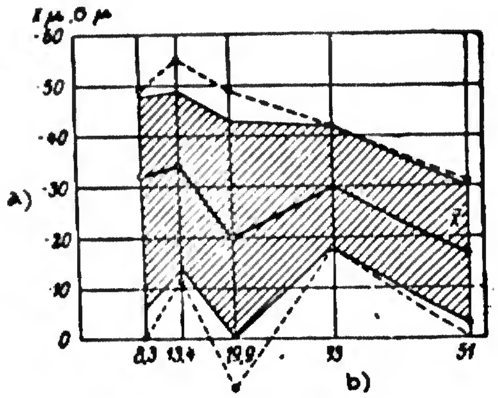

Fig.183 - Cutting Speed versus Hole Shrinkage after Flute-Reaming. Machining of alloy steels tempered to H_{R_C} = 49 - 54 at t = 0.2 mm and s = 0.275 mm/rev

a) Shrinkage of holes after flute-reaming, microns; b) Cutting speed v, m/min

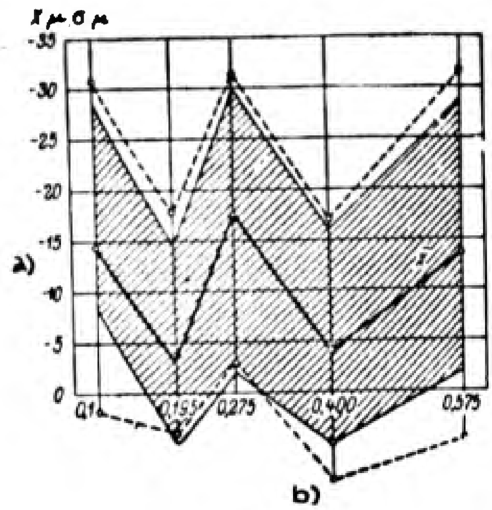

Fig.184 - Influence of Feed Upon Hole Shrinkage after Flute-Reaming. Machining of alloy steels tempered to H_{R_C} = 49 - 54 at t = 0.2 mm and v = 50 m/min

a) Shrinkage of holes after flute-reaming, microns; b) Feed s, mm/rev

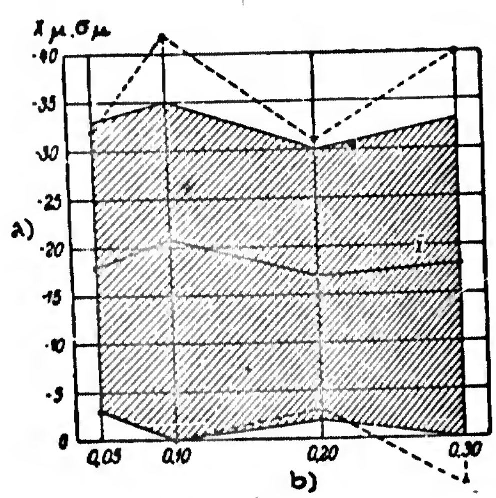

Fig.185 - Influence of Depth of Cut Upon Hole Shrinkage after Reaming. Machining of alloy steels tempered to H_{R_C} = 49 - 54 at s = 0.275 mm/rev and v = 52 m/min

a) Shrinkage of holes after flute-reaming, microns; b) Depth of cut t, mm the average deviation of the diameters of the flute-reamed holes is comparatively large. This value is considerably less at v = 51 m/min.

The least shrinkage of holes after reaming is achieved in the case of hardened alloy steels, at cutting speeds in excess of 20 m/min. The use of guides reduces the area of scatter of machined hole sizes to the 5 - 20 micron interval.

CHAPTER VII

ROSE-REAMING OF HARDENED STEELS

Rose Reamer Design and Jigs. The machining of holes in hardened steel parts with rose reamers requires the use of guides as does work with flute reamers. The tool is guided by means of a rear guide bushing, or by front and rear bushings. Dual guides are used in the following cases: when the length of the hole is more than two diameters; when several coaxial holes are being machined; when the axis of a previously machined hole has been substantially shifted relative to the axis of the guide bushings.

Holding fixtures for rose reamers should also have rotary guide bushings. In work with holding fixtures, the rose reamer is mounted by means of a floating arbor.

The design of the assembled type of rose reamer, tipped with carbide, is analogous to that of assembled flute reamers, differing from the latter only by the geometric parameters of the cutting part. The considerations in Chapter VI with respect to flute-reamer designs, and the methods of feeding the lubricant, are wholly applicable to rose reamers.

In the rose-reaming of hardened steels it is necessary to employ the lubricant and coolant fluid that yields the best results in flute-reaming, namely a 10% solution of emulsol in caustic +5% sulfofrezol.

The cutting conditions for rose-reaming, presented in Appendix V, will yield a finish of the machined surface as high as $\nabla\nabla 6$ and up to Class 4 accuracy.

Figure 186 presents the design of a rose reamer tipped with T15K6 alloy, with

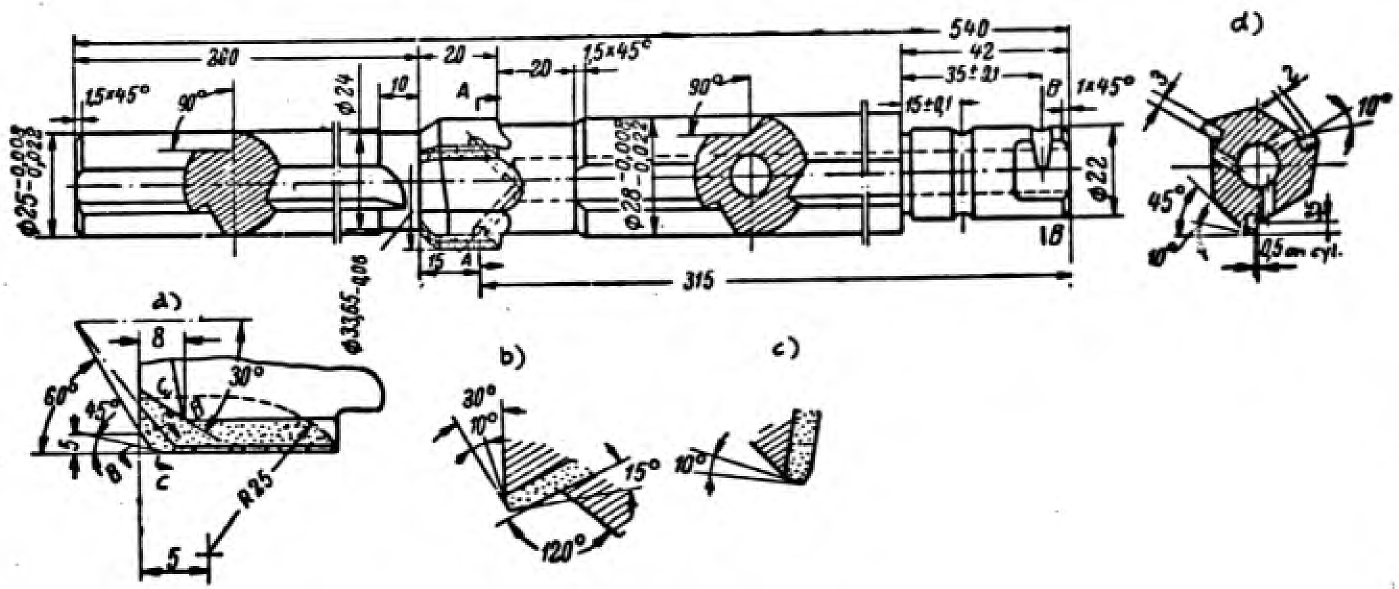

Fig.186 - Rose Reamer Tipped with T15K6 Alloy, Having Front and Rear Guide Bushings and Internal Lubrication

a) Axis of rose reamer; b) Section through B-B; c) Section through C-C
d) Section through A-A

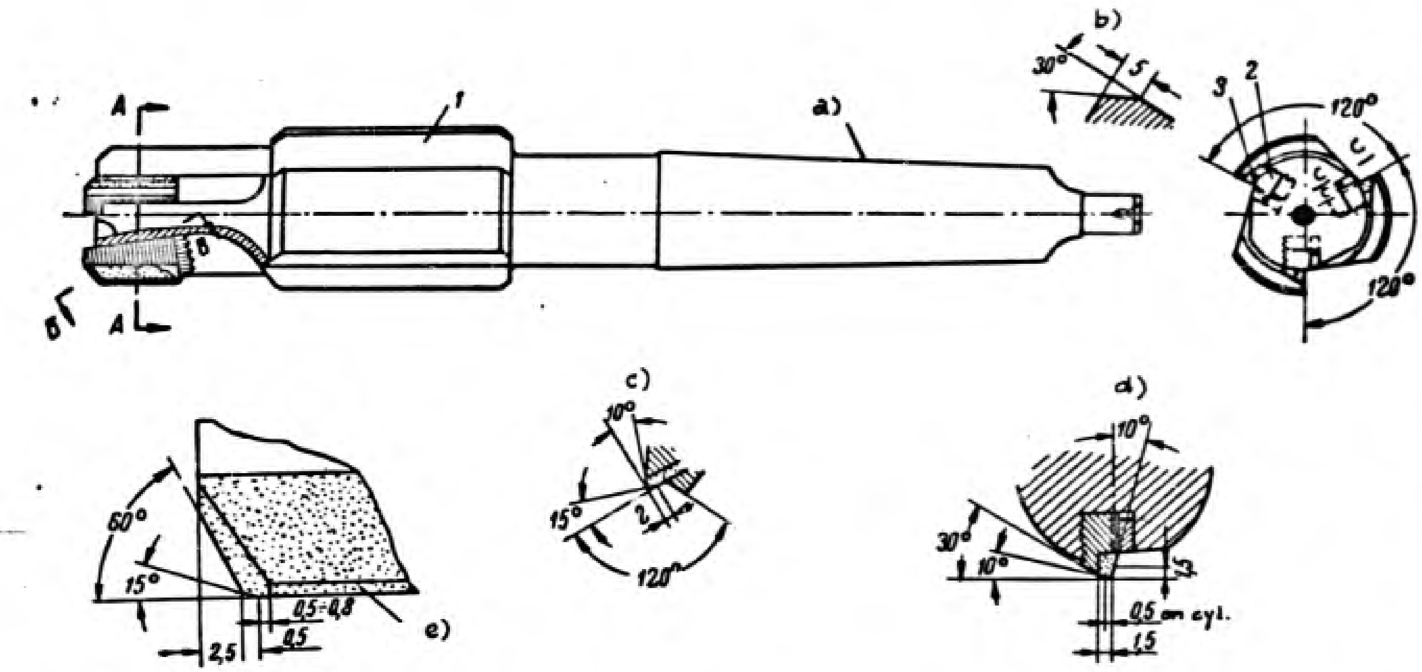

Fig.187 - Assembled Type of Rose Reamer, Made by the NIAT, with Rear Guide Bushing and Taper Shank

1 - Body; 2 - Inserted tooth; 3 - Wedge

a) Morse taper; b) Section through C-C; c) Section through B-B; d) Section through A-A; e) Back taper of 0.05 mm to shank dual guides and internal cooling. Figure 187 shows a rose reamer with rear guide and inserted teeth, as designed by the NIAT. These designs have proved satisfactory in the machining of hardened steels.

Geometry of Rose-Reamer Bit and Type of Carbide to be Used. Experiments have established that for machining hardened alloy steels of $H_{R_C} = 49 - 54$, rose reamers must have a true rake angle of $\gamma = -15^{\circ}$ and a working relief angle of $\alpha = 10^{\circ}$ (Fig.188). At a chamfer angle of $\varphi = 60^{\circ}$ and a second bevel of $\varphi_0 = 15^{\circ}$, the most

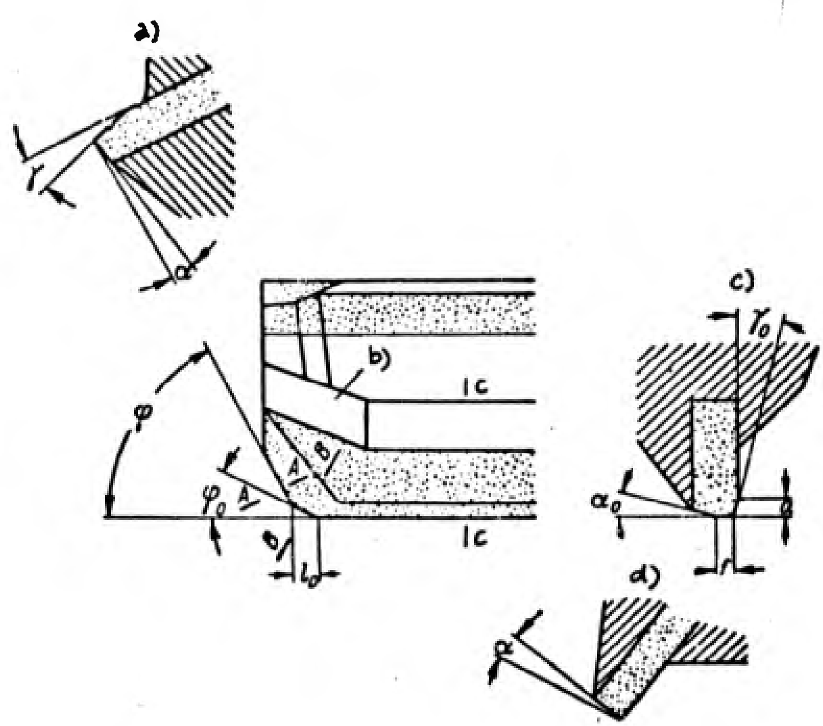

Fig.188 - Geometric Parameters of Cutting Portion of Rose Reamer

a) Section through A-A; b) Deflecting bevel; c) Section through C-C; d) Section through B-B

extensive wear of a rose reamer does not occur at the point of transition between the finishing and the entering edge but at the point of contact between the main cutting edge and the transitional cutting edge (Fig.189). The axial rake is taken to be $\lambda = 0^{\circ}$.

The main true rake angle γ, and its radial counterpart γ_0, both negative, are produced by a special recess (Fig.190). Point A denotes the point of contact between the main cutting edge on the entering edge and the transitional edge, while point B is the point of contact between the guiding land on the finishing edge with the transitional edge, and point C the intersection of the flat on the leading edge with the land. Figure 190a illustrate a recessing job properly done; Fig.190b and 190c show incorrect recessing; in the former instance the cutting edge is formed without a recess, whereas in the latter the guiding land is intersected.

Fig.189 - Wear of T15K6-Tipped Rose Reamer Along Flank of Entering Edge in the Machining of Hardened Alloy Steels, $H_{R_C} = 51$

The recess which forms the negative true rake angle also facilitates forward removal of chip, in the direction of the unmachined surface. Toward this purpose, a "deflecting bevel" (Fig.188) is formed on the flank of the rose-reamer blade immediately ahead of the one in question. As a result, the chip flowing off at high speed normal to the peripheral cutting edge (in the form of a straight ribbon) strikes the deflecting bevel, curls, and is directed forward.

Figure 191 shows curves for the relation between the cutting speed v and the life of a rose reamer T, for the hard alloys T15K6 and T5K10. The work material was hardened steel tempered to $H_{R_C} = 51$, machined at a cutting depth t = 0.65 mm and a feed s = 0.4 mm/rev. The diameter of the rose reamer was D = 25 mm. Obviously, the life of rose reamers tipped with T15K6 carbide is longer than that of reamers tipped with T5K10 alloy. For the rose-reaming of hardened alloy steels, the hard alloys T15K6 and T15K6T must be used.

Wear of Rose Reamers and Dulling Criteria. In the machining of hardened steels, the wear of a rose reamer occurs in approximately the same manner as that of a flute reamer. A rose reamer undergoes maximum wear at the point of intersection between the main peripheral and transitional cutting edges (Fig.189). The wear occurs along the flank and is insignificant on the face.

Figure 192 presents empirical data on the relationship between length of opera-

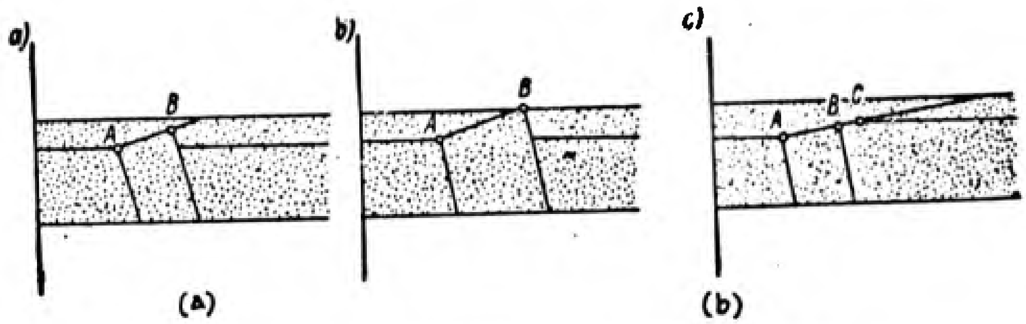

Fig.190 - Special Recessing of Rose-Reamer Face.
(a) Correct; (b) Incorrect

tion and flank wear of a rose reamer h, and also between taper and out-of-true of the hole after rose-reaming. The tests were made with rose reamers tipped with T15K6 carbide, at t = 0.65 mm, s = 0.4 mm/rev, and v = 60 m/min. As we see, the

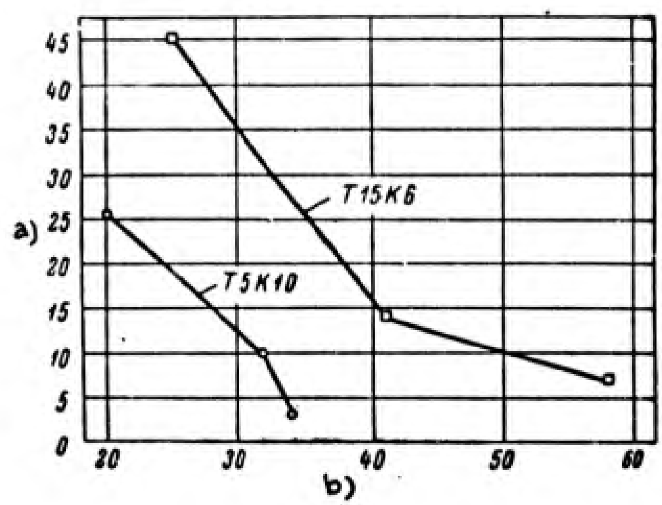

Fig.191 - Relation Between Cutting Speed v and Life T for Rose Reamers Tipped with Carbides T15K6 and T5K10

a) Life of rose reamer T, min; b) Cutting speed v, m/min

wear rises rapidly to a value of h = 0.6 mm and then stabilizes. Crumbling-out of the cutting edge begins on reaching h = 0.7 mm. The flank wear of a rose reamer has little effect upon the taper and out-of-true of the machined holes. The surface finish of the holes is not impaired with increase in wear of the reamer h.

Experiments show that flank wear of the rose reamer rises with an increase in the cutting speed. In the machining of steel tempered to $H_{R_C} = 51$ by rose reamers tipped with T15K6 alloy (geometry of cutting edge of reamers: $\gamma = -15^\circ$, $\alpha = 10^\circ$, $\varphi = 60^\circ$, $\varphi_0 = 15^\circ$), with t = 0.65 mm and s = 0.4 mm/rev, the flank wear after 15 min

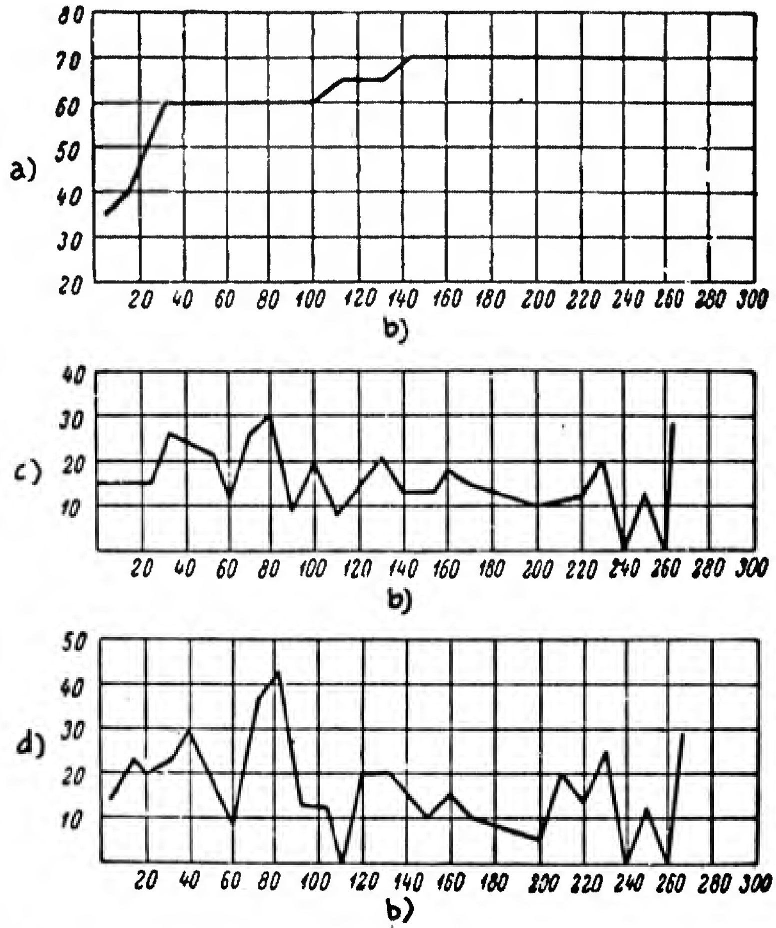

Fig.192 – Relationship of Flank Wear of Rose Reamer, Taper, and Out-of-True of Holes after Rose Reaming, to Duration of Work in the Machining of Steel Tempered to $H_{R_C} = 51$

a) Flank wear of rose reamer h, microns; b) Number of holes machined; c) Taper of holes after rose-reaming, microns; d) Out-of-true of holes after rose-reaming, microns

of work was h = 0.5 mm at a cutting speed of v = 20.7 m/min, h = 0.8 mm at a speed of v = 41.2 m/min.

In the case of reamers tipped with titanium-tungsten carbides, the dulling criterion employed in the machining of hardened alloy steels is h = 0.7 mm. Visible evidence of the dulling of a tool on rose-reaming, as in turning and flute-reaming, is offered by the fact that the removed chip takes on a goffered appearance.

An equation is presented for determining the cutting speeds in the rose-reaming of holes in alloy steel parts tempered to H_{RC} = 38 - 51:

$$v = \frac{C_v \cdot D^{0.6}}{T^{0.45} \cdot t^{0.3} \cdot s^{0.6}} \, m/min, \qquad (21)$$

where D is the diameter of the rose reamer, in mm;

T is the life of the reamer, in min;

t is the depth of cut, in mm;

s is the feed, in mm/rev;

C_v is a constant.

The following are the values adopted for C_v:

H_{RC} hardness of steel	Value of C_v
51	10
45	15.5
38	23

CHAPTER VIII

THREADING HARDENED STEELS

This Chapter gives results of an investigation conducted by the author into the process of threading our steel C tempered to $H_{R_C} = 65$. This investigation was started because of difficulties encountered in a machine-building plant in the course of

Fig.193 - Portion of Billet of C Steel, $H_{R_C} = 65$, With Thread

mastering this process. Under industrial conditions, thread cutting was characterized by the following data:

1) Work material steel tempered to $H_{R_C} = 60$;

2) External Whitworth thread, 8 threads per inch, root radially rounded at bottom, length of thread l = 20 mm;

3) Equipment - DIP-200 thread-cutting machine;

4) Cutting tool - single-point tool tipped with VK8 carbide, with no lapping

of cutting end, and rake angle of $\gamma = 0^{\circ}$. Setting of the tip below the lathe center line gave the cutter a rake angle of $\gamma = -5^{\circ}$ during the cutting process;

5) Cutting conditions: cutting speed v = 8 m/min, number of passes for threading a single part i = 30 - 35. Tool life T = 2 min. For threading a single part (l = 20 mm), 7 - 8 cutters (reamers).

The investigation was performed under laboratory conditions, with a specially

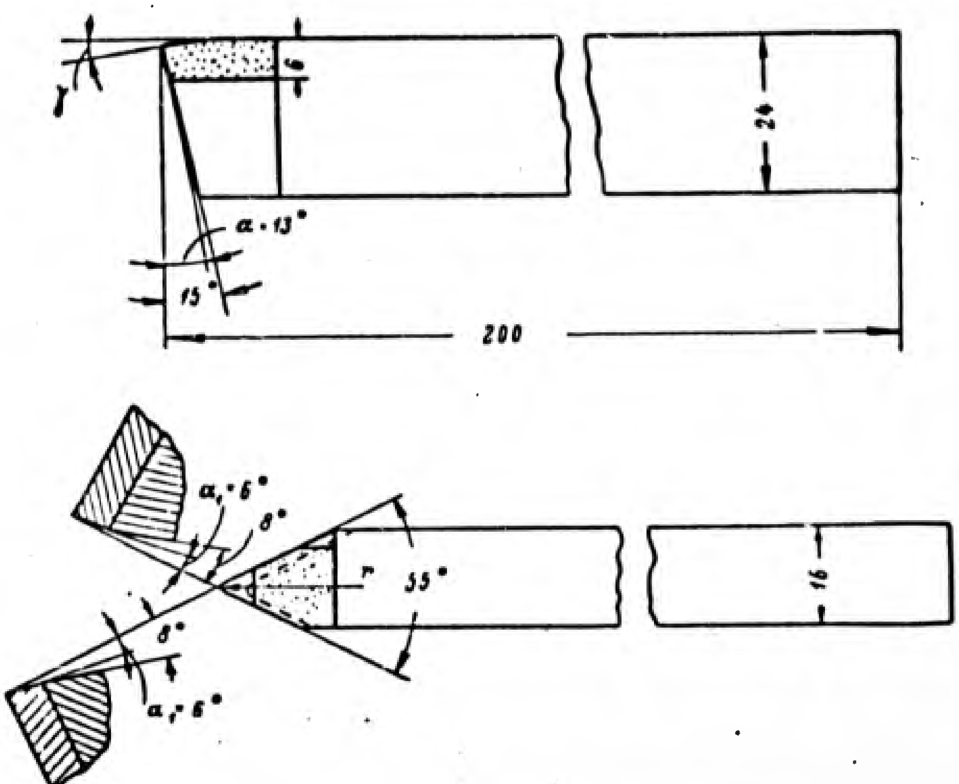

Fig.194 - Single-Point Thread Cutting Tool

prepared steel billet, L = 1150 mm, diameter D = 200 mm. The steel was tempered to H_{R_C} = 65.

Hardness testing was with a Rockwell tester, using a disk of 55 mm thickness cut from the billet. The hardness was determined at four points, at the following distances from the center of the disk: 30, 44, 79, and 88 mm (disk diameter D = = 198 mm). Hardness at all points was H_{R_C} = 65.

Subsequently, the hardness of the material was determined on the billet itself. This demonstrated deep penetration of hardness.

Three threads were studied: 12, 8, and 6 threads per inch, respectively. Rings of 20 and 40 mm were formed along the length of the billet. Grooves for the cutting tool to slide across were provided between each two rings. Figure 193 shows a portion of the threaded billet.

The cutting tool employed was a bar-type single-point tool (Fig.194), tipped with VK-8, T15K6, and T21K8 carbides. Most of the experiments were run on a DIP-300 lathe, and the others on a DIP-400 lathe.

The process is doubtless one of the most difficult in the machining of metals. The very high hardness of the material being machined, which approaches that of the cutting tool, is combined with large feed (over 4 mm when cutting 6 threads per inch) and a small tip radius, although this is the most critical part of the cutting edge of carbide-tipped tools. The cutter operates under "constrained" conditions, in which the entire profile of the cutting edge of the tool participates (in the finishing passes).

The results obtained in the investigation have demonstrated the possibility of significantly increasing the productivity of the process over that achieved in industrial practice.

33. Cutter Dulling Criteria

Flank wear and change in chip appearance may be taken as criteria of cutter dulling.

Flank Wear. This process is characterized by the fact that the major wear occurs on the curved portion of the cutter flank. This is clearly evident in finishing cutters, whose full profiles participate in the operation.

The operation of roughing cutters is such that their right-hand cutting edges hardly participate in the cutting process, so that they undergo flank wear similar in nature to that experienced by turning tools.

The permissible level of cutter wear depends upon the carbide with which it is

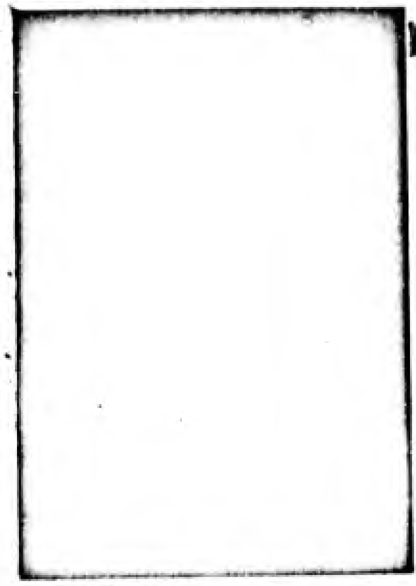

GRAPHIC NOT REPRODUCIBLE

Fig.195 - T21K8 Cutter Used until Normal Dulling. Geometry: $\alpha = 13^\circ$, $\alpha_1 = 6^\circ$, $\gamma = 0^\circ$, $\lambda = 0^\circ$, $r = 0.4$ mm.

tipped. The alloy VK8, being more ductile, will take considerably more wear than the alloys T21K8 and T15K6 before the danger of crumbling-out of the cutting edges of the tool arises.

Figure 195 shows a T21K8 cutter used to the stage of normal dulling. The cutter

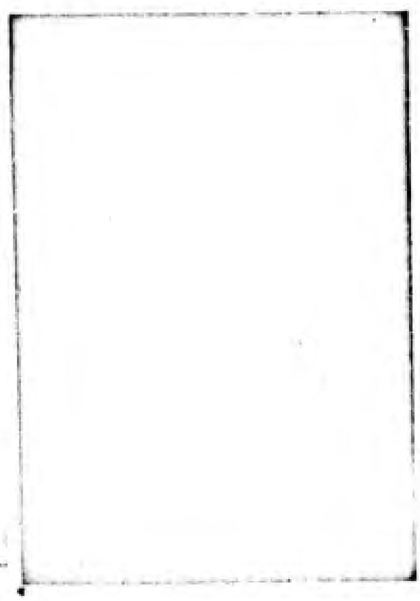

Fig.196 - T15K6 Cutter Used until Normal Dulling. Geometry: $\alpha = 13^\circ$, $\alpha_1 = 6^\circ$, $\gamma = -5^\circ$, $\lambda = 0^\circ$, $r = 0.4$ mm

would have crumbled out if it had not been taken out of operation. The wear along the curved portion of the flank had attained h = 0.27 mm. The wear of a VK8 cutter having the same geometry and used to normal dulling, was h = 0.5 mm. Both cutters were engaged along their full profiles.

In the case of the T15K6 cutter used to normal dulling (Fig.196), a wear of h = 0.52 mm resulted in no trace of crumbling-out. This substantial superiority of the life of T15K6 alloy over T21K8 alloy is due to the fact that the T15K6 cutter had a negative rake ($\gamma = -5^{\circ}$).

Change in Appearance of Chip. The appearance of the chip changes as the cutter gets duller. At the start of the cutting process, when the tool has as yet undergone little dulling, elementary chip comes off smoothly in the form of a spiral ribbon with an absolutely smooth outer surface - that being the surface of contact with the face. As the cutter becomes duller, the chip loses its spiral shape, and its external surface acquires a characteristic goffered appearance.

Figure 197 illustrates several chips produced at various stages in the dulling of a T15K6 roughing cutter. This cutter was used for T = 6.6 min before becoming completely dulled. The upper chip represents a life of T = 1.6 min, the second from the top of T = 4.4 min, and the bottom one of T = 6.2 min. Figure 198 illustrates a number of identical chips obtained in the final stage of dulling of a finishing cutter having the same geometry as the preceding example. This cutter, unlike the roughing cutter, worked over its entire profile and removed a chip of triangular cross section.

The following conclusions may be drawn from these experiments.

In the cutting of threads on hardened steels, the flank wear and change in the appearance of the chip may serve as the dulling criterion.

A change in the appearance of the chip - acquisition of a goffered appearance - is the most obvious criterion of cutter dulling, useful for application under industrial conditions.

Fig.197 - Effect of Stage of Cutter Dulling upon Chip Appearance ($\alpha = 13^\circ$, $\alpha_1 = 6^\circ$, $\gamma = 0^\circ$, $\lambda = 0^\circ$, r = 0.4 mm). The upper chip was produced at the start of operation of the cutter; the lower, at normal dulling

Fig.198 - Chip Resulting From Use of Finishing Cutter Along its Full Profile ($\alpha = 13^\circ$, $\alpha_1 = 6^\circ$, $\gamma = 0^\circ$, $\lambda = 0^\circ$, r = 0.4 mm)

In his investigation, the author employed both criteria jointly: the appearance of the chip being used for general purposes, and flank wear being used for control purposes.

Normal flank wear was taken to be as follows:

1) For roughing cutters, h = 0.3 to 0.5 mm (lower values for the cutters T15K6 and T21K8 and higher values for the cutters VK8);

2) For finishing cutters, h = 0.2 mm.

34. Determination of Optimum Number of Passes

The experiments to determine the number of passes were complex. The problem to be solved was that of producing a completely finished thread at the smallest number of passes, under simultaneous study of the influence of a number of factors upon the cutter life and upon the cutting process as a whole.

Let us agree to use the term cross feed s_1 to describe the depth of cut per pass in thread cutting on thread-cutting lathes. Various methods may be used to make the plunge cut (Fig.199).

When making a plunge cut in a direction normal to the axis of the part being cut (Fig.199a), the cutter is in the least favorable state since its entire profile participates in making the cut. This method has to be used in the final passes, in finishing the cut.

Figure 199b shows a method of plunging the cutter in which its right cutting edge is almost entirely non-participating. This is accomplished as follows: Having been given the required displacement in a direction normal to the axis of the part, the cutter is also edged leftward toward the headstock of the lathe.

Figure 199c illustrates the method of plunging the cutter at an angle. To accomplish this, the top slide of the carriage has to be turned through a 30° angle in the cutting of metric thread and through 27°30' in cutting Whitworth thread. When this method is employed, the right-hand cutting edge of the cutter is also eliminated from participation. The latter two methods are applicable only to rough threading cuts.

All three methods were employed in our investigation. The final finishing of

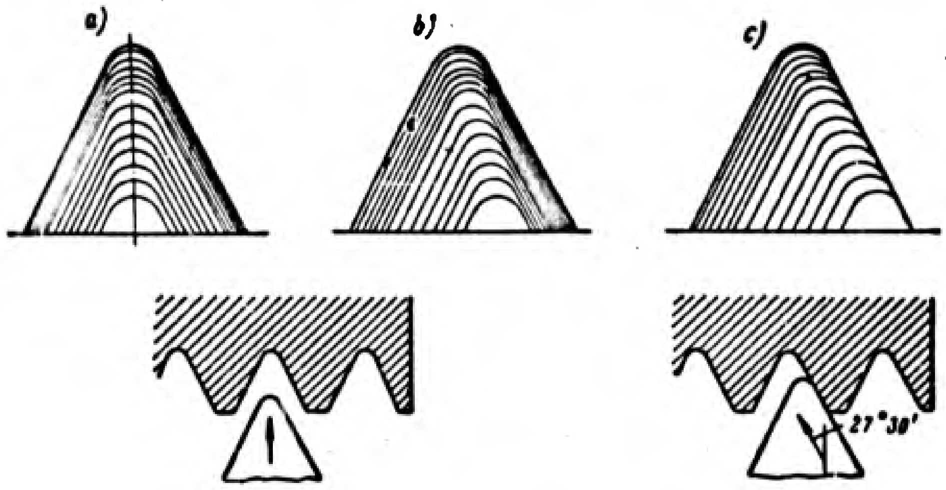

Fig.199 - Various Methods of Cross Feed (for Depth of Cut) in Thread Cutting

the thread was by the first method (Fig.199a); and the second and third methods were used in rough cutting (Figs.199, b and c).

Below we present the results of the tests made. Except for the tip radius r, the cutters were identical in geometry: $\alpha = 13^o$, $\alpha_1 = 6^o$, $\gamma = 0^o$, $\lambda = 0^o$.

Experiments in cutting thread with 8 thr/in were run on a length of $l = 20$ mm, and a cutting speed of v = 8.5 m/min. Roughing cutters had a tip radius of r = 0.6 mm, and the finishing cutters had r = 0.4 mm. The hard alloys VK8, T15K6, and T21K8 were employed. The second method was used in roughing cuts, and the first in finishing cuts.

The thread was finished on nine rings. This required 18 grindings of the cutters, or an average of two cutters (one roughing and one finishing) per ring. The total number of passes required to cut the nine rings was: a) 151 roughing passes for $s_1 = 0.10$ mm; b) 59 finishing passes for $s_1 = 0.10$ mm. Consequently, each ring was threaded on an average of seventeen roughing and seven finishing passes. The average life of the roughing cutter was T = 6.3 min, and that of the finishing cutter was T = 3.1 min.

The shorter life of the finishing cutters is due to the fact that their smaller radius r and due to their severe operating conditions (the entire cutter face participates in the cutting).

Experimental data illustrate the nature of the effect of the cross feed s_1 and the grade of carbide upon the life of the cutter. Whereas, at s_1 = 0.10 mm, the mean life of a VK8 roughing cutter (r = 0.6 mm) is 6.3 min, it will be only 1.5 min at s_1 = 0.15 mm, although cutters with s_1 = 0.15 mm underwent extreme dulling and crumbled out at their tips. Due to its high brittleness, the alloy T21K8 had a very short life.

Experiments in cutting 12 tpi thread were conducted over a length of l = 20 mm at v = 8.5 m/min. For the roughing cutters, the value was r = 0.4 and 0.6 mm and for finishing cutters, r = 0.3 mm. The cutter was plunged in the manner indicated in Fig.199b, except for two rings on which the plunging of roughing cutters was performed by the third method (Fig.199c). The thread was completely finished on eleven rings, and 31 cutters were required to accomplish this, of which 18 were for rough cuts and 13 were for finish cuts.

Each ring requires an average of three cutters, of which about 50% are roughers. The cutting of one belt required an average of 22 passes, of which 9 were roughing passes and 13 were finishing passes. The life of a single cutter was T = 5.1 min for a rougher, and T = 5.0 min for a finisher, on the average.

Thus, in our experiments, finishing cutters had the same life as roughing cutters (T = 5 min). However, roughing cutters operated at s_1 = 0.10 mm, and finishing cutters at s_1 = 0.05 mm. At an identical value s_1 the life of roughing cutters would be higher than that of finishers because of the fact that the tip radius of the roughing cutters is higher than that of the finishing cutters. It is important to note that the life of roughing cutters, in cutting 12 tpi thread, is lower than that of the same cutters in cutting 8 tpi thread. At identical feeds of $s_1 = 0.10$ mm, the mean life of a cutter in cutting 12 tpi thread (s = 2.12 mm) is T = 5.1 min, whereas it is T = 6.3 min in 8 tpi thread (s = 3.17 mm).

The apparent contradiction (since the cutter life should really rise with a reduction in pitch) can be attributed to the strong influence of the radius r on the life. A reduction in the radius r from 0.6 mm (roughing cutters for 8 tpi) to 0.4 mm (roughing cutters for 12 tpi) led to a reduction in the cutter life, despite the fact that the pitch diminished from 3.17 to 2.12 mm.

Experimental data reveal the T15K6 and VK8 cutters to have virtually identical life. At r = 0.6 mm and $s_1 = 0.10$ mm, the life of VK8 cutters on four rings was T = 5.3 and 6.0 min, and that of the T15K6 cutter was T = 6.6 min.

The two methods of cutting (Fig.199b and 199c) revealed virtually identical results. When the cutting was done in accordance with Fig.199b, the VK8 cutters (r = 0.4 mm and $s_1 = 0.10$ mm) had a life of T = 4, 7.9 and 7.3 min (three rings) when cut in accordance with Fig.199b, whereas the life of the VK8 cutter, when the cutting was done in accordance with Fig.199c, was T = 6 min.

Experiments in cutting 6 tpi thread were conducted over a length of l = 40 mm, at v = 7 m/min. A portion of the experiments were run with roughing cutters at r = 0.8 mm. In the other experiments, the cutters were of r = 0.6 mm. The roughing cutters were plunged by two methods. The thread was cut completely on seven rings.

Six rings were cut completely, for which seventeen roughing and eight finishing tools were required. Consequently, an average of two roughing and one finishing cutter, in 22 roughing and 16 finishing passes, were required to thread a single band (l = 40 mm). The life of a single cutter constituted on the average T = 6.3 min for a rougher, and T = 9.3 min for a finishing tool.

The average for the life of finishing cutters reflected the fact that the final passes on two bands were run at $s_1 = 0.05$ mm (all the other passes, both roughing and finishing were run at $s_1 = 0.10$ mm). Thus, as distinct from the results with 8 and

12 tpi threads, the finishing cutters were not inferior to roughing cutters in life when 6 tpi were cut. This is explained by the fact that the finishing cutters had the same large radius (r = 0.6 mm).

The life of the cutters proved to be higher for 6 tpi than for 8 and 12 tpi, due to the fact that 6 tpi thread was cut at v = 7 m/min, while the 8 and 12 tpi threads were cut at v = 8.5 m/min. This confirms the previous conclusion with respect to the approximately equal cutting capacity of the hard alloys VK8 and T15K6.

Table 80 contains systematized data on the number of passes required for complete cutting of 12, 8, and 6 tpi thread on twenty-six bands. As we see, the cutting of a single band required an average of 22 passes for 12 tpi, 24 for 8 tpi, and 38 for 6 tpi.

Due to the bounce caused by the radial force P_y, the actual depth to which the tool penetrates is less than the depth for which it is set at the start of the pass. Table 81 illustrates the degree of cutter bounce for twenty-seven bands. "Actual tool penetration" (column 9) was determined by direct measurement of the outside and inside diameters of the thread. "Total bounce" (column 10) was obtained by subtracting "actual tool penetration" from "nominal penetration" (column 8), which is the product of the actual number of passes by the nominal (rated) cross feed of the cutter (per pass). The average data on cutter bounce do not include bands 51 and 52, since they are not indicative.

Obviously, the cutter bounce is extensive and increases markedly with an increase in pitch. Due to the cutter bounce, the actual number of passes in cutting 6 tpi thread proved to be 35% larger than the number indicated by the depth of cut and the given cross feed of the cutter. Cutter bounce may be reduced by reducing the tip radius of the cutter r, but this shortens the life of the tool.

The experimental data were derived with a DIP-300 lathe, whose carriage is quite rigid. The author believes that, in determining the number of passes, it is necessary to begin with the average cutter bounce values (Table 81) except for 6 tpi

Table 80

Actual Number of Passes in Cutting 12, 8, and 6 tpi Thread

Thread	Thread length, in mm	Band No.	Actual Cutting Depth in mm	Actual number of passes: In rough cutting: Cutter r, in mm	In rough cutting: s_1, mm	In rough cutting: i	In finish cutting: Cutter r, in mm	In finish cutting: s_1, mm	In finish cutting: i	Total, i
12 tpi $s = 2{,}12$ mm	20	51	1,22	0,6	0,10	10	0,3	0,05	12	27
				0,4	0,10	5				
		52		0,4	0,10	14	0,3	0,05	10	24
		53		0,6	0,10	8	0,3	0,05	9	20
				0,4	0,10	3				
		54		0,44	0,10	11	0,3	0,05	9	20
		56		0,4	0,10	11	0,3	0,05	8	19
		57		0,6	0,10	9	0,3	0,05	9	18
		58		0,6	0,10	9	0,3	0,05	8	17
		59		0,6	0,10	9	0,3	0,05	9	18
		77		0,4	0,10	3	0,3	0,05	22	25
		78		0,4	0,10	3	0,3	0,05	22	25
		79		0,4	0,10	3	0,3	0,05	22	25
	Mean data (per band)			0,4 and 0,6	0,10	9	0,3	0,05	13	22
8 tpi $s = 3{,}17$ mm	20	30	1,90	0,6	0,10	19	0,4	0,10	5	24
		31		0,6	0,10	19	0,4	0,10	5	24
		32		0,6	0,10	17	0,4	0,10	7	24
		33		0,6	0,10	15	0,4	0,10	7	22
		34		0,6	0,10	15	0,4	0,10	6	21
		35		0,6	0,10	16	0,4	0,10	9	25
		36		0,6	0,10	17	0,4	0,10	7	24
		38		0,6	0,10	17	0,4	0,10	8	25
		45		0,6	0,10	16	0,4	0,10	8	24
	Mean data (per band)			0,6	0,10	17	0,4	0,10	7	24
6 tpi $s = 4{,}23$ mm	40	65	2,58	0,8	0,10	16	0,6	0,10	21	37
		66		0,8	0,10	27	0,6	0,10	15	46
							0,6	0,05	4	
		67		0,6	0,10	17	0,6	0,10	15	29
		68		0,6	0,10	33	0,6	0,10	15	48
							0,6	0,10	10	
		69		0,6	0,10	22				37
							0,6	0,05	5	
							0,6	0,10	7	
		70		0,6	0,10	20				32
							0,6	0,05	5	
	Mean data (per band)			0,6 and 0,8	0,10	22	0,6	0,05 and 0,10	16	38

Table 81

Bounce of the Cutter Due to the Influence of the Radial Force P_y

Band No.	Thread	Actual Number of Passes i			Nominal cutter penetration, in mm			Actual cutter penetration, in mm	Total cutter bounce, in mm	Ratio of total cutter bounce to nominal penetration, in %
		at s_1 = 0.10 mm	at s_1 = 0.05 mm	Total	at s_1 = 0.10 mm	at s_1 = 0.05 mm	Total			
51	12 tpi	15	12	27	1,5	0,60	2,10	1,22	0,88	42
52		14	10	24	1,4	0,50	1,90		0,68	36
53		11	9	20	1,1	0,45	1,55		0,33	21
54		11	9	20	1,1	0,45	1,55		0,33	21
56		11	8	19	1,1	0,40	1,50		0,28	19
57		9	9	18	0,9	0,45	1,35		0,13	10
58		9	8	17	0,9	0,40	1,30		0,08	6
59		9	9	18	0,9	0,45	1,35		0,13	10
77		3	22	25	0,3	1,10	1,40		0,18	13
78		3	22	25	0,3	1,10	1,40		0,18	13
79		3	22	25	0,3	1,10	1,40		0,18	13
	Mean data (per band)						1,42		0,20	14
30	8 tpi	24	—	24	2,4	—	2,40	1,90	0,50	21
31		24	—	24	2,4	—	2,40		0,50	21
32		24	—	24	2,4	—	2,40		0,50	21
33		22	—	22	2,2	—	2,20		0,30	14
34		21	—	21	2,1	—	2,10		0,20	10
35		25	—	25	2,5	—	2,50		0,60	24
36		24	—	24	2,4	—	2,40		0,50	21
38		25	—	25	2,5	—	2,50		0,60	24
45		24	—	24	2,4	—	2,40		0,50	21
	Mean data (per band)						2,37		0,47	20
64	6 tpi	44	5	49	4,4	0,25	4,65	2,58	2,07	45
65		37	—	37	3,7	—	3,70		1,12	30
66		42	4	46	4,2	0,20	4,40		1,82	41
67		29	—	29	2,9	—	2,90		0,32	11
68		48	—	48	4,8	—	4,80		2,22	46
69		42	5	47	4,2	0,25	4,45		1,87	42
70		27	5	32	2,7	0,25	2,95		0,37	12
	Mean data (per band)						3,98		1,40	35

Table 82

Recommended Number of Passes for Cutting 12, 8, and 6 tpi Thread Steel of Hardness $H_{R_C} = 65$.

Thread	Roughing cuts. Tool plunged as per Figs. 199b and c			Finishing cuts. Cutter plunged as per Fig.199a			Total Number of cuts, i
	Cutter r, in mm	s_1, in mm	i	Cutter r, in mm	s_1, in mm	i	
12 tpi	0,4	0,10	10	0,3	0,05	8	18
8 tpi	0,6	0,10	19	0,4	0,05	10	29
6 tpi	0,6	0,10	26	0,6	0,10	6	40
				0,6	0,05	8	

thread, for which the bounce may be taken as 1.0 mm. Table 82 presents the number of passes recommended for the threads studied.

Conclusions

1. The cutting of threads into hardened steels requires a large number of passes, increasing in proportion to the increase in pitch. The need for a large number of passes is due to the high hardness of the material machined, the brittleness of the carbides, and the considerable bounce of the tool. The latter is due to the high absolute and relative values of the radial force P_y.

2. With a reduction in the hardness of the tempered steel, the number of passes required diminishes.

3. The cutting of thread in hardened steels should be done on machine tools with highly rigid carriages.

35. Effect of Cutter Cross Feed Upon Tool Life

The experimental data discussed earlier provide a partial solution to the question of the relation between the cross feed of a cutter s_1 and its life T. To fill out the investigation, special experiments were run to determine the T versus s_1 relation in the rough cutting of 8 tpi thread at l = 20 mm and at a cutting speed of

$v = 8.5$ m/min. The tool was plunged as shown in Fig.199b. The cross feed was varied in the limits of $s_1 = 0.06$ to 0.12 mm. The tools had the following geometry: $\alpha = 13^\circ$, $\alpha_1 = 6^\circ$, $\gamma = 0^\circ$, $\lambda = 0^\circ$, and $r = 0.6$ mm.

Table 83 presents average values for the cutter life, at various feeds s_1. Obviously, in the cutting of threads into hardened steels, the cross feed exerts a significant influence upon the tool life. At $v = 8.5$ m/min, the relatively acceptable life of $T > 10$ min was achieved at $s_1 = 0.06$ mm. At $s_1 = 0.09 - 0.10$ mm, the life was less than 10 min. With a further rise in s_1, the life drops to a level that is no longer of any practical significance. In this connection, it should be borne in mind that the data for $s_1 = 0.06 - 0.10$ mm pertain to cutters that had undergone normal dulling, while at $s_1 > 0.10$ mm, the cutters underwent greater dulling, accompanied by crumbling-out of the cutting edges.

Table 83

Average Tool Life at Various Cross Feeds s_1

s_1, in mm	Grade of hard alloy	T, in mm
0,06	VK8	13,3
0,09		3,0
0,10		7,0
0,12		2,3
0,15		1,5
0,06	T15K6	13,7
0,10		6,6
0,15		0,9
0,10	T21K8	4,9

The VK8 and T15K6 carbides had approximately identical cutting properties. Due to the elevated brittleness of the alloy, cutters of T21K8 had a considerably shorter life, and the dulling was accompanied by crumbling-out of the cutting edges.

Experiments were made to determine the effect of the feed s_1 upon the tool life in cutting 6 tpi thread on a length of $l = 40$ mm at $v = 7$ m/min. The cutter geometry was the same as in the preceding series of experiments. The cross feed was changed over the range of $s_1 = 0.15$ to 0.20 mm. Table 84 gives data on the mean tool life.

As we see, cross feeds of $s_1 \leq 0.10$ mm are of practical significance in the cutting of 6 tpi thread at a cutting speed of $v = 7$ m/min. The hard alloys VK8 and T15K6 are characterized by identical cutting capacity.

No investigation was made of the effect of the tool-plunging method upon its life. However, the experience obtained in the course of the work and an analysis of experimental data with respect to 12 tpi thread, permit the conclusion that the plunge methods of Figs.199b and c show no superiority over each other. This is logical when taking into consideration the fact that the cutter operates under iden-

Table 84

Average Tool Life at Various Feeds s_1 6 tpi Thread.
Length of Threaded Section l = 40 mm; v = 7 m/min

s_1, in mm	Grade of Hard Alloy	T, in min	s_1, in m	Grade of Hard Alloy	T, in min
0,15	VK8	1,7	0,10	T15K6	6,7
			0,15		2,2
0,20		1,2	0,20		1,3

tical conditions in the two cases and that the right cutting edge virtually does not participate in the cutting.

When the method shown in Fig.199a is employed, the life of the cutter diminishes since it has to work with its entire profile under the severe conditions of "constrained" cutting.

Summary

1. In threading steel tempered to H_{R_C} = 65, the cross feed has a considerable effect upon the tool life.

For 8 and 6 tpi cutters, at a cutting speed v = 8.5 to 7 m/min and a cutter tip radius of r = 0.6 mm, a practically acceptable tool life is achieved at a feed of $s_1 \leq 0.10$ mm.

2. An increase in tool life is achievable when the cutting speed is reduced to $v < 7$ m/min.

3. The hard alloys VK8 and T15K6 have identical cutting capacity.

4. The method of plunging the tool shown in Fig.199a should be employed only in finish-threading during the final finishing of the thread.

36. Effect of Cutter Tip Radius and Cutter Rake Upon Tool Life

Experimental data show that the tip radius of the tool r exerts a significant influence upon its life. The tool life increases with an increase in the radius r. The radius r is the major factor limiting the field of application of the process of thread cutting of hardened steels for 12 tpi, at a pitch of s = 2.12 mm and a root radius of r = 0.3 mm. It is difficult to cut thread into high-hardness tempered steel whose root radius is r < 0.3 mm, when taking the considerable brittleness of modern cemented carbides into consideration.

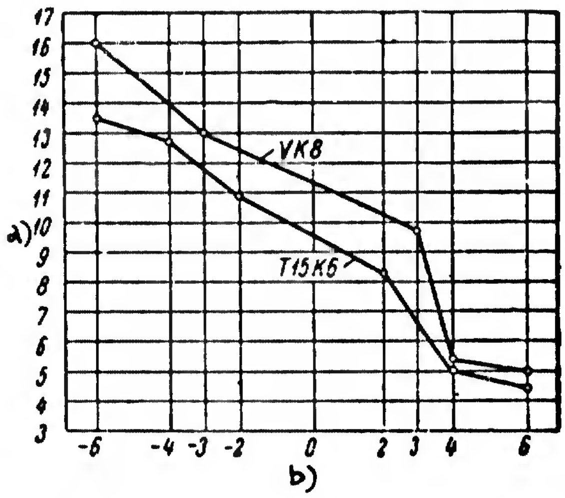

Fig.200 - Effect of Tool Rake γ Upon Life T. Machining of C steel of H_{R_C} = 65 at s_1 = 0.08 mm and v = = 8.5 m/min; 8 tpi thread. Length of threaded section l = 20 mm. Cutter geometry: α = 13°, α_1 = 6°, λ = 0°, r = 0.4 mm

a) Tool life T, min; b) Rake of tool γ°

Finish cutters should have a rake of γ = 0°. If the tool has a rake of more or less than 0°, distortion of the profile of the thread being cut will result. In the case of roughing cutters, which are plunged in the manner indicated in Figs.199b and c, the rake may be negative (γ < 0°). This problem will be discussed below.

Experiments have been made to determine the effect of the tool rake upon the tool life. Thread of 8 tpi was cut by VK8 cutters over a length of l = 40 mm and by T15K6 cutters over a length of l = 20 mm at a cutting speed of v = 8.5 m/min and a cross feed (in accordance with Fig.199c) of s_1 = 0.08 mm. The following was the geometry of the cutters: $\alpha = 13^\circ$, $\alpha_1 = 6^\circ$, $\lambda = 0^\circ$, $r = 0.4$ mm. The rake was varied from +6 to -6°.

Table 85 and Fig.200 present the relation of tool life to rake. The life of VK8 cutters is extrapolated to a thread length of l = 20 mm. Experiments with normal tool dulling are considered.

As we see, tool life diminishes as the rake increases. At high positive

Table 85

Cutter Life Versus Rake Angle γ

VK8 Cutters		T15K6 Cutters	
γ°	T in min.	γ°	T in min.
+6	5,0	+6	4,4
+4	5,4	+4	5,0
+3	9,6	+2	8,4
−3	13,0	−2	10,8
−6	16,0	−4	12,6
		−6	13,5

values γ, dulling of T15K6 cutters is accompanied by crumbling-out at the tip.

With a reduction in the angle γ there is an increase in the radial force P_y, which results in a rise in the tool bounce, making it necessary to increase the number of passes. From this viewpoint, the use of cutters with large negative rakes offers no advantage. The author believes that roughing cutters should be ground to a rake of $\gamma = -3^\circ$.

37. Choice of Hard Alloy

Three hard alloys were tested: tungsten carbide VK8 and titanium-tungsten carbides T15K6 and T21K8. Experimental data show that the hard alloys VK8 and T15K6 are characterized by approximately identical cutting properties. The cutting properties of the alloy T21K8 are lower because of its increased brittleness.

The results obtained differs from results in the turning of hardened steels (Ch.III). There the alloys T15K6 and T21K8 were considerably superior to the alloy VK8. This is explained by the fact that the radius r of the turning tools used was considerably higher than that of the threading tools. The brittleness of titanium-tungsten alloys, and particularly of T21K8 is manifested first in the most critical segment of the cutting portion of the tool, namely, its tip. The VK8 alloy, being the more ductile, is greatly superior to the alloy T21K8.

The merits of the alloy T15K6 include the fact that it yields a surface of higher quality than does the alloy VK8. The present investigation has confirmed that the cemented carbides made in this country make it possible to cut thread of fast pitch into steels hardened virtually to the limit for structural steels.

Alloys VK8 and T15K6 should be employed in cutting 12, 8, and 6 tpi thread into steels tempered to high hardness. The alloy VK8 may be recommended for roughing passes, and the alloy T15K6 for finishing.

38. Effect of Lapping the Cutting Elements on the Tool Life

Figure 201 illustrates the effect of lapping of the threading cutters upon their life. The experiments were made with T21K8 cutters in the finish-threading (as per Fig.199a) of 8 tpi thread over a length of l = 40 mm. The same cutters were tested, with and without lapping of their cutting elements. The experimental data indicates that the lapping of a cutter increases its life. It is of interest that, in cutting thread into hardened steels, lapping had less effect than when these same steels were turned. This can be explained by the fact that, in finish thread cutting, the cutter tip carries a larger load, and the quality lapping of the bit of the thread cutter is not high, since it is done by hand. At the same time, lapping gives evenness and smoothness to the straight cutting edges of a lathe tool as the result of using special jigs for the cutter face and flank.

The effect of lapping is greater in the case of roughing cutters of which only one cutting edge is used, in a manner analogous to the situation with turning tools.

39. Relation of Cutting Speed to Tool Life, Pitch, and Cross Feed

The process under study is characterized by low cutting speed and short cutter

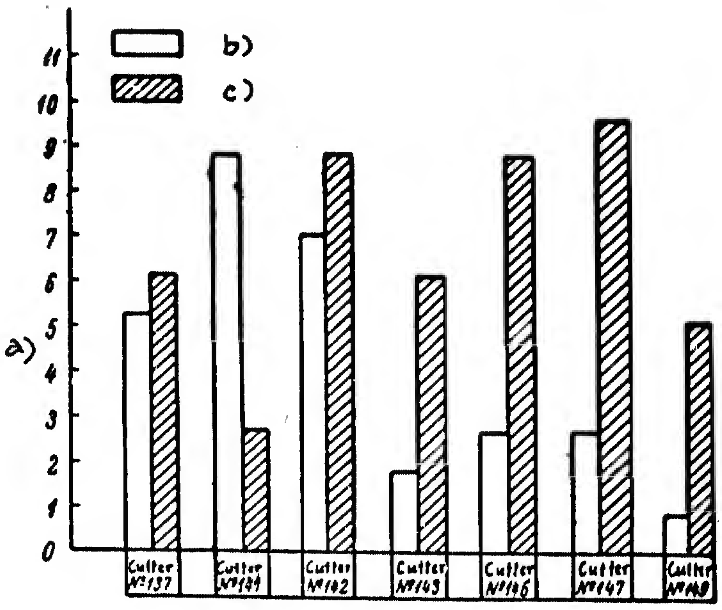

Fig.201 - Effect of Lapping of Cutter upon its Life. Machining of Steel C $H_{R_C} = 65$, at $s_1 = 0.10$ mm and $v = 8.5$ m/min. Length of threaded portion $l = 40$ mm. Geometry of T21K8 cutters: $\alpha = 13^\circ$, $\alpha_1 = 6^\circ$, $\gamma = 0^\circ$, $\lambda = 0^\circ$, $r = 0.4$ mm

a) Tool life T, min; b) Cutters without lapping; c) Cutters with lapping

life. This is due to the high hardness of the material being machined, the large feeds (pitches) and the small tool tip radius. The tool life found in the present study is considerably higher than the results obtained in practical production, as noted at the beginning of this Chapter. Nevertheless, the low tool life made it necessary to investigate the relation between cutting speed and cutter life to determine the conditions for increasing these factors. Table 86 contains the results of the experiments conducted to determine the ratio T - v for various cross feeds s_1.

As we see, the tool life may be increased by reducing the cutting speeds employed in the earlier tests. At increasing cutting speed, the life of the cutter

Table 86

Cutting Speed Versus Tool Life, Pitch and Cross Feed

Band No.	Thread	Thread pitch s, in mm	Cross feed of tool s_1, in mm	Number of passes, in i	Cutting speed v, in m/min	Tool life T, in min
182			0,05	18 16 19	8,5	16 15 17
183			0,05	24 28 27	7,5	24 28 27
184			0,05	44 53 45	6,5	52 62 53
185			0,08	13 13 12	8,5	12 12 11
186	8 tpi	3,17	0,08	18 23 22	7,0	20 25 24
187			0,08	29 32 35	6,5	34 38 41
188			0.10	8 9 8	8,5	7 8 7
189			0;10	15 14 16	7,0	16,5 15,5 17,5
190			0,10	28 26 30	6,0	36 33 38

Table 86 (Cont'd)

Band No.	Thread	Thread pitch s, in mm	Cross feed of tool s_1, in mm	Number of passes, in i	Cutting speed v, in m/min	Tool life T, in min
191			0,10	13 14 11,5	7,0	10 11 9
192	6 tpi	4,23	0,10	20 22 18	6,0	16 17 14
193			0,10	38 41 35,5	5,0	30 32 28
194			0,05	4 2 4	15	2 1 2
195	8 tpi	3,17	0,10	1 2 2	15	0,5 1 1
196			0,05	1 0,5 0,5	23	0,5 0,2 0,2
197	12 tpi	2,12	0,05	— — —	50	0 0 0
198			0,05	— — —	80	0 0 0

*Life stated at zero in cases of instantaneous dulling and crumbling-out of tools.

decreases. At $v = 23$ m/min, a life of no practical significance is achieved even for a 12 tpi thread ($s_1 = 0.05$ mm and $r = 0.6$ mm). Cutting speeds of $v > 23$ m/min result in instantaneous dulling and crumbling-out of the cutters.

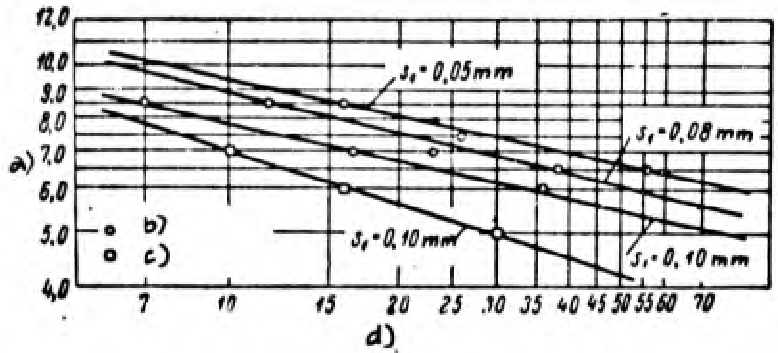

Fig.202 - Cutting speed v Versus Tool Life T for Various Threads s and Cross Feeds (at machining depth) s_1. Machining of steel C tempered to $H_{R_C} = 65$. Geometry of the VK8 tools: $\alpha = 13^\circ$, $\alpha_1 = 6^\circ$, $\gamma = 0^\circ$, $\lambda = 0^\circ$, $r = 0.6$ mm

a) Cutting speed v, m/min; b) Thread of 8 tpi; c) Thread of 6 tpi; d) Tool life T, min

Figure 202 presents the ratio T - v for various values s_1. The three upper curves pertain to 8 tpi thread, and the lower one to 6 tpi. Table 87 presents values for cutting speeds to attain a 30-minute cutter life (v_{30}) and gives the relative life indices m for various values s_1 and s.

Table 87

Values v_{30} and m for Various Values of s_1 and s

Thread	Pitch s, in mm	s_1, in mm	v_{30}, in m/min	m
8 tpi	3,17	0,05	7,4	0,19
		0,08	6,7	0,25
		0,10	6,2	0,21
6 tpi	4,23	0,10	5,0	0,32

The ratio of cutting speed to cutter life is expressed by the equation

$$v = \frac{C}{T^m}.$$

The magnitude of the m index depends upon the pitch. For 8 tpi pitch, the index m = 0.19 - 0.25, and for 6 tpi, m = 0.32.

The data in Table 86 have been employed to plot a curve for the relation between cutting speed v_{30} and cross feed of the cutter s_1 (Fig.203). This relation is expressed by the equation

$$v_{30} = \frac{C}{s_1^{0.25}}.$$

Figure 204 presents the relation between cutting speed v_{30} and pitch s for

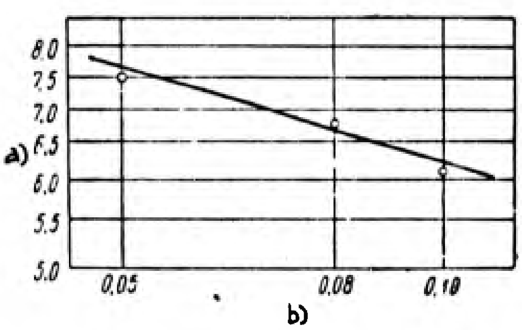

Fig.203 - Cutting Speed v_{30} Versus Tool Cross Feed s_1. Thread of 8 tpi. Machining of steel C tempered to H_{R_C} = 65. Geometry of VK8 cutters: $\alpha = 13°$, $\alpha_1 = 6°$, $\gamma = 0°$, $\lambda = 0°$, r = 0.6 mm

a) Cutting speed v_{30}, m/min; b) Cross feed of cutter s_1, mm

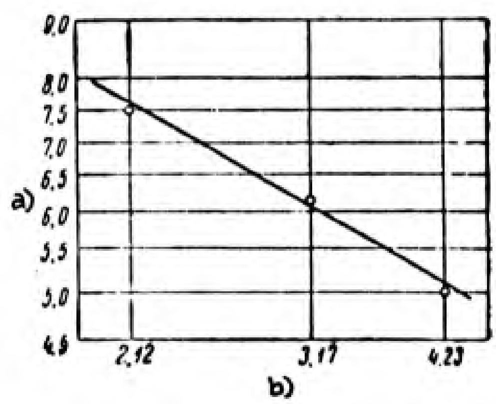

Fig.204 - Cutting Speed v_{30} Versus Thread Pitch s. Machining of steel C tempered to H_{R_C} = 65 at s_1 = 0.10 mm.

Geometry of VK8 cutters: $\alpha = 13°$, $\alpha_1 = 6°$, $\gamma = 0°$, $\lambda = 0°$, r = 0.6 mm

a) Cutting speed v_{30}, m/min; b) Thread pitch s_1, mm

s_1 = 0.10 mm. The values v_{30} for 8 and 6 tpi threads are derived from Table 87, and for 12 tpi from the test data for a cutter presenting a life of 18 min at v = 8.5 m/min. The curve makes it possible to relate v_{30} and s by the equation

$$v_{30} = \frac{C'}{s^{0.6}},$$

The equation relating v_{30}, s, and s_1 has the following form:

$$v_{30} = \frac{C_v}{s^{0.6} \cdot s_1^{0.25}} \ m/min, \qquad (22)$$

where C_v is a constant coefficient equal to 7.0.

It must be borne in mind that eq.(22) is valid only for roughing passes in which the cutter radius is r = 0.6 mm. Moreover, the exponent of s_1 (0.25) was derived for 8 tpi thread. For other threads and other r, the values of the exponents of s and s_1 may be other than this.

Equation (22) has more theoretical than practical significance, if we take into consideration the fact that the range of cutting speeds employed in the given process is quite narrow. This makes it possible to determine certain special features of thread cutting for hardened steels.

Here we adduce the equation, recommended by NIBTN, for the relation of cutting speed to the factors influencing it, for rough cutting of thread on unhardened structural steels (Bibl.66):

$$v = \frac{158\,470 \cdot t^{0,23}}{T^{0,2} \cdot s^{0,3} \cdot \sigma_t^{1,5}}.$$

A comparison of this equation with eq.(22) shows that, in the cutting of thread on hardened steels, the pitch plays a considerably greater role in determining the cutting speed than in cutting thread on unhardened steels. This follows from the fact that, in such steels, the exponent of s is considerably smaller than for hardened C steel.

The result obtained agrees with the author's conclusions with respect to turnings. In the machining of hardened steels, the feed has a more pronounced effect on the cutting speed than in the machining of unhardened steels.

Summary

1. The relation between cutting speed and tool life in the cutting of thread on

hardened steels is subject to the basic law of cutting theory, to the effect that the tool life is reduced as the cutting speed rises.

2. Thread may be cut in steels tempered to $H_{R_C} = 65$ and having a pitch of $s = 2.0$ to 4.0 mm, at low cutting speeds of $v < 10$ m/min. The use of higher cutting speeds leads to a rapid dulling and crumbling-out of the tools.

3. For such threads, the tool life is $T \approx 10$ min at a cross feed of $s_1 \leq 0.10$ mm and at $v = 7.0 - 8.5$ m/min.

An increase in life to $T = 30 - 60$ min is achievable by reducing the cutting speed to $v = 5 - 6$ m/min. Consequently, a 3 to 6-fold increase in the cutter life yields a reduction in the cutting speed and a consequent 20 - 25% increase in machine time.

4. In the cutting of thread on hardened steels, the cutting speed decreases with increasing pitch s and cross feed s_1.

As distinct from unhardened steels, the pitch has a greater influence upon the cutting speed than does the tool cross feed in thread cutting.

40. Summary

1. The material presented in this Chapter expands our knowledge of the cutting capacitites of cemented carbides. The cemented carbides made in our country have such high cutting properties as to make it possible to cut thread of more than 4 mm pitch into steel tempered to virtually the maximum obtainable for structural steels ($H_{R_C} = 65$).

The significance of the results obtained by the author is not diminished by the fact that this process has been very low in rate of output. It must be borne in mind that the productivity of the process will increase in the cutting of thread on steels tempered to a lesser degree of hardness.

2. The brittleness of hard alloys, which limits the possibilities for full utilization of their excellent cutting properties, is at the same time a factor

limiting the range of applicability of the process of thread-cutting in hardened steels. The minimum limit is a thread of $s = 2$ mm pitch. The present study has demonstrated in practice the possibility of cutting thread of $s = 4$ mm pitch into steel of $H_{R_C} = 65$. To determine the maximum limit of applicability of the process it is necessary to investigate thread of $s > 4$ mm pitch. It is obvious that the cutting of such thread will require cutting speeds of $v < 5$ m/min.

3. In Appendix VI we adduce the cutting conditions developed by the author for cutting 12, 8, and 6 tpi thread in steel tempered to $H_{R_C} = 35 - 65$.

4. A comparison of the results obtained by the author with the industrial data given at the beginning of this Chapter shows that the latter are sharply understated. It should be noted that the factory data pertain to steels tempered to a lower degree of hardness ($H_{R_C} = 60$).

Actually, under plant conditions, an average of 30 - 35 passes and 7 - 8 tools was required for the complete job of threading 8 tpi thread of $l = 20$ mm at a cutting speed of $v = 8$ m/min. The cutting conditions recommended by the author, and based on experimental data, specify the use of 24 passes and only two tools for this operation.

The fact that industrial tools have such a short service life can be explained chiefly by their poor grinding and the failure to lap the cutting elements. Tools must be lapped, and properly ground, if the process of thread cutting of hardened steels is to be performed properly.

CHAPTER IX

DISCUSSION OF PHYSICAL PHENOMENA IN THE MACHINING OF HARDENED STEELS

This Chapter presents some generalizing conclusions and ideas pertaining to the question of the physical principles of high-speed metal cutting, derived from an analysis of the process of machining hardened steels.

41. High-Speed Cutting of Hardened Steels

At present, the cutting speeds attained in the turning of steels by HSS cutters usually do not exceed 80 m/min, whereas carbide cutters permit cutting speeds of up to 300 - 400 m/min. Skilled workers are cutting at even higher speeds.

The machining of metals by carbide-tipped tools has come to be called "fast machining of metals".

The cutting speeds achieved in the experiments of the author and other investigators are lower than those employed in the fast machining of ordinary (unhardened) steels. However, if one consider the difference in hardness between hardened and ordinary steels, and the pronounced effect of the hardness of steel upon the permissible cutting speed, it becomes obvious that it was high-speed machining that actually took place in the experiments with hardened steels.

Let us present a validation of this proposition. It is obvious from the cutting conditions developed by the author (Appendix I) that the cutting speed of T15K6 cutters for steel A tempered to $H_{R_C} = 41$, at a depth of cut of $t = 1.0$ mm and a feed of $s = 0.2$ mm/rev, was $v_{60} = 82$ m/min.

Steel A (OKhN3M), which had been subjected to ordinary heat treatment (oil hardening at 840 - 860°C, followed by quenching at 580 - 600°C) acquires a hardness of H_{R_C} = 28 (H_B = 277). Consequently, the hardness of steel A in the tempered state exceeds the hardness of the same steel in the ordinary condition, by 13 Rockwell scale C units. It will be seen from Fig.77 that an increase in the hardness of tempered steel by 13 units in the interval from H_{R_C} = 41 to H_{R_C} = 54, will cause the $C_{v_{60}}$ constant to diminish from 50 to 22, i.e., by a factor of 2.27.

When using the same ratio for the hardness interval of interest to us, we will find that, when steel A is machined in the unhardened condition (at H_{R_C} = 28) and at the same t and s, it is possible to increase the cutting speed by a factor of 2.27 and to bring it to v_{60} = 82 × 2.27 = 186 m/min, corresponding to high-speed machining. In fact, under the conditions of high-speed cutting of nonferrous metals (Bibl.27), the v_{90} cutting speed is 197 m/min for alloy steels of σ_t = 85 kg/mm² at a cutting speed of t = 1.0 mm and a feed of s = 0.2 mm/rev. Let us introduce corrective factors for the shorter life (T = 60 min) K_T = 1.08, and for higher hardness (H_{R_C} = 28; σ_t = 100 kg/mm²) K_H = 0.87. In this situation, the cutting speed sought will be v_{60} = 197 × 1.08 × 0.87 = 185 m/min.

These considerations make it possible to state that, in the experiments with hardened steels performed in our country long prior to World War II, in which carbide cutters of negative rake were used, speeds corresponding to those of high-speed cutting were employed.

42. Surface Finish in the Machining of Hardened Steels

Let us first present the generalized data of scientific investigations (Bibl.47) which will offer an idea of the influence of surface finish upon the service characteristics of machine parts, determining their resistance to wear and fatigue strength.

The concept "surface finish" includes the geometric characteristics of the machined surface and the physical and mechanical properties of the surface layer of metal. In the cutting process, the surface layer undergoes extensive plastic deformations. Therefore, the properties of the metal of the surface layer differ significantly from the initial properties of the material machined. The metal in the surface layer increases in mechanical strength (becomes work-hardened); its hardness rises, and internal stresses develop.

Effect of Surface Finish Upon the Resistance of Machine Parts to Wear

Influence of Surface Microgeometry. Research has established that the microgeometry of machine parts exerts a significant influence upon the resistance to wear. If a pair of rubbing surfaces is to function successfully and for a long time, the contact areas should have microscopic roughnesses of a given optimum height. An increase or decrease in the height of the microscopic roughnesses, relative to the optimum value, will result in a reduction of wear resistance and in accelerated wear of the rubbing parts. The increase in wear is due primarily to the rapid abrasion, warping, and shear of excessively large microroughnesses, and secondly to leakage of lubricant as well to molecular adhesion and seizing of rubbing surfaces whose finish is excessively fine.

Influence of Work-Hardening of Metal. The work-hardening of a surface layer may significantly reduce the wear of rubbing parts. There are various hypotheses as to the influence of work-hardening upon the process of wear. However, the opinion of all investigators agrees in rating the wear due to seizing as the most intensive and dangerous form of wear, completely impermissible in normally operating machines. It may be hypothesized that pre-hardening of the metal in the surface layers of mating parts, which reduces their ductility, significantly reduces the amount of plastic deformation suffered by both rubbing surfaces, and prevents or reduces the seizing of metals.

Experiments on dry friction between steel specimens and a hardened disk of U8 steel demonstrated that, in all cases, the wear of specimens which were given preliminary work-hardening in the process of machining the samples will be much lower than the wear of specimens which have the same microroughnesses but, were preannealed in vacuum to remove work-hardening, prior to subjection to wear.

In addition to the existence of an optimum microgeometry of rubbing surfaces, there is an optimum microhardness of the surface layers of the rubbing parts. If a microhardness, optimum for the given conditions of friction, is created in the surface layers of the parts, the wear will reach a minimum and the microhardness of the surface layer of the rubbing parts will not change during the process of wear.

In the case in which the microhardness of the surface layer, after manufacture of the parts, is less than the optimum microhardness, intensified wear will occur during the run-in period, and this will continue until the plastic deformation of the surface layer raises its microhardness to the optimum level.

If, after manufacture of the parts, the microhardness of the surface layer is higher than optimum, normal wear of the surface layer will gradually eliminate the layers of elevated microhardness, subsequent to which optimum microhardness will set in, in the layers actively involved in friction.

It has been experimentally determined (Bibl.70) that the resistance of parts to wear is not dependent upon residual stresses in the surface layer of the metal.

Effect of Surface Finish upon Fatigue Strength of Machine Parts

Failure of machine parts due to metal fatigue starts at certain points on their surfaces. Therefore, the fatigue strength of machine parts is largely determined by the microgeometry of their surfaces and the physical conditions of the surface layer.

Influence of Surface Microgeometry. The presence, on the surface of parts operating under cyclic loads that change in sign, of various defects and microscopic roughnesses will lead to a concentration of stresses, whose magnitude may exceed the fatigue strength of the metal. In this case, the surface defects and machining cracks serve as nuclei for the development of submicroscopic discontinuities of the metal in the surface layer and for the development of crazings which, in turn, form starting points for fatigue cracks.

An increase in the height of microscopic roughnesses on the surfaces of parts subject to cyclic loadings is accompanied by a pronounced reduction in fatigue strength. Conversely, a decrease in the height of these microscopic roughnesses results in an increase in fatigue strength.

It follows from Table 88 that, on moving from polished to rough-turned finishes, there is a reduction by 10 - 20% in the fatigue strength of a given part, the reduction being 30% in the case of high-strength steel.

Table 88

Effect of Surface Finish of Steel Specimens Upon Ultimate Bending Strength

Type of Surface Machining	Tensile strength, σ_t, in kg/mm^2		
	47	95	142
	Endurance limit, %		
Fine-polishing	100	100	100
Rough-polishing	95	93	90
Finish-polishing and finish-turning	93	90	88
Rough-grinding or rough-turning	90	80	70

With an increase in the strength of the steel, a sharp increase occurs in the influence of the height of microroughnesses upon the fatigue strength. Not infrequently this effect may be greater than the positive effect upon fatigue strength of the increasing strength of the steel.

The service life of parts working under shock loadings is as highly dependent upon surface microroughnesses as is the service life of parts subject to loadings which change in sign. For example, a reduction from 8 to 5.7 microns in the height of the roughnesses in a steel part subjected to shock loading raised its service life by 60%.

The fatigue strength of hardened machine parts, in the case of contact loadings, depends upon the surface finish to the same degree as it does in shock loading. Under these conditions, microscopic roughnesses on working surfaces result in considerable contact stresses, tending to reduce the service life of the parts.

Effect of Work-Hardening of Surface Layer. Work-hardening of metal increases the fatigue strength of machine parts. Moreover, the creation, in the surface layer of the part, of a work-hardened crust inhibits the growth of existing, and the development of new, fatigue cracks. Experiments have shown that cyclic loading of parts with a work-hardened crust, by stresses exceeding the fatigue limit will result in the formation of fatigue cracks not on the surface of the part but deep within the surface layer, beneath the work-hardened crust. The nucleation and development of fatigue cracks underneath the strengthened layer occurs at higher stresses and at a larger number of cyclic loadings than in the case of no work-hardening.

Effect of Residual Stresses. The investigations by I.V.Kudryavtsev permit the following conclusions:

1. Residual stresses, set up in machine parts, affect the fatigue strength only when the metal of the part differs in tensile and compressive strength;

2. Residual tensile stresses reduce the fatigue strength less than compressive stresses of the same magnitude increase these stresses.

According to data by S.V.Serensen, the increase in fatigue strength due to compression is 50% higher, and reduction in the same factor when due to tension, is 30% lower, in the case of steels of elevated hardness.

3. Residual stresses have a greater effect upon changes in endurance limit in flexure, tension, and compression, and less in torsion;

4. The degree to which residual stresses influence the endurance limit depends not only upon the value and sign of the residual stresses but also upon their nature. The maximum influence upon the endurance limit is that due to three-dimensional

residual stresses, while the minimum is due to linear residual stresses.

It has been experimentally determined that the positive influence of compressive surface stresses is manifested particularly sharply when the surface of the part is grooved, has deep machining scratches, or other stress concentrations. The fatigue strength of parts is noticeably reduced upon the development of residual tensile stresses in the surface layer.

Higher surface finish specifications for critical machine parts have resulted in the development of special methods in work-hardening engineering: ball or bar burnishing, shot blasting, coatings of various types, etc.

However, the objectives pursued by hardening procedures are attainable by making use of the possibilities of cemented carbide (and mineroceramics) in the machining of hardened steels.

The experimental data presented in Section 17 of Chapter III permit the statement that machining of hard-alloy structural steels will result in such a microgeometry of the machined surface and in such physical and mechanical properties of the surface layer as to impart excellent service characteristics, both with respect to wear resistance and fatigue strength, to machine parts produced in this manner.

The high hardness acquired by steel in the tempering process rises in the surface layer of the part as the result of the work-hardening which takes place in the machining of steel. As has been shown in experiments by Ye.A.Belousova, hardened alloy steels of H_{R_C} = 50 - 65 undergo considerable work-hardening in the turning process - the level of work-hardening of the metal in the surface layer being 1.4 - 1.1.

It is obvious that where a contact load is involved, the service life of parts whose metal has such a high wear resistance will be quite long. Here, apparently, there is no need for special work-hardening operations.

The machining of hardened steels by carbide tools at low feeds yields a machined surface which is not inferior to a ground surface. As the hardness of the tempered steel increases, the conditions for obtaining a good surface finish are relaxed. In combination with the high hardness of tempered steels, which rises in the surface layer during the machining process, and with the formation of residual compressive stresses in this layer, this results in high indices of fatigue strength for parts of hardened steel. The same statement is true for machine parts working under contact loading.

Let us compare machining by a cemented-carbide tool and the grinding of hardened steels as to the quality of the surface layer of metal. Research (Bibl.30, 47, 71) shows that considerably better results are obtained by machining with a cemented-carbide tool.

No structural transformations occur in the work-hardened layer formed upon the turning of hardened steels (Bibl.30). The hardness of this layer diminishes smoothly from a maximum on the machined surface to the initial level acquired by the metal in work-hardening. The work-hardened layer is distributed uniformly over the entire machined surface and faithfully follows its profile.

In the grinding of hardened steels (Bibl.47, 71), structural changes occur in the surface layer of metal, due to the appearance of instantaneously high temperatures. As a result, after grinding, there frequently is an inhomogeneity in the hardness of the machined part in its cross section: a layer of highly tempered metal over the upper hardened stratum, this tempered layer proceeding with depth through all the stages of tempering to the initial hardened structure.

The stressed condition of the surface layer after grinding, resulting from structural changes in the metal, results in some cases in the appearance of grinding cracks.

The appearance of grinding cracks is also frequently observed when severe grinding conditions result in considerable emission of heat, and, in connection therewith, in local change in the microstructure of the metal, which is called grinding burns. The structure of the burned sections differs from that of the main mass of the metal, and is also lower in hardness (H_{R_C} = 45 to 55 instead of the normal H_{R_C} = 61 - 64). The depth of the burns is several millimeters.

The latest investigations have established (Bibl.47) that in high-speed grinding (the rate of rotation of the abrasive wheel is v_w = 50 m/sec instead of v_w = = 25 m/sec, as in ordinary grinding) of hardened steels at elevated rates of rotation and longitudinal feed of the part being machined, the quality of the surface layer of metal is higher than in ordinary grinding: the dimensions of the structurally changed zone of the surface layer diminish. Nevertheless, in this situation as well, machining with carbide tools offers significant advantages.

The investigations that have been performed thus far in the field of surface finish in the machining of hardened steels cannot be deemed sufficient for the presentation of practical recommendations. However, these studies make it possible to conclude that the machining of hardened steels by cemented carbide (and mineroceramic) tools is competitive with grinding in terms of the resultant surface finish.

43. Nature of Chip and Built-Up Edge on the Tool in the Turning of Hardened Steels

Nature of Chip. In the author's investigations, elementary chip was obtained under all cutting conditions, varying over a wide range (t = 0.1 to 2.4 mm, s = 0.5 to 0.61 mm/rev, and v = 6 to 81.5 m/min) in the turning of hardened steels whose hardness varied within the limits of H_{R_C} = 41 to 65. This type of chip was obtained under both high (v = 81.5 m/min) and low cutting speeds (v = 6 m/min). Investigating fine-turning of alloy steels, tempered to H_{R_C} = 50 to 69, Logak also obtained elementary chip. Chip of the same type was obtained in K.F.Romanov's experiments, in the finish-reaming of hardened steels.

We know from the theory of chip formation for ordinary (unhardened steels) that, in the machining of ductile metals, the formation of elementary chip is facilitated by high cutting speed, a high positive rake on the cutting tool, and low thickness of cut.

A considerable portion of the experiments with high-hardness tempered steels was performed with tools of negative rake and at low cutting speeds. From the viewpoint of the theory in question, the conditions for these experiments did not favor the production of elementary chip.

The steels investigated are characterized by high tensile strength and low elongation per unit length. Using the classification of metals and alloys into brittle (capable of failure without noticeable plastic deformation) and ductile (metals and alloys capable of withstanding considerable plastic deformation without failure), these steels have to be classified with the ductile types, when in the unhardened condition. In the hardened condition they occupy a position midway between the ductile and the brittle metals, and tempered steels of high hardness (for example, steel C) are typical brittle materials.

Thus, the conditions of investigation of hardened steels would be expected theoretically to result in continuous rather than elementary chip. In reality, however, it was elementary chip that was formed in the overwhelming majority of the experiments.

The fact that elementary chip was obtained in the machining of steels tempered to high hardness confirms the concepts of Ya.B.Fridman and B.Ya.Grozin (Chapter I) with respect to the ductility of brittle materials under given stressed conditions.

During the cutting process; the layer of metal being removed is in a state of stress in which the ductility properties are manifested in the class of brittle materials which includes steels tempered to high hardness.

Built-Up Edge. In the machining of ductile metals, a built-up edge appears in the cutting process. Ya.G.Usachev, the researcher who first provided an explanation for this phenomenon, offered forth the hypothesis that a built-up edge would facilitate the cutting process, since it creates a rake γ of the tool that is the most favorable for the machining of the given material. There is also another point of view to the effect that a built-up edge makes chip formation difficult and results in the formation of uneven spots and fissures.

In the author's experiments, there was no built-up edge in any of the machining schedules he employed or with any of the hardnesses of materials, and the surface was characterized by good finish.

The absence of a built-up edge in the machining of hardened steels is due to the fact that such steels occupy a position intermediate between the ductile and brittle metals. As we know, there is no built-up edge when brittle metals are machined.

The very good surface finish attainable in the machining of hardened steels is explained by the formation of elementary chip and the fact that the process is not accompanied by the appearance of a built-up edge.

44. Rake and Working Relief Angles of a Cutter in the Turning of Hardened Steels

Cemented carbides came into use as tool material about 25 years ago. The great superiority of cemented carbides over high-speed steel in terms of hardness, resistance to wear, and in particular to heat, created favorable conditions for their introduction into the field of large-scale machine-building. Nevertheless, for a number of years carbides had very limited application - somewhat more in the machining of cast iron, but to only a very limited degree in the machining of steels. This was explained by the elevated brittleness of carbides leading to the crumbling-out of the cutting edge of the tool in the cutting process. This pertained particularly to the use of titanium-tungsten carbides in the machining of steels.

In the past it was deemed axiomatic in both the theory and practice of machining that the tool had to have a positive rake, that the working relief angle had to be low, and that the higher the hardness of the material being machined, the lower the working relief angle should be. In the machining of hard steels it was recommended that cutters be given a working relief angle of not more than 6°.

These propositions, which were valid in general for high-speed tools, were extrapolated mechanically to cemented carbides. The result was that it became a general phenomenon for titanium-tungsten cutters to crumble out in the machining of steels. This largely destroyed the confidence of technical men in carbides, and inhibited extensive introduction thereof into production.

In the Mid-Thirties, the development of machine-building in our country at ever increasing rates posed new technical problems. The solution of many of these resulted in a sharp upgrading of the specifications for cutting tools. Specifically, the problem of the machining of special steels, tempered to high hardness, became pressing. At that time it was believed that hardened steel could be machined by grinding only. It goes without saying that the use of HSS tools was considered out of the question. The point was that in a number of cases the material being machined (the hardened steel) was harder than the cutting tool. And cemented carbides were the only materials in question.

The first experiments in the machining of hardened steels were run with carbide cutters with positive rakes. These ended in failure: The cutting edge of the tool crumbled out virtually at the very start of cutting. This led investigators to the idea of strengthening the cutting edge of the tool by grinding the face at an angle opposite to that generally employed. As expressed in the terminology subsequently adopted, cutters were ground at negative rake. Cutters with this geometry showed good results. The possibility of machining hardened steels of any hardness was demonstrated in practice.

No less interesting and important was the fact that the experimental cutting speeds were considerably higher than those used at the time in the machining of ordinary steels of low hardness by carbide-tipped tools. This served as proof of the fact that, in the machining of unhardened steels with hard-alloy cutters of negative rake, the cutting speeds may be increased considerably over those generally employed.

It was in this manner that the first steps were made in the high-speed machining of metals - one of the major achievements of modern engineering in the field of the machine-building.

The idea of a negative rake for carbide-tipped cutters did not appear by accident in the investigation of the machining of hardened steels. In the machining of these steels, the physical phenomena in question are clearly evident, and the regularities of the cutting process are more sharply defined than in the cutting of steels with the usual mechanical properties (unhardened steels).

The results of these experiments with hardened steels were published in the literature in our country as far back as 1938 - 1940 (Bibl.28, 72, 73). During the postwar period, highly valuable studies in the field of the machining of hardened steels have been published by P.P.Grudov (Bibl.29), V.A.Krivoukhov (Bibl.32), A.Ya.Malkin (Bibl.23), N.S.Logak (Bibl.21), N.N.Zorev (Bibl.22, 74), and others.

It must be noted that for a number of years after publication of these studies, the problem of the negative rake of carbide-tipped tools did not attract the attention of scientific workers. However, negative rake found practical application in industry in the machining of hardened steels.

Renewed interest in this question appeared in connection with the extensive development of high-speed methods of machining. There is a large number of scientific studies devoted to investigations of the influence of negative rake upon the process of machining. In some studies, negative rake was regarded as a necessary prerequisite for the success of the cutting process, out of relation to the problem of the brittleness of modern cemented carbides.

The erroneousness of this point of view must be noted. Cutters of negative rake have serious shortcomings. Their employment involves an increased load on the machine tool. All the cutting forces increase, particularly the radial force P_y which has a direct influence upon the precision of machining. It was shown in Chapter III that, in general, negative rake is only slightly superior to positive rake in terms of permissible cutting speed, but that it gives the cutting edge the required strength. Lacking this, it would be a practical impossibility to employ cutter tipped with carbides of the titanium-tungsten group in the machining of hardened steels due to the resultant crumbling-out of the carbide bars.

Negative rake in cutters should be regarded as a factor compensating for the still inadequate quality of modern carbides. With elimination of their brittleness, the need to provide a negative rake both in the machining of unhardened and hardened steels will disappear. It was noted in Chapter II that experimental studies for the development of new carbides, which would be midway between modern carbides and high-speed steels in bending strength, are already under way.

Let us turn to the matter of the working relief angle. As we have noted, it was taken for granted only a short time ago that the working relief angle for the machining of hard steels should not be in excess of 6°. Tests run by the author in the turning of hardened steels led to the opposite conclusion. It was found that the cutter life increased considerably with an increase in the working relief angle. The machining of steel tempered to $H_{R_C} = 65$ was performed successfully with cutters for which the working relief angle was $\alpha = 25°$. We know that larger working relief angles are now in wide use in the finish-machining of hardened and unhardened steels.

45. Theoretical Investigation of Cutting Forces in the Turning of Hardened Steels

Experimental investigations have shown that other relationships of the cutting forces P_x, P_y, and P_z are characteristic of the turning process than in the machining of unhardened steels. This feature of the machining of hardened steels found its theoretical explanation in the studies by N.N.Zorev (Bibl.74). N.N.Zorev's views on the cutting forces in the machining of hardened steels are discussed below.

Figure 205 presents a diagram of the forces acting upon the working faces of the cutting element under conditions of free rectangular cutting ($\gamma = 0°$). Acting upon the face OB are the normal force N and the tangential force F, which together yield the resultant R. The flank OA is acted upon by the normal force N' and the tangential force F', which together yield the resultant R'. Together, the forces R and R' yield the cutting force P. The magnitude and direction of this force in unconstrained machining has come to be characterized by its projections P_z and P_y

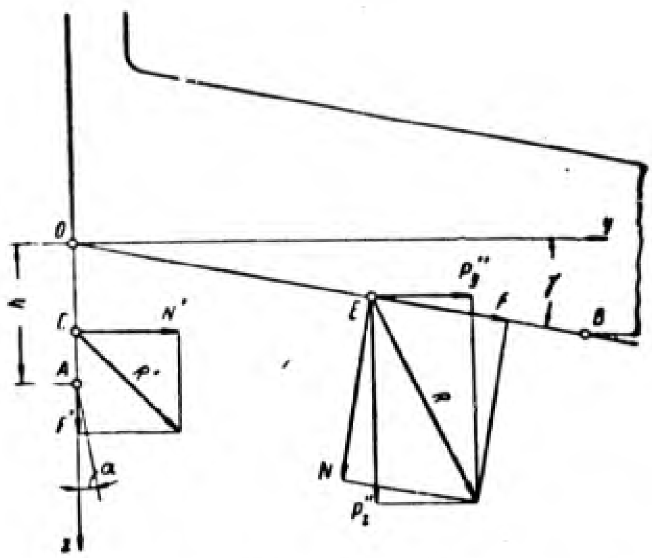

Fig.205 - Forces Acting upon Cutter Face and Flank

upon the z and y axes. Since the projections of the force P upon the z and y axes are equal to the sums of the projections of the forces R and R' upon these same axes, it follows that

$$P_z = P_z'' + P_z';$$
$$P_y = P_y'' + P_y'.$$

where P_z'' and P_y'' are the projections of the force R upon the z and y axes, or vertical and horizontal projections of the forces at work upon the face;

P_z' and P_y' are the projections of the force R' upon the z and y axis, or vertical and horizontal projections of the force acting upon the flank, where $P_z' = F'$ and $P_y' = N'$.

The forces acting upon the flank are related by the following expression:

$$F' = \mu' \cdot N',$$

where F' is the tangential force;

N' is the normal force;

μ' is the coefficient of friction.

In the cutting process, the flank of the cutting element is in contact with the workpiece unless this is not prevented by a built-up edge or a dead zone. Moreover, the flank absorbs the unit loads on contact, both normal q'_N and tangential q'_F, which are determined by the relations of the normal force N' and tangential force F' to the area of the wear flat f. Normal unit loadings develop as a result of the elastic reaction of layers of the work material underneath the surface of the cut. Unit tangential stresses are a consequence of friction between the work material and the flank of the cutting element. The sums of the normal and tangential unit loads represent, respectively, the normal and tangential forces at the flank.

If a dead zone at the face is either absent or minor, the forces at the flank will be chiefly dependent upon the yield point of the surface layer of the material being machined, the length and width of contact of the flank, and the coefficient of friction thereon. The forces on the flank increase with an increase in yield point and the scale of contact of the flank, and diminish with an increase in the coefficient of friction.

A strongly developed dead zone and - to an even greater degree - the presence of a built-up edge on the face of the cutting element significantly influence the conditions of contact between the flank and the workpiece. Moreover, the forces on the flank become dependent upon the action of factors that govern the development of dead-zone phenomena on the face: cutting speed, depth of cut, etc.

The effect of a built-up edge on the conditions of contact of the flank are similar to the effect of a dead zone, but manifest themselves more sharply. A built-up edge may project so far beyond the cutting edge that the resultant cutting plane may not touch the flank at all, which in turn will be completely free of contact loads.

Contrary to the forces on the face, those on the flank do not participate in the process of chip formation. The forces acting upon the face and flank are different in nature, so that the majority of factors influence the magnitude of these forces differently. For example, rake and thickness of cut seriously influence the forces acting upon the face but have only a minor effect upon those acting on the flank. The width of contact of the flank has little influence upon the forces acting upon the face, but greatly affect those acting upon the flank.

Inasmuch as the forces acting upon the flank and face of the cutting element depend upon different factors, or upon the same factors but to a different degree, the relation between the forces may vary within very broad limits. In the machining of soft materials with thick cuts by a tool in which there is little wear on the flank, the forces on this flank are negligible relative to those on the face. Conversely, in the machining of materials of high hardness with low thicknesses of cut, by an instrument that has undergone considerable flank wear, the forces on this flank may exceed those on the face.

The cutting force is the sum of forces acting upon the face and flank. Depending upon the relationship of forces acting upon the working edges of a tool, one encounters different laws governing the change in cutting force. In the majority of cases, the forces on the face are considerably greater than those on the back edge, and any change in the cutting force is determined by changes in forces on the face and, consequently, by changes in chip shrinkage. In some cases, however, when the forces on the back edge exceed those on the face, the change in the cutting force may not match that on the face or, consequently, the change in chip shrinkage.

In the machining of hardened steels by tools that have undergone considerable flank wear, the forces on this edge are a major factor in the cutting process. In contrast to the situation in the machining of unhardened steels, here the action of the forces on the back edge of the tool determines the general nature of the principles of change in cutting force, and the process of chip formation, while the forces on the tool face play a secondary role.

One of the methods of experimental determination of the forces acting upon the flank is the comparison of cutting forces under different conditions of tool wear. The forces on the flank relate to the cutting forces, as measured by a dynamometer, as follows:

$$P'_x = \Delta P_x \frac{h}{\Delta h};$$
$$P'_y = \Delta P_y \frac{h}{\Delta h};$$
$$P'_z = \Delta P_z \frac{h}{\Delta h},$$

where P'_x, P'_y, P'_z are the forces on the flank;

ΔP_x, ΔP_y, ΔP_z is the increase in cutting forces at different widths of wear flat on the flank;

h and Δh are the width of the wear flat, and the increase therein, respectively.

Inasmuch as, given a constant depth of cut, the area of the wear flat on the cutter flank is proportional to its width, these equations may be written as follows:

$$P'_x = \Delta P_x \frac{f}{\Delta f}; \quad (23)$$
$$P'_y = \Delta P_y \frac{f}{\Delta f}; \quad (24)$$
$$P'_z = \Delta P_z \frac{f}{\Delta f}, \quad (25)$$

where f and Δf are the area and the increase in area of the wear flat.

Experiments conducted by N.N.Zorev have shown that large forces develop on the cutter flank in the machining of hardened steels. Where steels of high hardness are concerned, they considerably exceed the forces acting upon the face.

Figures 206, 207, and 208 describe the effect of the area of the wear flat upon the cutting force in the machining of hardened steels 40KhNM2, 40KhNM3, and 9KhS3 whose hardnesses are, respectively, H_{R_C} = 35, 46, and 65. Table 89 presents data for the relationship of forces operating on the flank and face, at an area of the wear flat of $f = 1.8$ mm^2.

The magnitude of the forces P_x, P_y, and P_z is determined from the curves in

Figs.206 - 208, and the values of the forces on the flank P'_x, P'_y, and P'_z from eqs.(23) - (25). The magnitude of the forces on the face P''_x, P''_y, and P''_z represent

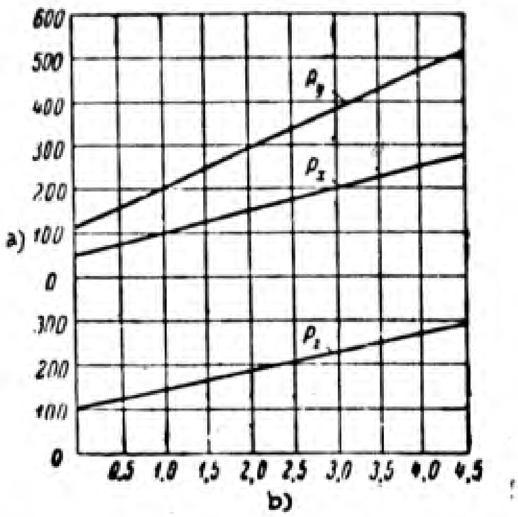

Fig.206 - Influence of Area of Wear Flat at the Flank Upon the Cutting Forces in the Turning of 40KhNM2 Steel Tempered to H_{R_C} = 35.

Cutting conditions: t = 2 mm; s = = 0.156 mm/rev; v = 75 m/min. Geometry of VK6 cutter: $\alpha = 12^\circ$, $\gamma = -10^\circ$, $\lambda = 0^\circ$, $\varphi = 30^\circ$, $\varphi_1 = 10^\circ$, r = 0.5 mm.

a) Forces P_x, P_y, P_z, kg; b) Area of wear flat on the flank f, mm^2

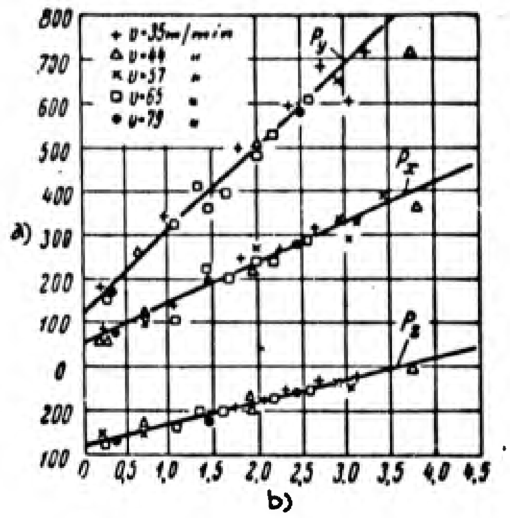

Fig.207 - Influence of Area of Wear Flat at the Flank Upon the Cutting Forces in the Turning of 40KhNM3 Steel Tempered to H_{R_C} = 46, at t = 2 mm, s = 0.156 mm/rev, and Various Cutting Speeds.

Geometry of VK6 cutter: $\alpha = 12^\circ$, $\gamma = -10^\circ$, $\lambda = 0^\circ$, $\varphi = 30^\circ$, $\varphi_1 = 10^\circ$, r = 0.5 mm.

a) Forces P_x, P_y, P_z, kg; b) Area of wear flat on the flank f, mm^2

the differences between the cutting forces and the corresponding forces on the flank:

$$P''_x = P_x - P'_x;$$
$$P''_y = P_y - P'_y;$$
$$P''_z = P_z - P'_z.$$

By way of example, let us calculate the forces P'_y and P''_y for 9KhS3 steel. Let us employ eq.(24).

We find, from Fig.208: for f = 1.8 mm^2 a force P_y = 850 kg, and for f = 1.0 mm^2, P_y = 515 kg.

$$\Delta P_y = 850 - 515 = 335 \text{ kg};$$

$$\Delta f = 1{,}8 - 1{,}0 = 0{,}8 \text{ mm}^2;$$

$$P'_y = \Delta P_y \cdot \frac{f}{\Delta f} = 335 \cdot \frac{1{,}8}{0{,}8} = 750 \text{ kg};$$

$$P''_y = P_y - P'_y = 850 - 750 = 100 \text{ kg}.$$

These data permit a number of conclusions. In the first place, we find confirmation of the proposition that high relative values of the radial force P_y and the longitudinal force P_x are characteristic of hardened steels, and that these increase with a rise in the hardness of the steel. Moreover, the force P_y is considerably larger than the tangential force P_z.

The radial force P'_y and the longitudinal force P'_x, acting upon the flank, considerably exceed the radial force P''_y and the longitudinal force P''_x acting upon the face. This excess rises with the steel hardness. For hardened steels of low and medium hardness (40KhNM2 and 40KhNM3), the tangential force on the flank is smaller than the tangential force on the face, whereas for 9KhS3 high-hardness steel, on the other hand, the force on the flank P'_z is 85% higher than the force P''_z acting on the face. With increase in the hardness of tempered steel, the radial force P'_y on the flank increases, and the radial force P''_y on the face diminishes somewhat.

Table 89

Relationship of Forces Acting Upon Cutter Face and Flank in the Turning of Hardened Steels

(Area of Wear flat on the flank f = 1.8 mm^2)

Steel	Hardness, H_{R_C}	P_x	P_y	P_z	$\frac{P_x}{P_z}$	$\frac{P_y}{P_z}$	P'_x	P'_y	P'_z	P''_x	P''_y	P''_z	$\frac{P'_x}{P''_x}$	$\frac{P'_y}{P''_y}$	$\frac{P'_z}{P''_z}$
		in kg					in kg								
40KhNM2	35	140	270	175	0,80	1,54	90	155	75	50	115	100	1,80	1,35	0,75
40KhNM3	46	215	460	210	1,02	2,19	160	340	90	55	120	120	2,90	2,80	0,75
9KhS3	65	350	850	285	1,23	2,98	300	750	185	50	100	100	6,00	7,50	1,85

Table 90

Normal q'_N and Tangential q'_F Unit Loads Upon Flank in the Machining of Hardened Steels

Steel	H_{R_C}	q'_N in kg/mm²	q'_F in kg/mm²	$\frac{q'_F}{q'_N} = \mu'$
40KhNM1	20	59	33	0,56
40KhNM2	35	107	38	0,35
40KhNM3	46	207	47	0,23
40KhNM5	58	295	80	0,27
9KhS3	65	445	110	0,25

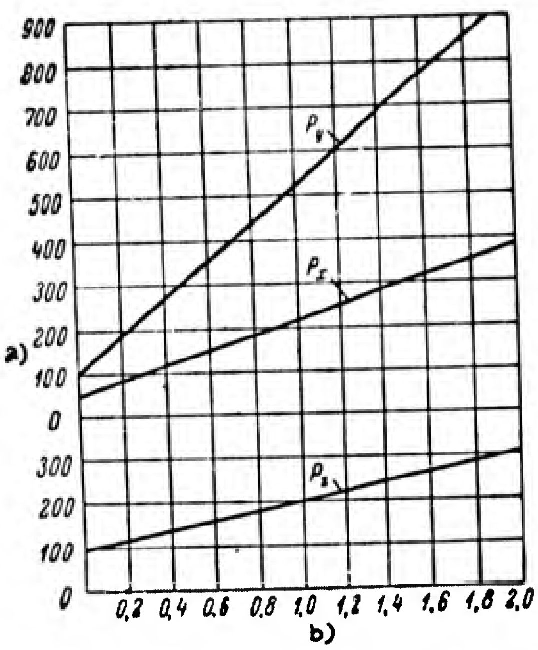

Fig.208 - Effect of Area of Wear Flat on Flank Upon the Cutting Forces in the Turning of 9KhS3 Steel Tempered to H_{R_C} = 65.

Cutting conditions: t = 1 mm; s = = 0.156 mm/rev; v = 12 m/min. Geometry of the VK6 cutter: $\alpha = 12^o$, $\gamma = -20^o$, $\lambda = 0^o$, $\varphi = 30^o$, $\varphi_1 = 10^o$, r = 0.5 mm.

a) Forces P_x, P_y, P_z, kg; b) Area of wear flat on flank f, mm²

The nature of the effect of the hardness of tempered steel upon the forces acting on the flank are more clearly seen in an analysis of the normal force q'_N and the tangential force q'_F of the unit loads upon the flank. Table 90 presents the values of q'_N and q'_F, as well as the coefficient of friction μ'.

We see from Table 90 that the unit loadings upon the flank of the cutter are quite high where hardened steels are concerned. For purposes of comparison, we note that, in the case of unhardened carbon steels of H_B = 97 - 185, the unit normal loading q'_N varies within the range of 37 - 61 kg/mm². Also notable is the fact that the coefficient of friction on the flank μ' diminishes with an increase in the hardness of the hardened steel.

Figure 209 illustrates the effect of the hardness of tempered steel upon the magnitude of unit contact loadings, and the coefficient of friction on the flank. It will be seen that, with an increase in the hardness of the steel, the tangential force q_F' and the normal force q_N' increase, the latter rise being the sharper.

On the basis of experimental data, N.N.Zorev believes that the excess in the tangential force P_z over the axial force P_y in the machining of hardened steels can be explained by the effect of intensive forces on the flank of the tool. The normal force on the flank N', determining the magnitude of the force P_y, is greater than the tangential force F' which influences the magnitude of the force P_z. With an increase in the hardness of the work material, increases occur in both forces, but the normal force N' increases more rapidly than does the tangential force F'. As a result, an increase occurs in the ratio $\frac{N'}{F'}$; in connection therewith, the ratio $\frac{P_y}{P_z}$ also rises. The influence of flank wear on the cutter is similar.

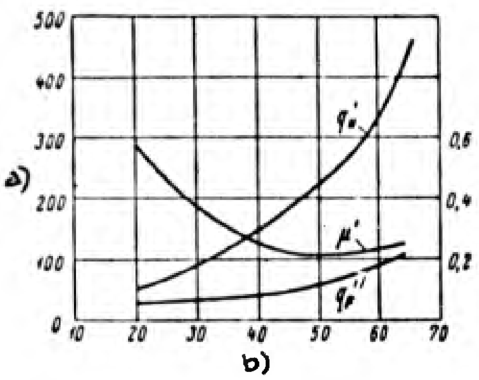

Fig.209 - Effect of Hardness of Tempered Steel Upon Unit Normal Load q_N' and Tangential Load q_F' and on the Coefficient of Friction on the Cutter Flank. Tests made at cutting conditions preventing the development of a built-up edge and a pronounced dead zone on the cutter face.

a) Unit load on flank q', kg/mm^2;
b) Hardness of work material, H_{R_C};
c) Coefficient of friction on flank, μ'

Let us proceed to the problem of the structure of the formulas for determining the cutting forces. In the turning of hardened steels, the influence of thickness of the cut upon the cutting force drops with an increase in the flank wear on the tool. This is obvious from Figs.210 and 211 which show the relationship of the forces P_z and P_y to the feed s and the tool wear h. The tests were run with VK6 cutters on 40KhNM5 steel of H_{R_C} = 58.

The dependence of the cutting forces upon the feed s (Figs.210 and 211) may be expressed by formulas of the general type:

At a width of the area of the cutter flank wear of h = 0:

$$P_z = C_{P_z} \cdot s^{0.8}, \quad P_y = C_{P_y} \cdot s^{0.6};$$

At h = 0.25 mm:

$$P_z = C_{P_z} \cdot s^{0.45}, \quad P_y = C_{P_y} \cdot s^{0.16}.$$

As we see, the exponent for the feed is largely dependent upon the flank wear h, so that the very nature of the cutting force relationships to feed changes with change in h. Therefore, N.N.Zorev believes the general type of equation ($P = C_P \cdot s^{y_P}$) to be unsuited to the case of hardened steels and instead suggests a formula of the following type:

$$P_x = C_{P_x} \cdot s^{y_{P_x}} + q'_N \cdot f \cdot \sin \varphi_{av};$$
$$P_y = C_{P_y} \cdot s^{y_{P_y}} + q'_N \cdot f \cdot \cos \varphi_{av};$$
$$P_z = C_{P_z} \cdot s^{y_{P_z}} + q'_P f.$$

where φ_{av} is the average complement of the side-cutting-edge angle. If the length of the nose is relatively small, the φ_{av} angle may be deemed to be equal to the complement of the side-cutting-edge angle φ.

The right-hand sides of these equations consist of two terms: the first terms represent the forces acting upon the cutter face, and the second the forces acting upon the flank. With this particular structure of the equations, the feed exponents are not dependent upon the amount of wear to which the tool has been subjected.

Let us consider the question of unit cutting force in the turning of hardened steels. N.N.Zorev suggests the following equation for determining the unit cutting force:

$$p = C_{P_z} \cdot a^{x_{P_z}-1} + q'_P \cdot \frac{h}{a}. \quad (26)$$

The second term on the right-hand side of eq.(26) characterizes the effect of the forces acting upon the cutter flank at unit cutting force. This influence rises with the wear h and with any reduction in the thickness of cut a. In the machining

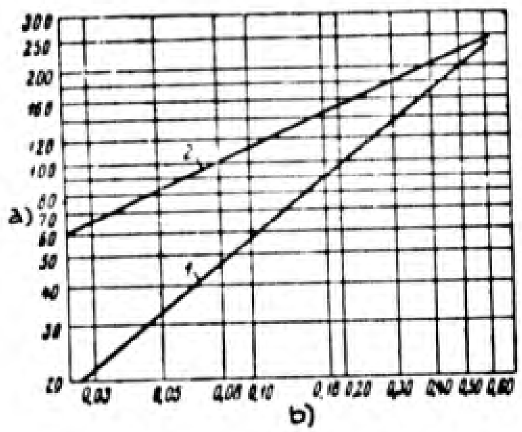

Fig.210 - Feed Versus Tangential Force P_z in the Turning of 40KhNM5 Steel Tempered to H_{R_C} = 58, with t = 1 mm and v = 17 m/min.

Geometry of VK6 cutter: $\alpha = 12^{\circ}$, $\gamma = -10^{\circ}$, $\lambda = 0^{\circ}$, $\varphi = 30^{\circ}$, $\varphi_1 = 10^{\circ}$, r = 0.5 mm.

1 - Flank wear h = 0; 2 - Wear h = 0.25 mm.

a) Force P_z, kg; b) Feed s, mm/rev

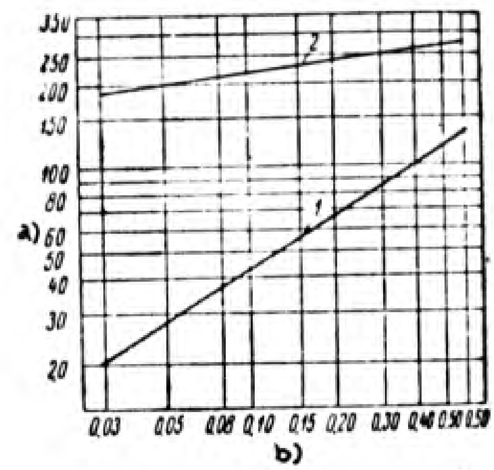

Fig.211 - Feed Versus Radial Force P_y in Turning 40KhNM5 Steel Tempered to H_{R_C} = 58, t = 1 mm and v = 17 m/min.

Geometry of VK6 cutter: $\alpha = 12^{\circ}$, $\gamma = -10^{\circ}$, $\lambda = 0^{\circ}$, $\varphi = 30^{\circ}$, $\varphi_1 = 10^{\circ}$, r = 0.5 mm.

1 - Flank wear h = 0; 2 - Wear h = 0.25 mm.

a) Force P_y, kg; b) Feed s, mm/rev

of steels tempered to high hardness, the unit cutting force p attains high values due to the large contact loadings q'_F and the low thicknesses of cut a. With respect to hardened 40KhNM5 steel of H_{R_C} = 58, the equation for determining the unit cutting force takes on the following form:

$$p = 171a^{-0.2} + 80\frac{h}{a}.$$

This equation has been used to plot curves (Fig.212) illustrating the influence of the width of the wear flat upon the unit cutting force, for three thicknesses of cut a = 0.02, 0.10, and 0.50 mm. The unit force p varies within very broad limits - from 210 kg/mm^2 when the cutter wear is low (h = 0.1 mm) and the thickness of cut is high (a = 0.5 mm) to 2370 kg/mm² when the wear is high (h = 0.5 mm) and the thickness of cut is low (a = 0.02 mm).

The unit cutting force is numerically equal to the unit work of cutting, and therefore eq.(26) may be considered as the formula for the unit work of cutting. The first term on the right-hand side of the equation represents the unit work of the forces acting upon the cutter face, i.e., the unit work of chip formation. The second term represents the unit work of the forces on the flank, i.e., the unit work of friction on the flank. When the cutter wear is high, the bulk of the work of cutting is comprised of the unit work of friction on the flank.

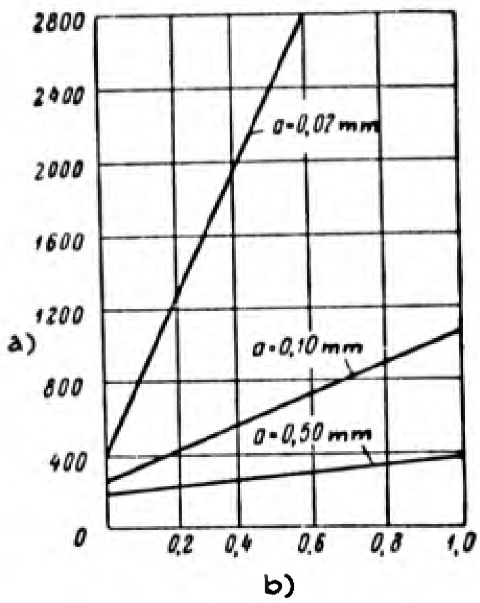

Fig.212 - Effect of Width of Wear Face and Thickness of Cut upon Unit Cutting Force in Turning of 40KhNM5 Steel, H_{R_C} = 58, at v = 17 m/min.

Geometry of VK6 cutter: $\alpha = 12^\circ$, $\gamma = -10^\circ$, $\lambda = 0^\circ$, $\varphi = 30^\circ$, $\varphi_1 = 10^\circ$, r = 0.5 mm.

a) Unit cutting force p, kg/mm²; b) Width of flank wear area h, mm.

For example, in the case of 40KhNM5 steel tempered to H_{R_C} = 58, at a = 0.1 mm and h = 0.8 mm, the unit work of cutting is 912 kg/mm², and the unit work of chip formation is 272 kg/mm², i.e., 30% of the former. The remaining 70% goes to unit work of friction on the flank.

46. Thermo-Velocity Hypothesis of the Machining of Hardened Steels

In the postwar period the hypothesis of fast machining advanced by N.I. N.I.Shchelkonogov (Bibl.28), which we term the "thermo-velocity" hypothesis for the machining of hardened steels, has attained wide recognition. This theory has been employed to find a physical basis for the fast machining of all steels, and not only of hardened steels. In some later studies, this hypothesis was rejected. However, it continues to be used in studies devoted to hardened steels.

Essence of the Hypothesis

In Fig.213 we present curves for the temperature of heating upon the tensile strength of steels of various strengths. The upper curve pertains to steels with σ_t = 160 - 180 kg/mm^2. As we see, upon heating to t = 100°C, the tensile strength σ_t diminishes. With further heating, σ_t increases, to attain a maximum at t = 300°C. Another increase in temperature results in a sharp drop in σ_t. At t = 800°C the tensile strength is approximately 20 kg/mm^2.

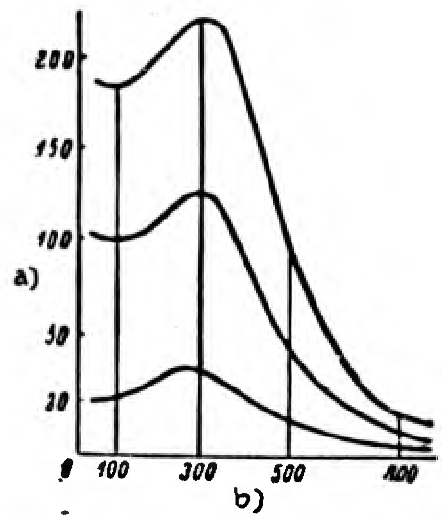

Fig.213 - Effect of Temperature of Heating upon the Tensile Strength of Steel.

a) Tensile strength σ_t, kg/mm^2;
b) Temperature of heating, t°

Moreover, Fig.213 shows that the influence of the temperature of heating upon changes in the tensile strength σ_t is manifested more strongly, the higher the tensile strength of the steel at room temperature.

Advocates of hypothesis are of the opinion that the machining of hardened steels requires establishing a certain temperature in the zone of origin of plastic deformations in the layer of metal being removed, high enough to provide the same change in the mechanical properties of the machined material as that obtained in artificial heating of steels to 700 - 800°C. As a result, the tool will actually not be cutting hardened steel of high hardness and strength and of low machinability, but ductile steel of low hardness and high machinability.

N.I.Shchelkonogov advanced his thesis on the basis of his investigation of the process of turning of hardened steels: structural steel (carbon No.40 and KhN alloy) of H_{R_C} = 49 - 52 and tool steel (U7, U10, and R18), of H_{R_C} = 56 - 64. The experiments were run with cutters tipped with VK8, VK6, T21K8 and with sergonite cutters*.

The following are the most interesting of N.I.Shchelkonogov's conclusions:

1) The machining of hardened steels is an exception to the general law of machining: with an increase in cutting speed (up to a given limit) the cutter life does not diminish, but rises;

2) In the machining of hardened steels, the cutting speed does not diminish as the hardness of the work material rises;

3) Machining of hardened steels can only be done at high cutting speeds.

For finish-turning of hardened steels, cutting speeds of not less than 150 m/min have to be employed.

Results of Experimental Verification of the Hypothesis

A large series of experiments conducted by the present author to determine the ratio T - v has disproved the thermo-velocity hypothesis. It was found that a slight increase in cutting speed resulted in a sharp drop in cutter life.

Numerous attempts made to cut at speeds of v = 100 - 150 m/min at low cutting depth t and feed s (process: turning of high-hardness steels) were unsuccessful - the cutters dulled and crumbled out instantaneously. Nevertheless, further experiments were run with A and C steels, of H_{RC} = 41 and 65, to determine the nature of the influence of cutting speed upon tool life, and also the possibilities for machining hardened steels at "super-high" speeds. Table 91 presents data on A steel of H_{RC} = 41. The experiments were conducted with lapped T21K8 and VK8 cutters of the following geometry: $\alpha = 6°$, $\gamma = 15°$, $\lambda = 0°$, $\varphi = 45°$, $\varphi_1 = 15°$, r = 1.15 mm. The cutters worked to normal dulling.

It follows from the experimental data that the familiar regularity also holds in the turning of hardened steels: The tool life diminishes with an increase in cutting speed.

*A titanium-tungsten carbide no longer manufactured: 74% WC, 18% TiC, 8% Co.

Table 91

Effect of Cutting Speed Upon Tool Life

Turning of A Steel, $H_{R_C} = 41$

Grade of Hard Alloy	Depth of Cut t, in mm	Feed s, in mm/rev	Cutting speed v, in m/min	Tool life T, in min
VK8	1,0	0,31	150	1,3
	1,0	0,31	100	5,5
	1,15	0,31	50	53
	1,30	0,31	30	126
T21K8	0,30	0,225	171	0,3
	0,30	0,225	130	0,2
	0,30	0,225	108	72

Table 92

Influence of Cutting Speed Upon Tool Life

Turning of C Steel, $H_{R_C} = 65$

Grade of Hard Alloy	Cutting Speed v, m/min	Tool Life T	Description of Experimental Results
VK3	100	Tools lasted a few seconds	Instantaneous dulling of tools and crumbling-out of cemented-carbide bar. Chip was bright red as it came off.
	75		
T21K8	100		
	75		
T15K6	100		
	75		

Table 92 presents the results of experiments with C steel of $H_{R_C} = 65$ ($t = 0.5$ mm, $s = 0.14$ mm/rev). The machining was done with lapped VK3, T15K6, and T21K8 cutters of the following geometry: $\alpha = 15^\circ$, $\gamma = -5^\circ$, $\lambda = 0^\circ$, $\varphi = 45^\circ$, $\varphi_1 = 15^\circ$, $r = 1.3$ mm.

The working relief angle of the tools was increased, with the purpose of improving their functioning. In view of the hardness of the work material (H_{R_C} = 65), the cutting speeds of v = 75 to 100 m/min must be regarded as quite high. It should be noted that, at the recommended cutting conditions (Appendix I) for steel of H_{R_C} = 65 with T15K6 carbide, t = 0.5 mm and s = 0.14 mm/rev, the v_{60} cutting speed is 8 m/min.

The cemented carbides tested were characterized by high cutting properties.

As we see, the cutter life was measured in seconds. Instantaneous dulling and crumbling-out of the cutters took place at the very outset of the machining process. This would indicate that the machining of steels of H_{R_C} = 65 at very high cutting speeds is impossible.

Analysis of the Hypothesis

Let us analyze the thermo-velocity hypothesis as it applies to unhardened and to hardened steels.

Fast Machining of Unhardened Steels. Let us briefly review studies on the fast cutting of unhardened steels, dealing with the question of the effect of the cutting-zone temperature upon the mechanical properties of the layer of metal being removed.

V.I.Rukavishnikov (Bibl.75) investigated the influence of the temperature of heating upon the machinability of steel (0.42% C, 0.75% Ni, 0.28% Mn, 0.28% Si, 0.30% Cr), possessing the following mechanical properties in the "cold" state: σ_t = 60 kg/mm^2, δ = 18%, H_B = 179. The experiments were run with cutters tipped with VK8 and T21K8 at t = 8 mm, s = 0.945 mm/rev, and v = 24.5 m/min. The investigation showed that, on heating the steel from zero to 560°C, the force P_z diminished from 1150 to 378 kg, i.e., by two-thirds.

According to the data by B.M.Askinazi and G.N.Babat (Bibl.75), the unit cutting force drops by a factor of 4.2 as the work-steel temperature is raised from zero to 900°C.

The data by M.M.Ioffe (Bibl.75) demonstrate that chromium steel (H_B = 320) is much more advantageously machined in the heated condition than in the ordinary way, in terms of tool life and the productivity of the process. Preheating of the work material to 700°C increased the tool life 5-fold, and the productivity of the process by 3.5 - 5 times.

In analyzing the data presented, P.P.Grudov (Bibl.75) notes that one cannot draw an analogy between "cold" machining at high speeds, and machining with preheating of the workpiece. A study of the process of cutting unheated steels at high temperatures, with the chip temperature attaining 800°C and more, may create the impression that here, as in the artificial heating of the work material, the layer of metal was heated both prior to and during the process of deformation to the same temperature attained in artificial heating and lost its mechanical properties, and that this is the decisive factor in the process and rate of machining. This is not actually the case since, if it were, we would be justified in expecting a reduction by a factor of 3 - 5 in the cutting force, and numerous experiments have shown that these forces diminish by only 20 - 40%.

In the opinion of P.P.Grudov, such a reduction in the cutting force (by 20 - - 40%) results not only from a change in the mechanical properties of the work material in the cutting zone, but also from a change in the condition of the rubbing surfaces. It may be assumed that, here, the second factor is of greater significance.

A.A.Avakov (Bibl.76) was the first to advance the idea that one cannot identify the machining of artificially heated steels with that of the same steels in the "cold" state, merely on the basis of the fact that the artificial heating of the metal brings it to the same temperature as that created in the cutting zone during the "cold" method of machining at high speeds.

In the machining of artificially heated steel, the tool is actually engaged in cutting softened metal at a unit cutting force that has been reduced several-fold. However, in the machining of "cold" metal at high speeds, heating has been localized in areas very small (in thickness) and directly in contact with the working edges of the tool. Between the two solids - the tool and the unsoftened portion of the chip - a layer of work metal with a high temperature due to the heat emitted in the cutting process is formed.

According to the calculations by A.A.Avakov, in the turning of steel of σ_t = 95 kg/mm^2, depth of cut t = 3 mm, feed s = 0.5 mm/rev, and cutting speed v = 230 m/min, the depth of penetration of heat into the depth of the chip is 24 microns in 0.0002 sec.

Experiments show that the increase in the thickness of the high-temperature layer of the chip sharply lags behind the growth in thickness of the chips themselves, and the thickness of the high temperature layer will be approximately identical both for thin and thick chip.

The heating of chip in depth to high temperatures (with the chip coming off red-hot), as sometimes observed in high-speed turning of steels, should, in the opinion of A.A.Avakov, be explained by the fact that the chip emerging from contact with the cutter face has already been subjected to the rubbing effect of this face.

Below we present data from research by E.I.Fel'dshteyn (Bibl.44), characterizing the heating conditions of the contact layers of the workpiece in the high-speed cutting of unhardened steels. Table 93 presents the mechanical properties and structure of the steels tested.

The experiments presented in Fig.214 (t = 1.5 mm, s = 0.2 mm/rev, v = 17 - 150 m/min for high-speed cutters and v = 150 - 550 m/min for cutters tipped with T15K6) show that, with the exception of a single instance, the sequence in the position of the steels with respect to v_{60} is identical both in ordinary and in high-speed cutting.

The good correspondence between the relative machinability indices obtained in the turning of various steels by high-speed cutters (i.e., under conditions in which there is no possibility of structural transformations of the workpiece - low cutting speed and therefore low temperature in the cutting zone) testify to the fact that

Table 93

Structure and Mechanical Properties of Steels, According to Data by E.I.Fel'dshteyn

Steel Grade and Identification	State	Structure	H_B	Tensile Strength σ_t, kg/mm²	Elongation per unit length, δ, %	Reduction in Area, ψ in %
10	Normalization	Ferrite and fine grains of thin lamellar pearlite	121	41,8	36,6	68,0
40	Normalization	Thin lamellar pearlite and ferrite in a coarse lattice; fine grain	179	63,9	25,1	4,0
40Kh-P	Annealing	Thin lamellar pearlite and ferrite in a lattice; fine grain	187	67,5	23,0	—
40Kh-3e	Hardening and high-temperature tempering	Granular (fine) pearlite with very fine grains of cementite	192	67,5	23,5	69,2
40KhN	Normalization (rolled products)	Sorbitic and fine lamellar pearlite and ferrite in the form of a fine and, in spots, broken lattice; coarse grain	248	85,5	15,3	33,0
30KhN3	Normalization	Thin lamellar pearlite and ferrite in the form of grains; ferrite ghost is encountered	207	—	—	—
35KhGS-P3e	Annealing	Lamellar pearlite changing in spots to granular; ferrite in lattice form; mixed grain size	217	76,5	18,6	42,0
35KhGS-P	Annealing	Lamellar pearlite and ferrite in lattice form; mixed grain size	217	77,1	21,8	40,0
35KhGS-3e	Annealing	Granular pearlite	197	68,5	23,7	53,6
35KhGS-U1	Quenching (tempered and annealed)	Sorbite	341	103,0	12,1	43,8

the nature of the influence of the initial properties of steels upon the cutter life remains the same in high-speed machining.

Consequently, in the fast machining of unhardened steels, the metal being worked undergoes no structural changes which would eliminate the differences in the machined steel due to special features of structure and properties in the initial state.

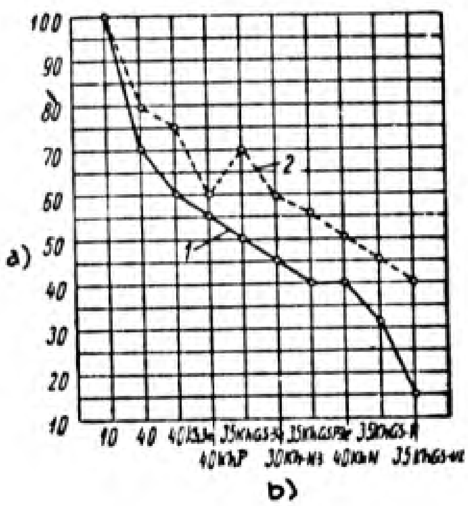

Fig.214 - Relative Machinability of Various Steels

1 - In turning with HSS tools;
2 - In very fast turning

a) Relative cutting speed v_{60}, %;
b) Conventional designations of steels tested

The most important conclusion which can be drawn from the data in Table 94 is the fact that high-speed machining retains the influence of various steel structures on the life of high-speed tools, working at relatively low cutting speeds and resulting in low temperatures in the cutting zone.

The data by E.I.Fel'dshteyn presented here pertain to experiments in which a given amount of flank wear was employed as the criterion for the dulling of carbide cutters.

E.I.Fel'dshteyn also investigated the nature of the face wear of cutting tools

Table 94

Relative Cutting Speeds v_{60} for Steels of Various Structures (in Percent)

Type of Machining	Conventional Designation of Steel					
	40Kh-P	40Kh-3e	35KhGS-P	35KhGS-3e	35KhGS-P3e	35KhGS-U1
Turning with HSS tools	100	109.5	100	125	147	50
Very fast turning	100	124	100	121	148	83

in the high-speed turning of 35KhGS steel, with a structure of granular pearlite, lamellar pearlite, and ferrite.

The experiments showed that the intensity of wear on the cutter faces, like that on their flanks, depends upon the structure of the work material in its initial state: With a granular pearlitic structure, the depth and width of the craters is significantly less.

These experimental data serve as proof of the fact that in very fast machining of steels the layer of metal removed, in direct contact with the cutter face, also undergoes no structural transformations.

E.I.Fel'dshteyn substantiated his conclusions by the following theoretical considerations: In the very fast machining of unhardened steels, the cutting temperatures are sufficiently high for structural transformations to occur. Data derived from numerous experiments show that the cutting temperature reaches not less than 700 - 800°C, and that actually the temperature at the interfaces between cutting tool and chip and the workpiece is even higher. The point is that in measuring the cutting temperature by the natural thermocouple method (the method in widest use), the results obtained are somewhat understated.

However, structural transformations need a certain amount of time to occur. Studies show that, at a temperature of 800 - 850°C, the time necessary for the transformation of pearlite to austenite to begin is at least tenths of a second. However, the duration of heating of the metal removed in very fast cutting is measured in ten-thousandths of a second. For example, at a contact length of l = 2 mm, a chip shrinkage of ξ = 2.0, and a cutting speed of v = 300 m/min, the contact time will be

$$\tau = \frac{60 l \xi}{1000 v} = \frac{60 \cdot 2 \cdot 2}{1000 \cdot 300} = 0{,}0008 \; sec.$$

It is obvious that, under these conditions of heating in the layer being removed, no structural transformations can occur.

Further, the heating of the contact layer of metal proceeds at a very high velocity in very fast machining. If we assume a temperature difference of 500°C and a contact time of 0.0008 sec, the rate of heating is

$$v_{heat} = \frac{500 \cdot 60}{0{,}0008} = 37\,500\,000 \text{ deg/min.}$$

We know that the temperature interval for transformation of pearlite into austenite increases with the rate of heating. An investigation of the nature of the behavior of steel in high-speed heating with high-frequency currents showed that, at rapid heating, the transformation of pearlite into austenite occurs at temperatures considerably in excess of the critical point A_{C_1}. This overheating is greater, the higher the rate of heating. For example, in heating at a rate of about 30,000 deg/min, the minimum hardening temperature exceeds by about 200°C the zone of hardening temperatures characteristic of slow heating.

Consequently, under conditions analogous to very fast cutting of metals, structural transformations will occur at temperatures considerably higher than the usual conditions of heat treatment of steels.

The data by P.P.Grudov, A.A.Avakov, and E.I.Fel'dshteyn refute the heat-and-velocity hypothesis for very fast cutting of unhardened steels. Let us now turn to the case of hardened steels.

Very Fast Machining of Hardened Steels. The data obtained by the author with steel C of H_{R_C} = 65 (Table 46) are of the greatest interest. The cutting conditions varied over a wide range: depth of cut t from 0.10 to 1.0 mm, feed s from 0.05 to 0.28 mm/rev, cutting speed v from 23.4 to 5.4 m/min. In the majority of cases the cutters had an acceptable tool life: T = 10 - 60 min.

An analysis of the experimental data yielded the following relation between cutting speed and cutter life:

$$v = \frac{C}{T^m}$$

or

$$T = \frac{C'}{v^{\frac{1}{m}}}.$$

Consequently, there is a regular reduction in tool life with rise in cutting speed. This indicates that the thermo-velocity hypothesis is not supported in the case of high-alloy chromium-nickel-molybdenum steel tempered to very high hardness (C steel).

The ratio $T = \frac{C'}{v^{\frac{1}{m}}}$ for steel C of $H_{R_C} = 65$ was derived for a range of relatively low cutting speeds.

As we see from Figs.61 - 64, a ratio T - v of identical nature was obtained for steel B of $H_{R_C} = 59$, for a range of higher cutting speeds v = 17.9 - 54 m/min, and also for steel B of $H_{R_C} = 49$, for cutting speeds of v = 30 - 75 m/min.

To this one may raise the objection that the hypothesis might find confirmation in the zone of even higher cutting speeds. However, this objection is invalidated by the experimental data presented in Tables 91 and 92. The data in Table 92 indicate that the machining of steel C of $H_{R_C} = 65$ at cutting speeds of v = 75 - - 100 m/min is unrealizeable, since instantaneous dulling of the cutter results.

It follows from Table 91 that the machining of steel A of $H_{R_C} = 41$, at high cutting speeds (v = 30 to 171 m/min) is also subject to the basic law of cutting theory, expressed by the equation $v = \frac{C}{T^m}$.

Nor is the thermo-velocity theory supported in the studies by P.P.Grudov (Bibl.29) and A.V.Alekseyev (Bibl.72), devoted to hardened steels.

These data on hardened steels permit the conclusion that in this case, as in the very fast machining of unhardened steels, no structural changes occur in the layer of metal being removed. This is also confirmed by the experimental data of the author and of P.P.Grudov, which indicate that the hardness of tempered steel exerts a powerful effect upon its machinability. It is obvious that if, in the cutting process, the work material underwent structural transformations (lost its hardness), then, regardless of its hardness, steel B would be characterized by an identical machinability, determined by the permissible cutting speed v_{60}. In fact, as we see from Table 49, steel B of $H_{R_C} = 59$, has a lower machinability than the same steel tempered to $H_{R_C} = 49$.

The author's observations of the cutting process of hardened steels show that the chip leaves the tool in a red-hot state only at high cutting speeds (speed high with respect to the hardness of the workpiece), low thicknesses of cut, and considerable dulling of the tool. At greater thickness of cut and low cutting speeds, the chip has a regular ("cold") appearance and only narrow strips of chip, immediately adjoining the leading edge of the cutter, will heat to red-hot heat and that merely at great dulling of the cutter. Numerous experiments with steel C hardened to $H_{R_C} = 65$ permitted to establish the fact that the chip did not undergo heating to red heat over a long period of tool operation, and that the cutting proceeded normally.

The fact that no structural transformations occur in the layer removed in the machining of hardened steels, similar to the very fast machining of unhardened steels, may be substantiated by data derived in the investigations by V.D.Sadovskiy, K.A.Malyshev, and B.G.Sazanov (Bibl.77). These writers note that the decomposition of martensite in the heating of hardened steel over a broad range of heating speeds proceeds in the temperature interval of 1000°C and higher and consequently lasts for not less than 0.5 sec, for example, when the heating speed is 200 deg/sec. However, the heating time τ of the removed layer of metal - if it is taken to be the same as the contact time between chip and tool face - will, at $v = 100$ m/min (a high speed for hardened steels) by only 0.0024 sec, or 0.008 sec at $v = 30$ m/min.

Hypothesis of A.Ya.Malkin. On the basis of theoretical and experimental investigations, A.Ya.Malkin (Bibl.23) further developed the hypothesis of N.I.Shchelkonogov and advanced a theory in accordance with which the basis for the machining of hardened steels is "control of heat during the cutting process". This theory has been encountered in recent studies of the machining of hardened steels (Bibl.30, 68).

In the opinion of A.Ya.Malkin, the problem of productive machining of hardened steels is successfully solved if proper utilization is made of the heat developed in the cutting process. This heat is required in order to produce an exceedingly brief reduction in the mechanical properti of the workpiece in the zone of chip formation.

According to the data by A.Ya.Malkin (Fig.215), the heat resulting from the

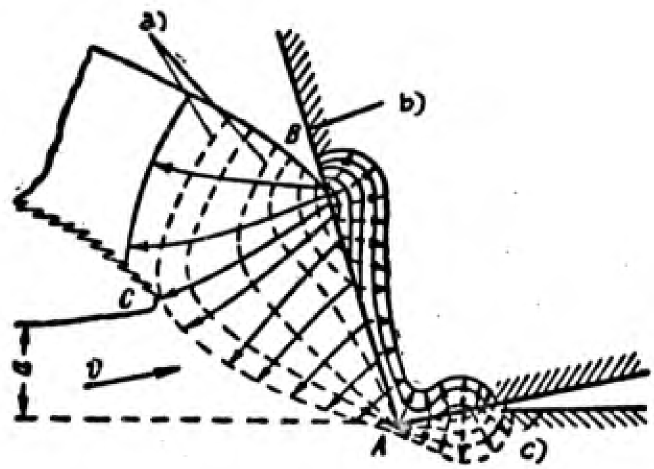

Fig.215 - Schematic of the Temperature Field in the Major Secant of the Plane, in the Machining of Metals

a) Isotherms of the temperature field (lines of equal temperature); b) Cutting edge; c) Machined surface

friction between the chip and the cutter face will cause the temperature in the segment AB to reach ~ 1000°C. In accordance with the law of heat exchange for the temperature field of a body limited on one side, a temperature of about 500°C may be expected in the zone ABC. The internal friction occurring as the result of deformation of layer of metal being removed, produces a rise of not less than 150 - 200°C in temperature in the zone ABC. As a result, the temperature of the chip coming off the tool face has to be not less than 650 - 700°C.

Since the amount of heat generated in the cutting process depends primarily upon the cutting speed v, the thickness of cut a, and the rake γ of the cutter (determining the position of the temperature field in the cutting process), a regulation of these factors will yield the desired temperature in the zone of chip formation.

Figure 216 illustrates these propositions of the Malkin hypothesis. Curve 3 expresses the relation between the cutting speed v and the life of the cutter T in

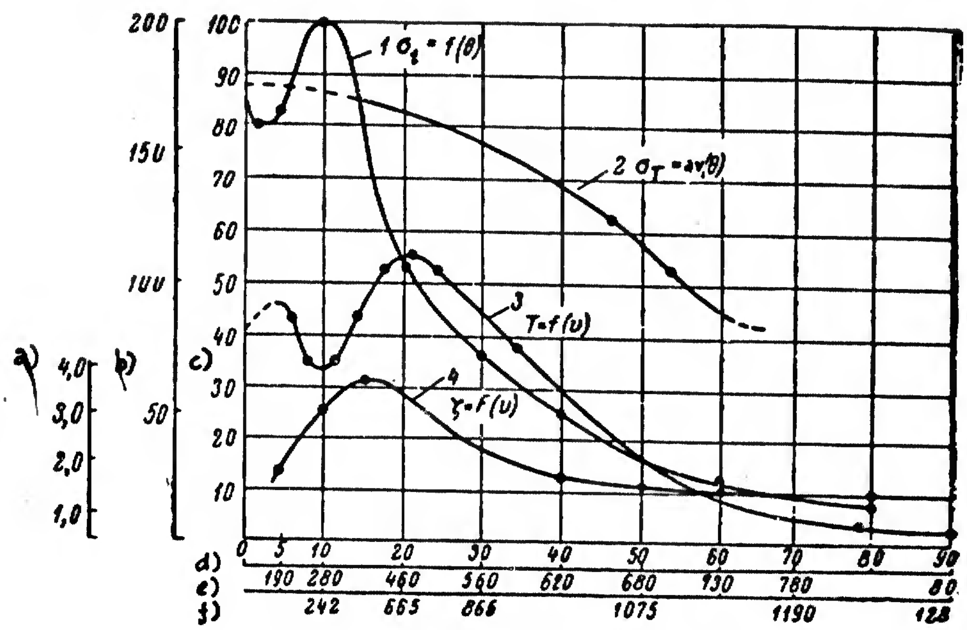

Fig.216 - Ratio of Cutting Speed to Tool Life in the Turning of Steel Tempered to H_{R_C} = 51 - 53. Data by A.Ya.Malkin

a) Longitudinal shrinkage of chip ξ; b) Tensile strength σ_t, kg/mm²; c) Tool life T, min; d) Cutting speed v, m/min; e) Chip temperature, °C; f) Temperature on cutter flanks, °C

the turning of hardened OKhN4M steel (H_{R_C} = 51 - 53) by tools tipped with VK8 alloy (h = 0.6 mm). Curves 1 and 2 describe the relation between the tensile strength σ_t of the steel and the strength σ_T of REN6 carbide on the one hand, and the heating temperatures θ and θ' on the other. The relation of the longitudinal shrinkage of the chip ξ to the cutting speed v is shown in curve 4.

The cutting speeds are laid off on the abscissa, and the chip temperatures θ and the tool flank temperatures corresponding to these cutting speeds are laid off on lines parallel to the abscissa. The temperature was measured with the aid of an optical pyrometer.

As we see, the cutting speed v = 10 m/min, at which the chip temperature is

θ = 300°C, corresponds to minimum tool life T and maximum tensile strength σ_t of the workpiece. A.Ya.Malkin believes that the tool life minimum is determined by the rise, at this temperature, of the σ_t strength of the work material.

Consequently, the Malkin hypothesis, like that of N.I.Shchelkonogov, is based on the concept that, under the influence of the heat generated in the cutting process, the layer removed loses its mechanical properties prior to being cut by the tool.

The erroneousness of this hypothesis is confirmed by the data of P.P.Grudov, E.I.Fel'dshtyen, the author, and other investigators. In fact, if the work were softened in the cutting zone, hardened steels of different degrees of hardness would have identical machinability since, upon heating to 700 - 800°C (which in Malkin's opinion is the temperature in the interval of onset of plastic deformation), these steels would differ little as to tensile strength and other mechanical properties.

Moreover, with an increase in cutting speed, the longitudinal shrinkage of the chip ξ should increase. However, as we see from Fig.216 (curve 4), it actually diminishes.

47. Relation Between Hardnesses of Work and Cutting Tool

As compared to the machining of ordinary (unhardened) steels, that of hardened steels is distinguished by a smaller difference in hardness between the material of the cutting tool and the material of the workpiece. In fact, in the machining with HSS tools of unhardened alloy steels of a hardness of $H_{R_C} \leq 30$ ($H_{Br} \leq 286$), the difference in hardness between the cutting tool (H_{R_C} = 64) and the work material is $H_{R_C} \geq 34$. When these steels are machined with cemented-carbide tools, this difference increases even further, attaining $H_{R_C} \geq 50$, for example, in the case of the hard alloy T15K6 (Bibl.50).

In the machining of hardened steels, the difference in hardness between the cutting tool and the work material diminishes to an insignificant level. In the case of the hardened alloy steels (H_{R_C} = 41 - 65) investigated by the author, the difference in hardness between tools tipped with T15K6 (H_{R_A} = 90 or H_{R_C} = 80) and the material of the workpiece varied from 39 to 15 units on the Rockwell C scale.

The experimental data presented in Chapters III and VIII demonstrate that the turning of steel C, tempered to H_{R_C} = 65, is performed successfully with tools tipped with any of the grades of carbide we have studied, including VK12, which is lowest in hardness H_{R_C} ≈ 73 (H_{R_A} = 86.5). Consequently, the hardness of VK12 tools exceeded that of the steel machined by only eight units on the Rockwell C scale. If we bear in mind the inaccuracy of readings on the Rockwell scale and in the Tables for conversion of hardness from one scale to another, it may be assumed that the difference in hardness was actually somewhat larger.

It is a question whether this difference in hardness between the tool and the material of the workpiece suffices for the cutting process to take place. This question arises with respect to steels hardened to high hardness, since in the cutting of ordinary and of hardened steels of only moderate hardness, the cutting tool is considerably harder than the work.

The difference in hardness noted ($H_{R_C} \geq 8$) pertains to the tool (VK12 carbide) and the work materials (hardened steel C) in their initial ("cold") condition, without consideration of the physical phenomena occurring in the cutting process. Due to thermal phenomena, the initial physical and mechanical properties of the tool and the work materials undergo specific changes in the cutting process. In our further reasoning, we proceeded from the proposition that high cutting temperature, leading to some reduction in the strength characteristics only of a very thin layer of work material, in contact with the tool face, does not, however, facilitate the conditions of work of the cutting edges. Their hardness, which diminishes under the action of the cutting temperature, must necessarily constantly exceed, in the cutting process, the initial hardness of the work material.

In the given instance, VK12 tools machined C steel, H_{R_C} = 65 at low speeds (v = 9 to 13 m/min at t = 0.5 mm and s = 0.14 mm/rev). The temperature in the cutting zone was low. Let us assume that it was 200°C. According to the data of N.F.Kazakov (Table 13), the hardness of the tool edges diminished in the cutting process from H_{R_A} = 86.5 to H_{R_A} = 80, corresponding to H_{R_C} = 64.

This unrealistic relation between the hardness of the tool (H_{R_C} = 64) and the work material (H_{R_C} = 65) in the cutting process is to be explained by the insufficient accuracy of the data of N.F.Kazakov, and also by the fact that the cutting temperature actually was apparently under 200°C. In any case, one may conclude that performance of the cutting process requires that the cutting tool must be somewhat harder than the work material.

At the same time, it must be noted that greater reliability attaches to the data of R.Kieffer and P.Schworzkopf than to those of N.F.Kazakov, and particularly those of A.I.Betaneli. If we proceed from the data of A.I.Betaneli (Table 13), we get even less probable results: the hardness of the work material H_{R_C} = 65, and the hardness of the cutting edge of the tool H_{R_C} = 54 (H_{R_A} = 76). Yet, a machining process actually took place.

From the data of Kieffer and Schworzkopf it would follow that in this instance the hardness of the tool material was H_{R_C} = 72 (H_{R_A} = 84).

In conclusion it should be noted that the machining of steels brought to high hardness has posed an interesting question with respect to the relationship between the hardness of the work material and the tool in the cutting process. The elaboration of this problem will demand further research.

APPENDIX

TURNING, END MILLING, DRILLING, ROUGH AND FINISH REAMING, AND THREAD CUTTING PRACTICE FOR HARDENED CONSTRUCTIONAL ALLOY STEELS

APPENDIX I

Table 1

Cutting Speeds, Cutting Forces and Effective Power in the Turning of Hardened Constructional Alloy Steels of H_{RC} = 38 with Tools Tipped with T15K6 Carbide

Tool shape: $\alpha = 15^\circ$ for $s \leq 0.2$ mm/rev, $\alpha = 10^\circ$ for $s > 0.2$ mm/rev; $\gamma = 0^\circ$, $\lambda = 0^\circ$, $\varphi = 45^\circ$, $\varphi_1 = 15^\circ$, r = 1 mm. Tool lapped with boron carbide.

a)	b)	c) 0,05	0,10	0,15	0,20	0,30	0,40	0,50	0,60	0,70	0,80
v_{60} in m/min	0,1	343	254	208	184	154	—	—	—	—	—
P_z in Kg		3	6	7	9	12	—	—	—	—	—
N_e in kw		0,17	0,25	0,24	0,28	0,30	—	—	—	—	—
v_{60} in m/min	0,2	288	212	175	154	12	—	—	—	—	—
P_z in Kg		6	9	13	17	23	—	—	—	—	—
N_e in kw		0,28	0,31	0,37	0,43	0,48	—	—	—	—	—
v_{60} in m/min	0,3	259	193	159	139	116	—	—	—	—	—
P_z in Kg		7	14	18	24	32	—	—	—	—	—
N_e in kw		0,31	0,44	0,48	0,54	0,61	—	—	—	—	—
v_{60} in m/min	0,5	—	170	140	122	102	90	—	—	—	—
P_z in Kg		—	21	30	38	52	65	—	—	—	—
N_e in kw		—	0,59	0,68	0,76	0,86	0,96	—	—	—	—
v_{60} in m/min	0,8	—	151	124	109	91	80	—	—	—	—
P_z in Kg		—	32	45	57	78	98	—	—	—	—
N_e in kw		—	0,81	0,92	1,01	1,16	1,28	—	—	—	—
v_{60} in m/min	1,0	—	143	117	102	86	76	69	—	—	—
P_z in Kg		—	40	56	70	95	120	143	—	—	—
N_e in kw		—	0,92	1,07	1,17	1,35	1,49	1,60	—	—	—
v_{60} in m/min	1,5	—	—	106	93	78	69	61	—	—	—
P_z in Kg		—	—	80	101	137	173	206	—	—	—
N_e in kw		—	—	1,38	1,52	1,73	1,95	2,06	—	—	—
v_{60} in m/min	2,0	—	—	—	85	71	63	58	53	—	—
P_z in Kg		—	—	—	132	178	224	267	310	—	—
N_e in kw		—	—	—	1,82	2,06	2,28	2,54	2,69	—	—
v_{60} in m/min	2,5	—	—	—	81	69	60	54	50	46	—
P_z in Kg		—	—	—	159	217	273	324	375	426	—
N_e in kw		—	—	—	2,12	2,42	2,67	2,82	3,06	3,22	—
v_{60} in m/min	3,0	—	—	—	—	65	58	51	48	44	41
P_z in Kg		—	—	—	—	255	323	383	445	503	565
N_e in kw		—	—	—	—	2 70	3,02	3,16	3,45	3,60	3,80

a) Characteristic; b) Depth of cut t, mm; c) Feed s, mm/rev

Table 2

Cutting Speeds, Cutting Forces and Effective Power in the Turning of Hardened Constructional Alloy Steels of $H_{R_C} = 41$ with Tools Tipped with T15K6 Carbide

Cutter shape: $\alpha = 15^\circ$ for $s \leq 0.2$ mm/rev, $\alpha = 10^\circ$ for $S > 0.2$ mm/rev; $\gamma = 0^\circ$, $\lambda = 0^\circ$, $\varphi = 45^\circ$, $\varphi_1 = 15^\circ$, r = 1 mm. Cutter lapped with boron carbide.

a)	b)	c)									
		0,05	0,10	0,15	0,20	0,30	0,40	0,50	0,60	0,70	0,80
v_{60} in m/min	0,1	274	203	167	147	123	—	—	—	—	—
P_z in Kg		3	6	8	10	13	—	—	—	—	—
N_e in Kw		0,14	0,20	0,22	0,24	0,26	—	—	—	—	—
v_{60} in m/min	0,2	230	170	140	123	103	—	—	—	—	—
P_z in Kg		6	10	14	18	25	—	—	—	—	—
N_e in Kw		0,23	0,27	0,32	0,36	0,42	—	—	—	—	—
v_{60} in m/min	0,3	207	154	127	111	93	—	—	—	—	—
P_z in Kg		8	15	20	26	35	—	—	—	—	—
N_e in Kw		0,27	0,38	0,42	0,47	0,53	—	—	—	—	—
v_{60} in m/min	0,5	—	136	112	98	82	72	—	—	—	—
P_z in Kg		—	23	32	41	56	70	—	—	—	—
N_e in Kw		—	0,51	0,59	0,66	0,75	0,83	—	—	—	—
v_{60} in m/min	0,8	—	121	99	87	73	64	—	—	—	—
P_z in Kg		—	35	49	62	84	106	—	—	—	—
N_e in Kw		—	0,70	0,80	0,88	1,01	1,11	—	—	—	—
v_{60} in m/min	1,0	—	114	94	82	69	61	55	—	—	—
P_z in Kg		—	43	60	76	103	130	154	—	—	—
N_e in Kw		—	0,80	0,93	1,02	1,17	1,30	1,39	—	—	—
v_{60} in m/min	1,5	—	—	85	74	62	55	49	—	—	—
P_z in Kg		—	—	86	109	148	187	222	—	—	—
N_e in Kw		—	—	1,20	1,32	1,50	1,69	1,79	—	—	—
v_{60} in m/min	2,0	—	—	—	68	57	50	46	42	—	—
P_z in Kg		—	—	—	142	192	242	288	334	—	—
N_e in Kw		—	—	—	1,58	1,79	1,98	2,18	2,30	—	—
v_{60} in m/min	2,5	—	—	—	65	55	48	43	40	37	—
P_z in Kg		—	—	—	172	234	295	350	405	460	—
N_e in Kw		—	—	—	1,84	2,11	2,32	2,46	2,66	2,80	—
v_{60} in m/min	3,0	—	—	—	—	52	46	41	38	35	33
P_z in Kg		—	—	—	—	275	348	413	480	543	610
N_e in Kw		—	—	—	—	2,35	2,63	2,74	3,00	3,12	3,30

a) Characteristic; b) Depth of cut t, mm; c) Feed s, mm/rev

Table 3

Cutting Speeds, Cutting Forces and Effective Power in the Turning of Hardened Constructional Alloy Steels of $H_{R_C} = 44$ with Tools Tipped with T15K6 Carbide

Cutter shape: $\alpha = 15^\circ$ for $s \leq 0.2$ mm/rev, $\alpha = 10^\circ$ for $s > 0.2$ mm/rev; $\gamma = -3^\circ$, $\lambda = 0^\circ$, $\varphi = 45^\circ$, $\varphi_1 = 15^\circ$, r = 1 mm. Cutter lapped with boron carbide.

a)	b)	c) 0,05	0,10	0,15	0,20	0,30	0,40	0,50	0,60	0,70	0,80
v_{60} in m/min	0,1	212	157	129	114	96	—	—	—	—	—
P_z in Kg		4	7	8	10	14	—	—	—	—	—
N_e in Kw		0,11	0,17	0,18	0,20	0,22	—	—	—	—	—
v_{60} in m/min	0,2	179	132	109	96	79	—	—	—	—	—
P_z in Kg		7	10	15	20	27	—	—	—	—	—
N_e in Kw		0,19	0,22	0,27	0,30	0,35	—	—	—	—	—
v_{60} in m/min	0,3	155	120	99	86	72	—	—	—	—	—
P_z in Kg		8	16	21	28	37	—	—	—	—	—
N_e in Kw		0,22	0,32	0,35	0,39	0,44	—	—	—	—	—
v_{60} in m/min	0,5	—	105	87	76	63	56	—	—	—	—
P_z in Kg		—	24	35	43	60	75	—	—	—	—
N_e in Kw		—	0,42	0,49	0,55	0,62	0,69	—	—	—	—
v_{60} in m/min	0,8	—	94	77	68	57	50	—	—	—	—
P_z in Kg		—	37	52	66	90	114	—	—	—	—
N_e in Kw		—	0,58	0,66	0,73	0,84	0,92	—	—	—	—
v_{60} in m/min	1,0	—	89	73	63	54	47	43	—	—	—
P_z in Kg		—	46	65	81	110	139	166	—	—	—
N_e in Kw		—	0,66	0,77	0,84	0,97	1,08	1,15	—	—	—
v_{60} in m/min	1,5	—	—	66	58	48	43	38	—	—	—
P_z in Kg		—	—	93	117	159	200	238	—	—	—
N_e in Kw		—	—	1,00	1,10	1,25	1,40	1,49	—	—	—
v_{60} in m/min	2,0	—	—	—	53	44	39	36	33	—	—
P_z in Kg		—	—	—	153	206	260	310	360	—	—
N_e in Kw		—	—	—	1,31	1,49	1,65	1,83	1,95	—	—
v_{60} in m/min	2,5	—	—	—	50	43	37	34	31	29	—
P_z in Kg		—	—	—	184	252	316	375	435	495	—
N_e in Kw		—	—	—	1,53	1,74	1,92	2,03	2,20	2,32	—
v_{60} in m/min	3,0	—	—	—	—	40	36	32	30	27	25
P_z in Kg		—	—	—	—	296	374	445	515	493	655
N_e in Kw		—	—	—	—	1,95	2,17	2,28	2,48	2,60	2,74

a) Characteristic; b) Depth of cut t, mm; c) Feed s in mm/rev

Table 4

Cutting Speeds, Cutting Forces and Effective Power in the Turning of Hardened Constructional Alloy Steels of $H_{R_C} = 47$ with Tools Tipped with T15K6 Carbide

Cutter shape: $\alpha = 15°$ for $s \leq 0.2$ mm/rev, $\alpha = 10°$ for $s > 0.2$ mm/rev; $\gamma = -3°$; $\lambda = 0°$; $\varphi = 45°$; $\varphi_1 = 15°$; $r = 1$ mm. Cutter lapped with boron carbide.

a)	b)	c) 0,05	0,10	0,15	0,20	0,30	0,40	0,50	0,60	0,70	0,80
v_{60} in m/min P_z in Kg N_e in Kw	0,1	185 4 0,12	137 7 0,16	112 9 0,17	100 11 0,18	83 15 0,21	— — —	— — —	— — —	— — —	— — —
v_{60} in m/min P_z in Kg N_e in Kw	0,2	155 7 0,18	114 11 0,21	95 16 0,25	83 21 0,29	68 29 0,32	— — —	— — —	— — —	— — —	— — —
v_{60} in m/min P_z in Kg N_e in Kw	0,3	140 9 0,21	104 18 0,31	86 22 0,31	75 30 0,37	62 40 0,41	— — —	— — —	— — —	— — —	— — —
$v_{1.0}$ in m/min P_z in Kg N_e in Kw	0,5	— — —	92 26 0,39	76 37 0,46	66 47 0,51	55 65 0,59	48 81 0,64	— — —	— — —	— — —	— — —
v_{60} in m/min P_z in Kg N_e in Kw	0,8	— — —	82 40 0,54	67 56 0,62	59 71 0,69	49 97 0,78	43 121 0,85	— — —	— — —	— — —	— — —
v_{60} in m/min P_z in Kg N_e in Kw	1,0	— — —	77 50 0,63	63 70 0,73	55 87 0,78	46 118 0,89	41 149 1,00	37 178 1,08	— — —	— — —	— — —
v_{60} in m/min P_z in Kg N_e in Kw	1,5	— — —	— — —	57 99 0,93	50 125 1,03	42 170 1;17	37 214 1,30	33 256 1,39	— — —	— — —	— — —
v_{60} in m/min P_z in Kg N_e in Kw	2,0	— — —	— — —	— — —	46 164 1,24	38 220 1,37	34 278 1,55	31 330 1,68	28 384 1,76	— — —	— — —
v_{60} in m/min P_z in Kg N_e in Kw	2,5	— — —	— — —	— — —	44 197 1,42	37 269 1,64	32 338 1,78	29 400 1,91	27 465 2,06	25 530 2,18	— — —
v_{60} in m/min P_z in Kg N_e in Kw	3,0	— — —	— — —	— — —	— — —	35 316 1,81	31 400 2,04	28 475 2,18	26 550 2,35	24 625 2,46	22 700 2,52

a) Characteristic; b) Depth of cut t, mm; c) Feed s in mm/rev

Table 5

Cutting Speeds, Cutting Forces, and Effective Power in the Turning of Hardened Constructional Alloy Steels of H_{R_C} = 50 with Tools Tipped with T15K6 Carbide

Cutter shape: $\alpha = 15^\circ$ for $s \leq 0.2$ mm/rev, $\alpha = 10^\circ$ for $s > 0.2$ mm/rev; $\gamma = -5^\circ$; $\lambda = 0^\circ$; $\varphi = 45$; $\varphi_1 = 15^\circ$; r = 1 mm. Cutter lapped with boron carbide.

a)	b)	c)									
		0,05	0,10	0,15	0,20	0,25	0,30	0,35	0,40	0,45	0,50
v_{60} in m/min	0,1	151	112	91	81	73	68	—	—	—	—
P_z in Kg		4	8	9	12	14	16	—	—	—	—
N_e in Kw		0,10	0,15	0,15	0,16	0,17	0,18	—	—	—	—
v_{60} in m/min	0,2	127	93	77	68	61	56	—	—	—	—
P_z in Kg		8	12	17	22	26	30	—	—	—	—
N_e in Kw		0,17	0,18	0,21	0,25	0,26	0,28	—	—	—	—
v_{60} in m/min	0,3	114	85	70	62	55	51	—	—	—	—
P_z in Kg		9	18	24	31	37	42	—	—	—	—
N_e in Kw		0,17	0,25	0,28	0,32	0,33	0,35	—	—	—	—
v_{60} in m/min	0,5	—	75	61	54	49	45	42	40	—	—
P_z in Kg		—	28	39	50	59	68	76	85	—	—
N_e in Kw		—	0,35	0,39	0,44	0,47	0,50	0,52	0,56	—	—
v_{60} in m/min	0,8	—	66	55	48	43	40	37	35	—	—
P_z in Kg		—	42	59	75	89	102	115	128	—	—
N_e in Kw		—	0,46	0,53	0,59	0,63	0,67	0,70	0,74	—	—
v_{60} in m/min	1,0	—	63	51	45	41	38	35	33	31	30
P_z in Kg		—	53	74	92	109	124	141	157	174	187
N_e in Kw		—	0,55	0,62	0,68	0,73	0,77	0,81	0,85	0,89	0,92
v_{60} in m/min	1,3	—	—	48	42	38	36	33	31	29	28
P_z in Kg		—	—	92	116	136	157	178	198	220	236
N_e in Kw		—	—	0,73	0,80	0,85	0,93	0,97	1,01	1,05	1,09
v_{60} in m/min	1,5	—	—	47	41	37	34	32	30	28	27
P_z in Kg		—	—	105	132	156	180	203	227	250	270
N_e in Kw		—	—	0,81	0,89	0,95	1,00	1,07	1,12	1,15	1,20
v_{60} in m/min	1,8	—	—	—	39	35	33	31	29	27	26
P_z in Kg		—	—	—	156	184	212	240	267	296	317
N_e in Kw		—	—	—	1,00	1,06	1,15	1,22	1,27	1,31	1,36
v_{60} in m/min	2,0	—	—	—	37	34	31	30	28	26	25
P_z in Kg		—	—	—	173	202	233	262	293	326	350
N_e in Kw		—	—	—	1,05	1,13	1,18	1,29	1,35	1,39	1,44

a) Characteristic; b) Depth of cut t, mm; c) Feed s in mm/rev

Table 6

Cutting Speeds, Cutting Forces, and Effective Power in the Turning of Hardened Constructional Alloy Steels of H_{RC} = 52 with Tools Tipped with T15K6 Carbide

Cutter shape: α = 15° for $s \leq 0.2$ mm/rev, α = 10° for $s > 0.2$ mm/rev; γ = -5°; λ = 0°; φ = 45°; φ_1 = 15°; r = 1 mm. Cutter lapped with boron carbide.

a)	b)	c)									
		0,05	0,10	0,15	0,20	0,25	0,30	0,35	0,40	0,45	0,50
v_{60} in m/min	0,1	134	99	81	72	65	60	—	—	—	—
P_z in Kg		4	8	10	12	15	16	—	—	—	—
N_e in Kw		0,09	0,13	0,13	0,14	0,16	0,16	—	—	—	—
v_{60} in m/min	0,2	112	83	68	60	54	50	—	—	—	—
P_z in Kg		8	12	18	23	27	32	—	—	—	—
N_e in Kw		0,15	0,16	0,20	0,23	0,24	0,26	—	—	—	—
v_{60} in m/min	0,3	105	75	62	54	49	45	—	—	—	—
P_z in Kg		10	19	25	33	38	43	—	—	—	—
N_e in Kw		0,17	0,23	0,25	0,29	0,31	0,32	—	—	—	—
v_{60} in m/min	0,5	—	66	55	48	43	40	37	35	—	—
P_z in Kg		—	29	41	52	62	71	80	89	—	—
N_e in Kw		—	0,31	0,37	0,41	0,44	0,47	0,49	0,51	—	—
v_{60} in m/min	0,8	—	59	48	43	38	35	33	31	—	—
P_z in Kg		—	44	62	78	93	107	121	135	—	—
N_e in Kw		—	0,43	0,49	0,55	0,58	0,62	0,66	0,69	—	—
v_{60} in m/min	1,0	—	56	46	40	36	34	32	30	28	27
P_z in Kg		—	55	77	96	114	130	148	165	182	196
N_e in Kw		—	0,51	0,58	0,63	0,67	0,73	0,78	0,82	0,84	0,87
v_{60} in m/min	1,3	—	—	43	37	34	32	29	28	26	25
P_z in Kg		—	—	96	122	143	164	187	208	230	247
N_e in Kw		—	—	0,68	0,74	0,80	0,86	0,89	0,96	0,98	1,01
v_{60} in m/min	1,5	—	—	41	36	33	30	28	27	25	24
P_z in Kg		—	—	110	138	163	188	212	237	262	282
N_e in Kw		—	—	0,74	0,82	0,88	0,93	0,98	1,05	1,08	1,11
v_{60} in m/min	1,8	—	—	—	34	31	99	27	25	24	23
P_z in Kg		—	—	—	163	192	222	250	279	310	332
N_e in Kw		—	—	—	0,91	0,98	1,06	1,10	1,15	1,22	1,26
v_{60} in m/min	2,0	—	—	—	33	30	28	26	24	23	22
P_z in Kg		—	—	—	181	211	244	274	306	340	366
N_e in Kw		—	—	—	0,98	1,04	1,12	1,17	1,21	1,28	1,32

a) Characteristic; b) Depth of cut t, mm; c) Feed s in mm/rev

Table 7

Cutting Speeds, Cutting Forces and Effective Power in the Turning of Hardened Constructional Alloy Steels of H_{RC} = 54 with Tools Tipped with T15K6 Carbide

Cutter shape: $\alpha = 15^{\circ}$ for $s < 0.2$ mm/rev, $\alpha = 10^{\circ}$ for $s > 0.2$ mm/rev; $\gamma = 7^{\circ}$; $\lambda = 0^{\circ}$; $\varphi = 45^{\circ}$; $\varphi_1 = 15^{\circ}$, r = 1 mm. Cutter lapped with boron carbide

a)	b)	c)									
		0,05	0,10	0,15	0,20	0,25	0,30	0,35	0,40	0,45	0,50
v_{60} in m/min	0,1	120	89	73	65	58	54	—	—	—	—
P_z in Kg		4	8	10	14	16	17	—	—	—	—
N_e in Kw		0,08	0,12	0,12	0,15	0,15	0,15	—	—	—	—
v_{60} in m/min	0,2	101	74	61	54	48	45	—	—	—	—
P_z in Kg		8	14	19	24	28	33	—	—	—	—
N_e in Kw		0,13	0,17	0,19	0,21	0,22	0,25	—	—	—	—
v_{60} in m/min	0,3	91	68	56	49	44	41	—	—	—	—
P_z in Kg		10	20	26	34	40	46	—	—	—	—
N_e in Kw		0,15	0,22	0,24	0,27	0,29	0,31	—	—	—	—
v_{60} in m/min	0,5	—	60	49	43	38	36	34	32	—	—
P_z in Kg		—	30	43	54	64	74	82	92	—	—
N_e in Kw		—	0,30	0,35	0,38	0,40	0,44	0,46	0,48	—	—
v_{60} in m/min	0,8	—	53	43	38	34	32	30	28	—	—
P_z in Kg		—	46	64	81	97	111	125	140	—	—
N_e in Kw		—	0,40	0,45	0,51	0,54	0,58	0,62	0,65	—	—
v_{60} in m/min	1,0	—	50	41	36	32	30	28	26	25	24
P_z in Kg		—	57	80	100	118	135	154	171	189	203
N_e in Kw		—	0,47	0,54	0,59	0,62	0,67	0,71	0,73	0,78	0,80
v_{60} in m/min	1,3	—	—	38	33	30	28	26	25	24	23
P_z in Kg		—	—	100	126	148	170	193	216	238	256
N_e in Kw		—	—	0,62	0,68	0,73	0,78	0,83	0,89	0,94	0,97
v_{60} in m/min	1,5	—	—	37	32,5	29	27	25	24	23	22
P_z in Kg		—	—	114	144	169	195	220	246	272	292
N_e in Kw		—	—	0,69	0,77	0,81	0,87	0,91	0,97	1,03	1,06
v_{60} in m/min	1,8	—	—	—	31	28	26	24,5	23	21,5	20,5
P_z in Kg		—	—	—	169	199	230	260	290	321	344
N_e in Kw		—	—	—	0,86	0,92	0,99	1,05	1,09	1,13	1,16
v_{60} in m/min	2,0	—	—	—	30	27	25	24	22	21	20,5
P_z in Kg		—	—	—	187	219	253	284	318	352	380
N_e in Kw		—	—	—	0,92	0,97	1,04	1,12	1,15	1,21	1,28

a) Characteristic; b) Depth of cut t, mm; c) Feed s in mm/rev

Table 8

Cutting Speeds, Cutting Forces and Effective Power in the Turning of Hardened Constructional Alloy Steels of H_{RC} = 56 with Tools Tipped with T15K6 Carbide

Cutter shape: $\alpha = 15^\circ$ for $s < 0.2$ mm/rev, $\alpha = 10^\circ$ for $s > 0.2$ mm/rev; $\gamma = -7^\circ$; $\lambda = 0^\circ$; $\varphi = 45^\circ$; $\varphi_1 = 15^\circ$; r = 1 mm. Cutter lapped with boron carbide

a)	b)	c)									
		0,05	0,10	0,15	0,20	0,25	0,30	0,35	0,40	0,45	0,50
v_{60} in m/min	0,1	110	82	67	59	53	49	—	—	—	—
P_z in Kg		4	8	10	13	16	18	—	—	—	—
N_e in Kw		0,07	0,11	0,11	0,13	0,14	0,14	—	—	—	—
v_{60} in m/min	0,2	92	68	56	49	44	41	—	—	—	—
P_z in Kg		8	13	19	25	30	34	—	—	—	—
N_e in Kw		0,12	0,15	0,18	0,20	0,22	0,23	—	—	—	—
v_{60} in m/min	0,3	83	62	51	44	40	37	—	—	—	—
P_z in Kg		10	21	27	35	41	47	—	—	—	—
N_e in Kw		0,14	0,21	0,23	0,25	0,27	0,29	—	—	—	—
v_{60} in m/min	0,5	—	55	45	39	35	33	31	29	—	—
P_z in Kg		—	31	44	56	66	77	85	96	—	—
N_e in Kw		—	0,28	0,33	0,36	0,38	0,42	0,43	0,46	—	—
v_{60} in m/min	0,8	—	48	40	35	31	29	27	25,5	—	—
P_z in Kg		—	47	66	84	99	115	129	144	—	—
N_e in Kw		—	0,37	0,43	0,48	0,51	0,55	0,57	0,60	—	—
v_{60} in m/min	1,0	—	46	38	33	29	27,5	26	24	23	22
P_z in Kg		—	59	82	103	122	140	159	176	196	210
N_e in Kw		—	0,44	0,51	0,56	0,58	0,63	0,68	0,70	0,74	0,76
v_{60} in m/min	1,3	—	—	35	30	28	26	24	22,5	21,5	20,5
P_z in Kg		—	—	103	131	153	176	200	224	247	265
N_e in Kw		—	—	0,59	0,65	0,70	0,75	0,79	0,83	0,87	0,89
v_{60} in m/min	1,5	—	—	34	29,5	26,5	25	23	22	20,5	19,5
P_z in Kg		—	—	117	148	175	202	228	254	280	303
N_e in Kw		—	—	0,65	0,72	0,76	0,83	0,86	0,92	0,94	0,97
v_{60} in m/min	1,8	—	—	—	28	25,5	23,5	22,5	21	20	19
P_z in Kg		—	—	—	175	206	238	269	300	332	356
N_e in Kw		—	—	—	0,81	0,86	0,92	1,00	1,03	1,09	1,11
v_{60} in m/min	2,0	—	—	—	27	25	23	22	20	19	18,5
P_z in Kg		—	—	—	194	226	262	294	328	364	392
N_e in Kw		—	—	—	0,86	0,93	0,99	1,06	1,08	1,14	1,19

a) Characteristic; b) Depth of cut t, mm; c) Feed s in mm/rev

Table 9

Cutting Speeds, Cutting Forces and Effective Power in the Turning of Hardened Constructional Alloy Steels of $H_{R_C} = 58$ with Tools Tipped with T15K6 Carbide

Cutter shape: $\alpha = 15°$ for $s < 0.2$ mm/rev, $\alpha = 10°$ for $s > 0.2$ mm/rev; $\gamma = -7°$; $\lambda = 0°$; $\varphi = 45°$; $\varphi_1 = 15°$; $r = 1$ mm. Cutter lapped with boron carbide.

a)	b)	c)										
		0,05	0,07	0,10	0,12	0,15	0,17	0,20	0,22	0,25	0,27	0,30
v_{60} in m/min	0,1	99	86	73	67	60	57	53	51	48	46	44,5
P_z in Kg		5	6	9	11	11	12	14	15	15	17	18
N_e in Kw		0,08	0,09	0,11	0,11	0,11	0,11	0,12	0,12	0,12	0,13	0,13
v_{60} in m/min	0,2	84	74	62	56	51	48	45	42,5	40	38,5	37
P_z in Kg		9	12	14	17	20	21	26	27	30	32	35
N_e in Kw		0,12	0,14	0,14	0,15	0,17	0,17	0,19	0,19	0,20	0,20	0,21
v_{60} in m/min	0,3	75	65	56	50	46	44	40	38	36	35	33,5
P_z in Kg		11	15	21	23	27	30	37	38	43	46	49
N_e in Kw		0,13	0,16	0,19	0,19	0,20	0,22	0,24	0,24	0,26	0,27	0,27
v_{60} in m/min	0,4	—	60	51	46	43	40	37	36	34	32	31
P_z in Kg		—	20	26	30	36	39	47	50	55	59	64
N_e in Kw		—	0,20	0,22	0,23	0,25	0,26	0,29	0,29	0,31	0,31	0,33
v_{60} in m/min	0,5	—	—	49	44	41	38	35	33	32	30,5	29,5
P_z in Kg		—	—	32	36	45	48	57	60	67	72	79
N_e in Kw		—	—	0,26	0,26	0,30	0,30	0,33	0,33	0,35	0,36	0,38
v_{60} in m/min	0,6	—	—	47	43	39	37	34	32	30	29	28,5
P_z in Kg		—	—	38	42	53	57	66	71	79	85	91
N_e in Kw		—	—	0,29	0,30	0,34	0,35	0,37	0,37	0,39	0,40	0,43
v_{60} in m/min	0,7	—	—	45	41	38	35	33	31	29,5	28,5	27,5
P_z in Kg		—	—	44	50	57	66	78	84	90	97	106
N_e in Kw		—	—	0,33	0,34	0,36	0,38	0,42	0,43	0,44	0,45	0,48
v_{60} in m/min	0,8	—	—	44	39	36	34	32	30	28	27	26,5
P_z in Kg		—	—	49	58	68	76	87	96	107	113	119
N_e in Kw		—	—	0,36	0,37	0,40	0,43	0,45	0,47	0,49	0,50	0,52
v_{60} in m/min	0,9	—	—	43	38,5	35,5	33	30	29	28	27	26
P_z in Kg		—	—	56	62	76	84	97	103	114	122	132
N_e in Kw		—	—	0,39	0,39	0,44	0,45	0,48	0,49	0,53	0,54	0,56
v_{60} in m/min	1,0	—	—	41,5	37	34	32	30	28	27	26	25
P_z in Kg		—	—	61	69	85	91	107	114	126	134	144
N_e in Kw		—	—	0,42	0,42	0,47	0,48	0,53	0,53	0,56	0,57	0,59

a) Characteristic; b) Depth of cut t, mm; c) Feed s in mm/rev

Table 10

Cutting Speeds, Cutting Forces and Effective Power in the Turning of Hardened Constructional Alloy Steels of $H_{R_C} = 60$ with Tools Tipped with T15K6 Carbide.

Cutter shape: $\alpha = 15^{o}$ for $s \leq 0.2$ mm/rev, $\alpha = 10^{o}$ for $s > 0.2$ mm/rev; $\gamma = -10^{o}$; $\lambda = 0^{o}$; $\varphi = 45^{o}$; $\varphi_1 = 15^{o}$; $r = 1$ mm. Cutter lapped with boron carbide.

a)	b)	c)										
		0,05	0,07	0,10	0,12	0,15	0,17	0,20	0,22	0,25	0,27	0,30
v_{60} in m/min P_z in Kg N_e in Kw	0,1	86 5 0,07	74 6 0,07	64 10 0,10	57 11 0,10	52 11 0,10	49 13 0,10	46 14 0,11	44 16 0,11	41 16 0,11	40 17 0,11	38,5 19 0,12
v_{60} in m/min P_z in Kg N_e in Kw	0,2	72 10 0,12	62 13 0,12	53 14 0,12	45 17 0,13	44 21 0,15	42 22 0,15	38,5 27 0,17	36,5 29 0,17	34,5 32 0,18	33,5 33 0,18	32 37 0,20
v_{60} in m/min P_z in Kg N_e in Kw	0,3	65 11 0,12	56 16 0,15	48 22 0,17	44 24 0,17	40 29 0,19	38 32 0,20	35 38 0,22	33 40 0,22	31 44 0,23	30 47 0,23	29 51 0,25
v_{60} in m/min P_z in Kg N_e in Kw	0,4	— — —	52 21 0,18	45 27 0,20	40 32 0,21	37 38 0,23	35 41 0,24	32 49 0,26	31 52 0,27	29 57 0,27	28 62 0,29	27 67 0,30
v_{60} in m/min P_z in Kg N_e in Kw	0,5	— — —	— — —	42 33 0,23	38 38 0,24	35 48 0,28	33 51 0,28	31 60 0,30	29 63 0,30	28 70 0,32	26,5 74 0,32	25,5 82 0,34
v_{60} in m/min P_z in Kg N_e in Kw	0,6	— — —	— — —	40 40 0,26	37 44 0,27	34 55 0,31	31 60 0,31	29 70 0,33	28 74 0,34	26 82 0,35	25 89 0,37	24,5 95 0,38
v_{60} in m/min P_z in Kg N_e in Kw	0,7	— — —	— — —	39 46 0,30	35 52 0,30	33 60 0,32	30,5 70 0,35	28 81 0,37	27 87 0,38	25,5 95 0,40	24,5 102 0,41	24 111 0,44
v_{60} in m/min P_z in Kg N_e in Kw	0,8	— — —	— — —	38 51 0,32	34 60 0,34	31 71 0,36	29 81 0,39	27 90 0,40	26 100 0,43	24 111 0,44	23,5 117 0,45	23 12[illegible] 0,47
v_{60} in m/min P_z in Kg N_e in Kw	0,9	— — —	— — —	37 59 0,35	33 65 0,35	30,5 79 0,39	28,5 87 0,41	26 101 0,43	25 108 0,44	23,5 118 0,45	23 126 0,48	22,5 137 0,51
v_{60} in m/min P_z in Kg N_e in Kw	1,0	— — —	— — —	36 63 0,37	32 71 0,37	29 89 0,42	28 95 0,44	25,5 111 0,46	24,5 119 0,48	23 131 0,50	22,5 139 0,52	21,5 150 0,53

a) Characteristic; b) Depth of cut t, mm; c) Feed s in mm/rev

Table 11

Cutting Speeds, Cutting Forces and Effective Power in the Turning of Hardened Constructional Alloy Steels of H_{R_C} = 62 with Tools Tipped with T15K6 Carbide

Cutter shape: $\alpha = 15^\circ$ for $s \geq 0.2$ mm/rev, $\alpha = 10^\circ$ for $s > 0.2$ mm/rev; $\gamma = -10^\circ$; $\lambda = 0^\circ$; $\varphi = 45^\circ$; $\varphi_1 = 15^\circ$; r = 1 mm. Cutter lapped with boron carbide.

a)	b)	c)										
		0,05	0,07	0,10	0,12	0,15	0,17	0,20	0,22	0,25	0,27	0,30
v_{60} in m/min	0,1	48	42	36	32	29	28	26	24,5	23	22	21,5
P_z in Kg		5	7	10	12	12	14	16	17	17	19	21
N_e in Kw		0,04	0,05	0,06	0,06	0,06	0,06	0,07	0,07	0,07	0,07	0,08
v_{60} in m/min	0,2	41	35	30	27	24,5	23	22	20,5	19,5	18,5	17,5
P_z in Kg		10	14	16	19	23	21	30	31	35	37	40
N_e in Kw		0,07	0,08	0,08	0,08	0,09	0,09	0,11	0,11	0,11	0,11	0,12
v_{60} in m/min	0,3	36	31,5	27	24	22	21	19,5	18,5	17,5	17	16
P_z in Kg		12	17	24	26	31	35	42	43	49	52	56
N_e in Kw		0,07	0,09	0,10	0,10	0,11	0,12	0,13	0,13	0,14	0,15	0,15
v_{60} in m/min	0,4	—	29	25	22,5	21	19,5	18	17	16	15,5	15
P_z in Kg		—	23	30	35	42	45	54	57	62	68	73
N_e in Kw		—	0,11	0,12	0,13	0,14	0,14	0,16	0,16	0,16	0,17	0,18
v_{60} in m/min	0,5	—	—	24	21,5	19,5	18,5	17	16	15,5	15	14
P_z in Kg		—	—	37	43	52	55	66	69	76	82	90
N_e in Kw		—	—	0,15	0,15	0,16	0,17	0,18	0,18	0,19	0,20	0,21
v_{60} in m/min	0,6	—	—	22,5	20,5	19	17,5	16	15,5	14,5	14	13,5
P_z in Kg		—	—	43	49	61	66	76	81	90	97	104
N_e in Kw		—	—	0,16	0,16	0,19	0,19	0,20	0,21	0,21	0,22	0,23
v_{60} in m/min	0,7	—	—	22	20	18,5	17	15,5	15	14	13,5	13
P_z in Kg		—	—	50	57	66	76	88	95	104	111	121
N_e in Kw		—	—	0,18	0,19	0,20	0,21	0,22	0,23	0,24	0,25	0,26
v_{60} in m/min	0,8	—	—	21	19	17,5	16,5	15	14,5	13,5	13	12,5
P_z in Kg		—	—	55	66	78	88	99	109	121	128	135
N_e in Kw		—	—	0,19	0,21	0,22	0,24	0,24	0,26	0,27	0,27	0,28
v_{60} in m/min	0,9	—	—	20,5	18,5	17	16	14,5	14	13	12,5	12
P_z in Kg		—	—	64	71	87	95	111	118	130	138	150
N_e in Kw		—	—	0,22	0,22	0,24	0,25	0,26	0,27	0,28	0,28	0,30
v_{60} in m/min	1,0	—	—	20	18	16,5	15,5	14	13,5	13	12,5	12
P_z in Kg		—	—	69	78	97	104	121	130	144	152	164
N_e in Kw		—	—	0,23	0,23	0,26	0,26	0,28	0,29	0,31	0,31	0,32

a) Characteristic; b) Depth of cut t, mm; c) Feed s in mm/rev

Table 12

Cutting Speeds, Cutting Forces and Effective Power in the Turning of Hardened Constructional Alloy Steels of H_{R_C} = 65 with Tools Tipped with T15K6 Carbide

Cutter shape: $\alpha = 15°$ for $s \leq 0.2$ mm/rev, $\alpha = 10°$ for $s > 0.2$ mm/rev; $\gamma = -10°$; $\lambda = 0°$; $\varphi = 45°$; $\varphi_1 = 15°$; r = 1 mm. Cutter lapped with boron carbide.

a)	b)	c)										
		0,05	0,07	0,10	0,12	0,15	0,17	0,20	0,22	0,25	0,27	0,30
v_{60} in m/min	0,1	19,2	16,6	14,2	12,9	11,7	11,1	10,3	9,7	9,3	8,9	8,6
P_z in kg		6	8	12	14	14	16	18	20	20	22	24
N_e in kW		0,02	0,02	0,03	0,03	0,03	0,03	0,03	0,03	0,03	0,03	0,03
v_{60} in m/min	0,2	16,2	14,0	11,9	10,8	9,8	9,3	8,6	8,2	7,7	7,4	7,1
P_z in kg		12	16	18	22	26	28	34	36	40	42	46
N_e in kW		0,03	0,04	0,04	0,04	0,04	0,04	0,05	0,05	0,05	0,05	0,05
v_{60} in m/min	0,3	14,5	12,5	10,8	9,7	8,9	8,4	7,8	7,4	7,0	6,7	6,5
P_z in kg		14	20	28	30	36	40	48	50	56	60	64
N_e in kW		0,03	0,04	0,05	0,05	0,05	0,06	0,06	0,06	0,06	0,07	0,07
v_{60} in m/min	0,4	—	11,6	10,0	9,0	8,3	7,9	7,1	6,9	6,5	6,2	6,0
P_z in kg		—	26	34	40	48	52	62	66	72	78	84
N_e in kW		—	0,05	0,06	0,06	0,07	0,07	0,07	0,08	0,08	0,08	0,08
v_{60} in m/min	0,5	—	—	9,5	8,5	7,8	7,4	6,8	6,5	6,2	5,9	5,7
P_z in kg		—	—	42	48	60	64	76	80	88	94	104
N_e in kW		—	—	0,07	0,07	0,08	0,08	0,09	0,09	0,09	0,09	0,10
v_{60} in m/min	0,6	—	—	9,0	8,2	7,6	7,1	6,5	6,2	5,9	5,6	5,5
P_z in kg		—	—	50	56	70	76	88	94	104	112	120
N_e in kW		—	—	0,08	0,08	0,09	0,09	0,09	0,10	0,10	0,10	0,11
v_{60} in m/min	0,7	—	—	8,8	7,9	7,3	6,8	6,3	6,0	5,7	5,5	5,3
P_z in kg		—	—	58	66	76	88	102	110	120	128	140
N_e in kW		—	—	0,08	0,09	0,09	0,10	0,10	0,11	0,11	0,12	0,12
v_{60} in m/min	0,8	—	—	8,4	7,6	7,0	6,6	6,1	5,8	5,5	5,3	5,1
P_z in kg		—	—	64	76	90	102	114	126	140	148	156
N_e in kW		—	—	0,09	0,09	0,10	0,11	0,11	0,12	0,13	0,13	0,13
v_{60} in m/min	0,9	—	—	8,2	7,4	6,9	6,5	5,9	5,6	5,3	5,1	5,0
P_z in kg		—	—	74	82	100	110	128	136	150	160	174
N_e in kW		—	—	0,10	0,10	0,11	0,12	0,12	0,13	0,13	0,13	0,14
v_{60} in m/min	1,0	—	—	8,0	7,2	6,6	6,2	5,7	5,5	5,2	5,0	4,8
P_z in kg		—	—	80	90	112	120	140	150	166	176	190
N_e in kW		—	—	0,10	0,11	0,12	0,12	0,13	0,13	0,14	0,14	0,15

a) Characteristic; b) Depth of cut t, mm; c) Feed s in mm/rev

Clarifications With Respect to Machining Practice

The cutting speeds indicated in Tables 1 - 12 are calculated according to eqs.(5) and (7).

The $C_{v_{60}}$ values are presented on p.173. It is assumed that: $x_v = 0.25$, $y_v = 0.45$, $n_v = 3$ for steels of $H_{R_C} \leq 60$; $n_v = 19$ for steels of $H_{R_C} > 60$.

The cutting speeds pertain to a life of T = 60 min and to cutters tipped with T15K6 carbide, which are the type most widely used in the turning of steels.

For conditions of work differing from those indicated in Tables 1 - 12, the v_{60} cutting speed has to be multiplied by corrective coefficients K_T, K_u, K_φ, K_α and K_r, representing differences in tool life (Table 13), carbide (Table 14), and in the values of angle φ (Table 15), the angle α (Table 16), and the radius r (Table 17).

The cutting speed sought is thus determined from the equality

$$v = v_{60} \cdot K_T \cdot K_u \cdot K_\varphi \cdot K_\alpha \cdot K_r \ m/min.$$

When working on scale, the cutting speeds selected have to be multiplied by a factor of 0.75.

The cutting speeds are determined in accordance with eqs.(1) and (2).

It is assumed that: $n_{P_z} = 1.0$ for steels of $H_{R_C} = 38$ to 60 hardness and $n_{P_z} = 3.0$ for steels of hardness $H_{R_C} > 60$.

The effective powers are calculated by means of eq.(6).

These values of the C_N factor for hardened steels of various hardnesses are presented on p.173.

The cutting forces indicated in the tabulations of machining practice pertain to tools with "sharp" cutting edges, or with edges that have been insignificantly dulled. The cutting force increases with tool wear, and attains, at normal dulling, about a 50% higher value than at the start of cutting. Correspondingly, the effective power also rises 50% over the data given in the Tables.

Table 13

Factor of Correction K_T Relative to Tool Life

a)	b)									
	10	20	30	40	60	90	120	150	180	240
	c)									
0,20	1,43	1,24	1,15	1,08	1,00	0,92	0,86	0,82	0,80	0,75
0,125	1,25	1,14	1,09	1,05	1,00	0,95	0,91	0,88	0,86	0,84
0,10	1,19	1,11	1,06	1,04	1,00	0,96	0,93	0,91	0,90	0,87
0,07	1,13	1,08	1,05	1,03	1,00	0,97	0,95	0,94	0,92	0,91

a) Relative life index, m; b) Tool life T, in min; c) Value of factor K_T

Table 14

Factor of Correction K_u Relative to Carbide Use in Tipping Tool

Carbide	Factor K_u
T30K4	1,30
T15K6	1,00
VK2	0,88
VK3	0,88
VK6	0,68
T5K10	0,65
VK8	0,65

Table 15

Factor of Correction K_φ Relative to Complement of Side-Cutting-Edge Angle

Complement of side-cutting-edge angle φ^o	Value of Factor K_φ
15	1,22
30	1,07
45	1,00
60	0,96
75	0,94
90	0,93

Choice of Cutting Practice

The choice of the cutting practice in the turning of hardened steels is performed in the same manner as in the machining of unhardened steels by carbide tools (Bibl.27).

The oversize is determined by the machining error in the preceding operation

Table 16

Factor of Correction K_α Relative to Working Relief Angle of Tool

Working Relief Angle α^o	$s \leq 0.2$ mm/rev	$s > 0.2$ mm/rev
	Values of factor K	
15	1,00	—
10	0,91	1,00
6	0,87	0,95

Table 17

Factor of Correction K_r Relative to Tool Nose Radius

Tool nose radius r, mm	Value of Factor K_r
0,5	0,95
1,0	1,00
2,0	1,07

and by the distortion (hog) of the part due to hardening. The oversize should be as small as possible. However, in the case of hardened parts of alloy steels it is not infrequently 5 - 6 mm and more (in diameter).

The effort should be to work at the greatest possible depth of cut. In determining the depth of cut for the first roughing pass (when oversize is large), it is necessary to remove the scale remaining on the part after heat treatment in that single pass. In fine work, the finish pass should be done at a depth of cut t = 0.2 to 0.3 mm.

To reduce the machining time, it is desirable to work with the largest possible feed. A feed permissible in terms of engineering considerations is chosen in accordance with the required surface finish and tolerance, and also in accord with the rigidity of the system comprising the machine tool, the workpiece and the tool.

In turning hardened steels, relatively small feeds are employed. However, the selection of the proper equipment is of major importance here. A machine tool of the required rigidity, and a reliable fastening of the tool, are essential. To avoid vibrations, the tool should project as little as possible. The tool should be installed in the machine tool in such fashion that its tip is on the center line or beneath it by 1% of the diameter of the workpiece.

Tools must be lapped regardless of whether they are to be used for finishing or for roughing passes.

At v = 60 m/min and higher cutting speeds, chip-breakers should be used.

In the turning of hardened parts, chip of low cross section is removed, and therefore the machine tool needs comparatively little power. As may be seen from the machining practice tables, the effective power for the generally employed depths of cut, and feeds, are at the level of N_e = 1.0 to 2.0 kw*. At the same time, the need to machine with a machine tool - workpiece - tool system of high rigidity means that lathes of not less than 7 kw power should be used to turn hardened parts.

In working at even comparatively low cutting speeds, the machine tool has to be equipped with a rotating back center.

The turning of hardened steels falls into the category of finishing processes in which high surface qualities are required. In this connection, the final passes must be made at very low feeds so as to produce a surface comparable to rough-ground, and in some cases to finish-ground. For the major passes, the feed is chosen in accordance with the hardness of the material machined: the higher the hardness, the lower the feed.

It must, however, be borne in mind that high surface finish may be produced on high-hardness hardened steel with a larger feed than on steel of lower hardness.

The appropriate cutting speed is determined in accordance with the depths of cut and the feed shown in the tables of practice.

The turning of hardened steels is usually performed without lubricant.

In the machining of steel parts on which scale is present, cutters tipped with carbides VK8, VK6 and T5K10 are to be used.

---

*The power N required to drive the machine tool exceeds the actual output N_e. The required power is obtained by dividing N_e by the actual efficiency of the machine tool η:

$$N = \frac{N_e}{\eta}.$$

The η factor is always less than unity. In practice, where turning lathes are concerned, it may be taken that η = 0.75.

APPENDIX II

Table 1

Cutting Speeds, Feeds per Minute and Effective Outputs in the End Milling of Hardened Alloy Constructional Steels of H_{RC} = 38 by Mills Tipped with T15K6 Carbide. $\frac{B}{D}$ = 0.6.

Shape of Cutting Portion of Mill: $\alpha = 15^\circ$, $\gamma = -5^\circ$, $\lambda = 15^\circ$, $\varphi = 60^\circ$, $\varphi_1 = 5^\circ$

Cutting

D	z	B	s_z	1				2			
				v	n	s_m	N_e	v	n	s_m	N_e
75	4	45	0,09	159	680	245	1,15	134	570	205	1,95
			0,07	174	740	208	1,00	146	620	174	1,70
			0,05	190	805	161	0,85	159	680	136	1,40
			0,03	222	940	113	0,65	186	790	95	1,10
90	6	54	0,09	159	560	303	1,70	134	475	257	2,95
			0,07	174	620	262	1,50	146	520	219	2,60
			0,05	190	670	202	1,25	159	560	168	2,10
			0,03	222	785	141	0,95	186	660	120	1,60
110	8	66	0,09	159	460	332	2,25	134	390	280	3,90
			0,07	174	505	284	2,05	146	420	236	3,45
			0,05	190	550	220	1,70	159	460	184	2,85
			0,03	222	640	154	1,30	186	540	130	2,15
130	8	78	0,09	159	390	270	2,25	134	325	233	3,90
			0,07	174	425	239	2,05	146	355	199	3,45
			0,05	190	460	184	1,70	159	390	156	2,85
			0,03	222	540	130	1,30	186	450	108	2,15
150	10	90	0,09	159	340	306	2,80	134	285	256	4,90
			0,07	174	370	260	2,55	146	310	216	4,30
			0,05	190	400	200	2,10	159	340	170	3,55
			0,03	222	470	141	1,60	186	400	120	2,70
200	10	120	0,09	159	250	225	2,80	134	215	194	4,90
			0,07	174	280	196	2,55	146	235	165	4,30
			0,05	190	300	150	2,10	159	250	125	3,55
			0,03	222	350	105	1,60	186	300	90	2,70
250	12	150	0,09	159	200	216	3,40	134	170	183	5,90
			0,07	174	220	185	3,05	146	185	156	5,15
			0,05	190	240	144	2,50	159	200	120	4,25
			0,03	222	305	110	1,90	186	235	84	3,25

D = mill diameter in mm; z = number of teeth on mill; B = milling width, mm; s_z = feed per mill tooth, mm; v = cutting speed at mill life T = 300 min, in m/min; n = mill rpm; s_m = feed in mm/min; N_e = actual output in kw.

The correction factors for other conditions of mill operation are given in Tables 7 – 11, and on pp.428 and 430.

Table 1 (Cont'd)

Depth in mm							
3				4			
v	n	$s_{м}$	N_e	v	n	$s_{м}$	N_e
121	510	184	2,65	113	480	173	3,35
132	560	157	2,35	123	525	147	2,95
143	610	123	1,25	135	575	116	2,45
168	710	85	1,50	158	670	80	1,85
121	425	230	4,00	113	400	216	5,05
132	465	197	3,55	123	440	186	4,45
143	510	153	2,90	135	480	144	3,70
168	595	106	2,25	158	555	99	2,80
121	350	252	5,35	113	325	234	6,70
132	380	214	4,70	123	360	202	5,90
143	410	164	3,90	135	390	156	4,90
168	485	118	3,00	158	450	108	3,70
121	300	216	5,35	113	275	199	6,70
132	320	178	4,70	123	305	170	5,90
143	350	140	3,90	135	330	132	4,90
168	410	99	3,00	158	380	92	3,70
121	255	230	6,70	113	240	216	8,40
132	280	197	5,90	123	265	187	7,40
143	305	153	4,85	135	290	145	6,10
168	360	108	3,75	158	335	102	4,65
121	195	175	6,70	113	180	163	8,40
132	210	148	5,90	123	195	136	7,40
143	230	115	4,85	135	215	118	6,10
168	270	81	3,75	158	250	75	4,65
121	155	168	8,00	113	140	152	10,00
132	165	140	7,10	123	155	131	8,90
143	185	111	5,80	135	170	102	7,35
168	215	78	4,50	158	200	72	5,55

Table 2

Cutting Speeds, Feeds per Minute and Effective Outputs in the End Milling of Hardened Alloy Constructional Steels of $H_{R_C} = 44$ by Mills Tipped with T15K6 Carbide. $\frac{B}{D} = 0.6$.

Shape of Cutting Portion of Mill: $\alpha = 15^o$; $\gamma = -5^o$; $\lambda = 15^o$; $\varphi = 60^o$; $\varphi_1 = 5^o$.

D	z	B	s_z	Cutting 1 v	1 n	1 s_M	1 N_e	2 v	2 n	2 s_M	2 N_e
75	4	45	0,09	116	495	179	1,05	98	415	151	1,75
			0,07	127	540	152	0,90	107	455	127	1,55
			0,05	139	585	118	0,75	116	495	100	1,25
			0,03	162	685	83	0,60	136	575	70	1,00
90	6	54	0,09	116	410	222	1,55	98	350	187	2,70
			0,07	127	450	190	1,40	107	380	159	2,35
			0,05	139	490	147	1,15	116	410	123	2,00
			0,03	162	575	103	0,85	136	480	87	1,45
110	8	66	0,09	116	335	242	2,05	98	285	204	3,55
			0,07	127	370	208	1,85	107	310	172	3,15
			0,05	139	400	160	1,55	116	335	134	2,60
			0,03	162	470	112	1,15	136	395	94	1,95
130	8	78	0,09	116	285	205	2,05	98	240	173	3,55
			0,07	127	310	175	1,85	107	260	146	3,15
			0,05	139	335	135	1,55	116	285	113	2,60
			0,03	162	395	95	1,15	136	330	79	1,95
150	10	90	0,09	116	250	223	2,55	98	210	188	4,45
			0,07	127	270	190	2,30	107	225	158	3,90
			0,05	139	290	147	1,90	116	250	125	3,25
			0,03	162	340	103	1,45	136	290	88	2,45
200	10	120	0,09	116	185	165	2,55	98	155	141	4,45
			0,07	127	205	144	2,30	107	170	121	3,90
			0,05	139	220	110	1,90	116	185	91	3,25
			0,03	162	255	71	1,45	136	220	66	2,45
250	12	150	0,09	116	145	158	3,10	98	125	134	5,35
			0,07	127	160	135	2,80	107	135	114	4,70
			0,05	139	175	105	2,30	116	145	89	3,90
			0,03	162	220	80	1,75	136	170	62	2,95

See Table 1 for symbols and factors of correction.

Table 2 (Cont'd)

Depth in mm							
3				4			
v	n	s_M	N_e	v	n	s_M	N_e
88	370	135	2,40	83	350	127	3,05
97	410	115	2,15	90	385	106	2,70
104	445	90	1,75	99	420	84	2,20
123	520	63	1,35	115	490	59	1,70
88	310	168	3,65	83	290	157	4,60
97	340	142	3,20	90	320	136	4,05
104	370	112	2,65	99	350	105	3,35
123	435	78	2,05	115	405	72	2,55
88	255	184	4,85	83	240	170	6,10
97	280	156	4,20	90	260	148	5,35
104	300	120	3,55	99	285	114	4,45
123	355	86	2,70	115	330	78	3,35
88	220	157	4,85	83	200	145	6,10
97	230	131	4,20	90	225	124	5,35
104	255	103	3,55	99	240	96	4,45
123	300	72	2,70	115	280	67	3,35
88	185	168	6,10	83	175	158	7,65
97	205	143	5,35	90	195	137	6,75
104	220	112	4,40	99	210	107	5,55
123	260	80	3,40	115	245	75	4,25
88	140	123	6,10	83	130	119	7,65
97	155	107	5,35	90	140	100	6,75
104	170	84	4,40	99	155	79	5,55
123	200	60	3,40	115	185	55	4,25
88	115	123	7,30	83	100	111	9,10
97	120	102	6,45	90	115	96	8,10
104	135	81	5,25	99	125	75	6,70
123	155	57	4,10	115	145	53	5,05

Table 3

Cutting Speeds, Feeds per Minute and Effective Outputs in the End Milling of Hardened Alloy Constructional Steels of H_{RC} = 49 by Mills Tipped with T15K6 Carbide. $\frac{B}{D}$ = 0.6.

Shape of Cutting Portion of Mill: $\alpha = 15^o$; $\gamma = -10^o$; $\lambda = 15^o$; $\varphi = 60^o$; $\varphi_1 = 5^o$.

D	z	B	s_z	Cutting 1				2			
				v	n	$s_м$	N_e	v	n	$s_м$	N_e
75	4	45	0,09	89	378	136	0,95	75	318	115	1,60
			0,07	97	412	115	0,80	82	348	98	1,40
			0,05	106	450	90	0,70	89	378	76	1,15
			0,03	124	525	63	0,55	104	440	54	0,90
90	6	54	0,09	89	315	170	1,40	75	265	143	2,40
			0,07	97	342	144	1,20	82	290	121	2,10
			0,05	106	375	113	1,00	89	315	95	1,70
			0,03	124	438	78	0,75	104	368	66	1,30
110	8	66	0,09	89	258	186	1,85	75	216	156	3,15
			0,07	97	280	156	1,65	82	237	132	2,80
			0,05	106	306	122	1,40	89	258	104	2,30
			0,03	124	359	86	1,05	104	300	72	1,75
130	8	78	0,09	89	218	157	1,85	75	183	132	3,15
			0,07	97	238	133	1,65	82	200	112	2,80
			0,05	106	260	104	1,40	89	218	88	2,30
			0,03	124	304	73	1,05	104	255	61	1,75
150	10	90	0,09	89	189	170	2,30	75	159	143	4,00
			0,07	97	206	145	2,10	82	174	122	3,50
			0,05	106	225	113	1,70	89	189	95	2,90
			0,03	124	264	80	1,30	104	222	67	2,20
200	10	120	0,09	89	141	127	2,30	75	119	107	4,00
			0,07	97	154	107	2,10	82	130	91	3,50
			0,05	106	168	84	1,70	89	141	71	2,90
			0,03	124	197	59	1,30	104	165	50	2,20
250	12	150	0,09	89	113	121	2,75	75	95	102	4.80
			0,07	97	123	104	2,50	82	104	87	4,20
			0,05	106	135	81	2,00	89	113	67	3,45
			0,03	124	158	57	1,55	104	132	48	2,65

See Table 1 for symbols and factors of correction.

Table 3 (Cont'd)

Depth in mm							
3				4			
v	n	s_M	N_e	v	n	s_M	N_e
68	289	104	2,15	63	267	96	2,70
74	313	88	1,90	69	292	82	2,40
80	340	68	1,60	76	322	64	2,00
94	400	48	1,20	89	378	45	1,50
68	240	129	3,25	63	222	121	4,10
74	262	110	2,90	69	244	102	3,60
80	282	84	2,35	76	268	81	3,00
94	332	60	1,85	89	315	48	2,30
68	197	142	4,35	63	182	130	5,45
74	214	120	3,80	69	198	110	4,80
80	231	92	3,15	76	220	88	4,00
94	272	66	2,45	89	258	62	3,00
68	166	120	4,35	63	154	111	5,45
74	181	102	3,80	69	169	95	4,80
80	196	79	3,15	76	186	75	4,00
94	230	56	2,45	89	218	52	3,00
68	144	130	5,45	63	133	120	6,80
74	157	110	4,80	69	146	102	6,00
80	170	85	3,95	76	162	82	4,95
94	200	60	3,05	89	189	57	3,80
68	108	97	5,45	63	100	90	6,80
74	118	83	4,80	69	109	76	6,00
80	127	64	3,95	76	121	60	4,95
94	149	45	3,05	89	141	43	3,80
68	87	95	6,50	63	80	87	8,10
74	94	79	5,75	69	88	74	7,20
80	102	62	4,70	76	96	57	5,95
94	119	44	3,65	89	113	41	4,50

Table 4

Cutting Speeds, Feeds per Minute and Effective Outputs in the End Milling of Hardened Alloy Constructional Steels of $H_{R_C} = 54$ by Mills Tipped with T15K6 Carbide. $\frac{B}{D} = 0.6$.

Shape of Cutting Portion of Mill: $\alpha = 20^{\circ}$; $\gamma = -10^{\circ}$; $\lambda = 15^{\circ}$; $\varphi = 60^{\circ}$; $\varphi_1 = 5^{\circ}$.

D	z	B	s_z	Cutting 1 v	1 n	1 s_M	1 N_e	2 v	2 n	2 s_M	2 N_e
75	4	45	0,09	71	303	109	0,85	60	255	92	1,40
			0,07	78	332	93	0,73	66	280	79	1,25
			0,05	85	362	73	0,62	71	303	61	1,00
			0,03	101	430	52	0,48	84	358	43	0,80
90	6	54	0,09	71	252	136	1,25	60	213	115	2,15
			0,07	78	276	115	1,10	66	234	98	1,90
			0,05	85	301	90	0,90	71	252	76	1,55
			0,03	101	358	65	0,70	84	298	54	1,15
110	8	66	0,09	71	205	148	1,65	60	173	125	2,85
			0,07	78	225	126	1,50	66	190	106	2,50
			0,05	85	245	98	1,25	71	205	82	2,10
			0,03	101	292	70	0,95	84	242	58	1,55
130	8	78	0,09	71	174	125	1,65	60	147	106	2,85
			0,07	78	191	107	1,50	66	161	90	2,50
			0,05	85	208	83	1,25	71	174	69	2,10
			0,03	101	248	59	0,95	84	206	49	1,55
150	10	90	0,09	71	151	136	2,05	60	127	114	3,60
			0,07	78	166	116	1,85	66	140	98	3,15
			0,05	85	181	91	1,55	71	151	77	2,60
			0,03	101	215	64	1,15	84	179	53	2,00
200	10	120	0,09	71	113	102	2,05	60	96	86	3,60
			0,07	78	124	87	1,85	66	105	74	3,15
			0,05	85	135	67	1,55	71	113	56	2,60
			0,03	101	161	49	1,15	84	134	40	2,00
250	12	150	0,09	71	90	98	2,50	60	77	84	4,30
			0,07	78	100	84	2,25	66	84	70	3,75
			0,05	85	108	65	1,85	71	90	54	3,10
			0,03	101	128	47	1,40	84	107	39	2,40

See Table 1 for symbols and factors of correction.

Table 4 (Cont'd)

Depth in mm							
3				4			
v	n	s_M	N_e	v	n	s_M	N_e
55	234	84	1,95	51	216	77	2,45
60	255	72	1,70	55	234	65	2,15
64	272	55	1,40	61	260	52	1,80
76	323	39	1,10	71	303	37	1,35
55	195	105	2,90	51	181	97	3,70
60	213	89	2,60	55	195	82	3,25
64	227	68	2,10	61	216	65	2,70
76	270	49	1,65	71	252	45	2,05
55	159	114	3,90	51	147	106	4,90
60	173	97	3,45	55	159	89	4,30
64	185	74	2,85	61	176	70	3,60
76	220	53	2,20	71	205	49	2,70
55	135	97	3,90	51	125	90	4,90
60	147	82	3,45	55	135	76	4,30
64	157	63	2,85	61	149	60	3,60
76	186	45	2,20	71	174	41	2,70
55	117	105	4,90	51	108	98	6,15
60	127	89	4,30	55	117	83	5,40
64	136	68	3,55	61	129	64	4,45
76	162	48	2,75	71	151	45	3,40
55	88	80	4,90	51	81	73	6,15
60	96	68	4,30	55	88	61	5,40
64	101	51	3,55	61	97	49	4,45
76	121	36	2,75	71	113	34	3,40
55	70	76	5,85	51	65	70	7,30
60	77	65	5,20	55	70	60	6,50
64	82	49	4,25	61	77	46	5,35
76	97	35	3,30	71	90	33	4,05

Table 5

Cutting Speeds, Feeds per Minute and Effective Outputs in the End Milling of Hardened Alloy Constructional Steels of H_{RC} = 58 by Mills Tipped with T15K6 Carbide. $\frac{B}{D}$ = 0.6.

Shape of Cutting Portion of Mill: $\alpha = 20^\circ$; $\gamma = -15^\circ$; $\lambda = 15^\circ$; $\varphi = 60^\circ$; $\varphi_1 = 5^\circ$.

D	t	B	s_z	Cutting 1 v	1 n	1 s_M	1 N_e	2 v	2 n	2 s_M	2 N_e
75	4	45	0,09	57	242	87	0,80	48	204	73	1,35
			0,07	63	268	75	0,69	53	225	63	1,15
			0,05	68	288	58	0,59	57	242	48	0,97
			0,03	80	340	41	0,45	67	285	34	0,76
90	6	54	0,09	57	202	110	1,15	48	170	91	2,00
			0,07	63	223	93	1,05	53	188	79	1,80
			0,05	68	241	72	0,86	57	202	61	1,45
			0,03	80	284	51	0,66	67	237	43	1,10
110	8	66	0,09	57	165	119	1,55	48	138	100	2,70
			0,07	63	182	102	1,40	53	153	86	2,40
			0,05	68	196	78	1,15	57	165	66	1,95
			0,03	80	231	56	0,90	67	193	46	1,50
130	8	78	0,09	57	140	101	1,55	48	118	85	2,70
			0,07	63	154	87	1,40	53	130	73	2,40
			0,05	68	166	67	1,15	57	140	56	1,95
			0,03	80	196	47	0,90	67	164	40	1,50
150	10	90	0,09	57	121	87	1,95	48	102	74	3,40
			0,07	63	134	75	1,75	53	112	63	2,95
			0,05	68	145	58	1,45	57	121	49	2,45
			0,03	80	170	41	1,10	67	142	34	1,85
200	10	120	0,09	57	91	83	1,95	48	77	70	3,40
			0,07	63	100	70	1,75	53	84	59	2,95
			0,05	68	108	54	1,45	57	91	46	2,45
			0,03	80	127	38	1,10	67	107	33	1,85
250	12	150	0,09	57	73	79	2,35	48	61	66	4,05
			0,07	63	80	69	2,10	53	67	57	3,55
			0,05	68	87	53	1,70	57	73	44	2,95
			0,03	80	102	37	1,30	67	85	31	2,25

See Table 1 for symbols and factors of correction.

Table 5 (Cont'd)

Depth in mm							
3				4			
v	n	s_M	N_p	v	n	s_M	N_n
44	187	67	1,85	41	174	63	2,30
48	204	57	1,60	44	187	53	2,05
52	221	44	1,35	49	208	41	1,70
61	260	31	1,05	57	242	29	1,30
44	156	78	2,75	41	145	78	3,50
48	170	72	2,45	44	156	66	3,10
52	184	55	2,00	49	174	53	2,55
61	216	39	1,55	57	202	36	1,95
44	127	91	3,70	41	118	83	4,60
48	138	77	3,25	44	127	71	4,05
52	150	60	2,70	49	141	55	3,40
61	176	42	2,10	57	165	40	2,55
44	108	77	3,70	41	100	72	4,60
48	147	65	3,25	44	108	61	4,05
52	127	51	2,70	49	120	48	3,40
61	149	36	2,10	57	140	33	2,55
44	83	67	4,60	41	87	63	5,80
48	102	57	4,05	44	93	52	5,10
52	111	45	3,35	49	104	42	4,20
61	130	31	2,60	57	121	29	3,20
44	70	63	4,60	41	65	59	5,80
48	77	54	4,05	44	70	49	5,10
52	83	41	3,35	49	78	39	4,20
61	97	29	2,60	57	91	28	3,20
44	56	61	5,50	41	52	57	6,90
48	61	51	4,90	44	56	48	6,15
52	66	41	4,00	49	62	38	5,10
61	78	28	3,10	57	73	27	3,80

Table 6

Cutting Speeds, Feeds per Minute and Effective Outputs in the End Milling of Hardened Alloy Constructional Steels of $H_{R_C} = 62$ by Mills Tipped with T15K6 Carbide. $\frac{B}{D} = 0.6$.

Shape of Cutting Portion of Mill: $\alpha = 20^\circ$; $\gamma = -15^\circ$; $\lambda = 15^\circ$; $\varphi = 60^\circ$; $\varphi_1 = 5^\circ$.

D	z	B	s_z	Cutting 1				2			
				v	n	s_M	N_e	v	n	s_M	N_e
75	4	45	0,09 0,07 0,05 0,03	36,5 40 43,5 51	155 170 185 217	56 48 37 26	0,58 0,50 0,43 0,33	31 33,5 36,5 42,5	132 142 155 180	48 40 31 21	0,98 0,85 0,70 0,55
90	6	54	0,09 0,07 0,05 0,03	36,5 40 43,5 51	129 142 154 180	70 60 46 33	0,85 0,75 0,63 0,48	31 33,5 36,5 42,5	110 119 129 150	60 51 39 27	1,50 1,30 1,05 0,80
110	8	66	0,09 0,07 0,05 0,03	36,5 40 43,5 51	105 115 125 147	76 64 50 35	1,15 1,00 0,85 0,65	31 33,5 36,5 42,5	90 97 105 123	65 54 42 30	1,95 1,75 1,40 1,10
130	8	78	0,09 0,07 0,05 0,03	36,5 40 43,5 51	90 98 106 125	65 55 43 30	1,15 1,00 0,85 0,65	31 33,5 36,5 42,5	76 82 90 104	55 46 36 25	1,95 1,75 1,40 1,10
150	10	90	0,09 0,07 0,05 0,03	36,5 40 43,5 51	77 85 92 108	65 60 46 33	1,40 1,30 1,05 0,80	31 33,5 36,5 42,5	66 71 77 90	60 50 38 27	2,45 2,15 1,80 1,35
200	10	120	0,09 0,07 0,05 0,03	36,5 40 43,5 51	48 64 69 81	53 45 34 24	1,40 1,30 1,05 0,80	31 33,5 36,5 42,5	49 53 58 68	44 38 29 21	2,45 2,15 1,80 1,35
250	12	150	0,09 0,07 0,05 0,03	36,5 40 43,5 51	46 51 55 65	50 43 33 24	1,70 1,50 1,25 0,95	31 33,5 36,5 42,5	39 43 46 54	42 36 28 20	2,95 2,60 2,10 1,60

See Table 1 for symbols and factors of correction.

Table 6 (Cont'd)

Depth in mm							
3				4			
v	n	s_M	N_n	v	n	s_M	N_n
28	119	43	1,30	26	110	40	1,70
30,5	130	37	1,20	28	119	33	1,50
33	140	28	1,00	31	132	27	1,20
39	165	20	0,75	36	153	19	0,90
28	100	54	2,00	26	92	50	2,50
30,5	108	46	1,80	28	100	42	2,20
33	117	36	1,45	31	110	33	1,85
39	138	25	1,15	36	127	23	1,40
28	81	58	2,70	26	75	54	3,35
30,5	88	49	2,35	28	81	46	2,95
33	95	38	1,95	31	90	36	2,45
39	113	27	1,50	36	104	25	1,85
28	68	49	2,70	26	64	46	3,35
30,5	75	42	2,35	28	68	38	2,95
33	81	33	1,95	31	76	31	2,45
39	95	23	1,50	36	88	21	1,85
28	60	54	3,35	26	55	49	4,20
30,5	65	45	2,95	28	60	42	3,70
33	70	35	2,40	31	66	33	3,05
39	83	25	1,90	36	77	23	2,30
28	44	40	3,35	26	41	37	4,20
30,5	48	34	2,95	28	44	31	3,70
33	52	26	2,40	31	49	24	3,05
39	62	19	1,90	36	57	17	2,30
28	36	39	4,00	26	33	36	5,00
30,5	39	33	3,55	28	36	30	4,45
33	42	26	2,90	31	39	24	2,65
39	50	18	2,25	36	46	17	2,80

Clarifications with Respect to Cutting Practice

Tables 1 - 6 contain the author's recommendation for practice in the end milling of hardened steels, of H_{R_C} = 38, 44, 49, 54, 58 and 62. The cutting speeds are calculated on the basis of eq.(13). Table 7 presents the author's values for rake angle γ.

Below we present the correction factors K_v with which determination may be made of the cutting speed for hardened steels of other hardnesses (not provided in the tabulations in practice), taking as unity the cutting speeds in the Table for steel of H_{R_C} = 38.

Hardness of work steel, H_{R_C}	38	41	47	51	56	60
Value of K_v factor	1.0	0.85	0.64	0.50	0.40	0.32

Table 7

Recommended Values of Rake Angle γ

Grade of Carbide	H_{R_C} Hardness of Work Steel		
	38–46	47–54	> 54
T30K4	−10	−15	−20
T15K6, T14K8, T5K10	−5	−10	−15

Table 8

Factor of Correction K_T Relative to Cutter Life T

Cutter life T, min	180	240	300	360	480	600	720	900
Values of correction factor K_T	1,13	1,05	1,0	0,95	0,88	0,84	0,80	0,75

The cutting speeds presented in the Tables are calculated for a cutter life T = 300 min and for T15K6 carbide.

For conditions of work other than those indicated in Tables 1 - 6, the cutting speed v_{300} may be multiplied by the correction factors K_T, K_u and K_B, which make provision, respectively, for other mill lives (Table 8), grades of carbide (Table 9), and $\frac{B}{D}$ ratios (Table 10).

Table 9

Correction Factor K_u In Terms of Carbide With Which Cutter Is Tipped

Carbide Grade	Value of K_u Factor
T5K10	0,73
T14K8	0,90
T15K6	1,00
T30K4	1,25

Table 10

Correction Factor K_B Relative to Ratio Between Milling Width B and Mill Diameter D

$\frac{B}{D}$	0,15	0,30	0,40	0,50	0,60	0,70	0,80	0,90
Value of Factor K_B	1,32	1,14	1,08	1,03	1,00	0,97	0,94	0,92

Table 11

Correction Factor K_{N_B} Relative to Ratio of Milling Width B to Mill Diameter D

$\frac{B}{D}$	0,15	0,30	0,40	0,50	0,60	0,70	0,80	0,90
Value of K_{N_B} Factor	0,33	0,57	0,72	0,86	1,00	1,13	1,25	1,38

The cutting speed sought is determined from the equation

$$v = v_{300} \cdot K_T \cdot K_u \cdot K_B \ m/min.$$

Actual outputs are defined in accordance with eq.(14).

Below we present correction factors K_N which permit determination of power for steels of other hardnesses than those in the Tables of practice. The tabular power for H_{R_C} = 38 steel is taken as unity.

Hardness of the machined steel H_{R_C}	38	41	47	51	56	60
Value of the K_N factor	1.0	0.96	0.85	0.78	0.70	0.65

At a $\frac{B}{D}$ ratio other than this, the actual outputs taken from Tables 1 - 6 must be multiplied by the correction factors K_{N_B} (Table 11).

In working with milling cutters having numbers of teeth z other than those listed in the machining-practice Tables, the feeds per minute s_m and actual outputs N_e must be increased or decreased in proportion to the change in the number of teeth. The machining speeds v and rpm n do not change.

In milling forgings and castings through scale, the cutting speeds v, rpm n, feeds per minute s_m, and actual outputs N_e must be multiplied by a factor of 0.85.

APPENDIX III

Table 1

Cutting Speeds, Axial Forces, Moments of Torque and Actual Output in the Machining of Alloy Constructional Steels Hardened to H_{R_C} = 35 to 65 With Drills Tipped With VK8

Cutting parameters	H_{R_C} Hardness of machined steel	Drill diameter D, in mm							
		10	12	14	16	20	24	28	30
Feed s, mm/rev	35—45	0,05	0,055	0,065	0,070	0,085	0,10	0,11	0,12
Cutting speed v_{30}, m/min		56	55	53	52	49	47	46	45
Drill rpm n, min		1780	1460	1205	1040	780	620	520	480
Axial force P_o, kg		520	645	820	975	1340	1740	2150	2400
Moment of torque, M_t, kgm		0,75	1,20	1,90	2,60	4,90	8,30	12,50	15,30
Actual output N_e, kw		1,30	1,80	2,35	2,80	3,90	5,30	6,70	7,50
Feed s, mm/rev	46—56	0,035	0,040	0,045	0,055	0,065	0,075	0,085	0,090
Cutting speed v_{30}, m/min		36	34	34	31	30	29	28	28
Drill rpm n, min		1140	905	770	615	475	385	320	295
Axial force P_o, kg		465	600	740	935	1270	1650	2050	2250
Moment of torque, M_t, kgm		0,70	1,10	1,70	2,60	4,70	7,80	12,00	14,40
Actual output N_e, kw		0,80	1,00	1,35	1,65	2,30	3,10	3,95	4,35
Feed s, mm/rev	57—65	0,030	0,035	0,040	0,045	0,050	0,060	0,065	0,070
Cutting speed v_{30}, m/min		25	24	23	22	22	21	21	20
Drill rpm n, min		800	635	520	435	350	280	240	210
Axial force P_o, kg		520	675	840	1020	1350	1760	2140	2400
Moment of torque, M_t, kgm		0,70	1,20	1,80	2,60	4,60	7,80	11,60	14,00
Actual output N_e, kw		0,60	0,80	0,95	1,15	1,65	2,25	2,85	3,00

Clarifications re Machining Practice

Cutting speeds are calculated in accordance with eq.(16).

The cutting speeds presented in the Table pertain to a drill life T = 30 min. For other lives, the cutting speed, as determined from the Table, must be multiplied by a correction factor K_T in accordance with Table 2. The relative life index m = 0.25.

The axial forces P_o were determined by means of eq.(17). The moments of torque were calculated by means of eq.(18).

The actual outputs have been determined according to the following formula:

$$N_e = \frac{M_{\kappa p} n}{716{,}2 \cdot 1{,}36} \; \kappa w.$$

Table 2

Factor of Correction K_T

Drill life T, min	15	18	21	24	30	36	40	45
Values of factors of correction K_T	1,19	1,13	1,09	1,06	1,00	0,96	0,93	0,90

APPENDIX IV

Table 1

Cutting Speeds v_{30} and Feeds per Minute s_m in the Finish Reaming of Hardened Alloy Constructional Steels of H_{R_C} = 38 by Flute Reamers Tipped with Carbide T15K6

Shape of cutting portion of reamers (Fig.152): $\alpha = 6^o$, $\gamma = -15^o$, $\gamma_o = -10^o$, $\lambda = 0^o$, $\varphi = 15^o$, $\varphi_o = 2^o$, f = 0.2 mm, a = 2 to 3 mm; l_o = 1.5 to 2.0 mm; t = 0.2 mm

Composition of lubricant-coolant fluid: 10% emul'sol in soda water + 5% sul'fofrezol

Feed s in mm/rev	Diameter of flute reamer D in mm								
	10			12			14		
	v_n m/min	n rpm	s_m mm/min	v_n m/min	n rpm	s_m mm/min	v_n m/min	n rpm	s_m mm/min
0,2	70	2230	446	73	1940	388	78	1770	354
0,3	59	1875	562	62	1640	491	65	1475	442
0,4	52	1655	662	54	1430	572	58	1320	528
0,5	46	1465	732	49	1300	650	53	1205	603
0,6	—	—	—	—	—	—	48	1090	654

Feed s in mm/rev	Diameter of flute reamer D, mm											
	16			18			20			25		
	v_n m/min	n rpm	s_m mm/min	v_n m/min	n rpm	s_m mm/min	v_n m/min	n rpm	s_m mm/min	v_n m/min	n rpm	s_m mm/min
0,2	82	1640	328	86	1520	304	90	1430	286	98	1250	250
0,3	69	1380	414	72	1275	383	75	1195	359	83	1060	318
0,4	61	1220	488	64	1130	452	67	1070	428	73	930	372
0,5	55	1100	550	58	1025	513	61	970	485	66	840	420
0,6	51	1020	612	54	955	573	56	890	534	61	780	468
0,7	—	—	—	—	—	—	—	—	—	57	725	507
0,8	—	—	—	—	—	—	—	—	—	54	690	552

Table 1 (Cont'd)

Feed s mm/rev	Diameter of flute reamer D, mm								
	30			35			40		
	v_n, m/min	n rpm	s_M mm/min	v_n, m/min	n rpm	s_M mm/min	v_n, m/min	n rpm	s_M mm/min
0,2	106	1130	226	113	1025	205	119	955	191
0,3	89	945	283	95	865	260	100	800	240
0,4	79	840	336	84	765	306	88	705	282
0,5	71	755	378	76	690	345	80	640	320
0,6	66	700	420	70	635	381	74	590	354
0,7	62	660	462	66	600	420	69	550	385
0,8	58	615	492	62	565	451	65	520	416

Feed s mm/rev	Diameter of flute reamer D, mm											
	45			50			55			60		
	v_n, m/min	n rpm	s_M mm/min	v_n, m/min	n rpm	s_M mm/min	v_n, m/min	n rpm	s_M mm/min	v_n, m/min	n rpm	s_M mm/min
0,3	104	735	221	109	692	208	113	652	196	117	620	186
0,4	92	650	260	96	610	244	100	578	231	104	550	220
0,5	84	595	298	87	555	278	91	525	263	94	496	248
0,6	78	550	330	81	515	310	84	485	291	87	460	276
0,7	73	515	360	76	483	338	79	456	319	81	430	301
0,8	69	490	392	71	451	362	74	427	342	77	407	326
0,9	65	460	415	68	433	390	71	410	370	73	386	347
1,0	62	438	438	65	413	413	67	338	388	70	370	370

Table 2

Cutting Speeds v_{30} and Feeds per Minute s_m in the Finish Reaming of Hardened Alloy Constructional Steels of H_{RC} = 45 by Flute Reamers Tipped With Carbide T15K6

Shape of cutting portion of reamers (Fig.152): $\alpha = 6^\circ$; $\gamma = -15^\circ$; $\gamma_0 = -10^\circ$; $\lambda = 0^\circ$; $\varphi_0 = 15^\circ$; $\varphi_0 = 2^\circ$; f = 0.2 mm; a = 2 to 3 mm; l_0 = 1.5 to 2.0 mm; t = 0.2 mm

Composition of lubricant-coolant fluid: 10% emul'sol in soda water + 5% sul'fofrezol

Feed s mm/rev	Diameter of flute reamer D, mm: 10			12			14		
	v, m/min	n, rpm	s_m, mm/min	v, m/min	n, rpm	s_m, mm/min	v, m/min	n, rpm	s_m, mm/min
0,20	47	1495	299	52	1375	275	54	1230	246
0,25	39	1240	310	43	1140	285	44	1000	250
0,30	35	1115	335	38	1005	302	40	910	273
0,40	29	890	356	31	823	329	32	727	291

Feed s mm/rev	Diameter of flute reamer D, mm: 16			18			20		
	v, m/min	n, rpm	s_m, mm/min	v, m/min	n, rpm	s_m, mm/min	v, m/min	n, rpm	s_m, mm/min
0,20	56	1115	223	59	1045	209	60	955	191
0,25	47	935	234	49	867	217	52	830	208
0,30	41	817	246	44	780	235	46	730	220
0,40	34	677	271	36	636	255	37	590	236
0,50	30	597	290	31	548	274	33	525	262

Table 2 (Cont'd)

Feed s mm/rev	Diameter of flute reamer D, mm: 25			30			35			40		
	v_D, m/min	n rpm	s_M mm/min	v_D m/min	n rpm	s_M mm/min	v_D, m/min	n rpm	s_M mm/min	v_D, m/min	n rpm	s_M mm/min
0,20	67	853	171	72	765	153	76	690	138	80	640	128
0,30	49	625	188	54	572	172	58	527	158	61	487	146
0,40	41	522	209	44	476	190	46	418	168	49	392	157
0,50	36	458	229	38	403	202	41	373	187	43	343	172
0,60	32	408	245	34	360	216	37	336	202	39	312	187
0,70	—	—	—	—	—	—	—	—	—	36	287	201

Feed s mm/rev	Diameter of flute reamer D, mm: 45			50			55			60		
	v_D, m/min	n rpm	s_M mm/min	v_D, m/min	n rpm	s_M mm/min	v_D, m/min	n rpm	s_M mm/min	v_D, m/min	n rpm	s_M mm/min
0,30	63	445	134	66	420	126	69	400	120	70	373	112
0,40	51	360	144	53	337	135	54	312	125	58	309	124
0,50	45	320	160	47	299	150	48	277	138	50	265	133
0,60	41	290	174	42	268	161	43	249	149	45	240	144
0,70	37	262	183	39	248	173	40	231	162	41	218	153
0,80	33	234	187	35	222	178	36	208	167	38	202	162

Table 3

Cutting Speeds v_{30} and Feeds per Minute s_m in the Finish Reaming of Hardened Alloy Constructional Steels of H_{RC} = 51 by Flute Reamers Tipped With Carbide T15K6

Shape of cutting portion of reamers (Fig.152): $\alpha = 6^o$; $\gamma = -15^o$; $\gamma_o = -10^o$; $\lambda = 0^o$; $\varphi = 15^o$; $\varphi_o = 2^o$; f = 0.2 mm; a = 2 to 3 mm; l_o = 1.5 to 2.0 mm; t = 0.2 mm

Composition of lubricant-coolant fluid: 10% emul'sol in soda water + 5% sul'fofrezol

Feed s mm/rev	Diameter of flute reamer D, mm								
	10			12			14		
	v m/min	n rpm	s_M mm/min	v m/min	n rpm	s_M mm/min	v m/min	n rpm	s_M mm/min
0,20	35	1145	229	39	1000	200	40	910	182
0,25	27	860	215	30	795	198	31	700	175
0,30	23	735	221	25	660	198	26	590	177
0,35	19	605	212	21	555	119	22	500	175
0,40	—	—	—	—	—	—	19	430	172

Feed s mm/rev	Diameter of flute reamer D, mm											
	16			18			20			25		
	v m/min	n rpm	s_M mm/min	v m/min	n rpm	s_M mm/min	v m/min	n rpm	s_M mm/min	v m/min	n rpm	s_M mm/min
0,20	42	835	167	44	780	156	45	720	144	50	640	128
0,25	33	655	164	34	600	150	36	570	142	39	495	124
0,30	27	537	161	29	515	155	30	480	144	32	410	123
0,35	24	475	166	25	440	154	26	415	145	28	355	125
0,40	20	400	160	21	370	148	22	350	140	24	305	122
0,45	—	—	—	19	335	150	20	320	144	22	280	126
0,50	—	—	—	—	—	—	—	—	—	20	255	128

Table 3 (Cont'd)

Feed s mm/rev	Diameter of flute reamer D, mm											
	30			35			40			45		
	v_M m/min	n rpm	s_M mm/min	v_M m/min	n rpm	s_M mm/min	v_M m/min	n rpm	s_M mm/min	v_M m/min	n rpm	s_M mm/min
0,20	54	575	115	57	518	104	60	480	96	63	447	89
0,25	42	445	111	45	410	102	47	375	94	50	353	88
0,30	35	372	111	38	345	104	40	320	96	41	290	87
0,35	31	330	115	33	300	105	34	270	95	36	254	89
0,40	26	276	110	27	246	98	29	232	93	30	213	85
0,45	23	243	109	25	227	102	26	206	93	24	190	85
0,50	21	220	110	22	200	100	23	183	92	24	170	85
0,60	17	180	108	18	165	99	19	152	92	20	142	85
0,70	—	—	—	—	—	—	16	128	90	17	120	84

Feed s mm/rev	Diameter of flute reamer D, mm								
	50			55			60		
	v_M m/min	n rpm	s_M mm/min	v_M m/min	n rpm	s_M mm/min	v_M m/min	n rpm	s_M mm/min
0,20	66	420	84	68	398	80	71	378	76
0,25	52	350	87	54	313	78	55	292	73
0,30	43	272	82	45	262	79	46	244	73
0,35	37	236	82	39	225	79	40	212	74
0,40	31	197	79	32	185	74	34	180	72
0,45	28	178	80	29	168	76	30	159	72
0,50	25	158	79	26	151	76	27	144	72
0,60	21	133	80	21	122	73	22	117	70
0,70	18	115	80	19	110	77	20	106	74

Clarifications Re Cutting Practice

Tables 1 - 3 present the recommended practices for the flute reaming of alloy steels hardened to H_{RC} = 38 to 51. For steels of H_{RC} = 51 and 38, cutting speeds are calculated in accordance with eqs.(19) and (20).

The cutting speeds for steels of H_{RC} = 45 were obtained by multiplying the cutting speeds for steel of H_{RC} = 51 by factors of correction K_v. Table 4 presents the values of factor K_v relative to feed s.

The rpm n of the flute reamer was determined in accordance with equation

$$n = \frac{1000\,v}{\pi D} \ rpm ,$$

and the feeds per minute s_m in accordance with equation

$$s_м = sn \ mm/min.$$

The cutting speeds presented in the Tables of practice are calculated on a

Table 4

Correction Factor K_v

Feed s, in mm/rev	0,20	0,25	0,30	0,35	0,40	0,45	0,50	0,60	0,70	0,80
Value of factor K_v	1,34	1,43	1,53	1,62	1,70	1,78	1,86	2,02	2,14	2,22

flute reamer life of T = 30 min, depth of cut t = 0.2 mm, and T15K6 carbide. The following values for the relative tool life index m are employed:

Hardness of work steel H_{RC}	38	45	51
Index m	0.40	0.60	0.85

For conditions of work other than those indicated, the cutting speeds selected from Tables 1 - 3 must be multiplied by the correction factors K_T and K_t, which allow for other tool lives (Table 5) and depths of cut (Table 6).

In working with flute reamers having T15K6T carbide tips, the cutting speeds selected from the Tables must be multiplied by the correction factor $K_u = 1.10$.

The feeds for flute reaming are selected from Tables 1 - 3 in terms of the conditions of maximum output, if the feed is not limited by the rigidity of the system comprising machine tool - workpiece - tool, the power of the machine tool, the strength of the tool, and other conditions.

In order to achieve Class 2 tolerance and surface quality superior to Class 9, the following feeds must be employed in the flute reaming of holes in steel parts whose hardness is $H_{R_C} = 49$ to 54: for $D < 20$ mm, s is up to 0.3 mm/rev; for $D > 20$ mm, s is up to 0.4 mm/rev. For hardened steels of lesser hardness, one may employ the same feeds, bearing in mind that machining here is at greater cutting speeds.

Table 5

Correction Factor K_T Relative to Life of Flute Reamer

Life of Flute Reamer T, min	Hardness of Work Steel		
	H_{RC} = 38	H_{RC} = 45	H_{RC} = 51
	Value of Factor K_T		
10	1,55	1,93	2,54
20	1,18	1,27	1,41
30	1,00	1,00	1,00
40	0,89	0,84	0,78
50	0,81	0,74	0,65
60	0,76	0,66	0,55
70	0,71	0,60	0,49
80	0,67	0,55	0,43
90	0,64	0,51	0,39
100	0,62	0,48	0,36
110	0,59	0,45	0,33
120	0,57	0,43	0,31

Table 6

Correction Factor K_t Relative to Depth of Cut

Depth of Cut t, mm	Hardness of Work Steel		
	H_{RC} = 38	H_{RC} = 45	H_{RC} = 51
	Value of Factor K_t		
0,05	1,30	1,73	2,83
0,10	1,14	1,30	1,68
0,15	1,06	1,10	1,25
0,20	1,00	1,00	1,00
0,25	0,96	0,91	0,86
0,30	0,93	0,84	0,74

APPENDIX V

Table 1

Cutting Speeds v_{30} and Feeds per Minute s_m in the Rose Reaming of Hardened Alloy Constructional Steels of H_{RC} = 38 by Rose Reamers Tipped With T15K6 Carbide

Rose reamer shape (Fig.188): α = 10°, α_o = 10°, γ = -15°, γ_o = -10°, λ = 0°, φ = 60°, φ_o = 15°, f = 0.3 to 0.5 mm; a = 1.5 to 2.0 mm, l_o = 0.5 to 1.0 mm; t = 1 mm

The coolant and lubricant is of the following composition: 10% emul'sol in soda water + 5% sul'fofrezol

Feed s mm/rev	Diameter of flute reamer D, mm											
	10			12			14			16		
	v m/min	n rpm	s_m mm/min	v m/min	n rpm	s_m mm/min	v m/min	n rpm	s_m mm/min	v m/min	n rpm	s_m mm/min
0,20	52	1650	330	59	1565	313	65	1475	295	69	1370	274
0,25	46	1465	366	52	1380	344	56	1270	318	60	1190	298
0,30	40	1270	380	44	1170	350	49	1110	333	53	1050	315
0,40	34	1080	432	38	1010	405	41	930	372	46	915	366
0,50	30	955	477	34	900	450	37	840	420	40	795	398

Feed s mm/rev	Diameter of flute reamer D, mm											
	18			20			25			30		
	v m/min	n rpm	s_m mm/min	v m/min	n rpm	s_m mm/min	v m/min	n rpm	s_m mm/min	v m/min	n rpm	s_m mm/min
0,30	57	1010	303	61	970	291	—	—	—	—	—	—
0,40	48	850	340	52	830	332	60	765	306	67	710	284
0,50	42	745	373	46	730	365	52	660	330	59	625	313
0,60	38	670	402	41	650	390	46	585	350	52	550	330
0,70	35	620	434	37	590	413	43	550	385	48	510	357
0,80	—	—	—	35	555	444	40	510	432	44	470	376
0,90	—	—	—	—	—	—	37	470	423	41	435	392

Table 1 (Cont'd)

Feed s mm/rev	Diameter of flute reamer D, mm											
	35			40			45			50		
	$v_з$ m/min	n rpm	$s_м$ mm/min	$v_з$ m/min	n rpm	$s_м$ mm/min	$v_з$ m/min	n rpm	$s_м$ mm/min	$v_з$ m/min	n rpm	$s_м$ mm/min
0,40	72	655	262	78	620	248	—	—	—	—	—	—
0,50	63	570	285	69	545	273	74	525	263	79	500	250
0,60	56	510	306	61	485	291	65	460	276	70	445	267
0,70	52	470	330	56	445	312	60	425	298	65	415	290
0,80	48	435	348	53	420	336	56	400	320	60	380	304
0,90	45	410	370	48	380	342	52	370	333	55	350	315
1,00	42	380	380	45	355	355	49	350	350	52	330	330

Table 2

Cutting Speeds v_{30} and Feeds per Minute s_m in the Rose Reaming of Hardened Alloy Constructional Steels of H_{R_C} = 45 by Rose Reamers Tipped With T15K6 Carbide

Rose reamer shape:(Fig.188): $\alpha = 10^\circ$; $\alpha_o = 10^\circ$; $\gamma = -15^\circ$; $\gamma_8 = -10^\circ$; $\lambda = 0^\circ$; $\varphi = 60^\circ$; $\varphi_o = 15^\circ$; $\lambda = 0^\circ$; f = 0.3 to 0.5 mm; a = 1.5 to 2.0 mm; l_o = 0.5 to 1.0 mm; t = 1 mm

The coolant and lubricant is of the following composition: 10% emul'sol in soda water + 5% sul'fofrezol

Feed s mm/rev	Diameter of flute reamer D, mm											
	10			12			14			16		
	$v_з$ m/min	n rpm	$s_м$ mm/min	$v_з$ m/min	n rpm	$s_м$ mm/min	$v_з$ m/min	n rpm	$s_м$ mm/min	$v_з$ m/min	n rpm	$s_м$ mm/min
0,20	35	1115	223	39,5	1050	210	43,5	990	198	—	—	—
0,25	31	990	248	35	930	232	38	865	216	41	815	204
0,30	27	860	258	30	795	239	33,5	760	218	36,5	725	218
0,35	25,5	810	283	28	740	259	31	705	247	33,5	666	233
0,40	23	735	294	26	690	276	28	635	254	31	615	246
0,45	21,5	685	309	24	635	286	26,5	600	270	28,5	565	254
0,50	—	—	—	—	—	—	—	—	—	27	535	267
0,60	—	—	—	—	—	—	—	—	—	24	475	285

Table 2 (Cont'd)

Feed s mm/rev	Diameter of flute reamer D, mm											
	18			20			25			30		
	v_n m/min	n rpm	s_M mm/min	v_n m/min	n rpm	s_M mm/min	v_n m/min	n rpm	s_M mm/min	v_n m/min	n rpm	s_M mm/min
0,30	39	690	207	41	650	195	—	—	—	—	—	—
0,35	35,5	625	219	38	605	212	43,5	555	195	—	—	—
0,40	32,5	575	230	35	555	222	40,5	515	206	45	480	192
0,45	31	550	247	32,5	515	232	35,5	450	202	42	445	200
0,50	28,5	505	252	31	495	247	35	445	222	39,5	420	210
0,60	26	460	276	27,5	440	264	31	395	237	35	370	222
0,70	—	—	—	25	400	280	29	370	259	32	340	238
0,80	—	—	—	—	—	—	—	—	—	30	320	256

Feed s mm/rev	Diameter of flute reamer D, mm											
	35			40			45			50		
	v_n m/min	n rpm	s_M mm/min	v_n m/min	n rpm	s_M mm/min	v_n m/min	n rpm	s_M mm/min	v_n m/min	n rpm	s_M mm/min
0,40	49	445	178	52,5	415	166	56,5	400	160	61	390	156
0,45	45,5	415	187	49,5	390	175	53	375	169	56,5	360	162
0,50	42,5	385	192	46,5	370	185	49,5	350	175	53,5	340	170
0,60	38	345	207	41	325	195	44	310	186	47,5	300	180
0,70	35	320	224	33	300	210	40,5	285	199	43,5	275	192
0,80	33	300	240	35,5	280	224	38	270	216	40,5	260	208

Table 3

Cutting Speeds v_{30} and Feeds per Minute s_m in the Rose Reaming of Hardened Alloy Constructional Steels of H_{RC} = 51 by Rose Reamers Tipped With T15K6 Carbide

Rose reamer shape (Fig.188): $\alpha = 10^{\circ}$; $\alpha_o = 10^{\circ}$; $\gamma = -15^{\circ}$; $\gamma_o = -10^{\circ}$; $\lambda = 0^{\circ}$; $\varphi = 60^{\circ}$; $\varphi_o = 15^{\circ}$; f = 0.3 to 0.5 mm; a = 1.5 to 2.0 mm; l_o = 0.5 to 1.0 mm; t = 1 mm

The coolant and lubricant is of the following composition: 10% emul'sol in soda water + 5% sul'fofrezol

Feed s mm/rev	Diameter of flute reamer D, mm											
	10			12			14			16		
	v_{30} m/min	n rpm	s_m mm/min	v_{30} m/min	n rpm	s_m mm/min	v_{30} m/min	n rpm	s_m mm/min	v_{30} m/min	n rpm	s_m mm/min
0,20	22,5	715	143	25,5	675	135	28	635	127	30	595	119
0,25	20	635	159	22,5	595	149	24,5	555	139	26,5	525	131
0,30	17,5	555	167	19,5	515	155	21,2	490	147	23,5	465	139
0,35	16,5	525	181	18	475	166	20	455	160	21,5	425	149
0,40	15	475	190	16,5	435	174	18	410	164	20	400	160
0,45	—	—	—	—	—	—	—	—	—	18,5	370	166
0,50	—	—	—	—	—	—	—	—	—	17,5	350	175

Feed s mm/rev	Diameter of flute reamer D, mm											
	18			20			25			40		
	v_{30} m/min	n rpm	s_m mm/min	v_{30} m/min	n rpm	s_m mm/min	v_{30} m/min	n rpm	s_m mm/min	v_{30} m/min	n rpm	s_m mm/min
0,30	25	440	132	26,5	420	126	—	—	—	—	—	—
0,35	23	405	142	24,5	390	137	28	355	124	—	—	—
0,40	21	370	148	22,5	360	144	26	330	132	29	310	124
0,45	20	355	160	21	335	151	23	290	131	27	290	131
0,50	18,5	330	165	20	320	160	22,5	285	143	25,5	270	135
0,60	—	—	—	—	—	—	20	255	153	22,5	240	144

Table 3 (Cont'd)

Feed s mm/rev	Diameter of flute reamer D, mm											
	35			40			45			50		
	v_t m/min	n rpm	s_M mm/min	v_t m/min	n rpm	s_M mm/min	v_t m/min	n rpm	s_M mm/min	v_t m/min	n rpm	s_M mm/min
0,40	31,5	285	114	34	270	108	36,5	260	104	—	—	—
0,50	27,5	250	125	30	240	120	32	225	113	34,5	220	110
0,60	24,5	220	132	26,5	210	126	28,5	200	120	30,5	195	117
0,70	22,5	205	143	24,5	195	136	26	185	130	28	180	126

Clarification With Respect to Cutting Practices

Tables 1 - 3 present the recommended practices for rose reaming of alloy steels hardened to H_{R_C} = 38 to 51. The cutting speeds are calculated in accordance with eq.(21).

The rose reamer rpm n and the feeds per minute s_m have been determined in accordance with the following formulas:

$$n = \frac{1000\,v}{\pi D}\ rpm\ ;$$
$$s_M = sn\ mm/min.$$

The cutting conditions presented in the Tables of practice are based on a rose reamer life of T = 30 min, depth of cut t = 1.10 mm, and T15K6 carbide.

For other conditions of work than these, the cutting speeds chosen from Tables 1 - 3 must be multiplied by correction factors K_T and K_t, which allow, respectively, for other rose reamer life (Table 4) and depth of cut (Table 5).

In the work with a rose reamer equipped with T15K6T carbide, the cutting speeds selected from the Tables must be multiplied by the following correction factor K_c = 1.10.

Table 4

Correction Factor K_T

Rose reamer life T, min	10	20	30	40	50	60	75	90	120	150	180
Value of Factor K_T	1,64	1,20	1,00	0,88	0,80	0,73	0,66	0,61	0,54	0,48	0,45

Table 5

Correction Factor K_t

Depth of cut t, mm	0,3	0,5	0,8	1,0	1,2	1,5
Value of factor K_t	1,43	1,23	1,06	1,00	0,95	0,89

APPENDIX VI

Table 1

Cutting Speed and Number of Passes in Cutting Thread on Alloy Constructional Steels Hardened to H_{R_C} = 35 to 65

Pitch s, mm	Thread Length l, mm	Hardness of Work Material H_{R_C}															
		35				45				55				65			
		Cutting Conditions															
		Passes				Passes				Passes				Passes			
		Rough		Finish		Rough		Finish		Rough		Finish		Rough		Finish	
		i	v	i	v	i	v	i	v	i	v	i	v	i	v	i	v
2	20	5	48	3	58	7	22	5	27	9	12	6	15	11	7,5	8	9
3	20	7	38	3	45	11	18	5	21	15	10	6	11	19	6	8	7
4	40	9	32	3	38	16	15	5	18	23	8	6	10	30	5	8	6

i - Number of passes; v - Cutting speed at tool life T = 30 min, in m/min

Clarification of Machining Practice in Cutting External Thread

The practices presented in Table 1 provide for:

1) Plunging the cutter in roughing passes by the methods illustrated in Figs.199b and c; in finishing passes by the method illustrated in Fig.199a;

2) For roughing cutters, the use of carbide VK8, and for finishing cutters the use of carbide T15K6;

3) For roughing cutters the rake angle $\gamma = -3^{\circ}$, for finishing cutters $\gamma = 0^{\circ}$;

4) For roughing and finishing cutters $\alpha = 13^{\circ}$, $\alpha_1 = 6^{\circ}$, $\gamma = 0^{\circ}$;

5) Lapping the cutters with boron carbide compound is absolutely essential;

6) Tip radius: r = 0.4 mm for roughing cutters in thread for which pitch s = 0.2 mm; r = 0.6 mm for thread in which pitch s = 3 and 4 mm; for finishing cutters r = 0.3 mm for thread in which pitch s = 2 mm; r = 0.4 mm for thread in which pitch s = 3 mm; r = 0.6 mm for thread in which pitch s = 4 mm.

7) For internal thread, the number of passes should be increased by 20% and cutting speed should be reduced by 15 - 20% as compared to the tabular data.

BIBLIOGRAPHY

1. - Encyclopedic Handbook: Manufacture of Machinery, Vol.3, Mashgiz (1947)

2. Kashchenko,G.A. - Principles of Metallography, Mashgiz (1956)

3. Kashchenko,G.A. - Principles of Metallography, Metallurgizdat (1950)

4. Fridman,Ya.B., and Volodina,T.A. - The Strength and Ductility of Hardened Steel, Dokl. AN SSSR, Vol.XLVIII, No.8 (1945)

5. Grozin,B.D. - The Mechanical Properties of Hardened Steel, Mashgiz (1951)

6. Kieffer,R., and Schworzkopf,P. - Hard Materials and Carbides. Springer, Vienna (1953)

7. Brokhin,I.S. - Modern Tool Carbides Made in Our Country, and Their Properties. Symposium: Skorostnyye metody obrabotki metallov, Doklady i tezisy dokladov na Moskovskoy konferentsii po skorostnym metodam obrabotki metallov, Mashgiz (1949)

8. Granovskiy,G.I. - The Resistance to Wear of Carbides and Hardened Tool Steels, MVTU Symposium: Rezaniye metallov i instrument. Mashgiz (1955)

9. Riskin,V.Ya. - Transactions of the First Conference on Cemented Carbides. Metallurgizdat (1933)

10. Betaneli,A.I. - The Hardness of Carbides and Cermet Materials in the Hot Condition, Vestnik mashinostroyeniya, No.4 (1953)

11. Kazakov,N.F. - An Investigation Into the Hardness of Tool Materials Upon Heating, Symposium of the Komissiya po tekhnologii mashinostroyeniya AN SSSR, "Treniye i iznos pri rezanii metallov", Mashgiz (1955)

12. Rassokhin,V.Ya. and Rura,M.A. - Foreign Carbides for Machining Tools. Stanki i instrument, No.6 (1957)

13. Kazakov,N.F., and Andrianova,M.N. - Determination of the Cutting Properties of Tungsten Carbides Employing Cobalt and Nickel Binders, Stanki i instrument, No.6 (1957)

14. Katsnel'son,V.Yu. - An Investigation of New Grades of Titanium Carbides in the Turning of Steel With Removal of Chip of Large Section. TsNIITMASh Symposium: Issledovaniya v oblasti tekhnologii obrabotki metallov rezaniyem. Mashgiz (1957)

15. - The Manufacture of Cemented Carbides. Sbornik ITEIN AN SSSR: Poroshkovaya metallurgiya v mashinostroyenii kapitalisticheskikh stran. (1955)

16. Rakovskiy,V.S., and others - Cemented Carbides in the Manufacture of Machinery. Mashgiz (1955)

17. Rakovskiy,V.S., and Anders,N.R., -Fundamentals of the Production of Cemented Carbides, Metallurgizdat (1951)

18. Mamayev,V.S. - Determination of the Most Profitable Conditions for the Utilization of Cermet Cutting Tools. Avtoreferat dissertatsii, MVTU imeni Baumana. (1957)

19. Kirillova,O.M. - An Investigation of the Cutting Properties of Tool Cermets. Avtoreferat dissertatsii, TsNIITMASh (1956)

20. - Instructions in the Manufacture and Employment of Cutters with Cermet Bars. BPTI transportnogo mashinostroyeniya (1956)

21. Logak,N.S. - The Fine Turning of Hardened Steels. TsNIITMASh Symposium: The Finish Machining of Constructional Metals. Mashgiz (1951)

22. Zorev,N.N. - Cutting Forces in the Turning of Hardened Steels. ITEIN AN SSSR, (1955)

23. Malkin,A.Ya. - The Fast Turning of Hardened Steels. Symposium: Skorostnaya obrabotka metallov rezaniyem. Oborongiz (1951)

24. Makarov,A.D. - An Investigation of Certain Components in Errors in Machining and the Height of Irregularities in the Finish Turning of Hardened Steels. Avtoreferat dissertatsii. Moskovskiy aviatsionnyy tekhnologicheskiy institut (1955)

25. Vul'f,A.M. - Fundamentals of Machining. Mashgiz (1954)

26. Maslov,A.A. - An Investigation of the Turning of Hardened Steels. Avtoreferat dissertatsii. Moskovskiy inzhenerno-fizicheskiy institut (1954)

27. - Ministerstvo stankostroyeniya SSSR - Fast Machining Practice in the Turning and Milling of Ferrous Metals with Carbide Tools. Mashgiz (1950)

28. Shchelkonogov,N.I. - The Machining of Hardened Steels with Carbide Tools and the Prerequisites for the Machining of Steel at Particularly High Cutting Speeds. Vestnik metallopromyshlennosti, No.1 (1938)

29. Grudov,P.P. - The Machining of Hardened Steels with Cutters Tipped with Carbides. Stanki i instrument, No.3 (1947)

30. Belousova,Ye.A. - An Investigation of the Surface Finish of High Hardness Steel After Machining on the Lathe. Avtoreferat dissertatsii, TsNIITMASh (1956)

31. Larin,M.N. - Determination of Optimum Rake and Working Relief Angles for Carbide Cutting Tools, Symposium: Progressivnaya tekhnologiya mashinostroyeniya. Part I, No.II. Mashgiz (1951)

32. Krivoukhov,V.A. - Instructions for Employment of the Method of Super-Fast Machining of Metals. izd. Ministerstva rechnogo flota (1948)

33. Bolotin,A.I. - Experiences in the Introduction of Fast Methods of the Machining of Metals at the Krasnyy Proletarii Plant. Symposium: Skorostnye metody obrabotki metallov. Opyt moskovskikh zavodov. Mashgiz (1949)

34. Turchaninov,I.G. - High-Speed Machining at the Borets Plant. Symposium: Skorostnye metody obrabotki metallov. Opyt moskovskikh zavodov. Mashgiz (1949)

35. Kapitel'man,V.I. - High-Speed Turning of Hardened Steel by Carbide Cutters. Stanki i instrument, No.6 (1948)

36. Nekrasov,S.S. - Turning Hardened Large Bearing Races on the Lathe. Vestnik mashinostroyeniya, No.12 (1950)

37. Rudnik,S.S. - The Laws of Cutting Speed for Cutters of Super-Hard Alloys. Sbornik dokladov konferentsii po rezaniyu metallov (1937)

38. Besprozvannyi,I.M. - The Physical Foundations of the Science of Machining. Oborongiz (1941)

39. Avakov,A.A. - Certain Problems of Tool Life. Trudy TbIIZhT, No.3 - 4 (1948)

40. Besprozvannyi,I.M. - An Investigation of Work in Finish Machining with Turning Tools. ONTI (1938)

41. Zverev,Ye.K. - Optimum Tool Shape, Orgainformatsiya, No.11 (1935)

42. Itkin,M.E. - An Investigation of Cutting Speed in the Finish Machining of Steels for Locomotive and Freightcar Axles by Cutters of Pobedit α-21. Vestnik metallopromyshlennosti, No.9 (1939)

43. Klushin,M.I. - High-Speed Machining. Mashgiz (1947)

44. Fel'dshteyn,E.I. - The Machinability of Steels. Mashgiz (1953)

45. Isayev,A.I. - The Process of Formation of a Surface Layer in the Machining of Metals. Mashgiz (1950)

46. Reznikov,N.I. - The Science of Machining. Mashgiz (1950)

47. Matalin,A.A. - Surface Finish and the Operating Properties of Machine Parts. Mashgiz (1956)

48. D'yachenko,P.A. and Yakovson,M.O. - Surface Quality in the Machining of Metals. Mashgiz (1951)

49. Sokolovskiy,A.P. - Scientific Fundamentals of Machinery Manufacture Engineering. Mashgiz (1955)

50. Silant'yev,A.V. - On Increasing the Work Rate in Lateral Profile Turning of Hardened ShKh15 Steel. Symposium of the Moscow Physical Engineering Institute: "Novyye issledovaniya v oblasti obrabotki metallov rezaniyem. Mashgiz (1957)

51. Zhikharev,V.I. - The Machining of Hardened Alloy Steels by Cutters with Plastic Bars. Vestnik mashinostroyeniya, No.7 (1955)

52. Khazhinskiy,N.M. - Fast Machining of Metals at the 1st State Ball-Bearing Plant. Symposium: "Skorostnyye metody obrabotki metallov. Opyt

moskovskikh zavodov" Mashgiz (1949)

53. Reznitskiy,L.M. - The Machining of Hardened Steels. Mashgiz (1949)

54. Reznitskiy,L.M. - The Turning of Hardened Steel. Lenizdat (1951)

55. Dawihl,W. and Dinglinger,E. - Handbook of Carbide Tools. Springer, Berlin (Goettingen) Heidelberg (1953)

56. Larin,M.N. and Maslov,A.A. - An Investigation of a Method of Machining Hardened Steels by Introducing Transformed Current into the Cutting Zone. Symposium "New Investigations in the Field of the Machining of Metals and Plastics", Mashgiz (1952)

57. - Carbide Tool Designs. Symposium of VNII, Mashgiz (1951)

58. - The Designing of Cutting Tools. Symposium of VNII, Mashgiz (1956)

59. - The Designing of End Mills Providing for the Grinding of Teeth Separately from the Body. Symposium of the VNII, Mashgiz (1954)

60. Markelov,P.A. - Fast Milling of Steels by End Mills. Oborongiz (1953)

61. Larin,M.N. - Optimum Geometrical Parameters of the Cutting Portion of Tools. Oborongiz (1953)

62. Shchegolev,A.V., and Others - High-Speed Milling. Mashgiz (1949)

63. Grudov,P.P., Volkov,S.I., and Vorob'yev,V.M. - Fast Milling of Steel. Symposium of VNII, TsBTI (1950)

64. Larin,M.N. - Fundamentals of Fast Milling, Symposium: "The High-Speed Machining of Metals". Oborongiz (1953)

65. Levin,V.G. - Drills with Carbide Bars. Oborongiz (1940)

66. Ministry of Machine Tool Manufacture of the USSR, NIBTN - Practice in Fast Machining for Drilling, Rose and Flute Reaming, and Thread Cutting of Ferrous Metals by Carbide Tools. Mashgiz (1951)

67. Ignatov,B.A. - An Investigation of the Drilling of Hardened Steels. Avtoreferat dissertatsii, TsNIITMASh (1956)

68. Romanov,K.G. - Fast Rose and Flute Reaming of Hardened Steels. Oborongiz (1952)

69. - The Machinery Builder's Handbook, Vols.I, II, and III. Mashgiz (1951)

70. Rystsova,V.S. - Changes in the Condition of the Surface Layer of Ground Specimens in the Process of Wear. LIEI Symposium: Surface Finish and the Life of Machine Parts, No.II (1956)

71. Podosenova,N.A. - An Investigation of the Quality of the Surface Layer in External Cylindrical Grinding of Hardened Steel. Avtoreferat dissertatsii, TsNIITMASh (1956)

72. Alekseyev,A.V. - On the Machining of Hardened Steels at High Speeds. Vestnik metallopromyshlennosti, No.1 (1939)

73. Reznitskiy,L.M. - The Machinability of Hardened Special Steels. Symposium of LONITOMASh: Materials for the Machining Conference (1940)

74. Zorev,N.N. - Problems of the Mechanics of the Machining Process, Mashgiz (1956)

75. Grudov,P.P. - Fast Machining. Symposium: Skorostnyye metody obrabotki metallov. Doklady i tezisy dokladov na moskovskoy konferentsii po skorostnym metodam obrabotki metallov. Mashgiz (1949)

76. Avakov,A.A. - The Physical Essence of Fast Machining. Symposium of Papers of the Vsesoyuzniy nauchno-inzhenerno-tekhnicheskoye obshchestvo zheleznodorozhnikov Tbilisi,(1954)

77. Sadovskiy,D.V., Malyshev,K.A., and Sazonov,B.G. - Phase and Structural Transformations in the Heating of Steel. Symposium: Metallovedeniye i termicheskaya obrabotka. Mashgiz (1955)

78. - Machining Tolerances and Methods for Their Improvement. Symposium of LPI im. Kalinina, Mashgiz (1951)

Table of Contents

Page